DRUGS AND THE PHARMACEUTICAL SCIENCES VOLUME 196

SECOND EDITION

Handbook of Drug Screening

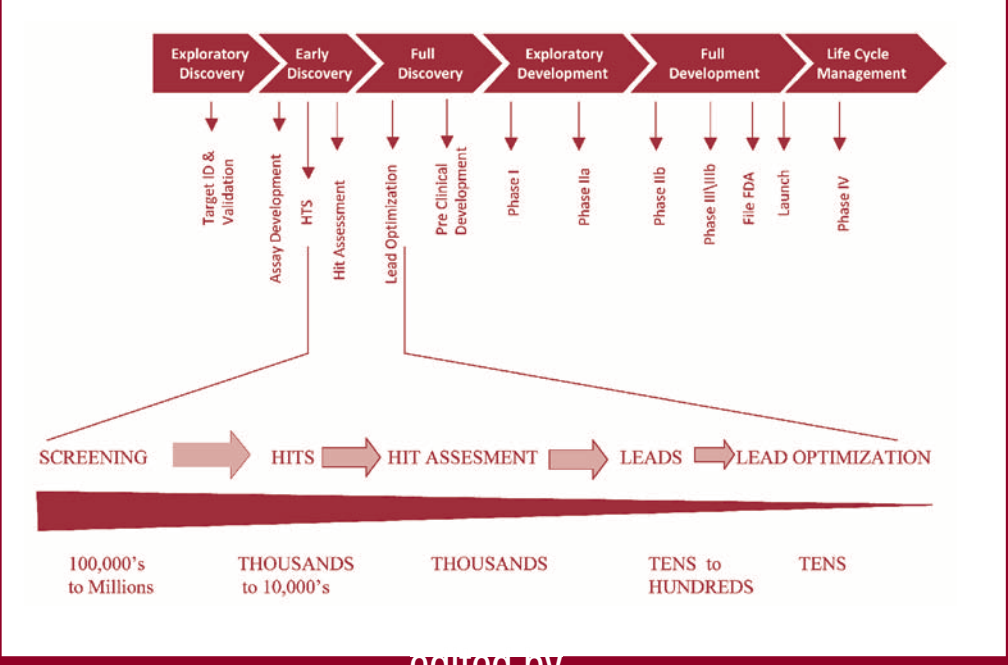

edited by
Ramakrishna Seethala
Litao Zhang

informa
healthcare

Handbook of Drug Screening

DRUGS AND THE PHARMACEUTICAL SCIENCES

A Series of Textbooks and Monographs

Executive Editor

James Swarbrick
PharmaceuTech, Inc.
Pinehurst, North Carolina

Advisory Board

For information on volumes 1–149 in the *Drugs and Pharmaceutical Science* Series, Please visit www.informahealthcare.com

150. Laboratory Auditing for Quality and Regulatory Compliance, *Donald Singer, Raluca-Ioana Stefan, and Jacobus van Staden*
151. Active Pharmaceutical Ingredients: Development, Manufacturing, and Regulation, *edited by Stanley Nusim*
152. Preclinical Drug Development, *edited by Mark C. Rogge and David R. Taft*
153. Pharmaceutical Stress Testing: Predicting Drug Degradation, *edited by Steven W. Baertschi*
154. Handbook of Pharmaceutical Granulation Technology: Second Edition, *edited by Dilip M. Parikh*
155. Percutaneous Absorption: Drugs–Cosmetics–Mechanisms–Methodology, Fourth Edition, *edited by Robert L. Bronaugh and Howard I. Maibach*
156. Pharmacogenomics: Second Edition, *edited by Werner Kalow, Urs A. Meyer and Rachel F. Tyndale*
157. Pharmaceutical Process Scale-Up, Second Edition, *edited by Michael Levin*
158. Microencapsulation: Methods and Industrial Applications, Second Edition, *edited by Simon Benita*
159. Nanoparticle Technology for Drug Delivery, *edited by Ram B. Gupta and Uday B. Kompella*
160. Spectroscopy of Pharmaceutical Solids, *edited by Harry G. Brittain*
161. Dose Optimization in Drug Development, *edited by Rajesh Krishna*
162. Herbal Supplements-Drug Interactions: Scientific and Regulatory Perspectives, *edited by Y. W. Francis Lam, Shiew-Mei Huang, and Stephen D. Hall*
163. Pharmaceutical Photostability and Stabilization Technology, *edited by Joseph T. Piechocki and Karl Thoma*
164. Environmental Monitoring for Cleanrooms and Controlled Environments, *edited by Anne Marie Dixon*
165. Pharmaceutical Product Development: In Vitro-ln Vivo Correlation, *edited by Dakshina Murthy Chilukuri, Gangadhar Sunkara, and David Young*
166. Nanoparticulate Drug Delivery Systems, *edited by Deepak Thassu, Michel Deleers, and Yashwant Pathak*
167. Endotoxins: Pyrogens, LAL Testing and Depyrogenation, Third Edition, *edited by Kevin L. Williams*
168. Good Laboratory Practice Regulations, Fourth Edition, *edited by Anne Sandy Weinberg*
169. Good Manufacturing Practices for Pharmaceuticals, Sixth Edition, *edited by Joseph D. Nally*
170. Oral-Lipid Based Formulations: Enhancing the Bioavailability of Poorly Water-soluble Drugs, *edited by David J. Hauss*
171. Handbook of Bioequivalence Testing, *edited by Sarfaraz K. Niazi*
172. Advanced Drug Formulation Design to Optimize Therapeutic Outcomes, *edited by Robert O. Williams III, David R. Taft, and Jason T. McConville*
173. Clean-in-Place for Biopharmaceutical Processes, *edited by Dale A. Seiberling*

174. Filtration and Purification in the Biopharmaceutical Industry, Second Edition, *edited by Maik W. Jornitz and Theodore H. Meltzer*
175. Protein Formulation and Delivery, Second Edition, *edited by Eugene J. McNally and Jayne E. Hastedt*
176. Aqueous Polymeric Coatings for Pharmaceutical Dosage Forms, Third Edition, *edited by James McGinity and Linda A. Felton*
177. Dermal Absorption and Toxicity Assessment, Second Edition, *edited by Michael S. Roberts and Kenneth A. Walters*
178. Preformulation Solid Dosage Form Development, *edited by Moji C. Adeyeye and Harry G. Brittain*
179. Drug-Drug Interactions, Second Edition, *edited by A. David Rodrigues*
180. Generic Drug Product Development: Bioequivalence Issues, *edited by Isadore Kanfer and Leon Shargel*
181. Pharmaceutical Pre-Approval Inspections: A Guide to Regulatory Success, Second Edition, *edited by Martin D. Hynes III*
182. Pharmaceutical Project Management, Second Edition, *edited by Anthony Kennedy*
183. Modified Release Drug Delivery Technology, Second Edition, Volume 1, *edited by Michael J. Rathbone, Jonathan Hadgraft, Michael S. Roberts, and Majella E. Lane*
184. Modified-Release Drug Delivery Technology, Second Edition, Volume 2, *edited by Michael J. Rathbone, Jonathan Hadgraft, Michael S. Roberts, and Majella E. Lane*
185. The Pharmaceutical Regulatory Process, Second Edition, *edited by Ira R. Berry and Robert P. Martin*
186. Handbook of Drug Metabolism, Second Edition, *edited by Paul G. Pearson and Larry C. Wienkers*
187. Preclinical Drug Development, Second Edition, *edited by Mark Rogge and David R. Taft*
188. Modern Pharmaceutics, Fifth Edition, Volume 1: Basic Principles and Systems, *edited by Alexander T. Florence and Juergen Siepmann*
189. Modern Pharmaceutics, Fifth Edition, Volume 2: Applications and Advances, *edited by Alexander T. Florence and Juergen Siepmann*
190. New Drug Approval Process, Fifth Edition, *edited by Richard A. Guarino*
191. Drug Delivery Nanoparticulate Formulation and Characterization, *edited by Yashwant Pathak and Deepak Thassu*
192. Polymorphism of Pharmaceutical Solids, Second Edition, *edited by Harry G. Brittain*
193. Oral Drug Absorption: Prediction and Assessment, Second Edition, *edited by Jennifer J. Dressman, hans Lennernas, and Christos Reppas*
194. Biodrug Delivery Systems: Fundamentals, Applications, and Clinical Development, *edited by Mariko Morista and Kinam Park*
195. Pharmaceutical Process Engineering, Second Edition, *edited by Anthony J. Hickey and David Ganderton*
196. Handbook of Drug Screening, Second Edition, *edited by Ramakrishna Seethala and Litao Zhang*

SECOND EDITION

Handbook of Drug Screening

edited by

Ramakrishna Seethala
Bristol-Myers Squibb
Princeton, New Jersey, USA

Litao Zhang
Bristol-Myers Squibb
Princeton, New Jersey, USA

informa
healthcare

New York London

Informa Healthcare USA, Inc.
52 Vanderbilt Avenue
New York, NY 10017

Printed in the United States of America on acid-free paper
10 9 8 7 6 5 4 3 2 1

International Standard Book Number-10: 1-4200-6168-2 (Hardcover)
International Standard Book Number-13: 978-1-4200-6168-0 (Hardcover)

Library of Congress Cataloging-in-Publication Data

Handbook of drug screening / edited by Ramakrishna Seethala, Litao Zhang. – 2nd ed.
p. ; cm. – (Drugs and the pharmaceutical sciences ; 196)
Includes bibliographical references and index.
ISBN-13: 978-1-4200-6168-0 (hardcover : alk. paper)
ISBN-10: 1-4200-6168-2 (hardcover : alk. paper) 1. Drug development–Handbooks, manuals, etc. 2. Drugs–Testing–Handbooks, manuals, etc. I. Seethala, Ramakrishna, 1947–II. Zhang, Litao. III. Series: Drugs and the pharmaceutical sciences ; 196.
[DNLM: 1. Drug Evaluation, Preclinical–methods. W1 DR893B v.196 2009 / QV 771 H2366 2009]
RM301.25.H36 2009
615′.19–dc22

2009012407

For Corporate Sales and Reprint Permissions call 212-520-2700 or write to: Sales Department, 52 Vanderbilt Avenue, 16th floor, New York, NY 10017.

Visit the Informa Web site at
www.informa.com

and the Informa Healthcare Web site at
www.informahealthcare.com

Preface

The success of "Handbook of Drug Screening" first edition and the profound advances in how drug screening is done today led us to the second edition of this book. Since the writing of the first edition, screening has matured and became one of the essential functions for drug discovery. Screening departments have carved out their place among the core scientific disciplines in pharmaceutical companies. The pace of drug discovery is increasing, leading to advances in target validation, compound screening, compound libraries, instrumentation, robotics, as well as data handling and mining. We hope that the second edition generates equal or more interest and satisfaction.

Some of the fundamental topics described in the first edition are retained and updated. In the last decade genomics, proteomics, assay technologies, structure-based drug design, automation, and medicinal chemistry have come together to improve the quality and efficiency of drug target validation and potential drug compound selection. New platforms for screening have been developed, with emphasis on reduction of assay cost and improvement of data quality and assay throughput. Since drug screening is a rapidly expanding science, several new chapters have been added including proteomics, microRNA, high-content screening, lead optimization, compound management, and quantitative high-throughput screening.

The completion of sequencing of the human genome has given a large amount of data for the identification of new drug discovery targets. The validation of new genes and protein function as drug targets is essential for the success of drug discovery programs. MicroRNA (miRNA) screening approach, a recent technology, has been widely used for target discovery and target validation by characterization of gene function. Homogenous systems have become the main stay of screening assays. New fluorescent probes and dyes have been used for developing assays for cellular responses and activation of signaling pathways, making it possible to screen multiple parameters in cells by high-content screening. The adaptation of nanofluidic devices and spectral and imaging technologies has led to complex systems that use multiple read-outs to examine interactions as well as multiple parameters. Miniaturization, applications of nanotechnology to screening that reduce the cost of drug discovery are described.

The clustering of the majority of drug targets around few target families such as the G-protein–coupled receptors (GPCRs), ion channels, proteases, nuclear hormone receptors, protein kinases, and phosphatases prompted target family directed screening that complements the traditional screening paradigm. Target family based panel screening allowed evaluation of the compound specificity to the target without any off-target effects. In addition to optimization of the lead

molecule against the target, safety and pharmacology must be examined. Screening methods to address ADMET (Absorption, Distribution, Metabolism, Excretion, and Toxicity), specific receptor panel and channels known to be the origin of some adverse effects in human are described.

The first edition gives the basic foundation of drug screening. This second edition describes advances and impacts of target validation, drug screening methods, target family based screening methods, cell-based assays, and quantitative high-throughput screening on drug discovery. The combination of these approaches improved efficiency to help the early stages of drug discovery in identifying suitable leads that fuel medicinal chemistry programs and reduced the time for preclinical development of drug candidates. Throughout this edition, the state-of-art technologies used in academic and industrial drug discovery process are discussed by experts in the field. We wish to thank all the contributors for contributing these elegant reviews.

Ramakrishna Seethala
Litao Zhang

Contents

Contributors

Arunmozhiarasi Armugam Department of Biochemistry, Yong Loo Lin School of Medicine, National University of Singapore, Singapore

Martyn N. Banks Lead Discovery, Profiling and Compound Management, Applied Biotechnology, Bristol-Myers Squibb, Wallingford, Connecticut, U.S.A.

Nathan W. Bays Department of Automated Lead Optimization, Merck Research Laboratories, Merck & Co., Boston, Massachusetts, U.S.A.

Mark Bowlby Neuroscience Discovery Research, Wyeth Research, Princeton, New Jersey, U.S.A.

Rathnam Chaguturu HTS Laboratory, University of Kansas, Lawrence, Kansas, U.S.A.

Moneesh Chatterjee Lead Discovery, Profiling and Compound Management, Applied Biotechnology, Bristol-Myers Squibb, Wallingford, Connecticut, U.S.A.

Francesca Civoli Department of Clinical Immunology, Amgen Inc., Thousand Oaks, California, U.S.A.

Mary Ellen Cvijic Lead Evaluation, Applied Biotechnology, Bristol-Myers Squibb, Princeton, New Jersey, U.S.A.

Haiteng Deng Proteomics Resource Center, Rockefeller University, New York, New York, U.S.A.

Sharon Diamond Incyte Corporation, Experimental Station, Wilmington, Delaware, U.S.A.

John Dunlop Neuroscience Discovery Research, Wyeth Research, Princeton, New Jersey, U.S.A.

Ian Foltz Department of Protein Sciences, Amgen Inc., Burnaby, British Columbia, Canada

Ralph J. Garippa Roche Discovery Technologies, Roche, Inc., Nutley, New Jersey, U.S.A.

Mark R. Harpel Heart Failure Biochemistry and Cell Biology, Metabolic Pathways Center of Excellence in Drug Discovery, GlaxoSmithKline, King of Prussia, Pennsylvania, U.S.A.

Wishva B. Herath Department of Biochemistry, Yong Loo Lin School of Medicine, National University of Singapore, Singapore

Ann F. Hoffman Roche Discovery Technologies, Roche, Inc., Nutley, New Jersey, U.S.A.

John G. Houston Applied Biotechnology and Discovery Biology, Bristol-Myers Squibb, Wallingford, Connecticut, U.S.A.

Ruili Huang NIH Center for Chemical Genomics, NHGRI, NIH, Rockville, Maryland, U.S.A.

James Inglese NIH Chemical Genomics Center, NHGRI, NIH, Bethesda, Maryland, U.S.A.

Ajit Jadhav NIH Center for Chemical Genomics, NHGRI, NIH, Rockville, Maryland, U.S.A.

K. K. Jain Jain PharmaBiotech, Blaesiring, Basel, Switzerland

Kandiah Jeyaseelan Department of Biochemistry, Yong Loo Lin School of Medicine, National University of Singapore, Singapore

Ilona Kariv Department of Automated Lead Optimization, Merck Research Laboratories, Merck & Co., Boston, Massachusetts, U.S.A.

Dwi S. Karolina Department of Biochemistry, Yong Loo Lin School of Medicine, National University of Singapore, Singapore

Ke Liu NIH Chemical Genomics Center, NHGRI, NIH, Bethesda, Maryland, U.S.A.

Peter R. McDonald University of Kansas, Lawrence, Kansas, U.S.A.

Kirk McMillan New Lead Discovery and Pharmacology, Exelixis Inc., South San Francisco, California, U.S.A

Christopher M. Moxham* Department of Automated Lead Optimization, Merck Research Laboratories, Merck & Co., Boston, Massachusetts, U.S.A.

Trung Nguyen NIH Center for Chemical Genomics, NHGRI, NIH, Rockville, Maryland, U.S.A.

Ravikumar Peri Neuroscience Discovery Research, Wyeth Research, Princeton, New Jersey, U.S.A.

Ashleigh Price University of Kansas, Lawrence, Kansas, U.S.A.

Anuradha Roy University of Kansas, Lawrence, Kansas, U.S.A.

Ramakrishna Seethala Bristol-Myers Squibb, Princeton, New Jersey, U.S.A.

Geetha Shankar Clinical Development, Exelixis Inc., South San Francisco, California, U.S.A.

Current affiliation: Department of Lead Generation/Lead Optimization, Eli Lilly and Co., Indianapolis, Indiana, U.S.A.

Pirthipal Singh Singh Consultancy, Shire Home, Wilmslow, Cheshire, U.K.

Nadya Smotrov Department of Automated Lead Optimization, Merck Research Laboratories, Merck & Co., Boston, Massachusetts, U.S.A.

Noel T. Southall NIH Center for Chemical Genomics, NHGRI, NIH, Rockville, Maryland, U.S.A.

Alexander A. Szewczak Department of Automated Lead Optimization, Merck Research Laboratories, Merck & Co., Boston, Massachusetts, U.S.A.

Byron Taylor University of Kansas, Lawrence, Kansas, U.S.A.

Yuhong Wang NIH Center for Chemical Genomics, NHGRI, NIH, Rockville, Maryland, U.S.A.

Yang Xu Center for Organelle Proteomics of Diseases, Zhejiang University School of Medicine, Hangzhou, and Center for Clinical Laboratory Development, Peking Union Medical College & Chinese Academy of Medical Sciences, Beijing, China

Swamy Yeleswaram Incyte Corporation, Experimental Station, Wilmington, Delaware, U.S.A.

Ge Zhang Lead Evaluation, Applied Biotechnology, Bristol-Myers Squibb, Princeton, New Jersey, U.S.A.

Linqi Zhang Comprehensive AIDS Research Center, Tsinghua University AIDS Research Center, Institute of Pathogen Biology, Chinese Academy of Medical Sciences and Peking Union Medical College, Beijing, China, and Aaron Diamond AIDS Research Center, Rockefeller University, New York, New York, U.S.A.

Litao Zhang Lead Evaluation and Mechanistic Biochemistry, Applied Biotechnology, Bristol-Myers Squibb, Princeton, New Jersey, U.S.A.

Wei Zheng NIH Chemical Genomics Center, NHGRI, NIH, Bethesda, Maryland, U.S.A.

1 Key Factors for Successful High-Throughput Screening

John G. Houston

Applied Biotechnology and Discovery Biology, Bristol-Myers Squibb, Wallingford, Connecticut, U.S.A.

INTRODUCTION

High-throughput screening (HTS) has gone through a series of significant changes over the last two decades, with many companies now describing the journey they have taken (1–4). It has evolved from an ad hoc set of lightly connected instruments and teams, producing a somewhat unpredictable end product, into a highly integrated, automated process capable of delivering a sustained, high-quality output (5). Not only has HTS managed to deliver on its core promise as a reliable platform for producing lead compounds, it has also been able to expand into academic research institutes, as scientists there seek specific compounds to probe disease models. In several companies, the technology platforms underpinning HTS have also been exported into lead optimization and drug safety teams, again showing the flexibility and maturity of the approach.

Of course, it has not all been smooth sailing, and the initial hype around HTS and its ability to transform R&D productivity has ultimately proven to be a significant hindrance in assessing where HTS can really be impactful. HTS alone was never going to be the answer to what ailed pharma companies in the late 1990s or even today. What it always had the potential to do was to provide a fast, reliable, high-capacity method for finding lead compounds and helping to profile and optimize them. Those companies that focused on delivering that type of service from their HTS platforms have probably been more successful and satisfied than those that hoped HTS would be the bedrock for generating more drugs into their late-stage pipelines. The fact that the sister technologies to HTS—genomics, proteomics, and combinatorial chemistry—also largely failed to live up to their early promise, left some observers with a somewhat jaundiced perspective on the drug discovery revolution that was expected, but seemingly failed to materialize (6).

However, the stuttering performance of most pharmaceutical companies and their R&D engines, over the last decade, cannot be placed solely at the door of discovery organizations; regulatory tightening, pricing control, access, IP, and generics have all played their part in changing the landscape for pharmaceutical companies, making it even more difficult for them to be successful. However, it cannot be denied that R&D productivity has significantly declined over a period of time when investment in R&D has been at a historical high. The answer to why that should be is no doubt complex but several scenarios that most thought would occur over the last 10 years or so have not panned out as expected.

The prediction that the human genome project would greatly improve our understanding of human disease and unleash a tsunami of targets amenable for drug intervention has not yet come to pass. Human biology and our understanding of disease mechanisms are just as complex and difficult today as they were 20 years ago (7). We may have more technologies and techniques for probing and trying to understand disease pathways of interest, but our ability to fully predict successful outcomes through drug intervention are still highly limited. In fact, the genes of interest that have come out of the genome project are so novel that one could argue that they have added to the burden of optimizing and developing drugs. More resources are needed to develop a deep understanding of the biology underpinning these targets compared to the fast follow on approaches seen with well-validated mechanisms. Although, novel gene targets offer the chance for break through medicines and the opportunity to be first in class, they come with a very high risk of failure.

We have also not significantly improved our ability to predict whether a particular drug and molecular target will be effective in the clinic. Using animal disease models as a surrogate for human disease has been an important staple of the drug discovery process over many years. The drive to show correlation between animal data and human clinical data has had some success but not enough to allow you to buy down the risk of a late-stage clinical failure. Predictive biomarkers of efficacy have fared no better outside the well-published impact of biomarkers in clinical oncology; for example, HER2/neu and Herceptin.

When you add in the initial failure of combinatorial chemistry to deliver the huge increase in high-quality small molecules, one can begin to see why the R&D new world order has not yet arrived. Nevertheless, this technology did evolve by using parallel array methodologies to start to deliver very useful focused libraries.

So, does HTS deserve to be added to this list of technologies that did not deliver?

In reality, for some companies, HTS has proven to be a great success and in others it has been an abject failure (8). So, why do we see such different outcomes for a process and technology platform that is largely similar in most companies? That is the big question and no doubt the answer will not be a simple equation or solution, but I think there are a few good pointers to show the path to success.

I believe there are several major factors or observations that can determine the ultimate success or failure of any HTS operation.

KEEP CUSTOMER FOCUSED AND DON'T PROMISE WHAT YOU CAN'T DELIVER

One of the fundamental errors any HTS organization can make is to not know or understand who its customers are. This may seem obvious but there are several examples in the industry of HTS and/or technology support teams who have built enterprises that do not deliver what is actually needed by their discovery organizations. An essential step in preventing this is to ensure that HTS goals are completely aligned with the goals of the therapeutic area project teams they are supporting. This can include short-term goals such as the number of targets,

timelines, and level of support needed by the discovery projects during any particular year, as well as longer term goals such as ensuring the compound deck has a deep supply of diverse structures against targets and target classes that are of current and future interest to therapeutic area teams. It is also very important to understand, up front, the major milestones for the project being supported. Those projects that are in backup mode can have a very different set of priorities and expectations than a program just starting out. Making sure that high priority targets are screened with speed and quality almost always aligns with the goals of the therapeutic area customer.

STANDARDIZE, INTEGRATE, AND ELIMINATE WASTE

Cost-disciplined science has become a major reality for most HTS organizations over the last few years. As corporate compound collections have continued to increase along side the demand for screening, the cost burden of running a large HTS infrastructure has grown significantly. By aggressive implementation of automation, miniaturized screening formats, and waste management processes, several HTS groups have been able to increase their overall productivity while keeping their costs flat. Automation of the HTS process has also allowed the full-time employees (FTE) burden to be reduced considerably compared to 10 years ago. Modular functionality, parallel processes, and standard user interfaces along side the general standardization of work flows have greatly increased the flexibility of HTS. Once this type of flexible, standardized functionality has been put in place, the ability to offer customized services is greatly increased and can be done in a nondisruptive, cost-managed way. A fully integrated work flow from lead discovery through profiling and optimization is the best way to ensure success. Ensuring that work streams and capacity flows are matched in the lead discovery phase is a really important factor for integration and streamlined operations. Keeping HTS capacity aligned with the growth in the compound deck, or vice versa, is a basic example of this impedance matching and integration.

However, global scalability and seamless integration of a process do not naturally go hand in hand and can be incredibly difficult, if not impossible to achieve. In this type of scenario, it is critical to have strongly, aligned leadership around the accountability and role of the HTS function.

For those large global companies that have tried to centralize and standardize their HTS operations, they have hit problems of scalability and lack of integration. In these situations, trying to deliver a rapid, high-quality service that fits the needs of every therapeutic area and project team is challenging at best. This has led several large companies to look at how they operate their R&D processes and to find ways of becoming more innovative and flexible. Breaking down large organizations into smaller, more nimble, and entrepreneurial units is one strategy being employed to reduce the burden of keeping large discovery units. Another approach, employed at Bristol-Myers Squibb is to use a centralized, fully accountable base organization that is able to standardize all the lead discovery and optimization platforms and have them "exported" to the other sites in a federated fashion. This has the benefit of local therapeutic area proximity and decision making plus global standardization and elimination of duplicated efforts.

USE TECHNOLOGIES THAT WORK: TRACK YOUR IMPACT, LEARN, AND EVOLVE

It is always tempting to use the latest and greatest new technologies to try and enhance your HTS capabilities or to solve a problem. However, in the transition from using state-of-the-art technologies to those that are cutting, or bleeding edge, one can run the risk of experiencing technology failures. Not all the technologies developed for HTS over the years have been able to deliver what they promised and not all have provided a clear return on investment. When bringing new technology platforms or services into play, it can be a huge help to have these systems run "off line" for a period of time to see if they actually can deliver what is promised. Don't implement a new service until it can.

Once implemented the only way to know if your HTS operation is truly having an impact is by asking, measuring, and tracking it over time. Comprehensive metrics showing operational efficiency gains and program impact are the most definitive way of finding out whether your discovery and optimization process are delivering. Using these metrics to assess whether a particular piece of technology or process change actually improved outcomes is a very useful learning tool. Being able to drop an ineffective technology platform or process can be a powerful method for improving efficiency and overall impact.

HIRE AND DEVELOP CROSS-FUNCTIONAL LEAD DISCOVERY SPECIALISTS

A critical factor in the success of several HTS operations has been the presence of cross-disciplined scientists such as biologist, chemists, informatics specialists, discovery technologists, and engineers housed in the same organization. This cross-pollination of backgrounds and ideas creates a real environment for innovation and problem solving. It encourages collaboration with external vendors to come up with technology solutions that work as well as develop specific customization of in-house platforms or processes. This type of embedding of highly specialized, cross-disciplined skill sets into the core lead discovery environment has also allowed the evolution of HTS platforms into different settings in biology, chemistry, and drug safety.

These are only a few observations that this author has found to be critical when trying to achieve success in the lead discovery and optimization process. I think they are key elements that will stand the test of time no matter what new technologies and innovations are introduced over the coming years. HTS approaches will continue to evolve and have impact beyond its home base, throughout the R&D process. This will be especially true if the lessons learned from HTS and the type of lean thinking and culture needed to be successful get exported along with the technology platforms.

REFERENCES

1. Snowden MA, Green DVS. The impact of diversity based, high-throughput screening on drug discovery: "Chance favours the prepared mind". Curr Opin Drug Discov Dev 2008; 11:553–558.
2. Pereira DA, Williams JA. Review: Historical perspectives in pharmacology. Origin and evolution of high throughput screening. Br J Pharmacol 2007; 152:53–61.

3. Lane SJ, Eggleston DS, Brinded KA, et al. Defining and maintaining a high quality screening collection: the GSK experience. Drug Discov Today 2006; 11:267–272.
4. Houston JG. Banks MN, Binnie A, et al. Case Study: Impact of technology investment on lead discovery at Bristol-Myers Squibb, 1998–2006. Drug Discov Today 2008; 13:44–51.
5. Banks MN, Cacace A, O'Connell J, et al. High throughput screening: Evolution of technology and methods. In: Shayne Cox Gad, ed. Drug Discovery Handbook. John Wiley and Sons, Inc., Hoboken, New Jersey, 2005:559–602.
6. Landers P. Human element: Drug industry's big push into technology falls short. Wall St J 2004, Feb 24.
7. Lindsay MA. Finding new drug targets in the 21st century. Drug Discov Today 2005; 10:1683–1687.
8. Fox S, Farr-Jones S, Sopchack L, et al. High-throughput screening: Update on practices and success. J Biomol Screen 2006; 11:864–869.

2 Critical Components in High-Throughput Screening: Challenges and New Trends

Litao Zhang

Lead Evaluation and Mechanistic Biochemistry, Applied Biotechnology, Bristol-Myers Squibb, Princeton, New Jersey, U.S.A.

Martyn N. Banks

Lead Discovery, Profiling and Compound Management, Applied Biotechnology, Bristol-Myers Squibb, Wallingford, Connecticut, U.S.A.

John G. Houston

Applied Biotechnology and Discovery Biology, Bristol-Myers Squibb, Wallingford, Connecticut, U.S.A.

INTRODUCTION

High-throughput screening (HTS) has become a mature and reliable component of the drug discovery process. It now has a proven, if somewhat variable, track record of impact on pipelines, and the technology is migrating into other parts of the drug discovery and optimization process as well as into academic institutes (1–7).

A recent survey of 58 HTS laboratories and 34 suppliers indicated that more than a 100 clinical candidates and 4 marketed products could trace their roots to past HTS approaches (8). In 2005, the National Institutes of Health (NIH), as part of the NIH Roadmap for Medical Research, funded ~$90 million in grants to nine screening centers to use HTS methods for identifying small molecule probes as research tools for drug discovery. Today, over 60 HTS screening centers have been established at academic laboratories and government institute laboratories in the United States. This trend of deploying screening technologies into academic environments should have an enabling impact for researchers and allow new breakthroughs to emerge. HTS technologies have also been implemented in parts of the R&D process that did not traditionally use HTS techniques such as lead optimization (9,10).

HTS has evolved over the last two decades from an expensive, slow, and random compound screening process, into a skill-based practice that balances chemical, biological, and technological inputs to purposefully screen compound collections built through planned synthesis and purchasing strategies (2,11,12). This approach will remain useful for both hit identification and tool identification for early drug discovery well into the next decade. The challenges ahead for HTS approaches will include capturing further gains in efficiency as well as providing continued impact in helping to discover and optimize drugs.

HTS originally emerged as a nascent technology platform for natural product extract screening in the 1980s (11). At that time, compound repositories were

a lot less defined than today, and screening campaigns took months to complete. With the advent of combinatorial chemistry in the early 1990s, there was a commensurate response by the HTS community, instrument manufacturers, and assay technology providers to meet the challenge of dealing with an exponential growth in the number of compounds available for test. This resulted in a drive for higher throughput, more reliable automation, with significant miniaturization of assays to conserve costs. Today the challenge for most HTS organizations is to continue to show their value by rapidly and consistently identifying good starting points for as many medicinal chemistry programs as possible, in a cost contained manner.

TACTICS USED IN HTS

There are now a number of screening approaches and tactics (2,9,10) used by discovery-based project teams for hit identification. The classic approach, which has been most utilized and optimized over the last two decades, is that of large-scale "random" or diversity-based screening. The chances of gaining a successful outcome through such a serendipity-based approach can be strongly influenced by a number of key factors including, but not limited to, the size of the deck, the storage conditions of the compounds, the structural diversity of the collection, the integration of the lead discovery process, and the quality of the bioassay used in the screen. It is apparent that a number of HTS organizations have had measurable success using this approach but a significant number have also had limited success. The burden of keeping a large HTS/compound management infrastructure in place as well as the cost of making, acquiring, and quality-assuring compounds in the deck have switched many lead discovery outfits to use alternate approaches to find chemical starting points.

A more focused approach that has gained a lot of traction is to screen a diverse, but limited, set of compounds that are representative of the entire compound collection. Screening hits are used to build Bayesian and/or 4D pharmacophore models (14–17); the models allow us to then "re-mine" the available compound inventory and a second set of compounds are selected for assay. By repeating this iterative cycle, compounds are chosen for progression into medicinal chemistry. Usually, mining of the internal deck is complemented by acquisition of specific compounds from commercial vendors. This sequential screening approach (14–17) can be a very efficient alternative to screening the entire compound inventory. The focused or sequential screening approach requires tight integration of compound management and screening processes to rapidly identify progressible chemotypes. Through the linked use of on-line compound stores and screening automation platforms, this particular loop can be closed.

Focused deck screening has become a widely used hit identification paradigm in early drug discovery (18), and this approach enables cost-effective and rapid hit identification.

One of the more stringent approaches currently used in lead discovery is called virtual screening (19–22). In this approach, computational models are used to help define the types of molecules that would be "expected" to bind to a particular target. This analysis is usually followed by the construction of a focused set of compounds based on these theoretical "leads" (18,23,24). This method is particularly useful if there are structural and medicinal chemistry datasets available to build a robust model. By decreasing, the stringency computational models

can also be used to select a set of compounds built around a target class, or target class–subset, for example, ion channels or specifically K^+ channels. These two approaches allow compound sets to be assembled independent of screening and be continuously upgraded with new compounds as new knowledge becomes available.

As the number of quality hits emerging from a screening campaign increases, there is an additional challenge—which compounds should be selected for further study (14,25)? Many HTS groups now supply additional assay data to support the prioritization of screening hits for future progression, for example, selectivity information and more detailed cellular data, etc. Carrying out an effective and well-integrated hit assessment phase has created a trend towards further centralization of screening teams to support in vitro lead optimization. The lead optimization screening infrastructure has benefited from the automation and miniaturization investments originally made in HTS. However, some of the challenges of this continuous flow approach from hit identification into lead optimization include overall process, assay, and data connectivity issues. There are many reasons why similar processes and assays can still generate different data sets, however, one can mitigate against these disconnects by prudent planning and introducing effective quality control into the overall HTS to lead optimization process.

HTS PROCESS

The efficiency, quality, and eventual successful outcome of a HTS process is dependent on several critically linked components (2,9), including generation and supply of reagents, compound supply and storage, bioassay methodology and reproducibility, integrated automation platforms, and comprehensive data acquisition and processing. In this section, we introduce some of the critical HTS components and discuss challenges and trends.

Generation and Supply of Reagents

Recombinant Proteins

The completion of the human genome sequence has enabled more rapid access to potential targets of interest for therapeutic area biologists to explore and for HTS teams to find leads for. In the current drug discovery paradigm, recombinant targets still represent one of the significant reagent sources for in vitro HTS assays. One of the challenges in developing recombinant reagents that are to be used in a HTS campaign is to express high enough levels of stable and functional proteins in vitro. Recently, numerous developments have been made to improve the production of soluble and active proteins in a variety of expression systems (26,27). These include modifications of the expression constructs, introduction of new and/or improved expression systems, and development of improved cell-free protein synthesis systems. Another challenge for reagent generation teams is aligning reagent development capacity and speed with the increased demand coming from HTS teams. The introduction of robotics for reagent selection and development has enabled a massive parallelization of expression experiments, thereby significantly increasing the speed of reagent generation.

Demand for over expression of recombinant receptors and secreted proteins is continually increasing. Transformed insect cell systems are receiving increasing attention from the research community and the biotechnology

industry. Baculoviruses (28–30) represent one of a few ideal expression systems that can produce recombinant, secreted, and membrane-anchored proteins. This is because such systems can enhance the yield of recombinant proteins with biologically relevant properties such as posttranslational modification.

Today, most recombinant proteins can be prepared and stored ready for assays at a future date, this removes the need to provide "just-in-time" reagents in house. This has created a trend to outsource such HTS supplies with the availability of a variety of recombinant proteins having greatly increased over the last few years in the catalogs of service vendors around the world.

Cellular Reagents

As the ratio of cell based to biochemical assays used in HTS continues to increase, especially as more complex targets are identified, there has been a growing need to build cellular technologies and an efficient infrastructure to supply cells for high-throughput assays.

A range of different technologies are currently available to facilitate the construction of recombinant cell lines and enhance reagent quality for HTS (27,31,32). The utility of various technologies in engineering cellular properties has clearly broadened our options for cell systems used in HTS (33–35). For instance, two genes, one encoding a type II membrane glycosylating sialyltransferase (siat7e) and the other encoding a secreted glycoprotein (lama4), were found to influence cellular adhesion, an essential mechanism for cells to attach to a surface in order to proliferate (34). A gene encoding a mitochondrial assembly protein (cox15) and a gene encoding a kinase (cdkl3) were found to influence cellular growth. Enhanced expression of either gene resulted in slightly higher specific growth rates and higher maximum cell densities for cell lines commonly used in HTS, for example, HeLa, HEK-293, and CHO cell lines (34).

Today, cell reagents used for HTS often come from different therapeutic area teams because specific expertise might be required to generate these cell reagents. Therefore, it is important to establish a rigorous QC/QA process for cell reagents before the cell lines are utilized for HTS campaign. For example, comprehensive characterization of G-coupled receptors (GPCR) in any given cell line depends on the background molecular biology used in the construction of the cell line and the pharmacology of the target itself. Because of these variables, a process for GPCR reagent characterization is recommended to ensure consistent outcomes in the screening process (Fig. 1). However, there are limitations in our ability to provide a comprehensive pharmacological characterization of certain GPCR cellular reagents. The limited pharmacological knowledge or availability of chemical tools for certain classes of GPCRs can impede our ability to differentiate pharmacological properties of receptor subtypes and mutants; lack of physiological ligands can also lead to unknown pharmacological properties of orphan GPCRs. Under these circumstances, we must depend on other molecular approaches to characterize cellular reagents.

For cellular HTS assays, there is often a need to supply cells directly to the screens. This dependency on the "just-in-time" supply of cellular reagents for assays is always challenging and can be resource intensive. This challenge can be largely solved by deployment of automation and two examples are shown in Figures 2 and 3 (10). The Cellmate™ (The Technology Partnership, Cambridge, U.K.) together with a flask loading mechanism and an incubator is ideal for a

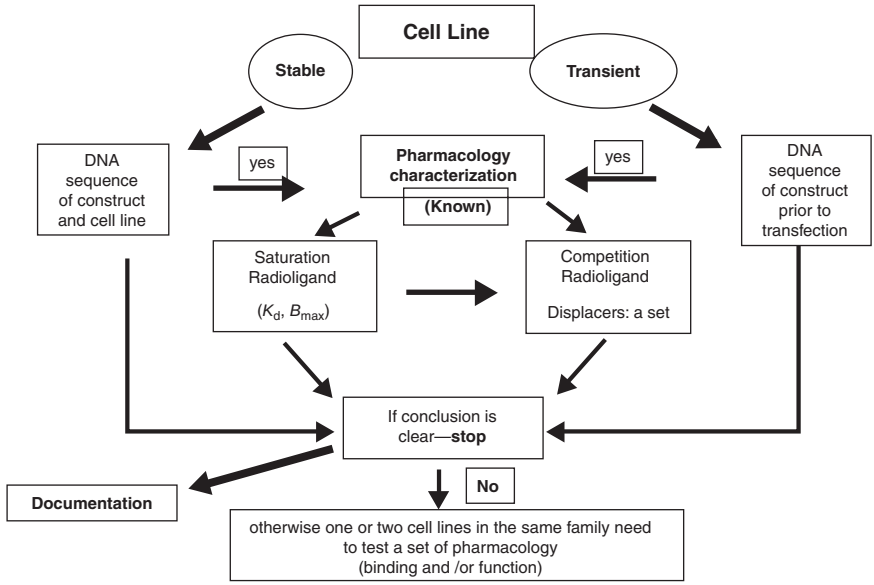

FIGURE 1 Cell line characterization process for GPCRs.

FIGURE 2 Photograph of the Cellmate™ robot built by The Technology Partnership, Cambridge, U.K. This robot performs cell seeding in either large T flasks or roller bottles, exchanges media, rinses cell sheets, purges gases, harvests cells by trypsinization or scraping, and supports transfections.

FIGURE 3 Photograph of the SelecT™ robot built by The Technology Partnership, Cambridge, U.K. This robot maintains between 1 and 50 cell lines, performs passaging, cell counting and viability measurements, and direct plating into microtiter plates for bioassay.

relatively large number of flasks for a single cell line used for HTS. In the authors hands a lot of the routine media changes and harvesting have been performed using this platform. The SelecT™ (The Technology Partnership) is one example of a more sophisticated platform that maintains upwards of 50 different cell lines. This system is capable of counting and dispensing cells directly into microplates ready for assay. At Bristol-Myers Squibb (BMS), both these automation platforms have significantly enhanced the capacity and throughput of cell-based HTS.

One new trend in cellular HTS is to avoid "just in time" cell supply and move to cryopreserved cell sources or division-arrested cells (36–36). These cryopreserved assay ready cells alleviate the need for daily cell culture supply and enhance cell-based assay support flexibility.

In the past, primary cells were not an option for HTS, because insufficient high-quality material could be made available to support an entire HTS campaign. To complete an HTS campaign, multiple batches of cells from different donors needed to be used and consequently donor-to-donor variation sometimes led to poor assay reproducibility. However, cryopreservation of pooled donor cells and assay miniaturization has enabled screening by using primary cells and minimized donor-to-donor variation.

Compound Supply

Efficient compound supply for HTS depends on a technology infrastructure that can support compound storage, compound tracking/retrieving, and assay

ready compound preparation. During the past two decades, technological- and informatics-based solutions for compound supply have been centered on enabling a variety of flexible screening approaches to be deployed as well as meeting the increased demands of screening ever increasing corporate compound collections (2,41–43). Continual improvements to the compound management process were necessary in order to keep pace with the growth of both targets and compounds that were becoming available for screening. From the 1980s to 1990s, most compound management organizations were focused on removing the bottlenecks around compound preparation for HTS including compound plate generation, compound plate replication, and compound storage/retrieval. For some, fully automated compound storage and retrieval systems were the key to enhance the speed and capacity of HTS. By automating the compound plate preparation and storage process, the linear, sometimes manual, connection between compound management and screening was reduced because full screening decks were made in advance. This new streamlined approach removed one of the major bottlenecks in the compound preparation process and significantly enhanced the productivity of HTS laboratories.

This increase in hit-finding capability has produced another potential bottleneck, as these compounds now have to be profiled and tested out in a wide array of secondary assays. This could result in significantly increased demand for customized compound plates for hit assessment and lead evaluation teams. Historically, a variety of plate formats with different compound starting concentrations and multiple freeze–thaw cycles of compound solutions were introduced into the compound preparation process to deal with the many different requests coming from therapeutic area scientists following up on their screening hits. This severely limited the efficiency of compound management because an entire catalogue of processes needed to be optimized and maintained. Today, in many lead discovery organizations, centralized teams for hit assessment and lead optimization have allowed compound management departments to minimize the variations in plate types and plate layouts for the compounds they supply.

Other issues that can affect the outcome quality of a compound management/screening outfit include compound stability and solubility. How compounds are formatted and stored has drawn broad attention and debate across the industry over a number of years (44–46)? In addition, issues such as precipitation of compounds in DMSO (dimethyl sulfoxide) screening stocks or HTS assays became a recognized problem (45,47,48). A number of solutions to these issues have been implemented by companies over the years (43,49–51), and most compound collections now have rigorous environmental and quality control systems in place.

At BMS, the increased demands on compound profiling and lead optimization led to some new challenges for compound management, that is, rapid compound depletion and frequent sample retrieving. This issue, in part, arose from an inefficient compound ordering and preparation process after HTS campaigns had been completed. New and/or unnecessary bottlenecks in the compound management process were created by having nonstandardized mechanisms for dealing with hit assessment and lead optimization. To overcome these issues at BMS, the centralized compound management organization was giving the accountability to support both hit identification and lead optimization as a standardized linked process. This change streamlined the hit identification to

lead optimization process, allowing more efficient tracking and usage of compounds as well as providing the added bonus of strengthening data connectivity and reproducibility between hit identification and lead optimization assays. This change also created more compound management flexibility, enhanced the speed for just-in time compound preparation, and reduced compound consumption.

Today, there is still a significant technology gap in the universal automation of dry compound dispensing. Dry compounds are mainly handled by a manual weighing process. Various automated technology solutions for weighing dry samples have been tried but none are sufficiently flexible to adapt to the wide range of different compound characteristics that can be experienced in a compound management setting.

The technology infrastructure around compound storage, tracking, and retrieving (41,52) has greatly matured over the last two decades and has created some very high-functioning well-integrated lead discovery units.

An alternate trend that has been adopted by some companies, who do not want to invest in an "in-house" infrastructure, is to outsource compound supply to external vendors. These companies use this service to enhance their screening ability and flexibility. More importantly, this new compound supply chain opens enormous opportunities for individual academic laboratories to conduct HTS and search for chemical probes to support exploratory biology research.

Bioassay Detection Methods

Bioassay detection techniques in HTS include a variety of fluorescent, luminescent, colorimetric, and radiochemical labels. Advanced bioassay detection methods will be discussed in other chapters of this book. In this section, we will mainly focus on the challenges and new trends of the bioassay detection methods for the HTS assay designer.

Today, one of the main challenges for an assay designer is how to minimize both false positives and false negatives in a screen (53–55). Each detection method has its strengths and weaknesses with regard to false positives; for example, fluorescence—interference due to light quenching or intrinsic fluorescence of compounds under test. False positives can be tolerated to a certain extent by using an alternate detection technique, or a secondary assay, during the hit-assessment phase of screening. False negatives are a more challenging event to overcome. For example, a compound maybe active against a molecular target but is also cytotoxic, and this cytotoxicity may dominate the cellular effect at the particular concentration under test and/or the incubation times used in the cell-based assay. There are certain approaches that can be used to minimize or mitigate false negatives; a HTS campaign could be run by using different formats and detection technology to allow cross comparison of hits, though this might not be considered cost-effective. Secondly, compounds that appear cytotoxic could be computationally compared to real positives to assess chemical similarity and thereby glean knowledge about the elements of the compound structure that may be causing cytotoxicity and/or *bona fide* activity.

The second challenge in assay design is that commonly reported assay designs are commonly engineered away from more physiologically relevant assay models of disease. For example, a neuronal GPCR overexpressed in a HEK cell used to look for allosteric modulation is significantly different from a primary neuron where basal levels of the receptor maybe in low abundance. One

future trend in bioassay detection methods is to move away from these "over-engineered" platforms to more physiologically relevant assays using primary or differentiated stem cells. That said, biochemical assays still have an important role in HTS.

Recently, high-content screening (HCS) (56–58) has become another powerful platform for HTS assay designers. This platform has enabled HTS scientists to discover new chemical entities that were difficult to discover using conventional HTS assays. The platform combines automated fluorescence microscopy and image analysis. It can be used to detect cellular events in both a static and dynamic mode. In the static mode, cells are fixed after compound treatment and relevant cellular markers stained with fluorescently labeled antibodies. High-content readers are used to scan the microtiter plate, collect, and process the image to yield quantitative spatial data. With current fluorescent labels multiple components can be detected at the same time increasing the information that can be gleaned from a single assay. The obvious disadvantage of a fixed cell is that a single time point needs to be preselected. Dynamic approaches in HCS overcome this impediment by using biosensors that are tracked in real time within the cell, for example, translocation of proteins to and from a range of cellular components. However, most of the biosensors are fluorescent conjugated proteins and therefore are not exactly physiological.

Another important trend in bioassay detection assay platforms is to remove the aforementioned labels completely and move toward direct measurement of the analyte (59–63). These label-free techniques, for example, mass spectroscopy, nuclear magnetic resonance, and other techniques, have the potential to eliminate the need for labels in HTS assays thereby eliminating false positives due to assay interference. Additionally, these techniques will also simultaneously detect many molecular species and facilitate the measurement of multiple assay end points. Most of these techniques are throughput limited today but the technology is evolving rapidly and may, in the not too distant future, provide a real alternative for HTS.

Automation Platforms

Automation platforms used to support HTS have gone through significant evolutionary changes over the last 15 years to fit the various needs of lead discovery organizations. Their major focus over these years has been to create capacity, drive process efficiency and flexibility, ensure data quality, and control costs. Almost all of the automation systems used over the years have contained a standard set of functional units and capabilities. Usually, a series of liquid handlers, methods for dispensing liquids over a wide range of volumes (5 nl to 250 μl), incubators, microtiter plate hotels, plate readers, imagers and other detectors, barcode readers, and plate sealers/de-sealers or lidding/de-lidding stations. In this section, we focus on two key components: liquid handlers and methods for moving plates on automation platforms. The detectors used in HTS are assay specific and are discussed in subsequent chapters.

Liquid Handlers

Liquid handlers are an essential component of HTS laboratories automation platforms. The key features of these devices are to aspirate or dispense both organic solvents and aqueous solutions into microplates. There are basically two classes

of liquid handler: contact and noncontact. A traditional contact liquid handler often includes a dragging action, such as a touch off technique against the solid surface of a vessel or a liquid surface. One disadvantage of this technique is that the surface tension of the last droplet will introduce assay reagent carryover and therefore assay imprecision. The new trend to solve this problem is to apply a noncontact liquid handler. These noncontact liquid handlers eliminate the need for pipette tips, pin tools, etc. A further advantage to noncontact dispensing is the reduction in reagent waste generation and ultralow-volume dispensing (i.e., nanoliter range) from and into microplates. More importantly, noncontact dispensing of compounds removes the need for aqueous intermediate dilution of compounds prior to assay. Intermediate dilution steps can result in compound precipitation due to poor solubility of compounds.

One of the challenges in evaluating a liquid handlers' performance is to develop consistent protocols by using a range of solvents and volumes required for HTS assays (64–66). Because of assay miniaturization, nanoliter dispensing liquid handlers are becoming more common and pose new challenges for routine quality control procedures. In our experience, the pipetting precision is better than some of the readers used to measure dye volumes, and gravimetric techniques have limitations in determining the CV of such low volumes. A broad range of QC/QA protocols need to be developed to gain confidence in HTS data generation.

Methods of Moving HTS Plates on Automation Systems

Methods for moving microtiter plates between a series of liquid handlers often determine the speed and capacity of an automation platform. There are four basic approaches for moving microtiter plates: manual, a static anthropomorphic robot arm, an anthropomorphic arm on a track, and a conveyor-based system. Examples of the later three are shown in Figure 4. One of the current challenges is how to effectively integrate compound preparation, reagent preparation, assay execution, and data analysis into these different automation platforms regardless of assay format.

FIGURE 4 Examples of automation platforms used in HTS. Part (**A**) is a static arm surrounded by instrumentation required to support a particular assay. In part (**B**), the real estate is expanded through the use of a robot on a track increasing instrument capacity on the system. Part (**C**) uses a conveyor belt to move microtiter plates between loaders that pick and place microtiter plates onto an instrument for processing.

Data Analysis and Data Reporting

HTS data analysis and data reporting processes have become one of the key elements for HTS operations success. Any changes made in bioassay detection methods and automation platforms have usually required some new informatics solution. During the past two decades, HTS dedicated informatics approaches have permitted rapid data capture, processing, analysis, and data reporting. These informatics solutions now play a critical role in ensuring good data quality, minimizing assay variability, and enabling facile decision-making steps. Statistical analysis software has been broadly utilized in HTS data analysis for some time now and various methods have been reported in the literature (67–69). These informatics-based approaches allow assay operators to examine in "real time" assay performance during the HTS campaign. More importantly, any systematic errors present in HTS data can be easily estimated and removed from the data sets. In order to deliver high-quality hits to the project teams, a broad profiling data set is often generated to guide decisions on hit to lead optimization. The volume of data generated by such profiles present a new challenge: how to effectively visualize HTS data sets and capture SAR trends from the HTS data reports.

To maximize the value of current and past HTS data, powerful informatics tools are required to rapidly retrieve and analyze the various data sets. A number of statistical techniques including cluster analysis, link analysis, deviation detection, and disproportionality assessment have been utilized to assess the quality of "live" and archived HTS data. To this end, HTS data mining (70,71) has now become a fast-growing field. This approach can enable discovery project teams to identify "tool" molecules early in the discovery process to help target validation and POC studies before they initiate a HTS campaign. In addition, it provides a cost-effective way for fast follow-on, SAR feasibility studies, toxicity, and selectivity prediction. HTS data mining demands could lead informatics software development for the next few years.

Today, the overall benefit and value of advanced HTS technology platforms depends in large part on the informatics infrastructure used for data analysis and data reporting. Recently, the new drive for HCS platforms has led to a new trend that is challenging the established informatics frameworks deployed across the discovery process (72). Because of the extremely large data volumes generated from HCS and the more complicated sets of data derived from the numerous HCS images, a new informatics infrastructure is necessary to support effective HCS platform implementation. It is clear that broad informatics tool development and integration that keeps pace with the changing needs of lead discovery processes will continually drive value for drug discovery and optimization approaches for the foreseeable future.

SUMMARY

Today, HTS is a well-established approach used in the pharmaceutical industry. However, HTS success is no longer defined as the number of hits identified from HTS campaigns. Advancing hits into the later stages of drug discovery and lead optimization have become the new area of influence for HTS. Implementation of technology platforms into the lead optimization phase of drug discovery is a recent trend across the industry and has helped streamline the approach of identifying and optimizing a set of lead molecules. Overall the successful conclusion of any HTS campaign depends on a number of critical factors: the

selection of target type to be screened, the choice of assay technology platform to be used, the quality of the hit to lead process, and the type of skill sets available to ensure all the component parts work together smoothly. HTS approaches have moved beyond their original scope, and the lessons learned by setting up discovery operations over the last 15 years have helped reshape current lead discovery teams and allowed them to become more productive, more comprehensive in their output, and more successful in their impact.

REFERENCES

1. Bender A, Bojanic D, Davies JW, et al. Which aspects of HTS are empirically correlated with downstream success? Curr Opin Drug Discov Devel 2008; 11(3):327–337.
2. Houston JG, Banks MN, Binnie A, et al. Case study, impact of technology investment on lead discovery at Bristol-Myers Squibb, 1998–2006. Drug Discov Today 2008; 13(1–2):44–51.
3. Inglese J, Johnson RL, Simeonov A, et al. High-throughput screening assays for the identification of chemical probes. Nat Chem Biol 2007; 3(8):466–479.
4. Carnero A. High-throughput screening in drug discovery. Clin Transl Oncol 2006; 8(7):482–490.
5. Fox S, Wang H, Sopchak L, et al. High-throughput screening 2002, moving toward increased success rates. J Biomol Screen 2002; 7(4):313–316.
6. Fox S, Farr-Jones S, Sopchak L, et al. High-throughput screening: Searching for higher productivity. J Biomol Screen 2004; 9(4):354–358.
7. Fox S, Wang H, Sopchak L, et al. High throughput screening: Early successes indicate a promising future. J Biomol Screen 2001; 6(3): 137–140.
8. Fox S, Farr-Jones S, Sopchak L, et al. High-throughput screening: Update on practices and success. J Biomol Screen 2006; 11:864–869.
9. Houston JG, Banks MN, Zhang L. Technologies for improving lead optimization. Am Drug Discov 2006; 3:1–7.
10. Banks MN, Zhang L, Houston, JG. Screen/counter-screen: Early assessment of selectivity. In: Bartlett PA, Entzeroth M, eds. Exploiting Chemical Diversity for Drug Discovery. London, U.K.: Royal Chemical Society Publication, 2006:315–335.
11. Houston JG, Banks MN. The chemical–biological interface: Developments in automated and miniaturized screening technology. Curr Opin Biotechnol 1997; 8(6):734–740.
12. Pereira DA, Williams JA. Origin and evolution of high throughput screening. Br J Pharmacol 2007; 152(1):53–61.
13. Mayr LM, Fuerst P. The future of high-throughput screening. J Biomol Screen 2008; 13(6):443–448.
14. Padmanabha R, Cook L, Gill J. HTS quality control and data analysis: A process to maximize information from a high-throughput screen. Comb Chem High Throughput Screen 2005; 8(6):521–527.
15. Johnson SR, Padmanabha R, Vaccaro W, et al. A simple strategy for mitigating the effect of data variability on the identification of active chemotypes from high-throughput screening data. J Biomol Screen 2007; 12(2):276–284.
16. Cloutier LM, Sirois S. Bayesian versus Frequentist statistical modeling: A debate for hit selection from HTS campaigns. Drug Discov Today 2008; 13(11–12):536–542.
17. Vedani A, Dobler M. Multi-dimensional QSAR in drug research. Predicting binding affinities, toxicity and pharmacokinetic parameters. Prog Drug Res 2000; 55:105–135.
18. Snowden M, Green DV. The impact of diversity-based, high-throughput screening on drug discovery: "Chance favors the prepared mind". J Biomol Screen 2006; 11(4):553–558.
19. Muegge I. Synergies of virtual screening approaches. Mini Rev Med Chem 2008; 8(9):927–933.

20. Tanrikulu Y, Schneider G. Pseudoreceptor models in drug design: Bridging ligand- and receptor-based virtual screening. Nat Rev Drug Discov 2008; 7(8):667–677.
21. Sun H. Pharmacophore-based virtual screening. Curr Med Chem 2008; 15(10):1018–1024.
22. Stahura FL, Bajorath J. Virtual screening methods that complement HTS. Comb Chem High Throughput Screen 2004; 7(4):259–269.
23. Valler MJ, Green D. Diversity screening versus focussed screening in drug discovery. Drug Discov Today 2000; 5(7):286–293.
24. Miller JL. Recent developments in focused library design: Targeting gene-families. Curr Top Med Chem 2006; 6(1):19–29.
25. Simmons K, Kinney J, Owens A, et al., Practical outcomes of applying ensemble machine learning classifiers to high-throughput screening (HTS) data analysis and screening. J Chem Inf Model 2008; 48(11):2196–2206.
26. Forstner M, Leder L, Mayr LM. Optimization of protein expression systems for modern drug discovery. Expert Rev Proteomics 2007; 4(1):67–78.
27. Horrocks C, Halse R, Suzuki R, et al. Human cell systems for drug discovery. Curr Opin Drug Discov Devel 2003; 6(4):570–575.
28. Murphy CI, Piwnica-Worms H. Overview of the baculovirus expression system. Curr Protoc Neurosci 2001; Chapter 4, Unit 4, 18.
29. Mäkelä AR, Oker-Blom C. The baculovirus display technology—An evolving instrument for molecular screening and drug delivery. Comb Chem High Throughput Screen 2008; 11(2):86–98.
30. Condreay JP, Kost TA. Baculovirus expression vectors for insect and mammalian cells. Curr Drug Targets 2007; 8(10):1126–1131.
31. Eglen RM, Gilchrist A, Reisine T. The use of immortalized cell lines in GPCR screening: The good, bad and ugly. Comb Chem High Throughput Screen 2008; 11(7):560–565.
32. Friedrich J, Eder W, Castaneda J, et al. A reliable tool to determine cell viability in complex 3-d culture: The acid phosphatase assay. J Biomol Screen 2007; 12(7):925–937. [Erratum in: J Biomol Screen 2007; 12(8):1115–1119].
33. Douris V, Swevers L, Labropoulon V, et al. Stably transformed insect cell lines: tools for expression of secreted and membrane-anchored proteins and high-throughput screening platforms for drug and insecticide discovery. Adv Virus Res 2006; 68:113–156.
34. Jaluria P, Chu C, Betenbaugh M, et al. Cells by design: A mini-review of targeting cell engineering using DNA microarrays. Mol Biotechnol 2008; 39(2):105–111.
35. Eglen RM, Gilchrist A, Reisine T. Overview of drug screening using primary and embryonic stem cells. Comb Chem High Throughput Screen 2008; 11(7): 566–572.
36. Kunapuli P, Zheng W, Weber M. et al. Application of division arrest technology to cell-based HTS: Comparison with frozen and fresh cells. Assay Drug Dev Technol 2005; 3(1):17–26.
37. Digan ME, Pou C, Niu H. et al. Evaluation of division-arrested cells for cell-based high-throughput screening and profiling. J Biomol Screen 2005; 10(6):615–23.
38. Cawkill D, Eaglestone SS. Evolution of cell-based reagent provision. Drug Discov Today 2007; 12(19–20):820–825.
39. Fursov N, Cong M, Federici M, et al. Improving consistency of cell-based assays by using division-arrested cells. Assay Drug Dev Technol 2005; 3(1):7–15.
40. Zaman GJ, de Roos JA, Blomenröhr M, et al. Cryopreserved cells facilitate cell-based drug discovery. Drug Discov Today 2007; 12(13–14):521–526.
41. Yasgar A, Shinn P, Jadhav A, et al. Compound management for quantitative high-throughput screening. J Assoc Lab Automation 2008; 13(2):79–89.
42. Benson N, Boyd HF, Everett JR., et al. NanoStore: A concept for logistical improvements of compound handling in high-throughput screening. J Biomol Screen 2005; 10(6):573–580.

43. Schopfer U, Engeloch C, Stanek J, et al. The Novartis compound archive—From concept to reality. Comb Chem High Throughput Screen 2005; 8(6):513–519.
44. Oldenburg K, Pooler D, Scudder K, et al. High throughput sonication: Evaluation for compound solubilization. Comb Chem High Throughput Screen 2005; 8(6):499–512.
45. Kozikowski BA, Burt TM, Tirey DA, et al. The effect of freeze/thaw cycles on the stability of compounds in DMSO. J Biomol Screen 2003; 8(2):210–215.
46. Quintero C, Rosenstein C, Hughes B, et al. Utility control procedures for dose–response curve generation using nanoliter dispense technologies. J Biomol Screen 2007; 12(6):891–899.
47. Di L, Kerns EH. Biological assay challenges from compound solubility: Strategies for bioassay optimization. Drug Discov Today 2006; 11(9–10):446–451.
48. Balakin KV, Savchuk NP, Tetko IV. In silico approaches to prediction of aqueous and DMSO solubility of drug-like compounds: Trends, problems and solutions. Curr Med Chem 2006; 13(2):223–241.
49. Pelletier MJ, Fabiili ML. Rapid, nondestructive near-infrared assay for water in sealed dimethyl sulfoxide compound repository containers. Appl Spectrosc 2007; 61(9):935–939.
50. Semin DJ, Malone TJ, Paley MT, et al. A novel approach to determine water content in DMSO for a compound collection repository. J Biomol Screen 2005; 10(6):568–572.
51. Delaney JS. Predicting aqueous solubility from structure. Drug Discov Today 2005; 10(4):289–295.
52. Schopfer U, Andreae MR, Hueber M, et al. Compound Hub: Efficiency gains through innovative sample management processes. Comb Chem High Throughput Screen 2007; 10(4):283–287.
53. Wu Z, Liu D, Sui Y. Quantitative assessment of hit detection and confirmation in single and duplicate high-throughput screenings. J Biomol Screen 2008; 13(2):159–167.
54. von Ahsen O, Schmidt A, Klotz M, et al. Assay concordance between SPA and TR-FRET in high-throughput screening. J Biomol Screen 2006; 11(6):606–616.
55. Gribbon P, Sewing A. Fluorescence readouts in HTS: No gain without pain? Drug Discov Today 2003; 8(22):1035–1043.
56. Mouchet EH, Simpson PB. High-content assays in oncology drug discovery: Opportunities and challenges. Invest Drugs 2008; 11(6):422–427.
57. Low J, Stancato L, Lee J, et al. Prioritizing hits from phenotypic high-content screens. Curr Opin Drug Discov Devel 2008; 11(3):338–345.
58. Haney SA, LaPan P, Pan J, et al. High-content screening moves to the front of the line. Drug Discov Today 2006; 11(19–20):889–894.
59. Shiau AK, Massari ME, Ozbal CC. Back to basics: Label-free technologies for small molecule screening. Comb Chem High Throughput Screen 2008; 11(3):231–237.
60. Gauglitz G, Proll G. Strategies for label-free optical detection. Adv Biochem Eng Biotechnol 2008; 109:395–432.
61. Neumann T, Junker HD, Schmidt K, et al. SPR-based fragment screening: Advantages and applications. Curr Top Med Chem 2007; 7(16):1630–1642.
62. Proll G, Steinle L, Pröll F, et al. Potential of label-free detection in high-content-screening applications. J Chromatogr A 2007; 1161(1–2):2–8.
63. Cooper MA. Non-optical screening platforms: The next wave in label-free screening? Drug Discov Today 2006; 11(23–24):1068–1074.
64. Albert KJ, Bradshaw JT, Knaide TR, et al. Verifying liquid-handler performance for complex or nonaqueous reagents: A new approach. Clin Lab Med 2007; 27(1):123–138.
65. Taylor PB, Ashman S, Baddeley SM, et al. A standard operating procedure for assessing liquid handler performance in high-throughput screening. J Biomol Screen 2002; 7(6):554–569.
66. Dunn D, Orlowski M, McCoy P, et al. Ultra-high throughput screen of two-million-member combinatorial compound collection in a miniaturized, 1536-well assay format. J Biomol Screen 2000; 5(3):177–188.

67. Gunter B, Brideau C, Pikounis B, et al. Statistical and graphical methods for quality control determination of high-throughput screening data. J Biomol Screen 2003; 8(6):624–633.
68. Kevorkov D, Makarenkov V. Statistical analysis of systematic errors in high-throughput screening. J Biomol Screen 2005; 10(6):557–567.
69. Makarenkov V, Zentilli P, Kevorkov D, et al. An efficient method for the detection and elimination of systematic error in high-throughput screening. Bioinformatics 2007; 23(13):1648–1657.
70. Harper G, Pickett SD. Methods for mining HTS data. Drug Discov Today 2006; 11(15–16):694–699.
71. Wilson AM, Thabane L, Holbrook A. Application of data mining techniques pharmacovigilance. Br J Clin Pharmacol 2004; 57(2):127–134.
72. Dunlay RT, Czekalski WJ, Collins MA. Overview of informatics for high content screening. Methods Mol Biol 2007; 356:269–280.

3 Hit-to-Probe-to-Lead Optimization Strategies: A Biology Perspective to Conquer the Valley of Death

Anuradha Roy, Byron Taylor, Peter R. McDonald, and Ashleigh Price
University of Kansas, Lawrence, Kansas, U.S.A.

Rathnam Chaguturu
HTS Laboratory, University of Kansas, Lawrence, Kansas, U.S.A.

INTRODUCTION

Central to the drug discovery process is gene identification followed by determination of the expression of genes in a given disease and understanding of the function of the gene products (1). This is the critical target identification and validation phase and is the first step in the drug discovery and development process. Linking a particular disease with cellular biology, deciphering the pathways involved, associating the genes participating in these pathways, pin pointing the critical genes involved, and identifying the therapeutic target require a multipronged approach. It takes a highly integrated and concerted effort by teams of scientists from biology and chemistry and quite often takes many years. Pharmaceutical industry relies primarily, but not exclusively, on academia for this invaluable information, and the potential for druggability then becomes the starting point for pharmaceutical research with an ultimate goal of developing a marketable product. From examining case histories for 35 important pharmaceutical innovations, a recent report co-authored by researchers from the Manhattan Institute and the Tufts Center for the Study of Drug Development strengthens the above assertion that National Institutes of Health (NIH)-sponsored research in academia tends to be concentrated on the basic science of physiology, biochemistry, molecular biology of disease pathways and may lead to the identification of biological targets that might prove vulnerable to drugs yet to be developed (2). Contributions by the pharmaceutical industry are more applied-in-nature, leading to the discovery and development of treatment and cure (drugs) for adverse medical conditions. The authors conclude that the NIH-sponsored and private-sector drug research are *complementary* to one another and are equally necessary in order to provide patients with better care and treatment (2).

Given the complexity of the research processes involved in developing a drug, it is not all too surprising that it takes approximately $800 million to make a new drug (3). A closer look reveals that the cost of one research program leading to a marketable drug is actually estimated at approximately $100 million, but jumps to more than $1 billion if one considers the terminated projects within the program and an astronomical $3 billion dollars if the cost of the capital is

included. The high cost and low productivity in the discovery and development of a new drug is often attributed to the dismal success rate (~25%) during the Phase 2 clinical trials compared to almost 60% to 70% success rate during Phase 3 and Phase 4 clinical trials (4). Most of the failures during Phase 2 clinical trials could be attributed to issues related to efficacy; absorption, distribution, metabolism, and excretion (ADME); and safety. Reasons for efficacy failure could easily be traced down to lack of confidence in the mechanism by which the "lead compound" acts, and in turn could be attributed to a fundamental lack of understanding in the pathobiology, and how the safety optimization approaches are implemented. Toxicity is still an issue at this stage. It could either be target site or metabolism related. This is where the "Hit to Probe to Lead" strategies play a critical role (Fig. 1). Until recently, it has generally been a linear and sequential approach in transforming chemical hits into leads, but because of the "industrialization" of the processes (target selectivity and specificity, efficacy and potency, pharmacokinetics (PK)/pharmacodynamics (PD), and ADME toxicology (ADME-T)); involved, one can now address all of these issues in a parallel and multiplexed manner. Such a multipronged, yet parallel and forward-integrated, approach certainly leads to a clear understanding of the chemical hit and an early assessment of its potential to become a successful probe and eventually a lead. The goal of the hit-to-lead stage in the drug discovery process is to identify lead compounds, which will not fail in expensive, later-stage preclinical and clinical testing. This requires an effective integration of chemical biology, counter screens, and ADMET studies. Because of the availability and affordability of what we consider to be "preclinical" assay technologies, these studies can now be undertaken and executed with much ease. We discuss justification for a forward integration of the preclinical studies to the hit-to-lead optimization phase to provide judicial guidance in conquering the so-called "valley of death." This means that critical decisions are made in a timely manner to "fail" undesirable compounds as early as possible, before significant resources are spent developing these to lead compounds.

A recent search in SciFinder Scholar for the term "hit–lead" yielded almost 1300 publications in peer-reviewed journals, spanning a period of 40 years. The majority deal with statistical and medicinal chemistry approaches to the implementation of structure–activity relationship (SAR) principles in optimizing chemical hits. Approximately 143 well-defined substituents are reported in the hit-to-lead literature. If all of them were used in just three positions of a putative pharmacophore, one would have 143^3 or 2,924,207 possible compounds. To complicate the scenario even further, there are ~400,000 pharmacophores according to the world drug index, a computerized database of 50,000 drugs. This highlights the fact that it would be impractical to make all the compounds possible to identify the best lead compound. Therefore, one resorts to the many quantitative design methodologies available to identify the best strategy for lead optimization (Table 1). The focus of this review is not to reiterate the chemoinformatic QSAR principles which have been previously defined and implemented by pharmaceutical discovery/medicinal chemists. We argue for a more holistic approach from a biology perspective as it is this area that we consider to be one of the root causes for the failures experienced during Phase 2 clinical trials. We propose a judgment-based (quantitative biology) approach to complement the predominantly rule-based (chemistry) efforts

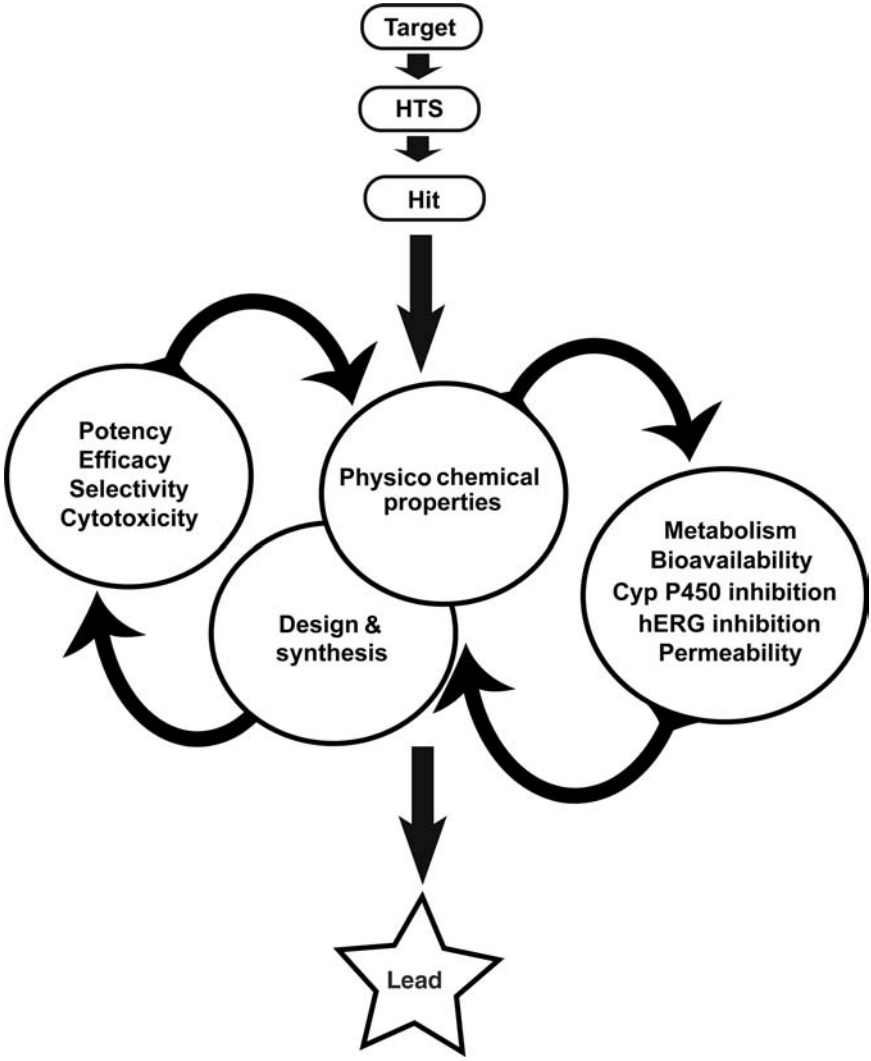

FIGURE 1 Hit-to-Lead Overview. This schematic shows an overview of the early drug discovery process and underscores the iterative nature of data flow between biological, pharmacological, and medicinal/computational chemistry domains.

that have been applied to implement the hit-to-probe-to-lead optimization strategies.

FORWARD INTEGRATION OF THE DRUG DISCOVERY STAGES

A paradigm shift has been taking place over the last decade, strengthening the drug discovery process by integrating many of the steps. Drug development flowcharts have gone from linear, step-by-step processes to parallel, multiplexed and multipronged, approaches. Decisions are made, not in a hierarchical way,

TABLE 1 Quantitative Design Methodologies Available for Identification of Best Strategy for Lead Identification

Design strategy	Comments
Topliss tree	Heuristic, knowledge based
	Fast biodata turn-around
Modified topliss	Heuristic, knowledge based
	Slow biodata turn-around
Fibonnaci search	For properties that reach an optimum
	Search strategy
Craig plots	Two-dimensional objective
	Good orthogonality and space coverage
Cluster analysis	Ideal substituent set; objective
	No guarantee of orthogonality or full parameter space
2n factorial design	Objective
	Sequential
SSO	Rapid optimization
	Biodata can be ranking
Central composite design	Ideal substituent set
	Resource expensive

but by project teams in a matrix setting. Molecular biology and biochemistry teams are coming together at the very inception of a project to participate in the target identification and validation phase. High throughput screening (HTS) groups (automation specialists) are working together during assay development and validation phase to ensure that the assay is high throughput screening ready, and thus reduce the time taken with the traditional "over the fence" approach to move projects from one phase to the next. Hit assessment is made in batch mode in real time to assess the quality of the screening data, and in setting and adjusting the hit selection criteria as appropriate. The Lipinski rule of five is implemented in assembling the screening libraries *a priori* rather than discarding the screen hits that do not meet the "rule of five" criteria after they have been screened (5,6). The hit selection is not made solely on the basis of efficacy and potency, but by including chemical tractability and intellectual property opportunities as well. Process chemists are working with discovery chemistry teams to provide guidance in charting out synthesis strategies to make lead molecules in high yield and with the fewest possible steps. The only disconnect during this much-aligned drug discovery process has been a lack of unanimity among the pharmaceutical scientists in understanding the pathobiology of the lead candidates. Hence, the use of preclinical data promotes guiding the progression of screen hits to the probe and lead development stage. Project teams involved in lead optimization have much to learn from the preclinical expectations, so it is highly desirable to have the preclinical teams and studies integrated in to the lead optimization stage to ensure that compounds fail or advance to clinical trials on the basis of solid experimental data. The National Toxicology Program of NIH rightly advocates moving the preclinical toxicology profiling studies from a mainly observational science at the level of disease-specific models to a predominantly predictive science focused on a broad inclusion of target-specific, mechanism-based, biological observations. With the industrialization of these

processes, we further advocate a HTS approach in addressing the preclinical-related issues during the lead-optimization stage to effectively and judiciously guide the clinical candidate drug selection.

HTS FOR TARGET SITE ACTIVES

HTS for target site actives is often referred to as searching for a needle in a haystack. HTS laboratories routinely screen large compound libraries, virtual compound collections, and vendor's databases, etc. Unless it is a "me-too chemistry" approach, we have a very limited knowledge of what we are looking for. We do not know the size or shape of the needle, or even if it is in the haystack. There is a distinct possibility, however, that we may end up finding more than one!

The primary objective of the HTS process is to find active compounds, usually screening at a single concentration. It comes as no surprise that more than half of late-stage drug discovery projects at leading pharmaceutical companies are now screening-derived. Hence, a robust selection process is key to provide chemical scaffolds for subsequent optimization by medicinal chemistry teams. Performance measures such as signal window, CV, Z' factor, and assay variability ratio, although mathematically similar but with different acceptance criteria, are employed at this stage. Because of great strides made in assay development and validation processes, the screening of compound libraries is usually done without replication. The objective of subsequent work with "actives" is to confirm the activity to differentiate compounds by employing potency and efficacy value thresholds. The compounds that pass through this stage are referred to as "hits," which then could be developed as molecular probes to investigate mechanistic aspects of the biochemical target site. Some of the nomenclatures widely used to describe compounds during the various stages of the HTS and hit validation process are given in Table 2. An "active" is a compound that shows a level of activity that is equal to or above the threshold set for the HTS campaign. Validated "hits" are molecules whose primary biological activity and structural integrity have been confirmed with selectivity towards its biochemical target. A "lead" is a molecular scaffold with congeners showing specificity and a well-defined quantitative structure–activity relationship, no significant ADME-T penalties, validated *in vitro* and *in vivo* correlation, and requiring significant resource commitment. "Probes" are hits to explore gene, pathway or cell function, and optimized for potency, efficacy, SAR, and selectivity against the target evidenced by the counter/secondary screen data. Probes are especially useful in exploring non-druggable targets such as rare diseases and inborn metabolic disorders.

The number of compounds that go through an HTS campaign is constantly being revised within the pharmaceutical industry. It is in direct response to the total number of compounds available, the spectrum of chemotypes present in in-house collections, internal research initiatives, portfolios of targets within a therapeutic area, lessons learned from previous screens, and finally the budget constraints. In the meantime, the chemical library vendors, mainly from Eastern Europe, have industrialized and perfected diverse chemical library synthesis. The size of commercially available chemical libraries has grown collectively to approximately 11 million compounds (Table 3), with considerable overlap among the libraries. Internal collections within the pharmaceutical companies' are in the range of 1 to 3 million compounds, and one company boasts

TABLE 2 Nomenclature and Characteristics of Compounds at Various Stages of Early Drug Discovery

	Active	Hit	Probe	Lead
A.				
Demonstrate minimal activity	☒	☒	☒	☒
Confirm activity	☒	☒	☒	☒
Eliminate false positives		☒	☒	☒
Verify structure and purity		☒	☒	☒
Attractive physicochemical properties		☒	☒	☒
Synthesis accessibility		☒	☒	☒
Potency and efficacy			☒	☒
Structure–activity relationship			☒	☒
ADME/Tox				☒
IP position				☒

Screen active	Qualified hit 12.0pt1,113.0pt	Validated hit 12.0pt1,194.0pt
B.		
Primary screen active	Purity and structure confirmed	Functional responses further validated in appropriate secondary screens
Activity confirmed	New tech sample active	Med chem initiated
Not autoluminescent	Minimum cytotoxicity	Analogs with reasonable SAR
Not autoflourescent	Active in a functional assay (preferably cell based)	Parallel assessment of ADMET
Not colored	Minimum Lipinski rule violations	Favorable pharmacodynamics (potency and selectivity)
Dose response w/EC_{50}	Analog synthesis feasible	Favorable pharmacokinetics (permeability, stability, preliminary tox studies)
Minimum cytotoxicity	Desired potency	Strong IP position regarding
	IP assessed	Composition of matter or use
↓	↓	↓
Qualified hit	Validated hit	Lead

(A) The compounds identified from an HTS assay have to meet certain requirements to be referred to as actives, hits, or leads. The table shows a few categories that must be met with at different stages of H2L phase. (B) Criteria for compound advancement from active to hit to lead.

TABLE 3 Size of Nonproprietary Compound Libraries Available from Some Commercial Vendors

Vendor	Library size
Molecular Diversity-MDPI	10,655
AnalytiCon	25,000
Key Organics	46,000
Maybridge	59,312
Tripos	80,036
Rare Chemicals	120,000
Otava Chemical	126,000
Asis Chem	160,000
TimTec	160,000
Vitas-M Laboratory	200,000
Moscow Medchem labs	200,200
Specs	214,937
Sigma-Aldrich	300,000
Asinex	400,000
AMRI	420,000
Interbioscreen	420,000
IBScreen	430,000
LifeChemicals	645,000
Chembridge	650,000
Chemdiv	1,000,000
Princeton Biomolecular research	1,000,000
Enamine	1,069,562
Aurora Fine Chemicals	3,700,000
Total	11,036,702

a staggering 7 million compound collection. In recent years, the quality of commercially available chemical libraries has vastly improved, and most adhere to Lipinski's rule of five concepts for bioavailability (5,6). They are largely devoid of undesirable compounds, such as known cytotoxic agents, chemically reactives, detergents, denaturing agents, mercaptans, oxidizing/reducing agents, heavy metals, and membrane disrupters. Chemically unattractive and synthetically difficult classes, such as beta-lactams, steroids, flavones, phospholipids, and carbohydrates, are also excluded. These chemical families have been removed because they are neither lead-like nor drug-like. The chemical libraries are continuously refined by implementing several structural filters for undesirable halides (sulfonyl, acyl, alkyl), halopyrimidines, aldehydes, imines, perhaloketones, aliphatic ketones, esters (aliphatic, thiol, sulfonate, phosphonate), epoxides, aziridines, etc. The chemical library collections, however, continue to have highly absorbent and fluorescent compounds, which need to be removed from the collections as they most frequently get triggered as actives (false positives) in the screening campaigns. Because of disappointing screen performance with in-house "historical" chemical libraries, which had been built up by organizations over time, the trend towards chemical libraries focused on a specific biochemical target or a specific gene family or a target class is increasing. Using in-house screening data, Lipkin et al. propose screening a minimum of 200 or 650 compounds derived from a focused library to identify two or five hits, respectively (7). These focused libraries are routinely being used to improve

the chances of finding actives, but with the inherent drawback that no novel and unique structures will be found from such a "focused" endeavor.

A successful screening effort will typically produce anywhere from 0.1% to 1% hit rate giving hundreds to thousands of molecules (depending on the size and quality of the library screened), representing several structural classes and with varying degrees of activity. The purpose of hit-to-probe-to-lead process is to turn this often overwhelmingly large and varied collection of molecules into a handful of manageable compounds that can then serve as starting points for the probe or lead optimization stage. This is done by subjecting each molecule to a series of secondary tests or "hurdles," which the compound must clear to become a lead molecule. The challenges include a series of robust and high-throughput assays to assess compounds for lead-like properties and to identify ones that have a high likelihood of success in preclinical and clinical phases. The strategies employed in a hit-to-lead process are largely determined by target-type, organizational infrastructure, intellectual property space, and budget. The process requires the integration of the efforts of medicinal chemists, biologists, statisticians, computational scientists, pharmacologists, and management. We offer here an outline of available hit-to-probe-to-lead strategies, especially from a quantitative biological perspective.

EVALUATION OF ACTIVES FROM THE HIGH-THROUGHPUT SCREEN

The primary objective of HTS data analysis is to (*i*) discriminate actives from inactives, (*ii*) relate biological similarity to chemical similarity, (*iii*) identify tractable hits from the screen based on medicinal chemist's "expert" knowledge, and (*iv*) identify multiple series of compounds that make attractive starting points for quantitative structure–activity relationship (QSAR)-based optimization (improvements in the hit quality), and manage the downstream capacity for the available chemistry resources. A typical linear regression strategy is provided in Figure 2. This strategy is usually followed by a multidimensional iterative analysis of structural diversity versus property diversity (Fig. 3).

The process of HTS and the subprocess of hit identification has generally been well developed (Fig. 4). When HTS technologies became widely available, the tendency was to screen the historical in-house chemical library in its entirety. Screening progressed from 96-well to 384-well microplates (in some instances, to 1536-well plates) and the size of compound libraries screened grew from ~100,000 to more than 1 million compounds. In the past, great emphasis was made with respect to the "hit rate," which typically varied from approximately 0.3% to ~1%. More recently, the hit rate has become a footnote to any discussion of the validity of a screening campaign, because it is simply a factor of the arbitrarily chosen activity threshold and the concentration at which the compounds were screened. Choosing an arbitrary threshold to define an active is rarely an effective strategy. For example, weakly active compounds can be valuable during these early stages if they represent scaffolds that are attractive and are not found in any of the more active compounds. The downstream processing capacity of the medicinal chemistry resource is most often the ultimate deciding factor as to how many compounds one can move from the screening stage to the "hit explosion" stage. However, with the industrialization of chemical library synthesis, improvements in the liquid handling technologies, signal detection platforms, and data mining and analysis routines, the constraints that once were

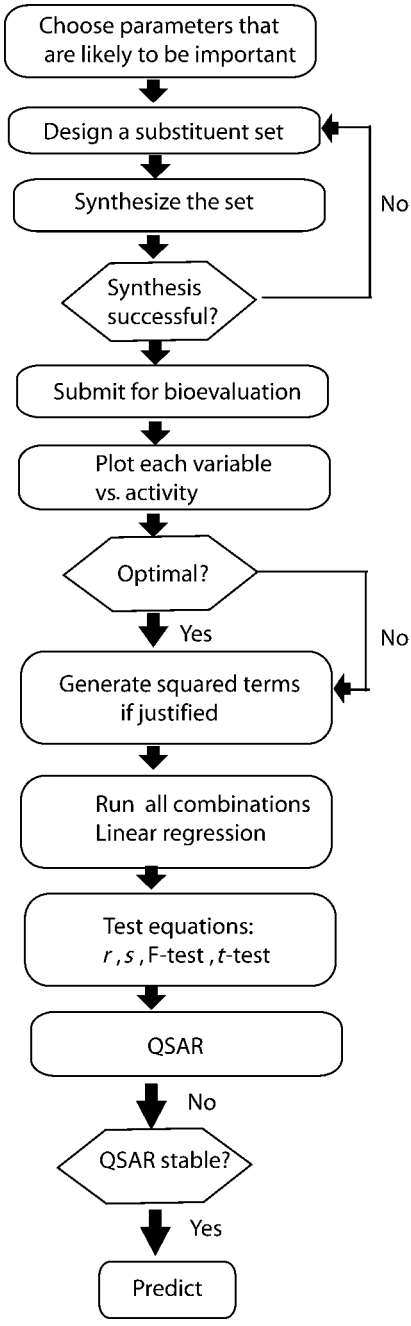

FIGURE 2 Linear regression analysis strategy for structure optimization.

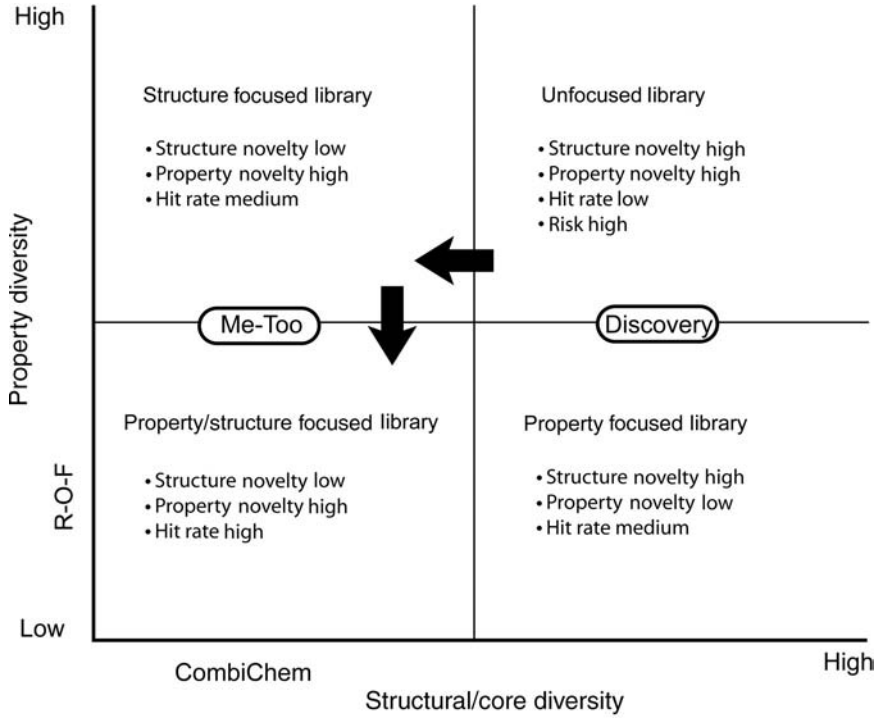

FIGURE 3 Multidimensional analysis of structural diversity versus property diversity.

thought to be insurmountable are no longer the limiting factors. The rigid activity threshold and the testing concentration may have served the purpose during the early evolution phase of HTS campaigns by yielding the most potent, efficacious, and high-quality compounds active at the concentration. However, it certainly restricted structural diversity within the portfolio of hits for medicinal chemistry optimization (Fig. 5). Again, with the industrialization of the many processes listed above, it is no longer necessary to limit the "hit" rate to ~0.3% to 1%. By providing the medicinal chemist with an HTS dataset comprising a wide variety of structural classes, the chemistry team can then determine, based on expert knowledge, which compounds or structural classes have the chemical tractability to pursue for a QSAR-based optimization.

False positives are a nuisance in any screen and waste significant resources if not removed from follow-up studies as early as possible during the hit evaluation process. A number of HTS actives tend to be false hits because they are either assay-format dependent or colloidal aggregates that nonspecifically bind and inhibit activity, especially in cell-free systems (8).

Promiscuous binders cause target inhibition using a nonspecific aggregation-type binding mechanism to proteins. These compounds should be removed from screening hit lists. Giannetti et al. (9) introduced a robust approach to identify these promiscuous binders using real-time surface plasmon

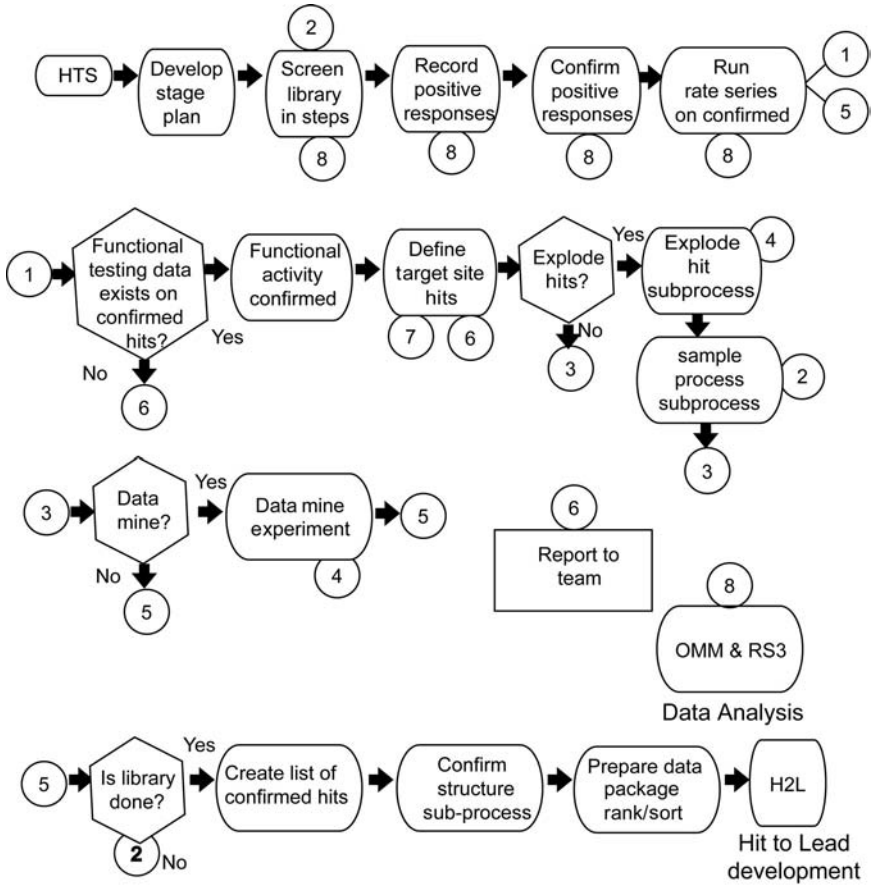

FIGURE 4 This flow chart shows the process of HTS and the subprocesses involved in hit identification.

resonance-based biosensors and offered a classification scheme that can be used to eliminate compounds with nonspecific mechanism of inhibition (9).

Many false positives also arise from interference with the assay or its readout, as is seen with intrinsic compound fluorescence and absorbance when the assay readout is fluorescence or absorbance-based, respectively. A recent assessment of compound interference in fluorescence assays found that approximately 2% of compounds in a screening library were fluorescent (10). Live cell assays are also susceptible to false positives. For example, a compound, which is an ionophore, or disrupts cell membranes, may appear as an active in an ion-channel modulator assay. If an assay measures inhibition of a cellular process or down regulation of any gene, toxic compounds will almost certainly appear as false positives. Some false positives are promiscuous (frequent hitters) because they are active against almost every screening target. The frequent hitters can be identified by comparing activity of a compound in all the different screens run using in-house databases or even in the PubChem bioassay database. Such issues

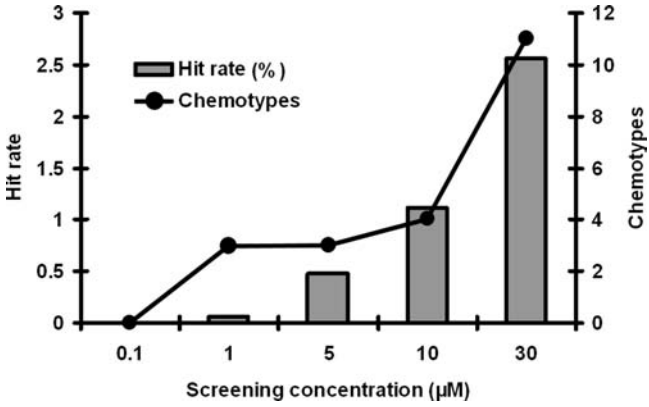

FIGURE 5 Chemotypes and hit rates. Hit portfolio as a function of the compound concentration. Approximately 100,000 compounds were screened against a target site at indicated concentrations.

are often resolved by using alternate secondary assays at the time of hit-to-lead analysis. For example, electrophysiology would be done to confirm hits in an ion-channel assay. The general toxicity of false positives would be exposed when other targets and cell lines are tested in selectivity and cytotoxicity assays.

Confirmation of structure and relative purity should be done as early as possible to rule out the contribution of an impurity or a degraded component of the compound. There may be other minor causes like compound registering errors and rotated plates. Of these, compound degradation is of major concern because of the hygroscopic nature of dimethylsulfoxide (DMSO), the universally accepted solvent for compound stock preparation (11). As a first step, the chemical purity of cherry-picked compounds is generally determined by using liquid chromatography-mass spectrometry (LC-MS) analysis. The active compounds may be repurchased from the vendor and the activity of new batches tested to confirm activity. If in-house analytical chemistry facilities are unavailable, the samples may be sent to companies that offer analytical and purification services like OpAns (www.opans.com) and Bruker Corporation (www.bruker.com).

The actives that are confirmed to be hits are evaluated by the medicinal chemistry team for hit explosion and subsequent structure optimization. The screening data are revisited for identification of compounds conforming to nearest neighbors and having common substructures, and selecting clusters based on relative activity in primary assay as well as synthetic accessibility. The *in silico* approach is routinely used for identification of pharmacophores and minimal structural scaffolds that are associated with a biological activity. The chemists may design a focused library based on the pharmacophores for rescreening in the primary assay. The focused library screen greatly improves the quality (and reduces the number) of compounds available for detailed profiling studies in hit-to-lead. The structures with undesirable chemical functionality or with synthesis challenges are generally eliminated at this stage. The hit-to-lead analysis is usually performed with at least five or more discrete chemotypes.

It is useful to define *a priori* the criteria of selection for an ideal lead candidate or a cluster of compounds that will effectively focus lead identification and development process. The lead molecules should be selective for the target (>100-fold) and should not cause general cytotoxicity. A suitable lead compound is generally expected to conform to Lipinski's rules for oral bioavailability and should have good potency (<500 nM) and efficacy (maximal effect) in cellular systems. The lead compounds should display a sound ADME/toxicology profile: permeability in Caco2 cells, stability in human and rat microsomes, and bioavailability (Table 5). Mechanism of action studies should be carried out and defined as early as possible in the hit-to-lead process. The patent space should be reasonable around the scaffold for it to be useful from an industry point of view.

STRATEGIES FOR HIT-TO-LEAD

It is at this stage we recommend the inclusion of a careful biological perspective, in addition to the well-established chemoinformatics principles, in guiding lead development. An example of hit analysis is given in Figure 6. A total of 130,000

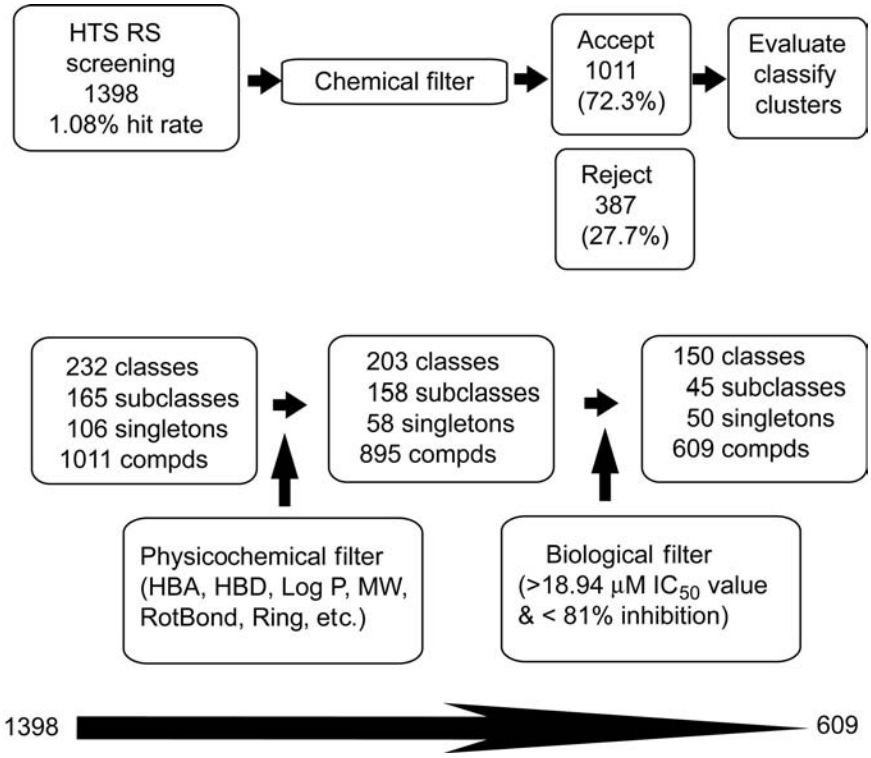

FIGURE 6 Use of physicochemical and biological filters for refining the HT screening confirmed "hit" portfolio.

highly diverse compounds were screened against a proprietary kinase target by using a fluorescence polarization-based assay. By employing chemical filters for unwanted chemistry, the number of confirmed hits was reduced by 28%. These compounds were clustered by using a chemistry-driven approach: (a) daylight substructural fingerprints as molecular descriptors, (b) Tanimoto coefficient as a measure of similarity, and (c) modified Jarvis–Patrick nonhierarchical cluster analysis to group compounds. By applying physicochemical as well as biological activity filters, the number of compounds for follow-up was reduced by 67% from a total of 1398 to 609, and the structural classes were reduced from 232 to 150 (Fig. 6). It has been our practice that the singletons, in the absence of their congeners, were usually ignored unless there was a compelling reason based on the uniqueness of the chemistry. These compounds were then grouped into four clusters based on *in vitro* (biochemical) and *in vivo* (cell-based) activities—low:low, low:high, high:low, and high:high. The highest priority was given to chemically tractable compounds with high *in vitro* and high *in vivo* activity (Fig. 7). This provided the initial synthesis starting points to the medicinal chemistry team, which

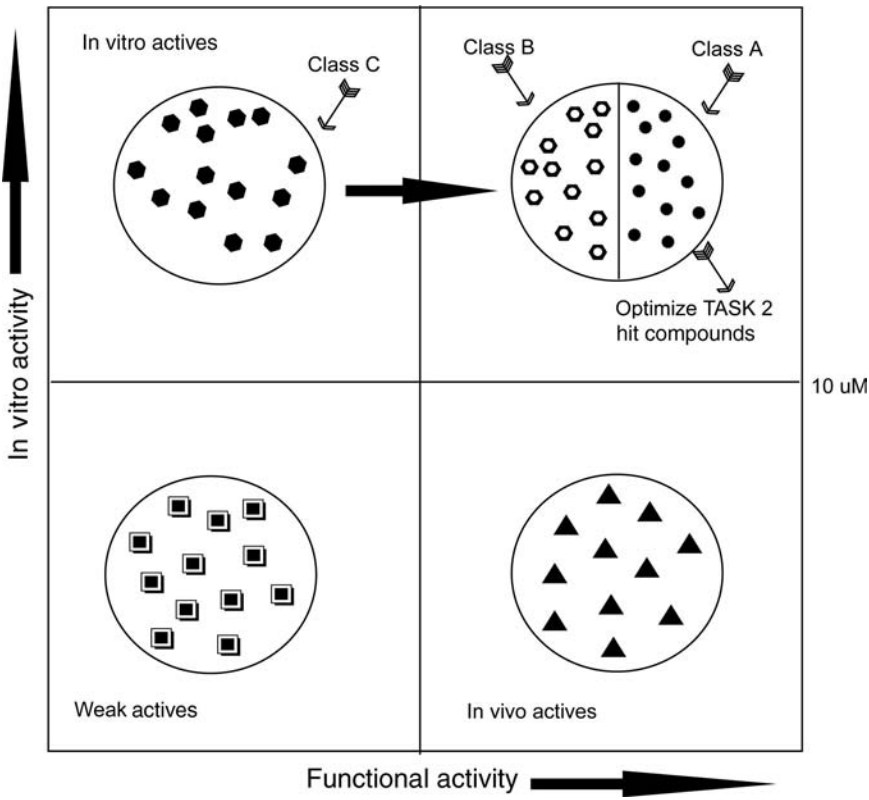

FIGURE 7 Hit clustering. Compounds identified as hits from an HTS screen were clustered based on *in vitro* and *in vivo* activities. Top priority was given to compounds with high *in vitro* and high *in vivo* activities.

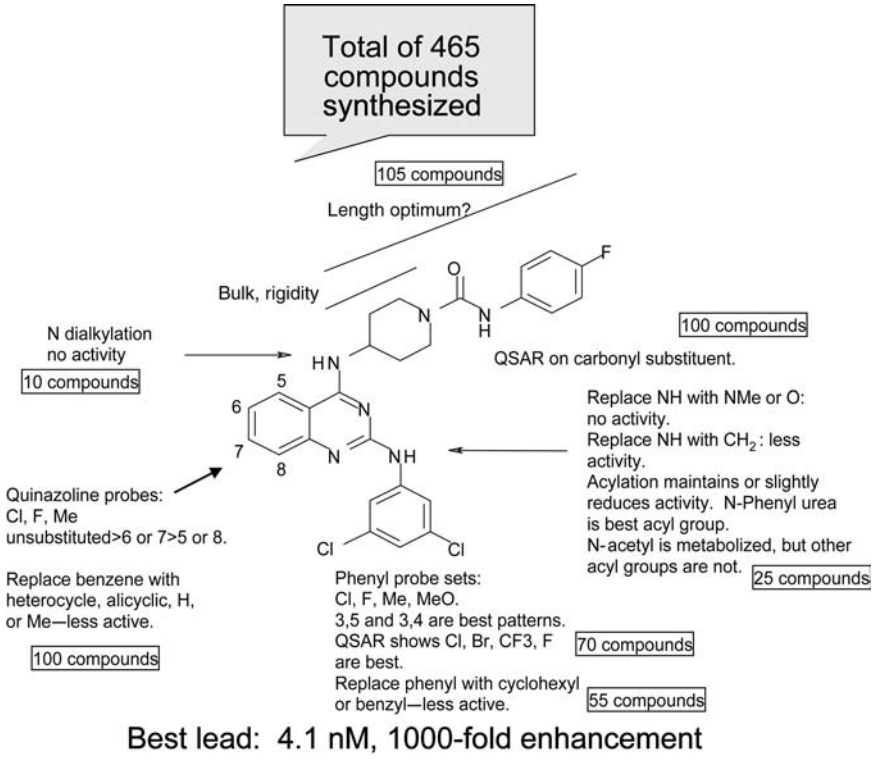

FIGURE 8 TSU 100. A quinazoline scaffold was predicted to show kinase-related activity. The enzyme activity showed clear *in vitro* and *in vivo* correlations. The scaffold was used to generate a focused library for rescreening with the HTS assay.

took a promising scaffold and improved the potency by approximately 1000-fold (Fig. 8).

After initial scrutiny of the reconfirmed HTS hits and hit-clustering into few minimal scaffolds by the chemistry team, the lead optimization process starts with the employment of new assays (secondary counter screens), which are different from those used in the primary screen. As mentioned previously, some of the false positives as well as frequent hitters will pass reconfirmation tests by using the primary assay, and these compounds should be tested by using alternative strategies, which are largely target-type dependent. Most of the secondary strategies should be developed quite early during the time of target validation. There are many biophysical and biochemical assays that can be used when information regarding the target is limited. Identification of meaningful assays that help establish a direct relationship between the target and the compound activity are vital to the success of hit-to-probe-to-lead identification and optimization. A flow chart indicating the various approaches for hit-to-lead development is shown in Figure 9. The new analogs should have improved potency, reduced off-target activities, and physiochemical/metabolic properties, predicting

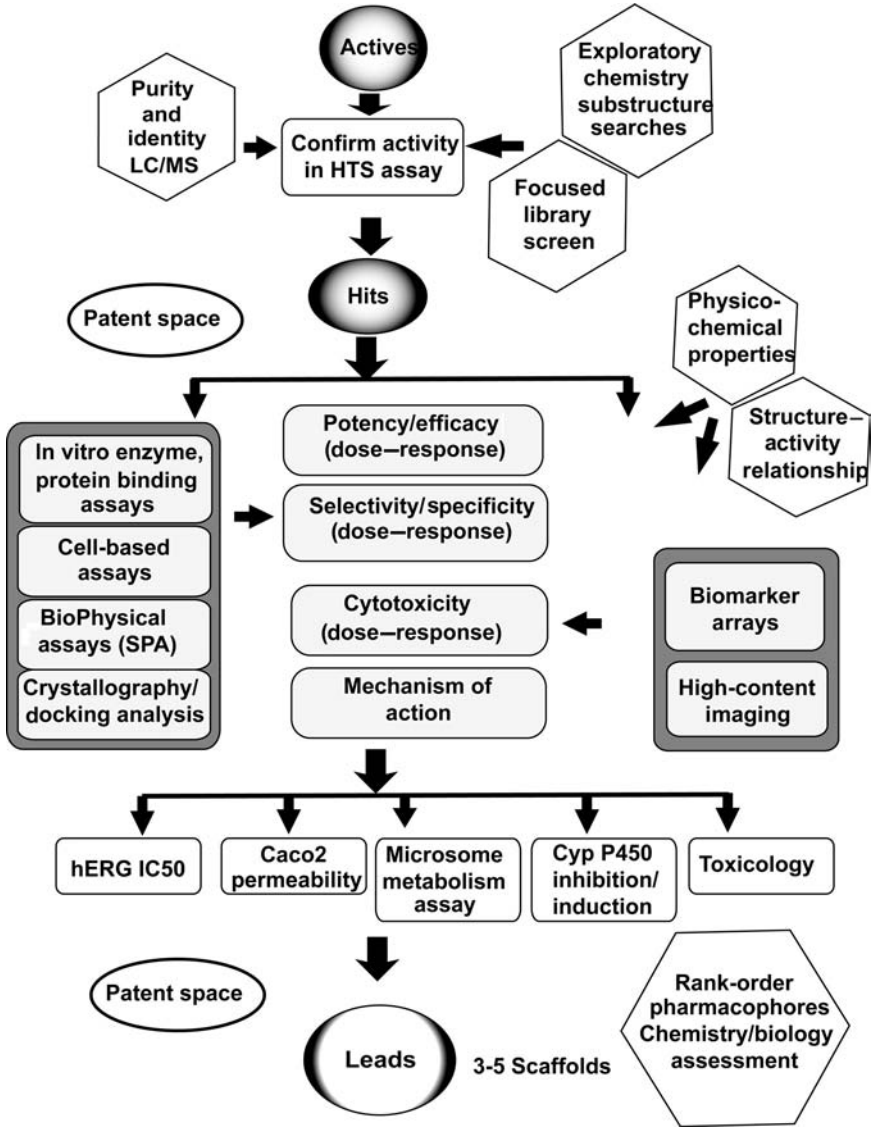

FIGURE 9 H2L flow chart detailed. The schematic shows all the steps involved in the evolution of lead molecules. The biological and pharmacological characterizations are accompanied with chemistry assessment of the structures and physicochemical properties.

reasonable *in vivo* pharmacokinetics. *In vitro* counter-assays that address cytotoxicity, permeability, and metabolic stability should be readily available to identify compounds with attractive biological activity profile. These counter-assays are designed to ensure that significant time and effort is not wasted on chemotypes with intrinsic liabilities at later stages of lead optimization.

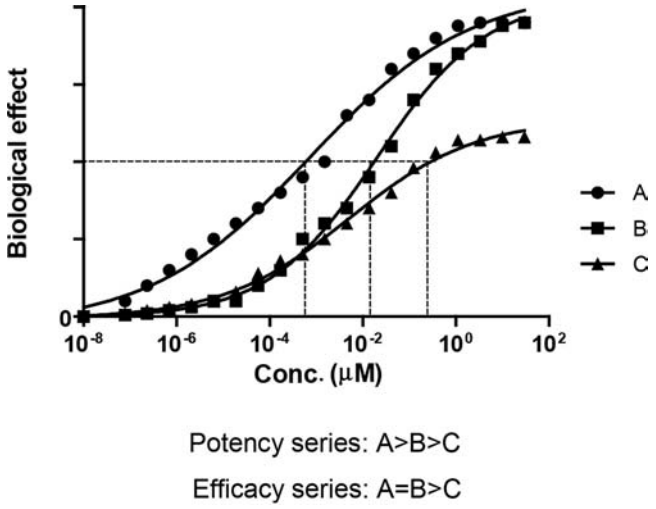

FIGURE 10 Potency versus efficacy. Three types of dose–response curves of compound activity are shown to highlight differences in potency and efficacy.

OPTIMIZATION OF BIOLOGICAL ASSAYS

Efficacy and Potency

As a first step, compound optimization is focused on defining the structure–activity relationship by testing analogs of the original structures. The efficacy of drug is the maximal response elicited by the compound. Potency is the effective dose concentration that measures how much compound is required to elicit a given response. Thus, in Figure 10, compound A is more potent than compound B, but both show same efficacy. Compound C shows lower potency and lower efficacy than compound A or B. A tentative ranking of hits is provided at the stage where there is a strong positive correlation between the structural features/groups with the biological activity of the compounds in any given assay. These parameters may be determined in both the primary HTS assay as well as in the secondary assays. The hits are usually tested in duplicates or triplicates in an 8 to 10-point dilution curve to calculate the EC_{50}/IC_{50} of a drug response. The efficacy and potency values are not sufficient enough parameters for lead series determination, and other properties (listed in Table 4/Fig. 9) need to be satisfied for a more comprehensive rank ordering of compounds (12).

Selectivity and Specificity

As most of the secondary assays used for compound prioritization are low-to-medium throughput, greater efficiency can be achieved if multiple assays are run in parallel and even multiplexed for compound profiling. The final choice of assays and the order in which they are performed depends on the size of chemical series, compound availability, and the target-type. Although the number and type of assays used for lead identification are generally dependent on the availability of resources and budget, screens should be selected to help focus on lead

TABLE 4 Criteria for Selection of a Lead Compound

MAssay	Measurement	Target value
Molecular properties	Molecular weight	$<$500 Da
	clogP	1–5
	H-bond donors	$<$5
	H-bond acceptors	$<$10
Potency	*In vitro*/cell-based assays, IC50 or fold changes	$<$1 μM or $>$4-fold change over basal values
Efficacy	*In vitro*/cell-based assays, IC50 or fold changes	$>$80% total inhibition or $>$4-fold modulation
Selectivity	Close homologs (EC50x/EC50 target)	$>$10 (family, function defined)
	Other proteins, enzymes, cells	$>$100 (distinct functions)
Cytotoxicity	(CC50/EC50 target) 24 hr, 72 hr	$>$100
In vitro ADME/Tox	Metabolism (mouse/human microsomes, 1 hr)	$<$30%
	Cyp P450 inhibition (IC50)	$>$5 μM
	hERG (5 inhibition at 5–10 μM)	$<$20%–30%
	In vitro Cyp P450 induction	$<$5-fold
	Permeability in Caco2 cells	$>100\ cms^{-1} \times 10^{-7}$
In vivo mini-PK studies	Plasma clearance	$<50\ mL{\cdot}min^{-1}{\cdot}kg^{-1}$
	Oral bioavailability	$>$25%

optimization and be able to demonstrate that the hits identified in the primary screen are target-dependent and largely target-specific.

Many proteins share homologies in the active sites or other domains, and belong to families with some functional and/or structural redundancy. This presents a problem for drug discovery efforts in terms of determining selectivity and specificity assays. Depending on the nature of the target, a unique panel of enzymes/receptors that can directly focus selectivity for a target is set up for early profiling of compounds in a hit-to-lead series.

For example, inhibitors that bind to the ATP-binding site of kinases generally inhibit all kinases because of the conservation of the ATP-binding site across all kinases. Despite the promiscuity, *in vitro* enzymatic assays are used against related or divergent kinases to define the activity across the family of kinases. The conversion of peptide to a fluorescent/luminescent phosphopeptide by a panel of purified kinases can also be monitored.

Like the kinases, caspases belong to the aspartate protease family, and the hits from a caspase HTS campaign are tested against a caspase panel (caspase 1–10) to select an apoptosis target that is more selective towards a given caspase isoform. Depending on the target and the disease, the selectivity panel may include either initiator caspases that are the first to be activated (caspases 2, 8, 9, and 10) or the downstream effector caspases (capsases 3, 6, and 7), which cleave, degrade, or activate other cellular proteins (13,14). The selectivity for anti-inflammatory compounds would require testing activity of caspases (capsases 1, 4, and 5), which are required for the processing of pro-inflammatory cytokines.

Like the kinases and the caspases, the matrix-metalloprotease (MMP) family consists of at least 20 enzymes that share considerable homology (30–50%) among their major domains (signal peptide, propeptide, catalytic, hinge, and hemopexin-like domains) (15). The inhibitors are screened for their activity

against several MMPs (MMP-1,-3,-2,-7,-8,-9,-13, and -12) with the ultimate goal of targeting MMPs in a particular cancer cell type. The selectivity panels require that the enzymes are functionally active and are relatively pure (>90%).

In the case of drug target-rich superfamily of ligand-gated ion channels, the 5-HT family and the nicotinic acetylcholine (nACh) family of receptors have very different functions, yet one of the nAChR subunits (α7) is very similar to one of the 5-HT subunits (5-HT_3). Not surprisingly, molecules having affinities for either of these receptors share chemical space. Several molecules, such as tropisetron, d-tubocurarine, and some quinuclidine derivatives, have high affinity to both subunits (16). Actives in ion-channel screens should be tested against a panel of ion channels. The activity should be confirmed via electrophysiological studies, preferably in primary cells in native cellular environment. A number of higher throughput techniques are available for monitoring ion-channel activity including fluorescent membrane potential and Ca^{++} dyes, increased fluorescence of GFP fused to channel subunits, ion flux across planar bilayers, microphysiometer readings of cell channel activation, and atomic absorption spectrometry to detect ions in whole cell lysate.

Cell-based assays are useful for confirmation of leads in an environment that mimics a live cell. While the high throughput screens using an *in vitro* enzymatic/reconstituted system assays provide a more direct insight into mechanism-of-action of the selected hits, the hit-to-lead prioritization should preferably include a cell-based system to address activity, membrane permeability, metabolism, and serum binding of compounds. The selectivity and secondary assays need to be set up early during target validation as these are critical steps in filtering sets of hits from high throughput screens. It is essential to define the cell-types that express the target and to determine the effects of target inhibition, selectivity, and off-target effects. These studies can be performed by using the powerful ability of small interfering RNAs (siRNAs) in selective gene silencing. A number of secondary/selectivity assays for drug prioritization can be set up based on the results from siRNA-mediated knockdown of a target. Does the knockdown (a) result in general cell toxicity or a decrease in growth rate or cell-cycle arrest? (b) elicit a perturbation in the expression or activation status (e.g. phosphorylation, dephosphorylation) of associated molecules in the signal transduction pathways? or (c) show similar effects on target-dependent and target-independent cell growth? The loss-of-function phenotypes, obtained when the cells are treated with high potency validated siRNAs, which show minimal off-target effects, may correlate with that expected from a target-specific small-molecule inhibitor. For example, Eggert *et al.* identified two phenotype classes, which were shared between the RNAi and small-molecule inhibitor studies on cytokinesis inhibitor proteins in Drosophila cell lines (17). Liu *et al.* demonstrated that expression of siRNA directed against cyclooxygenase-2 (COX-2) resulted in growth inhibition of human gastric carcinoma cells, which is comparable to the growth inhibition induced by treatment with the specific COX-2 inhibitor, Celcoxib (18). Further analysis showed that Celecoxib causes growth inhibition of gastric carcinoma cells by decreasing Bcl-2 of cyclooxygenase-2-dependent pathway and by increasing p21 (WAF1) and p27 (KIP1) of cyclooxygenase-2-independent pathway. These data could be used to set up selectivity screens for the identification of mechanism-based inhibitors of COX-2 by screening against the COX-2-dependent and -independent gastric carcinoma cell types.

Antimicrobial screens have historically targeted cell-wall synthesis, DNA gyrase, metabolic enzymes, RNA polymerase, and protein synthesis pathways. The increased availability of genomic sequences will help unravel novel targets and allow sequence comparisons to be made across species. Designing a drug discovery scheme for antimicrobial targets should be initiated with target validation (phenotypes associates with loss of function) and expression studies (19). The target should be expressed in the desired spectrum of gram-positive and gram-negative bacteria and be absent or be sufficiently distinct in mammalian cells for effective specificity and reduced toxicity in mammalian systems. For the compounds identified *in vitro*, key issues in hit-to-lead development arise from membrane permeability, compound availability, half-life, rates of efflux through ion-pumps, and metabolism in the bacterial cell. In addition, the bacteria acquire resistance to compounds with time due to mutations or changes in gene expression. Therefore, the assays for hit-to-lead development should include information on frequency of resistance at an early stage for compound prioritization. Some of the technologies available for characterizing the hits in biological systems will now be discussed.

Reporter Gene Assays

In recent years, there has been a growing trend and need toward cell-based assays as the preferred format for both HTS and hit-to-lead development. By definition, cell-based assays measure the effect of a test compound by monitoring a biological response of a wild-type or a genetically modified cell in which the therapeutic target site of interest has been engineered. Although executing a biochemical assay is relatively straightforward, designing a cell-based assay poses considerable challenges. Engineering a cell line (tester cell line) that expresses the protein of interest at sufficient levels to facilitate screening is a formidable task. The basic strategy is to transfect cells with a plasmid containing a reporter gene regulated by the promoter of interest and then treating the cells with test compounds. The expression of the reporter gene is quantitated and correlated with the activity of the promoter in question. The actives from such a screen are then tested on a cell line that does not have the promoter to assess the specificity and selectivity of the compound. Designing an appropriate control cell line lacking the promoter but comparable in size and nature with the tester cell line is extremely difficult. Attention needs to be paid with regards to variables such as the promoter length (short vs. long), promoter size (big or small), sequence (original vs. commercial), vector backbones (pSEAP2 vs. pGL4), and Kozak sites (NCO1 vs. ECOR1). Special care needs to be taken to be certain that the effect is not reporter specific (luciferase-Firefly vs. Renilla, β-galactosidase, alkaline phosphatase, green fluorescent protein, etc.) and that there are no transcriptionally relevant sites.

In a cell-based HTS effort utilizing a transient hTERT minimal promoter and luciferase reporter expression system, we identified compounds from a diversified small-molecule library of over 123,840 compounds that derepress the telomerase minimal promoter as evidenced by their ability to induce luciferase expression. When these compounds were tested for their specificity in the control cell lines that lacked the minimal reporter but replaced by a "nonsense or basic" promoter, there was sufficient luciferase expression and hence these "putative hits" were deemed to be rather nonspecific. However, as there were

TABLE 5 List of Various Constructs Tested for High Background Vector Expression in a Luciferase Reporter Assay

Construct	Description	Variable tested
To study effect of short vs. long promoter on Luc2 expression		
pSSI8412	Original Basic promoter expressing Luc2 in pSEAP2 backbone	Basic promoter length (short vs. long)
pSSI12038	Shorter Basic in pSEAP2 backbone	
pSSI12186	Long Basic in pSEAP2 backbone	
pGL4	Promega's pGL4 Basic promoter and backbone	
To study effect of Vector backbones on Luc2 expression		
pSSI12358	Original Basic promoter w/ ECOR1-Kozak in pGL4 backbone	Vector backbones on Luc2 expression (pSEAP2 vs pGL4)
pSSI12403	pGL4 Basic promoter w/ ECOR1-Kozak in pSEAP2 backbone	
pSSI12400	pGL4 Basic promoter w/ ECOR1-Kozak in pGL4 backbone	
pSSI12394	pGL4 Basic promoter w/o ECOR1-Kozak in pSEAP2 backbone	
To test Kozak sequences from NCOI vs. EcoRI in pGL4		
pSSI12400	pGL4 Basic promoter with ECOR1-Kozak in pGL4 backbone	Kozak sites (NCO1 vs. ECOR1) Vector (pSEAP2 vs. pGL4)
pSSI12540	Long Basic promoter with extra upstream NCO1-Kozak removed in pSEAP2 backbone	
pSSI12543	Long Basic promoter with Extra upstream TATA box and NCO1-Kozak removed in pSEAP2 backbone	
pSSI12458	Long-Basic + MP w/ECOR1-Kozak-Luc2pSSI12460 = Long-Basic + OBC w/ ECOR1-Kozak-Luc2	Use Long basic as an insulator for other promoters
pSSI12540	Long-Basic w/ ECOR1-Kozak-Luc2pSSI12455 = Long-Basic + SV40 w/ ECOR1-Kozak-Luc2	
pSSI12673	Long-Basic + RSV w/ ECOR1-Kozak-Luc2	

no reports in the literature about compounds that derepress the telomerase minimal reporter, the main goal of Sierra Sciences has been to find compounds that activate telomerase and reverse or delay aging and the age-related diseases, we painstakingly engineered a series of promoter-reporter plasmids of various combinations (Table 5) to create a mirror image of the tester cell line but lacking the minimal promoter. By adjusting the basic promoter length on a variety of vector backbones and removing translationally relevant sites, we were able to create the most appropriate control promoter-reporter plasmid (Fig. 11). Upon retesting, these compounds did not induce luciferase expression in the control cell lines transfected with the "right" basic promoter-reporter plasmid and were validated as true actives. The induction was not-reporter specific (i.e., promoter specific). Several of the active compounds were shown to induce hTERT mRNA expression (through real-time RT-PCR) as well as the associated telomerase activity (through the Telomere Repeat Amplification Protocol method). Had we not taken the time to engineer the most appropriate promoter-reporter plasmid system, not only for the tester cell line but also for the control cell line,

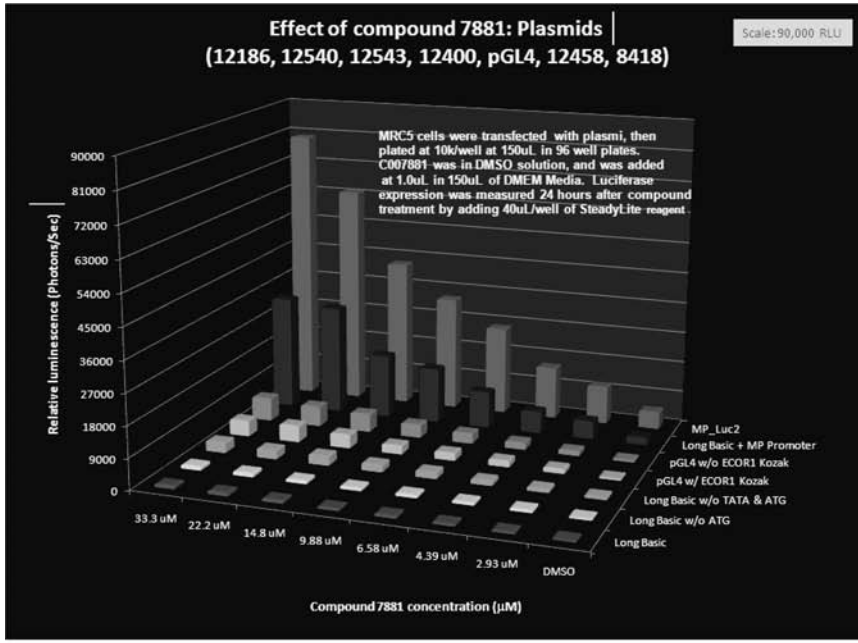

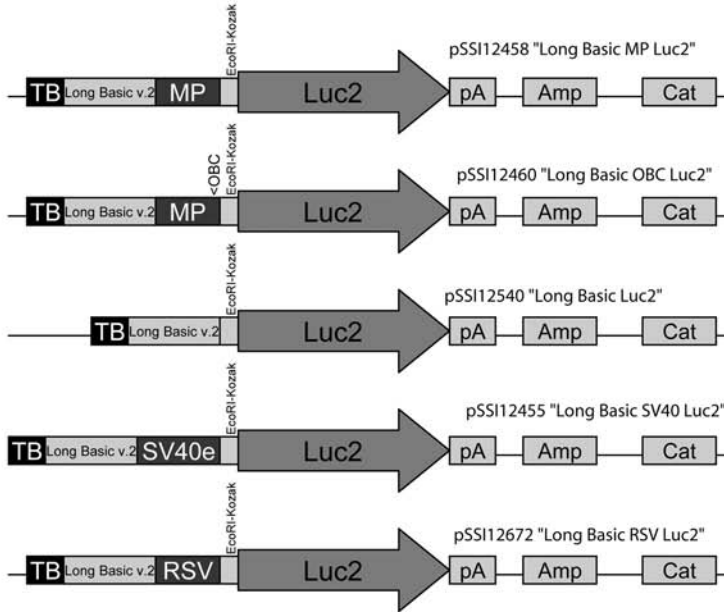

FIGURE 11 Plasmid comparison 2nd ATG site. Effect of a compound "7881" was tested by using cell-lines transfected with either the Luc2 construct expressing telomerase promoter or with various background vector constructs.

we would have missed these compounds, and hence the rare opportunity to find compounds that activate telomerase and reverse or delay aging and the age-related diseases. In a recent paper, Auld et al. further caution for due diligence in interpreting reporter activation results (20). They report that false activators may come from screening platforms using luciferase reporter–gene assays where the activity comes not from the promoter-activated reporter expression, but from the stabilization of the luciferase enzyme per se. It is reasonable to assume that this phenomenon could be universal to any gene–reporter assays. Although this study highlights an artifact inherent to luciferase or other reporter-based assays, one could account and eliminate this artifact by washing the cells to remove the compounds and then adding the signal-detection reagent. This suggests that extreme due diligence is needed in working with engineered cell lines for use in cell-based assays.

Immunoassays

The lead identification methods widely employ enzyme-linked immunosorbent assays (ELISA) for detecting expression levels of cellular targets. A number of relevant cell lines may be selected and the levels of target of interest are characterized using ELISAs. For compounds directed against a positive regulator of angiogenesis, relevant cell lines expressing one or more of the growth factors (e.g., VEGF, FGF, EGF, PDGF, angiopoietin, angiogenin, and IL-8) can be identified using ELISA kits and the activity of the anti-angigenic compound can be profiled. A large number of ELISA-based assay kits are currently available for oncoproteins, cell growth markers, apoptosis, etc., from various sources wherein the primary and secondary antibody combinations are already optimized.

When ELISA kits are not available commercially, the protein levels in various cell lines can be quantified using the specific antibody against a target using the Li-COR Odyssey system (http://www.licor.com/bio/odyssey). The in-cell western is an immunocytochemical assay performed in 96- or 384-well microplate format. Target-specific primary antibodies and infrared-labeled secondary antibodies are used to detect target proteins in fixed cells and fluorescent signal from each well is quantified. At least two different antibodies labeled with two spectrally different dyes may be used simultaneously, thus increasing the throughput of detection. A target-specific antibody could be used in combination with anti-actin, or anti-GAPDH antibody, and the effect of compound treatment be normalized against a housekeeping protein. In the example shown in Figure 12, in-cell western was performed in three cell lines treated with puromycin by using an antibody directed against eIF4E in combination with the secondary antibody to develop an eIF4E secondary assay. The small-molecule modulators of a target protein can easily be tested and specificity can be determined by parallel screening for some other marker of cell-proliferation (PCNA antigen) in the same well. The system allows analysis of protein signaling pathways, protein quantification, and cell-based determinations of IC_{50} concentrations for lead optimization and allows study of the effects of drug components on multiple points within one or more signaling pathways. A large number of reagent kits for the quantitative multiplexed assessment of cytokines, chemokines, and intracellular proteins involved in inflammation are available commercially.

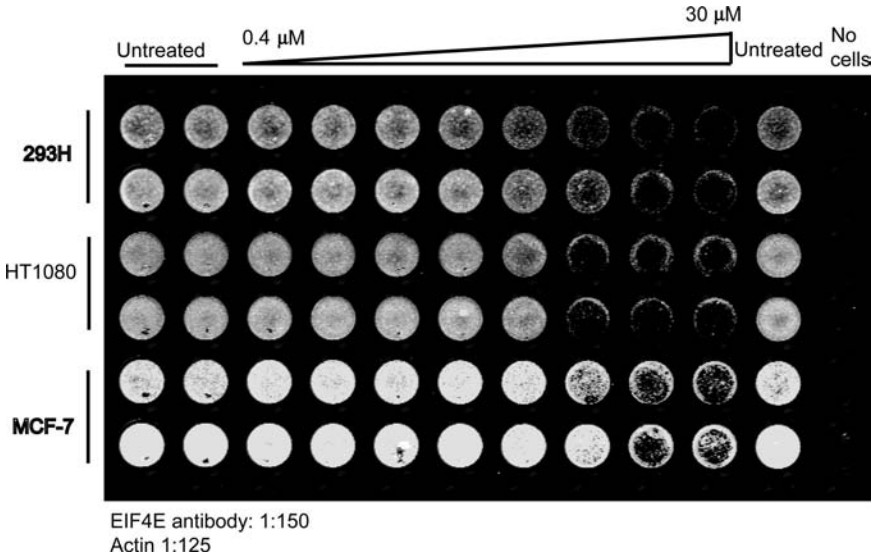

FIGURE 12 EIF4E in cell-western. Optimization of an in-cell western for screening hits against eIF4E. The effect of puromycin (a positive control, 0.4–30 μM) was tested in cell-lines (293H, HT1080, and MCF-7) plated at two different cell densities each. The image shows an overlay of signals from anti-eIF4E antibody and anti-actin antibody. The loss of both the actin and eIF4E signals at high puromycin concentrations indicate the general cytotoxicity of puromycin.

High-Content Analysis

High-content screening (HCS) is applied to the hit-to-lead process during orthogonal testing, by confirming hits using cell-based assays, which are more relevant to the target physiological condition that the inhibitor is addressing. HCS may also be used for secondary screening, by confirming hits with a functional cell-based assay using the actual cellular environment to test membrane permeability of labeled compounds. HCS has a wide range of applications for testing and confirming hits, such as measuring the ability of compounds to alter the protein that is being targeted in the screen, as illustrated in Table 6. For instance, hit series can be ranked and clustered based on the ability of compounds to trigger different forms of cell death and eliminate overly toxic compounds. Undesirable cellular effects of hits can be detected by HCS at this early secondary screening

TABLE 6 List of Some of the Application of High-Content Imaging (HCS) for Testing and Confirming Hits

Fluorescence intensity	Fluorescence distribution	Morphology	Cell movement
Calcium flux	Cytoplasm to nucleus	Neurite outgrowth	Chemotaxis/migration
Phosphorylation	Plasma membrane to organelle	Angiogenesis	Wound healing
Protein degradation	Receptor internalization	Cell differentiation	Metastasis/invasion
Image cytometry	Protein co-localization	Apoptosis	Long-term tracking

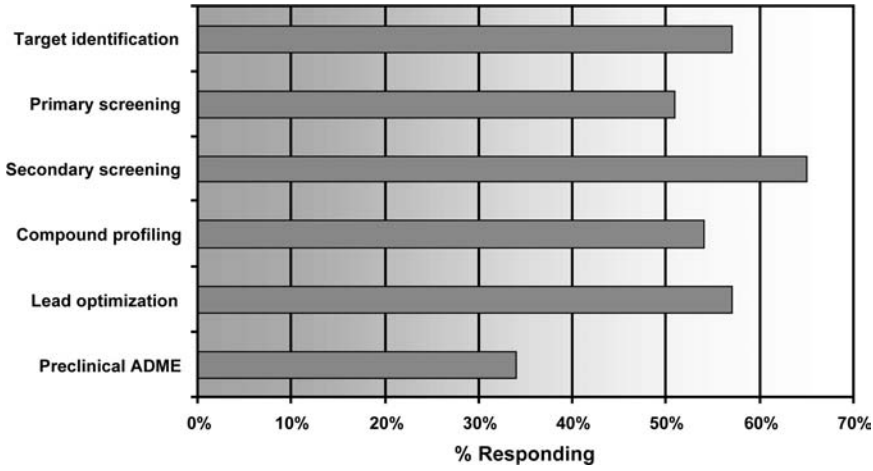

FIGURE 13 HCS in H2L. Use of high-content screening to different phases of drug discovery process from target identification, primary and secondary screening, compound profiling for hit-to-lead identification and profiling.

stage, making it possible to efficiently eliminate false positives (21). Fluorescently labeled hits can be visualized to quantify localization of the compound to the desired cellular compartment, or to view co-localization of the compound with its desired target protein. Live cell imaging further enables real-time monitoring of cellular response to compounds, such as stimulant response, receptor activation, and other transient events. The ability of HCS to quantitate even minute changes, on a cell-by-cell basis, allows it to capture small changes in subpopulations of cells, to produce accurate dose–response curves of an inhibitor in the target cell population. For instance, this subpopulation analysis can readily detect differences in the effects of a lead compound on one group of cells expressing a plasmid versus a second group of cells not expressing the plasmid, within the same well, even with expressing and nonexpressing cells being in close proximity to each other. A recent market survey of HCS in drug discovery by the independent market research consultancy agency, HTStec Limited, revealed that HCS is being applied widely to all phases of the drug discovery process, from target identification to preclinical candidacy [adapted from review by John Comley, with permission (Fig. 13); (22)]. The drug discovery process often requires quantitation of unique biological effects of multiple primary hits, a niche perfectly suited for HCS. The expansion of high-content analysis to screening has led to the development of a growing number of cell-based assays, enabling application of HCS to hit-to-lead studies. Typical hit compound advancement studies benefit from the ability of HCS to quickly characterize advanced hits for a given series of compounds in terms of potency and toxicity. In addition, high-content screens can be multiplexed, allowing analysis of multiple endpoints, simultaneously revealing the effects of compounds on multiple cellular pathways and targets, while identifying toxic effects of compounds. Alternatively, HCS can detect subpopulation effects off a drug on the same group of cells, such as an EC_{50}

concentration of compound altering a protein target in half of the cells, while being toxic to the other half.

Cytotoxicity Assays

When HCS is not available, the cytotoxicity assays may run in parallel with the selectivity assays to measure the general toxicity induced in cells treated with the test compounds in hit to lead development series. In addition to Cell-Titer Glo and MTT/MTS reagents, a large number of fluorimetric, bioluminescent, and colorimetric reagents and kits are available from companies such as Promega Inc., which can quantify the number of viable or dead cells or both in the same well. The effects of compounds on cytotoxicity are assayed in a panel of cells, which includes primary cells like peripheral blood mononuclear cells (PMBCs), as well as HepG2 or HuH cells to predict any potential drug-induced hepatotoxicity. If the target of interest is directly or indirectly related to angiogenesis (VEGF, etc.), HUVECs can be included in the screening panel. The cytotoxicity measurements are made in an 8 to 10-point dose–response curves on cells treated with the compounds for varying time-points (4, 24, 48, and 72 hours). The ratio of CC_{50} for activity to the EC_{50} of cytotoxicity defines a selectivity window, which is used for flagging and ranking compounds at an early stage in the hit-to-lead process. Thus, compounds showing a ratio >100 will be prioritized and this helps reduce the cost of identifying toxicity in expensive animal studies. The biomarkers for cytotoxicity can also be followed over time using HCS of cells treated with the test compounds. Alternately, activity assays can be performed by using caspase activation assays to quantify downstream apoptotic signal status. For anti-cancer drug development, clonogenic survival assays are often used as indicators of cell death and delayed growth arrest.

Many viral enzymes like polymerases, proteases, RTases, etc., are targeted in primary *in vitro* HT screens. The hits identified from an enzymatic/reporter assays can be assessed for their activity and cytotoxicity using cell-based assays, in which the cells express the basic replication unit of a virus. Thus, the identification of compounds active against RNA viruses like HCV is to use proprietary replicon systems (Apath, LLC; http://www.apath.com). Replicons are noninfectious subgenomic, self-replicating RNA molecules that contain all the nucleotide sequences required for RNA replication, transcription, and translation. The hits identified from any antiviral assay can be tested in the replicon to assess effects on the viral RNA levels (PCR-based detection) as well as on cytotoxicity. Compounds that effectively decrease viral RNA levels in the system without affecting the RNA levels of cellular actin or some other housekeeping gene and at the same time showing a window between activity and toxicity will be ranked higher than the ones for which such selectivity and specificity windows are small. Long- and short-term resistance against few scaffolds can be tested by exposing the replicons to the compounds for varying periods of time.

Label-Free Detection Technology

Currently, majority of HTS assays rely on the use of fluorescent or radioactive labels to monitor cellular responses or quantitating biochemical reactions in cell-free systems. However, labels can have adverse effects on the binding interactions, leading to false or misleading conclusions about binding properties of the

screening hits. When working with hard-to-drug targets or when a functional assay is unavailable, information for hit profiling can be obtained from the binding affinity measurements or other biophysical methods. A number of label-free optical and nonoptical biosensor technologies, based on thermal, electrical impedance, or refractive index, have evolved in recent years that could effectively be used in ranking hits as a function of their binding affinity profile and their selectivity towards the target of interest. A number of calorimetric systems are available to measure the differences in the heat released due to hit–protein interactions, and is used for determination of K_m turnover number in enzyme assays and binding constants and stoichiometry in binding assays. Surface plasmon resonance (SPR) is another technology that is gaining wider acceptance in advancing the lead optimization process and is useful in establishing a linear relationship between mass concentration of biologically functional molecules (such as proteins, sugars, and DNA) and resonance energy. The SPR signal is expressed in resonance units and is therefore a measure of mass concentration at the sensor chip surface. This means that ligand association and dissociation are used to calculate rate and equilibrium constants. The interaction quantification allows elimination of false positives and prioritization of hits using very low amounts of target protein. The HT SPR system (AP3000) from Fuji allows measurement of affinity and kinetics of biomolecular interactions in real time without labeling and provides information about complex formation and characterizing structure–function relationships. The binding affinity of 3840 analytes can be obtained within 24 hours using the AP-3000 system (http://www.fujifilm.com). Thermofluor, now a proprietary technology of Johnson and Johnson, is used to detect compounds that bind to unfolded proteins and thereby allowing selection of compounds that bind only to the folded state (23). The binding affinity is calculated from the ligand-dependent changes in the thermal stability of a target protein. This technology has been used at Johnson and Johnson for the prioritization of inhibitors of protein–protein interactions and to decrypt functions of previously uncharacterized proteins.

Conventional label and reporter-based cell assays are quite often prone to artifacts due to perturbation of the native cellular environment either by the label, overexpression of target protein of interest or promoter-mediated reporter gene expression. Label-free technologies are especially ideally suited for use with cell-based screening or hit-to-lead optimization platforms. Corning's Epic, SRU Biosystems' Bind, and ACEA Biosciences' and Celligence systems are some of the label-free detection platforms that are ideally suited for studying cell proliferation, drug and cell-mediated cytotoxicity, cell adhesion, receptor-mediated signaling, cell migration, and invasion, and have a unique place in hit-to-lead optimization phase of drug discovery and development.

Structure-Based Lead Selection

When the structural and electrostatic information for a target protein alone or one co-crystallized with ligand is available, computer-based *in silico* docking and scoring studies can be developed to identify which molecules have a complementary fit to the target-binding site and rank and direct analoging of compounds based on favorable small molecule/protein interactions (24). The crystal-structures of protein–ligand complexes are superimposed on the docking models of analogs from hit-to-lead series, to detect compounds that bind to

the protein target and can move forward into drug development. The X-ray crystallographic studies on the environment of interaction of chemical moieties with the binding sites on target provide high-resolution structural information that supports high-efficiency hit-to-lead development. Using this and other biophysical methods, novel ligand fragments are synthesized that improve binding kinetics of the hit being pursued. This fragment-based screening chemistry has been used successfully by Astex Therapeutics, Abbott and SGX Pharmaceuticals for both lead identification and lead generation for a number of diseases.

A good example of how a selectivity screening panel is organized and the power of co-crystallization methods in rapid attrition of hits at an early stage are illustrated in a recent publication on identification of selective B-Raf kinase inhibitors (25). A series of co-crystallization studies starting with low-affinity binders to several kinases led to identification of a compound, PLX4720, which inhibited oncogenic B-Raf^{V600E} specifically. The inhibitor was found to be >10-fold selective than wild type-B-Raf and showed higher selectivity against a diverse panel of 70 other kinases. The selectivity of the inhibitor was also studied in multiple tumor cell lines wherein the selectivity was >100-fold compared to enzymatic assays.

A number of low nanomolar, high potency specific inhibitors have been identified using fragment-based screens within few rounds of chemical synthesis, and are in later stages of drug development.

Biomarkers

Failing to measure the effects of lead compounds in physiological conditions leads to a high attrition rate during animal testing, amplifying the costs of drug discovery. However, recent advances in the application of biomarkers in early drug discovery can guide the hit-to-lead process to reduce the attrition rate of compounds in later preclinical and clinical testings. The Biomarkers Definitions Working Group define a biomarker as "a characteristic that is objectively measured and evaluated as an indicator of normal biological processes, pathogenic processes, or pharmacologic responses to a therapeutic intervention" (26). Biomarkers were first developed as biological readouts for detecting disease status in patients, but are now increasingly being applied to preclinical hit-to-lead studies to evaluate the safety and effectiveness of lead compounds (27).

Biomarkers can be used at three key points in the hit-to-lead process, as recently reviewed by Frank and Hargreaves (28). First, biomarkers can be used to detect if a series of screening hits actually hit the desired protein target. These studies can be performed with high-content screening to detect the biomarker indicator in response to the screening hits in the context of individual whole cells. Second, expression of biomarkers is detected through protein arrays, detecting the ability of lead compounds to alter the desired mechanism in the cell, indicative of a successful small-molecule inhibitor. Third, biomarkers can be applied in preclinical animal models to assess the ability of lead compounds to affect the target disease. This final stage is the most cost inhibitory, but yields valuable data about the expressed biomarkers in response to the compound. Only screening hits that alter the target and its pathophysiological mechanism would be expected to affect the disease state, thus biomarkers can guide the researcher in ranking compounds (28).

There are wide arrays of biomarker applications one could envision in hit-to-lead studies, ranging from studies in cell lines to animal models. One way to prioritize screening hits and lead series further development is by toxicity biomarker microarrays. In this application, the toxicity of compounds can be predicted to rank hits or series of hits for lead stratification. Compound advancement studies can be advanced by looking for gene expression of known biomarkers in response to compound hits, sorting compounds based on known or predicted molecular characteristics of successful drugs, based on factors such as solubility properties and metabolic products and the impact of metabolic products of a biomarker expression. An example of a biomarker is prostate-specific antigen (PSA). The effects of compounds on PSA levels can be measured by PSA protein levels to guide compound prioritization. Commercially available biomarker detection systems can be used to assist researchers automate and increase throughput of biomarker studies in drug discovery. One biomarker analysis platform, Invitrogen's ProtoArray, can monitor the levels of thousands of unique human proteins to generate disease signatures in response to lead compounds. The expression profiles of lead compounds can guide early triage of screening hits to prevent costly animal studies on toxic or ineffective hits.

Though the application of biomarkers to hit-to-lead studies is an emerging field, it has great potential to differentiate leads to reduce attrition rates in preclinical studies, thereby greatly decreasing the associated costs of drug discovery. The rich profile of data that can be derived from lead series through biomarkers ensures that these endpoints will increasingly be used routinely in hit-to-lead studies.

In short, the section above lists a variety of assays that allow a chemistry–biology assessment of hits based on their potency, selectivity, specificity, and cytotoxicity, and helps provide a preliminary ranking of compounds and scaffolds. This ranking is further influenced by the downstream analysis of pharmacokinetic attributes of these hits.

EARLY ADME ASSAYS

Most of the compounds fail to reach the market due to poor pharmacokinetic properties like poor solubility, permeability, and metabolic stability. A comprehensive knowledge of preclinical pharmacokinetic properties encompassing ADME-T are critical criteria that help determine the potential utility of a lead series and in later stages, for developing appropriate dosing regimens that result in optimal efficacy (see for more details chap. 16 in this book). A number of *in silico* methods as well as *in vitro* and/or *in vivo* studies are performed to provide a more comprehensive characterization of H2L series.

Physicochemical properties of compounds are important determinants of intestinal absorption, blood–brain barrier penetration, and metabolic stability. Poor oral bioavailability or duration of action can account for a significant number of failures in drug development. A number of computational methods are employed in pharmaceutical companies that allow cost-effective in silico prediction of the pharamcokinetic properties of a large number of compounds (29). In the first approach, compounds that meet Lipinski's rule of five are predicted to be orally bioavailable and permeable during passive transfer across biomembranes. These rules exclude the molecules that are substrates for active transporters. Another measure of predicting absorption is the plot of intrinsic lipophilicity

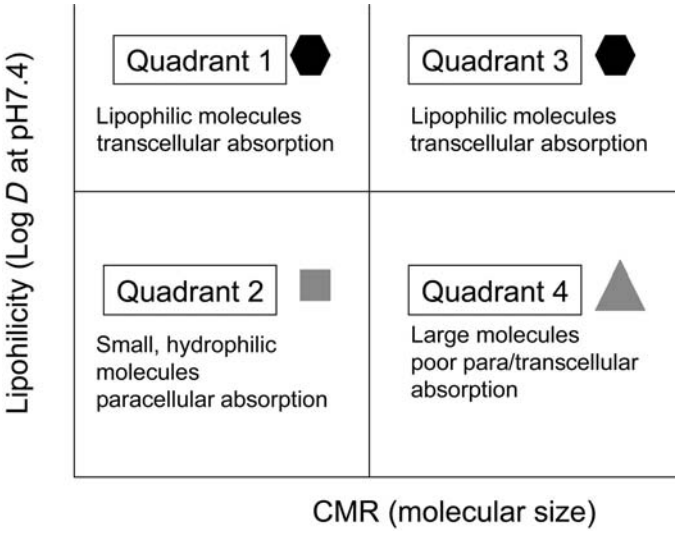

FIGURE 14 CMR versus pH. Predicting absorption of compounds by using a plot of intrinsic lipophillicity (Clog D, degree of ionization at physiological pH) versus molecular size calculated from molecular refraction (CMR).

(Clog D, degree of ionization at physiological pH) versus molecular size calculated from molecular refraction (CMR) (Fig. 14). The molecules in quadrants 1 and 3 are lipophilic and can be absorbed trans-cellularly. Molecules that are small and hydrophilic in quadrant 2 show para-cellular transport, but large hydrophilic molecules in quadrant 4 are predicted to show poor absorption. The probability of absorption can be determined from the quadrant distribution of a large number of test compounds by plotting lipophilicity and size parameters. In the third approach, compounds of MW $<$450 Da and polar surface area of $<$90 Å are predicted to cross the blood–brain barrier (29).

In addition to the *in silico* methods, several hundred compounds that cross the barriers of potency, selectivity, cytotoxicity, and chemical synthetic accessibility are routinely tested in the *in vitro* systems for assessing the following phamacokinetic properties.

Permeability, Absorption Through Caco2 Cells

A common *in vitro* method utilized to evaluate drug absorption through para- and trans-cellular transports is the use of human colon adenocarcinoma epithelial cells (Caco2 cells) (see for more details chap. 16 in this book). The permeability of compounds across a Caco2 cell layer correlates with *in vivo* oral absorption of drugs across the intestinal wall. The cells are grown in trans-wells or miniaturized formats, and the compound uptake is quantified by using LC-MS analysis. The apparent permeability (P_{app}) value of rate of transfer from the apical to basal side of the Caco2 monolayer is determined and the ones with a P_{app} coefficient of $>1 \times 10^{-6}$ cm^2/sec are predicted to have good oral absorption and are prioritized.

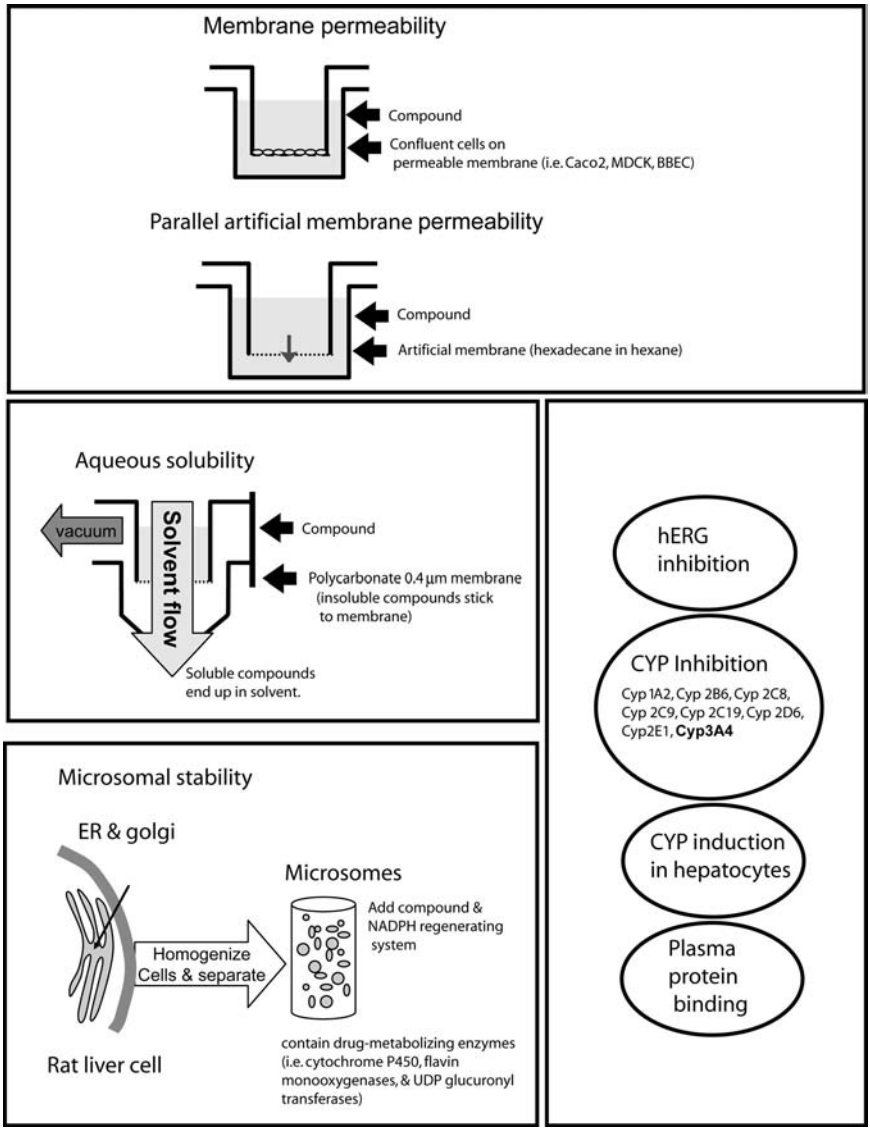

FIGURE 15 *In vitro* ADME assays. A schematic showing some of the *in vitro* ADME assays required for compound profiling and prioritization during hit-to-lead phase.

Metabolic Stability Using Liver Microsomes

The hepatic cytochrome P450 (Cyp P450) enzymes are mainly required for oxidation of drugs *in vivo*. The extent of metabolism of a drug by liver microsomes *in vitro* correlates with the *in vivo* metabolism of compounds. In hit to lead phase, several compounds are tested in 96-well formats for their ability to inhibit a panel of Cyp P450 enzymes expressed in mouse and/or human microsomes. The

analysis of parent molecule remaining is determined by LC-MS analysis, and the hits are prioritized compounds for a PK study. Compounds that are <25% metabolized (loss of parent per hour) in human liver microsomes are given higher priority and characterized further.

Cytochrome P450 Inhibition

In humans, five isoforms of the cytochrome P450 enzymes (CYP1A2, CYP2C9, CYP2C19, CYPD6, and CYP3A4) are responsible for the metabolism of approximately 95% of drugs. The inhibition of these enzymes by one drug is a major cause of drug–drug interactions with other drugs. CYP450 (BD Biosciences/Gentest CYP450 inhibitor screening kits containing cDNA-expressed p450 enzymes) are often used to prioritize compounds. At least 100 compounds can be tested in the CYP inhibition panel at single concentration (10 μM) for initial screening for cytochrome P450 inhibitors. For a large number of test compounds, inhibition of only one of the CYP enzymes (CYP 3A4), which processes 40% of all marketed drugs, can be tested at one or more concentrations.

hERG Ion Channel

A number of drugs are known to cause blockade of hERG (human ether-à-go-go-related gene) potassium channel. Inhibition of the hERG channel results in QT-interval prolongation, a defect in cardiac muscle repolarization. The potential of compounds to cause QT prolongation can be contracted out for e.g. ChanTest (Cleveland, OH) to assess inhibition of hERG potassium channel current using stably transfected HEK293 cells or can be determined using Patch Clamp electrophysiological methods. A fluorescence polarization assay is available from Invitrogen to determine activity of hERG channel. A red-shifted fluorescent tracer displays high polarization when bound to the hERG channel and a low polarization when displaced by compounds that bind to the channel. The results from the invitrogen Predictor™ assay showed a high correlation with those obtained from patch-clamp techniques.

Plasma Protein Binding

The extent of plasma protein binding is critical to predicting a drug's pharmacokinetic profile, the doses required for the drug, and possible drug–drug interactions. Most small molecules exhibit some level of protein binding affecting the amount of drug to reach the target tissue. Therefore, protein binding is generally determined by using a standard 96-well assay that utilizes a membrane filter to separate free from bound drug (Millipore, Bedford, MA).

So, while some of the pharmacokinetic properties of compounds can be determined, failure in the lead development and optimization stage may still occur due to unknowns such as affinity for P-glycoprotein and other transporter mechanisms *in vivo*. The parameters determined in ADME studies are used in conjunction with the potency and selectivity parameters to rank-order a hit to lead series. If resources are sufficient, top molecules in several hit to lead series may be further characterized. A variety of software packages are available to predict compound mutagenicity (30). Animal-free assays for mutagenicity include the Ames test, micronucleus assay, and chromosome aberration assays. Finally,

oral bioavailability in rodents and intravenous clearance studies can be done to determine the compound half-life *in vivo*.

PRELIMINARY PHARMACOKINETIC STUDIES

If resources are sufficient, compounds that are metabolically stable *in vitro* and demonstrate permeability across a Caco2 layer may be assessed for plasma exposure in mice after oral administration. The preliminary PK studies are generally designed to compare between 5 and 10 compounds in a single study for exposure. An experimental design might include assessing exposure at 15 minutes, 1 hour, 3 hours, 6 hours, and 24 hours after oral or SQ administration at 10 mg/kg. Compound levels in the plasma and in the liver tissue homogenates are measured by using LC/MS/MS technology. Compounds with poor oral exposure may not be assessed in animal models of disease. These properties will help identify a candidate that is:

- metabolically stable,
- sufficiently permeable,
- not genotoxic,
- not a hERG blocker,
- minimally inhibitory to the P450 enzymes in order to avoid drug–drug interactions, and
- safe and well tolerated in animals in which there is adequate exposure upon oral administration.

SUMMARY

As screening hits progress through the drug discovery gauntlet, many compounds fail due to lack of sufficient potency, efficacy, target site specificity, or a reasonable understanding of their pathobiology. The root cause of this attrition could be attributed to a lack of critical guidance in the implementation of the most appropriate counter screens, judicious progression of compounds through the hit-to-probe-to-lead stages, and most importantly a lack of adequate ADMET profile. With the industrialization of many of the secondary assays, it is no longer necessary to restrict the hit rate to an artificially low level. We recommend providing a wide variety of chemotypes to the medicinal chemistry team to select for optimization. There is no one way to define a generic hit-to-lead process that will work effectively for every target being pursued. We have attempted to define the logistics in the hit-to-lead phase and also discuss the tools available for a cost-effective hit-to-lead studies. We propose a judgment-based (quantitative biology) approach to complement the predominantly rule-based (chemistry) efforts that have been applied the hit-to-probe-to-lead optimization strategies. A multiplexed, multipronged, and parallel approach is advocated over a linear decision-making strategy to fail/advance compounds. These strategies are universally applicable among all target classes as well as lead chemistry types. We credit the medicinal chemistry teams for perfecting the lead optimization strategies within the drug-like space, and it is time for the "biologists" to measure up to their chemistry colleagues. The biology teams need to provide a better understanding of the selectivity and pathobiology profile at a very early stage of the drug discovery process. Because of the increasing availability and affordability

of preclinical assay technologies, these studies can now be undertaken with ease. We have provided justification for a forward integration of the preclinical studies into the hit-to-lead optimization phase to provide judicial guidance in conquering the so-called valley of death.

ACKNOWLEDGMENTS

The authors would like to thank their former colleagues at FMC Corporation and Sierra Sciences for the many years of collaboration in "hit-to-lead" research. The authors would like to thank Drs. Sitta Sittampalam and Scott Weir, Institute for Advancing Medical Innovation (IAMI) at the University of Kansas (KU) for their support; Drs. Roy Jensen, Barbara Timmermann, and George Wilson for their vision in promoting drug discovery research initiatives at KU and their commitment to the HTS laboratory's research priorities. KU-HTSL is a KU Cancer Center Shared Resource and is funded in part by NIH/NCRR COBRE grant P20 RR015563.

REFERENCES

1. Ohlstein EH, Johnson AG, Elliott JD, et al. New strategies in drug discovery. Methods Mol Biol 2006; 316:1–11.
2. Zycher B, DiMasi JA, Milne C. The truth about drug innovation: Thirty-five summary case histories on private sector contributions to pharmaceutical science. Med Prog Rep 2008; 6:1–48.
3. DiMasi JA, Hansen RW, Grabowski HG. The price of innovation: New estimates of drug development costs. J Health Econ 2003; 22(2:)151–185.
4. Kola I, Landis J. Can the pharmaceutical industry reduce attrition rates? Nat Rev Drug Discov 2004; 3(8:)711–715.
5. Lipinski CA. Drug-like properties and the causes of poor solubility and poor permeability. J Pharmacol Toxicol Meth 2000; 44(1:)235–249.
6. Lipinski CA, Lombardo F, Dominy BW, et al. Experimental and computational approaches to estimate solubility and permeability in drug discovery and development settings. Adv Drug Deliv Rev 2001; 46(1–3:)3–26.
7. Lipkin MJ, Stevens AP, Livingstone DJ, et al. How large does a compound screening collection need to be? Comb Chem High Throughput Screen 2008; 11(6:)482–493.
8. Feng BY, Simeonov A, Jadhav A, et al. A high-throughput screen for aggregation-based inhibition in a large compound library. J Med Chem 2007; 50(10:)2385–2390.
9. Giannetti AM, Koch BD, Browner MF. Surface plasmon resonance based assay for the detection and characterization of promiscuous inhibitors. J Med Chem 2008; 51(3:)574–580.
10. Simeonov A, Jadhav A, Thomas CJ, et al. Fluorescence spectroscopic profiling of compound libraries. J Med Chem 2008; 51(8:)2363–2371.
11. Kozikowski BA, Burt TM, Tirey DA, et al. The effect of freeze/thaw cycles on the stability of compounds in DMSO. J Biomol Screen 2003; 8(2:)210–215.
12. Wunberg T, Hendrix M, Hillisch A, et al. Improving the hit-to-lead process: Data-driven assessment of drug-like and lead-like screening hits. Drug Discov Today 2006; 11(3–4:)175–180.
13. Nuttall ME, Lee D, McLaughlin B, et al. Selective inhibitors of apoptotic caspases: Implications for novel therapeutic strategies. Drug Discov Today 2001; 6(2:)85–91.
14. Los M, Burek CJ, Stroh C, et al. Anticancer drugs of tomorrow: Apoptotic pathways as targets for drug design. Drug Discov Today 2003; 8(2:)67–77.
15. Haseneen NA, Vaday GG, Zucker S, et al. Mechanical stretch induces MMP-2 release and activation in lung endothelium: Role of EMMPRIN. Am J Physiol Lung Cell Mol Physiol 2003; 284(3:)L541–L547.

16. Werner P, Kawashima E, Reid J, et al. Organization of the mouse 5-HT3 receptor gene and functional expression of two splice variants. Brain Res Mol Brain Res 1994; 26(1–2:)233–241.
17. Eggert US, Kiger AA, Richter C, et al. Parallel chemical genetic and genome-wide RNAi screens identify cytokinesis inhibitors and targets. PLoS Biol 2004; 2(12:)e379.
18. Liu H, Huang P, Xu X, et al. Anticancer effect of celecoxib via COX-2 dependent and independent mechanisms in human gastric cancers cells. Dig Dis Sci 2008.
19. Coates AR, Hu Y. Targeting non-multiplying organisms as a way to develop novel antimicrobials. Trends Pharmacol Sci 2008; 29(3:)143–150.
20. Auld DS, Thorne N, Nguyen DT, et al. A specific mechanism for nonspecific activation in reporter-gene assays. ACS Chem Biol 2008; 3(8:)463–470.
21. Bowen WP, Wylie PG. Application of laser-scanning fluorescence microplate cytometry in high content screening. Assay Drug Dev Technol 2006; 4(2:)209–221.
22. Comley J. High content screening: Emerging importance of novel reagents/probes and pathway analysis. Drug Discov World 2005; 6:31–53.
23. Cummings MD, Farnum MA, Nelen MI. Universal screening methods and applications of ThermoFluor. J Biomol Screen 2006; 11(7:)854–863.
24. Joseph-McCarthy D, Baber JC, Feyfant E, et al. Lead optimization via high-throughput molecular docking. Curr Opin Drug Discov Devel 2007; 10(3:)264–274.
25. Tsai J, Lee JT, Wang W, et al. Discovery of a selective inhibitor of oncogenic B-Raf kinase with potent antimelanoma activity. Proc Natl Acad Sci U S A 2008; 105(8:)3041–3046.
26. Atkinson Jr AJ, Colburn WA, DeGruttola VG, et al. Biomarkers Definitions Working Group, Biomarkers and surrogate endpoints: Preferred definitions and conceptual framework. Clin Pharmacol Ther 2001; 69(3:)89–95.
27. Lewin DA, Weiner MP. Molecular biomarkers in drug development. Drug Discov Today 2004; 9(22:)976–983.
28. Frank R, Hargreaves R. Clinical biomarkers in drug discovery and development. Nat Rev Drug Discov 2003; 2(7:)566–580.
29. Spalding DJ, Harker AJ, Bayliss MK. Combining high-throughput pharmacokinetic screens at the hits-to-leads stage of drug discovery. Drug Discov Today 2000; 5(12 Suppl 1:)70–76.
30. Ringeissen S. Evaluation of (Q)SAR models for the prediction of mutagenicity potential. Proceeding of 6th World Congress on Alternatives & Animal Use in the Life Sciences, 2007; 14(special edition:)469–473.

4 Signal Detection Platforms for Screening in Drug Discovery

Ramakrishna Seethala
Bristol-Myers Squibb, Princeton, New Jersey, U.S.A.

INTRODUCTION

Drug discovery is a process by which drugs are designed and discovered through therapeutic target identification, efficacious assay development, identification of leads, lead optimization by synthesis, preclinical characterization, and drug safety assessment. The goal of drug discovery is to discover and develop safe and efficacious medicines for unmet medical needs. High-throughput screening (HTS) is an essential drug discovery strategy for biotechnology and pharmaceutical industries to find new leads that eventually will be developed into new drugs. HTS is an Enabling Technology for Drug Discovery and Biomedical Research. The goal of HTS is to accelerate drug discovery that relies on sound and best signal detection technologies. The preferred assay technologies therefore use homogeneous biochemical and cell-based assay formats that are adaptable for high-density microplate assays and automation. Advances in the assay technologies and instrument technologies are making it possible for the drug discovery marching towards ultra-HTS to keep pace with increasing demand to screen more targets in shorter time. Through this process one can rapidly identify active compounds or genes, which modulate a particular biomolecular pathway. The results provide starting points for drug lead discovery and design.

Drug therapy in 1990s was based on less than 500 molecular targets. Most of the blockbuster drugs are loosing exclusivity necessitating the pharmaceutical companies to replace their product pipeline with important drugs for unmet medical needs. To commensurate with the demand, the number of potential therapeutic targets is increasing exponentially with the advances in genomics, proteomics, and combinatorial chemistry (1). This rapid growth in targets necessitates increase in the pace and productivity of HTS to identify large number of new leads that will eventually transformed into promising therapeutics. Consequently, the number of screens and compounds being screened will be increasing.

Bulk of HTS screens before the year 2000 were run in 96-well plate formats (Table 1). At present, most of the assays are run either in 384- or 1536-well plate formats paving the way for ultra-HTS. To increase the throughput of screening, the assays must be very simple, robust, preferably homogeneous assays (add reagents, mix, and read) and amenable to miniaturization and automation, which will decrease the time and manpower required for completion of screening huge compound decks (>1 million compounds). There have been constant improvements in liquid-handling systems capable of delivering compounds and reagents in nanoliter volumes (with positive displacement, acoustic methods), detection

TABLE 1 Screening Throughput

Assay type	Assay plates	#Assays/day
Low-throughput assays	96-well plates	100s
Medium-throughpurt assays	96-well plates	1000s
High-throughput assays	384-well plates	10,000s
Ultra–high-throughput assays	1536-, 3456-, 9600-well plates	100,000s

instruments (multimode plate readers, imaging plate readers, and high-content imaging systems) informatics and data analysis software packages, high-density plates (generic or custom plates), high-quality reagents with recombinant expression (mammalian expression, bacculovirus expression of mammalian genes, Bacman expression systems), and assay technologies to be able to automate drug screening completely.

Drug discovery process is initiated with target identification (gene identification, expression of the genes in the pathophysiology, mutational and phenotype studies) followed by assembling reagents for developing a robust bioassay for HTS (Fig. 1). In HTS, one bioassay tests many compounds (>million) at one high concentration in a short time to identify the "hits" (normally the hit response is adjusted to have a hit rate of <1%), "hit" confirmation again in screening mode, followed by dose–response mode, which identifies thousands of compounds. Hit assessment in dose–response mode with a primary assay in lead optimization confirms hundreds of compounds. During lead optimization, small number of compounds (hundred to thousands) are tested against an array of assays for optimizing a drug candidate. Lead optimization assays use both biochemical and cell-based assays to identify lead compounds that can be

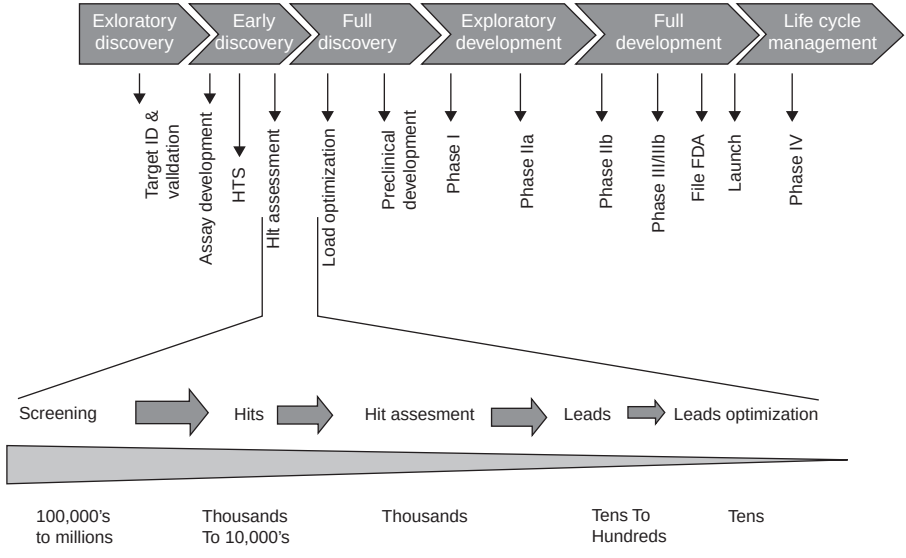

FIGURE 1 Drug discovery process in pharmaceutical and biotechnology industry.

tested in the in vivo assays. Finally, a compound with desirable pharmacokinetic and pharmacodynamic properties and desired therapeutic indication in animal models will be selected in Drug Discovery to promote for clinical development in human subjects. To reduce the attrition rate of compounds going from drug discovery process to human testing and approval as drugs, many pharmaceutical and biotechnology companies, although increasing the potency of lead compounds, have been including a panel of selectivity assay for the target and safety panel profiling assays to determine the off-target liability early on in the drug discovery.

In this chapter, various assay platforms for developing robust in vitro assays including cell-free (biochemical assays) and cell-based assays for HTS and lead optimization will be discussed. Selection of right screening technology for an effective "hit" seeking, "hit" assessment and lead optimization are needed. Robust, homogeneous assays can be developed for in vitro biochemical assays (Table 2). In vitro assays are advantageous because the assay can be targeted for a specific enzyme, receptor, or protein. The other advantages of in vitro assays include fast assays, less expensive, and more reproducibility of the assays as large amounts of the reactants and protein from same lot can be used for the screen. These assay technologies can also be applied for cell-based assays; however, cell-based assays tend to be resource and time-consuming. Cell-based assays were used as secondary and tertiary assays in 1990s, as these were time and resource consuming, labor intensive, and inherent variability. In cell-based assays, the concentration of test compounds in the cell depends on the permeability and efflux of the compound. The less-permeable compounds in mammalian cells may not be detected in whole-cell screen but may be an excellent chemotype affecting the target in a cell-free assay. Some chemotypes may be metabolized in the cell to inactive products and miss activity test. These chemotypes can

TABLE 2 Comparison of Heterogeneous Assays Vs Homogeneous Assays

Heterogeneous Assays	Homogeneous Assays (Mix and Measure)
Heterogeneous assays involve multi transfer, multi processing steps	The homogeneous assays are in general one-pot assays. There are no transfer and processing steps They are bead and non-bead based technologies
More processing steps, means more source of errors	Some times multi additions are used but do not effect signal.
Usually not amenable to automation	These are automation friendly
Create large biological or radioactive waste and environmentally not friendly	Environmental friendly. Waste generated is low.
Labor intensive, Time consuming	Easy and faster
Needs more FTE time (Takes Longer time)	Less FTE time is needed
CV is large	CV is low, reproducible data
Difficult to miniaturization	Amenable for miniaturization
Per Assay Cost is very high	Per Assay cost is lower as.
Reaction volumes are high and waste of reagents and compounds	Assay can be miniaturized into highdensity plates with small volumes saving on expensive reagents

Most of the new technologies use homogeneous assays for higher throughput and automation capabilities.

be detected in the in vitro biochemical assays and have the potential of being amenable to chemical modifications to increase the permeability or stability in the cell to obtain more potent compounds. Also, with the recombinant cells, the signal and response may change with the number of passage of the cell-line and cell biology reagents. Recent improvements in cell-based assays are making it possible to use these in primary screening in drug discovery. In the recent years with the availability of automated cell culture systems (MACCS^{TM} from Matrical and Select-T from The Technology Partnership, Cambridge, U.K.), use of cryopreserved cells in cell-based assays, new screening technologies, and bulk transfection methods, more and more cell-based assays are being used as primary assays for HTS. It should be noted that even cell-based assays are not predictive of in vivo outcomes in the animal.

Although conventional assays such as receptor–ligand binding, enzyme, and cell-based assays are multistep heterogeneous assays in the past, involving filtration, precipitation, or adsorption, and several wash steps to separate bound ligand from free ligand or product from substrate, recent years have seen newer homogeneous assay platforms that are robust consisting of reactions that are very rapid, taking minutes to reach equilibrium made it possible to develop HTS and ultra-HTS assays for biochemical and cell-based assays (Table 2).

In the homogeneous assay technologies, all the reaction components either in solution or some reagents attached to solid phase are incubated and read in a plate reader with no further processing steps. Major research efforts in the last few years produced several new radioactive-, fluorescence-, and luminescence-based homogeneous assay platforms that are compatible with automation for use in HTS and ultra-HTS. New nanotechnologies, including DNA array chips, quantum dots, nanoparticle technologies, are evolving that will be suitable for ultra-HTS in a very high-density format. In recent years, label-free detection technology platforms, which involve the use of a biosensor (transducer) that is capable of directly measuring some physical properties of a biomolecule or cell, are gaining prominence in drug discovery. The homogeneous radioisotope assays are based on scintillation proximity assay (SPA) platform, a widely used technology in which the radiolabeled biomolecule bound to an appropriate protein or antibody coated on SPA bead (a scintillant coated bead) comes into close proximity of the scintillant on the bead and produces scintillation signal. The fluorescence-based assays include (a) fluorescence intensity assays that include fluorogenic, fluorescence quench, and quench relaxation assays; (b) fluorescence polarization (FP) assay in which the signal is proportional to molecular volume (size); (c) fluorescence resonance energy transfer (FRET); (d) time-resolved fluorescence (TRF); (e) homogeneous time-resolved fluorescence (HTRF), homogeneous time-resolved fluorescence resonance energy transfer (TR-FRET), or Lance assay in which fluorescence resonance energy from a donor molecule is transferred to an acceptor molecule; (f) confocal fluorescence microscopy and fluorescence imaging analysis, and (g) fluorescent reporter systems such as green fluorescent protein (GFP) and β-lactamase reporter systems. Luminescence-based homogeneous assays have also been developed utilizing bioluminescence, electrochemiluminescence, or chemiluminescence. These homogeneous assays are discussed in greater detail in this chapter.

RADIOACTIVE ASSAYS

In the conventional radioactive assays, the product or bound ligand has to be separated from the radioactive substrate or free ligand by gel-filtration, precipitation, adsorption, or filtration and then washing. These procedures are not amenable for HTS and in addition generate large volumes of radioactive waste. Nevertheless, radioactive assays are very sensitive and robust assays. Reliable new homogeneous radioactive assays have been developed for HTS that do not require separation of bound radioactivity from free, thus increasing the throughput and greatly reducing radioactive waste.

Scintillation Proximity Assay (SPA)

Hart and Greenwald were the first to describe SPA in an immunoassay by using two polymer beads coated with antigen, one coated with flurophore and the other with ^{3}H (2). Antibody agglutination brings many of the ^{3}H beads into close proximity of the flurophore beads and excites them, and after very long incubations can be counted in a scintillation counter. Udenfriend et al. have improved with microbeads containing a flurophor and coated with antibody (3). [^{25}I]-labeled antigen binds to the antibody on the beads, and by its proximity the emitted short-range electrons of the [^{125}I] excite the flurophore in the bead, which can be measured in a scintillation counter without separation of unbound antigen. SPA technology was further developed by Amersahm International (now GE Healthcare Bio-Sciences Corp. Piscataway, NJ). SPA is a homogeneous assay platform that can be utilized for a variety of biological assays.

When ^{3}H atom decays, it releases β-particle with an average energy of 6 keV and has a mean path length of 1.5 μm in water and is ideally suited for SPA (4). The path lengths of [^{14}C], [^{35}S], [^{33}P], and [^{125}I] isotopes are 58, 66, 126, and 17.5 μm, respectively. If [^{3}H] β-particle meets a scintillant molecule within 1.5 μm of the particle being released, it will have sufficient energy to excite the scintillant into emitting light. On the other hand, if the β-particle of [^{3}H] travels longer distances of more than 1.5 μm, it will not have enough energy to cause scintillation. In SPA, if a radioactive molecule is bound to the SPA-bead directly or through a molecule coupled to the bead, it is brought in close proximity for the emitted radiation to pass through the solvent molecule, its energy is dissipated by collision with the solvent molecules that are elevated to an excited state. The excited solvent molecules transfer their energy to the scintillant molecules and emit this energy as photon of light (Fig. 2). Unbound radioactive molecules are too far away from the scintillant of the bead, and the energy released is dissipated and decays in the solution before reaching the bead and no light is produced (4). The amount of light produced is proportional to the amount of radioligand bound to the SPA bead and is detected by using photomultiplier tubes of scintillation counters or CCD imagers. As the bound radioligand only produces the scintillation signal and the unbound radioligand does not produce signal, hence there is no need for separation of free radioisotope in the assay. SPA method utilizes SPA beads or scintillant-coated plates (FlashPlate or Cytostar-T Plates) for the assays. Tritium β-particle with path length of 1.5 μM is ideally suited for SPA. [^{125}I] atom decays by electron capture giving rise to particles named Auger electrons that can be detected in SPA method. Although most of the SPA assays are preferably performed with ^{3}H, and ^{125}I β-emitters in aqueous buffers, ^{14}C, ^{35}S, and ^{33}P isotopes also have been used successfully with SPA.

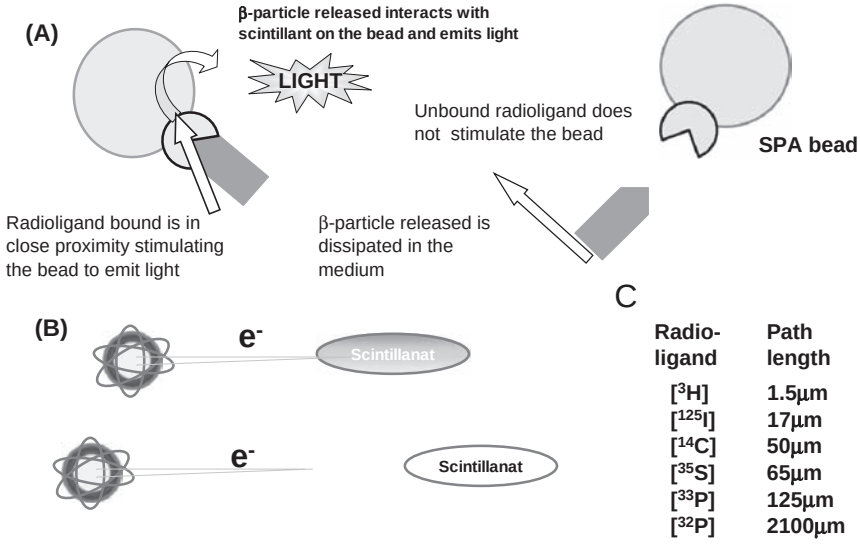

FIGURE 2 Scintillation proximity assay (SPA) principle. (**A**) When a radioligand binds to the acceptor molecule on the SPA bead, it is in close proximity of the scintillant on SPA bead. Radiation energy from the radioligand is absorbed by the scintillant on the bead and generates signal on the bead, whereas unbound radioligand will not be in close proximity of the bead scintillant and the β-particles released by radioligand will be dissipated in the medium and decays. (**B**) Scintillation proximity of various radioactive molecules. β-Particles of radioisotopes travel certain distances, and if they do not meet scintillant during their travel, they will be dissipated in the medium and decays. (**C**) Travel distances of β-particles of various radioisotopes. *Source*: Courtesy of GE Healthcare.

SPA Bead Assay

In the SPA bead method, the target of interest is immobilized to a small scintillant containing microspheres or fluoromicrospheres (SPA beads) of approximately 5 μm size. The fluoromicrospheres consist of a solid scintillant—polyvinyltoluene core coated with polyhydroxy film, which reduces the hydrophobicity of the particle. SPA beads coated with a wide range of biomolecules such as antibodies, streptavidin, receptors, enzymes and small molecules such as glutathione, copper ions are available. The SPA beads due to higher surface area have higher binding capacity and clearly have advantage over scintillant-coated plates. A choice of four different core bead types is available for development of SPA homogeneous assays. Two types of core SPA beads: polyvinyl toluene (PVT) and yttrium silicate (YSi) bead that contain scintillant, which emit light in the blue region of the visible spectrum, and the signal can be measured in a scintillation counter. SPA microsphere beads have been prepared from hydrophobic polymer such as polyvinyl toluene (PVT) and inorganic scintillators such as yttrium silicate (YSi) beads (4). The capacity of the YSi bead is higher compared to the PVT bead. YSi bead is denser than the PVT bead. The other two types of SPA beads are imaging beads, polystyrene (PS) and yttrium oxide (YOX) that contain scintillant, which emit light in the red region of the visible spectrum, and the signal can be measured in a CCD imager such as LEADseeker or ViewLux.

The SPA imaging beads have emission maximum of 615 nm and show very little quenching with colored (yellow) compounds in the assay.

Before developing an assay the compatibility of radioligands with SPA beads has to be tested. Also, the microplates have to be screened for low nonspecific binding of the radioligand. SPA has been applied to a wide variety of different assays including radioimmunoassays (RIAs), receptor binding assays, protein–protein interaction assays, enzyme assays, and DNA–protein and DNA–DNA interaction assays (5). SPA beads coated with protein A or secondary antibody capture the antibody–antigen complex and are quantitated in the radioimmunoassays (RIAs). The RIAs are used in clinical and pharmacological studies to measure drugs, the second messengers, prostaglandins, steroids, and other serum factors.

SPA beads with wheat germ agglutinin (WGA), polyethylimine WGA-PVT beads, or polylysine-coated YSi beads have been used for several membrane receptors including neuropeptide Y, galanin, endothelins, nerve growth factor, TGFα, TGFβ, Ach, EGF, insulin, angiotensins, β-adrenoceptors, somatostatin, bFGF, dopamine, interlukin receptors (6,7). SPA also has been utilized in designing screens for nuclear receptor binding assays with the ligand binding domain of the nuclear receptor expressed as a fusion protein with His-tag (His_6), radioligand, and nickel-SPA beads. The protein–protein interaction assays that have been developed by using SPA consists of SH2 and SH3 binding domains, Fos-Jun, Ras-Raf, selectin, and integrin adhesion assays (6,7). SPA has been used for protein–DNA binding interaction assays such as binding of transcription factor NF-κB to DNA. For enzymes such as acyl-coenzyme A:diacylglycerol acyltransferase, which have difficult traditional assays, a simple SPA bead–based HTS assay with polylysine-coated SPA beads has been developed (8).

FlashPlate™ Assay

FlashPlate™ is a white 96- or 384-well polystyrene microplate with plastic scintillator–coated wells (7,9–11). FlashPlate like other polystyrene microplates has hydrophobic surface for adsorption of protein. Because the scintillant is coated on the microplate, additional scintillant is not required for counting (Fig. 3). Image FlashPlate, a 384-shallow well microplate coated with a scintillant that emits in the red region, combines ultra miniaturization with superior sensitivity, the signal is read in an imaging plate reader (LeadSeeker or ViewLux) (9). FlashPlate or Image FlashPlate has to be precoated with a substrate, ligand, antibody, or secondary antibody before using for an assay. FlashPlate coated with antibodies, proteins, or peptide substrates have been used to develop one-step assays, reducing the amount of radioactive waste and time for assay. A SPA-based acetyl CoA carboxylase activity assay was developed by coupling to fatty acid synthase using phospholipid-coated FlashPlates and phospholipid-coated Imaging FlashPlates, and was then utilized for HTS compaign and lead optimization (9).

FlashPlate™ technology can be used in many assay formats: (a) enzyme assays such as protein kinase, chloramphenicol acetyl transferase (CAT), helicase, and reverse transcriptase (7); (b) receptor–ligand binding assays with soluble receptors (e.g., human estrogen receptor, interleukin-1 receptor) (11); G-protein–coupled receptors (e.g., endothelin receptors) (12); (c) radioimmunoassays (e.g., cyclic AMP, cyclic GMP, prostaglandin E2

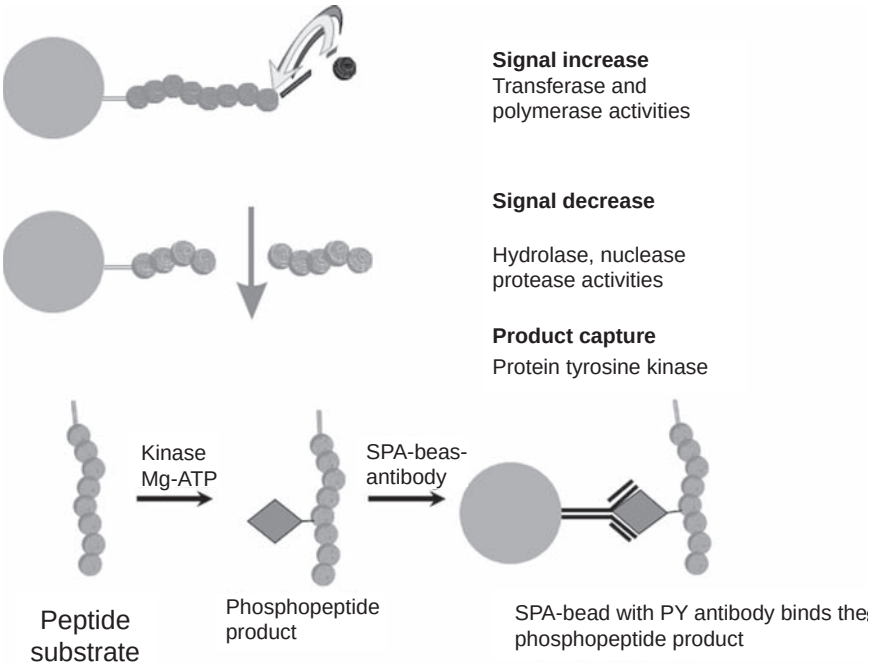

FIGURE 3 SPA enzyme assay formats. Schematic representation of the three enzyme assay formats 1. When a radiolabeled compound is added to a substrate attached to SPA bead, it results in signal increase. 2. When a radiolabeled substrate attached to SPA bead is cleaved releasing the radiolabel will result in signal decrease. 3. When a substrate forms a radiolabeled product in the reaction, the product can be captured on to the antibody-coated SPA bead and result in signal increase. *Source*: Courtesy of GE Healthcare.

(13); (d) functional assays with live cells (e.g., adenyl cyclase assay) (13); and (e) molecular biology techniques including sandwich hybridization assay and translation systems (13). FlashPlate technology can be used for a wide variety of applications such as enzyme, receptor binding, functional and immunoassays as well as in live cells. Commonly used radioisotopes (i.e., [^{3}H], [^{14}C], [^{35}S], [^{125}I], [^{32}P], [^{33}P], and [^{45}Ca]) can be used with FlashPlates. With low-energy β-emitters such as [^{3}H], [^{14}C], and [^{35}S] isotopes FlashPlates can be used in homogeneous format. However, with higher-energy β-emitters such as [^{32}P] and [^{33}P], the unbound radioactivity should be removed by aspiration and rinsing because these radioisotopes can be detected due to the long distance traveled by the strong β-particles and may interfere in the assay with high background. Availability of generic FlashPlates precoated with commonly used proteins such as streptavidin, protein A, antibody, and MBP and nickel chelate in assay ready format is an added advantage. Preparation of custom biomolecule bound to FlashPlate involves binding the biomolecule and several washings, which is labor intensive, and batch-to-batch variations may occur.

Cytostar-T™ Technology

Cytostar-T™ scintillating microplates (GE Life Sciences) are standard 96-well format, sterile, tissue culture–treated microplates. Cytostar-T plate is a polystyrene plate with a transparent base coated with scintillant. Upon addition of radioactive tracer to cells grown in the base of wells, the scintillant generates light when the tracer is bound to the cell membranes or taken up by the cell due to the close proximity of the radioactive isotope to the scintillant at the base of the plate and can be counted in a standard plate counter (14). The free radiolabel in the medium is physically too far from the scintillant to trigger a light reaction. Homogeneous cell-based assays have been performed in the Cytostar-T plate including receptor radioligand binding assays with intact cells, amino acid uptake into cells, DNA synthesis monitoring in cells in response to drug treatment and apoptosis measurements (15). Cytostar-T can be used for assays with live cells plated on the bottom of the well. Like with the FlashPlate assays, Cytostar-T assays can be used with weak β-emitters in homogeneous assay mode. When strong β-emitters or [^{125}I] are used, the plates need to be washed to remove unbound radioactivity.

SPA-based bead or FlashPlate assays can be grouped into three main formats (Fig. 4). (*i*) Signal removal: The radiolabeled substrate is linked to the streptavidin-SPA bead or plate via biotin and hydrolytic enzymes such as proteases, nucleases, phospholipases, and esterases, cleaves the radiolabel from the biotinylated substrate, resulting in a decrease in the signal. (*ii*) Signal addition: As in the case of synthetic enzymes such as transferases, kinases, and polymerases, the acceptor substrate is linked to the streptavidin SPA-bead or -plate through biotin, and the donor substrate is radiolabeled. Because of enzyme reaction, the radiolabel is transferred to the acceptor molecule on the bead from the donor, resulting in an increase in the signal. (*iii*) Product capture: In this assay format, the radiolabeled product of the reaction is captured by biospecific recognition to antibody as in the case of PTK. In the PTK assay, the phosphorylated product but not the substrate is captured specifically by anti-phosphotyrosine antibody that binds to protein A or secondary antibody coated on to the bead (4). SPA has also been used for quantification of PCR using biotinylated PCR primers and

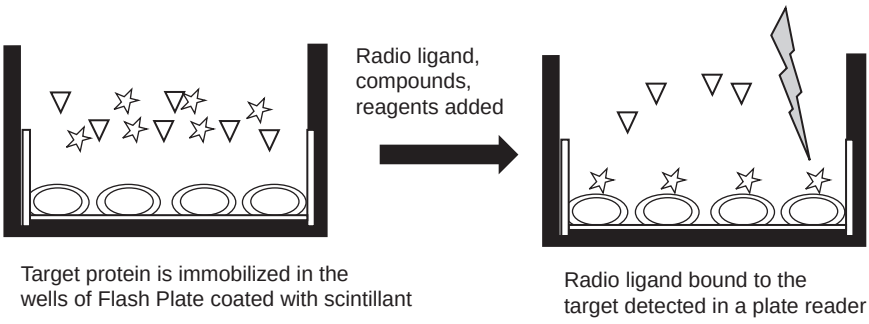

FIGURE 4 Schematic repesentation of FlashPlate technology. Receptor immobilized to 96- or 384-well FlashPlate is incubated with radioligand and compounds. Receptor bound radioligand is in close proximity with scintillant and is detected in a TopCount.

[^{3}H] dNTPs. The biotinylated [^{3}H] DNA produced is captured onto streptavidin-coated beads (4).

SPA is a very widely used homogeneous assay format for several different biological assays. The count time in scintillation counters for a 96- and 384-well plate is approximately 10 and 40 minutes, respectively, and this may restrict the throughput to some extent. SPA is applicable to HTS and can be adapted for automation. Assays are routinely performed in 96- and 384-well plates and for increased throughput in 1536-well plates. Assays in 384- and 1536-well plates using Imaging SPA beads or 384-well Imaging FlashPlates increase the throughput to 100,000 per day by reading in Imaging plate readers LeadSeeker or ViewLux, which images each plate within 10 minutes. The most commonly used radioisotopes in SPA are [^{3}H] and [^{125}I]. Recently, [^{33}P] is also being used in protein kinase assays. Although the path lengths of [^{35}S] and [^{14}C] are similar, because of the low specific activity [^{14}C]-labeled compounds (~60 mCi/mmol) have not been utilized as much in SPA. The signal-to-noise ratio in SPA is generally lower than the conventional filtration assays but may be adequate to use in HTS. Other critical issues associated with SPA are color quench and detection efficiency of scintillation counting.

ABSORBANCE ASSAYS

Absorbance assays based on photon absorption are commonly used, but they typically provide low sensitivity and are not adaptable to miniaturization and high throughput. Absorbance assays use chromogenic substrates. The sample is measured at a single wavelength, and the absorbance is dependent on extinction coefficient, path length, and concentration of the reagent (Beer–Lambert law). Absorbance-based assays can be miniaturized to suit HTS. These can be read as continuous kinetic mode or end point mode (provided convenient stopping reagent is available). Phosphate measurement based on malachite green method (A_{655} is measured) can be applied to ATPases, phosphatases (15). β-Lactamase assay uses nitrocefin, which is hydrolyzed to a product that can be detected at 490 nm. β-Glucorinadases or β-glucosidases use *p*-nitrophenyl glucuronide or *p*-nitrophenyl glucosides as substrates, respectively, and hydrolyze to yield *p*-nitrophenol that can be detected at 405 nm. Secreted alkaline phospahtase (SEAP) reporter assay can also be monitored with hydrolysis of *p*-nitrophenyl phosphate giving rise to *p*-nitrophenol that can be measured at 405 nm. Most of these colorimetric assays have been replaced with more sensitive, fluorogenic assays.

LUMINESCENCE

All processes that involve the emission of electromagnetic radiation are termed luminescence. Luminescence is general term that describes any process in which energy is emitted from a material at a different wavelength from that at which it is absorbed. Luminescence is due to the emission of light as a result of the excitation of atoms by energy other than heat, which is caused by chemical, biochemical, or crystallographic changes. Luminescence assays are based on photon emission, have greater sensitivity, broad adaptability to biological targets, and automation necessary for successful HTS.

Photon emission is achieved primarily through fluorescence and chemiluminescence (which includes bioluminescence). Although both processes create photons through energy transitions from excited states to their corresponding

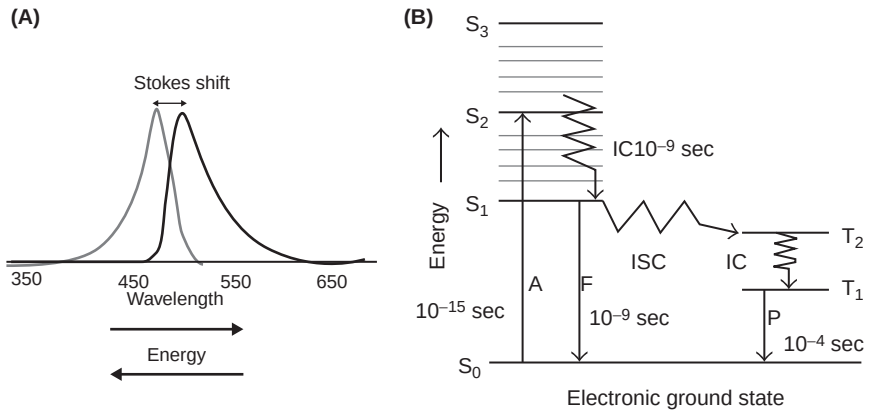

FIGURE 5 (**A**) Fluorescence spectrum. (**B**) Jablonski diagram. In the single state, electrons have an opposite spin orientation. In the triplet state, the electrons have the same orientation. Fluorescence is the observed radiation when an electron makes a transition from the excited state S_1 to the ground state S_0.

ground states, they differ in how the excited states are generated. In fluorescence, the energy needed for producing excited states is gained through the absorption of light, whereas in chemiluminescence, the energy results from exothermic chemical reactions.

A luminescence is a phenomenon in which electron de-excitation occurs almost spontaneously, and in which emission from a luminescent substance ceases when the exciting source is removed. In fluorescent materials, the excited state has the same spin as the ground state (Fig. 5). If A* denotes an excited state of a substance A, then fluorescence consists of the emission of a photon

$$A^* \rightarrow A + h\nu,$$

where h is Planck's constant and ν is the frequency of the photon.

The quantum yield of a fluorescent substance is defined by

$$\phi_{\text{quantum yield}} \equiv \frac{\#_{\text{photons re-emitted}}}{\#_{\text{photons absorbed}}}.$$

Bioluminescence

Bioluminescence Assays

Biolumenescence is chemilumenscence that occurs within an organism. Bioluminescent protease assays have been developed by using a peptide conjugated aminoluciferin as the proluminescent protease substrate and a stabilized firefly (*Photinus pyralis*) luciferase (Fig. 6) (16). High-throughput bioluminescence assays using either luciferase, ATP, or luciferin substrates as the limiting reagents for a luciferase-catalyzed reaction have been developed for ADME/Tox assays (17). Reporter gene assays limit the production of luciferase by tying it to a

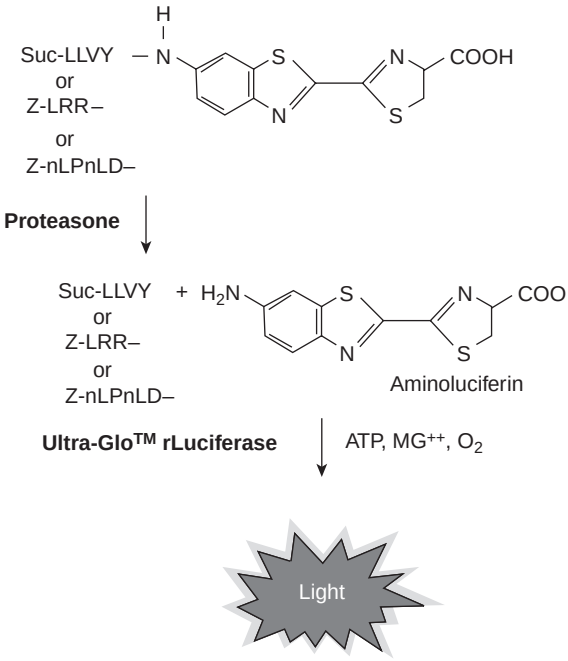

FIGURE 6 Scheme for the homogeneous bioluminescent, coupled enzyme protease assay in a single-step format. In this assay, the proluminescent protease substrate (conjugated aminoluciferin) is added along with stabilized luciferase in a single step. The protease cleaves the peptide from the peptide-conjugated aminoluciferin and luciferase, which immediately hydrolyzes the aminoluciferin in the coupled-enzyme.

promoter or DNA regulatory region of interest. Such assays can be used to study genes that are regulated by drugs and other xenobiotics. Bioluminescent assays in which ATP is the limiting reagent of the luciferase reaction can be designed to monitor cell viability or the activity of kinases. Bioluminescent assays in which the substrate is limiting can be designed so that the activity of a particular enzyme results in the production of a luciferin substrate that can, in turn, be acted upon by luciferase have been designed for proteases including caspase, P450 and MAO assays (18).

A Protease-Glo™ assay using a genetically engineered firefly luciferase (a circularly permuted firefly luciferase, the GloSensor™-10 F protein) with a protease recognition site as the protease substrate has been developed (19). Oligonucleotides encoding a protease recognition sequence are cloned into the GloSensor™-10 F gene located on a linearized vector. The GloSensor™ protein containing the protease site of interest is then synthesized in a cell-free protein expression system and subsequently used as a protease substrate. Cleavage of the protease recognition sequence leads to activation of the GloSensor™ protein and light emission, and the level of luminescence correlates to protease activity. Several ready kits for the luciferase bioluminescent kits are available from Promega.

Bioluminescent Reporter Assays

Bioluminescent reporters of genetic transcription provide rapid quantitative analysis of many cellular events that are important in drug discovery such as receptor function, signal transduction, gene expression, and protein–protein interaction. Firefly luciferase, a 62-KDa protein is the most widely used luminescent reporter enzyme for studying gene regulation and expression. As no endogenous luciferase activity is found in mammalian cells the background is very low. Bioluminescence is generated at 560 nm when luciferase converts the substrate luciferin to oxyluciferin in the presence of ATP and the half-life of the signal is few seconds. Developments in the luciferase assay increased the half-life from seconds (flash), to minutes (enhanced flash), and finally to hours (glow) (20). Homogeneous luciferase assays have been developed by adding reagent containing lysis buffer, enzyme stabilizer, and luciferin directly to the cells in culture media and measuring the chemiluminescence signal (21). Luciferase kits for homogeneous assays are available as Steady-Glo from Promega, LucScreen from Tropix, Luc Lite from PerkinElmer, and several others from other Manufacturers.

G_s-coupled GPCR can be monitored by using a cAMP response element (CRE) positioned upstream of a luciferase gene. Agonist activation of the receptor increases intracellular cAMP that activates protein kinase A to phosphorylate CRE binding protein. The phosphorylated CRE binding protein binds to the CRE sequence and increases the transcription rate of the luciferase gene and increases the concentration of luciferase (18). Calcium-regulated reporter assays are being developed by constructing transcription factors (NFAT, CREB) that become activated when there is a rapid rise in $[Ca^{2+}]_i$. The calcium-regulated promoter is fused to reporter gene luciferase, β-lactamase, or β-galactosidase. These transcription factors on activation bind to unique promoter and stimulate transcription of the reporter protein. CHO-K1 cells transfected with CCK1 receptor, a $G\alpha_q$-coupled GPCR along with NFAT-luciferase reporter gene, produced a dose–response signal curve with CCK-8, which was similar to that obtained using a fluorescent dye (22). For the nuclear receptor transactivation assays, the luciferase reporter is placed downstream of a promoter containing several repeats of a hormone response element. Binding of the nuclear receptor in the vicinity of the promoter activates luciferase gene expression (see also chap. 7 in this book).

Other Bioluminescence Reporters

Some other common reporter genes such as β-galactosidase (β-gal) and SEAP have been assayed traditionally with colorimetric reagents. The sensitivity of these reporter genes has been increased with the use of fluorescence substrates. The sensitivity of these enzymes has been remarkably enhanced (at least 3 orders) with chemiluminescent reporter gene assay reagents, galacto-star and galacto-light/plus for β-gal, and phospholight for SEAP from Tropix.

CLIPR System

The chemiluminescence imaging plate reader (CLIPR) is a product of Molecular Devices is an ultra–high-throughput luminometer system for 96-, 384-, 864-, and 1536-well microplates. The instrument can be used in HTS mode for cell-based assays and SPA-assays in microplates (23). CLIPR integrates a high-sensitivity CCD camera, telecentric lens, high-precision positioning mechanism, and computer system with software for instrument and record data. The CLIPR system

can be loaded manually or can have a plate stacker or can be integrated to linear robot line. The imaging plate reader system reads plates under a second and is possible to do kinetic studies.

Bioluminescence Resonance Energy Transfer (BRET) Assays

BRET has been used to study protein–protein interactions in living cells and in real time. BRET consists of coexpression of recombinantly fused proteins that link proteins of interest to a bioluminescent donor enzyme, a variant of Renilla luciferase (Rluc) or an acceptor flurophore, a green fluorescent protein (GFP) variant (24,25). Rluc and GFP upon coming into close proximity (10 nm), Rluc transfers energy (resulting from oxidation of its substrate coelenterazine) to the GFP variant producing BRET signal. When coelenterazine *h* is used as Rluc substrate, BRET signals can be detected up to 1 hour. When long-acting form of coelenterazine *h* called EnduRen is used, the signal lasts for several hours. With either Rluc substrates there is a substantial overlap in the donor and acceptor emission spectra. Another coelenterazine *h* analog called DeepBlueC produces emission at 400 nm when Rluc oxidizes and is separated from acceptor emission, and BRET signal is stable for several hours. In addition, the BRET signal was improved using novel forms of Rluc, namely, Rluc2 and Rluc8 when agonist (thyrotrophin releasing hormone) induced interaction between thyrotrophin releasing hormone receptor and β-arrestin 2 in HEK293 cells was measured (25).

Bioluminescent Calcium Flux (Aequorin Assays)

GPCRs represent a major group of potential therapeutical targets in drug discovery. For GPCRS coupling predominantly to G-proteins containing Gq-class Ga subunits, the functional activity is monitored by measuring intracellular calcium concentration $[Ca^{2+}]_i$. The intracellular $[Ca^{2+}]_i$ measurements have been mostly done with fluorescence-based assays. In recent years, luminescence-based assays are getting equally popular for HTS with the advances in imaging instrument technology. Intracellular $[Ca^{2+}]_i$ can be measured by using bioluminescent aequorin in a luminometer (22,26). Aequorin is produced in jellyfish *Aequorea Victoria*. It is a photoprotein composed of the apoaequorin protein bound to the prosthetic group coelenterazine and molecular oxygen. It has three EF-calcium binding sites and when calcium binds to these sites coelenterazine *h* is converted to coelenteramide, which results in the emission of blue light (470 nm). The signal in mammalian cells occurs within 30 seconds and the intensity of aequorin flash is proportional to Ca^{2+} concentration. The rank order of potency of m and d-opoid receptor selective analogs was similar in the bioluminescent aequorin calcium assay and the functional assay with isolated tissue preparations (guinea pig ileum and mouse vasdeferens, GPI/MVD) (27). The cell-based aequorin assay is extremly sensitive suggesting that the bioluminescent aequorin calcium assay therefore can differentiate the potency of opioid analogs much better than the GPI/MVD assay.

The aequorin signal, can be measured in LumiLux® (PerkinElmer), FDSS-6000 and -7000 (Hamamatsu Photonics), or CyBi™-Lumax (CyBio). Ca^{2+} measurement by aequorin assay, has been validated for many GPCRs and calcium channels, and the dose responses are similar to the values obtained with fluorescent dye methods. HEK293 cells stably expressing apoaequorin are co-transfected with serotinin receptors 5HT2a and 5HT2c, and when treated with

ligand 5HT dose-dependently stimulated the luminescence of aequorin. Comparison of aequorin luminescence-based calcium mobilization assay using various plate readers, the LumiLux® and FDSS-6000 plate readers or FDSS-6000 and CyBi™-Lumax (Fig. 7) by evaluating assay parameters including hit rate correlation, signal-to-noise ratio, and overall assay performance calculated by Z' and standard deviation suggested that they are comparable between different assay platforms (28).

Enzyme Fragmentation Complementation (EFC)

EFC is a homogeneous biochemical assay utilizing β-gal complementation technique. *Escherichia coli* β-gal is a tetramer with four identical subunits. Each monomer consists of 5 compact domains and 50 additional amino acids in the N-terminus, which are important for the activity. The deletion of the residues from N-terminus will result in inactive enzyme dimers serve as enzyme acceptors [EAs]. Supplementing the peptide containing missing residues deleted serve as enzyme donor [ED], the catalytic activity is restored. Individually, the EA and ED fragments are inactive (29–31). When they are combined, in the presence of ED, EA forms a tetrameric active enzyme by complementation.

$$2EA_2 + 4ED \rightarrow 2EA_2ED_2' \rightarrow 2EA_2ED_2 \rightarrow [EAED_2]_2$$

In EFC–analyte assay, analyte is conjugated to the ED fragment (which does not interfere with recognition of analyte by anti-analyte antibody) and the ED- analyte is capable of complementing with EA to form an active enzyme (29). Anti-analyte antibody used in the assay is optimally titrated so that the ED- analyte is fully complexed with the antibody and will not be able to associate with EA to form active enzyme (Fig. 8). Analyte in the cell lysate sample competes with ED-analyte in binding to the antianalyte antibody. The amount of free ED-analyte is proportional to the analyte in the sample. The free ED-analyte will complement with EA forming an active enzyme. Thus, analyte is measured as a function of the active tetrameric β-gal using luminescent substrate.

The PathHunter™ technology is an adaptation of EFC that provides a novel, generic cell-based assay format for detecting protein–protein interactions. The PathHunter system is a single addition homogeneous cell-based assay that utilizes EFC associated with a tagged protein. In this PathHunter assay approach, a small peptide from N-terminus of β-gal (β-gal ED, prolink) is expressed recombinantly on the intracellular C-terminus of the Receptor Tyrosine Kinase. One of the many different partner proteins containing SH2 domains (such as SHC1, SHC2, Grb2, PTPN6, PLCG1, or PLCG2) is co-expressed with complementary portion of β-gal (β-gal EA) (Fig. 9). Upon ligand binding to the receptor, ligand induces activation of the receptor, which causes either homo- or heterodimerization of the receptor resulting in cross-phosphorylation. The SH2-EA fusion protein then binds the phosphorylated receptor forcing complementation of the prolink and EA fragment, forming a functional β-gal enzyme that is capable of using chemiluminescentsubstrate producing luminescence signal (32).

Chemiluminescence

Chemiluminescence reaction produces molecule in electronically excited state.

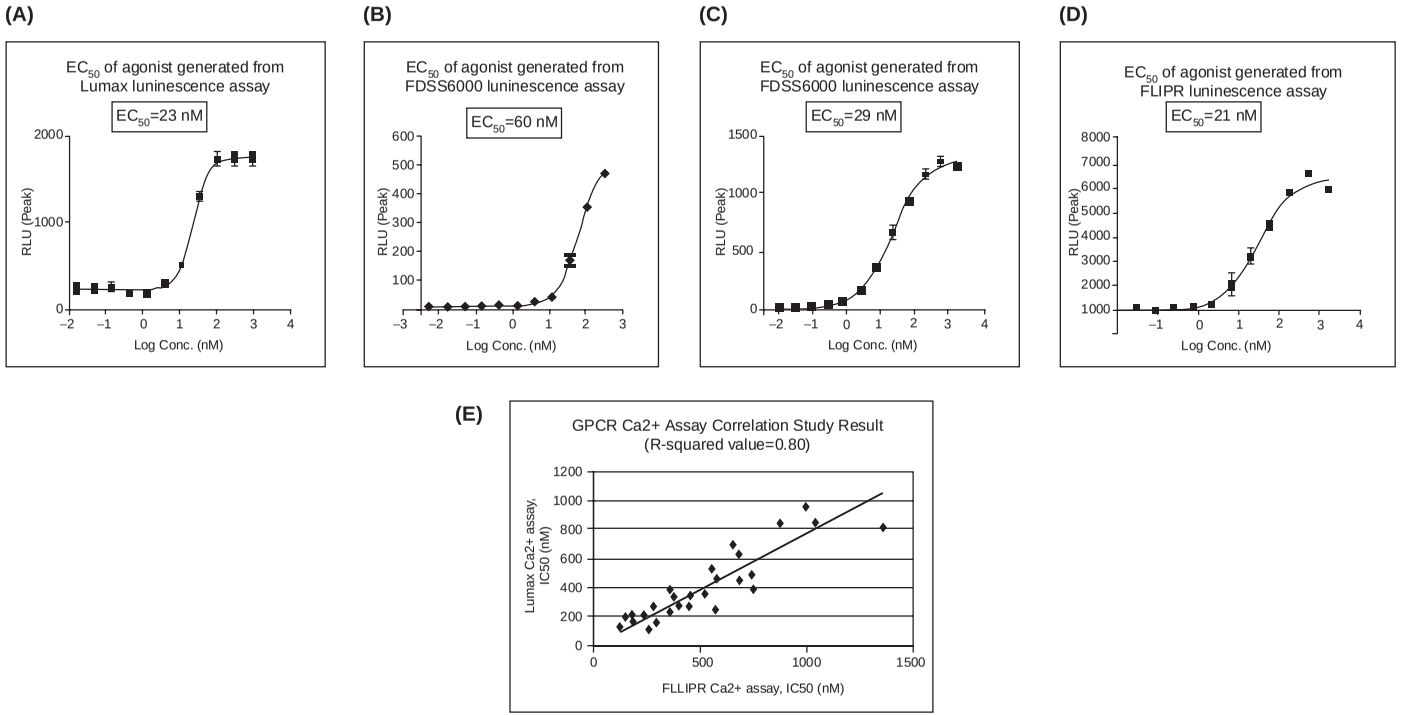

FIGURE 7 Agonist profiles in fluorescence and aequorin luminescence assays. HEK293 cell line expressing a recombinant GPCR was used to measure changes in intracellular calcium concentrations in the presence of agonist compound by luminescence assay with aequorin and another method using fluorescent dyes. The aequorin-based flash luminescence assay was performed (**A**) in the CyBi^{TM}-Lumax SD (CyBio) and (**B**) FDSS6000 (Hamamatsu Photonic Systems), and fluorescence assay was performed with fluorescence dye (**C**) FLUO 4AM in FLIPR (Molecular Devices) and (**D**) FDSS6000. The EC_{50} s determined in all the four calcium assays by flash luminescence or fluorescence dye (using FDSS6000, FLIPR, or Lumax) were comparable, which demonstrate consistency of EC_{50} values in various technology platforms. (**E**) The correlation of IC_{50} values of several antagonists between flash luminescence assay using Lumax and fluorescence dye assay using FLIPR showed that the IC_{50} values correlated reasonably well with a correlation coefficient 0.80. *Source*: Courtesy of Jing Chen and Mary Ellen Cvijic.

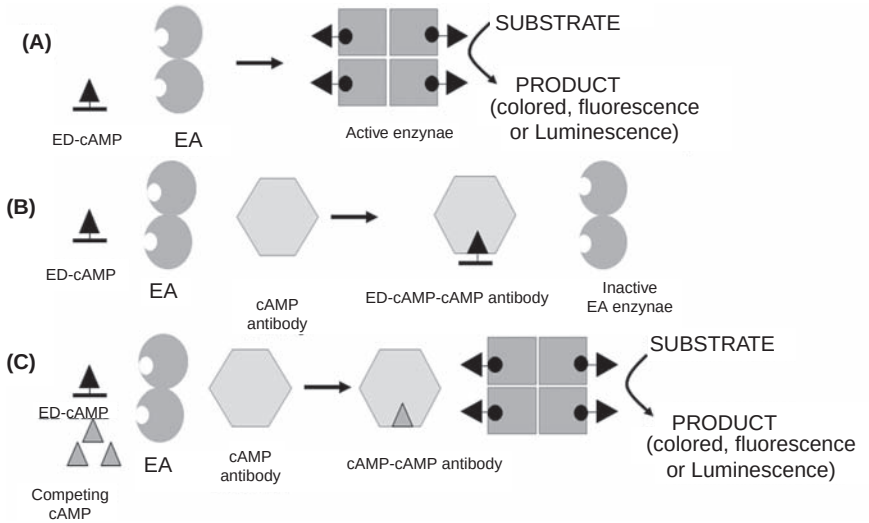

FIGURE 8 Schematic representation of the enzyme fragment complementation (EFC) cAMP assay. (**A**) β-Gal EFC. ED-cAMP complements with enzyme acceptor (EA) forming an active β-gal enzyme. The active tetrameric β-gal activity can be measured with luminescent or fluorescent substrates. (**B**) Inhibition of β-gal enzyme complementation by anti-cAMP antibody. Binding of ED-cAMP conjugate to the anti-cAMP antibody prevents from associating with EA and consequently inhibits formation of active β-gal. (**C**) Release of inhibition of β-gal enzyme complementation by cAMP in the sample. cAMP in the sample competes for binding sites on the anti-cAMP antibody and results in an increase in the free ED-cAMP, which complements with EA to form an active enzyme. β-Gal enzyme activity measured with luminescent or fluorescent substrate is directly proportional to the concentration of cAMP in the sample (30).

Electrochemiluminescence (ECL)

ECL assay utilizes stable ruthenium chelate (TAG), which, in the presence of tripropylamine, participates in a luminescent reaction that is triggered by the application of low voltage (33). In ECL, light is generated when low voltage is applied to an electrode, triggering a cyclical oxidation–reduction reactions of ruthenium metal ion (Ru^{2+}). The Ru^{2+} is bound in a chelate of *tris*-(bipyridine). Tripropylamine (TPA) present in molar excess is the second reaction component that is consumed in the oxidation process recycling the ruthenium chelate (Fig. 10). The tracer molecule, Ru-chelate is conjugated to antibody. Ru^{2+}-labeled component is captured on the surface of polystyrene magnetic beads and brought to the surface of an electrode by applying magnetic field through a movable magnet. TPA is introduced into the flow cell and a voltage is applied that oxidizes both ruthenium and TPA simultaneously (Fig. 10). TPA by losing a proton becomes a reducing agent and transfers electron to the ruthenium ion in an excited state and then decays to ground state releasing a photon in the process, which can be quantitated at 620 nm (33,34). The reduced Ru^{2+} is recycled, which along with TPA will intensify and amplify the ECL signal, and is read in ORIGEN® analyzer (BioVeris Corp, Gaithersburg, MD).

Ruthenium chelate conjugates TAG-NHS ester, TAG-amine, TAG-hydrazide, TAG-maleimide, and TAG-phosphoramidite, which are available

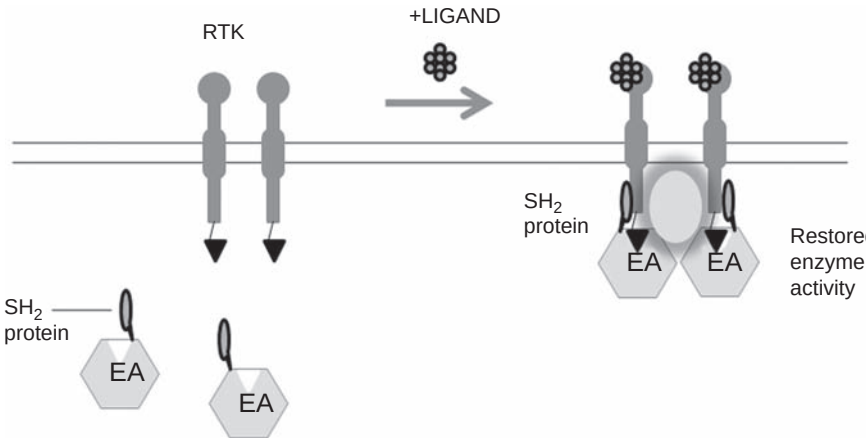

FIGURE 9 Schematic of PathHunter™ tyrosine kinase activity. The PathHunter™ technology is an adaptation of EFC in which a small peptide epitope (ED-β-gal or ProLink) is expressed recombinantly on the intracellular C-terminus of the receptor tyrosine kinase. SH_2 domains are co-expressed β-gal enzyme acceptor (EA-β-gal). Ligand-induced activation of the receptor causes either homo- or hetero-dimerization of the receptor, resulting in cross-phosphorylation. The SH_2–EA fusion protein then binds the phosphorylated receptor, forcing complementation of the Prolink (EA-β-gal) and EA fragment. This interaction generates an active β-galactosidase enzyme, which is detected by using a chemiluminescent substrate.

for convenient covalent linking to amine, carboxyl, carbohydrate, thiol, and oligonucleotide groups of biomolecules, respectively. ECL can be used for large and small molecule immunoassays such as hormones (35), second messengers, drugs (36); for enzyme–substrate interaction; for receptor–ligand interactions; for DNA–DNA, DNA–protein, and protein–protein interactions (37); for quantification of nucleic acids; and for PCR products (38). Screening can be performed using whole blood, culture medium, crude extracts, and membrane preparations. The ECL assays are easy to develop, have a wide dynamic range, and are very sensitive. ECL method utilizes nonisotopic small molecule label. In this assay, the sample passes through the flow cell and washed to remove free Ru^{2+}-labeled molecules resulting in a high signal-to-noise ratio. The ECL homogeneous assays can be adapted to HTS with 8-module instrument, which reads each plate in 10 minuntes. BioVeris is acquired by Roche Diagnostics.

ECL by Meso Scale Discovery (MSD®) technology (Gaithersburg, MD) platform enables sandwich immunoassays in microplates. MSD format enables multiplexed assays of several analytes, up to 4 in 384 plate and 10 in 96 plate can be measured in each well with carbon electrodes at the bottom of the each well. Each well of 96- and 384-microtiter plate can have 1 to 10 and 1 to 4 carbon electrode arrays per well, respectively. Ru-labeled antibodies are used in combination with the co-reactant tripropylamine added with the buffer. Upon application of current to the plate, electrochemical reaction occurs, which produces light signal 620 nm from Ru label bound to electrodes. The Ru counts from the Ru label bound at individual spots are measured with a charge-coupled device (CCD) camera without a wash step. MSD technology has been evaluated by measuring the changes in phosphorylation of AKT and glycogen synthase

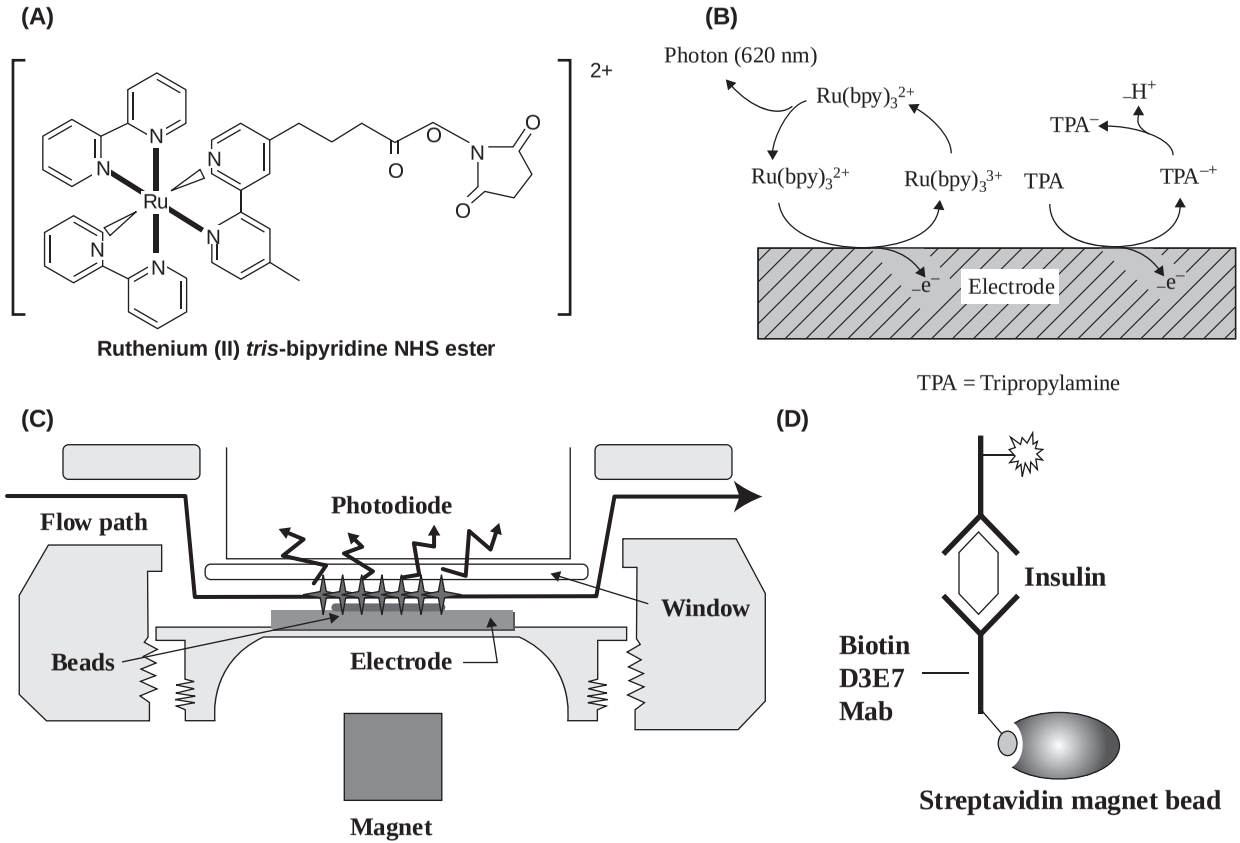

FIGURE 10 Electrochemiluminescence assay technology. (**A**) Structure of ruthenium (II)*tris*-(bipyridine) NHS ester. (**B**) Schematic representation of electrochemiluminescence reaction. (**C**) Schematic representation of ECL process. *Source*: Courtesy of BioVeris. (**D**) Schematic representation of an ECL insulin sandwich assay (36). *Source:* Courtesy of BioVeris.

kinase-3β in response to phosphoinositide 3-kinase in tumor cells as well as in human tumor xenografts (39). The applications of the MSD technology span from various biomarkers to cell signaling, cell and membrane binding assays, and metabolic assays (40).

Amplified Luminescent Proximity Homogeneous Assay (Alpha) Screen®

Alpha Screen™ is a bead-based nonradioactive proximity assay using two proprietary 200-nm–diameter latex donor and acceptor beads (41). When a biological interaction brings the beads into close proximity, a cascade of chemical reaction is induced that results in a greatly amplified signal. The beads are coated with hydrogel to prevent nonspecific interactions, self-aggregation, provide functionalized surface for covalent attachment and retain dyes. The donor beads contain a photosensitizer that absorbs light at 680 nm (laser excitation) and then converts ambient molecular oxygen to the excited singlet state that has a short lifetime of 4 μsec, allowing it to diffuse up to 200 nm in aqueous solution. When the acceptor bead is brought into close proximity (within 200 nm) by a molecular binding event, the singlet oxygen reacts with thioxene derivative of the acceptor beads generating chemilumenescence at 370 nm, which is immediately transferred to fluorescent acceptors in the same beads. The flurophores then emit light at 600 nm in high yield (Fig. 11). The half-life of the decay reaction is 0.3 second, allowing to operate in time-resolved mode. The singlet oxygen does not react with the unbound acceptor beads, they do not emit light.

As each donor bead contains high concentration of photosensitizers, each donor bead emits up to 60,000 singlet oxygen molecules per second that results in a very high amplification. The excitation at longer wavelength (680 nm) and emission at lower wavelength (500–600 nm) minimizes nonspecific excitation and reduces background. The beads are optimal size, too small to settle in aqueous buffers and large enough to be centrifuged. The effective distance between the donor and acceptor (R_0 value) is large ~200 nm, which overcomes the assay limitations of other FRET-based systems with weak interactions. Because of long life-time (0.3 second) of AlphaScreen fluorescence signal, measurements are made in time-resolved mode reducing the background. The AlphaQuest is a specific instrument for reading AlphaScreen signal and the signal *can also be* read in several multimode plate readers.

AlphaScreen technology has been applied to several different classes of assays including protein tyrosine kinases, serine-threonine kinases, proteases, helicases, receptor binding assays, protein–protein interactions, protein–DNA interactions, immunoassays for determining concentrations of small molecules, hormones, and cAMP functional assays for GPCRs (41).

AlphaScreen Surefire assays have been developed for rapid detection of full-length activated kinases in cell lysates even with difficult targets. AlphaScreen SureFire cellular kinase assays combines AlphaScreen® technology with TGR Biosciences' SureFire® cellular kinase assays provide an innovative solution for screening kinase activation in whole cells. The AlphaScreen Surefire assay utilizes AlphaScreen protein A–coated acceptor bead and streptavidin-coated donor bead. The phosphokinase is sandwiched between the two antibodies on the donor and acceptor bead and thus bringing the acceptor and donor beads to close proximity. Excitation at 680 nm results in the release of singlet oxygen from donor bead and transfers energy to thioxene derivative in the acceptor

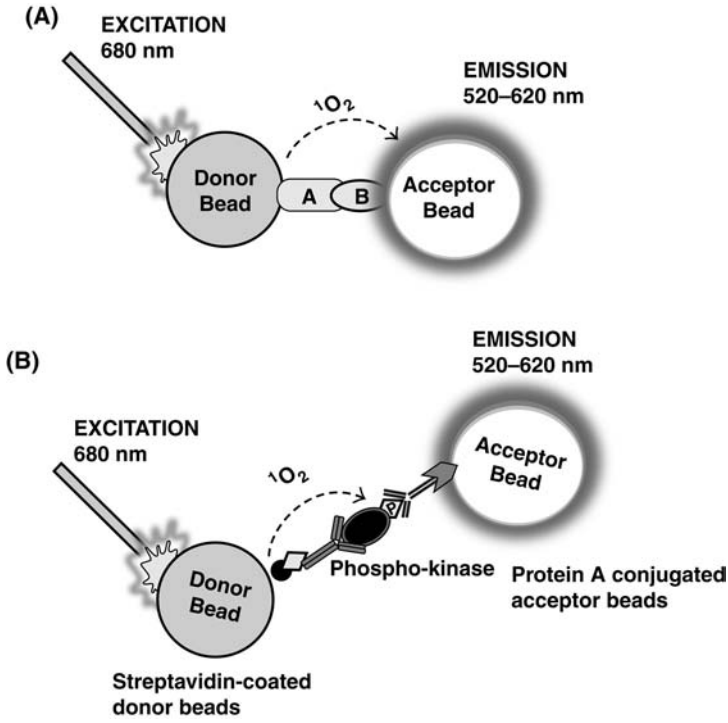

FIGURE 11 Principle of AlphaScreen assay. (**A**) Schematic of AlphaScreen assay. On laser excitation, the chemical signal (singlet oxygen $^1O_2$) generated by donor bead is amplified at the acceptor bead when it is brought into close proximity (200 nm) to the donor bead by specific biological interaction. (**B**) SureFire AlphaScreen assay. Ligand activation increases phosphrylation of kinase and the phosphorylated kinase binds to the phospho tyrosine antibody, which couples to the protein A acceptor bead. Upon excitation (at 680 nm) of streptavidin donor bead coupled with biotin tagged kinase antibody produces $^1O_2$, which is amplified at the protein A conjugated acceptor bead that is brought into close proximity (200 nm) to the donor bead by immuno sandwich of phosphorylated kinase between protein kinase antibody (on donor bead) and phosphotyrosine antibody (on protein A acceptor bead). The AlphaScreen signal is proportional to the activation (phosphorylation) of the protein kinase.

bead when they are in close proximity (<200 nm), resulting in emission of fluorescent signal at 520 to 620 nm (41,42).

AlphaElisa assay is modified AlphaScreen assay wherein streptavidin-coated donor bead and Eu-based acceptor bead whose emission is 605 to 625 nm are used. The analyte is sandwiched between the two antibodies on the donor and acceptor bead and thus bringing the acceptor and donor beads to close proximity (41). Excitation at 680 nm results in the release of singlet oxygen from donor bead and transfers energy to thioxene derivative in the acceptor bead when they are in close proximity (<200 nm), resulting in emission of fluorescent signal at 620 nm. The emission spectrum of AlphaElisa acceptor bead is narrower (600–625 nm) and thus gives stronger signal compared to AlphaScreen acceptor bead emission, which is very broad (520–620 nm) and less prone to matrix interferences (hemoglobin).

Fluorescence Assays

Fluorescent molecules (fluorophores) generally posses delocalized electrons, which are present in conjugated double bonds. An exception to this is with the lanthanides, Europium and Terbium. A photon of energy supplied by lamp or laser is absorbed by fluorophore, creating an excited electronic state (S1*). Energy of S1* is dissipated yielding a relaxed singlet excited state S1 from which emission originates. A photon of energy is emitted returning to its ground state. Stokes Shift is the energy difference between the lowest energy peak of absorbance and the highest energy of emission. Generally, the emission spectrum appears to be a mirror image of the absorption spectrum.

The flurophores are either intrinsic or extrinsic fluorophores. Several biological molecules contain naturally occurring flurophores (intrinsic fluorophores). Tryptophan is the most highly fluorescent amino acid in proteins and contributes more than 90% of fluorescence of a protein. Proteins absorb at 280 nm and the emission maximum ranges between 320 and 350 nm. Although tyrosine is fluorescent in solution, its emission in a protein is weaker. Nucleotides and nucleic acids are not fluorescent except yeast t-RNA^{phe}, which contains a highly fluorescent Y base. NADH is highly fluorescent, with absorption and emission maxima at 340 and 450 nm, respectively, but NAD^+ is nonfluorescent. The quantum yield of NADH increases 4-fold when bound to a protein. FMN and FAD are fluorescent with absorption and emission maxima at 450 nm and riboflavin at 515 nm (43).

When the intrinsic fluorescence of a macromolecule is not adequate, external flurophores are conjugated to them to improve spectral properties. In most of the biological assays, extrinsic fluorophores conjugated with biomolecules have been used. Fluorescein, rhodamine, Texas Red, and BODIPY dyes have been widely used for labeling proteins and nucleic acids. These fluorescent dyes have longer wavelengths of excitation and emission that minimize the background fluorescence of biological samples. 1-Anilino-8-naphthalenesulfonic acid (1,8-ANS), *bis*-anilino-8-naphthalenesulfonic acid (bis-ANS), and 2-*p*-toluidinyl-naphthalene-6-sulfonic acid (2,6-TNS) are nonfluorescent in water, but highly fluorescent in nonpolar solvents and when bound to proteins at hydrophobic pockets. Lipids in the membranes can be labeled with 9-vinyl anthracene, 1,6-diphenylhexatriene, or perylene. The probes are insoluble in water and partition into the lipid layer of membranes (43).

Although assay miniaturization increases throughput, it is important to use assay technologies that enable precise identification and quantification of the analytes with higher sensitivity. Recent advancements in the following fluorescence techniques: fluorescence intensity assays, fluorescence polarization, fluorescence resonance energy transfer, TRF, DELFIA, HTRF, TR-FRET or Lance, fluorescence correlation spectroscopy, fluorescence reporter assays (green fluorescent protein, β-lactamase), and fluorescence imaging (FLIPR, fluorescence confocal imaging, high content screening) will be discussed in this chapter.

Fluorescence Intensity Screens

The read-out of these assays is either increase or decrease in the fluorescence intensity. Fluorogenic assays and fluorescence quench relaxation assays are manifested in increase of fluorescence intensity whereas fluorescence quench assays show decrease (44).

Fluorogenic Assays

The reactants of the assay such as methylumbelliferyl derivatives, ANS (1-anilin-onaphthalene-8-sulfonic acid), bisANS (*bis*-1-anilinonaphthalene-8-sulfonic acid), nucleic acid specific dyes are not fluorescent, but the products generated are fluorescent and measured as an increase in fluorescence intensity. ANS in aqueous solution is nonflorescent. It becomes fluorescent when bound to membranes or proteins. 1,8-ANS and bis-ANS bind to nonpolar cavities (hydrophobic pockets) in proteins. ANS binding to GST-PPARγ-LBD results in an increase in fluorescence, which is dependent on ANS and PPARγ-LBD concentration (see Fig. 6 in chap. 7 in this book). This fluorescence signal of ANS-PPARγ binding is competed by PPAR ligands. In the human β-glucuronidase assay the fluorogenic substrate, 4-methylumbelliferyl-D-glucuronide (MUG) is hydrolyzed to fluorescent 4-methyl umbelliferone (4-MeU). The product 4-MeU is fluorescent only when the hydroxyl group is ionized (pK_a of this hydroxyl group is 8–9) and maximal fluorescence is obtained at pH >10. The enzyme activity is proportional to fluorescence signal and is measured in a fluorescence plate reader with excitation and emission λ of 355 and 465 nm, respectively (45,46).

Dyes (nonfluorescent or low intrinsic fluorescence) that specifically interact with double strand DNA (*ds*DNA), single strand DNA (*ss*DNA), or RNA and upon binding to the nucleic acids, exhibit several fold fluorescence enhancement and quantum yield increases. PicoGreen interacts with *ds*DNA and produces fluorescence signal, while *ss*DNA and RNA in the sample do not contribute to this fluorescence signal. PicoGreen is used for detection of picogram level of *ds*DNA in solution (47). OliGreen specifically binds to *ss*DNA and oligonucleotides and produces a fluorescence signal. RiboGreen binds specifically to RNA and has been used for quantitation of RNA in solution (48). Nuclease or polymerase assays using the specific nucleic acid binding dyes can be developed. PicoGreen binds to DNA in the intact DNA–RNA duplex, resulting in fluorescence signal. RNase H hydrolyzes the substrate poly r(A)-d$(T)_{12-18}$. As the RNA strand is hydrolyzed with the enzyme action, the double strand hybrid is depleted resulting in a decrease in the dye bound to the substrate. Thus, with the RNase H activity the fluorescence intensity is decreased. In a DNA polymerase assay, the *ds*DNA synthesized in the enzyme reaction binds the dye and increases the fluorescence signal, whereas the *ss*DNA substrate does not bind.

Fluorescence Quench Relaxation

In a fluorescence quench release assay, a fluorescent molecule when constrained by covalent modification of the reactive groups (substrate) the fluorescence is quenched. In the enzyme reaction, the covalent bond of the substrate is cleaved, releasing the free fluorescent dye, which increases the fluorescence intensity due to relaxation of quenching (46). Rhodamine 110 exhibits spectral properties similar to fluorescein with excitation and emission λ of 496 and 520 nm, respectively. Several fluorescent dyes have been used to measure activity in solution and living cells (47). The fluorescence of bisamide derivatives of rhodamine 110 (peptides covalently linked to the both amino groups of rhodamine thereby suppressing its absorption and fluorescence) that are used as specific substrates for protease is quenched (47). The nonfluorescent bisamide R-110 substrate is cleaved by protease to give fluorescent monoamide and further cleavage yields

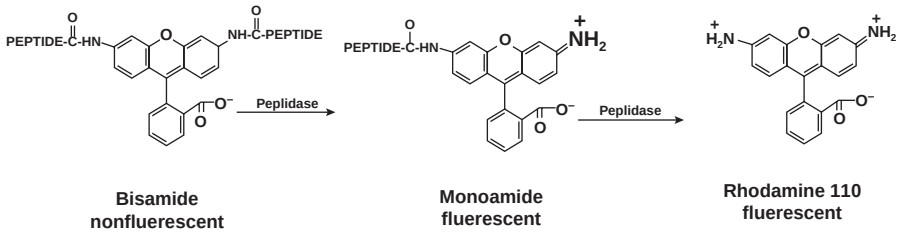

FIGURE 12 Fluorogenic peptidase assay. In this peptidase assay, the substrate, a nonfluorescent bisamide of rhodamine 110, was cleaved to the fluorescent monoamide and then to the highly fluorescent free rhodamine 110.

highly fluorescent R-110 (Fig. 12). The fluorescence intensity of the monoamide derivative and R-110 is constant between pH 3–9.

Fluorescence Quenching

IQ™ Technology (Pierce Rockford, IL) is a homogeneous assay platform based on fluorescence intensity quenching for direct measurement of the phosphorylation of the substrate. The assay incorporates an iron-containing compound that binds specifically to phosphate groups present on fluorescent dye-labeled phosphorylated peptides. The iron-containing compound upon binding to the phosphate group is brought into proximity to the flurophore and acts as a dark quencher of the fluorescent dye. A rhodamine derivative dye with excitation and emission λ of 569 and 592 nm, respectively, is used for labeling peptides. IQ™ Technology has been successfully applied for protein kinase and phosphatase assays. In the kinase or phosphatase enzyme reaction, the assay is terminated with the addition of IQ™ reagent working solution that stops the enzymatic reaction, and the fluorescence intensity is measured in a plate reader (49).

Several multimode plate readers from different manufacturers that can read fluorescence of 96-, 384-, and 1536-well microtiter plates with stackers are available (Table 3). The fluorescence assay can be fully automated in a robotic system, with liquid handlers, stackers, incubators, and a plate reader and the throughput can be increased to >100 K assay points per day.

Fluorescence Polarization (FP)

FP is a homogeneous technique in which FP signal is proportional to the molecular size of the fluorescent molecule in defined conditions. In 1926, Perrin first described the utility of FP to study the molecular interactions in solution (50). FP instrumentation was developed by Weber (51) and adapted to homogeneous assays by Dandliker et al. (52). FP is a powerful technology for the determination of molecular interactions in solution (51–61). For a detailed theory of polarization, see Ref. (46). When fluorescent molecules in solution are excited with polarized light, the degree to which the emitted light retains polarization reflects the rotation that the flurophore underwent during the interval between absorbance and subsequent emission. If the flurophore is small, it rotates or tumbles faster and the resulting emitted light is random with respect to the plane of polarization (depolarized) and will have lower FP value (Fig. 13). If the flurophore is large, it remains relatively stationary and the emitted light will remain polarized

TABLE 3 Different Plate Readers from Various Manufacturers

Plate reader	Plate reader
Acumen Explorer (TTP Lab Tech)	Insight (Evotec Technologies)
MF20/10S (Evotec Technologies)	IsoCyte (PerkinElmer)
Acquest™ (Molecular Devices)	Ion Works (Molecular Devices)
Analyst™ (Molecular Devices)	KineticScan (Cellomics)
Array Scan (Cellomics)	LEADseeker (GE HEalthcare)
Atto Pathway (Becton Dickinson)	LumiLux® (PerkinElmer)
CLIPR (Molecular Devices)	LUMIstar (BMG)
CyBi™-Lumax 1536 S(CyBio AG	NOVOstar (BMG)
Discovery 1 (Molecular Devices)	Opera (Evotec Technologies)
EIDAQ (Beckman Coulter)	Plate Screen (Carl Zeiss Jena)
EnspireTM	POLARstar (BMG)
Envision (PerkinElmer)	Q3DM (Beckman Coulter)
Explorer HTS (Acumen Biosciences)	RUBYstar (BMG)
FACS machine/ Flow cytometer	Safire (Tecan)
FDSS-6000 (Hamamatsu)	Spectromax L (Molecular Devices)
FDSS-7000 (Hamamatsu	Spectromax Gemni (Molecular Devices)
FLIP R^{TETRA} (Molecular Devices)	Spectromax Plus (Molecular Devices)
FLIPR^{384} (Molecular Devices)	Sector Imager 2400 and 6000 (Meso Scale Discovery)
FMAT 8100 (Applied Biosystems)	Top Count™ (PerkinElmer)
Fusion™ (PerkinElmer)	TriLux/Micro Beta (PerkinElmer)
ImageTrakTM (PerkinElmer)	Ultra Evolution (Tecan)
ImageXpress (PerkinElmer)	Ultra VIEW (PerkinElmer)
IN Cell analyzer 3000 (GE Healthcare)	Victor (PerkinElmer) X
IN Cell analyzer1000 (GE Healthcare)	Viewlux™ CCD Imager (PerkinElmer)

This list of plate readers is not a complete list available in the market. There may be several others that are not familiar to the author.

and will have higher FP signal (55,56). Theoretically, the minimum FP possible is "0" and the maximum is 500 mP for fluorescein. However, the real experimental minimum observed is 40 to 80 mP for small molecules and the experimental maximum for large molecules is 100 to 300 mP (56–59). This window of FP signal between the minimum and maximum is sufficient because the ratiometric FP signal is highly reproducible. Unlike other assays where the robustness of assay depends on the magnitude of signal-to-noise ratio, in FP assay ΔP (highest signal-lowest signal) is important. A ΔP of 100 mP in a FP assay is considered a good assay and $\geq$150 mP is considered a robust assay (58,59).

FP is a homogeneous technology consisting of simple mix reagents and read format. FP can be easily automated. The reactions are very rapid, reaching equilibrium very quickly. Fluorescein is the most common fluorescent derivatization reagents for covalent labeling. Fluorescein is a well-studied molecule that has high absorbtivity, excellent fluorescence quantum yield, good water solubility, and its maximum excitation closely matches the 488 nm spectral line of the argon-ion laser. A number of other fluorophore (BODIPY®, Texas Red™, Oregon Green®, Rhodamine Red™, Rhodamine Green™ etc.) derivatives are commercially available with various chemistries for making fluorescent bioconjugates (47). To reduce FP interference from compounds with autofluorescence, fluorescent dyes that absorb in the red region (higher wave length) have been used (62,63).

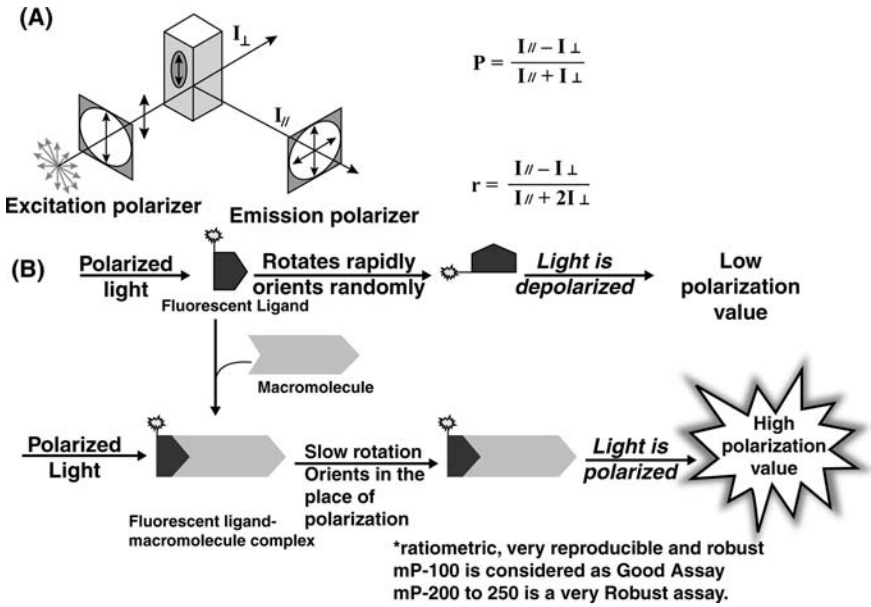

FIGURE 13 Principle of fluorescence polarization. Panel (**A**): Schematic illustration of fluorescence polarization. When fluorescent molecules are excited with polarize light, they can emit radiation in the same plane as polarized light. The degree to which they emit radiation in the same plane is dependent on the mobility of the fluorescent molecule. Panel (**B**): A small fluorescent molecule in solution rotates rapidly and orients randomly, the emitted light is depolarized and the polarization value is low. When a small fluorescent molecule binds to a macromolecule, the resulting fluorescent complex rotates slowly in solution, orients in the plane of polarization, and the emitted light is polarized giving high polarization value.

FP assays can be grouped into three different groups. In the first group there is an increase in size due to binding of a small molecule (containing fluorophore) to a macromolecule forming a larger fluorophore adduct, which gains polarization signal, for example, protein–DNA, antigen–antibody, DNA–DNA, DNA–RNA, protein–protein interactions, and receptor–ligand binding (46). In the second group relatively larger fluorescent molecules (fluorophore containing macromolecules) are cleaved to smaller fluorescent molecules, which incur loss of polarization signal, for example, nuclease, helicase, and protease assays (46). The third group represents facilitated (indirect) assays in which the fluorescent reactant molecule is coupled to antibody with acquisition or loss of FP signal: protein tyrosine kinases (PTKs), protein tyrosine phosphatases (PTPs). FP has been extensively used in the last decade in clinical laboratories in competitive immunoassays for the detection of drugs and hormones (46). FP assays representative of each of these groups are discussed below.

Size Increase

A fluorescent small molecule when binds to a protein increases the molecular size of the fluorescent containing molecule, resulting in a high FP value. Majority of HTS targets are receptors such as G-protein–coupled receptors (GPCRs) and

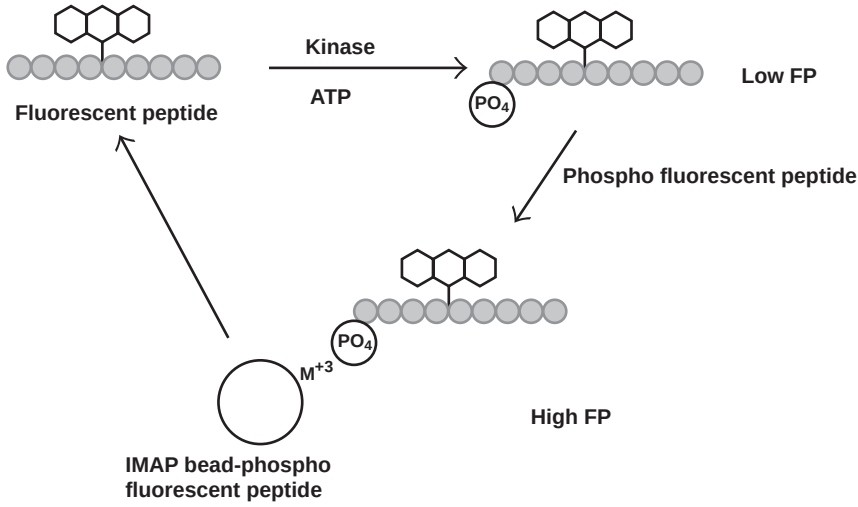

FIGURE 14 Schematic representation of IMAP FP technology. The IMAP technology is based on the high affinity binding of phosphate by immobilized metal (M^{III}) coordination complex. When fluorescent peptide kinase substrate is phosphorylated by kinase, the product, phosphorylated fluorescent peptide, binds to the immobilized metal (M^{III}) and increases the FP signal.

nuclear receptors. For successful application of FP method, a membrane receptor has to be expressed in a high copy number (~100000) in each cell (64). Theoretical and graphical methods to select optimal concentrations of ligand and receptor for development of FP binding assay have been detailed (65). FP assays have also been successfully used for nuclear receptor binding (66). A unique FP ligand binding assay for peroxisome proliferator activated receptor (PPAR) alpha and gamma using a PPARα/γ dual activator has been described (59). The FP-nuclear receptor and GPCR assays are discussed in a greater detail elsewhere in this volume (chaps. 6 and 7 in this book).

Size Reduction

The FP signal of the relatively large fluorescent substrate is high and when cleaved by protease action produces smaller labeled fragments that have low FP signal. To assay various proteolytic enzymes by FP, BODIPY-α-casein was used (67). A peptide substrate derivatized by biotinylation of a γ-aminobutyric acid modified amino terminus and labeled with 5-(4,6-dichlorotriazinyl) aminofluorescein at the carboxy terminus was used for cytomegalovirus protease (68). The substrate binds to avidin and thereby has higher FP signal. Enzyme action cleaves the substrate generating a fluorescein containing peptide separated from biotin that will not be able to interact with avidin resulting in the loss of FP signal. RNaseH hydrolizes RNA strand of RNA–DNA hybrid. fl-RNA–DNA-biotin hybrid substrate upon binding to avidin, increased FP signal from 105 to 350 mP (46). The ΔP of 245 mP is a robust signal for a FP assay. With the enzyme action the fl-RNA of the RNA–DNA hybrid is hydrolyzed, consequently there is a decrease in the fl-RNA, that couples to the avidin bound biotin-DNA strand

and hence the FP signal will decrease with increasing enzyme activity in this assay (46).

Facilitated Assays

Seethala and Menzel have developed the first robust FP-PTK assay (56–58). In the direct FP-PTK assay, the phosphorylated fluorescein-peptide (fl-phos-peptide) product formed in the reaction is measured by immunocomplexing with the anti-phosphotyrosine antibody (PY antibody), which results in an increase in the FP signal. The direct FP-PTK assay can only be used with a peptide substrate and requires large amounts of anti-phosphotyrosine antibody. To overcome these problems, FP-PTK competition immunoassay was developed (57,58). In this assay, phosphorylated peptide or protein produced by kinase reaction competes with the fluorescent phosphopeptide tracer for PY antibody. In this format, kinase activity results in a loss of the FP signal.

FP is a simple and reasonably predictive technology and can be used for a variety of different assays. FP is a robust homogeneous assay that can be applied to higher density 384- and 1536-plates. Only one component of the assay is required to be labeled with a fluorophore and is suitable for small ligands (<10 kDa). FP is insensitive to inner-filter effects. Because FP signal is a ratiometric measurement, it is less susceptible to quenching from colored compounds. However, autofluorescence compounds can interfere with FP assay. Some times, propellar effects on the fluorescent tag may restrict use of the FP assay.

Immobilized Metal Ion Affinity-Based Fluorescence Polarization (IMAP) Technology

IMAP technology (Molecular Devices) uses the specific binding of IMAP nanoparticles derivatized with trivalent metal ions to phosphate groups of fluorescent peptides and FP readout. IMAP trivalent nanoparticles are added to kinase reaction wherein the IMAP particles bind to the phosphorylated fluorescent peptides. The binding causes change in the motion of the peptide and results in an increase in the observed FP (Fig. 14). IMAP technology is independent of the sequence of the substrate peptides unlike the other kinase assays. The IMAP technology is also applicable to phosphatases and phosphodiesterases (69,70).

Fluorescence Resonance Energy Transfer (FRET) Assays

FRET is a phenomenon wherein excitation energy is transferred from a donor molecule to an acceptor molecule without emission of photon. FRET has been used for measuring the distances between interacting molecules under physiological conditions with near angstrom resolution (46,71–73). For FRET to occur, donor and acceptor molecules have to be in close proximity (10–100 Å), excitation of the acceptor must overlap with the emission of donor, and donor and acceptor transition dipole orientations must be parallel. The rate at which the energy is transferred from donor to acceptor is governed by the Förster equation (46).

In most cases, the donor and acceptor dyes are different and FRET can be detected as the quenching of donor fluorescence by the acceptor or appearance of the sensitized fluorescence of the acceptor. Typical Förster radius R_0 for donor–acceptor pair of fluorescein/tetra-methylrhodamine is 55 Å, 5-(2-aminoethylamino) naphthalene-1-sulfonic acid (EDANS) and 4-(4-dimethylamino-phenylazo)-benzoic acid (DABCYL) is about 33 Å and

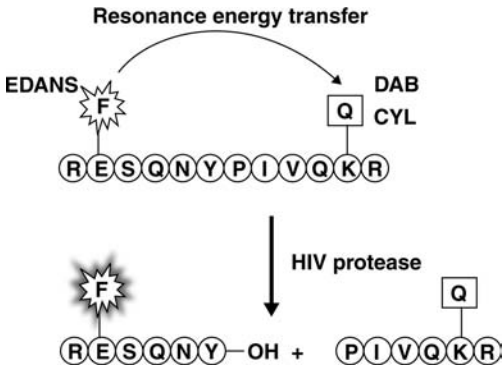

FIGURE 15 Schematic representation of FRET quench relaxation assay. In a peptide containing N-terminus EDANS and C-terminus DABCYL, the fluorescence of EDNAS is quenched by the acceptor DABCYL. Cleavage of this internally quenched fluorogenic substrate leads to an enormous increase in fluorescence intensity as the donor is separated from the acceptor. The fluorescence intensity is proportional to the hydrolysis of the substrate. Thus, the protease activity can be monitored by measuring the fluorescence intensity.

5-(2-iodo-acetyl aminoethylamino) naphthalene-1-sulfonic acid (IAEDANS) and fluorescein is 46 Å. FRET applications include quench and quench relaxation assays (46).

Protease Assay

In a FRET quench relaxation protease assay, peptide containing N-terminus EDANS and C-terminus DABCYL, the fluorescence of EDNAS is quenched by the acceptor DABCYL. Cleavage of this internally quenched fluorogenic substrate leads to an enormous increase in fluorescence intensity as the donor is separated from the acceptor (Fig. 15). The fluorescence intensity is proportional to the hydrolysis of the substrate. Thus, the protease activity can be monitored by the fluorescence intensity. Several protease assays (i.e., trypsin, HIV-1 protease, renin, hepatitis C virus protease, human cytomegalovirus protease) using FRET have been described (46).

HTRF™/LANCE™ (TR-FRET) Assays

Time-resolved fluorescence (TRF) is based on the long lifetime properties of lanthanides, europium (Eu), samrium (Sm), terbium (Tb), and dysprosium (Dy). Homogeneous time-resolved fluorescence (HTRF) as the name implies is a homogeneous assay method that uses fluorescence resonance energy transfer from europium kryptate (EuK) donor to an acceptor flurophore provided they are at a distance of less than 10 nm from one another and that the emission energy of donor overlaps with the excitation of the acceptor. HTRF™ technology is a trademark of Cis Bio International (Cedex, France) and this phenomenon is variously termed as time-resolved fluorescence resonance energy transfer (TR-FRET), Lance™ (Lanthanide Chelate Excitation) (PerkinElmer, Shelton, CT), or LanthaScreen (InVitrogen, Carlsbad, CA). For energy transfer, the donor and acceptor have to be brought into close proximity. The fluorescence lifetime of most of the fluorescent compounds is very short (typically few nanoseconds). The interference from assay components, microtiter plates, light scatter,

biological samples, and compounds are short-lived fluorescence (prompt fluorescence). To avoid interference from background fluorescence (compound and prompt fluorescence), lanthanide chelates with long life-times of 100 to 1000 μs (no polarization) are used as fluorescence energy donors. The common acceptor fluorophores used are modified allophycocyanine, a phycobiliprotein from red algae (XL665), Cy 5, fluorescein, or tetramethyl-rhodamine. The long-lived fluorescence of lanthanide due to Förster dipole–dipole energy transfer to the acceptor results in a long-lived fluorescence of the acceptor. The energy transfer emission has a decay time directly proportional to donor decay time and inversely to the distance between acceptor and donor. Time resolution in HTRF/Lance reduces scattering and prompt decay background interference from short-lived fluorescence due to delay in time of measurements of fluorescence.

The rare-earth elements, Eu^{+3}, Su^{3+}, Tb^{3+}, and Dy^{3+} are poor fluorophores by themselves, and to measure the lanthanide fluorescence, the lanthanides have to be complexed. Europium fluorescence is protected from decay by conversion to macropolycyclic compound, europium cryptate [Eu]K to enhance their fluorescence and cryptate to protect from fluorescence quenching (74–76). [Eu]K has convenient linker arms to covalently complex with peptides, proteins, nucleic acids, and other reagents. Also, selected generic reagents streptavidin, biotin, WGA, ConA, protein A, anti-DNP antibody labeled with XL665, and biotin, streptavidin, antiphospotyrosine antibody labeled with [Eu]K are available from CisBio. Chelates of Eu^{3+} and Tb^{3+} are available from CisBio that are used in Lance technology (74,77) and LanthaScreen uses Tb^{3+} chelates. The fluorescence resonance energy is transferred from Eu chelates emitting maximally at 613 nm to longer wavelength acceptor molecules such as allophycocyanins XL665 or Cy5 and from Tb chelates emitting at 492 and 545 nm to a variety of acceptors such as tetramethylrhodamine, xanthine dyes, GFP, or fluorescein (74,77). Some of the generic reagents available include Eu^{3+}- and Tb^{3+}-labeled antihuman, rabbit or mouse IgG, anti GST or anti-PY antibody, protein G and streptavidin, and APC-labeled streptavidin.

Essentially three types of labeling of macromolecules (direct, indirect, and semi-direct) can be performed with HTRF/Lance assays similar to labeling for FP (46). In direct labeling, the donor, lanthanide chelate, and the acceptor, allophycocyanin, rhodamine, or fluorescein, are directly labeled on molecule(s) involved in the reaction. In indirect labeling, the donor and acceptor flurophores are labeled to macromolecules involved in the secondary interactions such as antibody–secondary antibody binding, biotin–streptavidin interaction (Fig. 16). Semi-direct labeling is a combination of the direct and indirect labeling. HTRF/Lance assays have been successfully developed for reactions involving macromolecular interactions such as DNA–DNA, RNA–DNA, DNA–protein, protein–protein, receptor–ligand, for reactions involving hydrolysis of macromolecules such as nucleases or proteases, for reactions involving synthesis of macromolecules such as polymerases, and for other protein modification reactions such as kinases (74–78).

The applications for HTRF/TR-FRET technology have been rapidly growing. The applications include competitive immunoassays to measure hormones like prolactin, βhCG, tumor necrosis factor (79), receptor–ligand binding interactions: TNF receptor 1 (79), IL-2 receptor α (80), EGF–EGF, protein–protein interactions, for example, *jun-fos* heterodimerization (76), DNA-hybridization,

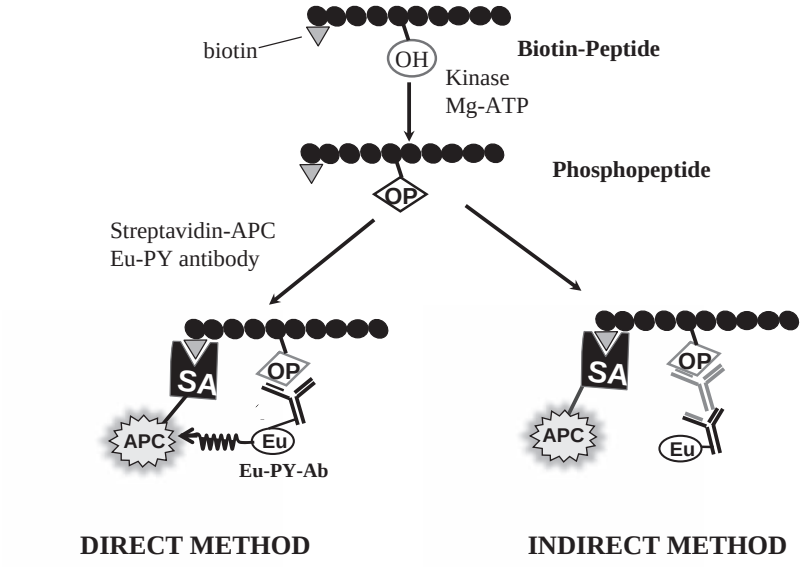

FIGURE 16 Schematic representation of TR-FRET protein tyrosine kinase assays. In direct assay, phosphorylated biotinyl-peptide is conjugated to Eu^{3+}-PY antibody and energy is transferred to APC-streptavidin bound to the phosphorylated biotinyl peptide. In the indirect assay, Eu^{3+}-protein A or Eu^{3+}-secondary antibody binds to the PY antibody conjugated to the phosphorylated biotinyl peptide and transfers energy to APC-streptavidin bound to the phosphorylated biotinyl peptide. *Source*: Courtesy of PerkinElmer.

enzymes helicase (46), carboxypeptidas (81), telomerase (82), 11β hydroxysteroid dehydro-genase (83), and GPCR functional assays for cAMP and inositol I phosphate assays (84,85).

HTRF/TR-FRET assays are homogeneous assays wherein interaction of two labeled binding partners is detected by the energy transfer from an excited donor to an acceptor dye and measurement of the emission signal from the acceptor dye. With appropriate delay time the background interference from scattering, compound and prompt fluorescence can be minimized and the emission of acceptor excited during excitation of donor can be eliminated and the pure energy transfer signal from acceptor can be measured. Energy transfer from lanthanide donor to allophycocyanin acceptor occurs when they are in proximity giving the long-lived decay at acceptor emission, the signal being specific for the biomolecular interaction. When acceptor (XL665) is not in proximity to donor, [Eu]K or lanthanide chelate gives a short-lived signal at 665 nm, which is discriminated by a time-delayed measurement. The interference from colored and florescent compounds in the assay can be eliminated by measuring the ratio of specific acceptor signal and the donor (Eu)K or lanthanide chelate signal. In the classical HTRF/TR-FRET assays, the acceptor dye used is allophycocyanin (APC) or XL665, which is light sensitive bulky molecule and can cause steric hinderance. To overcome these limitations, APC and XL665 acceptor dyes have been replaced with a new ULight^{TM} and D2 new acceptor dyes, respectively. ULight^{TM} and D2 are small acceptor dye molecules similar to APC suitable for direct labeling of

peptides and small molecules. These dyes are light resistant allowing easy handling of assay components and plates. Availability of several generic reagents with these new acceptor dyes as well as a series of several Eu-labeled reagents have been utilized to develop a variety of new high-throughput assays.

Dissociation-Enhanced Lanthanide Fluorescence Immune Assay (DELFIA)

DELFIA technology is well suited for binding assays and immunoassays based on heterogeneous approaches. In this technology, specific binding reagents such as antibodies or antigens are labeled with nonfluorescent labeling chelates. The bifunctional lanthanide chelates used in DELFIA are phenyl or benzyl isothicyanate derivative of EDTA, DTTA, DTPA, or pyridine tetraacetate. The key feature of DELFIA technology is dissociative fluorescence enhancement. The dissociation solution contains acidic buffer, which by lowering the pH (<3.5) dissociates the ions from the labeling chelates. The enhancement solution contains fluorogenic chelating reagent (b-NTA) that absorbs the excitation in the chelates and transfers the absorbed energy to the chelated lanthanide, TOPO, which replaces water molecules from the inner sphere of the chelates, enhances fluorescence, and prolongs decay time, and Triton X-100, which solubilizes the components for optimized fluorescence (86). DELFIA assays are separation assays built on coated microtitration plates or Acrowell filtration plates. Typical steps of an assay are binding of lanthanide chelates to a surface, washing excess of lanthanide chelate and dissociation of the lanthanide chelate, and enhancement of the signal (Fig. 17). The enhancement step is a unique proprietary feature of DELFIA technology and it is the key to high sensitivity. A prominent feature of the technology is the possibility to set up multiple label assays, which significantly increases the throughput as well as reducing the reagent costs (87). DELFIA technology is applied to immunoassays in determination of several different analytes in biological fluids and measurement of multiple analytes simultaneously.

Fluorescence Correlation Spectroscopy

Fluorescence correlation spectroscopy (FCS) is a biophysical technique used for unraveling molecular interactions in vitro and in vivo. FCS extracts information about a sample from the influence of thermodynamic equilibrium fluctuations on the fluorescence intensity. FCS gives information on molecular mobility and photophysical and photochemical reactions. By using dual-color fluorescence cross-correlation, highly specific binding studies can be performed. FCS monitors interactions of molecules present at miniscule concentrations in femtoliter volumes and thus offers the highest potential as the detection technique in the nanoscale in determination of molecular interactions in solution, on cell surfaces, or in the cells using homogeneous assays. In FCS, a sharply focused laser beam illuminates a very small volume element (typically femtoliter). Single molecules diffusing through the illuminated confocal volume produce bursts of fluorescent light quanta during the entire course of its journey (Brownian motion), and each individual burst is recorded in a time-resolved manner by a highly sensitive single-photon detector and is analyzed by using auto correlation techniques (88,89). This FCS autocorrelation function gives information on concentration, the diffusion time of all the individual molecules (related to the size and shape of the molecule), and the brightness of each molecule. Thus, autocorrelation of the

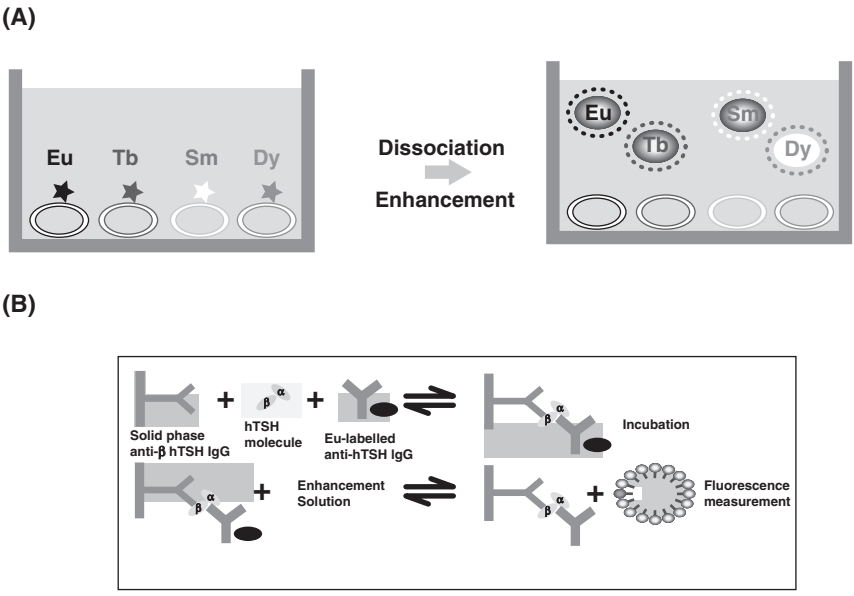

FIGURE 17 (**A**) Schematic of DELFIA assay. DELFIA assays are separation assays built on coated microtiter or Acrrowell filtration plates. Typical steps of DELFIA assay are binding of antibody or protein to microtiter plate surface, washing, dissociation, enhancement, and reading in a plate reader. (**B**) Schematic of DELFIA sandwich assay for quantitation of TSH. *Source*: Courtesy of PerkinElmer.

time-dependent fluorescence signal allows differentiation of slow and faster diffusing particles, and binding and catalytic activity can be directly calculated from the diffusion times and the ratio of faster and slower molecules. Variation to the established FCS is fluorescence cross-correlation spectroscopy (FCCS) that measures the temporal fluorescence fluctuations coming from two differently labeled molecules diffusing through a small sample volume (90). Cross-correlation analysis of the fluorescence signals from separate detection channels extracts information of the dynamics of the dual-labeled molecules. FCCS can be used for characterization of diffusion coefficients, determination of binding constants, kinetic rates of binding, and determining molecular interactions in solutions and cells.

FCS can be used for mass-dependent and independent fluorescence assays. Ligand–receptor binding assays can be performed by FCS at molecular level with membrane bound receptors in live cells on cell surface, membrane preparations, or cell-derived vesicles and nuclear receptors either based on fluorescence intensity or FP. In mass independent assays, the fluorescence of the substrate is quenched and the quenching is relieved in the product increasing the molecular brightness and the total fluorescence intensity. A quenched fluorescent protease substrate, tetramethylrhodamine (TMR)-quenched fluorescence peptide or streptavidin-quenched rhodaminegreen (RhGn)-peptide, when cleaved by protease leads to the relief of quenching, which results in an increase in fluorescence intensity, apparent particle number, and mean confocal intensity (91,92).

Although FCS was first described more than 30 years ago and used as analytical tool, the application of FCS technology for HTS is very recent with availability of commercial FCS readers. FCS can be used in micro-volume configuration (1–10 μl assay volumes) and adaptable for ultra-HTS. The read-times for vesicle assays are 5 to 10 seconds and for solution assays these are 1 to 2 seconds. FCS assays are based on the analysis of the molecular dynamics and the reaction kinetics of fluorescence labeled molecules that undergo temporal changes in their diffusion properties, allowing determination of the concentration of interaction parameters. A large number of simultaneously derived molecular parameters are obtained in FCS that allows selection of the most robust signal change for an assay. FCS can be used for several types of assays and for detection techniques monitoring intensity, particle number, polarization, energy transfer, and lifetimes increasing the scope of this technology. FCS can thus be used for most of the target classes of assays encountered in drug discovery.

FCS is a stable, reliable, and versatile technique that has become a standard method to monitor molecular interactions in vivo and in vitro. Single-channel measurements highlight photophysical phenomena, conformational changes, and mobility-related parameters. With multicolor applications, high spatial and temporal resolution, and multiplexing, it should be possible to find an ideal FCS variety for nearly any problem.

Fluorescent Reporter Assays

Cell-based assays are either used in conjunction with in vitro assays or in place of in vitro biochemical assays to examine output of specific cellular process. Reporter genes have been used in drug discovery for transcriptional studies as well as for characterization of receptor function and metabolic regulation (93). Agonist activation of a receptor or a ligand-gated ion channel produces changes in the transcription of a number of genes that can be readily measured by using gene fusions. A reporter gene construct consists of an inducible transcriptional element that controls the expression of reporter gene. Generally, a strong promoter (constitutively not active), which is controlled by desired response element that is regulated by receptor activation, is fused to the coding region of a reporter protein. Potential reporter proteins include green fluorescent protein (GFP), β-lactamase, luciferase, β-gal, chloramphenicol acetyltransferase, or SEAP (see also chaps. 6 and 8 in this volume). Reporter screens are sensitive and robust and are amenable to miniaturization and automation. One of the limitations of reporter screen is that receptor activation triggers gene transcription generating an indirect signal removed both spatially and temporally from the target.

Green Fluorescent Protein

Green fluorescent protein (GFP) is an autofluorescent protein originally isolated from the jellyfish *Aequorea victoria*. It is a 238 amino acid protein, which attains fluorescent state spontaneously and the fluorescence is stable (94,95). The wild GFP is relatively low in fluorescence intensity, has multiple absorption and emission maxima, and has about 4 hours lag-time between expression of protein and attaining full fluorescence. These drawbacks of GFP are remedied with the development of mutants of GFP with differing luminescent (increased brightness of fluorescence) and spectral properties, and mammalian cell compatible cloning vectors. Recently, monomeric forms of longer–wavelength-emitting

FIGURE 18 Schematic of FRET assay with green fluorescent protein (GFP). Example of a FRET protease assay between two linked variants of the GFP. C-terminus of a red-shifted variant of GFP (RSGFP4) was fused to N-terminus of a protein linker containing Factor Xa protease cleavage site, and N-terminus of a blue-variant of GFP (BFP5) was fused to the C-terminus of the protein linker. In the gene product, energy transfer occurs from BFP5 to RSGFP4. With Factor Xa protease action, the protein linker is cleaved and the two GFPs dissociate resulting in decrease in energy transfer. The emission ratio of the BFP5 (450 nm) and RSGF4 (505 nm) increases with the protease activity because FRET decreases.

proteins were created. Because of differing spectral properties of mutant GFPs, it is possible to follow two GFPs in the same cell and also can be used in FRET assays to study protein–protein interactions and other FRET-based assays. A FRET protease assay between two linked variants of the GFP has been described (94). C-terminus of a red-shifted variant of GFP (RSGFP4) was fused to N-terminus of a protein linker containing Factor Xa protease cleavage site and N-terminus of a blue-variant of GFP (BFP5) was fused to the C-terminus of the protein linker (Fig. 18). In the gene product, energy transfer occurs from BFP5 to RSGFP4. With Factor Xa protease action the protein linker is cleaved and the two GFPs dissociate resulting in decrease in energy transfer. The emission ratio of the BFP5 (450 nm) and RSGF4 (505 nm) increases with the protease activity because FRET decreases. A similar chymotrypsin assay using GFP FRET peptide in 3546-well nano well assay plates was reported (96).

β-Lactamase Reporter Assays

β-Lactamase from *E. coli* is a 29-kDa product of the ampicillin-resistant gene *Amp* that hydrolyzes pencillins and cephalosporins. A β-lactamase substrate CCF2/AM (6-chloro-7-hydroxy coumarin and fluorescein conjugated at 7 and 3′ positions of cephalosporin, respectively) provides a quantitative measure of gene transcription and thus allows the development of a transcription activation HTS assay with β-lactamase reporter (97). Excitation of coumarin at 409 nm by FRET results in emission from fluorescein a green fluorescence at 520 nm. When β-lactamase cleaves fluorescein on the 3′ position, it disrupts FRET and results in emission of coumarin at 447 nm, that is, blue fluorescence appears while green fluorescence of fluorescein is quenched. The measurement of β-lactamase activity as emission ratio at 450 nm/530 nm improves accuracy. A cell-based G-protein–coupled receptor assay using the β-lactamase reporter gene system in a 3456-nano well assay plate was described (97). In a functional screen with STAT5 regulated β-lactamase reporter gene in TF1 cells, GM-CSF–induced endogeneous wild type JAK2 activity has been determined by measuring β-lactamase activity (98). The β-lactamase reporter gene activation correlated with the target specific phosphorylation measured by LanthaScreen TR-FRET assay. In HEK-293 cells with β-lactamase reporter gene under control of NF-κB–responsive element, the TNFα-induced transcription of β-lactamase correlated well with TNFα-induced phosphorylation, ubiquitination, and degradation of IκBα assayed by LanthaScreen TR-FRET assays (98).

Fluorescence Imaging

In fluorescence imaging technology, unlike in a plate reader wherein the fluorescence signal is read one well at a time by PMT, all the wells of a microtiter plate (96-, 384-, 1536-well plates) are read simultaneously by imaging with a CCD camera and thus capable of recording kinetics in the sub-second range (99). Cellular imaging in combination with image-analysis tools is capable of visualizing cell population, single-cell, or subcellular structures (100). Because of the availability of flexible resolution and magnifications, fluorescence-based microscopy techniques can be used for various in vitro applications ranging from cell phenotype, proliferation, migration, and toxicity to intracellular molecular events such as nuclear translocation, mitosis, etc. Fluorescent Imaging Plate Reader (FLIPR) from Molecular Devices was developed to perform high-throughput quantitative optical screening for cell-based fluorescent assays (101). FLIPR measures fluorescence signals in all the wells of a microtiter plate simultaneously, with kinetic updates in the sub-second range. This permits determination of transient signals such as the release of intracellular calcium by using calcium indicators, calcium Green-1, Flura-2, Fluo-3AM, and Fluo-4AM. Leadseeker from GE Healthcare is a multichannel, line-scan confocal imager, which provides rapid data acquisition and analysis. Standard automated wide-field and confocal imaging microscopy platforms suitable for drug discovery include ArrayScan HCS from Cellomics, the laser-based Opera by Evotec Technologies, Discovery and ImageXpress Micro by Molecular Devices, Pathway 435 and 855 from BD Sciences, InCell Analyzer 1000 and 3000 from GE Healthcare, and Acumen Explorer, a laser scanning fluorescence microplate cytometer from TTP Lab Tech (Table 3).

High-Content Screening

High-content screening (HCS) is the analysis of complex cellular responses in a population of whole cells in parallel. HCS assays commonly use multiple fluorescence dyes (see also chaps. 6, 8, 15 in this volume). The HCS instruments extract spatial and temporal information of target activities within cells thus able to generate single-cell data for cells grown in microtiter plates (102). HCS yields information that will permit more efficient lead optimization before the in vivo testing. HCS assays are performed with either fixed cells using fluorescent antibodies, ligands, and/or nucleic acid probes or live cells using multicolor fluorescent indicators and biosensors.

Currently, there are three types of high-content instrumentation: flow cytometry, CCD imaging microscopy, and microplate cytometry (103). In flow cytometry, cell analysis is done by passing a stream of suspended cells through a fixed spot of laser light. Flow cytometry is a low-throughput platform that requires large number of nonadherent cells. CCD imaging microscopy gives high optical resolution for morphological readouts and high information data generating large data files (104). CCD imaging microscopy is best suited to target identification, validation, and lead optimization. The medium-throughput automated CCD imaging microscopy instruments are ArrayScan HCS and Discovery1, and the high-throughput instruments are Opera and INCell analyzer 3000. The emphasis of CCD imaging microscopy is high-content analysis for providing lot of information of each cell analyzed, and the assays are performed based on immuno-cytochemistry. Microplate cytometry offers high-throughput whole well high-content analysis and is applicable to hit identification and lead

optimization. Acumen Explorer uses a scanning laser for in situ analysis of cells at the bottom of clear-bottomed plates.

HCS can be very effectively applied to study drug-induced dynamic redistribution of intracellular constituents. Some of the high-content screens include cell adhesion, neurite growth, cell proliferation, cell viability, cell cycle analysis, cell migration, mitotic index, proteasome activity, P-glycoprotein activity, apoptosis, membrane potential, GPCR signaling, protein kinase activation, and GPCR translocation.

Fluorescent Imaging Plate Reader (FLIPR)

FLIPR system is developed to perform high-throughput quantitative optical screening for cell-based fluorescent assays (101). FLIPR measures fluorescence signals in all the wells of a microtiter plate simultaneously, with kinetic updates in the sub-second range. This permits determination of transient signals such as the release of intracellular calcium using calcium indicators. The FLIPR platform can use any of the several calcium dye indicators Fura-2, Fluo-3AM and Fluo-4AM, FLIPR Calcium 3 assay Kit, FLIPR no-wash calcium kit, BD calcium kit (105,106). It has also been used for measuring luminescence-based luciferase reporter assays. The FLIPR platform is very widely used for high-throughput calcium signaling for characterization of GPCRs coupled through G_q to the mobilization of intracellular calcium.

$FLIPR^{384}$ and $FLIPR^{TETRA}$ from Molecular Devices measure optical measurements on all wells of a 384 and 96-, 384-, 1536-well plates, respectively. $FLIPR^{TETRA}$ is optimized for use with fluorescent and luminescent assays capable of single or ratiometric kinetic cell-based reading (107). FLIPR can be used for measurements of intracellular calcium, intracellular pH, intracellular sodium, and membrane potential. (FLIPR assays are also discussed in chap. 6 in this volume). FLIPR has the ability to take readings in all the wells of a plate simultaneously, which enables study of real-time kinetics (Fig. 19). Real-time kinetic data gives additional pharmacological information for ranking relative potencies of drugs and gives information on the kinetics of the drug–receptor interaction. Functional response can be measured thus providing affinity, efficacy, and function of each drug and also can distinguish full agonists, partial agonists, and antagonists within a single assay. High-throughput functional screening assay was described for nonepinephrine transporter inhibitors using fluorescent substrate 4-(4-dimethylaminostyryl)-*N*-methylpyridinium in FLIPR system (107).

Functional Drug Screening System (FDSS)

FDSS-6000 and FDSS-7000 HTS instruments are from Hamamatsu Photonics capable of real-time kinetic analysis of various types of adherent and nonadherent cells. FDSS system is imaging-based plate reader for HTS cellular assays for evaluating compounds using cultured cells expressing receptor genes and reporter genes using various types of luminescent or fluorescent probes. FDSS system can be used for fluorescent, luminescent, FRET, and aequorin assays measuring calcium mobilization, membrane potential, and ion channel FRET. FDSS-6000 uses xenon lamps, enabling the use of fluorescent dyes ranging from UV to visible excitation wavelengths. It features two cameras: a photon detecting camera specifically designed for detecting flash aequorin signal and CCD

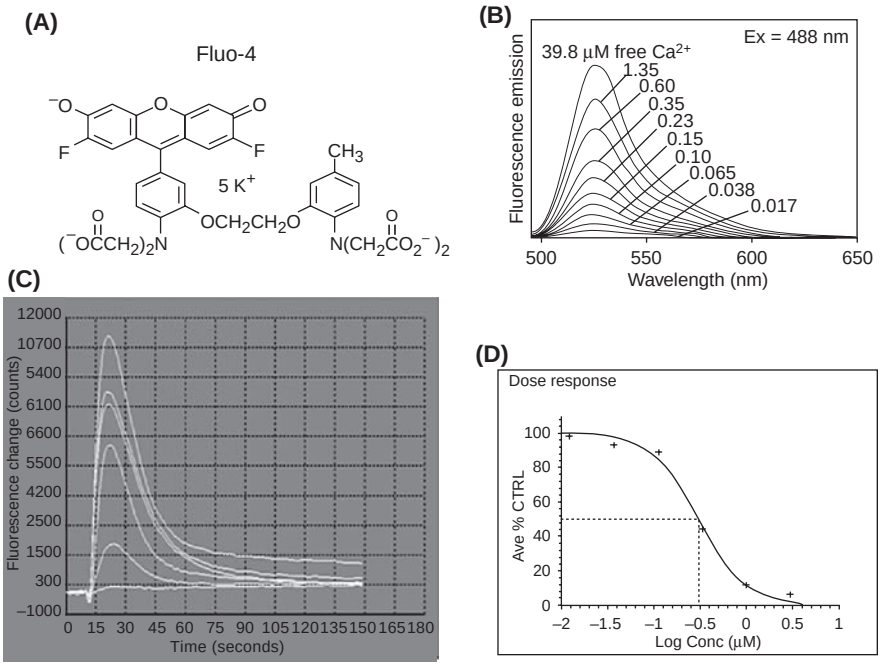

FIGURE 19 Fluorescence imaging plate reader (FLIPR) assay. (**A**) Structure of fluorescent dye Fluo 4 AM. (**B**) Calcium concentration response curves in FLIPR. (**C**) Measurement of intracellular Ca^{2+}. CHO cells stably expressing a desired GPCR are loaded with calcium sensing dye (Fluo 3 or Fluo 4), incubated with antagonist compounds, agonist is added, and the transient Ca^{2+} is measured in FLIPR. The individual Ca^{2+} curves in response to an antagonist concentration are given in the panel (**C**). (**D**) Dose–response curve of an antagonist on intracellular Ca^{2+} from which IC_{50} can be calculated.

camera specifically designed for detecting fluorescence up to 10 readings per second. FDSS-6000 can read 96- or 384-well plates and up to two excitation and emission wavelengths thus capable of multiplexing ex. the same cells can be loaded with the UV dye Fura-2AM and a no wash membrane potential dye thus measuring orthogonal cell responses, calcium mobilization, and membrane potential in the same assay (108). FDSS-7000 reads 1536-well plate and equipped with 1536 disposable tip head with better photon detector and luminescence detection system.

The changes in intracellular calcium concentrations in response to an antagonist in cells expressing a GPCR in HEK293 cell line were measured with fluorescent dye in FDSS-6000 and FLIPR and with aequorin assay in FDSS-6000 and CyBi Lumax (Cybio). In this antagonist fluorescence assays, the IC_{50} by FLIPR and FDSS system are similar (Fig. 7). In the luminescence assays in FDSS and Lumax systems, the IC_{50} s are also comparable.

Fluorometric Microvolume Assay Technology (FMAT™)

FMAT™ (PerkinElmer) is a homogeneous bead-based or cell-based assay and is compatible with various types of plate formats: 96-, 384-, and 1536-well plates.

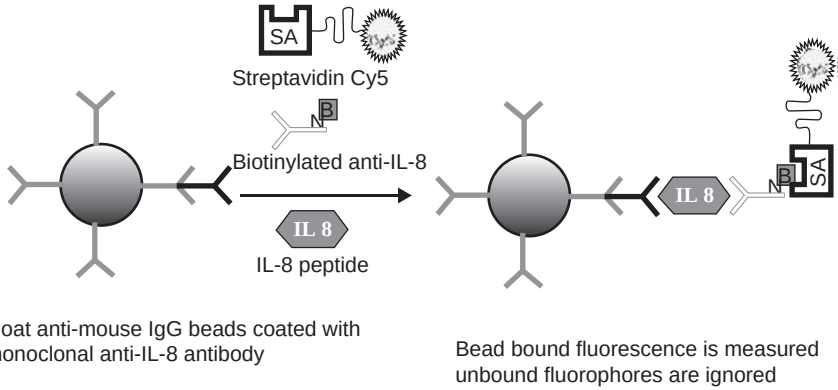

FIGURE 20 Schematic representation of FMAT interleukin-8 immunoassay. Goat antimouse beads coated with IL-8 monoclonal antibody bind IL-8 in the sample, then the second biotinylated IL-8 antibody (to a different epitope) will immunocomplex with IL-8. Streptavidin labeled with Cy5 will bind to biotin residue and bead bound fluorescence is measured. The unbound fluorophore is ignored and does not give a signal.

In a bead-based fluorescent-linked immunosorbent assay (FLISA), beads coupled with goat antimouse antibody are coated with the capture monoclonal antibody (109). The bead–antibody complex is then incubated with the sample, the biotinylated polyclonal antianalyte antibody, and Cy5-labeled streptavidin (Fig. 20). A sandwich is formed by the matched antibody pair when the analyte is present in the sample. The fluorescence associated with the bead complex is then detected by the FMAT system. In FMAT^{TM}, the laser (633 Helium/Neon) is focused on the bottom of the well of multiwell plate and the fluorescence associated with each cell or bead is detected over the unbound and background fluorescence. The analysis algorithm ignores background fluorescence. Specific signal is detected as areas of concentrated fluorescence surrounding a cell or a bead and the remaining background fluorescence is ignored in the final processing of the image data. FMAT is a homogeneous format for intact cell- and bead-based assays and does not require washing to remove unbound fluorophore. The FMAT^{TM} assays can be multiplexed using a two-color format with two PMTs to determine more than one receptor binding assays on a single cell or multiple markers on a cell or a bead.

FMAT^{TM} uses nonradioactive fluorescent tags and has been applied for cytotoxicity assays, functional assays such as ICAM-1 regulation by cytokines, and G-protein–coupled receptor binding assays, nuclear hormone receptor assays, tyrosine and serine/threonine kinases, protein–nucleic acid interactions, and protein–protein interactions (110). FLISA has been used for developing a high-throughput cell-based antibody-binding assay using FMAT platform (110). ELISA assays that are not HTS compatible due to the number of wash steps and incubation steps involved can be reformatted to bead-based homogeneous assays with FLISA. FLISA is a one-step incubation assay compared to multiple wash and incubation steps with ELISA, with equal or better sensitivity than ELISA.

LABEL-FREE DETECTION SYSTEMS

The vast majority of assay technologies used in drug discovery utilize fluorescence, or radiolabeled small molecules, proteins, or DNAs. These labels allow ultrahigh-throughput assay of molecular interactions. However, attaching these labels influence the conformation of the biomolecule thus may influence the way in which they interact with other biomolecules. However, label-free methods, which rely on optical, acoustic, thermal, potentiometric biosensors may improve the interactions. Although, label-free biosensor technology allows real-time, kinetic, affinity, and concentration analyses in analytical setting, achieving high throughput and sensitivity are important challenges. The instrument manufacturers are developing next-generation biosensors that can improve the throughput, reproducibility, and sensitivity to utilize the label-free technologies in cell-free and cell-based assays.

In a typical cell-free detection system, upon analyte binding to a target (proteins, antibodies, or ligands) or cellular material (living cells or tissues) on biosensor surface produces a change in electrochemical, pH, heat, light, magnetic, or mass, which is measured as electrical signal using an appropriate signal transducer such as electrode, semiconductor pH electrode, thermistor, photon counter, and piezoelectric device, respectively (Table 4) (111). These technologies can be used to assay development (antigen–antibody, ligand–receptor, DNA–protein), quantitation applications and in drug discovery (kinetic screening, affinity characterization, rank order affinities). Some of these emerging label-free technologies that use optical, acoustic, and calorimetric biosensors will be discussed.

Optical Sensors

A variety of optical biosensors such as surface plasmon resonance (SPR), resonant waveguide grating (RWG), resonant mirrors, and interferometry have been utilized in developing label-free detection methods. Among these, SPR and RWG have become popular methods for measuring biomolecular interactions.

Surface Plasmon Resonance (SPR)

SPR occurs when a prism directs a wedge of polarized light on to the sensor surface consisting of electrically conducting thin metallic film such as gold coated onto a glass support to excite surface plasmons (112,113). The light energy at a particular wavelength and angle of incidence are absorbed by free electron clouds in the gold layer generating surface plasmons causing alterations in the intensity of reflected light. The resonance (nonreflectance) angle is dependent on the refraction index in the vicinity of the metal surface, which in turn is dependent on the mass concentration. Molecules attaching to the sensor surface with gold film cause changes in the refractive index close to the surface resulting in a change in the SPR signal. Biomolecular binding events cause further changes in the refractive index that is detected as changes in the SPR signal (114,115).

Biomolecular interaction analysis in the Biacore is measured as the shift in the resonance angle with time. SPR technique can be used to precisely measure the kinetics of macromolecular interactions. Sensor surfaces can be functionalized to either directly capture different target molecules or affinity capture of the target molecules. SPR of macromolecules uses Au SPR film and a flow cell, which houses a chip coated with a thin layer of Au colloidal particles. Sensor chip CM5 (Biacore) has carboxymethylated dextran matrix surface to which ligand

TABLE 4 Label-Free Technologies

Category	Technology	Instrument	Throughput	Manufacturer
Optical biosensors	Surface plasmon resonance (SPR)	Biacore T-100	Medium	Biacore
	SPR	Plasmon Imager	Medium	Graffinity
	SPR	IBIS1 & II	Low	IBIS Technologies
	SPR	ProteomicProcesssso	Medium	Lumera
	SPR	Fuji AP3000	Medium	Fuji
Optical biosensors	SPR	ProteOn XPR 36	Medium	BioRad
	Resonance wave guide grating	Epic	High	Corning
	Resonant mirror	IAsys	Low	Thermo
	Interferometry	Octet & Octet Red	Medium	ForterBio
	Optical resonance grating	BIND	High	SRU Biosystems
Calorimetric Biosensors	Thermal	Autio ITC, iTC200	Low	Calorimetry Sciences Corp MicroCal (GE),
Acoustic	Resonant acoustic profiling	Rapid 4	Medium	Akubio
Piezoelectric	Real-time cell electronic sensing	ACEA	Medium	ACEA-Biosciences
	Cellular dielectric spectorscopy sensors	CellKey	Medium	MDS Sciex

The instrument, technology, and type of biosensrmation are listed.

can be immobilized through covalent derivatization through amine, thiol, aldehyde, or carboxyl groups. Different types of sensor surfaces are available that can be used for different assays: sensor chip CM5 (carboxymethylated dextran matrix surface) with immobilized ligand can be used for studying interaction with target molecules or affinity capture of alternative molecule, which interacts with the target molecule; sensor chip SA (streptavidin surface), which captures large biotinylated DNA fragments is used in nucleic acid interactions; sensor chip NTA (NTA-coated sensor surface) through nickel chelation captures histidine tagged biomolecules that can be used in receptor binding assays (116); sensor chip HPA (hydrophobic surface) to which membranes or liposomes containing receptors can be coated and used in receptor binding studies.

When light is reflected off the surface of the Au particle, the angle of reflection gives information about the mass bound to the matrix. A solution containing compounds that interact with the molecule bound to the chip (e.g., ligand to the receptor or antigen to the antibody) is passed over the surface of the chip. As these molecules interact, there is an effective change in surface roughness of a few nanometers on Au-SPR films and is easily detected. This allows a rapid and direct measurement of the binding kinetics of a broad variety of interactions in real time.

Single channel Biacore probe is used for fast detection and concentration of target biomolecules. In Biacore-probe, SPR occurs in the gold film at the tip of a sensor probe. Multichannel Biacore X, Biacore 2000, and Biacore 3000 can be used to study biomolecular-binding events in real time, allowing direct assessment of kinetic constants. Flow cells use as little as 5 μl sample. Biacore X is manual system with one continuous flow pump and two flow cells. Biacore 2000 and Biacore 3000 are automated systems with two auto-samplers and continuous flow pumps and four flow cells on one sensor, which allow immobilization of four different molecules and four different interactions can be monitored simultaneously.

A SPR developed by Bio-Rad uses a crisscrossing 6×6 array biosensor chip that allows 36 simultaneous measurements in ProteOn XP36. In ProteOn XP36, six parallel flow paths are oriented in the vertical direction for target immobilization. Six parallel flow paths are oriented in the horizontal direction for analyte injections of different concentrations (117).

Recent progress in SPR imaging technology led to development of few other commercial instruments. For SPR, imaging system employs a laser light source and a CCD camera to collect the reflected light intensity in an image. High-throughput SPR method Proteomic Processor™ was developed by Lumera Corporation by coupling with protein array technologies (118).

SPR measurements are based on refractive index changes, the analyte does not require any label or special characteristics. The SPR-based assays are homogenous assays though medium throughput, allow real-time monitoring of binding processes with accurate determination of kinetic constants. The sensitivity of SPR technology is sufficient for detection and characterization of binding events involving low–molecular-weight compounds and their immobilized protein targets. To increase the throughput of SPR, imaging technology with a CCD camera for detection can be used. As this technology develops, it will be a powerful tool for HTS to directly measure the binding of small molecule compounds to their drug targets.

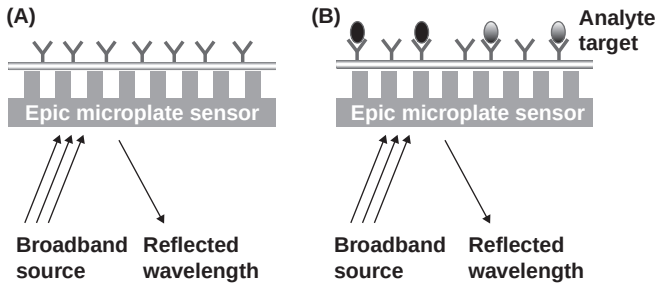

FIGURE 21 Schematic of measurement of refractive index changes in Epic^{TM}. (**A**) Each well of the Epic microplate contains a biosensor that has a surface chemistry layer, allowing for the attachment of biomolecules through amine chemistry. The target is immobilized to the plate. (**B**) Addition of a binding partner results in a change in refractive index.

Resonance Waveguide Grating

Corning's Epic system is a label-free detection system that features standard 96-, or 384-well microplate with optical biosensors and attachment chemistry in each well. Upon illuminating with broadband light, the resonant waveguide grating sensors reflect a specific wavelength that is a function of the index of refraction close to the sensor surface (Fig. 21). Epic system can be used for label-free direct binding in biochemical assays and detection of endogenous cell receptor response in cell-based assays. In biochemical assays, the plate surface (optical sensors) is coated with surface chemistry layer that attaches the target protein through primary amine group. When a small molecule (analyte) binds to immobilized target on the optical sensor, it changes the local index of refraction resulting in a shift in the wavelength of light that is reflected from the sensor (119). In cell-based assays, the cells are attached to the biosensor and a similar detection process takes place, a shift in response from the optical sensor indicates changes in the local index of refraction. The sensors detect index of refraction that takes place within the 200 nm from the sensor surface, which encompasses the bottom portion of the whole cells cultured on the sensor. The Epic system is sensitive to whole-cell movement.

Optical Resonance Grating

SRU Biosystems has developed a Biomolecular Interaction Detection (BIND) system that uses a guided mode resonance biosensor technology in which a total reflection at a single wavelength based on the energy field created at the site of binding (120–122). The sensor uses continuous sheets of plastic film that is incorporated into standard microtiter plates. The biosensor structure consists of a low refractive index plastic material surface structure that is over coated with a thin layer of high refractive dielectric material. When biomolecules or cells are immobilized on the surface of sensor, upon illumination of the surface with white light the wavelength of the reflected light is shifted to a higher value due to change in the optical path of light that is coupled into the grating. Real-time binding can be determined by measurement of the shift in Peak Wavelength Value (PWV) over time.

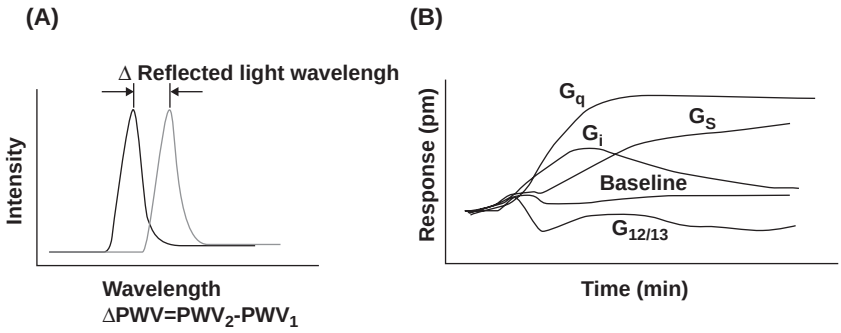

FIGURE 22 Label-free technology in the BIND reader. (**A**) The BIND signal. By mass attachment or detachment shifts in the peak wavelength value (PWV) are observed. (**B**) Temporal BIND patterns of four types of GPCR responses in HEK cells. Endogenous GPCR responses in HEK 293 cells with drugs are shown. The pattern of responses over time period can be distinctive with each type of receptor.

The SRU's BIND reader incorporates an imaging spectrometer that is capable of generating high-resolution spatial maps of the PWV on the photonic crystal surface. BIND reader can be used for label-free biochemical assays as well as cell-based assays. The standard Reader scans a 384-well plate in approximately 45 seconds and a 96-well plate in 15 seconds, and the Turbo Reader scans a 384-well plate in approximately 12 seconds and a 1536-well plate in 45 seconds, thus significantly increasing the throughput of the label-free technologies. The BIND system has been used for studying protein–protein interactions including antigen–antibody interactions, small molecule binding to protein, fragment screening, and cell-based assays including endogenous GPCRs, ion channels, and cell adhesion in primary cells (120–122). BIND gives signature responses to specific GPCR subtype agonists. As shown in Figure 22, the G_q, G_s, G_i, and $G_{12/13}$ GPCR subtypes have definitive kinetic profile responses. Native cells expressing endogenous GPCRs and cells overexpressing a particular receptor can be monitored in response to stimulus by specific ligands. From the characteristic G-protein functional coupling pathway triggered by each ligand in primary cells or cells containing expressed receptors or orphan receptors, the preference for one G-protein coupling type can be identified. The G-protein–coupling pathway triggered by each ligand is dependent on the cellular background (cell type) and mechanism of cell attachment. Thus, the kinetic data obtained in the BIND system measures quantitative response to stimulation or inhibition and the G-protein coupled signal transduction pathway.

Biolayer Interferometry

Biolayer interferometry is a label-free biosensor technology that enables measurement of molecular interactions. ForteBio technology is a label-free technology based on Biolayer Interferometry (BLI). The biosensor consists of a polished fiber optic embedded into a polypropylene hub with a sensor-specific chemistry at the tip. The biosensor has two-dimensional binding surface and the matrix minimizes nonspecific binding. This technology can be used for measuring binding kinetics (how specific, fast, and tight are the molecular interactions). Adding

molecules to the biological layer (binding) shifts the wavelength peaks to the right, whereas reducing the thickness of the biological layer (dissociation) shifts the wavelength to the left. The wavelength shift is a direct measure of the change in thickness of the biological layer. Only molecules binding to or dissociating from the biosensor layer can shift the wavelength of the interference pattern and generate a response profile in the Octet system. The Octet system measures the wavelength shift and gives the data for molecular interaction in real time (Fig. 23). Binding interaction at the biosensor surface does not require the use of detection labels. There are no labeling steps before the analysis, and there is no interference from fluorescent or chromogenic tags. No microfluidics in the system. Binding is only detected at the sensor surface, so there is minimal interference from biological sample media. Proteins can be assayed in crude mixtures (cell lysates or hybridoma sups) or in DMSO (<5%) thus minimizing interference.

FortreBio has two types of instruments, one capable of measuring protein–protein interactions (OctetK and Octet KQ) and the other measuring small molecule–protein interactions (OctetRed). OctetRed can be used to assay up to eight samples in parallel and up to 96 samples in unattended operation. The process is automated, simplifying the performance of multistep experimental protocols and complete data analysis. OctetRed can measure association rates (k_a), measure dissociation rates (k_d), and determine affinity constants (K_D).

Cellular Dielectric Spectorscopy (CDS)—Cellular Impedance

The application of electrical cell-substrate impedance sensing (ECIS) for real-time measurement of cellular process was first reported 25 years ago (123). Since then ECIS technology has been used for monitoring several cellular events. Cell sensor impedance technology allows for the noninvasive monitoring of cells in the entire experiment including cell attachment, spreading, proliferation, and compound treatments (124). The data are collected in real time to monitor the short-term and long-term cellular responses to treatment or manipulations of the cell.

Real-Time Cell Electronic Sensing (RT-CES) System

The RT-CES system from ACEA Biosciences is composed of four components: the electronic microtiter plates (EM plates); the EM plate station, which is placed in a tissue culture incubator; and an electronic sensor analyzer, which sends and receives the electronic signals; and the computer, which runs the RT-CES software and collects the real-time data (125). All the mammalian cells have very unique morphologies dictated by the architecture of the cellular cytoskeleton and the extracellular milieu. The factors that affect the internal physiology of the cell will bring about specific changes in the cell morphology. The EM plate contains integrated microelectrode arrays in the bottom of each well. The interaction of the adherent cells with microelectrodes leads to the generation of a cell-substrate impedance response. The electrical impedance generated is transferred to a computer and displayed as arbitrary unit of cell index. RT-CES system key applications for cell-based assays include cell proliferation and cytotoxicity, cell adhesion and spreading, functional assays for GPCRs, and receptor tysosine kinases (TRK), cell adhesion and spreading, endothelial barrier function and cell migration and invasion (126–128).

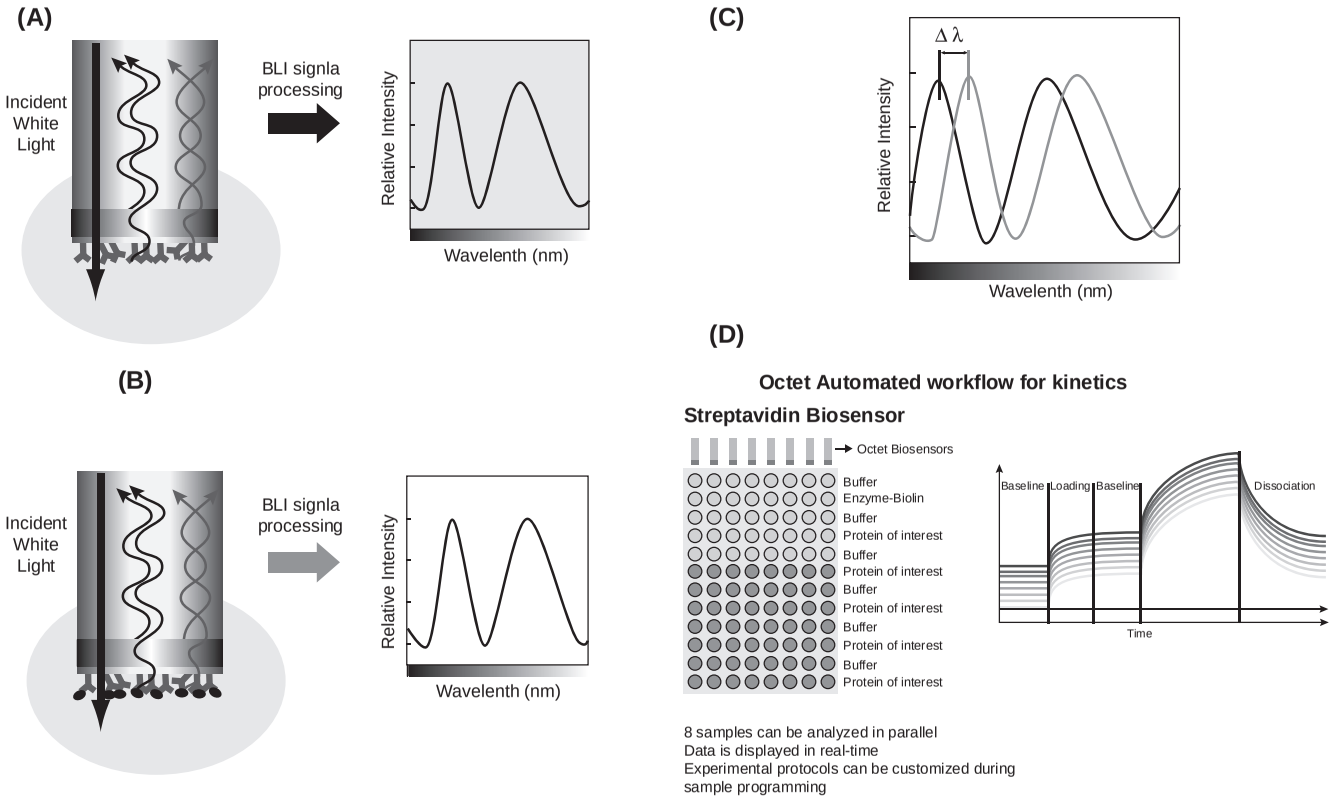

FIGURE 23 Biolayer interferometry technology in ForteBio's OctetRed. (**A**) A layer of molecules (target) attached to the tip of an optic fiber creates an interference pattern at the detector. (**B**) Analyte is bound to the target. (**C**) Analyte bound to the target causes shift in the wavelength and the $\Delta\lambda$. Only molecules binding or dissociating from the biological layer can shift the wavelength of the interference pattern and generate profile (nm). Adding molecules (binding) to the biological layer shifts the wavelength peaks to the right, and reducing the dissociation of molecules shifts the wavelengths peaks to the left. (**D**) Work-flow for kinetics. In the Octet system 8 samples can be analyzed in parallel. The tracings of baseline, loading the target, baseline, loading the analyte, and dissociation are represented. *Source*: Courtesy of ForteBio.

CellKey™ CDS System

CDS system is an emerging label-free technology that measures whole-cell responses. CellKey™ system (MDS Sciex, Foster City, CA) is a CDS-based instrument that is optimized for GPCR detection. CellKey has automated liquid handling in 96- and 384-microplate format that allows for reasonable throughput in lead generation and optimization. The CellKey™ 384 system sensitivity allows biorelevant measurements of receptor activity in cell lines and primary cells. The CellKey™ system provides a universal assay that can monitor the activity of different classes of GPCRs and TRKs and also differentiate between their signaling mechanisms. The response profiles directly correlate to receptor-mediated signal transduction pathways, thus enabling identification of the underlying mechanism of action of lead compounds. CellKey™ system is a simple assay platform that can measure functional activity of both GPCRs and TRKs (129).

The CellKey™ measurements have been generated even from endogenous receptors of primary cells in addition to cell lines suggesting that this CDS technology is sensitive enough to give pharmacological information under conditions of lower receptor density that is found in normal physiological conditions (Fig. 24) (130). Upon detecting GPCR activation, the CellKey™ system generates unique CDS response profiles that reflect the signaling pathways used by the cells. The profiles are characteristic of G_s-, Gi- or G_q- GPCRs and can be used to identify the G-protein coupling mechanism of unknown or orphan GPCRs. Supervised clustering of known or reference ligands can be used to generate the typical response profiles for G_s, G_q, and G_i GPCRs in the cell line of interest. The unique GPCR response profiles can also be used to deconvolute the pathway through which receptors transduce their signals. The CellKey™ system

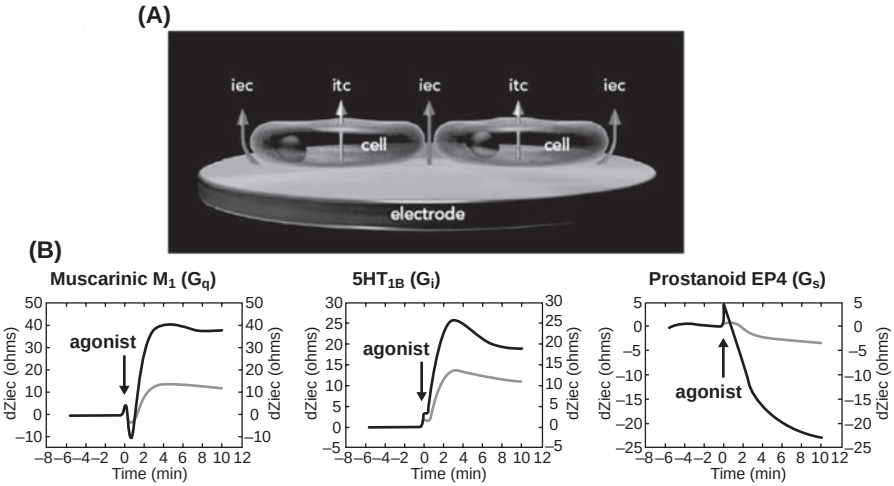

FIGURE 24 Label-free technology measuring cellular impedance by CellKey™. (**A**) Schematic representation of CellKey microplate well. (**B**) Characteristic responses of GPCRs in CellKey. The response for each type of receptor is different and is able to measure mixed/multiple signal pathways. *Source:* Courtesy of MDS SCiex

measures and analyzes downstream signaling events triggered by receptor activation.

Acoustic Biosensor Systems

Acoustic biosensors also have been utilized in the label-free detection of molecules and analysis of binding events. When molecules interact, result in changes in resonant frequency and resistance that are monitored by quartz crystal resonators in the acoustic biosensor systems. The acoustic technology can be used to monitor interaction between molecules as small as 200 Da. As with the other label-free detection technologies, acoustic biosensor systems also allow real-time monitoring of biomolecule interactions. Akubio (Cambridge, U.K.) uses a novel acoustic rupture event scanning (RES) technology to detect the sound of bonds breaking, as molecules are shaken off a vibrating resonator. RES can be used to size, separate, and detect particles. RES has been used to measure affinity of molecules as more strongly attached molecules detach at larger amplitude of oscillation. Akubio's RAPid4, a resonant acoustic profiling system is based on resonating quartz technology optimized for the detection of molecular interactions. RAPid4 can analyze up to four samples simultaneously and is capable of working with purified samples and complex mixtures. Akubio's sensor technology is the AKT-iv sensor cassette containing two resonating quartz crystal sensors and uses gold electrodes on the crystal surface to apply precise current (131). This drives the crystal and creates resonance, which is reduced in proportion to the molecules interacting on the surface. The crystal surface is coated with biologically inert chemical layer to which the biological targets are coupled. A variety of surface chemistries are available to couple the target to the biosensor. The coated crystal is encapsulated in a flow cell, which is used to add biological samples. This system couples acoustic detection with microfluidic delivery system to enable detection of analytes in real time. Analysis of the interaction data can be used to determine the "on" and "off" rates of binding events and the molecular affinity in the interactions and the concentrations of target molecules. The RAPid4 system has been used to determine the concentration of analytes, analysis of affinity, and kinetic characterization of antibody and antigen interaction and protein–protien interaction.

Calorimetric Methods

Traditionally, calorimetric methods are low-throughput assays for the determination of binding affinity and kinetic constants for the molecular interactions. However, calorimetric methods are the most reliable gold standard methods for characterizing molecular interactions. The conventional calorimetric methods required large sample amounts with low-throughput. Isothermal methods have been used to detect ligand binding. Isothermal titration calorimetry (ITC) is the preferred calorimetry method for determining ligand binding. ITC does not require immobilization of target and measures heat generated or absorbed when molecules interact. It provides the thermodynamic parameters such as the enthalpy of binding, the binding constant, and the number of binding sites of ligand–protein interactions. Binding is a process controlled by thermodynamics. Binding affinity is a combined function of the binding enthalpy and the binding entropy. Extremely high affinity requires that both enthalpy and entropy contribute favorably to binding and enthalpy/entropy balance affects selectivity of

a compound. SAR optimization has been driven by affinity; however, a multidimensional approach that also tracks the enthalpic and entropic contributions to affinity can yield faster and better results (132). Though, ITC is a high precision and reliable method with high reproducibility in determining molecular interactions, this method requires significant amounts of proteins in addition to being very time-consuming. Modern ITC instruments with improved data analysis make it possible to measure K_m and k_{cat}, in the ranges of 10^{-2} to 10^3 μM and 0.05 to 500 sec^{-1}, respectively. AutoITC (MicroCal LLC, Northampton, MA) can measure samples in a 96-well plate. ITC is now routinely used to directly characterize the thermodynamics of protein–ligand interactions and the kinetics of enzyme-catalyzed reactions (133).

Another calorimetric method is differential scanning calorimetry (DSC), which measures conformational changes in macromolecules. Miniaturization with the use of array with integrated microtemperature sensors at the bottom of each well enables determination of intermolecular activity by measuring the temperature in each well. Another calorimetric method is isothermal denaturation (ITD), which has been used to determine the stability and aggregation of proteins in physiological conditions. ITD assay method in 384-well plate format has been successfully used to determine the ligand binding and enzyme assays (134). ITD enabled screening libraries of large set of compounds and rapid detection of small stability differences between protein variants due to ligand binding.

OTHER METHODS

Microfluidics

Microfluidics is an innovative technology with numerous potential benefits in miniaturization of bioassays in drug screening. Microfluidic chips are small platforms with micro channel systems connected to fluid reservoirs capable of handling nanoliter volumes. Appropriate channel design coupled with separation technologies and surface pattern facilitates many operational steps by allowing reagents to successfully pass each unit. These individual steps include sampling, sample enrichment, mixing, reaction modules, product separation, and sensors and detectors for quantitation are miniaturized and integrated on-chip (135). Electrophoretic separation in channels has been optimized in microchip design, and microfluidic chips with entire measuring systems are now commercially available from many suppliers: Caliper Life Sciences, Agilent Technologies, Evotec Technologies, Hitachi, and Flidigm Technology (135).

Mobility-Shift Assay Technology

Mobility-shift assay technology from Caliper LifeSciences (Hopkinton, MA) is a microfluidic Lab-on-a-Chip technology for use in drug screening. The Caliper Off-Chip Mobility-Shift assay format combines the basic principles of capillary electrophoresis in a microfluidic environment to analyze enzymatic assays with or without the addition of a stop or quenching reagent, making it possible to determine real-time enzyme kinetics. The reaction samples are sipped onto the chip through small capillary. The movement of fluids and molecules is enabled via pressure or voltage and an integrated optical system detects the signal. Caliper Labchip 3000 platform employs microfluidic chips containing a network of miniaturized microfabricated channels through which fluids and chemicals

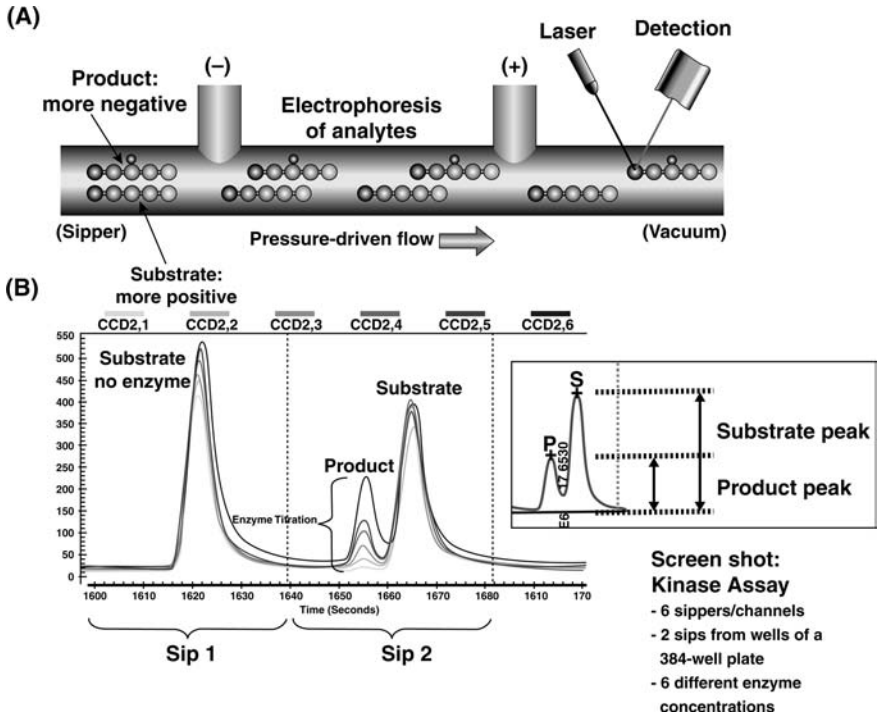

FIGURE 25 Mobility shift assay in Caliper LabChip. (**A**) The flow diagram for the Caliper LabChip-assay. The reactions are done in a microtiter plate and the samples are introduced into the LabChip into sippers and when electrical charge applied, the product is separated from the substrate and quantitated by reading in a laser reader driven detector. The Figure shows 6 channels of a 12 sipper-chip. (**B**) Trace of the output from a LabChip 3000. *Source:* Courtesy of Caliper.

are moved (Fig. 25). The reactions are run in a 96- or 384- well plate and samples are sipped through the 12 fused silica sippers located in the bottom of the chip. The fluorescent substrate and product are separated by applying an electrical potential across the separation channel. The fluorescence intensity signal of the substrate and product peaks is measured (Fig. 22). The sipping process can be repeated many times allowing a single chip to analyze thousands of samples automatically. This mobility-shift assay has been extensively used for screening assays for lipid kinases, protein kinases, phospatases, and proteases (136).

Agilents Lab-on-a-Chip

Agilent microfluidic Lab-on-a-Chip technology utilizes a network of channels and wells that are etched onto glass or polymer chips to build mini-labs. Pressure or electrokinetic forces move picoliter volumes in finely controlled manner through the channels. Lab-on-a-Chip enables sample handling, mixing, dilution, electrophoresis and chromatographic separation, staining, and detection on single integrated systems. The main advantages of Lab-on-a-Chip are ease of use, speed of analysis, low sample and reagent consumption and high reproducibility

due to standardization and automation. Agilent 5100 Automated Lab-on-a-Chip Platform (ALP) provides simultaneous electrophoretic analysis of four samples with unattended analysis of up to 10 standard well plates (96 or 384 formats).

Microarray Technologies

Microarray technology is developing very rapidly. The first use of microarrays was in immunological assays but the advent of genome sequencing microarray technologies have been mainly used for gene expression. Microarrays are typically glass slides on to which DNA, antibodies, protein, or peptide molecules are attached at fixed locations. It is very important to measure the levels of proteins in cells, tissues, extracts, and biological fluids in pharmaceutical research. The key purposes of these measurements are surrogates for organ activity, disease process, and drug action; proxies for activity when the measurement of tissue, organ, cell, and pathway are not possible; an end measure of the final protein product (137,138). Application of protein and peptide microarrays in drug discovery includes the identification of protein–protein, protein–small molecule, enzyme–substrate interactions. Protein microarrays include protein immobilized slides, slides imprinted with antibodies, slides etched with miniaturized wells with proteins or antibodies in solution in the flow chambers and detected by fluorescence labeling. Microarray technology has reduced reaction volumes to nanoliter volumes. Multiplexed protein measurement by microarrays has been utilized for protein measurement, for modeling networks and pathways, for biomarker development and have been finding important role in investigational new drug (IND) approval submissions and Phase IV studies (137).

A high-density homogeneous microarray system has been developed as the DiscoveryDot platform (Reaction Biology Corp, Malvern, PA) wherein peptides, proteins, and small molecule compounds are mixed with reaction mixture and then arrayed onto glass slides as individual reaction centers; the chip is activated by a fine aerosol mist of biological sample, the fluorescence signal is measured with a laser scanner or fluorescence microscope, and the data is analyzed with microarray software. This DiscoveryDot platform has been utilized for capsase-6 Factor Xa, protein kinase A, and protease reactions (138).

Micro Parallel Liquid Chromatography: Nanostream

Nanostream (Pasedena, CA) technology is a micro parallel liquid chromatography (μPLC) platform, which can analyze 24 samples simultaneously in a single run using a Brio cartridge that has 24 μPLC columns. The cartridge μPLC columns, which are 3 cm long with 0.5 mm inner diameter, are packed with Genesis C18 material. The assays are run in wells of 384-well plate and the samples are dispensed to 24-reservoirs on the Brio cartridge through an eight-channel sampler. The samples are separated by a binary gradient mobile phase delivered by the solvent delivery system and the samples eluted from each column of the cartridge pass through a set of capillaries that are led to a bank of UV detectors followed by a bank of fluorescence detectors. The data acquisition and analysis are performed with Nanostream's analysis software. The Nanostream platform is capable of detecting a broad range of substrate-to-product conversion and has been applied to a wide range of enzyme assays including kinases, phosphatases, and proteases (139,140). The μPLC also has been used to test the integrity of the

compounds used in HTS. The technology showed promising but closed its doors on March 2008.

Infrared Thermography

To measure thermogenesis in cell culture, infrared imaging system thermogenesis has been reported (141). The infrared-imaging system was shown to be a rapid, very sensitive (0.002°C) and effective method for measuring thermogenesis in cell culture in vitro. Thermogenesis increased in yeast expressing the mitochondrial uncoupling protein-2 after treating with an uncoupler of mitochondrial respiration and in adipocytes treated with rotenone, an inhibitor of mitochondrial respiration or β-adrenergic receptor agonists (141). A custom-made infrared thermography system consists of a thermo-electrically cooled Agema Thermovision 900 Infrared System AB (at a focal distance of 6 cm), equipped with a SW Scanner and a lens (40° × 25° lens) that detects 2 to 5.4 micron spectral response. Data analyzer consists of OS-9 advanced systems and ERIKA 2.00 software from Agema Infrared Systems. The sensitivity of this infrared thermography system is 0.002°C and robustness (96- as well as 384-well plates) makes this system very useful for HTS assays in detection of altered thermogenic responses in various cell types.

Quantom Dots and Nanoparticles

Quantom dots (nanocrystals) and other nanoparticles technology have been widely used in drug discovery and are extended to live cells, in vivo imaging, and diagnostics (142–145). Quantum dots are highly luminescent semiconductor (made of zinc sulfide–capped cadmium selelnide core) small nanoparticles that are covalently coupled to biomolecules (Fig. 26). The core of nanoparticles determines the color of the nanocrystal. The inorganic shell enhances the brightness of the nanoparticle. The polymer coating makes the nanocrystals stable and soluble

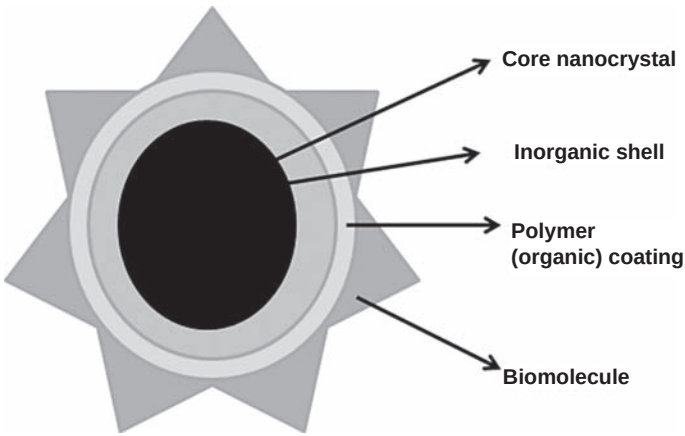

FIGURE 26 Schematic diagram of a Qdot. The core of nanoparticles determines the color of the nanocrystal. The inorganic shell enhances the brightness of the nanoparticle. The polymer coating makes the nanocrystals stable and soluble in aqueous soloution. Different biomolecules can be attached to different colored nanoparticles.

in aqueous soloution. Different biomolecules can be attached to different colored nanoparticles. These biomolecule conjugate Qdots are water soluble and biocompatible. When cells are exposed to the different colored nanoparticles containing various antibodies, each antibody binds only to its specific antigen on the cell surface. Depending on the presence of types of antigen on the cell surface, those colored nanoparticles are captured and others are washed away. Spectral readings at different wavelengths give information on the types of antigens present and amount of each antigen. Similarly, nanoparticles with different DNA probes can be used to identify a large number of gene sequences in blood and other biological samples. Semiconductor nanocrystals labeled with fluorescent probes have a narrow, tunable, symmetrical emission spectrum, broad continuous excitation spectrum and are photochemically stable and may prove to be superior to existing fluorophores and may have many applications in several different types of assays such as FP, FRET, SPR assays. The new generation of water-soluble nanocrystals and nanoparticles has great potential for the study of intracellular process at the single molecule level, high resolution in vivo cellular imaging, and cell trafficking, tumor targeting, neuroscience research for studies of neurons and glia, and diagnostics (143–145). Some of the companies developing nanoparticle technologies are Quantum Dot, Auspex, Biocrystals, Nanomat, Nanosphere, and Academic Labs.

Liquid Crystals

In this technology, liquid crystals are used to amplify and transduce receptor-mediated binding of proteins at surface into optical outputs. Liquid crystal sandwiched between two gold films supporting self-assembled monolayers containing ligands, upon binding of proteins to the specific ligands will change the surface roughness and trigger rapid changes in the orientations of 1 to 20 μm thick films of supported liquid crystals and changes the intensity of light transmitted through the liquid crystal, which can be further amplified and transduced into optical signals (146). The orientations of liquid crystals are sensitive to a wide variety of physicochemical properties of surfaces, suggesting that this approach can be used for detection of binding of small molecules to proteins and protein aggregates to surface. This approach does not need electroanalytical apparatus, provides spatial resolution of micrometers, and can be extended to assay the effect of spatially resolved chemical libraries on the ligand–receptor binding.

Microchip Technology

MicroChips are designed either for single or multiple use and consists of silicon and glass master chips combined with plastic injection molding or embossing produced by microfabrication technologies. Fluids are moved through microscopic channels by either electroosmosis or electrophoresis (microfluidics). Microfluidic capillary electrophoresis has been successfully used in several different types of HTS enzyme assays in MicroChips.

MicroChip technology has been used for enzyme assays and to determine the binding affinity of monoclonal antibody (147–149). In a MicroChip based protein kinase A assay, fluorescein-labeled Kemptide was used as substrate. The assay reagents are placed in wells on the Microchip, aliquots of the reagents are transported by electroosmosis into the network of etched channels and enzyme reaction is performed. The phosphorylated fluorescein-labeled

Kemptide product is separated from the substrate by on-chip capillary electrophoresis, and kinetic constants for ATP and peptide substrates (K_m) and inhibition constant (K_i) for inhibitor H-89 have been determined. This assay demonstrated the usefulness of the MicroChips for performing enzyme assays. Thus, MicroChip technology has potential for applications to immunoassays, nucleic acid assays, enzyme assays, and receptor-binding assays.

LC/MS/MS Analysis

Traditional and HTS assays rely on fluorescent or radiolabeled reagents and coupling assays for quantitation of enzyme reaction. LC/MS/MS methods offer a selective and sensitive analytical method for unlabeled substrate and products. LC/MS/MS methods enable elegant separation of substrate and products and quantitation precisely. It is a preferred method for difficult enzyme assays for which separation of the substrate and product molecules is not possible by other known assay methods. A high-throughput, simple, highly sensitive, and specific LC-MS/MS method (liquid chromatography coupled with tandem mass spectrometry or electrospray ionization method) can be developed for the estimation of analytes in the sample. LC/MS/MS methods also are being utilized for biomarker assays. The assay procedure involves direct precipitation with appropriate solvent such as acetonitrile, centrifugation to yield clean extracts from the matrix, separation of analytes on liquid chromatography (LC) followed by MS along with an internal standard gives the peak area of the product and substrate

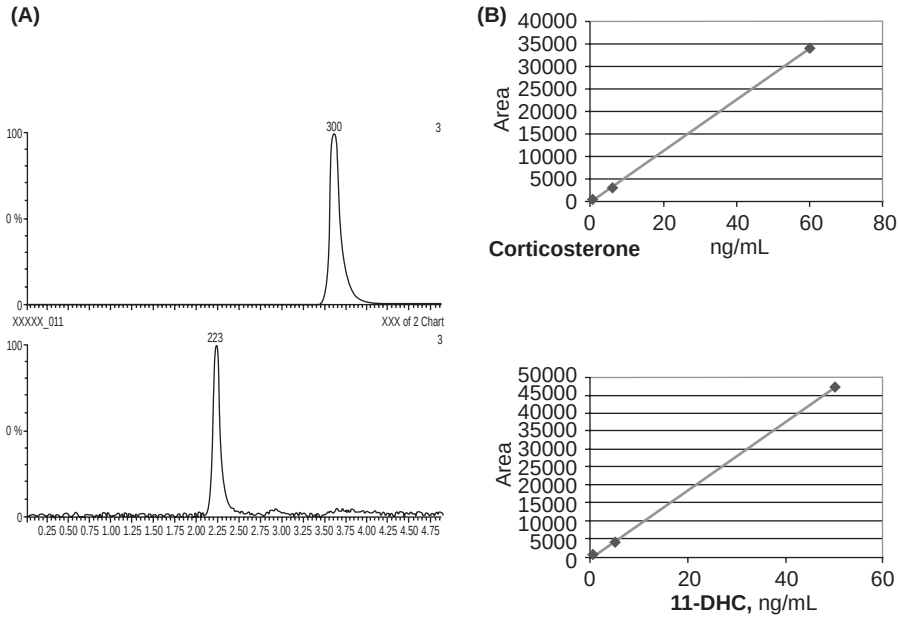

FIGURE 27 LC-MS/MS analysis of corticosterone and dihydrocorticosterone. (**A**) Corticosterone and dihydrocorticosterone are separated very well by LC-MS. (**B**) The standard curves of corticosterone and dihydrocorticosterones suggesting that the quantitiave analysis of the analytes is possible.

in each sample enabling quantitation of enzymatic reactions (Fig. 27). The total chromatographic run time generally is under 5 minutes and yields quality data. The LC/MS/MS assay gives high-quality data and has been utilized especially in the drug metabolism and pharmacokinetic studies (150,151). The assay can be multiplexed with four or eight channel electrospray ionization source interface for analyzing streams from four or eight LC systems. LC/MS/MS system can run up to twelve 96-well plates per day. This assay is a direct quantitative assay of the unlabeled substrates and products.

CONCLUSIONS

Robust, homogeneous fluorescence, chemiluminescence, radioactive, and label-free assays are described in this chapter, which do not require transfer, filtration, and washes. There is not a single universal assay format that can be used for various targets in drug screening. Traditional radioactive assays are generally very sensitive assays, but have handling problems, and generation of radioactive waste are of big concern. In the SPA bead, Flash Plate, Cytostar, and Leadseeker SPA methods, the amount of radioactive generated is reduced. SPA assays have been gaining popularity despite being radioactive methods. Nonradioactive fluorescence-based methods are getting more attention. FP assay format is comparatively simple, as only one labeled molecule is needed in the assay. HTRF/TR-FRET requires two-labeled molecules and with the availability of generic-labeled molecules an assay can be developed rapidly. Both FP and HTRF formats are very robust sensitive assays and added advantage being these are ratiometric methods hence less interference from colored compounds. Enzyme and receptors can be assayed with equal efficiency by more than one technology platform and it will be advantageous to go with an assay format that is already proven in the laboratory. Unless the new technologies offer substantial improvements over the existing platforms, it is counter intrusive to switch to a new technology. Several assay technologies based on fluorescence such as confocal microscopy, fluorescence correlation spectroscopy, fluorescence imaging, electrochemiluminescence, AlphaScreen, and FMAT have been developed to increase the throughput for HTS and ultra-HTS. Microassays using microchip technologies along with microfluidic array and imaging technologies are gaining importance in drug discovery. Label-free technologies with different biosensor platforms are gaining prominence to study the binding characteristics, and real-time kinetics of binding and instrument manufacturers are aiming at improving the throughput.

REFERENCES

1. Drews J. Drug discovery: A historical perspective. Science 2000; 287:1960–1964.
2. Hart HE, Greenwald EB. Scintillation proximity assay (SPA)–a new method of immunoassay. Direct and inhibition mode detection with human albumin and rabbit antihuman albumin. Mol Immunol 1979; 16:265–267.
3. Udenfriend S, Gerber LD, Brink L, et al. Scintillation proximity radioimmuno-assay utilizing 125I-labeled ligands. Proc Natl Acad Sci U S A 1985; 82:8672–8676.
4. Cook ND. Scintillation proximity assay: A versatile high-throughput screening technology. Drug Discov Today 1996; 1:287–294.
5. Bosworth N, Towers P. Scintillation proximity assay. Nature 1989; 341:167–168.
6. Glickman JF, Schmid A, Ferrand S. Scintillation proximity assays in high-throughput screening. Assay Drug Dev Technol 2008; 6(3):433–455.

7. Brown BA, Cain M, Broadbeat J, et al. FlashPlate^{TM} Technology. In: Devlin JP, ed. High Throughput Screening. New York, NY: Marcel Dekker, 1997:317–328.
8. Seethala R, Peterson T, Dong J, et al. A simple homogeneous scintillation proximity assay for acyl caoenzyme A diacylglyerol acyl transferase. Anal Biochem 2008; 383(2):144–150.
9. Seethala R, Ma Z, Golla R, et al. A homogeneous scintillation proximity assay for acetyl coenzyme A carboxylase coupled to fatty acid synthase. Anal Biochem 2006; 359:257–265.
10. Feau C, Arnold LA, Kosinski A, et al. A high-throughput ligand competition binding assay for the androgen receptor and other nuclear receptors. J Biomol Screen 2009; 14(1):43–48.
11. Haggblad J, Carlson B, Kivela P, et al. Scintillating microtitration plates as platform for determination of ^{3}H-estradiol binding constants for hER-HBD. BioTechniques 1995; 18:146.
12. Watson J, Selkirk JV, Brown AM. Development of FlashPlate^{TM} Technology to measure [^{35}S]GTPγS binding to Chinese hamster ovary cell membranes expressing the cloned human 5HT1B receptor. J Biomol Screen 1998; 3:101–105.
13. Watson S. In vitro measurement of the second messenger cAMP: RA vs FlashPlates^{TM}. Biotech Update 1995; 10:11.
14. Graves R, Davies R, Brophy G, et al. Noninvasivee real-time method for the examination of thymidine uptake events-application of the method to V-79 cell synchrony studies. Anal Biochem 1997; 248:251–257.
15. Cogan EB, Birrell GB, Griffith OH. A robotics-based automated assay for inorganic and organic phosphates. Anal Biochem 1999; 271(1):29–35.
16. O'Brien MA, Daily WJ, Hesselberth PE, et al. Homogeneous, bioluminescent protease assays: Caspase-3 as a model. J Biomol Screen 2005; 10(2):137–148.
17. Cali JJ, Niles A, Valley MP, et al. Bioluminescent assays for ADMET Expert. Opin Drug Metab Toxicol 2008; 4:103–120.
18. Fan F, Wood KV. Bioluminescent assays for high-throughput screening. Assay Drug Dev Technol 2007; 5:127–136.
19. Fan F, Binkowski BF, Butler BL,et al. Novel genetically encoded biosensors using firefly luciferase. ACS Chem Biol 2008; 3(6):346–351.
20. Lackey DB. A homogeneous chemiluminescent assay for telomerase. Anal Biochem 1998; 263:57–61.
21. Kolb AJ, Neumann K. Luciferase measurements in high throughput screening. J Biomol Screen 1996; 1:85–88.
22. Mattheakis LC, Ohler LD. Seeing the light: Calcium imaging in cells for drug discovery. Drug Discov Today 2000; Suppl 1:15–19.
23. Moleculardevices http://www.moleculardevices.com/product_literature/ family_links.php?prodid=13.
24. Maurullo S, Bouvier M. Resonance energy transfer approaches in molecular pharmacology and beyond. Trends Pharmacol Sci 2007; 28(8):362–365.
25. Kocan M, See HB, Seeber RM, et al. Demonstration of improvements to the bioluminescence resonance energy transfer (BRET) technology for the monitoring G protein-coupled receptors in live cells. J Biomol Screen 2008; 13(9):888–898.
26. Ungrin MD, Singh LMR, Stocco R, et al. An automated aequorin luminescence-based functional calcium assay for G-protein coupled receptors. Anal Biochem 1999; 272:34–42.
27. Fichna J, Gach K, Piestrzeniewicz M,et al. Functional characterization of opioid receptor ligands by aequorin luminescencebased calcium assay. J Pharmacol Exp Ther 2006; 317(3):1150–1154.
28. Menon V, Ranganathn A, Jorgensen VH, et al. Development of an aequorin luminescence calcium assay for high-throughput screening using a plate reader, the LumiLux. Assay Drug Dev Technol 2008; 6(6):787–793.
29. Golla R, Seethala R. A homogeneous enzyme fragment complementation cyclic AMP screen for GPCR agonists. J Biomol Screen 2002; 7(6):515–525.

30. Olson KR, Eglen RM β-Galactosidase complementation: A cell-based luminescent assay platform for drug discovery. Assay Drug Dev Technol 2007; 5(1):137–144.
31. Eglen RM. Enzyme fragment complementation: A flexible high throughput screening assay technology. Assay Drug Dev Technol 2007; 1(1):97–104.
32. Patel A, Murray J, McElwee-Whitmer S, et al. A combination of ultrahigh throughput PathHunter and cytokine seacretion assays to identify glucocorticoid receptor agonists. Anal Biochem 2009; 385(2):286–292.
33. Williams R. Electrochemoluminescence: A new assay technology. IVD Technology 1995; 28–31.
34. Deaver DR. A new non-isotopic detection system for immunoassays. Nature 1995; 377:758–760.
35. Golla R, Seethala R. A sensitive, robust high-throughput electrochemiluminescence assay for rat insulin. J Biomol Screen 204; 9(1):62–70.
36. Bohlm S, Kadey S, McKeon K, et al. Use of the ORIGEN electrochemiluminescence detection for measuring tumor necrosis factor-α in tissue culture. Biomed Prod 1996; 21:60.
37. Hughes SR, Khorkova O, Goyal S, et al. α2-Macroglobulin associates with β-amyloid peptide and prevents fibril formation. Proc Natl Acad Sci U S A 1998; 95:3275–3280.
38. Kenten JH, Casade J, Link J, et al. Rapid electrochemiluminescence assays for polymerase chain reaction products. Clin Chem 1991; 37:1626–1632.
39. Gowan SM, Hardcastle A, Hallsworth AE, et al. Application of Meso Scale Technology for the measurement of phosphoproteins in human tumor xenografts. Assay Drug Dev Technol 2007; 5(3):391–401.
40. Meso Scale Discovery: http://www.mesoscale.com/CatalogSystemWeb/WebRoot/literature/publications.aspx
41. AlphaScreen http://las.perkinelmer.com/Catalog/default.htm?CategoryID=AlphaScreen + Assays and Reagents.
42. Binder C, Lafayette A, Archibeque I, et al. Optimization and utilization of the SureFire phosphor-STAT5 assay for a cell-based screening campaign. Assay Drug Dev Technol 2008; 6(1):27–37.
43. Lakowicz JR. Principles of Fluorescence Spectroscopy. New York: Plenum Press, 1983.
44. Pope AJ, Haupts UM, Moore KJ. Homogeneous fluorescence readouts for miniaturized high-throughput screening: theory and practice. Drug Discov Today 1999; 4:350–352.
45. Rao AG, Flynn P. A quantitative assay for β-D-glucouronidase (GUS) using micrtotiter plates. Biotechniques 1990; 8:38–40.
46. Seethala R. Homogeneous assays for high-throughput and ultrahighthroughput screening. In: Seethala R, Fernandes PB, eds. Handbook of Drug Screening. New York: Marcel Dekker, 2001:69–128.
47. Haugland RP. Hand Book of Fluorescent Probes and Chemical Research, 6th ed. Molecular Probes Inc., 1996.
48. Jones LJ, Yue ST, Cheung C-Y, et al. RNA quantitation by fluorescence-based solution assay: RiboGreen reagent characterization. Anal Biochem 1998; 265:368–374.
49. McCauley TM, Mills SZ. Ahomogeneous, universal detection platform. Assay Tutorial: IQ Technology for kinase and phosphatase screening. Genet Eng News 2003; 23(8):32.
50. Perrin FJ. Poarisation de la lumiere de fluorescence vie moyenne des molecules dans letat excite. J Phys Radium 1926; 7:390–401.
51. Weber G. Fluorescence and Phosphorescence Analysis. New York: Wiley, 1966.
52. Dandliker WB, Chapiro HC, Meduski JW, et al. Applications of fluorescence polarization to the antigen–antibody reaction. Immunochem 1964; 1:165.
53. Jolley ME. Fluorescence polarization immunoassay for the determination of therapeutic drug levels in human plasma. J Anal Toxicol 1981; 5:236–240.
54. Jameson DM, Sawyer WH. Fluorescence anisotropy applied to biomolecular interactions. Meth Enzymol 1995; 246:283–300.

55. Jolley ME. Fluorescence polarization assays for the detection of proteases and their inhibitors. J Biomol Screen 1996; 1:33–38.
56. Seethala R, Menzel R. A homogeneous, fluorescence polarization assay for src-family tyrosine kinases. Anal Biochem 1997; 253:210–218.
57. Seethala R, Menzel R. A fluorescence polarization competition immunoassay for tyrosine kinases. Anal Biochem 1998; 255:257–262.
58. Seethala R. Fluorescence polarization competition immunoassay for tyrosine kinases. Methods 2000; 22:61–70.
59. Seethala R, Golla R, Ma Z, et al. A rapid, homogeneousfluorescence polarization binding assay for peroxisome proliferator activated receptors alpha and gamma using fluorescein-tagged dual PPARα/γ activator. Anal Biochem 2007; 363:263–274.
60. Owicki JC. Fluorescence polarization and anisotropy in high throughput screening: perspectives and primer. J Biomol Screen 2000; 5:297–306.
61. Jameson DM, Croney JC. Fluorescence polarization: Past, present and future. Comb Chem High Throughput Screen 2003;6:167–173.
62. Harris A, Cox S, Burns D, et al. Miniaturization of fluorescence polarization receptor-binding assays using CyDye-labeled ligands. J Biomol Screen 2003; 8(4):410–420.
63. Vedvik KL, Eliason HC, Hoffman RL, et al. Overcoming compound interference in fluorescence polarization–based kinase assays using far-red tracers. Assay Drug Dev Technol 2004; 2(2):193–203.
64. Allen M, Reeves J, Mellor G. High throughput fluorescence polarization: A homogeneous alternative to radioligand binding for cell-surface receptors. J Biomol Screen 2000; 5:63–69.
65. Nosjean O, Souchaud S, Deniau C, et al. A simple theoretical model for fluorescence polarization binding assay development. J Biomol Screen 2006; 11(8):949–958.
66. Parker GJ, Law TL, Lenoch FJ, et al. Development of high throughput screening assays using fluorescence polarization: Nuclear receptor–ligand binding and kinase/phosphatase assays. J Biomol Screen 2000; 5:77–88.
67. Schade SA, Jolley ME, Sarauer BJ, et al. BODIPY-α-casein: A pH-independent protein substrate for protease assays using fluorescence polarization. Anal Biochem 1996; 243:1–7.
68. Levine LM, Michner ML, Toth MV, et al. Measurement of specific protease activity utilizing fluorescence polarization. Anal Biochem 1997; 247:83–88.
69. Singh P, Lillywhite B, Bannaghan C, et al. Using IMAP technology to identify kinase inhibitors: Comparison with a substrate depletion approach and analysis of the nature of false positives. Comb Chem High Throughput Screen 2005; 8(4):319–325.
70. Sportsman JR, Gaudet EA, Boge A. Immobilized metal ion affinity-based fluorescence polarization (IMAP): Advances in kinase screening. Assay Drug Dev Technol 2004; 2(2):205–214.
71. Selvin PR. Fluorescence resonance energy transfer. Meth Enzymol 1995; 246:300–334.
72. Clegg RM. Fluorescence resonance energy transfer. Curr Opin Biotechnol 1995; 6:103–110.
73. Grahn S, Ullmann D, Jakubke HD. Design and synthesis of fluorogenic trypsin peptide substrates based on resonance energy transfer. Anal Biochem 1998; 265:225–223.
74. Kolb AJ, Burke JW, Mathis G. Homogeneous, time-resolved fluorescence method for drug discovery. In: Devlin JP, ed. High Throughput Screening. New York, NY: Marcel Dekker, 1997:345–360.
75. Mathis G. HTRF® technology. J Biomol Screen 1999; 4:308–310.
76. Alpha B, Lehn J, Mathis G. Energy transfer luminescece of Europium (III) and Terbium (III) cryptates of macrocyclic polypyridine ligands. Agnew Chem Int Ed Engl 1987; 26:266.
77. Hemmila I. Lance^{TM}: Homogeneous assay platform for HTS. J Biomol Screen 1999; 4:303–307.
78. Jia Y, Quinnn CM, Gagnon AL, et al. Homogeneous time-resolved fluorescence and its applications for kinase assays in drug discovery. Anal Biochem 2006; 356(2):278–281.

79. Hill DC. Trends in development of high-throughput screening technologies for rapid discovery of novel drugs. Curr Opin Drug Discov Dev 1998; 1:92–97.
80. Stenroos K, Hurskainen P, Eriksson S, et al. Homogeneous time-resolved IL-2-IL-2 R α assay using fluorescence resonance energy transfer. Cytokine 1998; 10:495–499.
81. Ferrer M, Zuck P, Kolodin G. Miniaturizable homogenous time-resolved fluorescence assay for carboxypeptidase B activity. Anal Biochem 2003; 317(1):94–98.
82. Gabourdes M, Bourgine V, Mathis G, et al. A homogeneous time-resolved fluorescence detection of telomerase activity. Anal Biochem 2004; 333(1):105–113.
83. Wang DY, Lu Q, Walsh SL, et al. Development of a high-throughput cell-based assay for 11beta-hydroxysteroid dehydrogenase type 1 using BacMam technology. Mol Biotechnol 2008; 39(2):127–134.
84. Gabriel D, Vernier M, Pfeifer MJ, et al. High throughput screening technologies for direct cyclic AMP measurement. Assay Drug Dev Technol 2003; 1(2):291–303.
85. Bergsdorf C, Kropp-Goerkis C, Kaehler I, et al. one-day, dispense-only IP-One HTRF assay for high-throughput screening of Galphaq protein-coupled receptors: towards cells as reagents. Assay Drug Dev Technol 2008; 6(1):39–53.
86. Hemmila I. Time-resolved fluorometry: Advantages and potentials. In: Devlin JP, ed. High Throughput Screening. New York, NY: Marcel Dekker, 1997:361–376.
87. Xu Y-Y, et al. Simultaneous quadruple-label flurometric immunoassay of thyroid stimulating hormone, 17α-hydroxyprogesterone, immunoreactive trypsin and creatine kinase MM isoenzyme in dried blood spots. Clin Chem 1992; 38:2038–2043.
88. Maiti S, Haupts U, Webb WW. Fluorescence correlation spectroscopy: Diagnostics for sparse molecules. Proc Natl Acad Sci U S A 1997; 94:11753–11757.
89. Lamb DC, Müller BK, Bräuchle C. Enhancing the sensitivity of fluorescence correlation spectroscopy by using time-correlated single photon counting. Curr Pharm Biotechnol 2005; 6(5):405–414.
90. Hwang LC, Wohland T. Recent advances in fluorescence cross-correlation spectroscopy. Cell Biochem Biophys 2007; 49(1):1–13.
91. Haustein E, Schwille P. Fluorescence correlation spectroscopy: Novel variations of an established technique. Annu Rev Biophys Biomol Struct 2007; 36:151–169.
92. Auer M, Moore KJ, Meyer-Almes FJ, et al. Fluorescence correlation spectroscopy: Lead discovery by miniaturized HTS. Drug Discov Today 1998; 3:457–465.
93. Finney NS. Fluorescence assays for screening combinatorial libraries of drug candidates. Curr Opin Drug Discov Dev 1998; 1:98–105.
94. Mitra RD, Silva CM, Youvan DC. Fluorescence resonance energy transfer between blue-emitting and red-shifted excitation derivatives of the green fluorescent protein. Gene 1996; 175:13–17.
95. Deo SK, Daunert S. Luminescent proteins from Aequorea Victoria: Applications in drug discovery and in high throughput analysis. Fresenius J Anal Chem 2001; 369(3–4):258–266.
96. Mere L, Bennet T, Coassin P, et al. Miniaturized FRET assays and microfluidics: Key components for ultra-high-throughput screening. Drug Discov Today 1999; 4:363–369.
97. Zlokarnik G, Negulescu PA, Knapp TE, et al. Quantitation of transcription and clonal selection of single living cells with β-lactamase as reporter. Science 1998; 279:84–88.
98. Robers MB, Machleidt T, Carlson CB, et al. Cellular LanthaScreen and β-lactamase reporter assay foor high-throughput screening of JAK2 inhibitors. Assay Drug Develop Technol 2008; 6(4):519–529.
99. Robers MB, Horton RA, Bercher MR, et al. High-throughput cellular assays for regulated posttranslational modifications. Anal Biochem 2008; 372:189–197.
100. Lang P, Yeow K, Nichols A, et al. Cellular imaging in drug discovery. Nat Rev 2006; 5:343–356.
101. Schroeder KS, Neagle BD. FLIPR: A new instrument for accurate high throughput optical screening. J Biomol Screen 1996; 1:75–80.
102. Giulliano KA, DeBiasio RL, Dunlay RT, et al. High-content screening: A new approach to easing key bottlenecks in the drug discovery process. J Biomol Screen 1997; 2:249–259.

103. Bowen WP, Wylie PG. Application of laser-scanning fluorescence microplate cytometry in high content screening. Assay Drug Dev Technol 2006; 4(2):209–224.
104. SW Paddock. Confocal laser scanning microscopy. BioTechniques 1999; 27:992–1004.
105. Zhang Y, Kowal D, Kramer A, et al. Evaluation of FLIPR calcium 3 assay kit—A new no-wash fluorescence calcium indicator reagent. J Biomol Screen 2003; 8:571–577.
106. Xin H, Zhang Y, Todd MJ, et al. Evaluation of no-wash calcium kits: Enabling tools for calcium mobilization. J Biomol Screen 2008; 12:705–714.
107. Wagstaff R, Hedrick M, Fan J, et al. High-throughput screening for nor epinephrine transporter inhibitors using the FLIPRTetra. J Biomol Scren 2007; 12(3):436–441.
108. Cassutt KJ, Orsini MJ, Abousleiman M, et al. Identifying nonselsctive hits from a homogeneous calcium assay screen. J Biomol Screen 2007; 12(2):285–287.
109. Miraglia S, Swartzman EE, Mellentin-Michelotti J, et al. Homogeneous cell and bead assays for high throughput screening using flurometric microvolume assay technology. J Biomol Screen 1999; 4:193–204.
110. Lee R, Tran M, Nocerini M. A high throughput hybridoma selection method using flurometric microvolume assay technology. J Biomol Screen 2008; 13(3):210–217.
111. Hitt E. Label-free methods are not problem free. Drug Discov Dev 2004, Sept:34–42.
112. Legay F, Albientz P, Ridder R. Bio-analytical applications of BIAcore, an optical sensor. In: Devlin JP, ed. High Throughput Screening. New York, NY: Marcel Dekker, 1997:443–454.
113. Salamon Z, Brown MF, Tollin G. Plasmon resonance spectroscopy: Probing molecular interactions within membranes. Trends Biochem Sci 1999; 24:213–219.
114. Willard FS, Sideroski DP. Covalent modification of histidine-tagged proteins for surface plasmon resonance. Anal Biochem 2006; 353:147–149.
115. Boozer C, Kim G, Cong S, et al. Looking towards label-free biomolecular interaction analysis in a high-throughput format: A review of new surface plasmon resonance technologies. Curr Opin Biotech 2006; 17:400–405.
116. Huber W, Mueller F. Biomolecular interaction analysis in drug discovery using surface plasmon resonance technology. Curr Pharm Des 2006; 12:3999–4021.
117. Gesellchen F, Zimmermann B, Herberg FW. Direct optical detection of protein–ligand interactions. Methods Mol Biol 2005; 305:17–46.
118. Bravman T, Bronner V, Lavie K, et al. Exploriing "one-shot" kinetics and small molecule analysis using the ProteON XPR6 array biosensor. Anal Biochem 2006; 358:281–288.
119. O'Malley SM, Xie X, Frutos AG. Label-free high-throughput functional lytic assays. J Biomol Screen 2007; 12(1):117–124.
120. Martin J. High-throughput optical-label-free in early drug discovery: From biomolecular interactions to cellular phenotypes. Am Drug Discov 2008; 3(4):12–20.
121. Cunnigham BT, Laing L. Microplate-based label-free detection of biomolecular interactions: applications in protemics. Expert Rev Proteomics 2006; 3(3):271–281.
122. Cunnigham BT, Li P, Schulz S, et al. Label-free assays on the BIND system. J Biomol Screen 2004; 9(6):481–490.
123. Giaever I, Keese CR. Monitoring fibroblast behavior in tissue culture with an applied elctric field. Proc Natl Acad Sci U S A 1984; 81:3761–3764.
124. Hug TJ. Biophysical methods for monitoringvcell–substrate interactions in drug discovery. Assay Drug Dev Technol 2003; 1(3):479–488.
125. Atienza JM, Yu N, Kirstein SL, et al. Dynamic and label-free cell-based assays using the real-time cell elctronic sensing system. Assay Drug Dev Technol 2006; 4(5):597–605.
126. ForteBio: http://www.fortebio.com/support_library.html.
127. Glamann J, Hansen AJ. Dynamic detection of natural killer cell-mediated cytotoxicity and cell adhesion by electrical impedance measurements. Assay Drug Dev Technol 2006; 4(5):597–605.
128. Solly K, Wang X, Xu X, et al. Application of real-time cell elctronnic sensing (RT-CES) technology to cell-based assays. Assay Drug Dev Technol 2004; 2(4):363–372.

129. Peters MT, Knappenberger KS, Wilkins D, et al. Evaluation of cellular dielectrric spectroscopy, a whole-cell, label-free technology for drug discovery on Gi-coupled GPCRs. J Biomol Screen 2007; 12(3):312–319.
130. Verdonk E, Johnson K, McGuinness R, et al. Cellular dielectric spectroscopy: A label-free comprehensive platform for functional evaluation of endogenous receptors. Assay Drug Dev Technol. 2006; 4(5):609–619.
131. Godber B, Frosley M, Rehaket al. Profiling of molecular interactions in real time using acoustic detection. Biosens Bioelectron 2007; 22(9–10):2382–2386.
132. Freyer MW, Lewis EA. Isothermal titration calorimetry: Experimental design, data analysis, and probing macromolecule/ligand binding and kinetic interactions. Methods Cell Biol 2008; 84:79–113.
133. Freire E. Do enthalpy and entropy distinguish first in class from best in class? Drug Discov Today 2008; 13(19–20):869–874.
134. Senisterra GA, Hong BS, Park H-W, et al. Application of high-throughput isothermal denaturation to assess protein stability and screen for ligands. J Biomol Screen 2008; 13(5):337–342.
135. Dittrich PS, Manz A. Lab-on-a-chip: Microfluidics in drug discovery. Nat Rev Drug Discov 2006; 5:210–218.
136. Perrin D, Fremaux C, Besson D, et al. A microfluidic-based mobility shift assay to discover new tyrosine phosphatase inhibitors. J Biomol Screen 2006; 11(8):996–1004.
137. Kingsmore SF. Multiplexed protein measurement: Technologies and applications of protein and antibody arrays. Nat Rev Drug Discov 2006; 5:310–321.
138. Ma H, Horiuchi KY, Wang Y, et al. Nanoliter homogeneous ultra-high throughput screening microarray for lead discoveries and IC50 profiling. Assay Drug Dev Technol 2005; 3(2):177–187.
139. Wu J, Barbero R, Vajjhala S, et al. Real-time analysis of enzyme kinetics via micro parallel liquid chromatography. Assay Drug Dev Technol 2006; 4(6):633–636.
140. Wu J, Vajjhala S, O'Connor S. A microPLC-based approach for determining kinase-substrate specificity. Assay Drug Dev Technol 2007; 5(4):559–566.
141. Paulik MA, Buckholz RG, Lancaster ME, et al. Development of infrader imaging to measure thermogenesis in cellculture: Thermogenic effects of uncoupling protein-2, troglitazone, and β-adrenoceptor agonists. Pharm Res 1998; 15:944–949.
142. Michalet X, Pinaud FF, Bentolila LA, et al. Quantum dots for live cells, in vivo imaging, and diagnostics. Science 2005; 307:538–544.
143. Pathak S, Cao E, Davidson MC, et al. Quantum dot applications to neuroscience: New Tools for probing neurons and glia. J Neurosci 2006; 26(7):1892–1895.
144. Ozkan M. Quantum dots and other nanoparticles: What can they offer to drug discovery? Drug Discov Today 2004; 9(24):1065–1071.
145. Medintz IL, Konnnert JH, Clapp AR, et al. A fluorescence resonance energy transfer-derived structure of a quantum dot-protein bioconjugate nanoassembly. Proc Natl Acad Sci U S A 2004; 101(26):9612–9617.
146. Gupta VK, Skaife JJ, Dubrovsky TB, et al. Optical amplification of ligand-receptor binding using liquid crystals. Science 1998; 279:2077–2080.
147. Cohen CB, Chin-Dixon E, Jeong S, et al. A microchip-based enzyme assay for protein kinase A. Anal Biochem 1999; 273:89–97.
148. Chiem NH, Harrison DJ. Monoclonal antibody binding affinity determined by microchip-based capillary electrophoresis. Electrophoresis 1998; 19:3040–3044.
149. Dolnik V, Liu S, Jovanovich S. Capillary electrophoresis on microchip. Electrophoresis 2000; 21:41–54.
150. Youdim KA, Lyons R, Payne L, et al. An automated, high-throuhput, 384well Cytochrome P450 cocktail IC50 assay using a rapid resolution LC-MS/MS end-point. J Pharm Biomed Anal 2008; 48(1):92–99.
151. Roddy TP, Horvath CR, Stout SJ, et al. Mass spectrometric techniques for label-free high-throughput screening in drug discovery. Anal Chem 2007; 79(21):8207–8213.

5 Proteomic Analysis in Drug Discovery

Haiteng Deng
Proteomics Resource Center, Rockefeller University, New York, New York, U.S.A.

Yang Xu
Center for Organelle Proteomics of Diseases, Zhejiang University School of Medicine, Hangzhou, and Center for Clinical Laboratory Development, Peking Union Medical College & Chinese Academy of Medical Sciences, Beijing, China

Linqi Zhang
Comprehensive AIDS Research Center, Tsinghua University AIDS Research Center, Institute of Pathogen Biology, Chinese Academy of Medical Sciences and Peking Union Medical College, Beijing, China, and Aaron Diamond AIDS Research Center, Rockefeller University, New York, New York, U.S.A.

INTRODUCTION

Proteins are the intermediaries between genetic codes and all forms of cellular activity. Analysis of the expression, interaction, and modification of proteins from a diseased population and preclinical experiments hold a great potential to provide insight into physiological and pharmacological mechanisms to accelerate systematic discovery of new drugs. The human proteome has been defined as all the proteins encoded in the human genome. The proteome differs from the genome in that the genome is relatively static, while the proteome is highly dynamic. The human genome encodes about 25,000 genes. The human proteome, however, presents a much deeper complexity as the result of alternative genomic splicing and posttranslational modifications (PTMs) of proteins (1–4). The human proteome also constantly changes in response to environmental stimuli and developmental instructions. Therefore, analysis of proteome is rather complex and challenging because proteins vary considerably in their physical, biochemical properties, and expression levels in addition to differently spliced variants and various PTMs. Over the last decade, the completion of the human genome project and advances in mass spectrometry and bioinformatics have made it possible to perform large-scale analysis of proteins from small amounts of biological samples. Despite many remaining technological challenges, the state of the technology allows reasonably comprehensive characterization of proteomes of biological samples including fluids, cells, and tissues from human and other model organisms. Mass spectrometry–based proteomics has evolved and become a systematic tool for studying diverse properties of individual proteins or a proteome (5–7). This has led to the generation of more comprehensive description of the differences between normal and diseased states and effects of drug treatment at the molecular level.

The process of drug discovery and development is rather complex and requires the integration of many disciplines. Key components of the drug discovery and development process include target identification and validation, lead design and optimization, and assessment of safety, toxicity, and efficacy of drug candidates (8–10). Proteomics that aims to characterize the protein changes from normal to diseased states and in responses to drug treatment holds the great promise to identify proteins that play important roles in disease initiation and progression and for understanding the underlying mechanism of treatments and toxicity (11–13). These proteins are potential biomarkers for early diagnosis and for assessment of drug efficacy and toxicity, as well as serving as potential targets for new therapeutic intervention (14–16). Libraries of small chemical compounds can be synthesized based on structural features of therapeutically targeted proteins. Subsequently, screening these compound libraries for drug leads can be achieved by targeted affinity mass spectrometry (TAMS) based on a combination of affinity chromatography and mass spectrometry (17–21). On the other hand, chemical proteomics uses derivatives of known drugs or drug candidates to screen for their cellular targets (22–25). These two-directional approaches have led to discovery of new drug leads and targets, and determination of drug efficacy and toxicity. Although it is still in its infancy, proteomics has great potential for acceleration of the current drug discovery process and will play an important role in the future health care program and personalized medicine.

MASS SPECTROMETRY–BASED PROTEOMIC ANALYSIS

Mass spectrometry (MS) has undergone revolutionary advances in recent years and has become the analytical tool of choice for a variety of research areas in drug discovery and development, ranging from drug metabolism to target identification. MS-based proteomics was established based on the development of the electrospray and MALDI ionization techniques that make biological molecules readily amenable to mass spectrometry (26–28). The most commonly used approach is the shotgun proteomics in which proteins are digested with trypsin, or other proteases, to generate peptide mixtures for subsequent analysis by MS.

Tandem Mass Spectrometry and Protein Identification

In routine shotgun proteomic analysis, protein mixtures are first separated by gel or liquid chromatography (LC)–based method followed by digestion with trypsin and other enzymes (29–31). The generated peptide mixture is then analyzed by a combination of nanoflow liquid chromatography and tandem mass spectrometry. Peptides are eluted from the stationary phase by using a linear gradient of organic solvents at a flow rate of 50 to 300 nL/min. The outlet of the nanocolumn is directly interfaced with a mass spectrometer. The amino acid sequence of the peptide ion can be determined by tandem mass spectrometry in which a peptide ion is isolated in the mass analyzer and subjected to dissociation to produce product ion fragments. A high-throughput method for searching the acquired MS/MS spectra has been pioneered by Yates (32,33), in which product ion spectra are directly compared with databases by cross-correlation analysis to identify the intact protein. This approach is especially suitable for searching the

data output comprising of tens of thousands of tandem mass spectra. Sequest and Mascot are the two most widely used searching algorithms (34).

As an alternative to gel- or LC-based protein separation, the elegant Multi-Dimensional Protein Identification Technology (MudPIT) has been established (35,36). In this approach, all proteins in a sample are digested directly into peptides without the prior gel- or LC-based separation. Generated peptide mixtures are analyzed by either a combination of a strong cation exchange (SCX) column and a reversed phase column in-line or a single column packed with two different separation matrices, both of which are interfaced directly with a mass spectrometer. Elution of peptides from the SCX column is achieved by step-increasing the concentration of the salt in the mobile phase to selectively elute classes of peptides binding to the SCX matrix. Each salt step is then followed by a reversed-phase chromatography, which separates those peptides according to their hydrophobicity. The eluents from the reversed-phase LC column is directly sprayed into a mass spectrometer capable of data-dependent data acquisition of MS/MS spectra. This technology allows a higher level of automation in sample handling, analysis, and data processing. The multiple-step elution and analysis result in the acquisition of hundreds to thousands of MS/MS fragmentation spectra for each individual sample. This approach is capable of identification of several thousands of proteins in a single sample including hydrophobic and membrane-spanning proteins.

The MS instrumentation used for these analyses is diverse. Ion trap has been the major mass analyzers for protein identification and characterization (37,38). An important characteristic of ion trap for protein identification is its mass spectrometer's data-dependent acquisition that isolates peptides as they elute and subjects them directly to collision-induced dissociation. Linear ion traps have a higher sensitivity than conventional 3D ion trap (39,40). The modest resolving power of ion trap instruments is offset by their ability to generate high-quality MS/MS spectra. The hybrid quadrupole-TOF, TOF-TOF, linear ion trap-Fourier-transform ion cyclotron resonance (LTQ-FT-ICR), and Orbitrap mass spectrometers that are capable of high resolution and precise measurement of the peptide masses greatly improve the confidence of assignment of peptide identity. TOF-TOF instruments typically use MALDI ionization. FT-ICR and Orbitrap mass spectrometers permit highly accurate peptide mass determination. The combination of accurate peptide mass measurement and chromatographic retention time has been used to identify a protein without MS/MS analysis (41).

Database-searching algorithms may create false-positive results because it always returns the best-matching peptide within the database for a given MS/MS spectrum. It is important to evaluate the reliability of peptide identities. Validation of peptides identified by database searching can be carried out by manual inspection and by searching proteotypic peptide sequence libraries (34). Libraries of proteotypic peptide sequences were compiled from the Global Proteome Machine Database for *Homo sapiens* and *Saccharomyces cerevisiae* model species proteomes. The cross-species protein sequence database searching can also be used to minimize the false-positive rate. To estimate the likelihood that a given protein could arise from a spurious random match, a decoy searching with a reversed database concatenated to the forward database has been used to estimate the rate of false-positive identification (42,43).

Quantitative Proteomics

The classical method for quantifying differentially expressed proteins in large-scale analysis of cellular extracts, biofluids, or tissues is two-dimensional (2D) polyacrylamide gel electrophoresis (2D PAGE), in which proteins are separated on a 2D gel and visualized by Coomassie Blue, Silver staining, or other methods. The spot density on the gel is used to assess relative quantification through comparison with "matched" protein spots on 2D gels run in parallel. However, the low reproducibility of 2D PAGE has limited its application. Difference gel electrophoresis (DiGE) is a modification of 2D PAGE in which two or three separate protein samples are labeled with different fluorescent dyes prior to separation. The labeled proteins are mixed and separated on the same 2D gel, enabling accurate analysis of differences in protein quantity between samples. The DiGE has an advantage over the classic 2D PAGE by elimination of gel-to-gel variation (44,45).

Because of the widely recognized limitations for 2D PAGE, MS-based quantitation methods have been developed and improved over the last several years. Isotope dilution methods including isotopic and isobaric labeling have enabled relative quantitation of proteins by mass spectrometry (46). The combination of shotgun approach and quantitative techniques has become the standard profiling tool for quantifying changes in protein expressions between samples from different cellular states (47–49). The major quantitation approaches include stable isotope labeling and label-free methods. The commonly used labeling methods are displayed in Figure 1, which include metabolic labeling such as stable isotope labeling by amino acids in cell culture (SILAC) (50,51), chemical labeling (52,53), and absolute quantitation (AQUA) strategy (54–56). Regardless of the method chosen for labeling, incorporation of the stable isotope atoms results in the separation of the same peptide in the mass spectrum and allows the intensities of the "heavy" and the "light" peptide to be compared and hence the relative quantity to be determined. It has found that deuterated peptides may elute out at different time from their counterparts in reversed-phase HPLC, and therefore the ^{13}C- and ^{15}N-based reagents are preferable. For metabolic labeling, growth and division of two cell populations are carried out in different media: one that contains a normal amino acid and the other with a heavy amino acid (50,51). Incorporation of the heavy amino acid into a peptide leads to a known mass shift compared with the peptide that contains the light version of the amino acid. For example, tryptic peptides from cells that are cultured in medium containing a "heavy" amino acid, ($^{13}C_6$)lysine will have 6 Da mass shift compared with the peptide from cells cultured in medium containing normal ($^{12}C_6$)lysine. This method is mainly applied to cell-based systems.

For in vitro labeling, chemically identical but isotopically distinct tags are used to covalently modify the peptide populations being compared (52,53). The labeling reaction can be carried out before or after proteolytic cleavage. The generated peptides are then pooled and analyzed in a single LC/MS or LC/MS/MS run. As the tags are chemically identical, the same peptides from both samples behave identically in terms of chromatographic time profile and ionization efficiency. Relative quantification is obtained by comparing the signal intensities of peptides with a defined, isotope-induced mass difference. Methods based on incorporating a "stable isotope" onto reactive amine groups and thiol groups have been established for relative quantification (46). Additionally, by performing the digestion in "heavy" water ($H_2{}^{18}O$), all tryptic peptides gain

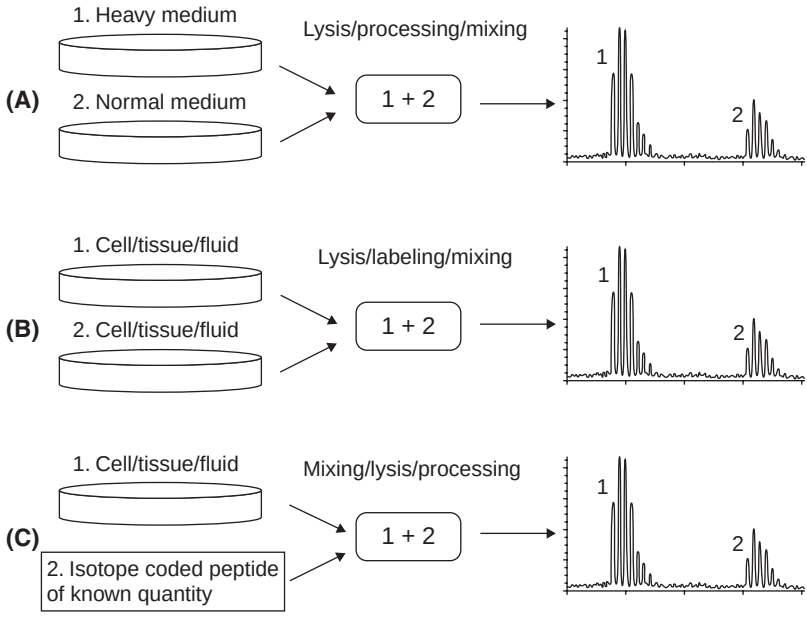

FIGURE 1 Isotope dilution methods in quantitative proteomics. Peptides from two different populations are quantified from ion intensities measured in mass spectra. (**A**) Metabolic labeling that uses normal medium and isotope-enriched medium for growth and division of two different cell populations. (**B**) Chemical labeling that uses light and heavy mass tag to chemically or enzymatically modify proteins or peptides from two different cellular populations. (**C**) Absolute quantitation by addition of a known quantity of a stable isotope-incorporated standard peptide to the sample of interest.

C-terminal ^{18}O, generating an apparent mass shift of 4 Da for relative quantitation (57). The amine-specific, multiplexed iTRAQ^{TM} (isobaric tags for relative and absolute quantitation) reagents have been widely applied to protein quantitation (58,59). The iTRAQ reagents allow analysis up to eight different biological samples simultaneously in a single experiment. The resulting peptide mixtures from different samples are labeled with the iTRAQ reagents. Upon completion of labeling, the samples are then combined and analyzed by LC/MS/MS or MudPIT. The intensity ratios of characteristic fragment ions are used for relative quantitation.

Absolute quantitation of proteins (AQUA) can be achieved by spiking a known quantity of an isotope-labeled synthetic peptide into the sample and subsequent comparison of the mass spectrometric signal to the endogenous peptide in the sample. Obviously, the choice of synthetic peptide standard is mostly determined empirically. However, a recent study suggests that it is possible to predict which of the protein's tryptic peptides will be most frequently observed for a given proteomic platform and thus can be used as a suitable quantification standard (60). High selectivity and sensitivity can be achieved by programming the triple quadrupole-based instrument to continuously monitor selected precursor to fragment ion transitions, which is termed as "selected reaction monitoring" (SRM) or "multiple reaction monitoring" (MRM). The combination of MRM and

AQUA increases the reliability of quantification by enhancing both the specificity and the accuracy of analysis by comparing signals from the exogenous isotopically labeled standards of known quantities and endogenous unlabeled species (61–63).

Label-free protein quantitation methods are a promising alternative (64–66). This method is based on comparison of the extracted ion current plotted over time or spectral count that represents the number of mass spectra identifying the same protein from two LC-MS analysis carried out under the identical experimental conditions. The major advantage of the label-free quantitation is that no labeling is needed. It has been demonstrated that mass spectral peak intensities of peptide ions correlate well with protein abundances in complex samples. An advantage of spectral counting is that relative abundances of different proteins in one sample can in principle be determined.

APPLICATION OF PROTEOMICS IN BIOMARKER DISCOVERY AND VALIDATION

Biomarkers are measurable surrogates, indicative of normal physiological or diseased status, or pharmacologic response to a therapeutic intervention (67,68). There are many types of biomarkers that are not only used as disease markers and surrogate endpoints, but they are also used to evaluate the toxicity, efficacy, and outcome of a drug treatment. The discovery of new biomarkers is often carried out by identifying the difference between samples from normal and disease stages or before and after treatment. It requires robust and high-throughout methods for simultaneous analysis of a large number of molecules from a small amount of sample. The combination of liquid chromatography (LC) separation, MS/MS, and sequence database searching has become the standard method for analysis of complex protein mixtures. Although there are no single platform that can satisfy all needs of biomarker discovery, the generic workflow for mass spectrometry–based protein profiling is displayed in Figure 2. In this workflow, samples from biological fluids, tissue, or cell extracts of two different populations are used to identify differences in protein expressions and modifications. Each step in this workflow is a complex process and needs to be carefully designed and optimized. The key aspects of application of MS-based proteomics in biomarker discovery will be reviewed and discussed in the following sections.

Research Design and Sample Preparation

Most biomarker studies have been carried out on samples from well-defined targeted and control populations (69). The sample includes biological fluids, and cell and tissue extracts. The projects have to be carefully designed based on the known disease mechanisms for selection of samples and workflow process. Sample preparation is a critical step for overall proteomic analysis. Well-prepared samples allow maximizing the detection of protein differences, while minimizing the sample number needed for analysis. The ideal samples should significantly differ from the control with respect to the condition of interest. In clinical studies, this can be done by using patients as their own controls, for example, before and after treatment. It is important to determine whether the sample must be collected in certain ways: if the sample will be collected in the fasting state or at a set time since some proteins exhibit significant circadian rhythm. Additives may affect measurements such as the anticoagulants used in serum and plasma

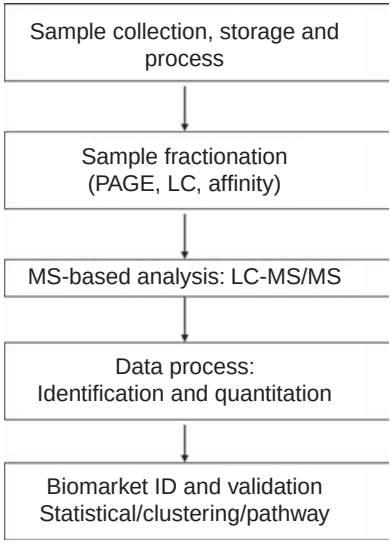

FIGURE 2 Workflow for biomarker discovery and validation. Samples from two populations, for example, healthy versus diseased or before and after therapeutic intervention are compared.

collection (70). Protein degradation is a major issue in sample preparation. One way to minimize protein degradation is by adding protease inhibitor cocktail (71). Acidic solution and heating have also been used to prevent protein degradation. Phosphatase inhibitors are used for preserving phosphorylated proteins. Short-and long-term storage conditions should be examined based on sample sources and analytic techniques.

Human plasma and serum are the most accessible and available biological material for disease diagnosis (72,73). However, the wide dynamic range in protein concentration has posed a major challenge in the development of diagnostic assays for identifying biomarkers in low abundance in the presence of high-abundance proteins. Albumin is the most abundant protein in serum and plasma and is present at 30 to 50 mg/mL concentration. In contrast, most of the potential biomarkers are secreted into the blood stream at low concentration. For example, cytokines and the prostate specific antigen (PSA) are present in the pg/mL levels. A practical and effective strategy is to remove most of the abundant proteins that are not diagnostically informative to enhance the detection sensitivity of the low-abundance proteins and to extend the coverage of the plasma proteome. The classical depletion strategy for albumin involves the use of the hydrophobic dye Cibacron blue (74,75). The immunoglobulins are the second most abundant proteins in the plasma or serum that can be removed by Protein A/G columns (76,77). Antibody affinity-based depletion methods have been used to remove 6 to 20 of the most abundant proteins, accounting for 98% to 99% of the total proteins in the plasma and serum (78–80). However, a limitation in these methods is that other proteins are concomitantly removed during depletion process due to nonspecific binding to the depleted proteins. A comparative study for comparing nondepleted serum and serum depleted of the six most abundant proteins has shown that some of the proteins were only found in the nondepleted serum (81). But nevertheless, the results strongly indicated that depletion of abundant proteins significantly increased the likelihood of identifying

minor protein components, which were otherwise undetectable in the nondepleted samples. Recently, a new method using hexapeptide library-bounded beads has been successfully applied to reduction of concentrations of high abundance proteins while enrichment of low abundance proteins for protein profiling and biomarker discovery (82).

Other biological fluids such as cerebral spinal fluid (CSF) (83,84), urine (85,86), saliva (87,88), interstitial fluid (89), amniotic fluid (90), follicular fluid, and platelet-derived microparticles in blood (91) have also been investigated for biomarker discovery. Among which, human saliva is an attractive biological fluid for disease diagnosis and prognosis because saliva testing is simple, safe, low cost, and noninvasive. Comprehensive analysis of the proteomic content in human whole saliva has identified more than 1000 proteins or their fragments secreted in saliva (92). Because composition of saliva temporally reflects the metabolic activity of the secretary proteins, saliva is therefore the potential source for development of clinical diagnosis (93). In addition, proteomic profiles of human tissues like the brain, heart, liver, lung, muscle, pancreas, spleen, and testis have been explored. Furthermore, protein profiling of disease models such as cell lines and genetically homogenous animals is important for testing the analytical methodology, screening for new biomarkers, and understanding the disease mechanism, and drug efficacy and toxicity.

Protein concentrations in the biological samples need to be determined before proteomic analysis (94,95). It remains a challenge to obtain the accurate measurement of protein concentrations because samples are frequently treated with urea, thiourea, and other reagents prior to proteomic analysis. A widely used method for measuring protein concentration is Bradford assay that uses the Coomasie Blue G250 for protein binding (96,97). Other useful methods include ninhydrin- and amido-black–based assays and fluorescence assay (98–100). Furthermore, proteomic analysis can be conducted on individual sample or pooled samples. This should be determined based on sample size as well as complexity. Analysis of pooled samples is not just for reducing the cost and complexity of data analysis, but also for minimizing biological variability. A study on liver proteomics demonstrated that the individual variations had no significant impact to the whole pool when more than seven samples were pooled (101). However, sample pooling will reduce the power of statistical comparison of changes between each individual samples and can result in a loss of information.

Protein Fractionation and Separation

The goal of biomarker discovery is to find proteins that are indicative of a disease or effectiveness of therapeutic intervention. These proteins are likely to be present in tissues and body fluids at relatively low abundance. The current technique is not able to characterize the complete proteome due to the limited dynamic range and detection sensitivity of mass spectrometry. For highly complex samples, protein separation and enrichment of target proteins are critical to detect low-abundance proteins and characterize biologically important differences. The more separation steps in the process, the more likely it will reveal low-abundant proteins. The commonly used separation strategies include gel electrophoresis and LC-based separation.

2D SDS PAGE combined with mass spectrometry is the classic method for profiling of protein expression from various samples (31,102,103). 2D SDS PAGE

provides the ability to resolve proteins from complex mixtures and visualize these components via gel staining. In this method, proteins are separated by their isoelectric point through a pH-gradient gel matrix (IPG) and then by molecular weight in the second dimension. The two-dimensional approach allows for separation of several thousand proteins. The protein spots of interest can be excised and analyzed by mass spectrometry. Generally speaking, the 2D gel electrophoresis approach is limited in sensitivity and can be inefficient when analyzing hydrophobic proteins or those with very high or low molecular weight. On the other hand, the combination of 1D gel electrophoresis and LC-MS/MS has become a powerful approach owing to facile separation of proteins on 1D SDS PAGE followed by the shotgun proteomic analysis (104). In this approach, proteins are first separated by size on standard polyacrylamide gels to reduce the complexity of a sample. After separation, the gel is removed and the lanes containing the sample of interest will be excised into a number of gel slices compatible with multiple sample handling procedures. The gel slices will then be treated with digestion enzymes and the generated peptides can be analyzed by LC-MS/MS. As the gel slices contain many different proteins that are digested into peptides, protein reassembly is required. One advantage of this workflow is that common 1D gel equipment are available to broad researchers and one gel can accommodate many samples.

An alternative to gel-based protein separation is to separate proteins with LC-based techniques (105). Various LC techniques have been used for separation of proteins, including size-exclusion, gel filtration, ion exchange, affinity chromatography, hydrophobic interaction chromatography, and reversed-phase chromatography. Selection of suitable LC-method is dependent on the characteristics of the target biomolecules to be separated including size, charge, hydrophobicity, function, or specific content. The advantages for LC-based separation include easy automation and large dynamic range. Different sizes of proteins have different elution volume and retention times in size exclusion chromatography. Affinity chromatography purifies biological molecules according to the specific interactions between their chemical or biological structure of the molecules and the suitable affinity ligand. Separation of proteins by ion-exchange chromatography based on the electrostatic interactions between the ion-exchange matrix and the proteins is an efficient method of purification of proteins, polypeptides, nucleic acids, polynucleotides, and other charged molecules. Reversed-phase chromatography separates biological molecules according to the hydrophobic interactions between the molecule and a chromatographic support matrix. High-resolution separation can be achieved by manipulating the nature of the sample buffer, the salt and salt concentrations, and solvents used for mobile phase. Conditions such as pH, temperature, the selection of salt, organic solvents, and addition of chaotropic agents have a significant effect on the resolution of the proteins. Recently, a combination of two or more chromatographic methods has been developed for separation of proteins at a higher resolving power. For example, the ProteomeLab PF 2D protein fractionation is able to separate thousands of proteins by pI-based chromatofocusing and hydrophobicity-based reversed-phase chromatography. In PF-2D, fractions from the first dimension are collected and automatically injected into a second dimension and separation generates both one- and two-dimensional maps of the expressed protein profiles (106,107).

Biomarker Identification and Validation

Shotgun proteomic analysis usually generates a list of proteins whose expressions have two fold or greater difference in two populations, for example, healthy versus diseased or before and after treatment. These differentially expressed proteins are candidate biomarkers. Differences in protein expression may come from the analytical and biological variation inherent to instruments and samples being studied. The significant protein variations among individuals were found in a recent study that demonstrated the extent of protein diversity in the human population and provided important information in clinical proteomics/biomarker studies (108). Clustering analysis reveals the most distinguishably changed proteins, and these proteins will be classified by gene ontology analysis into different functions including antioxidant, binding, enzyme, enzyme regulator, motor activity, signal transducer, transporter, and structural molecules, or are subjected to pathway analysis. This may provide important information for understanding the underlying mechanisms of pathogenesis and drug actions. The next critical step is to find a few proteins from this list that have performance characteristic to be developed into clinical assay. Validation of candidate biomarkers is carried out on a subset of qualified candidates. The selection is based on biological knowledge, marker performance, and reagent availability. Validation has been largely carried out by using antibody-based assays including ELISA, radioimmunoassay, or western blot (109,110).

In the case that antibodies against the newly discovered biomarker candidates are not available, verification by multiple reaction monitoring (MRM)/stable isotope dilution (SID) MS using a triple quadrupole mass spectrometer is an efficient alternative (111,112). MRM on the triple quadrupole mass analyzer has been fully used for developing MS-based methods for quantification of small-molecule drugs and analytes (113). MRM methods provide both structural specificity and quantitation of analyte concentration with enhanced sensitivity and linearity. In the MRM, experiments carried out on a triple quadrupole mass spectrometer, the precursor ion is selected with the first mass filter Q1, and fragmented in Q2 by collisions with a neutral gas. One of the resulting product ions of the selected precursor is mass selected and analyzed using the third quadrupole Q3. Only 10 to 30 ms is needed to survey each precursor–product transition, and 30 to 100 candidate biomarkers can be simultaneously targeted and measured. This enables high throughput and high multiplexing capability for analysis of a large number of samples required for biomarker verification and has a potential to be developed into a screening method for early diagnosis and assessment of drug efficacy and toxicity.

For quantification of low-abundance proteins, antipeptide antibodies are used to enrich for the signature peptides before MRM analysis (114,115). Immunoaffinity peptide enrichment improves both sensitivity and specificity, facilitating throughput by permitting analysis in complex matrices with little or no fractionation. This method has also been applied to study the cellular signaling network by monitoring 222 tyrosine phosphorylated peptides (116).

APPLICATION OF PROTEOMICS IN DRUG DISCOVERY AND DEVELOPMENT

Proteins differentially expressed in healthy and diseased populations are not only the potential biomarkers for early diagnosis, but they may also allow

construction of the cellular control circuitry to identify the potential targets for drug intervention. These targets can aid rational drug design to identify the potential low-molecular-weight binding partners through efficient structure–activity relationship studies. The in silico analysis can lead to design and synthesis of libraries of chemical compounds. Targeted affinity MS uses proteins of interest to screen for drug leads from a collection of small molecules and is an important tool for identification of promising drug candidates (17–21).

However, many identified drug candidates fail in the development due to their toxicity (12,16). A common mechanism of drug toxicity is bioactivation of drug molecules to form reactive metabolites. The reactive species modify proteins to disrupt their functions, cause cell and tissue death, and elicit immune response. Proteomic analysis has been applied to identification of the drug-induced changes in protein expressions and the reactive metabolite-modified proteins. It has a potential to play an important role for assessment of drug toxicity at the early stage of the drug development and for identification of toxicity markers.

Although protein profiling is an efficient method to identify changes of proteome in pathogenesis and in responses to drug treatment, it suffers from a number of limitations like identification of low abundance proteins and characterization of protein isoforms and modifications. Chemical proteomics focuses on a subset of proteome or a class of proteins that is isolated and purified by affinity chromatography. One application of chemical proteomics is to identify and characterize intracellular targets of low-molecular-weight chemical compounds. This is important since targets of a large number of drugs are unknown and their pharmacological mechanisms are not well understood. This strategy plays important roles for understanding the underlying pharmacological mechanisms of drug actions. The simplified workflow of applications of TAMS and chemical proteomics to drug discovery is displayed in Figure 3 and some examples will be discussed in the following sections.

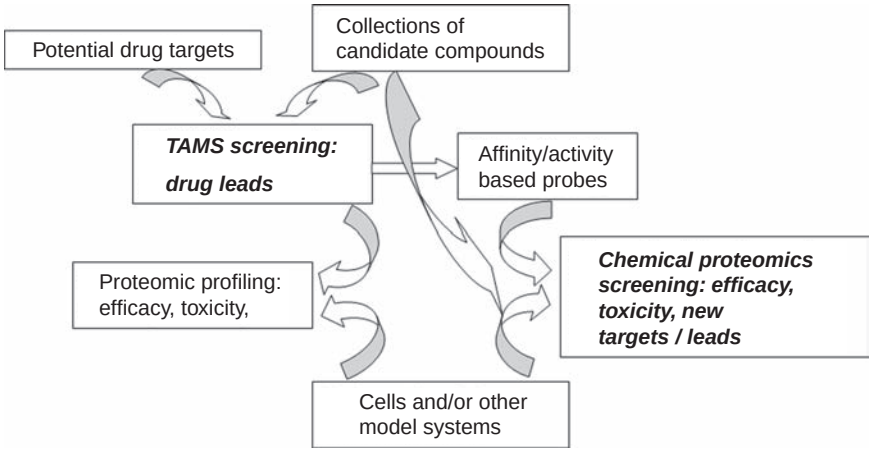

FIGURE 3 Role of proteomics in the drug discovery and development process.

Targeted Affinity Mass Spectrometry (TAMS) Screening for Drug Discovery

TAMS has many advantages in studying interactions of therapeutically important proteins and their ligands over the other detection methods. No labeling is needed for TAMS. TAMS has high sensitivity and specificity over a large mass range and provides both qualitative and quantitative information for protein–ligand interactions. In some cases, high-throughput screening can be achieved with TAMS. The key step in TAMS is the affinity selection to form the target–ligand complexes in solution phase or on a solid surface. MS can be used to directly detect complexes formed in solution. Electrospray ionization is the major method for detection of strongly bound noncovalent protein complexes or covalent complexes, such as those formed by fragment-based lead assembly (117). Enhanced sensitivity has been achieved with nanospray MS (118,119). The lead compound for the targeted protein can be identified by the mass shift or by tandem mass spectrometry. TAMS is able to screen for the low-molecular-weight binding partners for the single protein as well as multimeric protein complexes (120,121). However, this method is not applicable to weakly bound protein complexes that do not survive the transfer process from solution to the gas phase or complexes that are formed in solution with nonvolatile salts, complex buffers, or detergents.

Various methods have been developed for separating the target-bound protein complexes from the unbound compounds including size-exclusion chromatography (122), ultrafiltration (123,124), and gel permeation (125). Then, lead compounds from the bound complexes are eluted and analyzed by both MALDI- and ESI-mass spectrometry. With these screening methods, lead compounds against many therapeutically important molecules have been identified. The alternative approach for screening lead compounds uses immobilized proteins on a surface. Frontal affinity chromatography (FAC) was established for lead discovery, in which a set of ligands is passed through a column onto which a receptor has been immobilized (126–128). Potential ligands are continuously infused into the column, and the ligands are detected in the column effluent with different breakthrough volumes based on their interaction with an immobilized protein. MS is used to monitor a representative ion that elute at different breakthrough times in either MS or tandem MS mode. The frontal affinity chromatography MS enables ranking of ligand binding strength and K_d determinations of binder molecules. Up to 200 compounds can be screened in a single run and up to 10,000 compounds can be screened in 24 hours (126). Details of TAMS have been extensively reviewed in recent published literatures (17–21,126–128).

Proteomic Methods for Assessment of Drug Toxicity

One of difficulties in drug development is the adverse effect of drug toxicity. In many cases, drug toxicity forces candidate drugs to be abandoned late in the drug development process: in the preclinical phase on animal models or in clinical trials on human patients. New techniques for assessment of drug toxicity in the early stage of drug development are greatly needed. It is anticipated that development of proteomic technologies should facilitate a comprehensive understanding of the molecular mechanisms of drug toxicity and lead to better predictive models of toxicity for use in drug development. One factor contributing to

the drug toxicity is the covalent modification of proteins and other molecules by reactive drug metabolites. These reactive species may trigger specific signaling pathways, leading to cellular toxicity and stress responses. Protein profiling has been used to identify the differentially expressed proteins upon drug treatment. For example, 110 liver proteins were identified that displayed altered levels in mice following treatment with a candidate drug. These proteins were grouped in different functional categories, suggesting their involvement in the xenobiotic metabolism of drugs and in toxicity (129). Proteomic profiling was also used to study the toxicological effects of other drugs (130,131).

Upregulation of some metabolizing enzymes has been identified due to drug-induced oxidative stress or chemical modification of sensor proteins (132). Reactive intermediates are mainly produced by P450 enzymes that are the most important part of the primary drug metabolism pathway. Targets of reactive intermediates have been identified by a combination of radioisotope labeling and protein profiling. The early study identified 23 protein targets for acetaminophen reactive metabolites including cytosolic and mitochondrial proteins (133). This finding was consistent with the occurrence of mitochondrial dysfunction reported during the early stage of acetaminophen toxicity. A late study showed overdose of acetaminophen (APAP) causes severe centrilobular hepatic necrosis in humans and experimental animals and this toxicity was a direct action of its known reactive metabolite NAPQI, rather than a consequence of gene regulation (134). Protein profiling has been used to identify the potential biomarkers of drug toxicity from plasma and biles (135,136). LC-MS-MS analysis of bile from rats treated with the model hepatotoxin 1,1-dichloroethylene (DCE) revealed DCE-derived adducts on biliary proteins. Several toxicity biomarkers have been identified including alpha-glutathion S-transferase, thioredoxin, NF-κB (16). Studies with appropriate model systems and development of affinity capture methods for identification of reactive metabolite-modified proteins will help to define targets or pathways that are subject to modulation by drug candidates and to establish the prediction models of drug toxicity.

Chemical Proteomics in Target Discovery and Efficacy Evaluation

Determination of the in vivo selectivity of the lead compounds and identification of their intracellular targets constitute a prerequisite and a crucial step for drug development. This not only enhances understanding of underlying mechanisms of drug actions, but it also provides information for prediction of its potential efficacy and toxicity. Chemical proteomics based on a combination of affinity chromatography and MS has been developed to identify drug-targeted proteins and pathways. The key steps in chemical proteomics include derivation of a chemical compound of interest, affinity selection of targeted proteins from biological samples, and identification of targeted proteins by mass spectrometry. The sample preparation methods discussed in the previous section are also applicable to samples used for chemical proteomic analysis. The sample complexity should be reduced, and interfering substances and highly abundant proteins should be removed before proteomic analysis (24).

Identification of the drug targets can be carried out by the affinity- or activity-based chemical proteomics. In affinity-based chemical proteomic approach, a derivative of a compound of interest is synthesized that is suitable

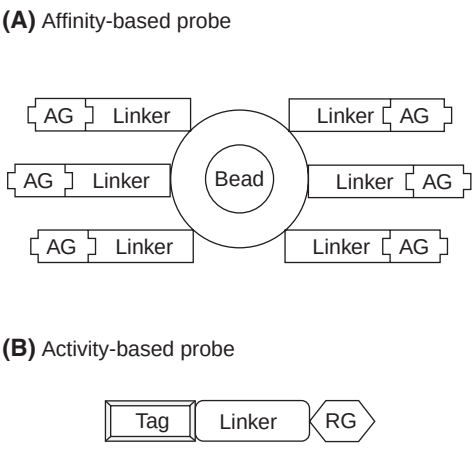

FIGURE 4 Structures of affinity- and activity-based probes. *Abbreviations*: AG, affinity group; RG, reactive group.

for affinity chromatography to isolate the interacting proteins. In most cases, noncovalent complexes are formed. The activity-based proteomics uses small molecules that can covalently attach to catalytic residues in an enzyme active site. The selectivity of the chemically reactive group allows distinct enzyme families to be tagged, purified, and analyzed. The affinity-based probe has three components: a linker, a spacer, and an affinity group as shown in Figure 4(A). The affinity group is the analogy of the drug or inhibitor molecule of interest that noncovalently binds to the targeted proteins. The spacer is used to eliminate the steric hindrance and it should not interfere with the biological activity of the drug molecule of interest. The linker can be an affinity tag like biotin, or a reactive group for immobilization on a surface. The affinity-based method has been widely applied for screening targets of kinase inhibitors. For example, a purine compound, (*R*)-roscovitine, has been found to inhibit cyclin-dependent kinases by competing with ATP at the ATP-binding site (137,138). Using (*R*)-roscovitine–linked Sepharose beads, several kinases were isolated and identified including CDK5, pp44MAPK/Erk1, p42<APK/Erk2, and pyridoxal kinase. For maximizing the binding efficiency and elimination of nonspecific binding, the length and hydrophobicity of the linker need to be optimized. A polyethylene glycol (PEG) has been frequently used as the spacer to link the lead compound with Sepharose beads. Other affinity beads for identification of drug receptors have also been developed, such as the latex beads composed of a glycidylmethacrylate and styrene copolymer (139).

Activity-based protein profiling (ABPP) has been developed to characterize a set of related enzymes for drug discovery and development (22,23,140). The activity-based probes (ABPs) also have three components: the tag, the affinity linker, and the reactive group as shown in Figure 4(B). Most reactive groups are electrophiles or photoreactive reagents that covalently modify the targeted enzymes. The affinity linkers have similar structures as mechanism-based inhibitors or affinity labeling reagents that direct the reactive group onto the active site of enzyme. The tag is used for identification or purification. The most commonly used tags are biotin, or a reporter that is fluorescent or radioactive.

ABPs have been successfully applied to identification of potential drug targets. For example, cysteine proteases that are important in apoptosis, cataract formation, and malarial infection have been identified by chemical proteomics (141–143). Furthermore, an ABP-based screening method for identification of small-molecule inhibitors of a specific enzyme target has also been established. Using a chemical probe DCG-04, a small library of inhibitors was screened for identification of the leading drug candidate for cathepsin proteases (144). A scheme of application of ABPs to assessment of drug efficacy has also been proposed (140).

The power of the combination of chemical proteomics and quantitative proteomics in drug discovery was demonstrated in a recent publication (145,146). The kinobeads onto which a mixture of seven kinase inhibitors was immobilizd have been used to screen for their targeted kinases from multiple cell lines and tissues. A total of 307 kinases were identified, indicating the broad selectivity of kinobeads. By pretreating cells or cell lysates with three selected kinase inhibitors at varying concentrations before incubation with the kinobeads, their targets and binding affinities were identified and determined based on quantitative proteomics. The discoidin domain receptor 1 (DDR1) was identified as the new kinase target, and NADPH-dependent oxidoreductase (NQO2) was identified as a nonkinase target of imatinib. Using iTRAQ labeling and mass spectrometric quantitation, IC_{50} values were determined for each target protein of each of the three kinase inhibitors based on the competing binding of kinase to kinbeads and the selected inhibitors over nine different concentrations. This technique represents the state of the art of proteomic approach in drug discovery and development. Improvements in targeted affinity enrichments and the sensitivity of the MS methods will lead to the detection and quantification of more targets at lower abundance. This technique can be applied for other protein classes of interest, such as phosphatases, proteases, and lipase.

CONCLUSION AND PROSPECTS

Proteomic analysis has proven its value to be a powerful approach for biomarker and drug discovery and development. Proteomic approach will play more important role in all areas of drug discovery, from target identification to assessment of drug efficacy and toxicity in preclinical and clinical situations. Advances in instrumentation for achieving larger dynamic range and higher sensitivity will enable a deeper and more complete measurement of the proteome to fulfill the promise of proteomics in delivering clinically significant results. It is expected that arrays of biomarkers for diagnosis of various diseases and for assessment of drug efficacy and toxicity will be discovered in the near future that will open a new avenue for high-throughput drug screening. The advancement and development of proteomics-based technologies will ultimately fulfill our quest for safer, more effective, more cost-effective, and more personalized medicines.

ACKNOWLEDGMENTS

Great appreciation is expressed to Dr. Chandramouli and Fernandez of the Rockefeller University for critically reading the manuscript and offering many helpful suggestions.

REFERENCES

1. International Human Genome Sequencing Consortium. Finishing the euchromatic sequence of the human genome. Nature 2004; 431:931–945.
2. Brett D, Pospisil H, Valcarcel J, et al. Alternative splicing and genome complexity. Nat Genet 2002; 30:29–30.
3. Modrek B, Lee C. A genomic view of alternative splicing. Nat Genet 2002; 30:13–19.
4. Creasy DM, Cottrell JS. Unimod: Protein modifications for mass spectrometry. Proteomics 2004; 4:1534–1536.
5. Patterson SD, Aebersold RH. Proteomics: The first decade and beyond. Nat Genet 2003; 33(Suppl):311–323.
6. Yates JR III. Mass spectrometry. From genomics to proteomics. Trends Genet 2000; 16:5–8.
7. Cox J, Mann M. Is proteomics the new genomics? Cell 2007; 130:395–398.
8. Terstappen GC, Schlüpen C, Raggiaschi R, et al. Target deconvolution strategies in drug discovery. Nat Rev Drug Discov 2007; 6(11):891–903.
9. Egner U, Krätzschmar J, Kreft B, et al. The target discovery process. Chem Biochem 2005; 6(3):468–479.
10. Sams-Dodd F. Target-based drug discovery: Is something wrong? Drug Discov Today 2005; 10:139–147.
11. Stoughton RB, Friend SH. How molecular profiling could revolutionize drug discovery. Nat Rev Drug Discov 2005; 4:345–350.
12. Ulrich R, Friend SH. Toxicogenomics and drug discovery: Will new technologies help us produce better drugs? Nat Rev Drug Discov 2002; 1:84–88.
13. Hong ML, Jiang N, Gopinath S, et al. Proteomics technology and therapeutics. Clin Exp Pharmacol Physiol 2006; 33(5–6):563–568.
14. Hanash S. Disease proteomics. Nature 2003; 422(6928):226–232.
15. Rifai N, Gillette MA, Carr SA. Protein biomarker discovery and validation: The long and uncertain path to clinical utility. Nat Biotechnol 2006; 24:971–983.
16. Liebler DC, Guengerich FP. Elucidating mechanisms of drug-induced toxicity. Nat Rev Drug Discov 2005; 4(5):410–420.
17. Zehender H, Mayr LM. Application of high-throughput affinity selection mass spectrometry for screening of chemical compound libraries in lead discovery. Expert Opin Drug Discov 2007; 2:285–294.
18. Deng G, Sanyal G. Application of mass spectrometry in early stages of target based drug discovery. J Pharm Biomed Anal 2005; 40:528–538.
19. Zehender H, Mayr LM. Application of mass spectrometry technologies for the discovery of low-molecular weight modulators of enzymes and protein–protein interactions. Curr Opin Chem Biol 2007; 11(5):511–517.
20. Hofstadler SA, Sannes-Lowery KA. Applications of ESI-MS in drug discovery: Interrogation of noncovalent complexes. Nat Rev Drug Discov 2006; 5:585–595.
21. Annis DA, Nickbarg E, Yang X, et al. Affinity selection-mass spectrometry screening techniques for small molecule drug discovery. Curr Opin Chem Biol 2007; 11(5):518–526.
22. Barglow KT, Cravatt BF. Activity-based protein profiling for the functional annotation of enzymes. Nat Methods 2007; 4(10):822–827.
23. Campbell DA, Szardenings AK. Functional profiling of the proteome with affinity labels. Curr Opin Chem Biol 2003; 7(2):296–303.
24. Opiteck GJ, Scheffler JE. Target class strategies in mass spectrometry-based proteomics. Expert Rev Proteomics 2004; 1(1):57–66.
25. Hopf C, Bantscheff M, Drewes G. Pathway proteomics and chemical proteomics team up in drug discovery. Neurodegener Dis 2007; 4(2–3):270–280.
26. Fenn JB, Mann M, Meng CK, et al. Electrospray ionization for mass spectrometry of large biomolecules. Science 1989; 246:64–71.
27. Karas M, Hillenkamp F. Laser desorption ionization of proteins with molecular masses exceeding 10000 daltons. Anal Chem 1988; 60:2299–2301.

28. Tanaka K, Ido Y, Akita S, et al. Detection of high mass molecules by laser desorption time-of-flight mass spectrometry. In: Matsuda H, Xiao-Tian L, eds. Proceedings of 2nd Japan–China Joint Symposium on Mass Spectrometry, Osaka, Japan, 1987:185–188.
29. Aebersold R, Mann M. Mass spectrometry-based proteomics. Nature 2003; 422:198–207.
30. Chait BT. Chemistry: Mass spectrometry: Bottom-up or top-down? Science 2006; 314:65–66.
31. Gygi SP, Corthals GL, Zhang Y, et al. Evaluation of two-dimensional gel electrophoresis-based proteome analysis technology. Proc Natl Acad Sci U S A 2000; 97:9390–9395.
32. McCormack AL, Schieltz DM, Goode B, et al. Direct analysis and identification of proteins in mixtures by LC/MS/MS and database searching at the low-femtomole level. Anal Chem 1997; 69:767–776.
33. Eng JK, McCormack AL, Yates JR III. An approach to correlate tandem mass spectral data of peptides with amino acid sequences in a protein database. J Am Soc Mass Spectrom 1994; 5:976–989.
34. Nesvizhskii AI, Vitek O, Aebersold R. Analysis and validation of proteomic data generated by tandem mass spectrometry. Nat Methods 2007; 4(10):787–797.
35. Link AJ, Eng J, Schieltz DM, et al. Direct analysis of protein complexes using mass spectrometry. Nat Biotechnol 1999; 17:676–682.
36. Wolters DA, Washburn MP, Yates JR III. An automated multidimensional protein identification technology for shotgun proteomics. Anal Chem 2001; 73:5683–5690.
37. Syka JE, Coon JJ, Schroeder MJ, et al. Peptide and protein sequence analysis by electron transfer dissociation mass spectrometry. Proc Natl Acad Sci U S A 2004; 101(26):9528–9533.
38. Qin J, Chait BT. Identification and characterization of posttranslational modifications of proteins by MALDI ion trap mass spectrometry. Anal Chem 1997; 69(19):4002–4009.
39. Schwartz JC, Senko MW, Syka JE. A two-dimensional quadrupole ion trap mass spectrometer. J Am Soc Mass Spectrom 2002; 13(6):659–669.
40. Douglas DJ, Frank AJ, Mao D. Linear ion traps in mass spectrometry. Mass Spectrom Rev 2005; 24(1):1–29.
41. Liu T, Belov ME, Jaitly N, et al. Accurate mass measurements in proteomics. Chem Rev 2007; 107(8):3621–3653.
42. Benjamini Y, Hochberg Y. Controlling the false discovery rate—A practical and powerful approach to multiple testing. J R Stat Soc Ser B. Methodol 1995; 57:289–300.
43. Elias JE, Gygi SP. Target-decoy search strategy for increased confidence in large-scale protein identifications by mass spectrometry. Nat Methods 2007; 4:207–214.
44. Unlu M, Morgan ME, Minden JS. Difference gel electrophoresis: A single gel method for detecting changes in protein extracts. Electrophoresis 1997; 18;2071–2077.
45. Kondo T, Hirohashi S. Application of highly sensitive fluorescent dyes (CyDye DIGE Fluor saturation dyes) to laser microdissection and two-dimensional difference gel electrophoresis (2D-DIGE) for cancer proteomics. Nat Protoc 2006; 1:2940–2956.
46. Ong SE, Mann M. Mass spectrometry-based proteomics turns quantitative. Nat Chem Biol 2005; 1(5):252–262.
47. Zhou H, Boyle R, Aebersold R. Quantitative protein analysis by solid phase isotope tagging and mass spectrometry. Methods Mol Biol 2004; 261:511–518.
48. Chelius D, Bondarenko PV. Quantitative profiling of proteins in complex mixtures using liquid chromatography and mass spectrometry. J Proteome Res 2002; 1:317–323.
49. Jin M, Bateup H, Padovan JC, et al. Quantitative analysis of protein phosphorylation in mouse brain by hypothesis-driven multistage mass spectrometry. Anal Chem 2005; 77(24):7845–7851.
50. Oda Y, Huang K, Cross FR, et al. Accurate quantitation of protein expression and site-specific phosphorylation. Proc Natl Acad Sci U S A 1999; 96:6591–6596.

51. Ong SE, Mann M. A practical recipe for stable isotope labeling by amino acids in cell culture (SILAC). Nat Protoc 2006; 1(6):2650–2660.
52. Munchbach M, Quadroni M, Miotto G, et al. Quantitation and facilitated *de novo* sequencing of proteins by isotopic N-terminal labeling of peptides with a fragmentation-directing moiety. Anal Chem 2000; 72:4047–4057.
53. Regnier FE, Julka S. Primary amine coding as a path to comparative proteomics. Proteomics 2006; 6(14):3968–3979.
54. Stemmann O, Zou H, Gerber SA, et al. Dual inhibition of sister chromatid separation at metaphase. Cell 2001; 107:715–726.
55. Kuhn E, Wu J, Karl J, et al. Quantification of C-reactive protein in the serum of patients with rheumatoid arthritis using multiple reaction monitoring mass spectrometry and ^{13}C-labeled peptide standards. Proteomics 2004; 4:1175–1186.
56. Gerber SA, Rush J, Stemman O, et al. Absolute quantification of proteins and phosphoproteins from cell lysates by tandem MS. Proc Natl Acad Sci U S A 2003; 100:6940–6945.
57. Yao X, Freas A, Ramirez J, et al. Proteolytic ^{18}O labeling for comparative proteomics: Model studies with two serotypes of adenovirus. Anal Chem 2001; 73:2836–2842.
58. Ross PL, Huang YN, Marchese JN, et al. Multiplexed protein quantitation in Saccharomyces cerevisiae using amine-reactive isobaric tagging reagents. Mol Cell Proteomics 2004; 3(12):1154–1169.
59. Aggarwal K, Choe LH, Lee KH. Shotgun proteomics using the iTRAQ isobaric tags. Brief Funct Genomic Proteomic 2006; 5(2):112–120.
60. Mallick P, Schirle M, Chen SS, et al. Computational prediction of proteotypic peptides for quantitative proteomics. Nat Biotechnol 2007; 25(1):125–131.
61. Anderson L, Hunter CL. Quantitative mass spectrometric MRM assays for major plasma proteins. Mol Cell Proteomic 2006; 5:573–588.
62. Unwin RD, Griffiths JR, Leverets MK, et al. Multiple reaction monitoring to identify sites of protein phosphorylation with high sensitivity. Mol Cell Proteomics 2005; 4(8):1134–1144.
63. Barnidge D, Goodmanson M, Klee G, et al. Absolute quantification of the model biomarker prostate-specific antigen in serum by LC-MS/MS using protein cleavage and isotope dilution MS. J Proteome Res 2004; 3:644–652.
64. Old WM, Meyer-Arendt K, Aveline-Wolf L, et al. Comparison of label-free methods for quantifying human proteins by shotgun proteomics. Mol Cell Proteomics 2005; 4(10):1487–1502.
65. Wang W, Zhou H, Lin H, et al. Quantification of proteins and metabolites by mass spectrometry without isotopic labeling or spiked standards. Anal Chem 2003; 75:4818–4826.
66. Jin S, Daly DS, Springer DL, et al. The effects of shared peptides on protein quantitation in label-free proteomics by LC/MS/MS. J Proteome Res 2008 Jan; 7(1):164–169.
67. Baker M. In biomarkers we trust? Nat Biotechnol 2005; 23(3):297–304.
68. Frank R, Hargreaves R. Clinical biomarkers in drug discovery and development. Nat Rev Drug Discov 2003; 2(7):566.
69. Vitzthum F, Behrens F, Anderson NL, et al. Proteomics: From basic research to diagnostic application. A review of requirements and needs. J Proteome Res 2005; 4(4):1086–1097.
70. Evans MJ, Livesey JH, Ellis MJ, et al. Effect of anticoagulants and storage temperatures on stability of plasma and serum hormones. Clin Biochem 2001; 34(2):107–112.
71. Castellanos-Serra L, Paz-Lago D. Inhibition of unwanted proteolysis during sample preparation: Evaluation of its efficiency in challenge experiments. Electrophoresis 2002; 23(11):1745–1753.
72. Anderson NL, Anderson NG. The human plasma proteome: History, character, and diagnostic prospects. Mol Cell Proteomics 2002; 1(11):845–867.

73. Anderson N, Polanski M, Pieper R, et al. The human plasma proteome: A nonredundant list developed by combination of four separate sources. Mol Cell Proteomics 2004; 3:311–316.
74. Travis J, Bowen J, Tewksbury D, et al. Isolation of albumin from whole human plasma and fractionation of albumin-depleted plasma. Biochem J 1976; 157:301–306.
75. Travis J, Pannell R. Selective removal of albumin from plasma by affinity chromatography. Clin Chim Acta 1973; 49:49–52.
76. Bjorck L, Kronvall D. Analysis of bacterial cell wall proteins and human serum proteins bound to bacterial cell surfaces. Acta Pathol Microbiol Scand B 1981; 89:1–6.
77. Guss B, Eliasson M, Olsson A, et al. Structure of the IgG-binding regions of streptococcal protein G. EMBO J 1986; 5:1567–1575.
78. Pieper R, Su Q, Gatlin CL, et al. Multi-component immunoaffinity subtraction chromatography: An innovative step towards a comprehensive survey of the human plasma proteome. Proteomics 2003; 3(4):422–432.
79. Tirumalai RS, Chan KC, Prieto DA, et al. Characterization of the low molecular weight human serum proteome. Mol Cell Proteomics 2003; 2:1096–1103.
80. Schuchard MD, Melm CD, Crawford AS, et al. Immunoaffinity depletion of 20 high abundance human plasma proteins. Removal of approximately 97% of total plasma protein improves identification of low abundance proteins. Origins 2005; 21:17–23.
81. Yocum AK, Yu K, Oe T, et al. Effect of immunoaffinity depletion of human serum during proteomic investigations. J Proteome Res 2005; 4(5):1722–1731.
82. Guerrier L, Righetti PG, Boschetti E. Reduction of dynamic protein concentration range of biological extracts for the discovery of low-abundance proteins by means of hexapeptide ligand library. Nat Protoc 2008; 3(5):883–890.
83. Pan S, Zhu D, Quinn JF, et al. A combined dataset of human cerebrospinal fluid proteins identified by multi-dimensional chromatography and tandem mass spectrometry. Proteomics 2007; 7(3):469–473.
84. Pasinetti GM, Ungar LH, Lange DJ, et al. Identification of potential CSF biomarkers in ALS. Neurology 2006; 66:1218–1222.
85. Thongboonkerd V. Practical points in urinary proteomics. J Proteome Res 2007; 6(10):3881–3890.
86. Hortin GL, Sviridov D. Diagnostic potential for urinary proteomics. Pharmacogenomics 2007; 8(3):237–255.
87. Hu S, Loo JA, Wong DT. Human saliva proteome analysis. Ann N Y Acad Sci 2007; 1098:323–329.
88. Helmerhorst EJ, Oppenheim FG. Saliva: A dynamic proteome. J Dent Res 2007; 86(8):680–693.
89. Magi B, Bargagli E, Bini L, et al. Proteome analysis of bronchoalveolar lavage in lung diseases. Proteomics 2006; 6(23):6354–6369.
90. Hampton T. Comprehensive "proteomic profile" of amniotic fluid may aid prenatal diagnosis. JAMA 2007; 298:1751.
91. Smalley DM, Root KE, Cho H, et al. Proteomic discovery of 21 proteins expressed in human plasma-derived but not platelet-derived microparticles. Thromb Haemost 2007; 97(1):67–80.
92. Fang X, Yang L, Wang W, et al. Comparison of electrokinetics-based multidimensional separations coupled with electrospray ionization-tandem mass spectrometry for characterization of human salivary proteins. Anal Chem 2007; 79:5785–5792.
93. Malamud D. Salivary diagnostics: The future is now. J Am Dent Assoc 2006; 137(3):284–286.
94. Ramagli LS, Rodriguez LV. Quantitation of microgram amounts of protein in two-dimensional polyacrylamide gel electrophoresis sample buffer. Electrophoresis 1985; 6:559–563.
95. de St SF, Webster RG, Datyner A. Two new staining procedures for quantitative estimation of proteins on electrophoretic strips. Biochim Biophys Acta 1963; 71: 377–391.

96. Bradford MM. A rapid and sensitive method for the quantitation of microgram quantities of protein utilizing the principle of protein–dye binding. Anal Biochem 1976; 72:248–254.
97. Diezel W, Kopperschläger G, Hofmann E. An improved procedure for protein staining in polyacrylamide gels with a new type of Coomassie Brilliant Blue. Anal Biochem 1972; 48(2):617.
98. Schaffner W, Weissman C. A rapid, sensitive, and specific method of the determination of protein in dilute solution. Anal Biochem 1973; 56:502–514.
99. Stephenson JR, Jones MA. Advancement in fluorescent detection of protein following electrophoresis. Anal Biochem 2005; 346(2):342–343.
100. Agnew BJ, Murray D, Patton WF. A rapid solid-phase fluorescence-based protein assay for quantitation of protein electrophoresis samples containing detergents, chaotropes, dyes, and reducing agents. Electrophoresis 2004; 25(15):2478–2485.
101. Zhang X, Guo Y, Song Y, et al. Proteomic analysis of individual variation in normal livers of human beings using difference gel electrophoresis. Proteomics 2006; 6(19):5260–5268.
102. O'Farrell PH. High resolution two-dimensional electrophoresis of proteins. J Biol Chem 1975; 250:4007.
103. Bjellqvist K, Ek PG, Righetti E, et al. Isoelectric focusing in immobilized pH gradients: Principle, methodology and some applications. J Biochem Biophys Methods 1982; 6:317.
104. Breci L, Hattrup E, Keeler M, et al. Comprehensive proteomics in yeast using chromatographic fractionation, gas phase fractionation, protein gel electrophoresis, and isoelectric focusing. Proteomics 2005; 5:2018.
105. Neverova I, Van Eyk JE. Role of chromatographic techniques in proteomic analysis. J Chromatogr B Analyt Technol Biomed Life Sci 2005; 815(1–2):51–63.
106. Barré O, Solioz M. Improved protocol for chromatofocusing on the ProteomeLab PF2D. Proteomics 2006; 6(19):5096–5098.
107. Levreri I, Musante L, Petretto A, et al. Separation of human serum proteins using the Beckman-Coulter PF2D system: Analysis of ion exchange-based first dimension chromatography. Clin Chem Lab Med 2005; 43(12):1327–1333.
108. Nedelkov D, Kiernan UA, Niederkofler EE, et al. Investigating diversity in human plasma proteins. Proc Natl Acad Sci U S A 2005; 102(31):10852–10857.
109. Kingsmore SF. Multiplexed protein measurement: Technologies and applications of protein and antibody arrays. Nat Rev Drug Discov 2006; 5:310–320.
110. Thomson DMP, Krupey J, Freedman SO, et al. The radioimmunoassay of circulating carcinoembryonic antigen of the human digestive system. Proc Natl Acad Sci U S A 1969; 64(1):161–167.
111. Desiderio D, Kai M, Tanzer F, et al. Measurement of enkephalin peptides in canine brain regions, teeth, and CSF with HPLC and mass spectrometry. J Chromatogr 1984; 297:245–260.
112. Barr J, Maggio VL, Patterson DG Jr, et al. Isotope-dilution mass spectrometric quantification of specific proteins: Model application with apolipoprotein A-1. Clin Chem 1996; 42:1676–1682.
113. Roschinger W, Olgemoller B, Fingerhut R, et al. Advances in analytical mass spectrometry to improve screening for inherited metabolic diseases. Eur J Pediatr 2003; 162:S67–S76.
114. Anderson NL, Anderson NG, Haines LR, et al. Mass spectrometric quantitation of peptides and proteins using stable isotope standards and capture by anti-peptide antibodies (SISCAPA). J Proteome Res 2004; 3:235–244.
115. Whiteaker JR, Zhao L, Zhang HY, et al. Antibody-based enrichment of peptides on magnetic beads for mass-spectrometry-based quantification of serum biomarkers. Anal Biochem 2007; 362(1):44–54.
116. Wolf-Yadlin A, Hautaniemi S, Lauffenburger DA, et al. Multiple reaction monitoring for robust quantitative proteomic analysis of cellular signaling networks. Proc Natl Acad Sci U S A 2007; 104(14):5860–5865.

117. Erlanson DA, Hansen SK. Making drugs on proteins: Site directed ligand discovery for fragment-based lead assembly. Curr Opin Chem Biol 2004; 8:399–406.
118. Zhang S, Van Pelt CK, Wilson WD. Quantitative determination of noncovalent binding interactions using automated nanoelectrospray mass spectrometry. Anal Chem 2003; 75:3010–3018.
119. Benkestock K, Van Pelt CK, Akerud T, et al. Automated nano-electrospray mass spectrometry for protein-ligand screening by noncovalent interaction applied to human H-FABP and A-FABP. J Biomol Screen 2003; 8:247–256.
120. Cheng X, Chen R, Bruce JE, et al. Using electrospray ionization FTICR mass spectrometry to study competitive binding of inhibitors to carbonic anhydrase. J Am Chem Soc 1995; 117:8859–8860.
121. McCammon MG, Scott DJ, Keetch CA, et al. Screening transthyretin amyloid fibril inhibitors: Characterization of novel multiprotein, multiligand complexes by mass spectrometry. Structure 2002; 10:851–863.
122. Annis DA, Athanasopoulos J, Curran PJ, et al. An affinity selection-mass spectrometry method for the identification of small molecule ligands from self-encoded combinatorial libraries: Discovery of a novel antagonist of *E. coli* dihydrofolate reductase. Int J Mass Spectrom 2004; 238:77–83.
123. Comess KM, Schurdak ME. Affinity-based screening techniques for enhancing lead discovery. Curr Opin Drug Discov Devel 2004; 7:411–416.
124. Cloutier TE, Comess KM. Library screening using ultrafiltration and mass spectrometry. In: Wanner K, Hofner G, ed. Mass Spectrometry in Medicinal Chemistry. Wiley-VCH, Weinheim 2007:157–184.
125. Siegel MM. Drug screening using gel permeation chromatography spin columns coupled with ESI-MS. In: Wanner K, Hofner G, ed. Mass Spectrometry in Medicinal Chemistry. Wiley-VCH, Weinheim 2007:65–120.
126. Slon-Usakiewicz JJ, Ng W, Dai JR, et al. Frontal affinity chromatography with MS detection (FAC-MS) in drug discovery. Drug Discov Today 2005; 10(6):409–416.
127. Zhu L, Chen L, Luo H, et al. Frontal affinity chromatography combined on-line with mass spectrometry: A tool for the binding study of different epidermal growth factor receptor inhibitors. Anal Chem 2003; 75:6388–6393.
128. Besanger TR, Hodgson RJ, Guillon D, et al. Monolithic membrane-receptor columns: Optimization of column performance for frontal affinity chromatography/mass spectrometry applications. Anal Chim Acta 2006; 561:107–118.
129. Nordvarg H, Flensburg J, Rönn O, et al. A proteomics approach to the study of absorption, distribution, metabolism, excretion, and toxicity. J Biomol Tech 2004; 15(4):265–275.
130. Bandara LR, Kelly MD, Lock EA, et al. A correlation between a proteomic evaluation and conventional measurements in the assessment of renal proximal tubular toxicity. Toxicol Sci 2003; 73:195–206.
131. Ishimura R, Ohsako S, Kawakami T, et al. Altered protein profile and possible hypoxia in the placenta of 2,3,7,8-tetrachlorodibenzop-dioxin-exposed rats. Toxicol Appl Pharmacol 2002; 185:197–206.
132. Kaplowitz N. Drug-induced liver injury. Clin Infect Dis 2004; 38(Suppl 2):S44–S48.
133. Qiu Y, Benet LZ, Burlingame AL. Identification of the hepatic protein targets of reactive metabolites of acetaminophenin in vivo in mice using two-dimensional gel electrophoresis and mass spectrometry. J Biol Chem 1998; 273:17940–17953.
134. Ruepp SU, Tonge RP, Shaw J, et al. Genomics and proteomics analysis of acetaminophen toxicity in mouse liver. Toxicol Sci 2002; 65:135–150.
135. Gao J, Ann Garulacan L, Storm SM, et al. Identification of in vitro protein biomarkers of idiosyncratic liver toxicity. Toxicol In Vitro 2004; 18:533–541.
136. Jones JA, Kaphalia L, Treinen-Moslen M, et al. Proteomic characterization of metabolites, protein adducts, and biliary proteins in rats exposed to 1,1-dichloroethylene or diclofenac. Chem Res Toxicol 2003; 16:1306–1317.

137. Guiffant D, Tribouillard D, Gug F, et al. Identification of intracellular targets of small molecular weight chemical compounds using affinity chromatography. Biotechnol J 2007; 2(1):68–75.
138. Meijer L, Raymond E. Roscovitine and other purines as kinase inhibitors. From starfish oocytes to clinical trials. Acc Chem Res 2003; 36(6):417–425.
139. Shimizu N, Sugimoto K, Tang J, et al. High-performance affinity beads for identifying drug receptors. Nat Biotechnol 2000; 18(8):877–881.
140. Jeffery DA, Bogyo M. Chemical proteomics and its application to drug discovery. Curr Opin Biotechnol 2003; 14(1):87–95.
141. Faleiro L, Kobayashi R, Fearnhead H, et al. Multiple species of CPP32 and Mch2 are the major active caspases present in apoptotic cells. EMBO J 1997; 16(9):2271–2281.
142. Baruch A, Greenbaum D, Levy ET, et al. Defining a link between gap junction communication, proteolysis, and cataract formation. J Biol Chem 2001; 276(31):28999–29006.
143. Greenbaum DC, Baruch A, Grainger M, et al. A role for the protease falcipain 1 in host cell invasion by the human malaria parasite. Science 2002; 298(5600):2002–2006.
144. Greenbaum D, Baruch A, Hayrapetian L, et al. Chemical approaches for functionally probing the proteome. Mol Cell Proteomics 2002; 1(1):60–68.
145. Bantscheff M, Eberhard D, Abraham Y, et al. Quantitative chemical proteomics reveals mechanisms of action of clinical ABL kinase inhibitors. Nat Biotechnol 2007; 25(9):1035–1044.
146. Ong SE, Schenone M, Margolin AA, et al. Identifying the proteins to which small-molecule probes and drugs bind in cells. Proc Natl Acad Sci U S A 2009 Mar 24; 106(12):4617–4622.

6 Screening and Characterization of G-Protein–Coupled Receptor Ligands for Drug Discovery

Ge Zhang and Mary Ellen Cvijic

Lead Evaluation, Applied Biotechnology, Bristol-Myers Squibb, Princeton, New Jersey, U.S.A.

INTRODUCTION

Since the pioneering work of Langley (1) and Enrlich (2) at the beginning of 20th century, identification and understanding of receptors, especially G-protein–coupled receptors (GPCRs) and their ligands, have grown to be one of the most important research areas of the academic environment and pharmaceutical industry. GPCRs are the largest family of integral membrane proteins that mediate most of the cell–cell communication in humans. GPCRs have evolved to recognize a broad variety of extracellular stimuli such as neurotransmitters, hormones, peptides, amino acids, lipids, and ions, and act to transmit messages encoded in stimuli from the exterior to the interior of the cells. GPCRs are also called seven transmembrane (7TM) receptors because they share a common feature of seven transmembrane domains (Fig. 1), and couple to cellular heterotrimeric guanine–nucleotide-binding protein (G-proteins) to elicit cellular responses. Because GPCRs are expressed on the cell membrane, signaling through GPCRs in the central nervous and peripheral systems underscores the physiological importance of this receptor family. It has been shown that numerous diseases and disorders have been linked to mutation and dysfunction of G-proteins and GPCRs (3,4), and some inherited endocrine diseases can be treatable with specific ligands targeting specific GPCRs (3).

The GPCR family members can be grouped into three major categories (Table 1) mainly based on sequence and structure similarity as well as the pharmacological nature of endogenous ligands (5–8). Class A (Family 1) GPCRs are referred to as the rhodopsin-like family and represent the largest subgroup containing receptors for odorants, small molecules, peptides, and glycoproteins. Class A GPCRs are characterized by a short N-terminus, some highly conserved amino acids mainly in transmembrane domains and a disulphide bridge that links the first extracellular (ECL1) and second extracellular (ECL2) loops of GPCRs. The majority of Class A receptors also have palmitoylated cysteines in the carboxyl-terminal tail. Class B (Family 2) GPCRs are the secretin-like receptors, having six conserved cysteins and a hormone-binding domain in their relatively long N-terminus. The Class B receptor family binds to large peptide ligands such as glucagon, corticotropin releasing factor (CRF), vasoactive intestinal peptide (VIP), parathyroid hormone (PTH), growth hormone releasing hormone, gastric inhibitory polypeptide and calcitonin. The receptor members in the Class B family are coupled to Gs proteins and enhance cAMP-mediated

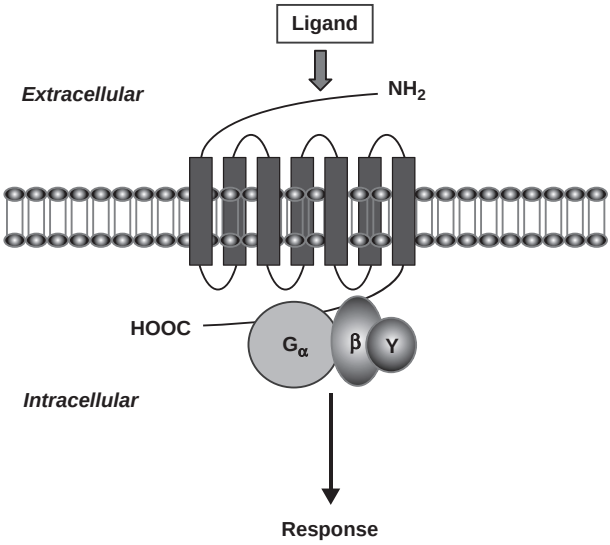

FIGURE 1 G-protein–coupled receptors sharing common feature of seven transmembrane domains. The seven transmembrane domains are abbreviated as TM1, TM2, TM3, TM4, TM5, TM6, and TM7 from the left to the right, respectively. The amino terminus is located outside of the cell, and carboxyl terminus is located inside of cell. The three extracellular loops are named as ECL1, ECL2, and ECL3 from the left to the right, respectively. The three intracellular loops are named as ICL1, ICL2, and ICL3, respectively. Heterotrimeric guanine–nucleotide-binding proteins (G proteins) consist of three subunits, α, β, γ, and couple to the GPCR after ligand stimulation. G-proteins mediate downstream effects following receptor activation.

TABLE 1 Subfamily of GPCRs (5–8)

Class	Endogenous ligand	Example	Receptor feature
Class A (I)	Biogenic amines	Adrenergic	Short N-terminus
		Dopaminergic	
		Serotoninergic	
		Histaminergic	
	Peptides	Opioids, Angiotensins	
	Peptide hormones	Galanin, Melanocortins	
	Lipid messengers	Cannabinoids	
	Nucleotides	ATP (P2Y12)	
	Chemokines	CXCR1, CCR9	
	Protease receptors	Thrombin (PARs)	
Class B (II)	Large peptide	Glucagon	Long N-terminus
		Calcitonin	G_S-coupled
		PTH	
		GHRH	
		CRF	
Class C (III)	Glutamate	mGLU-Rs	Long N-terminus
	Calcium	Calcium sensors	Long C-terminus
		T1R	

Class A represents rhodopsin-like family and contains many members, which are coupled through different G-proteins and 2nd messengers. Class B is a glucagon/calcitonin family, where the endogenous ligand is a large peptide and all receptor members are coupled to G_S and enhance cAMP-mediated signaling. Class C is a metabotropic glutamate and chemosensor family.

signaling. Class C (Family 3) GPCRs are the metabotropic glutamate receptor-like receptor family and contain metabotropic glutamate receptors, calcium-sensing receptors, and $GABA_b$ receptors. These receptors in the Class C family are characterized by a long amino terminus and a long carboxyl tail. In addition, a unique characteristic of Class C receptors is that the third intracellular loop is short and highly conserved. With exception of two cysteines in ECL1 and ECL2 that form a putative disulphide bridge, Class C receptors do not share any key features with Class A and Class B receptors (5–8).

GPCRs constitute the largest membrane receptor gene family of the human genome. The number of GPCRs within the human genome has been estimated to be as many as 800 to 1000 and the analysis of predicted GPCR gene structure has, so far, identified approximately 650 genes (8–10). Roughly 190 of these are categorized as "known" GPCRs because they are known to be activated by identified ligands. A large percentage (∼50%) of today's prescription drugs (30% of the top 50 best sellers) act through GPCR receptors, with the majority of these drugs targeting the Class A family via agonist- and antagonist-based mechanisms. Based on the percentage of receptors having an available full-length sequence, Class A represents 76% receptors (37% known and 39% orphan), Class B has 11% receptors (6% known and 5% orphan), and Class C occupies 3% receptors (2% known and 1% orphan) (8). Although historical and current success in drug discovery has made GPCR-targeting drugs as 50% of the market, today's clinically successful GPCR-based drugs have only targeted a small number (∼30%) of known GPCRs (8–11). Therefore, the molecular cloning efforts, in combination with the complete sequencing of the human genome have afforded a huge opportunity to identify receptor subtypes of known GPCRs and entirely novel GPCRs as well as their biological functions. These new receptors, concepts, and approaches offer great promise for the search of novel GPCR-based therapeutics (5–7,9–22) and have been the center point of increasing attention from the pharmaceutical industry.

The aim and scope of the present chapter is to give a brief introduction of GPCR receptor pharmacology, provide the screening strategy for agonist-, antagonist-, and modulator-based targets, and describe the in vitro pharmacological approaches and technologies to screen and advance lead compounds, especially focusing on characterizing compounds in the lead optimization process. In addition, we describe selectivity screening analysis in the early stage of structure–activity relationship (SAR) studies in order to detect unwanted side effects, potential liability issues, as well as to increase the rate of moving leads to go through in vivo proof-of-principle studies. This overview provides insight into the characterization of small-molecule ligand interaction with specific and different GPCR receptor families and describes the screening strategy to design for therapeutic agents for treatment of various GPCR-related disorders.

BASIC RECEPTOR PHARMACOLOGY

Identification and understanding of GPCRs have become the central focus of investigation of drug effects and their mechanisms-of-action that is referred to as pharmacodynamics (23). The receptor is the receptive component of a cell that interacts with an endogenous ligand or drug and initiates the chain of biochemical or biophysical events, leading to the drug's observed effects (23). Many drugs and endogenous ligands bind to receptor macromolecules as **agonists** that

activate the receptor and change receptor function. Pharmacological receptor **antagonists**, however, bind to the receptor without directly altering the receptor's function (23). Thus, the effect of a receptor antagonist on a cell depends entirely upon preventing the binding and blocking the biological responses of the natural ligand. Receptors largely determine the quantitative relations between dose or concentration of drug and pharmacologic effect. The receptor affinity for binding a drug determines the concentration of drug required to form a significant number of drug–receptor complexes, and the total number of receptors often limits the maximal effect a drug may produce (23). The receptor affinity for a given drug and a total receptor number in a given biological system can be experimentally determined (23–29) and will be described later in this chapter.

The relationship between drug concentration and biological response can be estimated and described by the concentration–response curve or dose–effect curve (23,24). If an agonist drug interacts reversibly with its receptor, the resultant effect is proportional to the number of receptors occupied and can be given by the following reaction equation:

$$\text{Drug (D)} + \text{Receptor (R)} \rightarrow \text{DR} \rightarrow \text{Effect}$$

This drug and receptor reaction sequence is analogous to the interaction of substrate with enzyme reaction, and the magnitude of effect can be analyzed in a manner similar to that for enzymatic product formation (23,24). The applicable equation can be represented similar to Michaelis–Mention equation:

$$\text{Effect} = \frac{\text{Maximal effect}\,[D]}{K_{\text{D}} + [D]}$$

where $[D]$ is the concentration of free drug and K_{D} is the dissociation constant for the drug–receptor complex. This equation describes a simple rectangular hyperbola. It is frequently convenient to plot the magnitude of effect verus log$[D]$, because a wide range of drug concentrations is easily displayed on the log scale, and the central portion of the concentration–response curve is more linear (23,24). In this case, the result is the familiar sigmoidal log dose–effect curve, which is the standard dose–response curve and routinely used for pharmacological analysis for drug screening. The potency (EC_{50}) and efficacy maximal response (E_{max}) of a drug are generally estimated by fitting the dose–response data to the four parameter logistic equation through nonlinear regression analysis (23,24), where

$$Y = \text{Bottom} + \frac{(\text{Top} - \text{Bottom})}{1 + 10^{(\text{Log EC}_{50} - X)\,\text{Hill Slope}}}$$

Y is the effect and X is the concentration of drug. EC_{50} is the concentration of agonist, which induces half of the maximal effect. E_{max} or intrinsic activity is the ability of an agonist to produce the maximal response after all receptors are occupied by agonists. Hill slope is the slope obtained from the concentration–response curve.

$$\text{Intrinsic activity} = \frac{\text{Maximum response of test agonist}}{\text{Maximum response of a full agonist at the same receptor}}$$

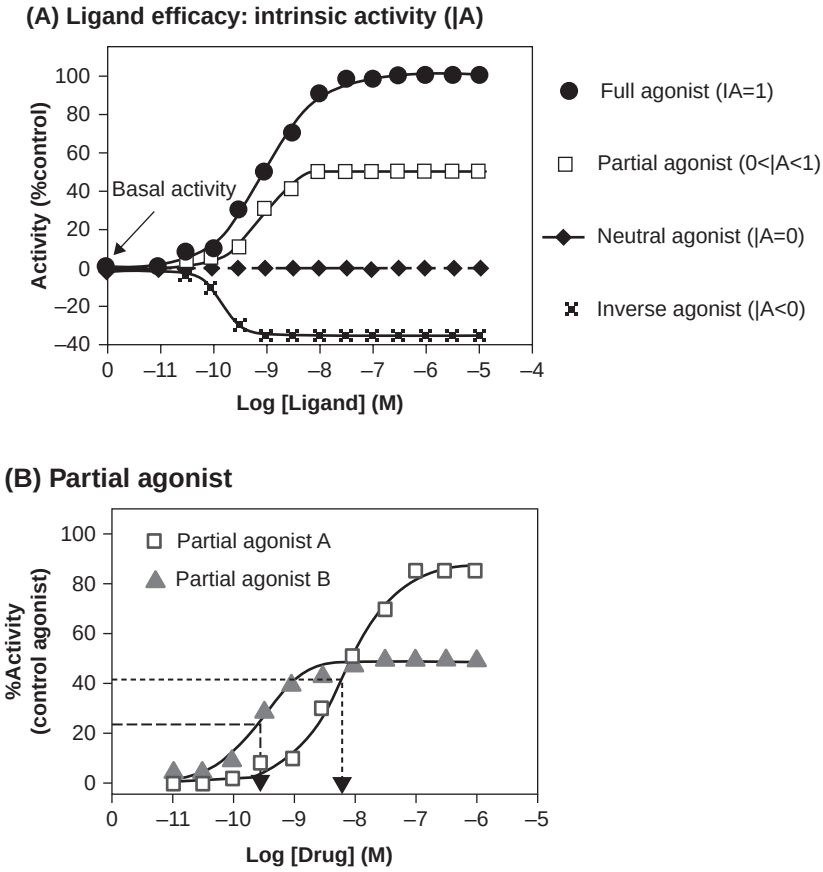

FIGURE 2 Intrinsic activity (IA) or efficacy of full agonist, partial agonist, antagonist, and inverse agonist (**A**) (23,24). The agonist activity is derived from compound activity, which is normalized to the full agonist (control). The inverse agonist decreases the basal activity. Partial agonists can display different potency and efficacy (**B**).

Based on the maximal pharmacologic response that occurs when all receptors are occupied, agonists can be divided into two classes (23): One is the partial agonists that produce a lower maximal response or demonstrate lower intrinsic activity at full receptor occupancy than do full agonists (Fig. 2). In terms of intrinsic activity, efficacy for a full agonist is considered to be 1.0, while the efficacy of a pure neutral antagonist is zero (23). Partial agonists have efficacies between 0 and 1.0. Some drugs as competitive antagonists are in fact weak partial agonists (14,23). The second is the **inverse agonist** that produces a negative intrinsic activity, decreasing the basal constitutive activity of the receptor (12,13,30). The negative efficacy of inverse agonists in the constitutive activity of GPCRs is described in detail in recent reviews (12,13). The recombinant cell line expressed mutant GPCR with constitutive activity has attracted attention in the drug discovery community to specifically search for inverse agonists (13,14,31).

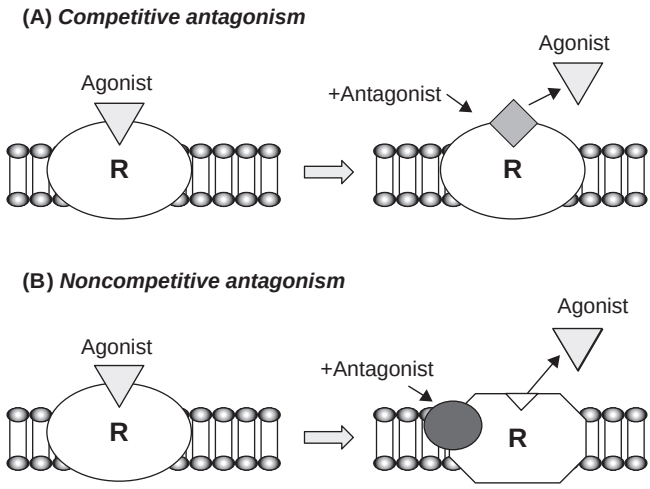

FIGURE 3 Competitive and noncompetitive antagonisms (23,24). (**A**) The competitive antagonist binds the orthosteric site, where an endogenous agonist binds to the receptor, to form competitive inhibition with agonists. (**B**) The noncompetitive antagonist binds an allosteric site, which is distal from orthosteric site, to alter receptor conformation and prevent agonist binding and/or agonist coupling to the receptor.

Antagonists can be divided in general into **competitive** and **noncompetitive** antagonists (Fig. 3) (23,24,32). A simple competitive antagonist binds to the agonist site and functions by hindering the agonist from binding to the receptor, while initiating no effect by itself (efficacy = 0). The antagonist action of simple competitive antagonists depends upon the law of mass action by inhibiting the activity of agonist applied to the system (23). Because of an antagonist's competitive nature with the agonist for the receptor-binding site, the inhibition from antagonist application can be overcome by increasing the concentration of the agonist, ultimately achieving the same maximal effect (23). Therefore, the parallel rightward shift of an agonist dose–response curve is observed in the presence of a competitive antagonist and depicts decreasing agonist potency without significant change in their maximal response (Fig. 4). In contrast, a noncompetitive antagonist binds the allosteric site, which is distal from an endogenous agonist binding site on the receptor, alters the receptor conformation, and may prevent agonist binding and/or inhibit agonist-induced signaling (23), acting in an irreversible or nearly irreversible fashion (Fig. 3). Because of alteration of the agonist binding or coupling, the maximal effect of the agonist is reduced with a noncompetitive antagonist in a concentration-dependent manner (Fig. 4).

Another characteristic of receptors is that they are responsible for selectivity of drug action (23). The molecular size, shape, and electrical charge of a drug determine whether it will bind to a particular receptor among the vast array of chemically different binding sites available in a biological system (6,8,23,28,33,34). Accordingly, changes in the chemical structure of a drug can dramatically increase or decrease the new drug's affinity for different classes of receptors and/or its functional behaviors as agonist and antagonist, with

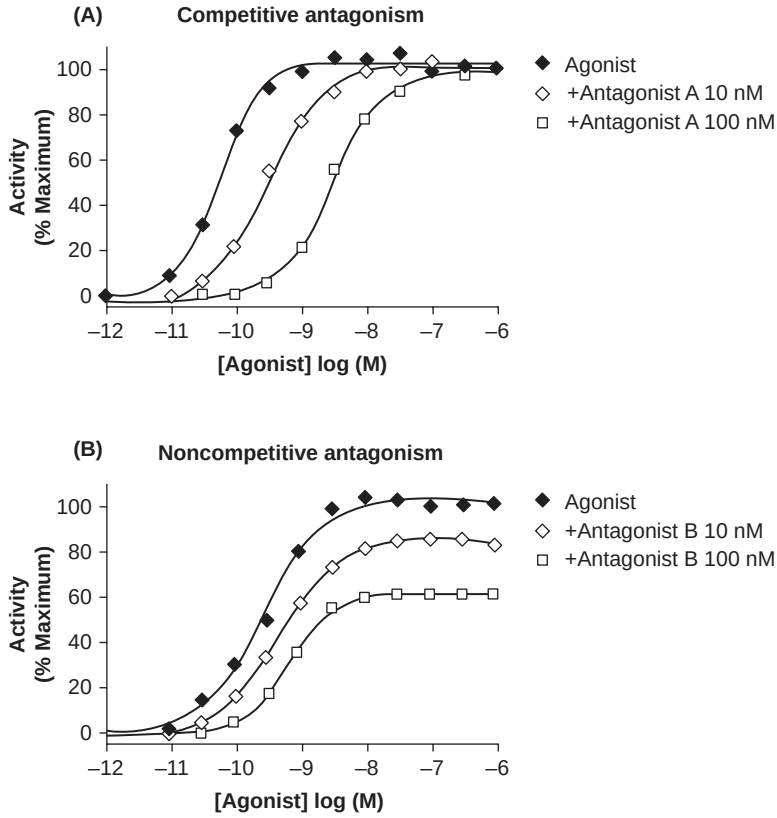

FIGURE 4 The agonist concentration–response analysis in absence and presence of competitive (**A**) and noncompetitive antagonists (**B**), respectively (23,24). The agonist concentration–response relationship was examined in 12 concentrations of either agonist alone (*solid symbols*) or agonist plus one fixed concentration of the antagonist (*open symbols*).

resulting alterations in therapeutic and toxic effects. Therefore, the SAR study is a very important aspect and represents a major effort for lead optimization preclinical drug discovery (6,8,21,23,28,33,34,).

GPCR SIGNAL TRANSDUCTION AND RECEPTOR REGULATION

Agonist ligand binding to GPCR promotes conformational changes leading to G-protein coupling, the initiation of signaling pathways, and the activation of downstream effectors via second messengers to produce cellular responses (24,30). GPCRs have a similar topology consisting of a core of 7TM-spanning α-helices with three hydrophilic intracellular and three hydrophilic extracellular loops (ECLs). The N-terminus is located extracellularly and the C-terminus is located intracellularly. GPCRs contain a region involved in ligand binding and another region involved in G-protein coupling. The ligand receptor binding involves hydrogen bond, ion pair, and hydrophobic interactions. The ligand

and receptor interaction in GPCR subfamilies has its own characteristics and unique regions based on the structural diversity of the endogenous ligands (8,30). Many small agonists such as biogenic amines bind within the transmembrane segments. In contrast, peptide hormones often bind to the N-terminus and extracellular sequences joining the transmembrane regions of receptors. However, the size of the ligand is not the only factor that predicts the location of the binding site. For instance, glycoprotein hormones in the Class B family and glutamate and calcium (Ca^{2+}) in the Class C family activate their respective receptors by binding to relatively large amino terminal domains (8,30). It is interesting to note that it has been possible to identify small-molecular-weight allosteric modulators that bind within the TM regions for many GPCRs that bind their native agonists on the extracellular loops or the amino terminus (35). The intracellular domains of GPCRs contain several regions responsible for receptor coupling to signal transduction systems. The contact regions of GPCRs for G-protein coupling exist predominantly on the second and third intracellular loops as well as on the C-terminal tail (8,30,36).

The G-protein serves as the molecular switch for linking receptor stimulation to effector system activation (8,30,36,37). G proteins consist of three subunits, α, β, γ, but they function in essence as dimers because the signal is communicated by either the G_α or $G_{\beta\gamma}$ complex. There are more than 16 different α subunits, 6 β subunits, and 11 γ subunits. Despite the great diversity of ligand types, the receptor function is generally very modular, receptors couple to a subset of the heterotrimeric G protein subtypes, which are functionally grouped into four broad families: G_s, $G_{i/o}$, G_q, and G_{12} (36,37), based on sequence homology and functional similarities of their α subunits (Table 2). These G-proteins in turn regulate a relatively small number of intracellular effectors such as adenylate cyclase, phosphoslipase C, and ion channels. Once a GPCR is occupied by its ligand, it undergoes a conformational change and binds directly to a heterotrimeric G protein, leading to the nucleotide exchange of GDP for GTP bound to the G_α subunit and the dissociation of the G_α subunit from the $G_{\beta\gamma}$ complex. Subsequently, the G_α and $G_{\beta\gamma}$ subunits can relay signals to a wide variety

TABLE 2 Subtypes of G-Protein Subunits (8,30,36,37)

Class	Subtypes	Toxin Sensitivity	Function
α Subunit	α_s (~4 subtypes)	CTX	Activate adenylate cyclase
	α_i (~3 subtypes)	PTX	Inhibit adenylate cyclase Open K^+ channel
	α_o (~2 subtypes)	PTX	Inhibit Ca^{2+} channel
	α_q/α_{11} (~5 subtypes)	-	Activate PLC α_{16}-Universal PLC transducer
	α_z	-	Couples to same receptors as $G_{i/o}$
	α_{olf}	CTX	Activate adenylate cyclase
	α_t (~2 subtypes)	CTX, PTX	Activate PDE in retina
	α_{Gust}	CTX, PTX	Involved in taste transduction
β/γ subunits	β (~20 subtypes) and γ (~11 subtypes)		Can activate effectors after dissociation from α: activate PLC and GIRK, inhibit Ca^{2+} channel

Abbreviations: CTX- cholera toxin; PTX- pertussis toxin; PDE- phosphodiesterase; PLC- phospholipase C, GIRK- G-protein coupled inwardly rectifying potassium channel.

of downstream effectors (36). G-proteins serve as the substrate of different toxins (36,37). For pertussis toxin (PTX), the substrates are the $G_{\alpha i}$, $G_{\alpha o}$, and also other G-proteins such as transducin and gustucin. ADP-ribosylation by PTX maintains the G-protein in the GDP-bound state, preventing the interaction between G-protein and receptor. Thus, PTX results in blocking of $G_{i/o}$-mediated signal transduction. For cholera toxin (CTX), the substrates are $G_{\alpha s}$, $G_{\alpha olf}$, transducin, and gusducin. The effect of CTX on $G_{\alpha s}$ is manifest as prolonged activation of adenylate cyclase and a consequently large rise in intracellular cAMP in cells. These toxins are useful tool molecules for identifying G-protein–coupled transduction pathways following agonist-mediated receptor activation (31,36).

The essential function of the subunit is to recognize specific receptors and couple these to specific effector systems (8,30,35–37). The G_s protein activates the effector adenylate cyclase, resulting in increased intracellular cAMP production, with subsequent activation of protein kinase A (PKA) and the Epac family of cAMP-regulated guanine nucleotide exchange factors, both of which have multiple downstream effectors (36,37). The G_i protein has the ability to inhibit adenylate cyclase via $G_{\alpha i}$ but it also signals via $G_{\beta\gamma}$, which couples to phospholiase C-β (PLC-β), K^+ channel, Ca^{2+} channel, adenylate cyclase, and phosphatidylinositol 3-kinase (PI3K). The G_q pathway stimulates PLC-β to produce inositol 1,4,5-triphosphate (IP_3) and diacylglycerol (DAG). The 2nd messenger IP_3 triggers the release of Ca^{2+} from the endoplasmic reticulum, whereas DAG activates protein kinase C (PKC). Because $G\alpha_{16}$ recognizes a large number of GPCRs, it has been widely used in orphan receptor cell lines to efficiently link receptor activation to Ca^{2+} mobilization for HTS hit identification campaigns (38). Many cell- based assays have been developed to monitor these conventional signaling pathways after GPCR activation following agonist application. These assay technologies have been utilized in drug screening to search for agonists and antagonists in pharmaceutical industry (11,18,22) and will be introduced in this chapter.

GPCRs also undergo different modifications such as posttranscriptional and translational modifications, as well as receptor dimerization. Recent studies also suggest that GPCRs may function as homodimers or oligomers and can form heterodimers or hetero-oligomers with closely related receptor subtypes or even GPCRs belonging to different classes (15–17,39–41). These dimerizations may be involved in transducing signals from the receptor and it has been postulated that oligomerization of GPCRs may play a role in the biosynthesis and trafficking of nascent GPCRs to the cellular membrane (42). Following synthesis, GPCRs undergo processing and folding in the endoplasmic reticulum where they form homo- or heterodimeric structures. GPCRs then transit through the Golgi where they undergo modifications such as oligosaccharide processing. It is in the Golgi where GPCRs are packaged to exocytic transport vesicles called endosomes and are targeted to the cellular membrane. Additional proteins are involved in GPCR stability in the phospholipid membrane microenvironment (8,30,42).

Many GPCRs undergo ligand-dependent homologous desensitization accompanied by aggregation of the receptor followed by internalization. This process occurs on the order of minutes after receptor activation (42). After ligand binding, GPCR kinases (GRKs) phosphorylate agonist-activated GPCRs on serine and threonine residues on the carboxyl-terminal tail. The phosphorylated

GPCR then binds to arrestin, which leads to uncoupling of the GPCR from the cognate G-protein resulting in loss of sensitivity to the ligand (43–46). The uncoupled, desensitized receptors are then targeted to clathrin-coated pits and internalized to an early-endosomal compartment via endocytosis. From the endosome, the GPCR is either recycled back to the plasma membrane or degraded in the lysosome (47). Receptor ubiquitination also plays a part in GPCR degradation via lysosomes.

In addition, GPCRs activate and cross talk with many diverse signaling pathways including mitogen-activated protein kinase (MAPK) cascades (8,37,48,49). The biological relevance of these nonconventional pathways for GPCR-targeted drug discovery is currently under investigation. Furthermore, despite a large amount of growing knowledge regarding structure, signaling, trafficking, and regulation of GPCR function, much remains to be known on these molecular mechanisms and their therapeutic usefulness. Better understanding of the complex modulation and biologically relevant endpoints may provide novel approaches to search for molecular targets of GPCR and screening of GPCR ligands (8,37,50,51).

ASSAY AND TECHNOLOGY FOR SCREENING GPCR LIGANDS FOR LEAD OPTIMIZATION

Ligand–Receptor Binding

The radioligand binding assay is a standard method to directly measure ligand binding affinity for a given receptor and has been applied to GPCR ligand screening for many years (23,24). The bimolecular interaction between the ligand and receptor is characterized by saturability, pharmacological specificity, stereoselectivity, reversibility, and molecular receptor cloning. As there are a finite number of receptors per cell or per tissue, it follows that a dose–response relationship for the binding of a ligand should exhibit saturability (23,24). In this case, no more binding is observed even through increasing ligand concentration. In general, specific binding of a ligand to a receptor is characterized by a high affinity and low capacity, whereas nonspecific binding usually displays high-capacity and low-affinity binding that is virtually nonsaturable. This phenomenon can be revealed in radioligand saturation binding analysis (23–29,52). Specificity is one of the most important and difficult criteria to fulfill, especially using tissues in binding studies because of the enormous mass of nonspecific binding sites compared with specific receptor sites in a given tissue. However, the overexpression of a specific receptor in a recombinant cell line makes the investigation of receptor pharmacological profile more manageable (23,25–28,52). For best practice, it is necessary to explore the displacement of the labeled ligand with a series of agonists and antagonists from various chemical structures and pharmacological properties as the competing ligand in a competition experiment. In addition, the characteristic of specific receptor binding can be demonstrated with stereoselectivity using a pair of stereoisomers (23,27). It is of obvious importance to demonstrate that one isomer is a more potent displacer than another isomer at the same receptor in competition binding. Because transmitters, peptides, hormones, and most drugs act in a reversible manner, it follows that the binding of these ligands to receptor should be reversible in the dissociation kinetic study. It is also to be

expected that the ligand of a reversible receptor should be not only dissociable but also recoverable in its natural form. From the law of mass action, the binding of ligand (L) to its receptor leads to the following equation (23,24):

$$L + R \underset{k_{-1}}{\overset{k_{+1}}{\rightleftarrows}} LR$$

$$\text{Thus, } K_D = \frac{k_{+1}}{k_{-1}} = \frac{[L][R]}{[LR]}$$

where k_{+1} = association rate constant, k_{-1} = dissociation rate constant, [L] = free-ligand concentration, [R] = concentration of free receptors, [RL] = concentration of ligand bound receptors, K_D = dissociation equilibrium constant.

Since the total receptor population $[R_T] = [R] + [RL]$; so $[R] = [R_T] - [RL]$

$$\text{Therefore, } K_D = \frac{[RT - RL][L]}{[RL]}$$

where RL = Bound, R_T = Maximal binding site (B_{max}), L = free ligand.

The K_D and B_{max} can be calculated from saturation data using the equation

$$\text{Bound} = \frac{[B_{max}][L]}{[L] + K_D}$$

In general, the main goals of ligand–receptor binding studies are threefold in the common practice of drug screening. The first goal is to determine the thermodynamic dissociation constant (K_D) of radioligand binding to a given receptor and also quantify the total number of binding sites (B_{max}) in a given tissue or cell line (23,24). This initial characterization of membrane receptor and radioligand properties in saturation studies is critical in order to estimate the parameters for subsequent binding and functional studies. Saturation analysis is conducted routinely following protein titration and time course evaluation in ligand binding studies. The saturation experiment is performed in which the receptor concentration is kept constant and 8 to 12 radioligand concentrations are applied in the absence and presence of a fixed concentration of cold ligand to define nonspecific binding (23–27,53), then the ligand specifically bound to receptor is plotted versus [L] (Fig. 5). The maximal binding (B_{max}) and dissociation constant (K_D) are determined by fitting the data to a one site hyperbola saturation equation through nonlinear regression analysis (23,24) by using Prism software (GraphPad Software, Inc). K_D is sometimes characterized by on-rate and off-rate kinetic binding experiments (23–26,28,53) as presented in Figure 6.

The second goal for performing binding assays is to determine conformational changes of receptor following the treatment when a proper methodology is utilized. For instance, the shift from a high-affinity binding to a low-affinity binding state of an agonist can be detected in the presence of GTP analogues in radioligand binding assays (8,23,25,27,28,52). The third goal of ligand–receptor binding assays is to determine binding constants and/or binding mechanisms for other ligand molecules (23,24,28). In this case, the radioligand is a tool probe to label specific receptors, and a series of test compounds with different affinities competes with this radioligand in the competition experiment (23–25,27). In an indirect way, the binding potency (IC_{50}) and/or binding affinity (K_i) to the receptor for a large set of compounds can be easily accomplished in one

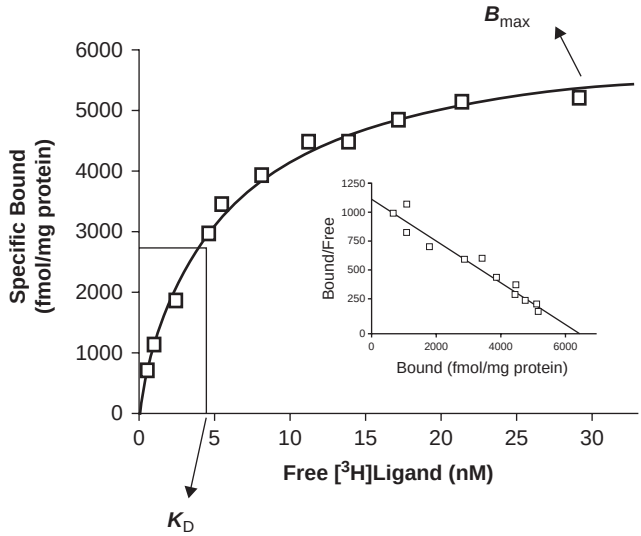

FIGURE 5 Saturation isotherm of specific radioligand binding to membranes of cells expressing a human GPCR. K_D and B_{max} values were determined from nonlinear regression analysis of the data using the one-site model (23,24,54). *Inset*: Scatchard plot of transformed saturation data. Specific binding was obtained by subtracting nonspecific binding from total binding at each concentration. Nonspecific binding was defined as that occurring in the presence of a cold ligand (1–10 μM).

competition experiment as illustrated in Figure 7. Therefore, competition binding is the most useful and practical screening format in binding assays to search for potent binders to a specific GPCR target.

The competition binding is performed under equilibrium conditions. The receptor concentration and radioligand concentration are kept constant in the presence of increasing concentrations of unlabeled competing ligands, which is usually kept in a half log scale of the dilution factor (23–26,28).

$$\text{Bound} = \frac{[B_{max}][L]}{[L] + K_D(1 + I/K_i)}$$

where K_D is the equilibrium dissociation constant for radioligand and K_i is the equilibrium dissociation constant for inhibitor.

The decrease in radioligand binding to a given receptor by high concentrations of unlabeled ligand occurs in a concentration-dependent manner. The potency (IC_{50}) of an unlabeled ligand is determined as the ligand concentration that displaces half the amount of specific binding of radioligand based on fitting the binding data to the sigmoid-shaped competition binding curve on a semi log scale (23,24). It is important to note that the IC_{50} value is a relative potency of ligand, which is dependent upon a fixed concentration of radioligand used in the competition assay. For a simple competitive interaction, a high concentration of radioligand is used and a high IC_{50} value is received according to the law of mass action and the competitive nature of binding to the same binding site (23).

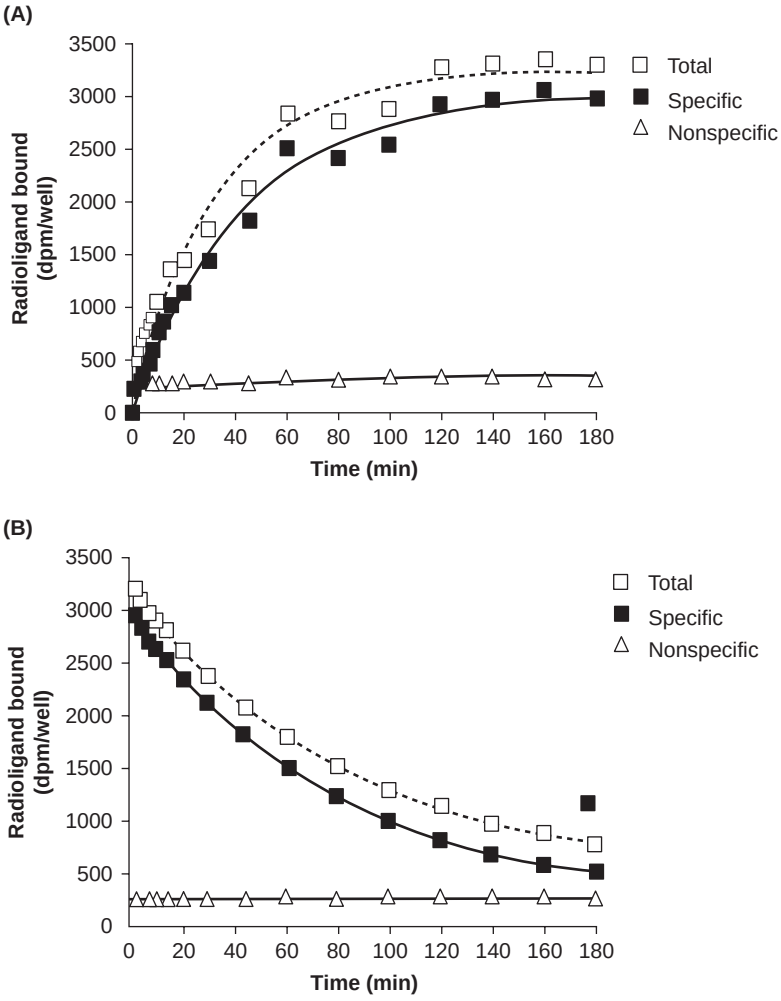

FIGURE 6 Kinetic equilibrium binding of radioligand (23,24,54) to membrane prepared from recombinant human cells expressing a GPCR of interest. (**A**) Equilibrium association of radioligand binding to the GPCR to determine on-rate. (**B**) Dissociation of radioligand binding to a given GPCR to determine off-rate. Nonspecific binding was defined at each time point by cold ligand (1–10 μM). The equilibrium dissociation constant K_D obtained from off rate/on-rate kinetic studies is comparable to the K_D derived from saturation analysis as in Figure 5.

Binding affinity data for the competitive inhibitors is analyzed by using Cheng and Prusoff (55) equation used for kinetic analysis of enzyme inhibitors (23,24).

$$K_i = \frac{IC_{50}}{1 + [L]/K_D}$$

For the competition experiment, the radioligand concentration is kept within the range of $1/5K_D$ to K_D concentrations (23–28,52,53). As the K_D concentration is

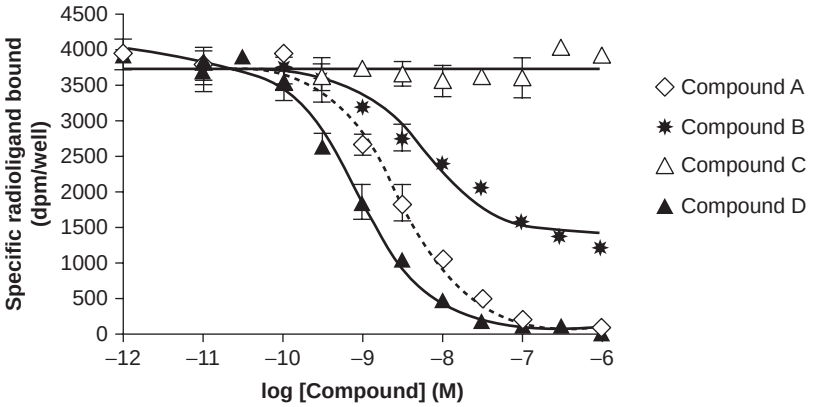

FIGURE 7 Competition of a radioligand binding (23,24,32,54) to membrane prepared from recombinant cells expressing a GPCR of interest. The radioligand is a small-molecule antagonist radiolabel for a specific binding site on the GPCR, and a set of cold compounds with increasing concentrations was included in the assay to compete for the binding site. Nonspecific binding was defined at each time point by a cold ligand (1–10 μM). The IC_{50} values for this set of compounds can be determined by fitting the data using the nonlinear competition analysis described in the Graph Pad Prism software.

usually used for the competition binding study, the IC_{50} value of the cold ligand is equal to two times the K_i number. However, the competitive nature of a test ligand with the radioligand at the receptor is unknown and not investigated in a routine drug screening process. Therefore, the IC_{50} value instead of the K_i value for a test compound should be reported as long as the radioligand concentration is kept constant among experiments and indicated in competition experiments. With computer-assisted nonlinear regression analysis, saturation data is no longer needed to transform to the linear Scatchard plot for accurate K_D and B_{max} determinations (23,24). The same is true for competition data analysis using nonlinear regression fitting of the original data to the four-parameter logistic equation without data transformation (23–28,52,53).

Receptor Preparation for Ligand Binding Studies

In high-throughput screening (HTS), binding assays are usually carried out with crude preparation in total particulate fraction that includes cell membrane, cytosolic, and nuclear components (23–28,52,53). If the tissue or cell line has a low level of receptor expression, the membrane fraction with enriched membrane preparation (29,56) is required to detect specific binding. The Chinese hamster ovary (CHO) or human embryo kidney (HEK) cell lines, which stably express a given GPCR, are generated and commonly used in drug screening (11,18,25,28,33,53). However, tissue from animal species is another alternative receptor source, particularly when the endogenous receptor in the target tissue is preferred for biological relevance (26,28,29,57,58). The 96-well harvester (Packard 96-well Unifilter) is a popular format in screening but has a protein limit (50–60 μg protein/well) for even filtration during the wash step to separate free ligand from bound ligand (25,26,28,58,59). The application of whole cells in the

binding assay is another format in GPCR ligand screening (8,11,23,25,58). Inclusion of 120 mM NaCl in the assay buffer is required to maintain osmolarity to prevent cell lysis during binding (23,25). The receptor concentration should be tested in protein or cell titration experiments by using a constant concentration of radioligand to achieve a robust assay window to be able to separate specific binding to receptors from nonspecific binding (23–26,28). It is also crucial to adjust protein concentration to maintain less than 10% of radioligand bound to the receptor in order to avoid the free ligand depletion issue in ligand–receptor binding assays (23,24). Nonspecific binding is defined experimentally with an excess amount of cold ligand where the concentration is over 100- to –1000-fold of the ligand affinity for the receptor.

Radioligand Selection

In developing ligand–receptor binding assays, a high-affinity radioligand with high-specific activity is usually needed for detecting specific binding in a given cell line or tissue. Radioligands with binding affinity below 10 nM are preferred because a high-affinity ligand is tightly bound to the receptor and there is little ligand dissociation from the receptor after the binding reaction is terminated during a quick separation process (23,24,26,28,58,59). In addition, the isotope choice for the radioligand should be considered based on several factors such as alteration of the biological activity of the ligand, radioactivity decay, and receptor expression level in cellular or membrane reagents (Table 3). The chemical stability and purity of the ligand is also a very important factor to establish a successful binding assay with long-term stability (8,23,24,60). For tissue and cell preparations with low-receptor density (B_{max} below 200 fmol/mg protein), it is preferable to have a [^{125}I]-radioligand (2200 Ci/mmol) with high-specific activity whenever possible (23–29,52,53). It offers almost 100 times higher sensitivity compared to a [^{3}H] ligand. Furthermore, [^{125}I] radiolabeling of an endogenous large peptide agonist is also the radioligand choice to screen for small-molecule antagonists from all chemotypes (25,26,28). The disadvantages of using [^{125}I] ligands are their short half-life, the potential for altering the bioactivity of small molecules, and its degradation problems (11,23,24,58,59,61,). The most commonly used radioisotope in receptor–ligand screening is [^{3}H]-ligands and it is the radioligand of choice for labeling small-molecule agonist and antagonist compounds (11,23–28,52,53). The advantage of [^{3}H] ligands is that they are less likely to alter the biological activity of either peptides or small molecules compared to [^{125} I] ligands. The typical specific activity if incorporating one mole [^{3}H] per mole ligand roughly equals 30 Ci/mmol (23,24,58,59,61). The modest specific activity can provide efficient detection for radioligand receptor binding

TABLE 3 Isotope Types of Radioligands for Ligand–Receptor Binding Assays (61,59)

Isotope	Half-life ($T_{1/2}$)	Specific radioactivity (Ci/mmol)	Comments
[^{3}H]	12.3 yr	29–87	Less likely to alter bioactivity
[^{125}I]	60 day	2225	Useful when receptor density is low
[^{35}S]	87.9 day	100	Useful with sulfur containing compounds
[^{32}P]	14.3 day	9760	Short half-life limits utility
[^{14}C]	5730 yr	0.064	Inadequate sensitivity

in a high assay volume assay (23,24,27,29). In a high-throughput miniaturized format, a ^{3}H-ligand below 30 Ci/mmol of specific radioactivity may not provide adequate sensitivity for the binding assay, especially using a membrane reagent with low-receptor expression (23,24,28).

For best practice, the radioligand added to saturation and competition assays should be counted in terms of counts per minute (cpm or dpm) per aliquot for each preparation then converted back to the radioligand concentration (i.e., nM) before the binding data is analyzed (23,24,59). This calculation of ligand concentrations is different from regular biochemical assays, which are based on the mathematic dilution factor for substrate concentration determination. The femtomole of radioligand bound to receptor (i.e., fmol/mg protein) can be calculated from the specific radioactivity of radioligand and membrane protein amount assuming 50%, 70%, and 80% counting efficiency for [^{3}H], [^{35}S], and [^{125}I], respectively (59,61).

The evaluation of radioligand selectivity is very important, and a highly selective ligand is utilized when performing binding in the tissues with expression of multiple receptors (23,24,26,28,29). For a recombinant receptor system, a nonselective radioligand for a receptor subtype has the advantage to streamline multiple subtypes of binding assays with the same radioligand on workstation or robotic platform (23,24,26,53). For example, the opioid mu, kappa, and delta receptor binding assays can be conducted with the same radioligand [^{3}H]-naloxone or [^{3}H]-diprenorphine. Screening of ligands in competition studies, the selection of either agonist radioligand or antagonist radioligand should be made cautiously depending upon the individual situation in terms of technical factors and biological rationale (23,24,27,28,53).

Assay Conditions

Because many parameters have substantial effects on the ligand binding reaction, the establishment of appropriate assay conditions is critical for accurate measurement of a ligand–receptor binding interaction (11,23,24,58,61). The different assay conditions include various factors to be evaluated in assay development such as determination of assay buffers, binding temperature, and reaction incubation time (23–26,28). The radioligand receptor binding reaction is performed under equilibrium conditions at which association and dissociation of the ligand from the receptor reach a state of equilibrium. For a saturation binding experiment, it is important to keep the incubation time long enough to make sure that the lowest concentrations of radioligand achieve binding equilibrium. Otherwise a short incubation time may cause low binding at lower concentrations of the radioligand, resulting in an underestimation of affinity with a high K_D value (23,24). For a competition experiment, a time course study with a fixed concentration of radioligand is recommended to determine the binding reaction time during the initial step of assay development and optimization (23–26,28).

For ligand–receptor binding assays, the optimal assay buffer conditions have to be determined especially dealing with a difficult binding assay (23,25,26). Normally, an isotonic or hypotonic buffer is used, with 50 mM Tris buffer or 25 mM HEPES buffer being the most popular in binding assays (23–28,33,52,53). A buffer pH of 7.4 to 7.5 is typically used to mimic physiological conditions. The requirements of monovalent cations such as Na^{+} or divalent cations should be

determined, and the inclusion of Mg^{2+} in the assay buffer is routinely used in order to promote high-affinity binding for agonists because the receptor coupling with G-proteins to form tertiary complexes is often Mg^{2+} dependent. In peptide binding assays, BSA is often included in the buffer to stabilize peptide ligands and prevent nonspecific binding of peptide ligands to the surface of test tubes or assay plates (23–28,33,52,53). BSA also reduces protease activity and increases stability of membrane or cells. The optimal temperature for the binding reaction should be determined and room temperature is normally preferred in HTS screening (11,23,24,27,28,29,53,61). In a whole-cell–binding assay, the binding reaction can be carried out at 4°C to minimize internalization of the ligand with receptor from the membrane surface (23,25,58,61).

Binding Assay Format

Radioligand receptor binding assays can be conducted in many formats including centrifugation, vacuum filtration, and equilibrium membrane dialysis. The binding assay formats commonly used to date are filtration and scintillation proximity assays (SPA) for GPCR targets in the pharmaceutical screening environment (11,23–29,33,52,53,61). The filtration assay is a very efficient and sensitive method for separating signal from noise to achieve a good assay window and is considered to be the "gold standard" method. The separation of ligand-bound receptor from free ligand is performed through filtration using a 96-well cell harvester. In order to reduce nonspecific binding and increase signal/noise ratio, optimal times of washing and wash buffer volume should be examined during assay development (23,25,28,29). Since the binding reaction is terminated after incubation by several ice-cold washes on a filtration apparatus, bound ligand can be dissociated from the receptor if prolonged washing occurs. Filtration time allowed during washing step is based on the dissociation constant for a given ligand, and allowable times to avoid ligand dissociation are described in Table 4 (32,54). A low-affinity ligand (K_D > 10 nM) may be dissociated from the receptor binding sites during the period of the wash filtration step (Table 4). However, drastically reduced temperature with an ice-cold buffer during washing will slow down the dissociation process (23–29,52,53).

The scintillation proximity assay (SPA) has been successfully applied to ligand–receptor binding by immobilizing receptors directly to SPA beads by a number of coupling methods (11,25,58,61). SPA is a homogenous HTS binding

TABLE 4 Relationship Between Steady State Dissociation Constant (K_D) of Ligands and Allowable Separation Time (32,54) for Filtration and Wash Steps

K_D (M)	K_D (nM)	Allowable separation time
10^{-12}	1 pM	1.2 day
10^{-11}	10 pM	2.9 hr
10^{-10}	100 pM	17 min
10^{-9}	1 nM	1.7 min
10^{-8}	10 nM	10 sec
10^{-7}	100 nM	0.10 sec
10^{-6}	1000 nM	0.01 sec

method and is an alternative of the traditional filtration format in [^{125}I] and [^{3}H] ligand binding assays (see chap. 4 in this book for more details). When the radioligand binds to the receptor immobilized on the SPA beads, it will be in close proximity to stimulate the scintillant in the beads to emit light, whereas the unbound radioligand is too distant from the beads to transfer energy and goes undetected (11,58,61). Therefore, there is no need to separate free radioligand from the receptor-bound radioligand. SPA beads and radioligands are available from vendors including GE Healthcare. Two generic beads called wheat-germ agglutinin (WGA)-PVT or polylysine (PL)-YS beads have been used for ligand–receptor binding assays (11,58,61). It is important to confirm that there is little or no specific interaction of radioligand with the beads. The optimum bead to membrane ratio has to be examined at a fixed concentration of radioligand around K_D to obtain highest specific binding. With a good radioligand having a low nonspecific binding and membrane with high receptor expression, this homogenous format has enabled 384-well SPA binding assays (11,58) and has maintained consistent rank order of potency and pharmacology for a large set of compounds (Fig. 8). In addition, SPA methods are more amenable to automated platforms compared to filtration binding assays (58,61). However, validation of pharmacological profile of test set of compounds in SPA is a necessary process to ensure that the rank order of potency remains consistent with the data obtained from the filtration format (23,25,58,61).

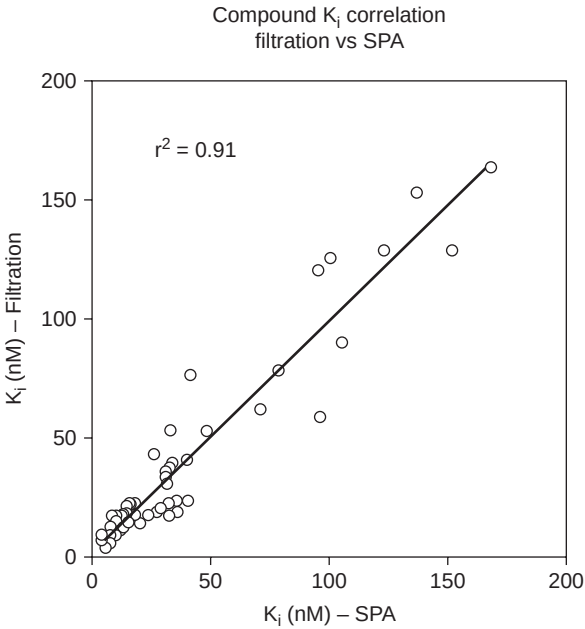

FIGURE 8 Comparison of compound K_i values between a 96-well filtration binding assay and a 384-well scintillation proximity assays (SPA) using receptor membranes expressing a GPCR of interest. A significant correlation is observed for compound K_i values between the two assay formats.

Nonradioactive ligands have been developed by tagging fluorescent probe to GPCR ligands (62), and nonradioactive binding assays can be conducted through a washing-separation format (11,61,62). As a fluorescence probe can be large and has the potential to alter the affinity and bioactivity of a ligand, the evaluation of a fluorescence-labeled ligand in routine competition binding and functional assays is necessary prior to establishment of the nonradioactive binding assay. The evaluation of a ligand binding assay to the human melanocortin-4 receptor by using dissociation-enhanced lanthanide (Europium) fluoroimmunoassay (DELFIA) technology (PerkinElmer Lifescience) has been successfully developed in a 96-well format (11,61–63). The competition assay data are comparable between the DELFIA and [^{125}I] radiolabeled binding assay (62). DELFIA provides an attractive alternative to the traditional radiolabeled ligand binding assays for peptide-GPCR interactions in terms of throughput, cost savings, and biohazards.

FUNCTIONAL ASSAY PLATFORMS

Lead optimization requires homogenous and high-throughput GPCR functional cell-based assays for rapid pharmacological characterization of GPCR agonists or antagonists (11,18). For the lead optimization process, receptor binding screens can identify small molecules interacting with receptors at binding sites or allosteric sites (23). However, analysis in GPCR cell-based assays is necessary to further characterize the functional activity of a molecule before progressing it into in vivo PK and PD models (11,18,28,33). Upon ligand binding to the receptor, a series of signaling pathways is activated, leading to downstream intracellular interactions. For example, agonist binding to GPCRs may result in cellular responses such as the stimulation or inhibition of adenylate cyclase, activation of phospholipase C and generation of inositol triphosphate (IP_3), activation of protein kinase C, and an increase in intracellular calcium concentrations (8,11,18,36,) (Fig. 9).

GTPγS Assays

The downstream event from ligand binding is the receptor–G-protein interaction followed by G-protein activation. In the resting state, where receptor is uncoupled from the agonist ligand, the heterotrimeric G-protein is in an inactive state with GDP bound to G_α and in this state there is a low basal rate of GDP–GTP exchange (8,64). After agonist stimulation of the GPCR, the G_α protein-bound GDP is exchanged for GTP, which triggers conformational changes and dissociation of the G-protein α-subunit from the βγ subunits and elicits downstream signal transduction events (64). Subsequently, intrinsic GTPases are activated thus cycling the activated G_α protein back to the GDP-bound basal state. This nucleotide exchange process forms the basis of this GPCR functional assay through direct binding measurements of [^{35}S]GTPγS, a GTPase resistant GTP analogue, to the activated G_α in cell membranes or native tissues (64).

The advantage of this platform is that guanine nucleotide exchange is a proximal event to receptor activation and is less subject to signal amplification or regulation by other cellular processes than more distant events such as second messenger signaling or reporter gene assays. The limitation of [^{35}S] GTPγS binding assays is that the platform is generally limited to the $G_{i/o}$-coupled

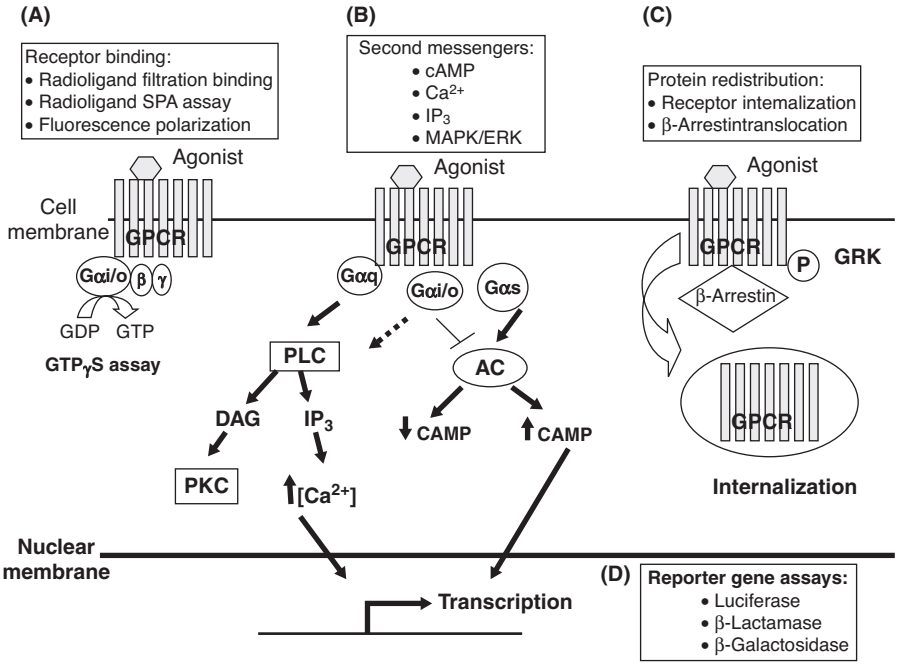

FIGURE 9 Summary of GPCR screening platforms (8,11,18,23,54). (**A**) GPCR activity can be measured at the level of the receptor through ligand binding filtration, SPA, and fluorescence polarization assays. Proximal to the receptor, the nucleotide exchange process occurring at $G_{\alpha i/o}$ forms the basis of the functional GTPγS assay, which is a direct binding measurement of a GTPase resistant GTP analogue such as $[^{35}S]GTP\gamma S$ to the activated $G_{\alpha i}$. (**B**) Agonist binding to GPCRs results in functional cellular responses from the signaling of second messengers. $G_{\alpha q}$- and $G_{\alpha i/o}$-coupled GPCRs stimulate the activity of phospholipase C (PLC) to form IP_3, which binds IP_3 receptors on the endoplasmic reticulum to release intracellular Ca^{2+} stores that can be measured by fluorescent-based dyes or bioluminescence technologies such as aequorin. G_s-coupled receptors stimulate adenylate cyclase activity, which converts ATP to cAMP whereas G_i-coupled receptors are inhibitory to adenylate cyclase acting to decrease intracellular cAMP concentrations after agonist stimulation. Many assay formats can monitor cAMP accumulation and are based on competition between cellular cAMP and a labeled form of cAMP for binding to an anti-cAMP antibody. (**C**) Protein redistribution assays are a secondary assay for screening GPCRs. β-Arrestins mediate desensitization of GPCRs after ligand activation through direct interaction with the GPCR C-terminus, which has been phosphorylated by GPCR kinases (GRKs). β-Arrestin binding leads to uncoupling and GPCR internalization into the endosome, which can be visualized by high-content screening technologies or fluorescence microscopy. (**D**) Calcium or cAMP-regulated reporter assays are another platform for the functional screening of GPCRs and are based on transcription factors (i.e., NFAT, AP-1, CREB) that become activated with rises in intracellular levels of the second messengers. Reporter assays are based on the ability of GPCR-mediated second messengers to activate or inhibit responsive elements upstream of a promoter regulating in the expression of a reporter protein such as luciferase, β-lactamase, or β-galactosidase.

GPCRs (18). $G_{i/o}$ is the most abundant G-protein in most cells and has substantially higher rates of GDP–GTP exchange than other G proteins (65). Therefore, standard [^{35}S]GTPγS binding assays using G_s- or G_q-coupled receptors often result in high assay background since agonist stimulation would result in only a small or insignificant level of GTP binding above basal levels (18,65). Another disadvantage is that the GTPγS binding assay usually has a low assay window (1.5–3 fold) and it is not easily amenable to a 384-well screening format (65). High cost and low signal prevents this assay application for library screening for hit identification (11).

In the standard GTPγS binding radioactive assay format, the amount of [^{35}S]GTPγS bound to G_α is measured by separation of the membrane-bound fraction from the free by a filtration step followed by scintillation counting to quantify the amount of radioactivity (66). This filtration step can be a limiting factor to assay throughput. To enhance assay throughput, the homogeneous SPA [^{35}S]GTPγS binding assays can be used with wheat-germ agglutinin-coated SPA beads that capture the GPCR and the [^{35}S]GTPγS bound to the receptor comes in close proximity to the scintillant on the bead to yield the assay signal (67). In addition to the SPA bead assay, FlashPlate™ technology can be used as a HTS method in which the receptor-membrane preparation is immobilized on the surface of the FlashPlate (68). The membrane fraction is incubated with [^{35}S]GTPγS in the well of the microplate and centrifuged after incubation. The supernatant is discarded and the plate is counted on the Trilux™, Viewlux™ or TopCount™ scintillation plate readers for the quantitation of GTP binding.

Several recent approaches have extended the utility of the GTP binding assay as a measure of functional activation of G_s- and G_q-coupled GPCRs and allow the reduction of the high background observed for these G proteins. These include coexpression of G proteins and receptors in Sf9 insect cells, construction of GPCR-G_α fusion proteins, and the use of antibody-capture for [^{35}S]GTPγS SPA format (65,69). This SPA method combines the immunocapture of the G_α subunit following [^{35}S]GTPγS binding with SPA technology. The activated G_α bound [^{35}S]GTPγS is captured by the primary anti-G_α antibody, and the G_α–antibody complex is captured by anti–IgG-coated SPA beads (69). The proximity of the [^{35}S]GTPγS excites the scintillant on the SPA beads to give off light that can be read in a microplate scintillation counter.

Additionally, the PerkinElmer DELFIA technology gives a nonradioactive alternative for GTP binding assays (63). This GTP binding approach uses time-resolved fluorescence (TRF) and a lanthanide chelate technology with a europium-labeled GTP to measure the binding of GTP to G_α upon GPCR activation (63). However, this approach still requires a filtration and wash step (18). The results from conventional filtration, SPA and DELFIA assays correlate very well and have been validated for GPCRs from the adrenergic, serotonin, and muscarinic receptor families (70).

All of the GTP binding assays described here allow for determination of traditional pharmacological parameters of potency, efficacy, and affinity without the agonist-induced amplification that may occur by measuring parameters downstream of the receptor (64). Furthermore, the [^{35}S]GTPγS binding assay can be used for orphan GPCRs where ligand and signaling pathways are not known and for other GPCRs for which signal transduction mechanisms are not

well characterized. This approach can identify not only full and partial agonists but also inverse agonists because the basal activity is sufficiently high (64).

cAMP Second Messenger Assays for G_s- and $G_{i/o}$-Coupled Receptors

cAMP is an important second messenger that mediates diverse physiological cellular responses (8). Intracellular cAMP concentrations are controlled by adenylate cyclase, which converts ATP to cAMP, and inorganic pyrophosphate and phosphodiesterase, which degrades cAMP into AMP. Adenylate cyclase activity is regulated by GPCRs through direct binding of $G_{\alpha s}$ or $G_{\alpha i}$ G-proteins (8,11,18,36,). Following G_s-coupled GPCR activation, $G_{\alpha s}$ acts to stimulate adenylate cyclase activity increasing cAMP production, whereas $G_{\alpha i}$ is inhibitory to adenylate cyclase resulting in a decrease in intracellular cAMP levels. Screening G_s-coupled receptors is straightforward but $G_{i/o}$-coupled receptor screening requires forskolin stimulation of adenylate cyclase to maximize the inhibition signal (18). Historically, intracellular cAMP was measured after agonist administration by using radioisotopic methods with competition of a radiolabeled cAMP (71). Additionally, luciferase reporter gene assays under the transcriptional control of a cAMP responsive element have been utilized (72). However, several homogenous assay platforms measuring cAMP accumulation are commercially available (see chap. 4 in this book) and many studies comparing assay formats have been conducted (73,74). The principle of these cAMP accumulation assays is that changes in intracellular cAMP are detected by competition between cellular cAMP and a labeled form of cAMP for binding to an anti-cAMP antibody.

HTRF cAMP Assays

Homogeneous time-resolved fluorescence (HTFR) technology (Cis Bio, France) uses cAMP that is labeled with allophycocyanin and the anti-cAMP antibodies are labeled with europium cryptate (75). When these two fluorescent molecules are in close proximity, fluorescence resonance energy transfer (FRET) occurs, in which the excited energy of the donor europium cryptate is transferred to the acceptor allophycocyanin and fluorescence is emitted at two different wavelengths (Fig. 10). After receptor stimulation and cell lysis, intracellularly produced cAMP competes with the fluorescent cAMP for limited binding sites on the europium labeled anti-cAMP antibody. Hence, when the two-labeled molecules are separated by competition with cellular cAMP, no FRET occurs and only emission from the europium is detected. A decrease in signal is obtained by increasing amounts of intracellular cAMP produced. This assay involves ratiometric data analysis and is dependent on normalization to a cAMP standard curve for accurate agonist EC_{50} measurements.

Fluorescence Polarization (FP)

FP technology kits (PerkinElmer, Molecular Devices and GE Healthcare) are based on the measurement of depolarization of emission from fluorescently labeled cAMP irradiated with a polarized light source. Fluo-cAMP is a small fluorescent molecule that rotates rapidly in solution, whereas fluo-cAMP bound to an anti-cAMP antibody is a large complex with slow rotation, orients in the plane of polarization, and the emitted light is highly polarized (77,78). At the starting point, a high polarization is measured when fluo-cAMP is bound to the cAMP monoclonal antibody. Agonist-stimulated cAMP displaces fluo-cAMP

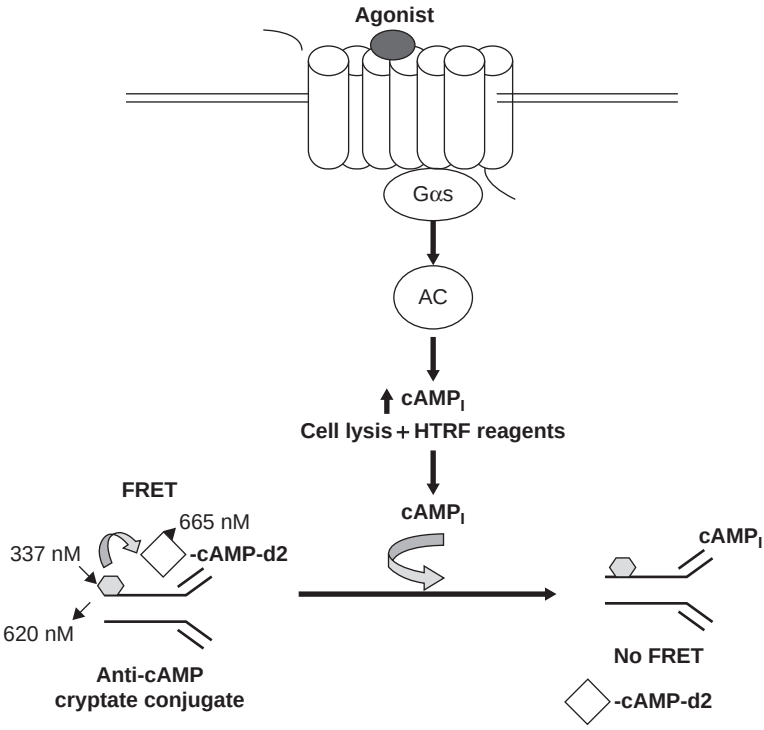

FIGURE 10 Detection of cAMP accumulation. Homogeneous time-resolved fluorescence (HTRF) cAMP assays measure a decrease in signal due to displacement of exogenous cAMP-d2 conjugate by increased endogenous cAMP ($cAMP_i$) production in response to agonist stimulated G_S signaling and activation of adenylate cyclase (AC). The cAMP-d2 tracer binding is visualized by a monoclonal anti-cAMP antibody labeled with europium cryptate such that when the two fluorescent molecules are in close proximity, fluorescence resonance energy transfer (FRET) occurs in which excited energy of the donor europium cryptate is transferred to the d2 acceptor and fluorescence is emitted at two wavelengths. When the two labels are separated by competition with intracellular cAMP, no FRET occurs. The signal is inversely proportional to the concentration of cAMP in the sample. *Source*: From Ref. 76.

from the anti-cAMP antibody binding sites and produces a decrease in polarization signal (77). Although this is a homogenous assay amenable to miniaturization and automation, this technology requires purified receptor source to yield a detectable signal-to-noise ratio and may be limited by interference of autofluorescent or yellow/brown compounds in the screening process (74,77,78).

Flashplate and Scintillation Proximity Assays

FlashPlate technology is an ELISA-based SPA competition of cAMP with [^{125}I]-cAMP for binding to a cAMP monoclonal antibody conjugated to scintillant-coated microtiter plate wells (71,79). In the absence of intracellular cAMP, the antibody sequesters the [^{125}I]-cAMP, which brings it close to the scintillant coated on the plate producing light that can be measured in a plate reader. Agonist-stimulated cAMP displaces [^{125}I]-cAMP from the antibody, leading to a reduc-

tion in signal. In addition to FlashPlate technology, SPA bead assay is based on the same principle of competition of cAMP with [^{125}I]-cAMP binding to an anti-cAMP antibody conjugated to SPA beads (80). A loss of signal is due to reduced proximity of [^{125}I]-cAMP and the SPA bead resulting from endogenous cAMP competition.

ALPHAscreen

The amplified luminescent proximity homogeneous assay (ALPHAscreen by PerkinElmer) uses proximity interaction between donor and acceptor beads (81). This format is based on competition of cellular cAMP and exogenously added biotinylated cAMP, which binds to high-affinity streptavidin-coated donor beads. When a monoclonal antibody conjugated to an acceptor bead captures the biotinylated cAMP bound to the streptavidin bead, free-radical oxygen is transferred, which is able to produce a chemiluminescent signal within the acceptor bead (82,83). Agonist-stimulated cAMP displaces biotinylated cAMP from anti-cAMP antibodies immobilized on acceptor beads resulting in a decrease in signal.

HitHunter Enzyme Fragment Complementation (EFC)

The DiscoveRx HitHunter assay kit is based on a β-galactosidase immunoassay complementation technology by using fluorescent or luminescent substrates (84–86). This system uses a cAMP molecule tagged with a β-galactosidase donor component, which is still recognizable by an anti-cAMP antibody and spontaneously combine with β-galactosidase acceptor component to form active enzyme. In the absence of cellular cAMP, the cAMP-enzyme donor is sequestered by an anti-cAMP antibody, which does not allow formation of an active enzyme complex when mixed with its counterpart enzyme acceptor component. The presence of cellular cAMP competes with the enzyme donor cAMP for the antibody, which then allows the free cAMP-tagged donor enzyme peptide fragment to recombine with the enzyme acceptor moiety to restore enzymatic activity that can be detected via substrates that generate a luminescent or fluorescent product.

Electrochemiluminescence (ECL)

Meso Scale Discovery's ECL technology uses cAMP tagged with a ruthenium derivative captured on carbon electrode multiarray plates by anti-cAMP antibodies (87). An electrical charge is applied following addition of a substrate, which initiates a reaction resulting in light produced from the labeled cAMP. Cellular cAMP competes for the anti-body and displaces ruthenium-tagged cAMP, which is no longer in proximity to the electrode and is not excited or detected. Background signals are minimal for this technology because the stimulus mechanism (electrical current) is decoupled from the signal output (light).

DELFIA

PerkinElmer's DELFIA technology is a heterogeneous time-resolved fluorometric immunoassay and is based on the competition between a Europium-labeled cAMP and endogenous cAMP for binding sites on rabbit cAMP polyclonal antibodies, which are immobilized to a solid surface through anti-rabbit IgG antibodies (88). The competition reaction is performed at room temperature for one hour followed by a wash step to remove unbound cAMP. An enhancement solution

dissociates europium ions from the labeled antigen in solution to form highly fluorescent chelates. The europium fluorescence can be detected on a plate reader with time-resolved fluorescence capability (88).

The cAMP accumulation assay technologies described above have been applied for the investigation of many G_s- and G_i-coupled GPCRs, with commonly used methods including HTRF, SPA, EFC, and DELFIA (11,18,73,74). The platforms can be used with recombinant or endogenously expressed receptors in many different cell types and these assays can be miniaturized to be amenable to the HTS format. HTRF and DELFIA have higher sensitivities to measure low levels of cAMP on the cAMP standard curve and EFC has amplification to enhance the assay window (18,73,74).

Inositol Phosphate Accumulation Assay

Following activation of a GPCR by agonist binding, G-protein–mediated signal transduction activates phospholipase C (PLC) to hydrolyze the lipid precursor phosphatidylinositol 4,5-bisphosphate to give second messengers diacyl glycerol (DAG) and inositol (1,4,5)-triphosphate (IP_3) (8,11). DAG activates protein kinase C and regulates cellular functions. IP_3 is a second messenger that controls many cellular processes by generating internal calcium (Ca^{2+}) signals. IP_3 binds to IP_3 receptors on the endoplasmic reticulum to mobilize stored Ca^{2+}. G_q-coupled GPCRs trigger the release of Ca^{2+} from internal stores via the PLC/IP_3 pathway. IP_3 accumulation assays, therefore, have been used to develop functional screens for Gq-coupled receptors. Traditional approaches measured the total accumulation of inositol phosphates including IP_3 and its metabolites D-myo-inositol bisphosphate (IP_2) and D-myo-inositol monophosphate (IP_1) after labeling cells with tritiated myo-inositol (89). Additionally, a radioreceptor IP_3 assay was developed to quantify IP_3 production in which a sample containing IP_3 competes a fixed amount of tracer (radioactive IP_3) for a fixed number of IP_3 receptor binding sites. These approaches suffer from the limitation that IP_3 production is very transient, reaching a peak 10 to 15 s after receptor activation followed by a rapid decay and this short lifetime makes the timing of the assay difficult for application to an HTS screen (90). SPA technology has also been employed to leverage higher throughput, homogeneous assays for IP accumulation. These SPA assays have been designed to use metal ion SPA beads that bind tritiated IP via their phosphate groups or yttrium silicate SPA beads that bind IPs (91,92).

In the nonradioactive HitHunter IP_3 fluorescence polarization detection kit, cells are treated with ligand to increase intracellular IP_3 levels and then quenched by perchloric acid (93). A fluorescent IP_3 tracer and a binding protein are added so that IP_3 from cell lysates competes for the IP_3 binding protein. IP_3 tracer bound to IP_3 binding protein will rotate more slowly in solution to give a high polarization signal. This polarization signal is inversely proportional to the amount of IP_3 contained in the cell lysates.

To circumvent the problem of rapid turnover of IP_3, Cisbio has developed the IP-One assay, which uses IP_1 as a surrogate of IP_3 to measure G_q-coupled receptor activation (90). This assay is based on the knowledge that LiCl leads to IP_1 accumulation after receptor stimulation by inhibiting inositol monophosphatase, the final enzyme in the IP_3 metabolic cascade. The IP-One assay is HTRF-based competitive immunoassay that uses europium cryptate–

labeled anti-IP_1 monoclonal antibody and d2-labeled IP_1 (90). The detection of IP_1 is a two-step process. During the first step, IP_1 is accumulated in cells after GPCR stimulation with agonist compounds in the presence of LiCl. The second step involves the sequential addition of HTRF reagents (acceptor d2-labeled IP_1 and FRET donor europium cryptate–labeled anti-IP_1 antibody) in a cell lysis buffer to allow detection of IP_1. Because of competitive binding to the anti-IP_1 antibody of d2-labeled IP_1 by the IP_1 accumulated after cell stimulation, results in a decrease in FRET signal. The advantage of IP_1 accumulation assays versus the traditional Ca^{2+} assays is the ability to measure inverse agonist activity in addition to agonism and antagonism.

Ca^{2+} Mobilization Assays for G_q and $G_{i/o}$ Receptors

One of the most widely applied cell-based techniques for measuring GPCR function is the monitoring of ligand-mediated activation or inhibition of intracellular calcium flux.

Agonist activation of GPCRs that can couple to the G_q and $G_{i/o}$ classes of G-proteins increases transient cellular Ca^{2+} concentrations. Although the Ca^{2+} concentration of mammalian cells is very high (1 mM), the cytosolic Ca^{2+} concentration is low (10–100 nM) and stimulation of a GPCR can increase the cytosolic Ca^{2+} to 400 to 1000 nM and activate calcium responsive events (61). Calcium mobilization can be measured by fluorescence-based dyes or bioluminescence methods (Figs. 11 and 12).

Fluorescence-Based Calcium Assays

The fluorescent calcium dyes Fluo3, Fluo4, and calcium green-1 are visible wavelength calcium dyes that are essentially nonfluorescent unless bound to Ca^{2+} and undergo a 100-fold increase in fluorescence upon binding Ca^{2+} (61). These dyes that are used in HTS intracellular calcium flux assays excite at a wavelength of 488 nm and emit at a wavelength of 500 to 560 nm (61). Fluorescence Imaging Plate Reader (FLIPR, Molecular Devices) is the main instrument used to perform high-throughput quantitative optical screening for cell-based fluorescent assays (94). The FLIPR is an automated, real-time charge-coupled device (CCD)–based fluorescent plate reader. In addition to intracellular calcium measurements, the FLIPR has also been employed in various applications to measure intracellular pH, intracellular sodium levels, and membrane potential in ion channel assays (61). The FLIPR measures fluorescence signal in all wells of a 96- or 384-well plate simultaneously by imaging with kinetic updates in the subsecond range (Fig. 11). Typically, a plate is read every one second for the first two minutes and every six seconds later up to 10 minutes. The Ca^{2+} spikes are predictable for each receptor and cell type, and the Ca^{2+} response is measured between certain time periods with blank subtracted.

For a FLIPR assay, cell lines expressing the GPCR of interest are grown as monolayers and loaded with Ca^{2+}-sensitive fluorescent dyes such as Fluo4 and Fluo3 AM and excess dye is washed out. The Calcium-3 fluorescent dye kit from Molecular Devices allows cellular dye loading without the need for subsequent wash steps (18). For agonist assays, different concentrations of agonistic compound is added to each well simultaneously by the FLIPR and the dye bound to Ca^{2+} is measured and is proportional to the transient increases in intracellular Ca^{2+} concentrations. For antagonist assays, the antagonist activity of a

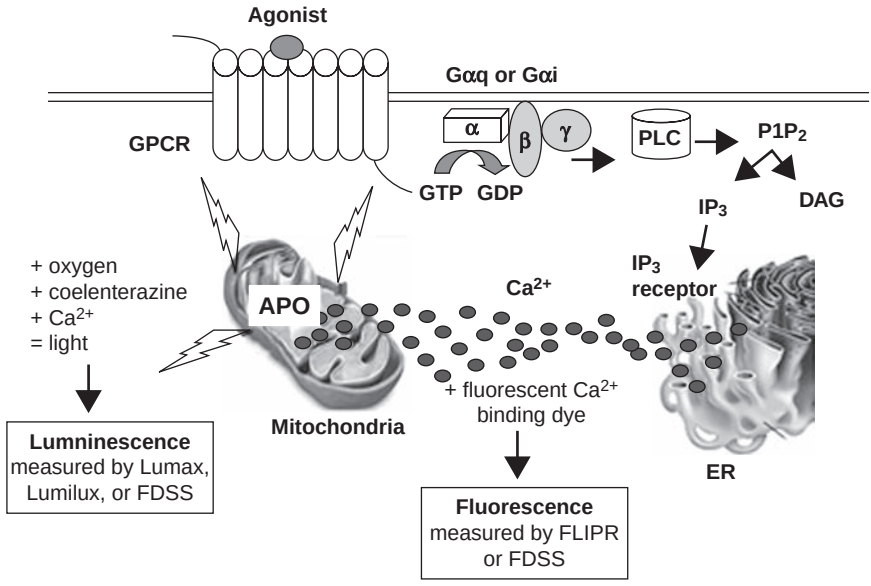

FIGURE 11 Luminescent and fluorescent technologies for measurement of intracellular Ca^{2+} signaling. Agonist activation of GPCRs that couple to $G_{\alpha q}$ and $G_{\alpha i/o}$ increase intracellular calcium concentrations through activation of phospholipase C (PLC), which hydrolyzes $P1P_2$ into the second messengers IP_3 and DAG. IP_3 binds to receptors in the endoplasmic reticulum (ER) to release intracellular Ca^{2+} stores, which can be measured by FLIPR or FDSS6000 via binding of fluorescent Ca^{2+} binding dyes. Aequorin technology is based on engineered cell lines expressing a mitochondrial-targeted apoaequorin (APO). Upon binding of Ca^{2+} to apoaequorin, a conformational change converts the protein into an oxygenase, which oxidizes the luminophore coelenterazine into coelenteramide with production of CO_2 and emission of light which can be measured by the Lumax, Lumilux, or FDSS6000 platforms.

compound is measured after dye loading and incubation with test compound followed by the addition of a standard agonist. The antagonist decreases the Ca^{2+} transient induced by agonist stimulation. The data output in ASCI form is imported into an appropriate database and the percentage of maximal response with a standard agonist is calculated against agonist concentration to obtain an EC_{50} value or plotted against antagonist concentration to obtain an IC_{50} value. Measurement of a functional response provides data on drug potency, efficacy, and function. It can characterize and distinguish full or partial agonists and antagonists within a single assay.

Luminescence-Based Calcium Assays

Intracellular calcium concentrations can also be measured by using bioluminescent aequorin and a luminometer such as the CyBio CyBi™-Lumax or the PerkinElmer Lumilux. Aequorin is a calcium-binding photoprotein originating from the jellyfish *Aequorea victoria* (95). Aequorin is composed of a 22-kDa apoprotein (apoaequorin), a luminophore called coelenterazine and molecular oxygen. Upon binding of calcium to three EF-hand calcium-binding sites, aequorin undergoes a conformational change that converts it into an oxygenase

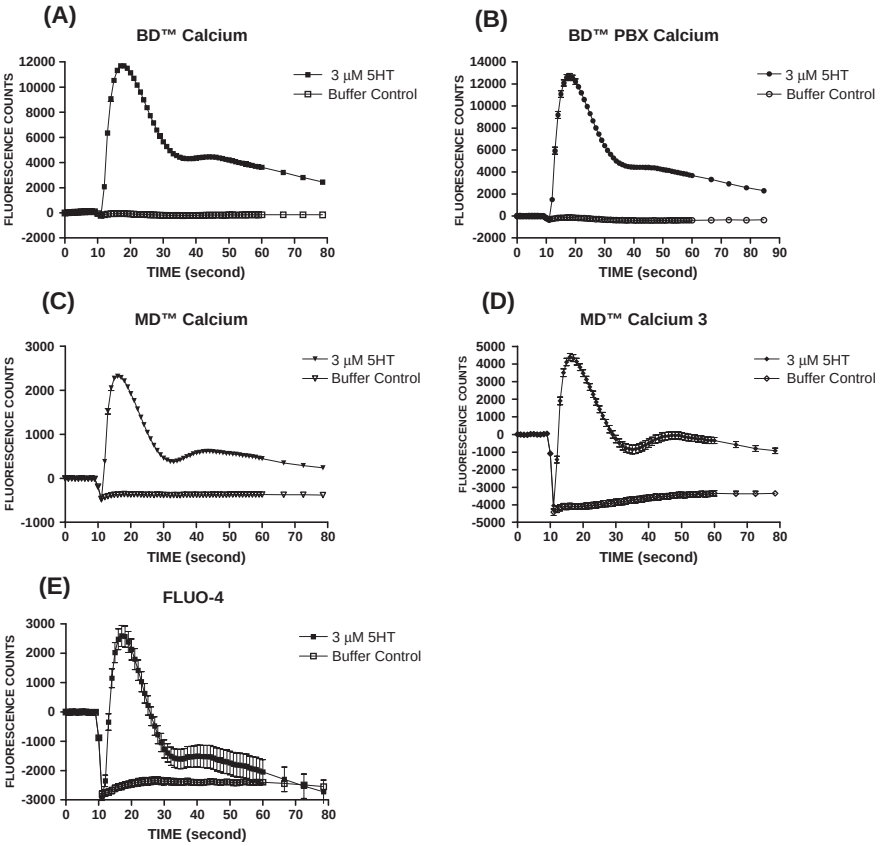

FIGURE 12 Measurement of intracellular Ca^{2+} using a fluorescent imaging plate reader (FLIPR). Real-time fluorescence image trace of the maximum agonism response from serotonin (5HT) in 384-well homogenous FLIPR assays using HEK293 cells expressing human $5HT_{2B}$ receptors. The mean response and standard error plotted in the graph was achieved from 5HT at the concentration of 3 μM and buffer control containing the same concentration of DMSO from 16 replicates tested in the same assay plate. (**A**) Calcium Kit [Becton Dickinson (BD)], (**B**) PBX Calcium Kit (BD), (**C**) Calcium Kit [Molecular Devices (MD)], (**D**) Calcium 3 Kit (MD), and (**E**) Nonwash FLUO-4 method. Agonist addition is at the time of six seconds.

and oxidizes coelenterazine into coelenteramide with production of CO_2 and emission of blue light (470 nM; Fig. 12) (96,97).

For aequorin studies, the cell line must be created to stably express the receptor of interest and the mitochondria-targeted apoprotein. Euroscreen has a product line of engineered cell lines called AequoScreen™ in which a mitochondrially targeted apoaequorin is expressed together with GPCRs with or without promiscuous ($G_{\alpha 15/16}$) or chimeric G proteins (98,99). During the assay, cultured cells are detached and incubated with coelenterazine to reconstitute active aequorin. In the agonist mode, cells are added to agonistic compounds in a 384-well plate followed by kinetic read of the resulting luminescence. In the antagonist mode, light is emitted upon agonist activation of the GPCR and antagonist activity is reflected by the inhibition of light emission during a kinetic read

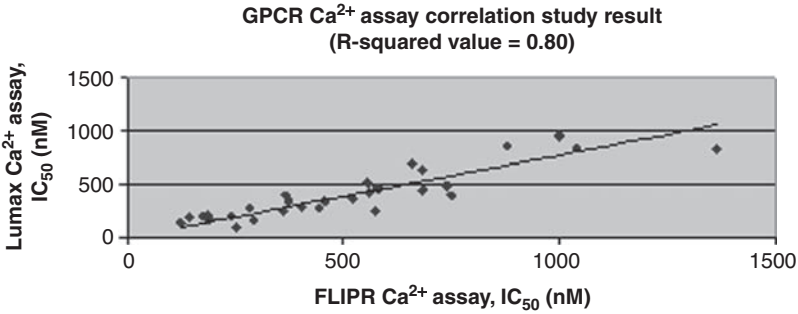

FIGURE 13 Assay correlation of luminescence- and fluorescence-based Ca^{2+} mobilization assays. The activity of 30 antagonists of a G_i-coupled GPCR was assessed using Ca^{2+} binding fluorescent dyes with FLIPR analysis and aequorin luminescence technology with Lumax analysis. IC_{50} assessments covering a range of potencies show a significant correlation between luminescence and fluorescence technologies for this GPCR target as measured by the Pearson correlation coefficient (r^2). r^2 reflects the degree of linear relationship between two variables with one being a perfect relationship (100). These data suggest that the aequorin luminescence assay results are comparable with FLIPR fluorescence assay results for antagonist mode assays (101).

on a luminometer. The signal in mammalian cells occurs within 30 seconds and the intensity of the aequorin flash is proportional to the Ca^{2+} concentration (61). Calcium assay optimization studies for luminescence-based assays include titrations for cell number, agonist, and DMSO concentrations as well as incubation time courses and coelenterazine titrations.

Another technology platform called the Hamamatsu Photonic Systems FDSS6000 Functional Drug Screening System has capabilities to measure both fluorescence and luminescence read-outs (98). Ca^{2+} measurements by aequorin assay have been validated for many GPCRs and the dose–responses are similar to the values obtained with fluorescent-dye methods. As indicated in Figure 13, the IC_{50} values for the majority of antagonists tested for a $G_{\alpha i}$-coupled receptor in the aequorin luminescence assay are comparable with FLIPR fluorescence assay results.

The advantages of fluorescent technologies are that primary cell lines can be used, a high-intensity emission is achieved, and intracellular Ca^{2+} is directly measured. The disadvantages of fluorescent technologies are that the dyes can be toxic to cells, wash steps associated with dye removal, assay sensitivity to factors affecting cell performance, and artifacts from the interference of autofluorescent test compounds. The pros for aequorin luminescent technology are that no toxic dye is needed for measurement, cells are stable for many hours, and it is a homogenous mix-and-read assay that is sensitive over large dynamic ranges with low background and no interference from test compound autofluorescence. The cons of aequorin technology are that expression of a photoprotein is required, short emission times, low quantum yield, and an indirect measurement of intracellular Ca^{2+} levels through the mitochondria. Assay performance parameters and pharmacological characterization of antagonists (IC_{50}) have been evaluated in both luminescent and fluorescent formats (Fig. 13) and the results have indicated that calcium assays can be transferred among the technology platforms (98).

Calcium Reporter Assays

Calcium-regulated reporter assays are another platform for the functional screening of GPCRs and are based on transcription factors (NFAT, AP-1) that become activated when there is a rapid rise in intracellular calcium levels. These reporter assays are based on the ability of second messengers such as calcium to either stimulate or inhibit responsive elements (NFAT or AP-1 response elements) upstream of a calcium-regulated promoter driving a reporter gene such as luciferase, β-lactamase, or β-galactosidase (18). These transcription factors on activation bind to the unique promoter and stimulate transcription of the reporter protein. The drawback to this approach is the long incubation times required for transient transfection studies and the fact that a downstream event is being measured very distal to the receptor that may result in a higher false-positive rate.

β-Arrestin Technologies

As previously described in this chapter, β-arrestins mediate the desensitization and internalization of GPCRs after ligand activation through direct interaction with the GPCR C-terminus (8,11,44–47). DiscoveRx's PathHunter β-arrestin Flash Detection technology (102) uses cell lines transfected with a GPCR of interest fused to an EFC tag comprised of a portion of an inactive β-galactosidase protein. The cell line is also transfected with a fusion protein of β-arrestin with a second EFC β-galactosidase component essential for chemiluminescent detection of an agonist or antagonist response. After ligand activation, the GPCR–arrestin interaction combines the two β-galactosidase components, which interact only when in close proximity to form an active β-gal enzyme capable of converting a substrate into a chemiluminescent detection signal.

Invitrogen's Tango™ GPCR assay system is also a cell-based GPCR–arrestin interaction technology (103). After GPCR activation by a ligand, a desensitization process is triggered, which is mediated by recruitment of β-arrestin proteins to the activated receptor. Tango technology is based on the interactions between intracellular arrestins and the GPCR C-terminus. Upon receptor stimulation, a protease-tagged arrestin cleaves a protease site fused to the C-terminus of a given GPCR that has been tethered to a nonnative transcription factor. Cleavage of this site releases the transcription factor that enters the nucleus and regulates transcription of a β-lactamase reporter construct, which is measured upon substrate addition after FRET reaction. In the absence of β-lactamase expression, cells generate a green fluorescence signal, but in the presence of β-lactamase, cells generate a blue fluorescence signal due to substrate cleavage. The blue to green fluorescence ratio obtained correlates to receptor modulation by agonists and antagonists tested in the system.

There are several advantages gained from the usage of the Tango System (103). First, the read-out obtained is specific for the target GPCR expressed, which ensures a selective read-out. Second, the measurement is proximal to the site of receptor activation and minimizes false positives associated with downstream signaling events. Finally, this technology is applicable to all classes of GPCRs independent of G-protein coupling, which enables the study of any GPCRs including orphans (103). Molecular Devices' Transfluor technology also uses the β-arrestin pathway.

High-Content Screening for GPCR Targets

High-content screening (HCS) is a combination of fluorescence microscopy and automated image analysis algorithms to extract biologically meaningful measurements from cellular images. HCS allows scientists to quantitatively measure interactions between biological targets and molecules in living cells and dependencies of activities on their physical and chemical environments. HCS technology enables the measurement of multiple assay variables at the same time in cell-based assays. HCS assays for the functional activation of GPCRs typically rely on measurements of protein translocation, receptor internalization, and trafficking (104,105). The broad application of GPCR internalization assays is based on the GPCR desensitization process (106) described previously in this chapter. Many GPCRs undergo ligand-dependent homologous desensitization accompanied by aggregation of the receptor followed by internalization into endosomes. From the endosome, the GPCR is either recycled back to the plasma membrane or degraded in the lysosome (47).

HCS platforms are imaging systems developed to analyze multiple fields of cells in microtiter plate wells simultaneously. For GPCR internalization assays, specific algorithms measure the appearance and intensity of intracellular fluorescent patches or aggregates. There are several means to monitor the internalization of a GPCR including the co-internalization of a specific, fluorophore-labeled ligand, or a fluorescent antibody directed against an amino- or carboxyl-terminal tag of the GPCR (107). Another means to monitor receptor internalization is by construction of stable cell lines expressing recombinant GPCR-green fluorescent protein (GFP) fusion conjugates. For example, in an unstimulated cell, the majority of a GFP-tagged GPCR is localized on the cell membrane, resulting in a green fluorescent halo around the cell periphery. In an agonist-stimulated cell, the GFP-tagged GPCR internalizes in a time- and concentration-dependant manner into endosomes and appears as punctuate dots throughout the cytosol (108). Furthermore, it is possible to also measure recycling of the GPCR back to the cell membrane.

Molecular Devices' Transfluor technology is also a fluorescence high-content assay used to screen GPCR activation (109). This platform is based on the receptor desensitization pathway whereby β-arrestin proteins bind to the activated GPCR. The cellular location of the receptor–arrestin complex is monitored by attaching a fluorescent label to the β-arrestin. After receptor activation, β-arrestin translocation and subsequent receptor recycling provide a method to detect GPCR activation (110). Receptor stimulation induces movement of the fluorescence to pits within seconds and to endocytic vesicles within minutes (111). Using genetically engineered cell lines that express the fluorescently tagged beta-arrestin and GPCR of interest, the Transfluor technology has been validated for all GPCR classes (I, II, III) independent of G-protein coupling.

The most widely used automated cellular imaging platforms employing automated fluorescent microscopy are the ArrayScan™ HCS (Cellomics) and Discovery 1™ (Molecular Devices) with plate handling, CCD cameras, data point storage linked to the cell image, which generated it, and medium throughput of <50,000 data points per day (112). The Opera™ (Evotec Technologies) and the INCell Analyzer™ (GE Healthcare) utilize confocal microscopy with very high throughput (>1 million data points per day). These cellular imaging devices are primarily used for secondary screening and lead optimization

and their easy-to-use features and user-friendly software require minimal supervision (112). These high-content screening platforms are a homogeneous format that can be used to study GPCRs in the context of intracellular signaling transduction events and subcellular localization.

Label-Free Cell-Based Assays to Study GPCRs

Label-free cellular dielectric spectroscopy (CDS) technology is a universal platform for the pharmacological evaluation of different classes of endogenous GPCRs with the ability to differentiate between GPCR subtypes without the development of separate assays to monitor secondary messengers associated with G-protein coupling. The underlying principle of this technology is the fact that GPCR signaling activates the Rho family of GTPases, which are involved in regulation and maintenance of the actin cytoskeleton framework (113). Because GPCRs couple to and modulate cytoskeletal changes and cell morphology, it is possible to measure the changes in cell adherence, cell shape, cell size and volume, and cell-to-cell interaction to evaluate cell responses as a result of ligand-dependent GPCR activation (114–116).

CDS technology measures the changes in dielectric impedance of a cell layer that occur in response to GPCR stimulation. For measurements using the CellKey^{TM} system (MDS Sciex, Concord, Ontario, Canada), cells are seeded on microtiter plates containing electrodes imbedded in the bottom of the well (115,117). The instrument applies small voltages to the electrodes over different measurement frequencies once every two seconds (115). At low frequencies, extracellular currents (iec) are induced that pass around individual cells, while at high frequencies, voltages induce transcellular currents (itc) that penetrate the cell membrane (115). The impedance (Z) is measured as the ratio of the applied voltage to the measured current in accordance with the Ohm's law equation.

When cells are stimulated with agonist or test compounds, GPCR signaling events lead to changes in the actin cytoskeleton and these changes affect the flow of the iec and itc currents, which affect the impedance. Using CDS technology, it is possible to determine the G-protein coupling of a specific GPCR since differently coupled GPCRs generate different effects on cell morphology that affect cellular impedance measurements. For example, activation of G_q- and G_i-coupled GPCRs leads to increased actin polymerization resulting in increased impedance, whereas stimulation of G_s-coupled GPCRs lead to actin depolymerization, resulting in a decrease in impedance (118–121). These affects can be observed in as little as 30 seconds after receptor stimulation (115). The general characteristics of CDS responses for GPCR activation are depicted in Figure 14. CDS results from the CellKey correlated with agonist and antagonist data obtained using classical methods such as cAMP and [^{35}S]GTPγS binding and have been characterized with many different receptors.

There are several major advantages of employing CDS technology (114–117). First, this approach is noninvasive (where both ligand and receptor are label free) and provides real-time kinetic data for measuring cellular responses to ligand or drug treatment (114,117). Second, the platform is versatile with respect to assay conditions and has minimal assay-specific cell line requirements (117). The sensitivity of the CDS technology is capable of detecting responses with both exogenously expressed receptors and the lower expression levels associated with endogenous receptors and, therefore, enables the use of disease-relevant primary

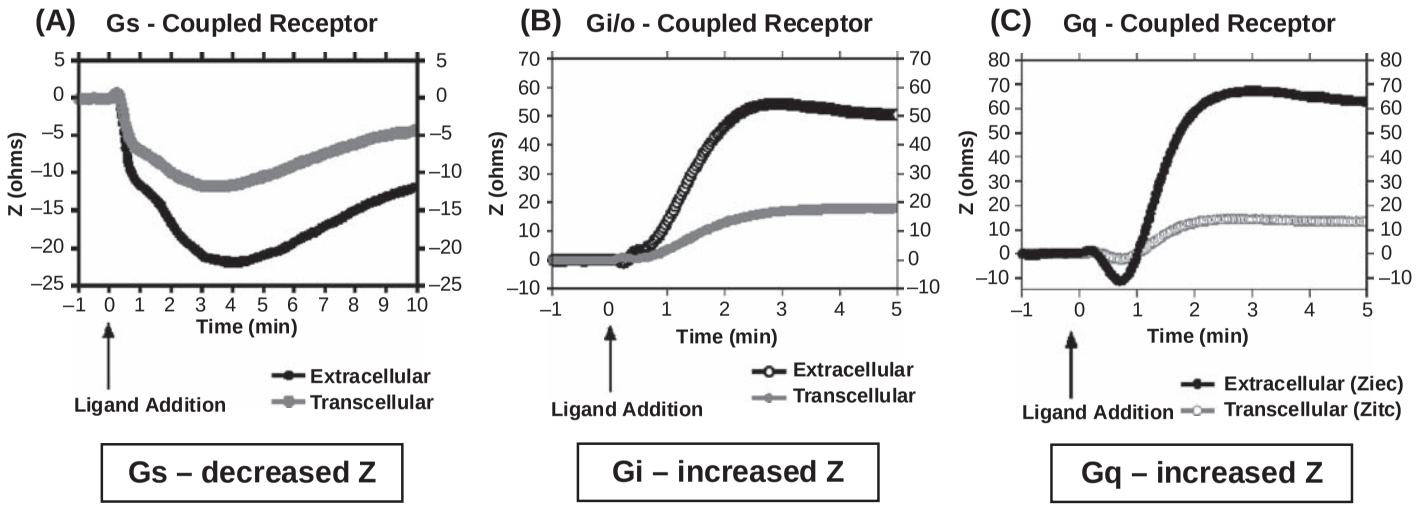

FIGURE 14 General characteristics of CDS responses for GPCR activation. GPCRs with different G-protein coupling generate different effects on cell morphology that affect cellular impedance (Z) measurements and yield different graphical signatures by CellKey CDS technology (115). (**A**) Characteristic G_S-coupled response after agonist stimulation resulting from decreased impedance due to actin depolymerization. (**B**) Characteristic $G_{i/o}$-coupled response resulting from increased impedance due to actin polymerization. (**C**) G_q-coupled receptors also demonstrate increase impedance due to actin polymerization and are characterized by a downward shift at the beginning of the reading.

cell lines (115). As a result, there is no need to engineer the cells with promiscuous G proteins or overexpressed receptors or label the cells with dyes (116). CDS can measure endogenous receptors that are undetectable with other functional assays (115). Third, multiple stimulation with the same or different ligands can be conducted to assess receptor desensitization or receptor cross-talk. Finally, this universal platform can be used to measure G_q-, G_i-, and G_s-coupled receptors (115–117).

The CDS platform does present several technological challenges, and assay development and optimization are important for use of this technology. CDS assays are very sensitive to many factors including cell health in culture, cell density, DMSO concentration, BSA purity, buffer pH, and temperature. In addition, CDS measures the downstream events distal from receptor activation and second messenger signaling. Therefore, selective receptor antagonists and specific signaling blockers are recommended in validation of assays and interpretation of CDS pharmacological data (116,117). Nonetheless, combined with other technologies, this label-free universal platform may have broad impacts on multiple stages of preclinical drug discovery such as identification of G-protein–coupling mechanism of orphan GPCR receptors, cataloging functional endogenous receptors, de-convolution of signaling transduction of unknown ligands, and pharmacological analysis of GPCR receptors (115,116,122).

The RT-CES™ system (Acea Biosciences, San Diego, CA) also uses electronic cell sensor arrays and cell-electrode impedance measurements for real-time monitoring of minute changes in cellular morphology as a result of ligand-dependent GPCR activation (114,116). The pharmacological profiles of GPCR ligands obtained from the RT-CES system are comparable with data from direct measurement of second messengers in conventional functional assays (114,116). In addition to measurement of GPCR activation, the RT-CES system can monitor cell attachment, growth, proliferation, and cytotoxicity. However, this technology, unlike CDS, does not provide a unique signature pattern for G_q, G_s, and G_i signaling.

In addition to cell-substrate impedance technologies, the Corning Epic™ System optical biosensor technology, which uses resonant waveguide grating, has also been employed as a label-free approach to detect functional activation of GPCRs (123). Other label-free technologies including quartz microbalance biosensor technology, surface plasmon resonance, optical ellipsometry, and refractive index measurements are also a means to monitor live cell status in response to GPCR activation (124–128).

SCREENING STRATEGY AND CONSIDERATION FOR THE GPCR TRAGET FAMILY

HTS has become a mainstay of pharmaceutical research. Through a combination of advances in assay development, robotic instrumentation, compound library development, and liquid handling technologies, the pharmaceutical industry has become dependent upon HTS methods as a primary approach for identifying hit compounds that interact with a specific pharmacological target. The hit identification process for the GPCR target family is primarily driven by cell-based functional assays for both agonist and antagonist targets (11,18,21,22,129–131). Completion of a full deck library screening in a short-time period (a couple of weeks or months) requires the most efficient means, where speed, signal, and

cost are clearly appropriate criteria by which an HTS lead discovery group may evaluate various assays. After the identification of hits from a HTS campaign, lead optimization is a time-consuming process (21,22,129–131). From early hit advancement to the drug candidate stage usually takes several years of SAR effort in preclinical drug discovery. The understanding of signaling pathways and biological relevance in order to establish efficient and biologically meaningful approaches at the early stage of SAR is a very important investment. Along with better understanding of in vitro and in vivo data connectivity for lead compounds in terms of efficacy and side effect profiles, the in vitro screening strategies need to be adjusted accordingly.

Screening of GPCR Agonists and Antagonists

The approaches used to discover GPCR agonists and antagonists over the last 20 years primarily involved biochemical methods, such as radioligand binding assays (8,23). GPCR ligand binding technologies are employed to screen for drugs against any GPCR for which a high-affinity radilogand is available. Collectively, many FDA-approved GPCR drugs on the market were first identified in a primary screen by using radioligand binding techniques (8,11). At present, assessment of agonist activity in functional assays should be considered as an essential primary screening (8,11,18,23) to support lead optimization studies for any GPCR agonist targets (Fig. 15). In contrast, the binding assay can be performed as a secondary and confirmatory assay or conducted in parallel because the binding assay only provides the compound information of binding affinity with receptor, without any insight into compound agonist activity (11,18,23,33). The structure–activity relationship (SAR) is driven by designing

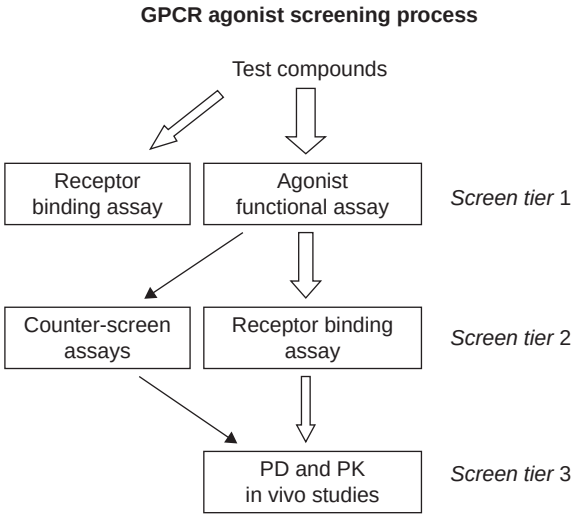

FIGURE 15 Proposed compound progression of GPCR agonist screening strategy (8,10,11,13,18,11,34,130). Functional activity assessment and binding determination for screening agonist compounds can undergo parallel approaches or go through a linear 1st and 2nd tier sequential process. *Abbreviations*: PD, pharmacodynamics; PK, pharmacokinetics.

compounds that are not only potent receptor binders but also display efficacious and potent agonist activity. The agonist-driven approach requires the compound to induce receptor conformation changes to trigger downstream signaling events in a manner consistent with full agonist-induced changes. Recent studies from Wacker et al. (33) have shown that a disconnectivity for $5HT_{2C}$ agonist compounds between binding potency (K_i) assessed in ^{125}I-DOI binding and agonist potency (EC_{50}) obtained in FLIPR Ca^{2+} mobilization assays, demonstrating that compounds with the same affinity can have differential agonist potencies as well as efficacies even with minor changes are made in the structure for certain chemotype compounds (33). Furthermore, today's HTS capacity and efficiency in GPCR functional assay technology (11,18,22) are enabling parallel searches based on both functional and binding parameters for agonist determination.

Recently, more and more orphan GPCR receptors are up and coming as novel agonist targets (10,11). Agonist functional assays for study of these orphan receptors represent a main driver for the screening of compounds from de novo direct synthesis due to lack of known endogenous agonists or a high-affinity ligand as radioligands. When a potent lead compound is available, it can be radiolabeled to use in binding assay to ensure specific interaction between drug and receptor (10,11,23,28) and this approach can be implemented as a secondary screen or spot check. Examination of the competitive nature of the new radioligand with receptor and other chemotypes is highly recommended prior to application of the binding assay for primary screen (23,26,28).

Unlike the development of binding assays, agonist activity and assay stability can be affected by many factors, including receptor expression level, cell background, and assay format (8,11,18,23,25,28,57). For example, agonist potency and efficacy can be overestimated in a cell system with a huge number of spare receptors reserved and, therefore, data interpretation should be made cautiously (23,25,34). Careful evaluation and characterization of cell lines prior to assay development is needed in order to select appropriate cell lines and assay formats for the agonist screen. In addition to assay conditions, signaling pathway analysis in terms of understanding the biological relevance of differential transduction pathways should be fully investigated prior to selecting the agonist assays to drive SAR screening (8,11,14,23,57,58,132). The agonist-directed trafficking phenomenon was introduced in the GPCR research field many years ago but current interest has been heightened with a focus on functional selectivity in recent reviews (14,34,132). Basically, many agonist ligands can differentially activate multiple signaling pathways through a single receptor via coupling with different G-proteins, demonstrating differential agonist potency and efficacy for these cellular responses (8,11,14,23,132). For example, a $5HT_{2A}$ compound can be a full agonist in G_q-mediated Ca^{2+} response but display weak partial agonist activity in G_i-mediated arachidonic acid release (132). Another agonist compound may behave equally potent and efficacious in triggering both G_q- and G_i-signal pathways. The biased agonism can be explained by different receptor conformational changes induced by different agonists. However, understanding of individual pathways relevant to compound efficacy and side effect profiles will guide the meaningful monitoring and screening of lead compounds for compound advancement in the lead optimization phase and proof-of-principle studies for drug discovery.

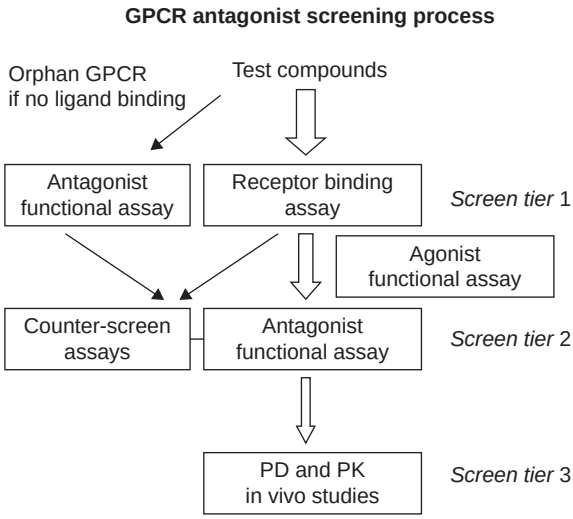

FIGURE 16 Proposed compound progression of GPCR antagonist screening strategy (8,11,18,134–136). *Abbreviations*: PD, pharmacodynamics; PK, pharmacokinetics.

The approaches used to discover GPCR receptor antagonists are mainly driven by ligand–receptor binding screening. This strategy is still a very useful approach today based upon the assumption that the compound is a high affinity binder without agonist activity and, therefore, must be the receptor antagonist (Fig. 16). In general, the rank order of potency for antagonist compounds from competition binding studies using the endogenous agonist as a radioligand probe correlates well with the data from functional antagonist IC_{50} determination (133). The antagonist potency determination can be a second tier assay in the compound progression scheme. However, in the case of orphan GPCRs, it is difficult to establish the radioligand binding assay because an endogenous agonist radioligand is not available or not useful due to a low potency or high nonspecific binding. In this case, IC_{50} determination from a functional antagonist assay becomes a main driver for SAR studies (11,18). After a potent antagonist lead is found, the labeling of this small-molecule antagonist compound can be achieved in some cases and the compound can be evaluated in a radioligand binding assay to ensure specific ligand–receptor interaction (23,28).

In the early phase of SAR or with any new chemotypes as antagonist lead molecules, it is important to check for any agonist activity of the compounds (11,23,28,62). The agonist properties of compounds could desensitize the receptor and therefore lead to false-positive antagonist data from compounds with intrinsic agonist activity (8,23). The screen of agonist activity for any antagonist compounds is a necessary step for all compounds until there is no agonist activity found for the chemotypes and compounds in the late stage of SAR. At this point, the agonist screen can then be retired as a second tier assay to spot check for lead compounds (8,23,28,135,136).

Screening of GPCR Allosteric Modulators

GPCR-based drug discovery has focused on the development of more selective and potent molecules either functioning as an agonist or an antagonist that act at the receptor's orthosteric site, that is, the same binding site recognized by the endogenous agonist (7,23,33). However, some GPCR subfamilies share high sequence homology within the orthosteric binding domain across receptor subtypes, making the development of a subtype-selective orthosteric ligand very difficult. There is a growing interest in the pharmaceutical industry to search for allosteric modulators of GPCR targets based on several advantages of allosteric modulator over orthosteric ligands (7,11,19,23,33,137,138). First, greater GPCR selectivity might be obtained by targeting an allosteric site. Second, allosteric modulators have no effect in the absence of the orthosteric ligand, and act only to either "turn up" or "turn down" the signaling responses of the orthosteric ligand. Third, these allosteric modulators may have a ceiling to their effect with a potential of reduced toxicity. Allosteric modulators are defined as ligands that bind to a site on the receptor that is topographically distinct from the orthosteric binding site (137). After binding to the receptor, allosteric modulators termed "allosteric enhancers" enhance the orthosteric ligand's activity and mediate their effect by increasing orthosteric agonist ligand affinity or function. Allosteric modulators are able to activate the receptor even in the absence of the orthersteric ligand are termed "allosteric activators" or "allosteric agonists" (138). In contrast to the positive effect of the allosteric enhancer, allosteric modulators can also be referred to as "allosteric inhibitors" or "allosteric antagonists" because they act to inhibit agonist activation after binding to the allosteric site of the receptor (138).

There is now an increasing body of evidence demonstrating that GPCRs do indeed possess extracellular allosteric binding sites and allosteric modulating compounds have arisen from drug discovery efforts and are described in recent reviews (19,20,138). For the screening of allosteric inhibitors, the cell-based functional antagonist assay is typically utilized in hit identification and the competition binding assay is employed for assessing compound rank order of potency in the lead optimization process (7,19,21,137,138). These paradigms are aligned with approaches used for orthosteric antagonists (competitive antagonists). Allosteric inhibitors can fully inhibit agonist radioligand binding in the competition binding experiment by altering receptor conformation and preventing agonist binding to the receptor (8,11,23,28). In general, the allosteric inhibitor can be evaluated and screened with the same method used for competitive antagonists for SAR determination. In the same way, the potency (IC_{50}) of allosteric inhibitors can be determined in cell-based functional assays in the presence of a fixed concentration of the agonist (8,11,23,28). However, the noncompetitive nature of allosteric inhibitors should be evaluated experimentally in three modes—Schild analysis, reciprocal binding, and binding kinetic studies—in order to confirm the mechanism of inhibition (8,19,23,137,138). Even though a compound shows the competitive pattern in a Schild analysis where a receptor overexpressed recombinant cell line is used (Fig. 17), the inhibition nature of the compound should be followed up with an endogenous, physiologically relevant system, and off-rate agonist binding studies (23,28). Greater success and validation may be achieved by using a dissociation kinetic binding assay. This assay takes advantage of the fact that allosteric changes in receptor confirmation will lead to changes in the rate of orthosteric ligand dissociation, irrespective

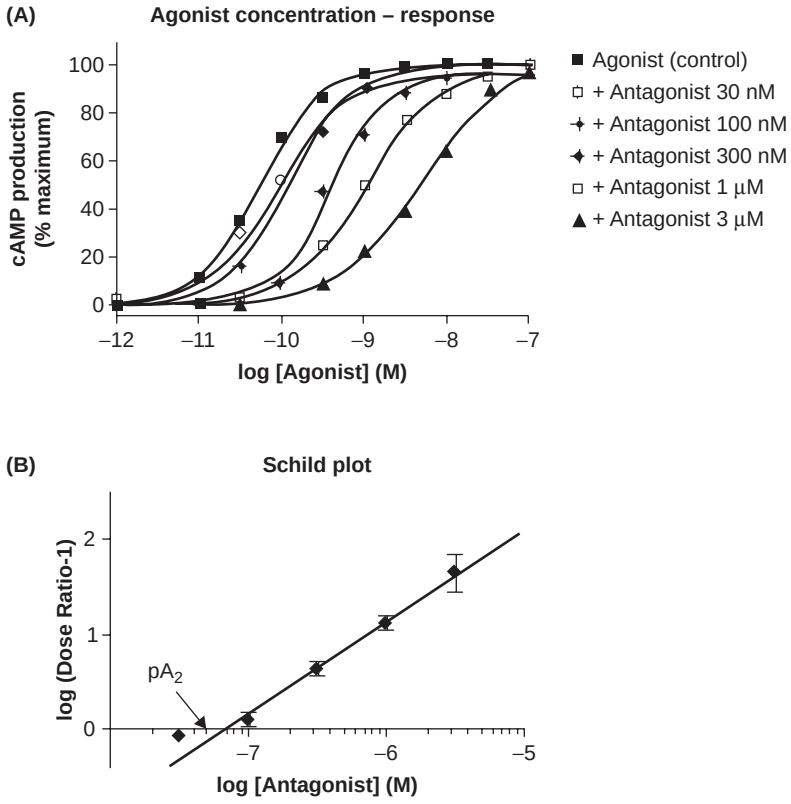

FIGURE 17 The agonist concentration–response analysis in the absence and presence of an antagonist which was examined in a GPCR overexpressing cell line. (**A**) A parallel shift pattern of agonist concentration–response curves observed in the presence of the antagonist. (**B**) The antagonist potency constant K_B can be calculated from PA_2 value from the Schild plot (23,24).

of whether the cooperativity at equilibrium is positive or negative. However, this approach is low throughput with many limitations as a primary screening approach for selecting leads from SAR studies, as it requires significant expenditure of time and money for quality and quantitative analysis (8,19,23,137,138).

For allosteric activators and positive modulators, the functional assay is preferred in an initial screening paradigm. Functional assays have a potential to detect a wider spectrum of compounds that either activate the receptor by itself or enhance endogenous agonist activity, the only prerequisite being that the compounds perturb receptor signaling irrespective of where they are binding (8,11,18,19,23,137,138). In binding assays, the probe is always a surrogate-radiolabeled chemical that displays high affinity and selectivity for a specific orthosteric site on the GPCR of interest. Thus, binding assays are biased towards the detection of orthosteric agonist drugs because an allosteric interaction might be clearly apparent using one probe, and the observed interaction can be negligible using another probe in the binding assay. For the screening of allosteric enhancers, functional assays are performed with surrogate chemical probes

(i.e., agonists) to test for positive modulator molecules (8,11,18,19,23,137,138). Many of the properties of GPCR allosteric positive modulators that make them therapeutically attractive also present the greatest challenge for in vitro screening to drive SAR studies due to low assay window and low throughput (11,19,137,138). However, targeting of allosteric modulators towards GPCRs will represent an attractive and challenging approach to drug discovery for the pharmaceutical industry in the near future.

Determination of Compound Specificity

As ligand binding assays cannot differentiate between agonist, antagonists, and inverse agonists, lead optimization utilizes both biochemical and cell-based assays for assessing compound potency and selectivity for a given GPCR target. Lead compounds then progress to in vivo efficacy studies and the process requires strong assay connectivity between in vitro and in vivo studies. Through the panel screening strategy, which includes an array of drug safety and selectivity profiles, rapid, high-throughput lead optimization data enables the drug discovery project teams to compare compounds against a multiparameter matrix. The tracking of a full data package of potency, selectivity, and properties directs project teams in the identification of the most promising preclinical drug candidates (21,2,131).

Ligand Specificity Assessment

Small-molecule agonists or antagonists that are developed against one GPCR often show off-target selectivity or cross-reactivity with other members of the same family. The chemokine receptor family of GPCRs, which are responsible for activation and mobilization of immune cells, is a prime example of cross-talk between receptor family members. With at least 19 chemokine receptors and over 45 chemokine ligands, significant promiscuity exists in the chemokine binding within the family (134,139). Some of the chemokine receptors share high homology, that is, CCR2/CCR5, CCR1/CCR3, CXCR1/CXCR2 (139). The challenge for a drug discovery program is to ensure highly selective antagonists for a given chemokine receptor. Therefore, during the lead optimization process, it is necessary to assay a panel of closely related targets concurrently with the advantages being not only to identify a selective lead series but to query a number of potential drug targets simultaneously that may lead to program cross-fertilization by serendipitous discovery of drug-like compounds for another target (21).

Target Specific Liability

Lead molecules for a given GPCR target may also have cross-reactivity with receptors of different GPCR families. For example, chemokine receptor antagonists often display activity at the biogenic monoamine GPCR receptor classes, including dopamine, adrenergic, histamine, muscarinic, and serotonin receptors, which may result in liability issues surrounding cardiac and central nervous system functions (135,136). These target specific liability issues can therefore preclude the therapeutic use of these chemokine antagonists for specific indications. Therefore, emphasis on early detection of cross-reactivity at receptors associated with harmful side effects can increase the probability of success of a lead molecule (21).

Species Specificity

Commonly, there are potency and/or efficacy differences among different species for a given GPCR target. For example, a major challenge of small-molecule chemokine antagonist programs is having poor affinity for nonhuman receptors such as mouse, rat, rabbit, and Cynomologous monkey, which complicates efficacy testing in the appropriate animal model (140). Some reasons for the lack of relevant animal models for chemokine receptors include differences in amino acid sequence, species differences in expression levels of chemokine receptors, differences in expression patterns, that is, CCR1 is expressed on neutrophils in rat but in humans CCR1 is expressed on monocytes, T cells, immature dendritic cells but not on neutrophils (141), differences in selectivity due to receptor conformation or activation states, and differences in components of downstream signaling pathways. Therefore, species selectivity panels are necessary to progress leading compounds and to interpret in vivo data. Automated, high-throughput primary and secondary selectivity assays run in parallel for different species can provide more comprehensive data packages to expedite discovery program decisions on advancing drug candidates (22). Ligand and species specificity and selectivity are important determinants for priming in vivo assessment and building correlation between in vitro and in vivo studies (21).

RECEPTOR MUTAGENESIS STUDIES

The combined use of site-directed mutagenesis techniques and molecular modeling approaches has provided detailed insights into the molecular mechanisms of GPCR ligand binding, receptor activation, and G-protein signaling as evidenced by many publications including studies with the rhodopsin, adrenergic, serotonin, neurotensin, purinergic, and chemokine receptors (142–149). Currently, the only means for validation of GPCR structural models is through design and testing of mutant receptors married with small molecule SAR. The yield of information from such studies can provide detailed insight into receptor folding, ligand/receptor affinity and selectivity, G-protein coupling, and regulation of signal transduction (150). The resulting data has proven invaluable in progressing modeling efforts to feed compound design efforts and enhance compound potency, selectivity, and properties.

To select amino acids for mutation, prior knowledge about the receptor or related receptors is required. Examples include information from computer-modeling–derived structure, sequence alignment, homology modeling, and other mutation data (151). Site-directed mutagenesis of key residues followed by binding or functional tests elucidates the functional consequences of the mutation by measurement of a significant change on an order of magnitude for drug affinity for the receptor (151). These studies can be used to define structural determinants specifying high-affinity ligand binding at extracellular GPCR domains, subtype selective binding, and species differences in ligand binding. Specific objectives for applying mutagenesis techniques to study a target GPCR include the confirmation of binding hypotheses generated through GPCR modeling (i.e., virtual screens, pharmacophore modeling, and QSAR) (150). From specific mutations, we can establish biologically relevant binding conformations, elucidate new areas for potency and selectivity, and enable new insight into new chemotype design (143). Mutagenesis studies taking into consideration species homology can be used to define residues contributing to

potency loss in animal models and can influence the design of broadly active analogs (152). The demonstration of small-molecule binding at a receptor can also rule out nonreceptor mediated effects.

The general requirements for a successful mutagenesis study revolve around compound selection, a sensitive assay, and reagent generation. A diverse set of lead compounds spanning multiple chemotypes is required and these compounds should feature high receptor binding affinity (150). The assay should be a robust ligand binding assay with a cell line conducive to transient transfection as well as functional assays for agonist and potentiator programs (142,153–155). A means for monitoring receptor expression in the model system is needed in addition to rapid cDNA reagent generation (150). An iterative procedure involving molecular modeling, site-directed mutagenesis, in vitro ligand binding experiments, and cell-based functional assays is a means to improve the accuracy of receptor models and rationalize SAR pharmacological profiles (143,150). Expedited receptor mutagenesis studies will have significant impact on new chemotype design and the lead optimization process.

Despite extensive efforts, high-resolution GPCR structural information has been limited to the bovine rhodopsin crystal structure for use in homology modeling approaches for mutagenesis studies (156). Recently, the crystal structure of the human β2 adrenergic receptor has been obtained and represents a key milestone in the understanding of how GPCRs work at a molecular level (157–159). The β_2 adrenergic crystal structure can now be used for ligand docking computer programs and homology-based models for in silico screening (160). New GPCR modeling techniques will undoubtedly evolve through evaluation and refinement of the β_2 adrenergic receptor models, which can be applied to newly generated mutagenesis study data to gain further insights into GPCR ligand binding and functionality.

CONCLUSION

The majority of the drug discovery efforts for the GPCR target family have been focused on agonist and antagonist discovery. The HTS functional assay using recombinant cell lines for monitoring a specific signaling pathway has been heavily used in hit identification over the last 10 years. In contrast, in the lead optimization stage, the radioligand binding assay as a primary screen is still a major driver for many GPCRs regardless of an agonist and antagonist target. With numerous HTS second messenger assays available, the implementation of cell-based assays as primary screens has become an important and popular approach for hunting lead compounds, especially for agonist SAR studies. Because of the nature of agonist-biased trafficking and coupling to different downstream effectors, the understanding of pharmacologically relevant signaling cascades and the building of in vitro and in vivo connectivity becomes more challenging and complex but is necessary for finalizing the signaling assay for functional selectivity in the drug screening process. In addition, for recombinant cell lines employed with current technology for high-throughput and miniaturized studies, the data may not reflect the in vivo or disease state and, therefore, careful evaluation is needed to validate the cellular reagents, screening format, and strategy. Although allosteric modulators and inverse agonists have been attracting much attention in the pharmaceutical industry, after the initial hit identification stage, no clear solutions exist to decipher rank order potency of compounds for advancing leads

along with SAR studies. Breakthroughs in technology and experimental strategy in these areas will bring many opportunities and advantages for developing new and novel ligands for known and orphan GPCRs.

ACKNOWLEDGMENTS

The authors would like to thank Dr. Ramakrishna Seethala and Dr. Litao Zhang for helpful suggestions on this manuscript. We acknowledge our colleagues Sarah Malmstrom, Jing Chen, Rajasree Golla, and Stephen Jefcoat for their efforts in collecting data for some of the figures and illustrations presented in this chapter. We also thank Dr. Andrew Tebben for his collaboration and helpful discussions on receptor mutagenesis studies.

REFERENCES

1. Langley JN. On nerve endings and on special excitable substances in cells. Proc R Soc 1906; B78:170–194.
2. Enrlich P. Chemotherapeutics: Scientific principles, methods and results. Lancet 1913; 2:445–451.
3. Spiegel AM. Inherited endocrine diseases involving G proteins and G protein-coupled receptors. Endocr Dev 2007; 11:133–144.
4. Salazar NC, Chen J, Rockman HA. Cardiac GPCRs: GPCR signaling in healthy and failing hearts. Biochim Biophys Acta 2007; 1768:1006–1018.
5. George SR, O'Dowd BF, Lee SP. G-protein-coupled receptor oligomerization and it's potential for drug discovery. Nat Rev Drug Discov 2002; 1:808–820.
6. Tyndall JD, Pfeiffer B, Abbenante G, et al. Over one hundred peptide-activated G protein-coupled receptors recognize ligands with turn structure. Chem Rev 2005; 105:793–826.
7. May LT, Leach K, Sexton PM, et al. Allosteric modulation of G-protein-coupled receptors. Annu Rev Pharmacol Toxicol 2007; 47:1–51.
8. Schwartz TW, Holst B. Molecular structure and function of 7TM G-protein-coupled receptors. In: Foreman JC, Johansen J, eds. Textbook of Receptor Pharmacology. Boca Raton, Florida: CRC Press LLC, 2003:81–108.
9. Chalmers DT, Behan DP. The use of constitutively active GPCRs in drug discovery and functional genomics. Nat Rev Drug Discov 2002; 1:599–608.
10. Civelli O. GPCR deorphanizations: The novel, the known and unexpected transmitters. Trends Pharmacol Sci 2005; 26:15–19.
11. Eglen RM, Bosse R, Reisine T. Emerging concepts of quinine nucleotide-binding protein-coupled receptor (GPCR) function and implications for high throughput screening. Assay Drug Dev Technol 2007; 5:425–451.
12. Costa T, Cotecchia S. Historical review: Negative efficacy and the constitutive activity of G protein-coupled receptors. Trends Pharmacol Sci 2005; 26:618–624.
13. Smit MJ, Vischer HF, Bakker RA, et al. Pharmacogenomic and structural analysis of constitutive G-protein-coupled receptor activity. Annu Rev Pharmacol Toxicol 2007; 47:53–87.
14. Kenakin T. New concepts in drug discovery: Collateral efficacy and permissive antagonism. Nat Rev Drug Discov 2005; 4:919–927.
15. Park PS, Filipek S, Wells JW, et al. Oligomerization of G protein-coupled receptors: Past, present and future. Biochemistry 2004; 43:15643–15656.
16. Prinster SC, Hague C, Hall RA. Heterodimerization of G protein-coupled receptors: Specificity and functional significance. Pharmacol Rev 2005; 57:289–298.
17. Maggio R, Innamorati G, Parenti M. G protein-coupled receptor oligomerization provides the framework for signal discrimination. J Neurochem 2007; 103:1741–1752.
18. Thomsen W, Frazer J, Unett D. Functional assays for screening GPCR targets. Curr Opin Biotechnol 2005; 16:655–665.

19. May LT, Leach K, Sexton PM, et al. Allosteric modulation of G-protein-coupled receptors. Annu Rev Pharmacol Toxicol 2007; 47:1–51.
20. Milligan G, Smith NJ. Allosteric modulation of heterodimeric G-protein-coupled receptors. Trends Pharmacol Sci 2007; 28:615–620.
21. Zhang L, Banks M. Screening strategy for lead optimization. Am Drug Discov 2006; 1:1–4.
22. Houston JG, Banks MN, Binnie A, et al. Technologies for improving lead optimization. Am Drug Discov 2006; 3:1–7.
23. Jenkinson DH. Classical approaches to the study of drug-receptor interaction. In: Foreman JC, Johansen J, eds. Textbook of Receptor Pharmacology. Boca Raton, Florida: CRC Press LLC, 2003:3–80.
24. Motulsky H, Christopoulos A. Fitting models of biological data using linear and non-linear regression—A practical guide to curve fitting. GraphPad PRISM Version 4.0, 2003. www. graphpad.com.
25. Fitzgerald LW, Patterson JP, Conklin DS, et al. Pharmacological and biochemical characterization of a recombinant human galanin GALR1 receptor: Agonist character of chimeric galanin peptides. J Pharmacol Exp Ther 1998; 287:448–456.
26. Rominger DH, Rominger CM, Fitzgerald LW, et al. Characterization of [125I] sauvagine binding to CRH2 receptors: Membrane homogenate and autoradiographic studies. J Pharmacol Exp Ther 1998; 286:459–468.
27. Bunzow JR, Zhang G, Bouvier C, et al. Characterization and distribution of cloned rat mu-opioid receptor. J Neurochem 1995; 64:14–24.
28. Zhang G, Huang N, Li YW, et al. Pharmacological characterization of a novel nonpeptide antagonist radioligand,(±)-N-[2-methyl-4-methoxyphenyl]-1-(1-(methoxymethyl)propyl)-6-mehtyl-1H-1,2,3-triazolo[4,5-c]pyridine-4-amine([^{3}H]SN003) for corticotrophin-releasing factor1 receptors. J Pharmacol Exp Ther 2003; 305:57–63.
29. Zhang G, Lagrange AH, Rønnekleiv OK, et al. Tolerance of hypothalamic beta-endorphin neurons to mu-opioid receptor activation after chronic morphine. J Pharmacol Exp Ther 1996; 277;551–558.
30. Kobilka BK. G-protein coupled receptor structure and activation. Biochim Biophys Acta 2007; 1768:794–807.
31. Cacace A, Banks M, Spicer T, et al. An ultra-HTS process for the identification of small molecule modulators of orphan G-protein-coupled receptors. Drug Discov Today 2003; 8:785–792.
32. http://www.dcb-server.unibe.ch/groups/reymond/education/urwyler/Chapter%203.pdf
33. Wacker DA, Varnes JG, Malstrom SE, et al. Discovery of (R)-9 ethyl-1,3,4-tetrahydro-7-trifluoromethylpyrazino[2,1-α]isoindol-6(2H)-one, a selective, orally active agonist of the 5-HT2c receptor. J Med Chem 2007; 50:1365–1379.
34. Kenakin T. Efficacy at G-protein-coupled receptors. Nat Rev Drug Discov 2002; 1:103–110.
35. Knoflach F, Mutel V, Jolidon S, et al. Positive allosteric modulators of metabotropic glutamate 1 receptor: Characterization, mechanism of action, and binding site. Proc Natl Acad Sci U S A 2001; 98:13402–13407.
36. Neves SR, Ram PT, Lyengar RG. Protein pathways. Science 2002; 296:1636–1639.
37. Brown DA. G-proteins. In: Foreman JC, Johansen J, eds. Textbook of Receptor Pharmacology. Boca Raton, Florida: CRC Press LLC, 2003:183–212.
38. Liu AM, Ho MK, Wong CS, et al. $G\alpha_{16/z}$ Chimeras efficiently link a wide range of G-protein-coupled receptors to calcium mobilization. J Biomol Screen 2003; 8:39–49.
39. Park PS, Wells JW. Oligomeric potential of the M2 muscarinic cholinergic receptor. J Neurochem 2004; 90:537–548.
40. Terrillon S, Bouvier M. Roles of G-protein-coupled receptor dimerization. EMBO Rep 2004; 5:30–34.

41. Baragli A, Alturaihi H, Watt HL, et al. Heterooligorization of human dopamine receptor 2 and somatostatin receptor 2 co-immunoprecipitation and fluorescence resonance energy transfer analysis. Cell Signal 2007; 19:2304–2316.
42. Drake MT, Henoy SK, Lefkowitz RJ. Trafficking of G protein-coupled receptors. Circ Res 2006; 99:570–582.
43. Prossnitz ER. Novel roles for arrestins in the post-endocytic trafficking of G protein-coupled receptors. Life Sci 2004; 75:893–899.
44. DeWire SM, Ahn S, Lefkowitz RJ, et al. β-arrestins and cell signaling. Annu Rev Physiol 2007; 69:483–510.
45. Shenoy AK, Lefkowitz RJ. Multifaceted roles of β-arrestins in the regulation of seven-membrane-spanning receptor trafficking and signaling. Biochem J 2003; 375: 503–515.
46. DeFea K. β-Arrestins and heterotrimeric G-proteins: Collaborators and competitors in signal transduction. Br J Pharmacol 2008; 153:S298–S309.
47. Marchese A, Paing MM, Temple BRS, et al. G protein-coupled receptor sorting to endosomes and lysosomes. Annu Rev Pharmacol Toxicol 2008; 48:601–629.
48. Pierce KL, Premont RT, Lefkowitz RL. Seven-transmembrane receptors. Nat Rev Mol Cell Biol 2002; 3(9):639–650.
49. Delcourt N, Bockaert J, Marin P. GPCR-jacking: From a new route in RTK signaling to a new concept in GPCR activation. Trends Pharmacol Sci 2007; 28:602–607.
50. Dong C, Filipeanu CM, Duvernay MT, et al. Regulation of G-protein-coupled receptor export trafficking. Biochim Biophys Acta 2007; 1768:853–870.
51. Yeagle PL, Ren PG, Avsian-Kretchmer O, et al. G-protein coupled receptor structure. Biochim Biophys Acta 2007; 1768:808–824.
52. Brown DA. G-Proteins. In: Foreman JC, Johansen T, eds. Textbook of Receptor Pharmacology. Boca Raton, Florida: CRC Press, 2003:213–236.
53. Zhang G, Murray TF, Grandy DK. Orphanin FQ has an inhibitory effect on the guinea pig ileum and the mouse vas deferens. Brain Res 1997; 772:102–106.
54. Qume M. Overview of ligand-recpeotr binding techniques. In: Mary Keen, ed. Receptor Binding Techniques. Clifton, NJ: Humana Press, Inc., 1999:3–23.
55. Cheng Y, Prusoff WH. Relationship between the inhibitor constant (K_I) and the concentration of inhibitor which causes 50 percent inhibition (IC_{50}) of an enzymatic reaction. Biochem Pharmacol 1972; 22:3099–3108.
56. Orchinik M, Murray TF, Moore FL. A corticosteroid receptor in neuronal membranes. Science 1991; 252:1848–1851.
57. Eglen RM. Emerging concepts in GPCR function—The influence of cell phenotype on GPCR pharmacology. Proc West Pharmacol Sci 2005; 48:31–34.
58. http://las.perkinelmer.com/content/featured/gpcrnews/200803/spa.html.
59. http://las.perkinelmer.com/Catalog/default.htm?CategoryID = Radioactivity
60. Quigley DI, Arttamangkul S, Allen RG, et al. Integrity of tritiated orphanin FQ/nociceptin: Implications for establishing a reliable binding assay. Peptides 2000; 21;1111–1118.
61. Seethala R. Receptor screens for small molecule agonist and antagonist discovery. In: Seethala R, Fernandes PB, eds. Handbook of Drug Screening. Marcel Dekker, Inc., 2001:189–264.
62. Handl HL, Vagner J, Yamamura HI, et al. Lanthanide-based time-resolved fluorescence of in cyto ligand–receptor interactions. Anal Biochem 2004; 330:242–250.
63. http://las.perkinelmer.com/content/applicationnotes/app_delfiagproteincoupled-receptors.pdf. Application notes: Time-resolved fluorescence based GTP binding assay for G-protein coupled receptors, 2002.
64. Harrison C, Traynor JR. The [^{35}S]GTPγS binding assay: Approached and applications in pharmacology. Life Sci 2003; 74:489–508.
65. Milligan G. Principles: Extending the utility of [^{35}S]GTPγS binding assays. Trends Pharmacol Sci 2003; 24:87–90.
66. Stanton JA, Beer MS. Characterization of a cloned human 5-HT_{1A} receptor cell line using [^{35}S]GTPγS binding. Eur J Pharmacol 1997; 320:267–275.

67. Ferrer M, Kolodin GD, Zuck P, et al. A fully automated [^{35}S]GTPγS scintillation proximity assay for the high-throughput screening of G_i-linked G protein-coupled receptors. Assay Drug Dev Technol 2003; 1:261–273.
68. http://las.perkinelmer.com/content/applicationnotes/fsp_file14useforinvitro125i-labeled. pdf. Application notes: Use of FlashPlate technology for in vitro measurement of [^{35}S]-GTPγS binding in CHO cells expressing the human 5-HT_{1B} receptor.
69. DeLapp NW. The antibody-capture [^{35}S]GTPγS scintillation proximity assay: A powerful emerging technique for analysis of GPCR pharmacology. Trends Pharmacol Sci 2004; 25:400–401.
70. Frang H, Mukkala VM, Syysto R, et al. Nonradioactive GTP binding assays to monitor activation of G protein-coupled receptors. Assay Drug Dev Technol 2003; 1:275–280.
71. Kariv I, Stevens ME, Behrens BL, et al. High throughput quantitation of cAMP production mediated by activation of seven transmembrane domain receptors. J Biomol Screen 1999; 4:27–32.
72. Kemp DM, George SE, Kent TC, et al. The effect of ICER on screening methods involving CRE-mediated reporter gene expression. J Biomol Screen 2002; 7:141–148.
73. Gabriel D, Vernier M, Pfeifer MJ, et al. High throughput screening technologies for direct cyclic AMP measurement. Assay Drug Dev Technol 2003; 1:291–303.
74. Williams C. cAMP detection methods in HTS: Selecting the best from the rest. Nat Rev Drug Discov 2004; 3:125–135.
75. http://www.htrf.com/files/resources/Cisbio%20cAMP%20SBS2000.pdf. Degorce F, Achard S, Preaudat M, et al. A new HTRF assay for the direct assessment of cyclic AMP in high throughput screening, 2001; CISbio International.
76. Cisbio HTRF application note—cyclic AMP: A functional second messenger for assaying GPCR target activation. http://www.htrf.com/files/resources/cAMP_second_messenger.pdf.
77. Prystay L, Gagne A, Kasila P, et al. Homogeneous cell-based fluorescence polarization assay for the direct detection of cAMP. J Biomol Screen 2001; 6:75–82.
78. Sportsman JR, Leytes LF. Miniaturization of homogeneous assays using fluorescence polarization. Drug Discov Today 2000; Suppl 1:27–32.
79. http://las.perkinelmer.com/content/applicationnotes/fsp_file1noveladenylylcyclaseactassay. pdf. Kasila PA. A novel adenylyl cyclase activation assay on FlashPlate (FlashPlate File #1, Application Note). PerkinElmer Life Sciences, 1998.
80. http://las.perkinelmer.com/content/applicationnotes/app_topcounthtscampformation.pdf. Horton JK, Smith L, Ali A, Baxendale PM. High throughput screening for cAMP formation by scintillation proximity radioimmunoassay. PerkinElmer Application Notes TCA-021, 1995.
81. http://las.perkinelmer.com/content/relatedmaterials/posters/sps_s4026galphacoupledgpcral phascreencamp.pdf. Bouchard N, Robitaille E, Wenham, D. Functional characterization and screening of $G_{\alpha i}$-coupled GPCRs using AlphaScreen cAMP detection technology. PerkinElmer Life Sciences, 2002.
82. Ullman EF, Kirakossions H, Singh S. Luminescent oxygen channeling immunoassay: Measurement of particle binding kinetics by chemiluminescence. Proc Natl Acad Sci U S A 1994; 91:5426–5430.
83. Glickman JF, Wu X, Mercuri R, et al. A comparison of ALPHAScreen, TR-FRET, and TRF as assay methods for FXR nuclear receptors. J Biomol Screen 2002; 7:3–10.
84. Eglen RM, Singh R. Beta galactosidase enzyme fragment complementation as a novel technology for high throughput screening. Comb Chem High Throughput Screen 2003; 6:381–387.
85. Eglen RM. Enzyme fragment complementation: A flexible high throughput screening assay technology. Assay Drug Dev Technol 2002; 1:97–104.
86. Golla R, Seethala R. A homogeneous enzyme fragment complementation cyclic AMP screen for GPCR agonists. J Biomol Screen 2002; 7:515–525.

87. http://www.mesoscale.com/CatalogSystemWeb/WebRoot/technology/ecl/walkthrough.htm.
88. http://las.perkinelmer.com/content/applicationnotes/app_delfiaassaymeasurecamp.pdf. Bjork S, Vikstrom S. A DELFIA assay for measuring cAMP in plasma. Application Notes (006986–01-APP). PerkinElmer Life Sciences, 2004.
89. Berridge MJ, Dawson RM, Downes CP, et al. Changes in the levels of inositol phosphates after agonist-dependent hydrolysis of membrane phosphoinositides. Biochem J 2003; 212:473–482.
90. Trinquet E, Fink M, Bazin H, et al. D-myo-inositol 1-phosphate as a surrogate of D-myo-inositol 1,4,5-tris phosphate to monitor G protein-coupled receptor activation. Anal Biochem 2006; 358:125–135.
91. Liu JJ, Hartman DS, Bostwick JR. An immobilized metal ion affinity adsorption and scintillation proximity assay for receptor-stimulated phosphoinositide hydrolysis. Anal Biochem 2003; 318:91–99.
92. Brandish PR, Hill LA, Zheng W, et al. Scintillation proximity assay of inositol phosphates in cell extracts: High-throughput measurement of G-protein-coupled receptor activation. Anal Biochem 2003; 313:311–318.
93. http://www.discoverx.com/products.php?.p=3
94. Schroeder KS, Neagle BD. FLIPR: A new instrument for accurate, high throughput optical screening. J Biomol Screen 1996; 1:75–80.
95. Shimomura O, Johnson FH, Saiga Y. Extraction, purification and properties of aequorin, a bioluminescent protein from the luminous hydromedusan, Aequorea. J Cell Comp Physiol 1962; 59:223–224.
96. Kendall JM, Badminton MN. *Aequorea victoria* bioluminescence moves into an exciting new era. Trends Biotechnol 1998; 16:216–224.
97. Shimomura Q, Johnson FH. Regeneration of the photoprotein aequorin. Nature 1975; 256:236–238.
98. Le Poul E, Hisada S, Mizuguchi Y, et al. Adaptation of aequorin functional assay to high throughput screening. J Biomol Screen 2002; 7:57–65.
99. Coward P, Chan SDH, Wada HG, et al. Chimeric G protein allows a high-throughput signaling assay of G_i-coupled receptors. Anal Biochem 1999; 270:242–248.
100. Pearson K. Determination of the coefficient of correlation. Science 1909; 30:23–25.
101. Chen J, Zhang G, Malmstrom S, et al. Comparison of fluorescent and luminescent cell-based calcium flux assays: An antagonist case study using Lumax, FLIPR and FDSS6000 for a GPCR target. Poster #PST1A031, 2007, Society of Biomolecular Screening 13th Annual Conference, Montreal, Canada. http://s19.a2zinc.net/clients/sbs/sbs07/public/SessionDetails.aspx?SessionID=1429
102. http://www.discoverx.com/products.php? p=68.
103. http://www.invitrogen.com/content.cfm?pageid=12147.
104. Milligan G. High content assays for ligand regulation of G-protein-coupled receptors. Drug Dispos Today 2003; 8:579–585.
105. Granas C, Lundholt BK, Heydom A, et al. High content screening for G protein-coupled receptors using cell-based protein translocation assays. Comb Chem High Throughput Screen 2005; 10:476–484.
106. Ferguson SSG. Evolving concepts in G protein-coupled receptor endocytosis: The role in receptor desensitization and signaling. Pharmacol Rev 2001; 53:1–24.
107. Haasen D, Schnapp A, Valler MF, et al. G protein-coupled receptor internalization assays in the high-content screening format. Methods Enzymol 2006; 414:121–139.
108. http://www.bioimage.com/pdf/assay_application_notes/07–04-86v01.01%20M1%20 Assay%20Application%20Note.pdf.
109. Garippa RJ, Hoffman AF, Gradl G, et al. High-throughput confocal microscopy for beta-arrestin-green fluorescent protein translocation G protein-coupled receptor assays using the Evotec Opera. Methods Enzymol 2006; 414:99–120.
110. Hudson CC, Oakley RH, Sjaastad MD, et al. High-content screening of known G protein-coupled receptors by arrestin translocation. Methods Enzymol 2006; 414:63–78.

111. http://www.moleculardevices.com/pages/reagents/transfluor.html.
112. Lang P, Yeow K, Nichols A, et al. Cellular imaging in drug discovery. Nat Rev Drug Discov 2006; 5:343–356.
113. Etienne-Manneville S, Hall A. Rho GTPases in cell biology. Nature 2002; 420:629–635.
114. Atienza JM, Yu N, Kirstein SL, et al. Dynamic and label-free cell-based assays using the real-time cell electronic sensing system. Assay Drug Dev Technol 2007; 4:597–607.
115. Verdonk E, Johnson K, McGuinness R, et al. Cellular dielectric spectroscopy: A label-free comprehensive platform for functional evaluation of endogenous receptors. Assay Drug Dev Technol 2006; 4:609–619.
116. Yu N, Atienza JM, Bernard J, et al. Real-time monitoring of morphological changes in living cells by electronic cell sensor arrays: An approach to study G protein-coupled receptors. Anal Chem 2006; 78:35–43.
117. Peters MF, Knappenberger KS, Wilkins D, et al. Evaluation of dielectric spectroscopy, a whole-cell, label-free technology for drug discovery on G_i-coupled GPCRs. J Biomol Screen 2007; 12:312–319.
118. Pierce KL, Fujino H, Srinivasan D, et al. Activation of FP prostanoid receptor isoforms leads to Rho-mediated changes in cell morphology and in the cell cytoskeleton. J Biol Chem 1999; 274:35944–35949.
119. Schraufstatter IU, Chung J, Burger M. IL-8 activates endothelial cell CXCR1 and CXCR2 through Rho and Rac signaling pathways. Am J Physiol Lung Cell Mol Physiol 2001; 280:L1094–L1103.
120. Salterelli D. Heterotrimeric $G_{i/o}$ proteins control cyclic AMP oscillations and cytoskeletal structure assembly in primary human granulosa-lutein cells. Cell Signal 1999; 11:415–433.
121. Martineau LC, McVeigh LI, Jasmin NJ, et al. P38 MAP kinase mediates mechanically induced COX-2 and PG EP_4 receptor expression in podocytes: Implications for the actin cytoskeleton. Am J Physiol Renal Physiol 2004; 286:F693–F701.
122. http://www.cellkey.com.
123. Fang Y, Ferrie AM, Fontaine NH, et al. Resonant waveguide grating biosensor for living cell sensing. Biophys J 2006; 91:1925–1940.
124. Cooper M. Label-free screening of bio-molecular interactions. Anal Bioanal Chem 2003; 377:834–842.
125. Hug TS. Biophysical methods for monitoring cell-substrate interactions in drug discovery. Assay Drug Dev Technol 2003; 1:479–488.
126. Ramsden JJ, Li SY, Heinzle E, et al. Optical method for measurement of number and shape of attached cells in real time. Cytometry 1995; 19:97–102.
127. Zhou T, Marx KA, Warren M, et al. The quartz crystal microbalance as a continuous monitoring tool for the study of endothelial cell surface attachment and growth. Biotechnol Prog 2000; 16:268–277.
128. Marx KA, Zhou T, Montrone A, et al. Quartz crystal microbalance biosensor study of endothelial cells and their extracellular matrix following cell removal: Evidence for transient cellular stress and viscoelastic changes during detachment and the elastic behavior of the pure matrix. Anal Biochem 2005; 343:23–34.
129. Bleicher KH, Böhm HJ, Müller K, et al. Hit and lead generation: Beyond high-throughput screening. Nat Rev Drug Discov 2003; 2:369–378.
130. Kenakin T. Predicting therapeutic value in the lead optimization phase of drug discovery. Nat Rev Drug Discov 2003; 2:429–438.
131. Banks MN, Zhang L, Houston JG. Screen/counter screen: Early assessment of selectivity. In: Bartlett PA, Entzeroth M, eds. Exploiting Chemical Diversity for Drug Discovery. London, U.K.: Royal Chemical Society Publisher, 2006:315–335.
132. Urban JD, Clarke WP, Zastrow MV, et al. Functional selectivity and classical concepts of quantitative pharmacology. J Pharmacol Exp Ther 2007; 320:1–13.
133. Swinney DC. Biochemical mechanisms of drug action: What does it take for success? Nat Rev Drug Discov 2004; 3:801–808.
134. Carter PH. Chemokine receptor antagonism as an approach to anti-inflammatory therapy: 'Just right' or plain wrong? Curr Opin Chem Biol 2002; 6:510–525.

135. Onuffer JJ, Horuk R. Chemokines, chemokine receptors and small-molecule antagonists: Recent developments. Trends Pharmacol Sci 2002; 23:459–467.
136. Horuk R. Development and evaluation of pharmacological agents targeting chemokine receptors. Methods 2003; 29:369–375.
137. Christopoulos A. Allosteric binding sites on cell-surface receptors: Novel targets for drug discovery. Nat Rev Drug Discov 2002; 1:198–210.
138. May LT, Christopoulos A. Allosteric modulators of G-protein-coupled receptors. Curr Opin Pharmacol 2003; 3:551–556.
139. Olson TS, Ley K. Chemokines and chemokine receptors in leukocyte trafficking. Am J Physiol Regul Integr Comp Physiol 2002; 283:R7–R28.
140. Liang M, Rosser M, Ng HP, et al. Species selectivity of a small molecule antagonist for CCR1 chemokine receptor. Eur J Pharmacol 2000; 389:41–49.
141. Gao JL, Wynn TA, Chang Y, et al. Impaired host defense, hematopoiesis, granulomatous inflammation and type1-type 2 cytokine balance in mice lacking CC chemokine receptor 1. J Exp Med 1997; 185:1959–1968.
142. Vaidehi M, Schlyer S, Trabanino RJ, et al. Prediction of CCR1 chemokine receptor structure and BX471 antagonist binding followed by experimental validation. J Biol Chem 2006; 281:26613–26620.
143. Kristiansen K. Molecular mechanisms of ligand binding, signaling, and regulation within the superfamily of G-protein-coupled receptors: Molecular modeling and mutagenesis approaches to receptor structure and function. Pharmacol Ther 2004; 103:21–80.
144. Moro S, Guo D, Camaioni E, et al. Human P2Y1 receptor: Molecular modeling and site-directed mutagenesis as tools to identify agonist and antagonist recognition sites. J Med Chem 1998; 41:1456–1466.
145. Mialet J, Dahmoune Y, Lezoualc'h F, et al. Exploration of the ligand binding site of the human 5-HT4 receptor by site-directed mutagenesis and molecular modeling. Br J Pharmacol 2000; 130:527–538.
146. Labbee-Jullie C, Barroso S, Micolas-Eteve D, et al. Mutagenesis and modeling of the neurotensin receptor NTR1. J Biol Chem 1998; 279:16351–16357.
147. Shi W, Osawa S, Dickerson CD, et al. Rhodopsin mutants discriminate sites important for the activation of rhodopsin kinase and G_t. J Biol Chem 1995; 270:2112–2119.
148. Ostrowski J, Kjelsberg MA, Caron MG, et al. Mutagenesis of the β2-adrenergic receptor: How structure elucidates function. Annu Rev Pharmacol Toxicol 1992; 32:167–183.
149. Berkout TA, Blaney FE, Bridges AM, et al. CCR2: Characterization of the antagonist binding site from a combined receptor modeling/mutagenesis approach. J Med Chem 2003; 46:4070–4086.
150. Flower DR. Modelling G-protein-coupled receptors for drug design. Biochim Biophys Acta 1999; 1422:207–234.
151. Beukers MA, IJzerman AP. Techniques: How to boost GPCR mutagenesis studies using yeast. Trends Pharmacol Sci 2005; 26:533–539.
152. Gros J, Manning BS, Dietri-Rouxel F, et al. Site directed mutagenesis of the human beta 3-adrenoreceptor transmembrane residues involved in ligand binding and signal transduction. Eur J Biochem 1998; 251:590–596.
153. Fujiwara Y, Osborne, DA, Walker MD, et al. Identification of the hydrophobic ligand binding pocket of the S1P1 Receptor. J Biol Chem 2007; 282:2374–2385.
154. Kapur A, Hurst DP, Fleischer D, et al. Mutation studies of Ser7.39 and Ser2.60 in the human CB_1 cannabinoid receptor: Evidence for a serine-induced bend in CB_1 transmembrane helix 7. Mol Pharmacol 2007; 71:1512–1524.
155. Scarselli M, Li B, Kim SK, et al. Multiple residues in the second extracellular loop are critical for the M_3 muscarinic acetylcholine receptor activation. J Biol Chem 2007; 282:7385–7396.
156. Palczewski K, Kumasaka T, Hori T, et al. Crystal structure of rhodopsin: A G protein-coupled receptor. Science 2000; 289:739–745.

157. Rasmussen SGF, Choi HJ, Rosenbaum DM, et al. Crystal structure of the human β_2 adrenergic G-protein-coupled receptor. Nature 2007; 450:383–387.
158. Cherezov V, Rosenbaum DM, Hanson MA, et al. High-resolution crystal structure of an engineered human beta2-adrenergic G protein-coupled receptor. Science 2007; 318:1258–1265.
159. Rosenbaum DM, Cherezov V, Hanson MA, et al. GPCR engineering yields high-resolution structural insights into beta2-adrenergic receptor function. Science 2007; 318:1266–1273.
160. Kobilka B, Schertler GF. New G-protein-coupled receptor crystal structures: Insights and limitations. Trends Pharmacol Sci 2008; 29:79–83.

7 Nuclear Hormone Receptor Screening in Drug Discovery

Ramakrishna Seethala

Bristol-Myers Squibb, Princeton, New Jersey, U.S.A.

Litao Zhang

Lead Evaluation and Mechanistic Biochemistry, Applied Biotechnology, Bristol-Myers Squibb, Princeton, New Jersey, U.S.A.

NUCLEAR RECEPTOR SUPERFAMILY

Nuclear receptors (also known as nuclear hormone receptors or intracellular receptors) are ligand-regulated transcription factors that regulate expression of genes that are involved in a number of physiological functions, metabolism, development, and reproduction. Nuclear receptors (NRs) represent important drug discovery targets for therapeutic applications in inflammation, cancer, and metabolism. There are 48 genes in the human genome that comprise NR superfamily (1,2) (Table 1). More than 20 of these NRs have been utilized as drug targets. The first NR cloned was human glucocorticoid receptor followed by estrogen receptor, thyroid receptor, and retinoic acid receptor (3–7).

Nuclear Receptor Classes

Nuclear receptors can be classified by different methods. NRs can be grouped into five classes based on DNA binding and dimerization properties (Table 1). Although some NRs bind to DNA as monomer and activate transcription of their target genes, most other NRs bind as homodimers or heterodimers bound to retinoid X receptor (RXR) (Fig. 1). Cytoplasmic steroid receptors including glucocortioid receptor (GR), androgen receptor (AR), mineralcorticoid receptor (MR), estrogen receptor (ER), and progesterone receptor (PR) are active as homodimers and undergo nuclear translocation from cytoplasm upon ligand binding. The RXR heterodimeric receptors including thyroid hormone receptor (TRα,β), vitamin D receptor (VDR), ecdysone receptor (EcR), peroxisome proliferator-activating receptors (PPARs), FXR, LXR, CAR, and retinoic acid receptor (RAR) bind the transcription elements as heterodimers with RXR and are retained in the nucleus regardless of the presence of ligands (8,9). There are several orphan NRs that lack known physiological ligands for these orphan receptors when they were identified. The homodimer orphan receptors are RXRα,β,γ hepatocyte nuclear factor 4 (HNF-4) α,β,γ chicken ovalbumin upstream promoter transcription factor (COUP-TF), GCNF, PNR, TR2,4; the monomeric orphan receptors are RORα,β,γ, ERRα,β,γ, TLX, NURR 1,77, NOR1, SF-1, SXR; and orphan receptors lacking DBD (DNA-binding domain) are DAX and small heterodimer partner (SHP).

TABLE 1 Classification of Nuclear Receptors

Class	Name	Members	Ligands	Dimerization	DNA binding (repeat type)
I	Steroid receptors	GR, AR, MR, ERα,β, PR	Glucocorticoid, androgen, mineralcorticoid, estrogen, progesterone	Homodimers	Inverted
II	Retinoid X receptors (RXR) heterodimers	TRα,β, RARα,β,γ , VDR, PPARα,γ,δ, LXRα,β, FXR, PXR, CAR	T3, atRA, vitamin D fatty acids, 15d-PGJ2, cPG1 oxysterol bile acids, PCN (xenobiotics) androstane	Heterodimers	Direct
III	Orphan dimeric receptors	RXRα,β,γ, HNF-4 α,β,γ, COUP-TFα,β,γ, GCNF, PNR, TR2,4	9-cis RA fatty acids	Homodimers	Direct
IV	Orphan monomeric receptors	RORα,β,γ, ERRα,β,γ, TLX, NURR 1, 77, NOR1, SF-1, SXR, NGFI-B	Cholesterol, estrogen ?, phospholipids	Monomers	Extended
V	Orphan receptors lacking DBD	DAX, SHP		Lacks DBD	

Ligands for Nuclear Receptors

The current market for NR-targeted drugs is estimated to be 10% to 15% of the global market. Because NRs are important drug discovery targets, they have resulted in the discovery of ligands that modulate the activity of these receptors (Table 2) (10). Ligands for NRs can be classified into naturally occurring ligands and synthetic ligands. The natural nuclear receptor ligands [such as 17-β-estradiol for ER, testosterone for AR, progesterone for PR, cortisol for GR, aldosterone for MR, all-trans retinoic acid for RAR, and L-3.5,3′-L-triiodothyronine (T3) for TR, 9-*cis*-retinoic acid (RXR), and 1,25-dihydroxy vitamin D3 for VDR] are small, fairly rigid, and hydrophobic molecules that can easily diffuse across cell membranes. Ligands (agonist and antagonists that either activate or repress transcription in transient transfection reporter gene assays) of NRs have been used in many important clinical areas to treat diseases such as cancer, inflammation, dyslipidemia, atherosclerosis, metabolic syndrome, diabetes, and osteoporosis. However, these NR ligands also may result in side effects that limit the utility of these as drugs. Some ligands function as agonists in certain tissues and antagonists in others (11–13). Yet some other ligands can bind to NRs as partial (or mixed) agonists (or antagonists) with lower affinity than full agonists

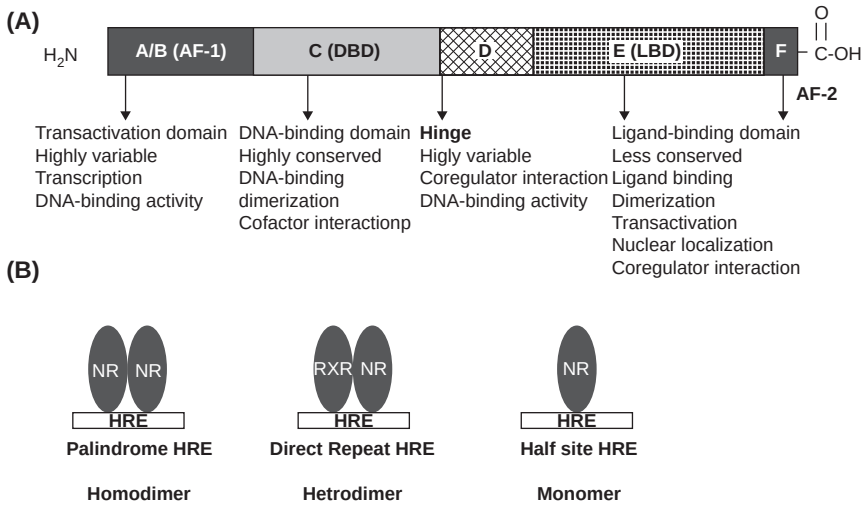

FIGURE 1 (**A**) Schematic domain structure of a nuclear hormone receptors. The highly conserved DBD (C) is flanked by less–well-conserved N-terminal and C-terminal regions. Ligand binds to the LBD (E), which is moderately conserved. Dimerization functions are located in the C and E regions. Ligand-dependent (AF-2) and independent (AF-1) transactivation functions are located in the receptor A/B and E domains, respectively. DNA binding is regulated by residues in the DBD (C) in cooperation with residues in the N-terminal (A/B) region and hinge region (D). (**B**) Schematic illustration of dimerization of NRs.

and induce unique conformational changes in the receptors, resulting in specific biological response. The ability to selectively modulate the receptors in different tissues has led to the search for selective nuclear receptors such as selective estrogen receptor modulators (SERMs), selective androgen receptor modulators (SARMs), selective liver X receptor modulators (SLRMs), selective peroxisome proliferator-activated receptor (PPAR) modulators, and selective thyroid receptor modulators (STRMs). Together, these make NRs attractive drug targets (14,15). The SERMs tamoxifen (Nalvodex) and Raloxifene (Evista) act as antagonists of ER in breast and uterine tissues and are used for the treatment of estrogen-dependent breast cancer and act as agonist in bone (Table 2).

Orphan Nuclear Receptors

Molecular cloning identified several orphan receptors sharing similar structure to the nuclear receptors (Table 1); however, the natural ligands for these orphan receptors are not known at present. Identification of novel ligands for orphan nuclear receptors will lead to discovery of new drugs. Some of the orphan nuclear receptors have been recently matched with physiological ligands such as 9-*cis*-retinoic acid that was found to bind and activate three of the nuclear receptors classified originally as orphan receptors and later named as retinoic acid receptor RARs (2). Similarly, the physiological ligands of other orphan nuclear receptors have not been identified earlier, but they provided potentially important drug targets—peroxisome proliferator-activated receptor-γ (PPARγ) role in adipogenesis and discovery of thiazolidinedione ligands in the

TABLE 2 Nuclear Receptor Drug Targets

Receptor	Function	Disease target
ERα,β	Antagonist breast & uterine tissue, agonist (SERM) in bone	Breast cancer, osteoporosis
PR	PR agonist, PR antagonist	Breast cancer, fertility abortion
AR	Antagonist prostate, agonist in muscle	Prostate cancer, anti-ageing anabolic steroids, male hormone replacement
GR	GR agonist	Immunology & inflamation, Metabolic, Asthama
TRα,β,		Atherosclerosis, obesity, metabolic syndrome, diabetes
RARα,β,γ		Cancer, dermatology
RXRα,β,γ		Cancer, atherosclerosis, metabolic syndrome, diabetes
PPARα,γ,δ		metabolic syndrome, diabetes, dyslipidemia, atherosclerosis
VDR		Osteoporosis
LXRα,β		Atherosclerosis, Alzheimers disease, diabetes
Nurr 1		Parkinson's disease
Nurr77		Apoptosis
FXR		Dyslipidemia, liver disease
CAR		Xenobiotic sensor
SXR		Xenobiotic sensor
PXR		Xenobiotic sensor

treatment of noninsulin-dependent type II diabetes and regulation of cholesterol metabolism by steroidogenic receptor (SF-1), liver X receptor α (LXRα), and farnesoid X receptor (FXR). Subsequently, the endogenous ligands of these orphan receptors have been identified—fatty acids and fatty acid metabolites as the ligands of PPARs, oxysterols for LXR, and bileacids for FXR (16–21).

Ligand identification for the orphan receptors have been done by various methods: (*i*) cell-based assays using cultured mammalian cells transfected with LBD (ligand-binding domain) fused to Gal4 DBD (DNA binding domain) used as the receptor; (*ii*) receptor immobilization on solid support, incubation with compounds or cell lysates, elution of the putative ligands, and characterization; (*iii*) ligand screening by ligand dependent nuclear receptor–coactivator interaction; (*iv*) crystal structures of receptor LBDs have been used to identify the ligands of the orphan receptors.

Structure Features of Nuclear Receptors

NRs are modular proteins of ~50 to 100 kDa that share six functional and structural domains including one DBD and one LBD (Fig. 1) (9). The N-terminal A/B domains (50–500 amino acids) contain a cell- and promoter-specific transactivation domain termed as activation function 1 domain (AF-1), which is the least conserved domain (<15% sequence homology) across the superfamily. The centrally located DBD (C domain ~70–80 amino acids) has highly conserved sequence (>50% sequence homology). It contains conserved cysteine residues that form two zinc fingers that are involved in DNA recognition and binding in concert with residues in N-terminal (A/B domains) and hinge (D domain)

regions (22,23). The DBD also contains nuclear localization sequences. DBD is also important in the dimerization of the receptor. The linker D region contains the nuclear localization signal and a flexible hinge between C and E regions. The C-terminal LBD (domain E) though is similar in length (~250 amino acids) between receptors, the sequence is highly variable across the family (sequence homology only 15–60%) and is responsible for ligand specificity and transactivation. At the C-terminus, LBD contains a second activation function domain (AF-2), which is involved in hetero- and homodimerization and binding of heat shock proteins to inactive receptor. The function of the C-terminus F domain is not clearly understood and is not present in all receptors.

NUCLEAR RECEPTOR ACTIVATION OF TRANSCRIPTION

Corepressors and coactivators regulate NR function (Fig. 2). The NRs recruit corepressors and form a corepressor complex at the promoters of target genes followed by chromatin condensation causing the gene repression, thus silencing the NR activity. Ligand binding induces conformational change in NR LBDs and dissociation of the NR from these corepressors results in chromatin decondensation, which is believed to prepare target gene promoters for transactivation. Following chromatin decondensation, a second coactivator complex is assembled that is able to establish contact with the basal transcription machinery, resulting in transcription activation of the target gene. This general mechanism is not universal for all the NRs, since some NRs may act as activators without a ligand, whereas others are unable to interact with target gene promoter in the absence of ligands (10–11).

NRs in the absence of ligand binding are associated with other proteins either in cytoplasm or nucleus. In the absence of ligand, steroid receptors form quaternary complexes with chaperones like heat shock proteins that prevent their interaction with DNA. In a classical steroid receptor function, ligand binds to LBD of cytosolic NR complex containing the receptor and chaperone proteins, changes protein conformation in the C-terminus dissociating the corepressor proteins from the transcription complex followed by recruitment of coactivators. This protein– protein interaction occurs between the AF-2 domain of the

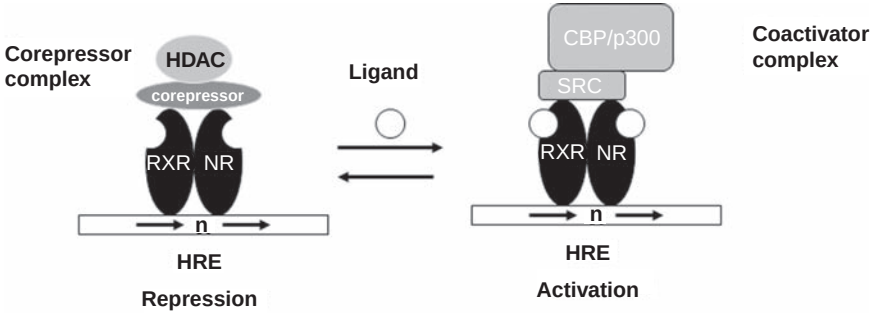

FIGURE 2 Schematic illustration activation of nuclear receptor by ligand binding. NR is associated with corepressor and the NR–corepressor complex is repressed. Ligand binding releases corepressors from NR and recruits coactivators to form NR–coactivator complex and results in transcription activation.

LBD and the short α-helical LXXLL motifs (NR box) within the coactivator. The LXXLL motifs and the sequences flanking this motif of the coactivators determine the specificity to the receptors. The liganded receptor is translocated to the cell nucleus where the activated receptor protein binds directly to specific DNA sequences of hormone response elements (HREs) symmetrical repeats of 5′-AGAACA-3′ (5′-AGGTCA-3′ for ER) with one nucleotide spacing contained in the enhancer and promoter regions of target genes, resulting in transcriptional activation (24). With the green fluorescent protein (GFP)-tagged steroid, NRs are able to monitor real-time intracellular trafficking in living cells (25). The RXR heterodimer receptors bind to direct repeats of hexad consensus sequence 5′-AG(G/T)TCA-3′ but with a spacing of one to four nucleotides (9). Although the DNA binding of monomers is the same as for the RXR heterodimers, the flanking sequences at the 5′end determines the selectivity.

EXPRESSION OF NR LBD

The streptavidin–biotin interaction and histidine-tagged proteins and nitrilotriacetic acid (NTA) can be utilized for facilitating biochemical assays of proteins. Recombinant NR LBDs have been produced by using the hexahistidine (His_6) tag approach (26). This is the most commonly used recombination expression system that facilitates purification of the recombinant protein via their His_6 tag NTA binding. In this system, the cDNA encoding the receptor protein is cloned in frame with a linker encoding hexahistidines with the pET15b vector. The expression of this fusion protein is driven by the bacteriophage T7 RNA polymerase in bacterial strains that carry T7 RNA polymerase on an episomal plasmid under control of the lactose repressor (LacR). This allows for the regulatable expression of the fusion protein on the addition of isopropylthiogalactoside (IPTG). A standard strain for this purpose is the BL21(DE3) series. The His_6 recombinant protein is purified by adding the cell extract to nickel NTA column. His_6 reversibly binds divalent nickel cation chelated by NTA. The nickel–NTA His_6 complex can be disrupted by imidazole, thus releasing His_6 protein from the nickel–NTA gel.

NR LBD can be recombinantly expressed with glutathione S-transferase (GST) fusion protein tag as an amino-terminal fusion tag (27). DNA encoding the receptor is cloned into the pGEX expression vector under the control of IPTG-inducible T7 promoter in *Escherichia coli* BL21 strain. The GST-tagged protein is purified on glutathione column.

Biotinylated NR can also be prepared enzymatically that can be used for NR binding studies and crystallization studies. The NR-LBD fused to an N-terminal biotinylation signal sequence is cloned and coexpressed in *E. coli* with biotin ligase that catalyzes the covalent addition of a biotin moiety to a lysine residue in the signal sequence (28). Alternatively, the NR-LBD fused to a N-terminal biotinylation signal sequence is cloned in *E. coli* and the cell extracts expressing NR with biotinylation site can be biotinylated with a purified biotin ligase. Thus, the site-specific biotinylated NR can be purified by affinity chromatography on avidin or streptavidin gels and used for binding assays.

The purified recombinant NRs can be used for nuclear receptor ligand-binding studies and crystallization studies to determine the structure of binding pocket.

NUCLEAR RECEPTOR BINDING ASSAYS

Members of the NR superfamily regulate gene expression by binding to *cis*-active elements in target genes and either activating or repressing transcription. Ligand binding to NRs modifies the DNA-binding and transcriptional properties of these receptors, resulting in the activation or repression of target genes. Ligand binding induces conformational change in NRs and promotes association with diverse nuclear proteins that may function as coactivators of transcription through a conserved sequence motif present in the coactivators (Fig. 3). The coactivator proteins that associate with NRs in a ligand-dependent manner varied from 2 for estrogen receptor (ERAP) to 12 for vitamin D receptor (DRIPS). In addition to the receptor binding assays, transcription, DNA binding, and coactivator binding assays are used for functional screens of NRs (Table 3).

Members of NR family have a conserved LBD of about 250 amino acids in the carboxy-(C-)terminal region of the receptor. LBD is responsible for the selective binding ligands. The LBD has an extensive secondary structure consisting of alpha helices and beta sheets. Natural and synthetic ligands bind to the LBD by either activating or repressing the receptor. Purified NR-LBD subunit can bind the ligands and have been extensively used to determine the affinities of compound binding to the receptor. Radioactive and fluorescence methods have been used to determine the affinity of compounds to the NR.

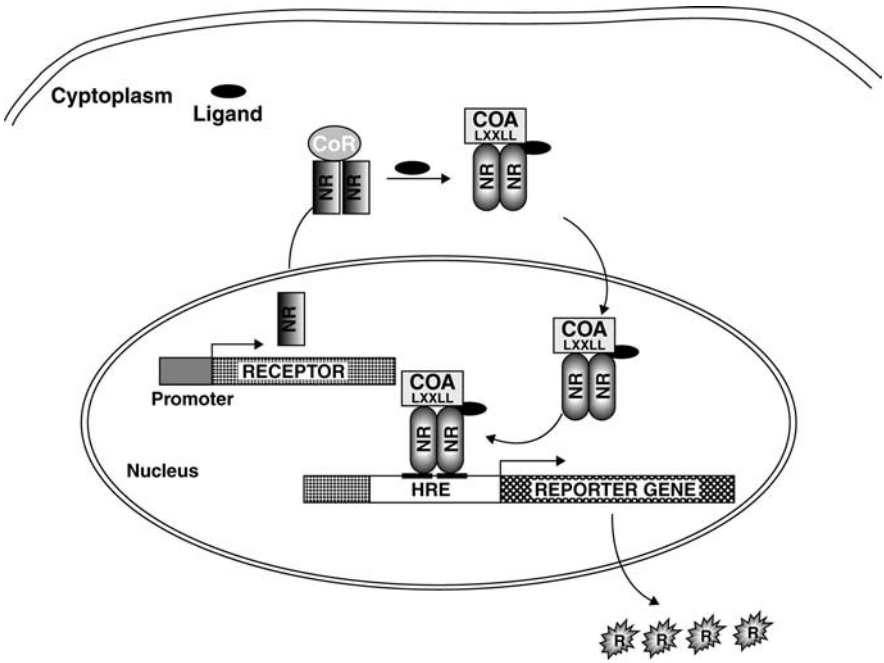

FIGURE 3 Schematic illustration of regulation of gene expression by nuclear receptor (NR). Upon binding of ligand, NR undergoes conformational changes and translocates into nucleus where it binds to HRE as a dimer and activates gene expression.

TABLE 3 The Bioassay Techniques Used to Characterize Ligand Specificities for NRs

Purpose	Assay type	Assay techniques	Sensitivity	Throughput
Primary	Cell-free binding assay	Filtration	High	Low
		SPA	High or medium	High
		FP	High or medium	High
Secondary		FRET	High or medium	High
	Cell-free coactivator recruit assay	FP	High or medium	High
		AlphaScreen	High or medium	High
		Bind (label-free)	High or medium	Medium
	Reporter transcription assay	β-Galactosidase	High	Medium
		Lucerferase	High	Medium
		Secreted alkaline phosphatase	High or medium	Low
Tertiary	Gene induction through mRNA detection	Taqman	High	Low
		bDNA	Medium	Medium

Radioligand Binding Assays

For the radioligand binding assays, a ligand with high affinity is needed. Where a radioligand specific for a particular receptor is available, a radioligand binding assay can be developed. In the radioligand binding assay, it is important to choose appropriate receptor concentration, where the radioligand and the competing compound are not depleted. Assessment of the radioligand bound receptor can be made with any of the several heterogeneous methods involving separation of the receptor-bound ligand from the free ligand (29,30)

Charcoal Adsorption Assays

This method is useful for the assay of ligand binding to soluble receptors. The binding reaction is done in a well of a 96-well microtiter plate. At the end of incubation, charcoal suspension in buffer is added, mixed vigorously, incubated on ice for 30 minutes and centrifuged. The free ligand binds to charcoal and the receptor bound ligand stays in solution (29). To aliquots of supernatant transferred to another microtiter plate, scintillant is added, mixed, and counted in a plate reader. This is a low-throughput assay and is not amenable for HTS.

Filtration Assay

When employing native or recombinant mammalian cells expressing the nuclear receptor, the radioligand binding to the receptor can be assayed by filtration assay. The binding reaction is performed by incubating the cells with [^{3}H]-ligand in 100 μl volume in a 96-well microtiter plate (29). The reaction contents are filtered rapidly on to a 96-well GF/C, GF/B, or GF/F plate (pretreated with 0.1% polyehyleneimine to reduce NSB) in a cell-harvester (PerkinElmer) or filtration unit (Millipore) and washed (5× with buffer). The washed plate is air-dried—the bottom of the plate is sealed, scintillant is added, and counted in a scintillation

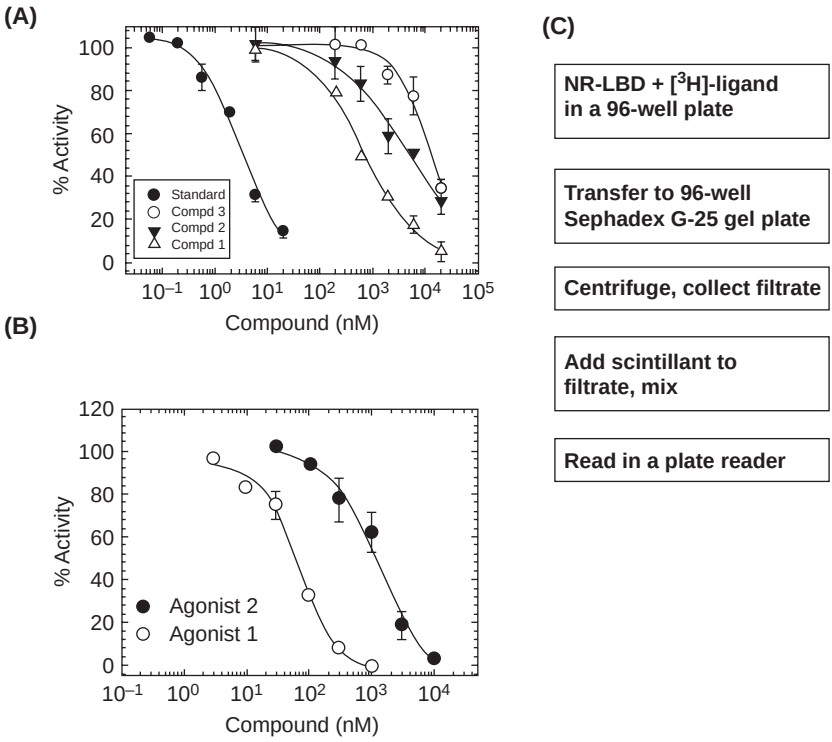

FIGURE 4 (**A**) NR whole-cell filtration binding assay. The cells stably expressing the NR reacted with a [^{3}H]-radioligand, filtered on to GFC-filtration plates, washed and air dried, scintillant added and the radioligand bound to the cells was determined in a TopCount or MicroBeta plate counter. (**B**) Determination of binding affinities of agonists by gel-filtration (exclusion chromatography) assay. Purified NR-LBD is incubated with [^{3}H]-radioligand, the NR–radioligand complex is transferred to 96-well gel-filtration plate. The flow through containing NR-radioligand complex is collected in 96-well plate, scintillant added, and counted in a TopCount or MicroBeta plate counter (27) (**c**) Assay flow chart of Gel-Filtration assay.

plate counter (Fig. 4). To increase the throughput, the assay can be automated in a 384-microtiter plate format by using Embla washer unit on an automation robot. This automated 384-microtiter filtration assay can be used as a primary assay with reasonable higher throughput.

Gel-Filtration Assay

When using cell-free extracts of full length NR or NR-LBD expressed in *E. coli* or purified NR or NR-LBD, the receptor bound radioligand is separated from the unbound radioligand by rapid size-exclusion chromatography on Sephadex G-25 (gel-filtration assay) (27,29,30). Specific binding is determined by competition with an excess of unlabeled ligand. The gel-filtration assay is performed in a 96-well plate by adding to each well of the plate NR or LBD in binding buffer, compound to be tested and initiating the reaction with the addition of the radioligand. After incubation, the reaction is transferred on to the top of the gel in

the wells of a 96-well gel-filtration block packed with Sephadex G-25 (previously centrifuged for one minute at $800\times g$ to drain the excess buffer). The gel-block is placed over a 96-collection plate, centrifuged at $1000\times g$ for four minutes to collect the flow-through (containing radioligand bound receptor). Scintillant is added, the plate is sealed, mixed thoroughly for 30 minutes on a plate shaker and counted in a plate reader to determine the radioligand bound receptor (Fig. 4). This heterogeneous assay is a sensitive assay but at best a low-throughput assay that involves filtration and transfer steps.

Scintillation Proximity Assay (SPA)

Scintillation proximity assay has been successfully used for receptor-binding assays by immobilizing receptors directly to SPA beads (30,31). NR or LBD expressed as fusion protein with His_6 or GST can be immobilized on to copper-SPA bead or GST-SPA bead, respectively, and with availability of a radioligand, a HTS-SPA method can be devised for ligand–receptor binding. When the radioligand binds to the receptor immobilized on the SPA bead, the radioligand will come into close proximity of scintillant on the bead to stimulate the bead to emit light thus producing a signal [Fig. 5(A)]. The unbound radioligand will not come in close proximity to the scintillant on SPA bead hence not able to yield signal, thus eliminating separation of the unbound radioligand from radioligand bound receptor. The SPA binding assay gave binding affinities for compounds similar to those obtained by gel-filtration binding assay (27,31). The apparent K_i values obtained by SPA assay correlated ($r^2 = 0.92$) very well with the K_i values obtained by traditional gel-filtration binding assay for ERα and ERβ receptors [Fig. (5B)]. The SPA binding assay is a homogeneous assay with the addition of reagents to a well of microtiter plate, mixed, and count in a plate reader (for more details see chap. 4 in this volume).

When polyvinyl toluene (PVT) or yttrium silicate (YSi) SPA bead (blue shifted bead) is used, 96- or 384-microtiter plate assays can be run and the signal is read in a plate reader (384 plate is read in ~2 hours). If polystyrene (PS) or yttrium oxide (YOX) (red shifted bead) is used, 384- or 1536-plate assays can be run and the signal is read in an imaging plate reader (read each plate in five minutes). This homogeneous radioactive method can be miniaturized to 384- or 1536-plate assays thus increasing the throughput, and reducing radioactive waste generated compared to conventional radioactive (filtration) receptor-binding assays.

Fluoresecnce-Based Assays

Anilinonapthalene-1-Sulfonic Acid (ANS) Binding Assay

ANS and bisANS in aqueous solutions are nonfluorescent, however, when they bind to protein become fluorescent. This assay measures fluorescence emission from ANS/bis-ANS following binding to NR ligand binding pocket ($ex\lambda$ = 360 nm, $em\lambda$ = 460 nm). Any compound that competes with the same binding site will decrease the fluorescence intensity from the dye (Fig. 6). The assay can be miniaturized to 384- or 1536-well microtiter plates. The limitation of this method is that the dye can also bind nonspecifically to any hydrophobic regions of proteins (not necessarily the ligand binding pocket) thus can give false positives. The compounds may not completely displace the dye, suggesting there is nonspecific binding of the dye. Also, color compounds can cause interference in the readout.

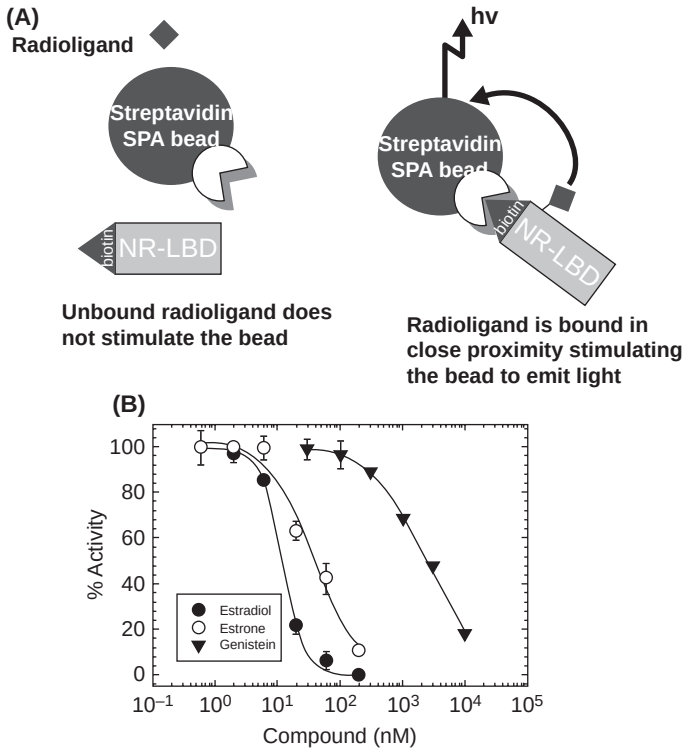

FIGURE 5 (**A**) Schematic representation of an SPA ligand schematic presentation of SPA receptor ligand binding assay. Biotinylated NR-LBD binds to streptavidin SPA bead due to biotin–streptavidin interaction. When the radioligand binds to the receptor attached to the SPA bead, it will be in close proximity to the scintillant on the bead, generating photons, which can be measured in a TopCount of MicroBeta plate counter. When a compound competes with radioligand in binding to the receptor, the radioligand is displaced by the competitor and will have reduced signal. The radioligand unbound to the SPA bead will not be in close proximity of the scintillant and will not give signal. (**B**) Competition of [^{3}H]-estradiol binding to ERα in SPA binding assay by estrdiol, estrone, and genistein.

Fluorescent Fatty Acids in PPAR Binding Assays

Fluorescent fatty acids have been used in binding assays of fatty acid binding protein (32). Fatty acids serve as ligands to all the three isoforms of PPAR and have been shown to bind to PPARs. When *cis*-Parinaric acid (CPA) binds to PPARγ-LBD, there is a spectral shift from 319 to 329 nm. The ratio of 319 and 329 nm for CPA in solution is 3 and changes to 1 when bound to PPARγ-LBD. However, instead of using the spectral changes, a more sensitive fluorescent reading (exλ = 318 nm and emλ = 410 nm) has been used to determine the IC_{50} for the compounds. The CPA method can be used for determining low-affinity compounds, needs highly purified receptor, the CPA–PPAR complex is temperature sensitive and color compounds interfere in the assay. Other fluorescent fatty acids also have been used for PPAR assays (32).

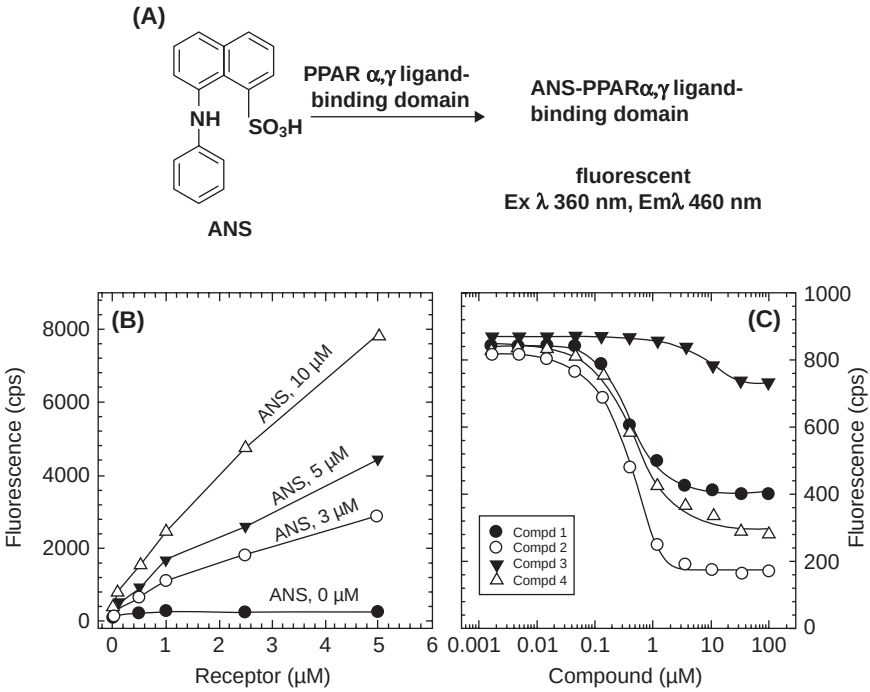

FIGURE 6 An NR ligand binding assay using anilinonaphthalene sulfonic acid (ANS). ANS in aqueous solution is nonfluorescent and when binds to protein yields fluorescence. (**A**) Schematic of ANS binding reaction. (**B**) Dose-dependent response to receptor concentration. Fluorescence signal increased with increasing ANS and the receptor concentrations. (**C**) Competition binding of ANS by agonists (29).

Fluorescence Polarization (FP) Binding Assay

FP ligand–receptor binding assay with appropriate fluorescent ligand (or agonist or antagonist) have been used in HTS (27,33). A small fluorescent ligand in solution freely rotates and is depolarized, whereas the fluorescent ligand when bound to the receptor protein is oriented in the plane of polarization producing high polarization signal. FP is a homogeneous assay wherein all the components of the reaction are added into a well of microtiter plate, incubated, and without further processing the FP signal is read in a FP plate reader (for more details see chap. 4 in this volume). A potent agonist (ligand) labeled with a fluorescent molecule (fluorescein, TAMARA, BODIPY), which still retains good binding affinity to the receptor, will be used as ligand for the FP binding assay (27,33) (Fig. 7). Briefly, in the FP homogeneous assay, to the test compound NR-LBD is added, followed by fluorescent ligand to each well of a microtiter plate (100, 30, and 8 μL total volume in a 96-, 384-, and 1536-well microtiter plate assay, respectively). The reaction mixture is incubated at room temperature and FP signal is read in any multimode plate reader. The agonist/antagonist compounds displace specifically the fluorescent ligand, making it possible to determine the binding affinity of the compounds to the receptor.

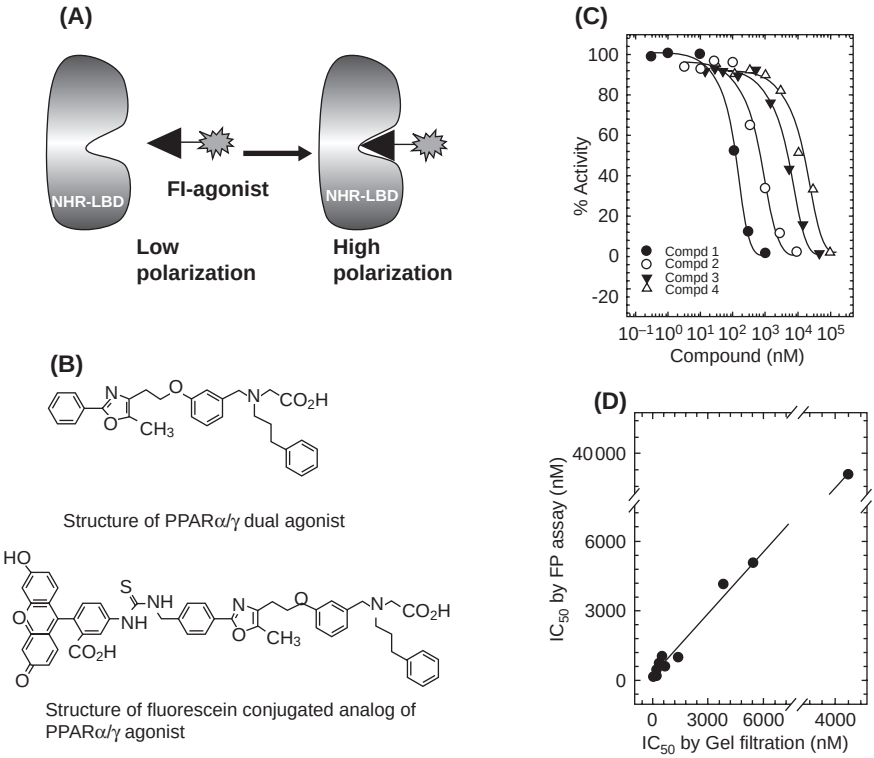

FIGURE 7 (**A**) Schematic of FP binding assay. (**B**) Structure of PPARα/γ agonist and fluorescein conjugated agonist. (**C**) FP competition binding assay for PPARγ by PPARγ agonists. (**D**) Correlation of binding affinity between PPARγ FP binding assay and gel-filtration assay. There is a good correlation between these two assays ($r^2 = 0.99$) (27).

COACTIVATOR/COREPRESSOR INTERACTION ASSAYS

The docking of ligand into the hydrophobic binding pocket of the LBD induces conformational changes in the NR specifically in the position of the AF-2 helix in the C-terminus of the receptor to form a specific coactivator binding pocket and permits the NR to interact with a consensus sequence of LXXLL (NR-box) motifs present in all coactivators. Coactivators fall into certain families: the p-160 family consists of steroid receptor coactivator-1, 2 (SRC-1, -2), transcriptional intermediary factor-2 (TIF2) or glucocorticoid receptor-interacting protein 1 (GRIP1), and receptor-associated coactivator 3 (RAC3); the CRE binding protein (CBP)/p300; and the TRAP220/DRIP205/PBP complex. There are three LXXLL (NR-box) motifs within the receptor interaction domain of p160 coactivator. Although, LXXLL motifs are sufficient for interacting with LBD, sequences flanking LXXLL motif are important for the receptor specificity (34).

The corepressors are bound to NRs inhibiting NR activity by limiting the cellular proteins recruited to NRs to mediate transcriptional repression in the absence of ligand. Upon ligand binding to NR, the corepressors dissociate from the NR, paving the way to the recruitment of coactivators that trigger

transcriptional activation. Similar to the consensus LXXLL motifs present in coactivators, the repressors share a common sequence motif of I/L-X-X-I/V-I (CoRNR box). The I/L-X-X-I/V-I motif and the adjacent residues flanking the CoRNR box are important for the interaction with NRs.

Several fluorescence-based assays have been used for coactivator interaction with NRs and will be discussed below.

FP Assay

Coactivators or peptides containing the LXXLL motif labeled with a fluorescent tag and NR-LBD have been used for identification of ligands. The ligand binding to the NR facilitates the binding of coactivator (35). The unbound fluorescent coactivator tumbles rapidly when excited with polarized light and emits depolarized light, resulting in low FP signal. When the fluorescent coactivator peptide (with LXXLL motif) interacts with the NR, and the resulting fluorescent coactivator-NR orients in the plane of polarization, resulting in higher FP signal (Fig. 8). The recruitment of the fluorescent coactivator by the receptor is dependent on agonist concentration and thus the FP signal increases with increasing concentration of agonist. This FP assay format can be utilized to identify agonists for orphan NRs. This FP assay is a robust homogeneous assay that can be performed in high-density plates, thus allowing a high-throughput assay that can be developed as an automated assay.

Time-Resolved Fluorescence Resonance Energy Transfer (TR-FRET) Assay

The interaction between NRs and their coactivators can be determined by using TR-FRET assay. The reagents required are purified NR LBD with myc or FLAG tag, europium (Eu)-labeled myc or FLAG antibody, biotinylated peptide containing LXXLL motif, and streptavidin-labeled APC (Fig. 9). The order of addition of the reagents should be determined in the optimization studies. Tagged receptor and Eu-labeled antitag antibody are first incubated for one hour, similarly, biotinylated coactivator protein and streptavidin APC are incubated for the same time. Then the two reaction mixtures are combined in the presence of the test compound (agonist), incubated for additional one hour

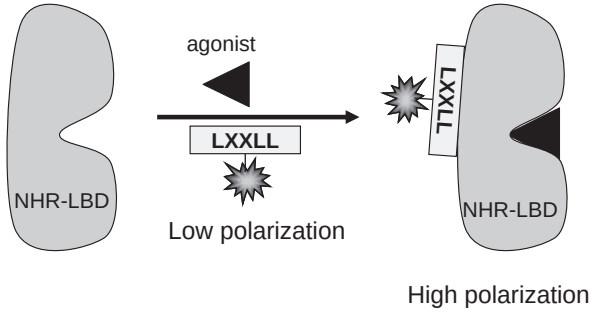

FIGURE 8 Schematic illustration of FP assay for detecting ligands for NR using a fluorescent coactivator peptide (containing LXXLL motif). Agonist-bound NR can recruit fluorescent coactivator peptide resulting in higher FP value.

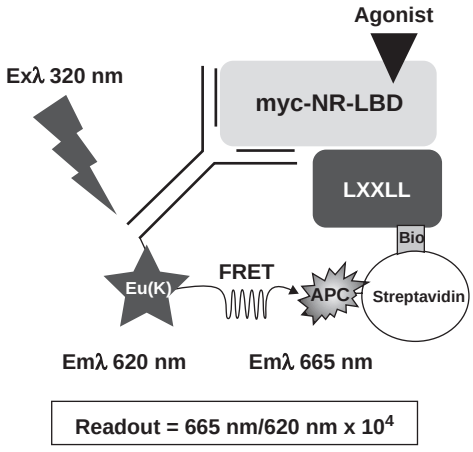

FIGURE 9 Schematic diagram for TR-FRET assay for detecting ligands for NR using a biotinylated coactivator peptide (containing LXXLL motif). In the illustration, myc-tagged NR-LBD and biotinylated coactivator peptides are used. Eu-labeled myc antibody is incubated with myc-NR-LBD, and biotinylated coactivator is incubated with APC-tagged streptavidin. In the presence of agonist, Eu-myc Ab—myc-NR-LBD recruits biotin-coactivator—streptavidn-APC thus bringing donor Eu flurophore in close proximity of the acceptor flurophore APC. Excitation of Eu at 320 nm results in emission 620 nm, and the emission at 665 nm from APC is detected when agonist-induced NR–LXXLL interaction occurs.

and the FRET signal is measured in a plate reader. Upon biotinylated coactivator binding to the NR in the presence of ligand, Eu on the anti-tag antibody comes close to APC of streptavidin and due to the close proximity of the donor Eu and acceptor APC molecules FRET occurs. Thus when excited at 320 nm, Eu transfers energy to APC due to FRET and FRET signal is measured at 665 nm (see chap. 4 in this book for TR-FRET assay principle) in a plate reader. This is a robust homogeneous assay that can be performed in a 96-, 384-, or 1536- plate in a total volume of 100, 30, or 8 μl, respectively, and can be developed as an automated assay (36).

Alphascreen Assay

The ligand-activated interaction between NR and the coactivator can be detected by AlphaScreen assay by using AlphaScreen beads (36,37) (see chap. 4 in this book for AlphaScreen assay principle). Depending on the reagent, availability a direct, indirect, or sandwich assay format can be used (Fig. 10). For the direct assay, the required reagents are a biotinylated coactivator peptide, streptavidin donor beads, GST-tagged NR LBD, and anti-GST acceptor beads. For the indirect assay, the required reagents are a biotinylated coactivator peptide, streptavidin donor beads, NR-LBD, antireceptor antibody, and protein A acceptor beads. For the sandwich assay, the reagents required are streptavidin donor beads, biotinylated anti-GST antibody, GST-tagged coactivator, NR, anti-NR antibody, and protein A acceptor bead. In the sandwich assay format, the NR-coactivator interaction is sandwiched between two antibodies. One of the binding partner (GST-tagged coactivator peptide) is captured by a biotinylated anti-GST antibody, which binds to the streptavidin donor bead and the other partner (NR) is captured by NR antibodies preadsorbed to protein A–coated acceptor beads. Upon ligand activation of NR (bound to acceptor bead), coactivators (bound to donor bead) are recruited and the donor bead and acceptor bead come in close proximity yielding signal. The AlphaScreen NR assay is a homogeneous nonradioactive assay that can be used for HTS assay.

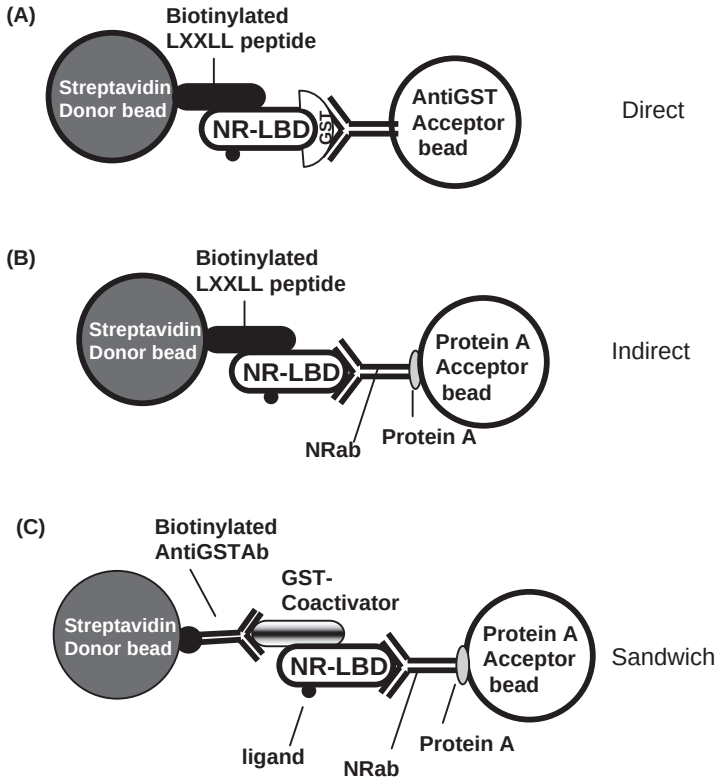

FIGURE 10 Schematic representation of different formats of AlphaScreen assays for agonist-induced NR–LXXLL interaction. (**A**) Direct assay. Biotinylated coactivator peptide is captured by streptavidin donor bead, and GST-tagged NR-LBD is captured by anti-GST Ab acceptor bead. When agonist-induced NR–LXXLL interaction occurs, donor bead and acceptor bead into close proximity give alpha signal. (**B**) Indirect assay. Biotinylated coactivator peptide is captured by streptavidin donor bead, NR-LBD is captured by anti-NR-LBD preadsorbed to protein A acceptor bead Ab. (**C**) Sandwich assay. Coactivator is captured by biotinylated anticoactivator Ab bound to streptavidin donor bead, and NR-LBD is captured by anti-NR-LBD preadsorbed to protein A acceptor bead Ab, thus NR–LXXLL are sandwiched between two antibodies.

Label-Free Nuclear Receptor Assay

The above-described methods use fluorescent and/or biotin or other tagged reagents. In a label-free assay technology using optical biosensor and BIND reader (SRU Biosystems), the target is immobilized to the optical biosensor and compounds binding to the target will shift the peak wave value and are measured in Bind reader (see chap. 4 in this book for more details) (38). In the coactivator binding assay, the NR LBD is immobilized to the biosensor surface. The agonist or antagonist is added to the biosensor and read till a steady state is obtained. Then the coactivator peptide is added and the signal is monitored. In the sample where agonist is present, coactivator is recruited to the NR on the biosensor and this binding increases the signal, whereas in the sample where antagonist is present there is no binding of coactivator and no change in the signal (Fig. 11).

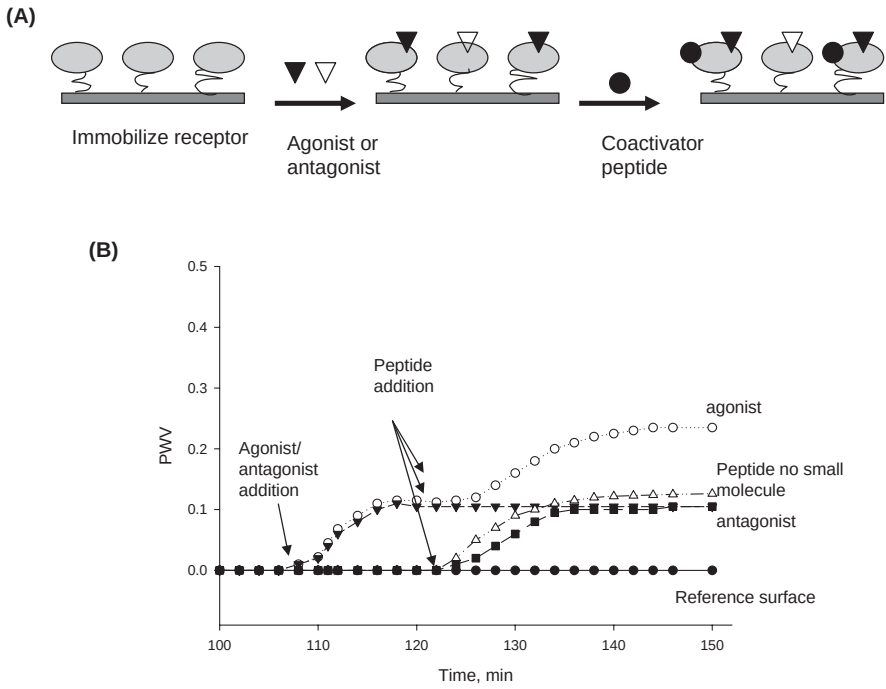

FIGURE 11 Label-free BIND® (SRU Biosystems) assay for agonist induced NR–coactivator interaction. (**A**) Schematic of BIND® assay format. Receptor protein is immobilized to the biosensor surface. Small molecule agonist or antagonist is added and after steady state, the cofactor peptide is added. (**B**) Agonist and antagonist bind to the NR on the biosensor and the PWV increases. When peptide is added, the signal increased only with agonist, and no change is observed with antagonist, as the antagonist does not interact with the coactivator.

CELL-BASED ASSAYS

Reporter genes have been extensively used in cell-based assays to monitor promoter activation and receptor function. Conventional screens for receptor ligands usually depend on transcriptional activity and reporter assays. The ligands for NR on entering the cells, bind to their cognate receptors with high affinity and induce a conformational change that activates the receptor. In some cases, the receptor may dissociate from heat shock proteins and conformational changes that allow the receptor to bind with other proteins involved in transcriptional regulation. Activated receptors bind to specific DNA sequences called hormone response elements (HRE) and increase transcription of the linked downstream genes (39).

Functional Transcription Assays

A typical reporter construct consists of either a single or multiple copies of the responsive element placed upstream of a minimal but functional promoter, which controls the expression of the reporter gene. Cell-based high-throughput transcription assays require introduction of DNA construct into a cell line by

either transient or stable transfection from an expression vector. In cell-based reporter assay, the target NR (or LBD) is expressed in a cell line under certain selection of antibiotic, together with a reporter gene under the control of a promoter containing appropriate HRE under selection of a second antibiotic. Incubation of the cell with a ligand activates the expressed NR receptor, dimerizes, and translocates into nucleus where it binds to the HREs in the reporter plasmid and induces the expression of the reporter gene (Fig. 12). The agonist-induced expression of the reporter gene results in the increased production of the reporter gene-product, which can be quantitatively assayed. The common reporters used for this purpose include firefly luciferase enzyme, secreted alkaline phosphatase (SEAP), β-lactamase, green fluorescent protein (GFP), and β-galactosidase. Luciferase activity can be assayed as a homogeneous assay by any of several kits, LucLite from PerkinElmer, LucScreen from Tropix, Steady-Glo from Promega, or others. Similarly, SEAP activity can be assayed with attophos kit and β-galactosidase with fluorescence detection kits. β-Lactamase reporter assay involves a membrane-permeant ester derivative CCF2/AM (6-chloro-7-hydroxy coumarin and fluorescein conjugated at 7 and 3′ positions of

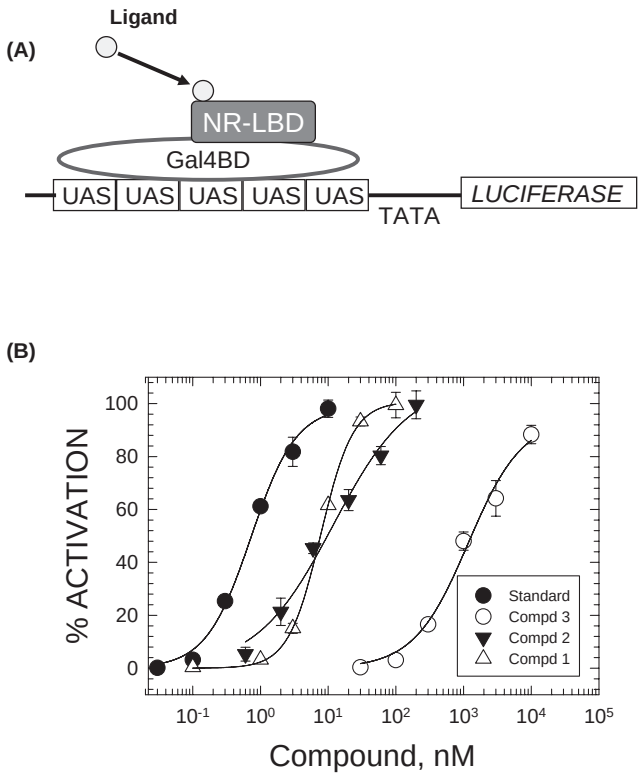

FIGURE 12 NR transactivation assay. (**A**) Schematic illustration of NR transactivation system. (**B**) Cell-based NR transactivation assay. In the luciferase reporter assay, the agonists stimulated transactivation activity comparable to their binding affinities.

cephalosporin, respectively), a β-lactamase substrate, provides a quantitative measure of gene transcription and thus allows the development of a homogeneous transcription activation HTS assay with β-lactamase reporter (40) (The reporter assays are described in chap. 4 in this book).

Agonists for PPARγ can be assayed by using stably transfected human embryonic kidney (HEK) 293 cells. The cells stably express a chimera consisting of a synthetic promoter with five tandem repeats of the yeast GAL4 binding site, controlling the expression of the *Photinus pyralis* (American firefly) luciferase gene (Fig. 12). The cells are subsequently transiently transfected with a plasmid (pcDNA3.1) consisting of a chimeric construct of the yeast GAL4 DNA binding domain upstream from the human PPARγ LBD. These cells will express the luciferase protein dependent on agonist concentration due to activation of PPAR. Luciferase activity is then determined by cell lysis and catalysis of luciferin substrate to yield luminescence signal. To have uniform transient expression, a bulk transient transfection protocol has been developed, wherein cells are grown in T-150 flask, washed with phosphate buffered saline, and then appropriate medium (without phenol red) is added followed by DNA/lipofectamine mixture. After five to six hours incubation at 37°C in 5% CO_2–95% O_2, the cells are harvested and added to each well of a 384-well microtiter plate. Transiently transfected cells are treated in the presence and absence of agonists for 18 hours at 37°C in 5% CO_2–95% O_2, cells are lysed with the addition of SteadyGlo and assayed for the luciferase enzyme activity, and the luminescence signal is read in a plate reader. The agonists increased the reporter activity in a dose-dependent manner (Fig. 12). The agonists with different binding affinities increased the transcription (activation) activity proportional to their relative affinity.

Binding of NR to NR Response Element

When ligand binds to the NR, the complex translocates into nucleus where it acts as a transcription factor binding to NR responsive elements NRRE in the DNA and modulates cellular functions. About 50 base pair double stranded DNA to which fluorescein attached is used as substrate for binding to NR in a FP assay format. Binding of increasing concentration of estrogen receptor to 1 nM fluorescein-labeled estrogen response element increased the signal from 60 to 260 milliP with a K_d of 4.5 nM for estrogen receptor. This is a homogeneous assay that can be miniaturized to high-density plates (29).

Translocation Assays

The binding assay identifies compounds that bind to the target NR. As purified receptor proteins are used in the binding assay in the absence of the appropriate cofactors, there is a greater chance of these being false positives or negatives. Upon ligand binding the steroid receptors translocate from the cytoplasm to nucleus where they bind to their specific HREs in the promoter region of the target genes. Different coregulators are present in each different cell line, which regulate the transciptional activity in response to ligand activation of the receptor. So, the modulator screen for each receptor should use appropriate cell line. The transcription assays and proliferation assays are time-consuming assays and are used as secondary screens.

Translocation Assay with Green Fluorescent Protein (GFP)-Fused NR

Some unliganded NRs (steroid NRs) are predominantly in the cytoplasm, and upon ligand binding these cytoplasmic receptors are translocated to nucleus. Receptors that are predominantly nuclear when unliganded need to be reengineered for retention in cytoplasm to use in a translocation screen. Only the pure agonists and selective modulators can trigger downstream transcription activity, whereas the translocation activity can be triggered by a variety of ligands (pure agonist, antagonists, and selective modulators). The receptor fused with GFP can be used to monitor the movement of the receptor from cytoplasm to nucleus (39). Because GR is constitutively cytoplasmic in uninduced cells, GR can be used to construct chimeras between GR (N-terminus, DBD, and partial LBD) and constitutively nuclear receptor (41).

The cytoplasmic receptors and chimeric NRs are engineered with GFP at the N-terminus, and the stable cell lines with GFP-fused receptors have been generally used fluorescence-based primary translocation assays. Cell-based assay for NR translocation by modulators can be measured by high-content screening with any of several imaging systems that are equipped with cytoplasmic to nuclear translocation algorithms in their software packages [INCell analyzer (General Electric), ArrayScan from Cellomics, Disocvery from Universal Imaging, and IC 100 from Q3DM].

Enzyme Fragment Complementation (EFC) Translocation Assay

The PathHunter system (DiscoveRx) is a homogeneous assay that utilizes EFC associated with labeled target protein. In the PathHunter assay a small peptide from N-terminus of β-gal (β-gal ED) fused to NHR is expressed recombinantly in the cell, and the complementary portion of β-gal (β-gal EA) is expressed in the nucleus (Fig. 13). Upon ligand binding the receptor causes either homo- or heterodimerization of the receptor and translocation to nucleus, allowing the β-gal EA to interact with β-gal ED and form a functional β-gal enzyme that is capable of using chemiluminescent substrate producing luminescence signal (42). The assay has been performed by adding cells and compound in 1.6 μL volume in 3456-format or 4 μL in 1536-format and incubated at 37°C for three hours (in 5% CO_2/95% O_2) followed by addition of 0.6 or 3 μL of PathHunter detection reagent, respectively, and incubated at room temperature for one hour and the luminescence is read in ViewLux (PerkinElmer).

Protein–Protein Interaction Assay

Pull-Down Assays

The interaction between NRs and coactivators are traditionally measured in vitro by "pull-down" assay using ^{35}S-coactivator protein or by nonradioactive "pull-down" assay with GST-coupled coactivators (43). These "pull-down" assays are not amenable to screening large number of agonists and antagonists.

A variety of methodologies have been applied to determine protein–protein interactions. One of the most extensively used techniques is "pulldown" assay. The GST-tagged coregulator proteins are immobilized on glutathione agarose, which serves as bait protein in the filtration assay. [^{35}S] Radiolabeled receptor proteins are prepared in vitro by use of a phage RNA polymerase–coupled transcription/translation serve as "prey" proteins. The immobilized GST-fusion protein is incubated with [^{35}S] radiolabeled receptor proteins in a

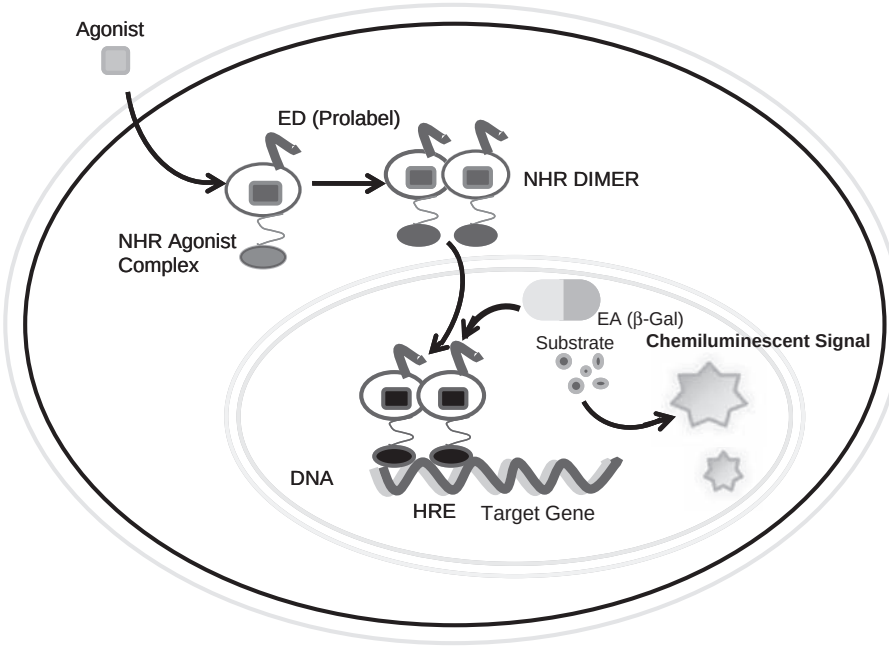

FIGURE 13 The PathHunter NR translocation assay. In CHO cells the N-terminal β-gal peptide (β-gal ED, prolabel) is stably expressed on the NR and the complimentary β-gal (β-gal EA) is expressed in the nucleus. When ligand binds to the receptor, prolabel dimerizes and translocated to the nucleus and the prolabel interacts with β-gal EA in the nucleus and forms a functional β-gal enzyme that can act on the chemiluminescent substrate producing luminescent signal, which can be measured in a plate reader.

96-well Multiscreen-HV filter plate (Millipore). GST-pulldown microplate method displayed well-behaved saturable binding and NR displayed binding to the GST-coactivator that fit two-component protein–protein interaction (44). Alternatively, GST-pulldown assay can be performed on glutathione-coated microplates (45). However, the maximum GST binding capacity of 10 ng/well (compared to 5 μg/μL GST agarose resin), which is considerably lower binding capacity that restricts its suitability to only very higher affinity interactions.

Mammalian Two-Hybrid Assay

The yeast two-hybrid system has been utilized to identify many coactivators and corepressors of steroid receptors. The mammalian two-hybrid system is based on the principle of yeast two-hybrid system. The two-hybrid system is a useful approach for detecting protein–protein interactions in cells. This two-hybrid system method with the transcription assay has the potential to identify ligands that are dissociated in promoter transactivation from certain coactivator interaction. In the mammalian two-hybrid assay, the LXXLL peptide or full receptor interaction domain of coactivator is fused to Gal4DBD and a plasmid containing GAL4 response elements upstream of luciferase gene and the NR or NR-LBD is fused to VP16 transactivation domain (AD). The Gal4DBD-peptide fusion is

bound to Gal-4 response element upstream of the TATA-driven luciferase. Agonist binding to NR-LBD interacts with LXXLL/coactivator forming NR–LXXLL complex, and the VP16 AD activation in this complex promotes the assembly of RNA polymerase II complex at the promoter enhancing transcription activation of the luciferase reporter gene (46).

This strategy can also be applied to the receptor dimerization assay, as most of the nuclear receptors form homodimers or heterodimers with RXR.

Optical Probes for Modulators of NR

A selective NR modulator (SNRM) is able to promote the receptor activity in one tissue acting as a full or partial agonist and block the receptor activity in another tissue acting as an antagonist. This tissue-selective activity of SNRM is due to different distribution of cellular coregulators in different tissues interacting with the ligand-bound NR. The molecular details of an SNRM binding to a NR, accompanying conformational changes, recruitment of coregulators, and translocation are important features for understanding SNRM action in the cell and tissue. An intramolecular FRET assay was reported that can be used to identify NR modulators in the cell (47–49). NR LBD connected to the NR interacting sequence from coactivator or corepressor protein via a flexible linker sequence and at the N-terminus fused with cyan fluorescent protein (CFP) serves as donor and at the C-terminus fused with yellow fluorescent protein (YFP) (Fig. 13). The excitation and emission spectra of CFP and YFP are suitable for FRET. The fusion protein functions as a fluorescent probe for imaging ligand-induced conformational changes in the NR and interaction of NR and coregulator protein in live cells. In the absence of ligand, the FRET partners CFP donor and YFP acceptor, which are at the either end of the NR LBD, do not come into close proximity. Upon ligand binding, conformational changes occur in NR LBD. The ligand bound NR-LBD interacts with the intramolecular coactivator/corepressor peptide. Consequently, YFP is oriented in close proximity to CFP, resulting in FRET signal response (Fig. 14). The cells can be monitored with exλ 440 nm (for CFP), emλ 480 nM (for CFP), and emλ 535 nm (for YFP). The emission ratio of CFP/YFP can be measured to follow the FRET changes. With the modulator interaction with the NR LBD, the CFP/YFP ratio decreases in a dose-dependent manner. The FRET responses can be read in any imaging plate reader. Thus, the fluorescent probe allows monitoring ligand-induced NR/coregulator interactions in a living cell in real time.

Epigenetic Regulators

The cellular enzymes Histone deacytylase (HDAC) and DNA methyl transferases (DNMT) mediate epigenetic events and have become important molecular targets. The level of DNA methylation, histone acetylation, methylation, and phosphorylation determines the level of chromatin compaction in the cell, which in turn determines the accessibility of transcription factors to their target genes. Methylated DNA and hypoacetylated histones prevent transcription, and unmethylated DNA and acetylated histones at promoter site favor transcriptional activity. Mammalian cell lines, which expresses HDACs and/or DNMTs and responsive to chemical epigenetic modulators, are cotransfected with an expression vector for a GFP-tagged receptor driven by a constitutively active CMV promoter and with a gene for antibiotic resistance (50). Cells that survived

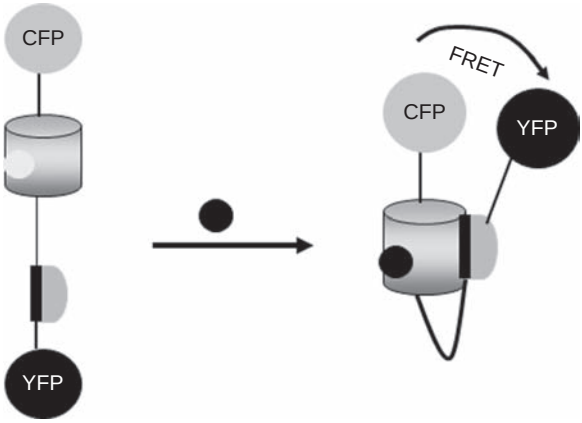

FIGURE 14 Ligand-induced coactivator/corepressor recruitment to the NR LBD in living cells using fluorescent probes. NR-LBD is linked to coactivator/corepressor peptide through a linker and fused with CFP and YFP at N-terminus and C-terminus, respectively. Ligand-dependent interaction between the NR LBD and coactivator facilitates intramolecular FRET by orienting YFP in close proximity to CFP.

in the presence of antibiotic but did not express GFP but express GFP by treatment with inhibitors of HDACs or DNMTs are selected. These cells give a robust cellular response to inhibitors of HDACs or DNMTs and can be imaged in image plate readers like Discover-1 (Molecular Devices).

CONCLUSIONS

NRs have been utilized as drug targets to develop therapies to treat myriad diseases. The NRs and orphan NRs continued to be important drug targets in pharmaceutical drug discovery. The challenge will be in discovering better ligands that target specific NRs without overlapping activities on other NRs and do not alter the metabolism of other genes. Several radiometric- and fluorescence-based binding assays and cell-based functional assays are available for NR assays, however, it is not clear which assay technology is optimal for a specific NR. In addition to agonists or inhibitors of specific NR, increased focus is being given in the identification of selective nuclear receptor modulators (SNRMs) in different tissues to avoid unwanted effects of the NRs. The availability of very sensitive high-throughput assays is making it possible to identify SNRMs.

REFERENCES

1. Tobin JF, Freedman LP. Nuclear receptors as drug targets in metabolic diseases: New approaches to therapy. Trends Endocrinol Metab 2006; 17(7):284–290.
2. Robinson-Rechavi M, Capentier AS, Duffraisse M, et al. How many nuclear receptors are there in human genome? Trends Genet 2001; 17 (7):554–556.
3. Weinberger C, Hollenberg SM, Ong ES, et al. Identification of human glucocorticoid receptor complementary DNA clones by epitope selection. Science 1985; 228:740–742.
4. Green S, Walter P, Greene G, et al. Cloning of human oestrogen receptor cDNA. J Steroid Biochem 1986; 24:77–83.

5. Greene GL, Gilna P, Waterfield M, et al. Sequence and expression of human estrogen receptor complementary DNA. Science 1986; 231:1150–1154.
6. Sap J, Munoz A, Damm K, et al. The c-erb-A protein is a high-affinity receptor for thyroid hormone. Nature 1986; 324:635–640.
7. Petkovich M, Brand NJ, Krust A, et al. A human retinoic acid receptor which belongs to the family of nuclear receptors. Nature 1987; 330:444–450.
8. Aranda A, Pascual A. Nuclear hormone receptors and gene expression. Physiol Rev 2001; 81(3):1269–1304.
9. Mangelsdorf J, Evans RM. The RXR heterodimers and orphan receptors. Cell 1995; 83:841–850.
10. Weatherman VR, Fletterick RJ, Scanlan TS. Nuclear-receptor ligands and ligand-binding domains. Annu Rev Biochem 1999; 68:559–581.
11. Fancis GA, Fayard E, Picard F, et al. Nuclear receptors and the control of metabolism. Annu Rev Physiol 2003; 65:261–311.
12. MacGregor JI, Jordan VC. Basic guide to the mechanism of antiestrogen action. Pharmacol Rev 1998; 50(2):151–190.
13. Gustafsson JA. Therapeutic potential of selective estrogen receptor modulators. Curr Opin Chem Biol 1998; 2(4):508–511.
14. Sladek FM. Nuclear receptors as drug targets: New developments in coregulators, orphan receptors and major therapeutic areas. Expert Opin Ther Targets 2003; 7(5):679–684.
15. Valledor F, Ricote M. Nuclear receptor signaling in macrophages. Biochem Pharmacol 2004; 67:201.
16. Xu HE, Lambert MH, Montana VG, et al. Molecular recognition of fatty acids by peroxisome proliferator-activated receptors. Mol Cell 1999; 3:397–403.
17. Kliewer SA, Sundseth SS, Jones SA, et al. Fatty acids and eicosanoids regulate gene expression through direct interactions with peroxisome proliferator-activated receptors α and γ. Proc Natl Acad Sci U S A 1997; 94:4318–4323.
18. Lehmann JM, Kliewer SA, Moore LB, et al. Activation of the nuclear receptor LXR by oxysterols defines a new hormone response pathway. J Biol Chem 1997; 272:3137–3140.
19. Janowski BA, Willy PJ, Devi TR, et al. An oxysterol signalling pathway mediated by the nuclear receptor LXR alpha. Nature 1996; 338:728–731.
20. Parks DJ, Blanchard SG, Bledsoe RK, et al. Bile acids: Natural ligands for an orphan nuclear receptor. Science 1999; 284:1365–1368.
21. Wang H, Chen J, Hollister K, et al. Endogenous bile acids are ligands for the nuclear receptor FXR/BAR. Mol Cell 1999; 3:543–553.
22. Hard T, Kellenbach E, Boelens R, et al. Solution structure of the glucocorticoid receptor DNA-binding domain. Science 1990; 249:157–160.
23. Luisi BF, Xu WX, Otwinowski Z, et al. Crystallographic analysis of the interaction of the glucocoticoid receptor with DNA. Nature 1991; 352:497–505.
24. Mangelsdorf DJ, Thummel C, Beato M, et al. The nuclear receptor superfamily: The second decade. Cell 1995; 83:835–839.
25. Walker D, Htun H, Hager GL. Using inducible vectors to study intracellular trafficking of GFP-tagged steroid/nuclear receptors in living cells. Methods 1999; 19:386–393.
26. Tamrazi A, Katzenellenbogen JA. Site-specific fluorescent labeling estrogen receptors and structure–activity relationships of ligands in terms of dimer stability. Methods Enzymol 2003; 364:37–53.
27. Seethala R, Golla R, Ma Z, et al. A rapid, homogeneous, fluorescence polarization binding assay for peroxisome proliferator-activated receptors alpha and gamma using a fluorescein-tagged dual PPARα/γ activator. Anal Biochem 2007; 363:263–274.
28. Chapman-Smith A, Cronan JE Jr. The enzymatic biotinylation of proteins: A post translational modification of exceptional specificity. TIBS 1999; 24:359–363.
29. Seethala R. Receptor screens for small molecule agonist and antagonist discovery. In: Seethala R, Fernandes P, eds. Handbook of Drug Screening, Marcel Dekker, NY 2001:189–264.

30. Jones SA, Parks DJ, Kliewer SA. Cell-free ligand binding assays for nuclear receptors. Methods Enzymol 2003; 364:53–71.
31. Nichols JS, Parks DJ, Consler TG, et al. Development of a scintillation proximity assay for peroxisome proliferator-activated receptor γ ligand binding domain. Anal Biochem 1998; 257:112–119.
32. Adamson JA, Palmer CNA. Fluorescenc-based ligand binding assays for peroxisome proliferator-activated receptors. Methods Enzymol 2003; 364:188–197.
33. DeGrazia MJ, Thompson J, Heuvel JPV, et al. Synthesis of a high-affinity fluorescent PPARγ ligand for high-throughput fluorescence polarization assays. Bioorg Med Chem 2003; 11:4325–4332.
34. Chen T, Xie W, Agler M, et al. Coactivators in assay design for nuclear hormone receptor drug discovery. Assay Drug Dev Technol 2003; 1(6):835–842.
35. Mettu NB, Stanely TB, Dwyer MA, et al. The nuclear receptor–coactivator interaction surface as a target for peptide antagonists of the peroxisome proliferator activated receptors. Mol Endocrinol 2007; 21(10):2361–2377.
36. Wu X, Glickman JF, Bowen BR, et al. Comparison of assay technologies for a nuclear receptor assay screen reveals differences in the set of identified functional anatagonists. J Biomol Screen 2003; 8(4) 381–392.
37. Rouleau N, Turcotte S, Mondou M-H, et al. Development of a vesatileplatform for nuclear receptor screening using AlphaScreen™. J Biomol Screen 2003; 8:191–197.
38. Cunningham BT, Laing L. Microplate-based label-free detection of biomolecular interactions: Applications in proteomics. Expert Rev Proteomics 2006; 3(2):1–11.
39. Lamb P, Rosen J. Drug discovery using receptors that modulate gene expression. J Recept Signal Transduct Res 1997; 12:302–313.
40. Chin J, Adams AD, Bouffard A, et al. Miniaturization of cell-based β-lactamase-dependent FRET assays to ultra-high throughput formats to identify agonists of human liver X receptors. Assay Drug Dev Technol 2003; 1(6):777–787.
41. Martinez E, Hager GL. Development of assays for nuclear receptor modulators using fluorescently tagged proteins. Methods Enzymol 2006; 414:37–50.
42. Patel A, Murray J, McElwee-Whitmer S, et al. A combination of ultrahigh throughput PathHunter and cytokine secretion assays to identify glucocorticoid receptor agonists. Anal Biochem 2009; 385(2):286–292.
43. Bakker O, VanBeeren HC, Emrich T, et al. Interaction between nuclear hormone receptors and coactivators analyzed using a nonradiactve "puldown" assay. Anal Biochem 276:105–106.
44. Goodson ML, Farboud B, Privalsky ML. An improved high throughput protein–protein interaction assay for nuclear hormone receptors. Nucl Recept Signal 2007; 5:e002.
45. Murray AM, Kelly CD, Nussey SS, et al. Production of glutathione-coated microtiter plates for capturing recombinant glutathione S-transferase fusion proteins as antigens in immunoassays. J Immunol Methods 1998; 218:133–139.
46. Larson JC, Osburn DL, Schmitz K, et al. Peptide binding identifies an ERα conformation that generates selective activity in multiple in vitro assays. J Biomol Screen 2005; 10(6):590–598.
47. De S, Macara I, Lannigan DA. Novel biosensors for the detection of estrogen receptor ligands. J Steroid Biochem Mol Biol 2005; 96:235–244.
48. Awais M, Sato M, Umezawa Y. Optical probes to identify the glucocorticoid receptor ligands in living cells. Steroids 2007; 72:949–954.
49. Awais M, Sato M, Umezawa Y. Imaging of selective nuclear receptor modulator-induced conformational changes in the nuclear receptor to allow interaction with coactivator and corepressor proteins in living cells. Chembiochem 2007, 8(7):737–743.
50. Martinez AD, Dull AB, Beutler JA, et al. High-contnet fluorescenc-based screening for epigenetic modulators. Methods Enzymol 2006; 14:21–36.

8 Emerging Novel High-Throughput Screening Technologies for Cell-Based Assays

Ilona Kariv, Alexander A. Szewczak, Nathan W. Bays, Nadya Smotrov, and Christopher M. Moxham*

Department of Automated Lead Optimization, Merck Research Laboratories, Merck & Co., Boston, Massachusetts, U.S.A.

INTRODUCTION

This chapter reviews advantages and shortcomings of cell-based assays for high-throughput screening (HTS) and identifies emerging trends in information-rich cell-based formats with throughput comparable to traditional cell-free biochemical screens. During the last decade, HTS has become an integrated part of the drug discovery engine for lead identification. Technological advances in assay miniaturization now enable screens in excess of one million member compound libraries in a short period of time, thus producing multiple starting points for medicinal chemistry (1,2). Because many active molecules can be identified quickly during primary HTS campaigns, hit assessment and prioritization of the target-specific chemical entities becomes a next critical step. The major challenge during lead optimization is to generate quantitative and predictive results to yield high-quality leads. The increasing sophistication of compound testing in biologically relevant cell-based assays encompassing complex functional systems enhances the probability of success by aligning in vitro and in vivo assessment of compound activity. A recent survey of 58 HTS laboratories and 34 suppliers reported that cell-based screens comprise on average 50% of all the assays currently utilized in support of drug discovery (3).

Traditionally HTS platforms utilize immortalized and/or genetically engineered cell lines to ensure assay reproducibility and to ensure a ready and rapid supply of cells to conduct the HTS. However, under these conditions, the cellular context may be inappropriate (i.e., the interaction of the targeted protein with other critical players within the interrogated pathway might be affected by the nonphysiologic protein expression levels in genetically engineered cell lines) and subsequently the results from the small molecule screen might be misinterpreted. An example of a cellular surrogate disease model might include a specific mutation, deletion, or gene amplification associated with a cancer cell phenotype, such as ras-activating mutations, or mutations causing inactivation of p53. The resulting phenotype represents a lack of normal cell cycle regulation and resistance to apoptosis (4). Another example illustrates the use of in vitro biological selection for a transformed phenotype in response to either direct target modulation

Current affiliation: Department of Lead Generation/Lead Optimization, Eli Lilly and Co., Indianapolis, Indiana, U.S.A.

or in tandem with a cotransfected helper gene to probe chemogenomic space (5). More recently complimentary RNAi screening, where in theory one specifically modulates the expression of the targeted protein, has become a powerful tool for the validation of cellular models (6–8). Profiling of small molecules against a broad panel of genetically engineered cell lines provides another useful approach in identifying preferentially sensitive cells. Recent publications highlight advantages of systematically linking information from extended panels of different cell-line responses with powerful data analysis methods (9–10). With the improvement in software and hardware tools allowing the use of smaller number of cells to statistically quantify cellular transformation and differentiation processes, one might envision extending these techniques to probe primary or stem-cell–derived cell populations (11–13).

There are many technical and practical considerations in implementing cell-based assays. Technical considerations in setting up cell-based assays include sufficient cell density required to generate a detectable signal without inducing cell death due to cell culture overcrowding, efficient cell dispensing of high numbers of cells in a relatively small volume without inducing cellular stress responses, media evaporation control during assay plate incubation, concentration of the organic solvent used for compound dissolution, and many others. Although successful assay adaptation required to achieve ultrahigh throughput has been demonstrated for many cell-free assays, only limited numbers of the cell-based assays formats have been successfully miniaturized (1,2,14–16).

Traditionally, cell surface receptors provide excellent targets for cell-based primary screens because their extracellular ligand binding pockets preclude the need for cell permeability, and agonist/antagonist binding to cell surface receptors has been extensively utilized in HTS formats and remains useful today. This review will primarily focus on novel functional assays including second-generation reporter screening assays, high-content screening (HCS) imaging platforms, recent advancements in G-protein–coupled receptor (GPCR), and ion channel cell-based functional assays, multiparametric apoptosis quantification, emerging technologies to evaluate protein–protein interactions, cell–cell interactions, and other selective cell-based biochemical, binding, and morphological screens. As we continue to understand that the biological systems, which we wish to interrogate, are far more complex than first imagined, these recent advances in HTS technology help scientists probe the interface between chemical and target/pathway space. For example, several research publications emphasize development of HCS technologies as the most innovative approach to bridge functional responses at the molecular target level with the regulation of other proteins in pathways or networks within the cell. HCS uses cellular imaging assays to extract multiparameter data quantifying biological processes within cells (17,18). This powerful technique allows the simultaneous measurement of multiple biologically relevant parameters, including receptor internalization, protein trafficking, cell cycle status, cellular morphology, cellular toxicity, protein expression levels, phosphorylation states, apoptotic responses, cellular differentiation, and many other properties (4,19,20). Broadly speaking, the major advantage of high-content assays is that they provide a wealth of biological information within a relevant cellular context. It is also important to emphasize that any effort to provide a comprehensive overview of all emerging technologies will be ultimately incomplete due to the rapid innovation pace in this field.

VIABILITY ASSAYS

Viability assays have been extensively applied to discover compounds with novel anticancer activity (4,20) and to identify agents with cytotoxic off-target effect as a follow-up strategy (14). There are a number of assays that can be utilized in the HTS setting to quantify multiple biochemical and morphological changes associated with apoptosis and necrosis processes. Traditionally, in vitro cytotoxicity assays relied on either the extent of the cellular contents as evidenced by the crystal violet or sulphorodamine B staining (21,22), or the measurement of cellular mitochondria metabolic function by using reduction of the tetrazolium salts. The result is the generation of intensely colored formazan dyes, which can be readily quantified using homogenous assay formats (23,24). More sensitive approaches to quantify mitochondria functional status and thereby cellular toxicity and viability measure the levels of ATP and ATP:ADP ratios and have been developed as a reliable predictor of cell viability (22). More recent study of mitochondrial function using nonchemical quantification of oxygen levels by phosphorescent oxygen-sensitive probes demonstrated that this direct measurement of the electron transport chain can be adapted to HTS (25).

A different marker of cell viability has been to measure apoptotic changes within cells. A hallmark characteristic of the apoptotic process is induction of caspase (cysteine aspartate–specific proteases)-mediated proteolytic activity in response to either the activation of death receptor signaling or the release of the apoptosis-inducing factors from mitochondria, such as cytochrome *c* (20,26). An advantage of using caspase activity as a specific apoptotic marker is that it is one of the earliest responses during apoptosis and is required for multiple subsequent events. One such caspase-mediated downstream effect is an increased exposure of phosphatidylserine to the outer membrane caused by membrane flipping. The increase in phosphatidylserine on the cell surface is detected by measuring annexinV binding. Activation of caspases is an irreversible event because proteolytically digested molecules can be only replaced by de novo synthesis. Elucidation of this apoptotic mechanism lead to the development of novel cell-permeable fluorogenic caspase substrates to measure caspase activity, primarily focusing on caspase-3, as an indication of the induction of apoptosis (11,27). These probes consist of a peptide containing a consensus cleavage sequence conjugated to rhodamine 110 (R110), which becomes fluorescent upon caspase-mediated cleavage. Low fluorescence of the uncleaved probe and the longer excitation and emission wavelength of R110 allow for easy adaptation to HTS (28).

A limitation of the apoptosis detection assays described above is that the majority of these assays are limited to a single biochemical factor. A recent trend in studying apoptosis is to associate these biochemical parameters with morphological changes by using HCS measurements. Examples of apoptotic markers including cytoplasmic condensation, nuclear fragmentation, and formation of apoptotic bodies are further described in this chapter. The ability to implement extensive HTS data handling algorithms to measure cellular morphological changes and cell cycle arrest in conjunction with cellular biochemical modifications has enabled the elucidation of mechanistic target-specific effects in the context of complex cellular changes empirically associated with anti-cancer activity.

CELL-BASED BIOCHEMICAL ASSAYS

Well-defined enzymatic assays are advantageous as primary screens in identifying and characterizing target-specific modulators. However, determining activity in the whole-cell system is important to confirm specific target engagement in a physiologically relevant environment. Direct quantification of proximal signaling events can serve as a specific biomarker of target function. The most commonly used read-out is kinase-mediated autophosphorylation and/or phosphorylation of the immediate downstream cellular substrates. The utility of monitoring the degree of phosphorylation to identify small-molecule inhibitors has been reported for the mTOR signaling network (29) and for the Checkpoint kinase 1 (ChK1) (30) using different immunostaining procedures. Dickey et al. have demonstrated that measuring levels of MARK-specific tau phosphorylation in the whole cell by using the In-Cell® western platform (Li-Cor, Lincoln, NB) provides more sensitive measurements compared to traditional Western blots (31). An advantage of this detection platform is its capability to quantify signal in the infrared wavelength range ($\lambda em = 680$ and 800 nm), thus overcoming fluorescence quenching by cellular components. Furthermore, we have validated In-Cell® western technology in an HTS format as a critical compound-filtering assay (32).

To expand our repertoire of cell-based measures of kinase signaling, we have employed an additional HTS platform for the identification of inhibitors of cellular phosphorylation by using a homogenous assay based on the amplified luminescence proximity homogenous assay (Alpha Screen®) technology offered by PerkinElmer (Waltham, MA). A major advantage of AlphaScreen® is that it is a nonradioactive and homogeneous proximity assay. Solution binding of bead-captured analyte molecules leads to energy transfer from one bead to another. Upon laser activation of photosensitizers present in the donor bead, ambient oxygen becomes singlet state oxygen, which can diffuse up to 200 nm and react with redox-sensitive fluorophores in the acceptor bead. This reaction of donor bead–generated singlet oxygen with the redox-sensitive acceptor bead produces a luminescence signal ($\lambda ex = 520$–620 nm). If the donor and acceptor beads are separated by a distance greater than 200 nm, the singlet state oxygen is not able to reach the acceptor bead, and no signal is generated. The high sensitivity observed in AlphaScreen® is because the donor bead may carry up to a few thousand streptavidin molecules, and a single protein A–coated acceptor bead can bind up to a few hundred antibodies. Therefore, the binding signal is dependent not only on the binding affinity of one pair of interacting partners, but also on the cooperative avidity of hundreds of molecules. Because of its homogenous format, AlphaScreen® can be easily automated and miniaturized for uHTS applications. AlphaScreen® is also highly versatile due to the availability of a wide range of compatible antibodies. Validation using AlphaScreen® technology with cell lysates has been reported for discovery of inhibitors of endogenous JNK kinase activity (33).

In our laboratories, we have utilized AlphaScreen® technology to develop a novel cell-based assay to measure in situ c-Met tyrosine phosphorylation in GTL-16 cells, a human gastric tumor cell line reported to possess abnormally high c-Met protein kinase activity (34–36). In this assay, AlphaScreen® streptavidin-coated donor beads were combined with biotinylated anti–c-Met antibodies to capture total c-Met, while acceptor beads coated with an

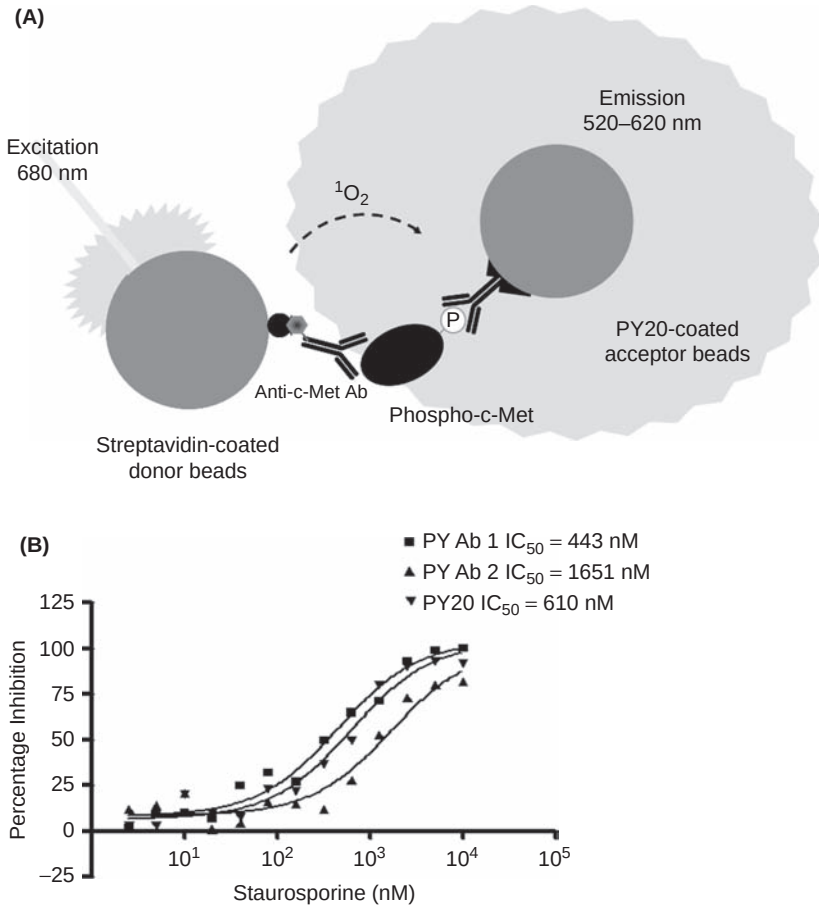

FIGURE 1 In situ analysis of c-Met phosphorylation. (**A**) Schematic representation of detection of global c-Met phosphorylation using AlphaScreen® technology. Streptavidin-coated AlphaScreen® donor beads are used to capture biotinylated anti–c-Met antibody bound to c-Met protein obtained from cell lysates. Detection of phosphorylated residues on c-Met is accomplished by using the anti-phosphotyrosine pan antibody PY20 captured by protein A–coated acceptor beads. (**B**) Potency determination of Staurosporine treatment. Cells were treated with the pan-kinase inhibitor, Staurosporine, at increasing concentrations, starting from 0.2 nM. Total c-Met phosphorylation was assayed by using pan-PY20 antibody, and specific phosphorylation events were quantified with specific Abs. All dose–response curves were plotted using calculated % inhibition versus inhibitor concentration. % Inhibition was calculated as % INH = (average of positive control − average of sample)/(average of positive control − average of negative control) × 100. IC_{50} values for inhibitors were determined from four-parameter curve fitting by GraphPad Prism software.

anti-phosphotyrosine antibody PY20 (37) were used to detect phosphorylated c-Met [Fig. 1(A)]. The assay was miniaturized to a 384-well format with excellent performance as demonstrated by a signal-to-background ratio of 15 and Z′ value (38) of 0.8. In addition, we took advantage of the availability of antibodies recognizing different autophosphorylation sites on c-Met and extended this application to quantify site-specific receptor tyrosine autophosphorylation. To do

so, the original assay was modified by substituting the PY20 antibody with site-specific antibodies, PYAb1 or PYAb2, bound to the protein-A coated acceptor beads. In the site-specific phosphorylation assay, the donor bead configuration remained the same with identical streptavidin-coated beads capturing the same biotinylated anti–c-Met antibody. Protein A–coated acceptor beads also remained the same, differing only in the antibody captured by the acceptor beads. To simplify assay development and allow comparison with the global phosphorylation assay using PY20, we used the same cell lysis conditions, bead concentrations, and anti–c-Met antibody concentrations as the PY20 assay. Both the global and site-specific c-Met phosphorylation assays were evaluated for their ability to determine compound potency. Figure 1 illustrates representative IC_{50} value determinations for Staurosporine, a nonselective pan-kinase inhibitor. In all three assays, Staurosporine displayed dose-dependent inhibition of the different c-Met autophosphorylation sites.

Additional application of this technology was demonstrated for elucidation of the functional GPCR-mediated response. GPCRs have been shown to activate numerous kinase pathways including the canonical ERK pathway. Using AlphaScreen® technology as its foundation, TRG Biosciences (Thebarton, Australia) has recently introduced an assay kit that allows one to screen for ERK activation as a measure of GPCR function in both cells overexpressing and those expressing endogenous levels of receptor. In contrast to traditional approaches using Western blotting to measure ERK activation, which are extremely low throughput and time-consuming, the Surefire™ assays are homogeneous and thus are highly amenable to HTS and can be miniaturized to 1536 well format if the signal window is sufficiently robust. As with other technologies, one can measure the full spectrum of functional modalities with either adherent or suspension cells.

REPORTER GENE ASSAYS

Different reporter gene models have been characterized for use in a multitude of HTS applications during the last decade, including luciferase, β-lactamase, aequorin, alkaline phosphatase (AP), secreted AP (SEAP), and other read-outs (15,39–43). Because of the maturity of the reporter gene technology, these assays are also widely used as follow-up functional models for primary biochemical screens.

The firefly luciferase is chosen for many screens as a reporter enzyme of choice due to the high-detection sensitivity and selectivity ($\lambda em = 510$ nm) as well as the amplification provided by the luciferase-mediated enzymatic reaction. The luminescence signal is generated by the light produced from the ATP and Mg^{2+}-dependent cleavage of the luciferin substrate. In addition, different systems have been recently described that lead to significant signal amplification and production of steady light or "glow." Other luciferase reporter genes can also be utilized, including the enzyme cloned from *Renilla reniformis* ($\lambda em = 480$ nm), which is ATP and Mg^{2+}-independent for dual glow signal in the same cell. However, the use of the latter luciferase gene is limited by its short half-life. The disadvantage of the luciferase reporter assay is that signal generation requires cell lysis, and therefore is not amenable for continuous kinetics studies.

Taking advantage of the above-described properties of the luciferase reporter assay, we have previously demonstrated a successful miniaturization of an assay in 1536-well plate format using total volume of 3 μL/well for

identification inhibitors of the NFκB pathway (14). This system utilizes a human T cell line transfected with the luciferase reporter gene under the control of the promoter of the gene of interest. In another example, an interesting modification of the luciferase gene reporter assay was recently adapted for screening of ubiquitin-proteosome pathway inhibitors by expressing a ubiquitin-luciferase construct (44). Moreover, the use of a luciferase reporter has been extended to the 3D cultures critical to assess Hepatitis C virus (HCV) infection efficiency in complex 3D aggregate models of human tissue (45). In this model, quantitative measurement of dual-luciferase reporter gene activity was normalized to the total DNA content as evaluated by Hoechst 33258 dye in the same lysates.

The β-lactamase reporter gene is also widely used in HTS format. Several commercially available β-lactamase substrates, cleaved by the enzyme to produce either fluorescent or chemiluminescent products, generate a reasonable signal and are adaptable to a miniaturized format. A β-lactamase fluorogenic substrate has been described for use in live cell kinetic studies, applying Förster resonance energy transfer (FRET) technology (46). Recent development of β-lactamase expression using FRET principals significantly improves quantitation of this measurement. In this system, β-lactamase cleaves the CCF2 substrate labeled with coumarin and flourescein, or similar fluorophore pair, on the N- and C-terminus, respectively, thus disrupting energy transfer. This technology was utilized for the identification of signal transduction pathway utilized by orphan GPCRs (47). Another demonstration of the FRET format was a report to identify inhibitors of the oncogenic transcription factor AP-1 in stably transfected CEllSensor AP-1-bla HEK293T cell line (Invitrogen, Carlsbad, CA) (48).

A well-designed study by Coppola et al. demonstrated the use of secreted alkaline phosphatase for noninvasive cellular measurements for Golgi-resident protease activity (49). In this work, a fused reporter gene construct consisting of SEAP, a Golgi specific recognition and cleavage site, and the cytoplasmic and transmembrane domain of a β-site precursor protein (APP)-cleaving enzyme (BACE), is retained in the trans-Golgi network until it is cleaved by a specific protease. Protease-mediated cleavage releases SEAP into the supernatant where measurement of protease activity occurs in real time.

Green fluorescent protein (GFP) and a multitude of GFP derivatives are alternatives for noncatalytic fluorescent reporters (42,50) (Invitrogen). This system allows noninvasive tagging and monitoring of cellular proteins. Because miniaturization of these assays requires a high level of GFP expression, the choice of gene promoter is limited to strong viral promoters such as SV40 or CMV, and the technology is usually less suitable for "native" mammalian promoters. However, because expression of fluorescent proteins can be directly monitored in intact cells, the utility to different assay read-outs can be extended to novel applications. An elegant approach taking advantage of the unusual feature of some fluorescent proteins that contain an alternate reading frame lacking stop codons was employed to elucidate alternative splicing mechanisms (51). In this screen, the ratio between two different reporter genes, enhanced GFP (EGFP), and dsRED, expressed from the same reporter allowed quantification of the alternative splicing that resulted in different protein expression.

These examples clearly emphasize that reporter gene assays will continue to be utilized for the screening of multiple biological functions. False positive hits due to interference with enzymatic activity and/or nonspecific inhibitors of

transcriptional/translational machinery can be easily identified in the appropriate counter screens. Examples of more recent applications of reporter gene platforms for the elucidation of protein–protein interactions are further discussed in this review.

IN SITU PROTEIN–PROTEIN INTERACTION ASSAYS

Physical interactions between proteins drive the transduction of critical signals inside and outside all cells, but the predominant methods for the evaluation of these protein–protein interactions are in vitro biochemical assays (52). Only recently have satisfactory cell-based methods emerged to assay protein–protein interactions in cells. Examples of cell-based assays to study protein–protein interaction may include transcriptional reporters, "two-hybrid" assays, fluorescence/bioluminescence resonance energy transfer assays, "split" reporter (or protein fragment complementation) assays and the use of positional biosensors. Transcriptional reporter assays to monitor protein–protein interactions in a two-hybrid yeast model have the longest track record and have been extensively used for numerous applications, including interaction of mammalian proteins assayed in yeast strains (53–58). However, the following section will focus on recent innovations for quantifying protein–protein interactions in mammalian cells that would be amenable to the HTS format.

Cellular FRET Assays

FRET assays allow the direct measurement and even visualization of protein proximity by means of energy transfer between a fluorescent donor and fluorescent acceptor. Although FRET is readily accomplished in vitro by a wide range of small-molecule fluorophores including the highly useful suite of molecules capable of time-resolved fluorescence (59), the in vivo FRET repertoire is much more limited. Notable and useful exceptions to the use of small-molecule fluorophores in cells are cases where proteins of interest can be studied on the cell surface and/or these proteins are endocytosed. To date, the most popular FRET system in cells employs "enhanced" GFP variants from *Aequorea victoria*: cyan fluorescent protein (CFP) and yellow fluorescent protein (YFP) (60). The pair does meet the criteria for successful FRET: (*i*) overlap between CFP emission and YFP excitation spectra, (*ii*) acceptable quantum yield of CFP and YFP fluorophores, and (*iii*) ability to report proximities to ~10 nm in distance (61). Although CFP and YFP have been used extensively in FRET experiments, CFP/YFP is far from a perfect FRET pair. First, there is significant overlap between the emission spectra of CFP and YFP that is further complicated by a broad "two-peak" emission spectrum for CFP. The resulting crosstalk can confound results, including an accurate assessment of assay statistics for HTS. Second, CFP is not particularly bright (GFP is almost three times as bright as CFP; see Table 1 for spectral data). Third, GFP and its variants (CFP) can form dimers (albeit weakly), potentially affecting the interaction between proteins of interest in the FRET assay. Recent advances in FRET technology improve on these three weaknesses of CFP/YFP and expand the available toolbox for FRET assays.

The most abundant new FRET tools are new fluorescent proteins suitable for FRET. For example, replacement of CFP with cerulean fluorescent protein and YFP with venus fluorescent protein results in higher FRET efficiency (Table 1) and allows a 10% increase in distance between the interacting proteins of

TABLE 1 Spectral Properties of FRET Pairs in Cellular Protein–Protein Interaction Assays

FRET pair (donor/acceptor)	Donor		Acceptor		Quantum yield		Extinction coefficient (M^{-1} cm^{-1})		Brightness (QY × EC, mM^{-1} cm^{-1})		Ref.
	Ex	Em	Ex	Em	Donor	Acceptor	Donor	Acceptor	Donor	Acceptor	
BFP/GFP	383	447	488	507	0.2	0.6	13,500	56,000	2.7	34	60
EBFP2/GFP	383	448	488	507	0.56	0.6	32,000	56,000	18	34	60,67
CFP/YFP	433	475	514	527	0.4	0.6	32,500	83,400	13	51	60,140
Cerulean/Venus	433	475	515	528	0.62	0.57	43,000	92,200	27	53	62,141
CyPet/YPet	435	477	517	530	0.51	0.77	35,000	104,000	18	80	142
TealFP/YFP	462	492	514	527	0.85	0.6	64,000	83,400	54	51	63
miCyan/KOrange	472	495	548	559	0.9	0.6	27,200	51,600	24	31	64
GFP/TMP-Hex	488	507	535	556	0.6	0.9	56,000	96,000	34	86	60
GFP/Far Yellow	488	507	510	538	0.6	n/a	56,000	n/a	34	n/a	60,68

interest (62). Another alternative to CFP itself is a monomeric teal fluorescent protein (mTFP1) with improved brightness, sharper emission peak, and high photostability (63). To illustrate FRET proof-of-concept for mTFP1, Ai et al. used mTFP1 as the donor and YFP as acceptor in a Ca^{2+}-sensing FRET reporter (63). In this application, mTFP1 showed higher FRET efficiency than that of CFP or cerulean fluorescent protein. Another FRET pair of interest is represented by the Midori cyan (miCy) and Kusabira orange (KO) fluorescent proteins (64). miCy has a higher quantum yield and a more narrow emission peak compared to CFP (although miCy still exhibits significant emission overlap with KO). Both miCy and KO are available in monomeric form. The fluorescence of both proteins is fairly insensitive to pH, unlike CFP (acid-sensitive quantum yield) and YFP (acid-sensitive extinction coefficient), making this pair suitable for use in acidic organelles such as lysosomes.

Although GFP from *A. victoria* pioneered the now vast family of fluorescent proteins, it still resides convincingly in the top tier of fluorescent proteins with high brightness and photostability. GFP has also been successfully expressed as a fusion partner with tens of thousands of proteins, and many of these fusions have been characterized extensively (65). It is therefore not surprising that researchers have long sought to construct FRET assays using GFP as either a FRET acceptor or donor to take advantage of existing GFP fusions. Unfortunately, GFP-compatible FRET partners with robust fluorescence properties have proven elusive. Blue fluorescent protein (BFP), discovered soon after GFP, has an appropriate spectral overlap to be a FRET donor to a GFP FRET acceptor, but BFP is very dim and subject to rapid photobleaching (60). Azurite and EGFP are alternatives to BFP that are much brighter and more photostable (66,67). All of these blue fluorescent proteins require excitation at ~380 nm, a region where compound interference can be substantial. Acceptable GFP-compatible FRET acceptors are also rare, but some notable candidates have emerged, including a far-yellow fluorescent protein displaying ideal overlap of its excitation spectrum with GFP emission spectrum (68).

An alternate strategy to take advantage of GFP as a FRET donor is to simply forego the use of a fluorescent protein acceptor entirely in favor of small molecules like hexachlorofluorescein (HEX) or rhodamine with superior fluorescent properties. To accomplish this for intracellular proteins, a fusion partner like dihydrofolate reductase (DHFR) can be used. DHFR fusions take advantage of the observation that the competitive DHFR inhibitor trimethoprim (TMP) exhibits >1000-fold higher affinity for DHFR from *Escherichia coli* (eDHFR) than DHFR from mammals (mDHFR) (69). A consequence of this differential affinity is that when eDHFR is expressed in mammalian cells, nanomolar concentrations of trimethoprim bind efficiently to eDHFR while leaving mammalian DHFR active. This is useful in protein labeling because trimethoprim can be fused to fluorescent molecules like hexachlorofluoroscein (HEX) to form a high-affinity fluorescent eDHFR ligand (69). In FRET experiments, this allows the use of GFP and TMP-HEX as a FRET pair with ideal spectral properties including red-shifted fluorescence spectra more suitable for compound library screening. Additionally, control experiments (including assessment of crosstalk) can be easily performed with the same cells prior to and after the addition of TMP-HEX.

Clearly, the number of FRET acceptor and donor options is growing. What is not so clear is which new FRET combinations will prove to be the most

useful in HTS applications. Therefore, judicious experimentation with several options will likely be required in order to develop the most robust HTS assays—especially with more challenging protein targets. It is also important to note that just as important options for FRET reagents have grown in number, so have options in instrumentation capable of reading FRET in cells. Standard PMT- and CCD-based plate readers used in HTS can accommodate many FRET pairs with little difficulty, although alternative excitation options (laser or LED) may offer additional opportunities to obtain signal from difficult targets (those with transient interactions, low expression, etc.). One drawback in using standard plate readers to measure cell FRET assays is that any cell-to-cell heterogeneity of expression in either FRET acceptor or donor can create false positives or false negatives if this heterogeneity is not known or well understood. Automated microscope-based or laser-scanning imagers can be valuable in avoiding these problems.

A laser-scanning plate reader is available with the capability to measure anisotropy in cells (IsoCyte, Blueshift Biotechnologies, Sunnyvale, CA). Because anisotropy decreases as FRET increases, anisotropy measurement provides an alternate read-out for FRET distinct from fluorescence intensity. Using anisotropy to measure FRET should be highly useful in discriminating actual FRET from the myriad of possible artifacts. Anisotropy is especially useful in HTS as compound interference is often reduced due to the ratiometric read-out.

Bioluminescence resonance energy transfer (BRET) assays comprise especially useful variant of FRET assays for HTS applications. In BRET, a luminescent protein is used as the donor in the BRET pair rather than the fluorescent protein used in FRET. This is a significant advantage for HTS assays as no excitation light is required—eliminating problems with donor photobleaching, cell autofluorescence, phototoxicity, and perhaps most importantly, compound interference. By far, the most common BRET pair employs firefly luciferase as the BRET donor and GFP as the BRET acceptor, and the use of these two robust reporters generates high signal:background ratios in BRET assays (70). BRET assays are also amenable to HTS automation and standard HTS detection systems. In fact, BRET has been successfully used in a number of HTS screens for a wide array of drug targets (5,71–74). Previously, BRET had not been amenable to cell imaging assays due to low sensitivity in these detection systems. Advances in imaging technology have lowered this barrier and now allow imaging read-outs of BRET assays (75).

Split "Reporter Assays

"Split" reporters are the most recent addition to cell assays for protein–protein interaction, and the addition is quite welcome as these assays combine key strengths of both the two-hybrid and FRET assays while overcoming several of their fundamental weaknesses. Split reporters are enzymes or fluorescent proteins that can be "split apart" and expressed as two (or more) separate, nonfunctional polypeptides that can then later re-associate to form a functional protein. For protein–protein interaction assays, it is critical that each fragment of the split reporter have very little or no affinity for each other so that the re-association to form a functional reporter is driven not by the fragments of the reporter

itself but by the binding of target proteins expressed as fusions to the reporter fragments (76).

Split reporter assays employing split enzymes, also called protein fragment complementation assays (PCA), are ideally suited for HTS as they can use robust HTS-friendly enzyme reporters. Available split enzymes include luciferase (from firefly, *Gaussia princeps*, or *Renilla* species.) β-galactosidase, β-lactamase, and dihydrofolate reductase (77–81). These split enzymes allow an amplification of signal and thus a potentially large signal-to-background ratio. This is important for HTS assays that seek to monitor disruption of protein–protein interaction, as these are loss-of-signal assays in a split reporter context. Because the split reporters are already pre-formed in the cell at the start of the assay, their association and dissociation can be reliably monitored in minute timescales (81).

A broad spectrum of split fluorescent proteins is also available, including a robust split-GFP reporter (82). This bi-fragment complementation (BiFC) approach has been successfully used to study the interactions of diverse proteins including ion channels, GPCRs, kinases, phosphatases, and cystokeletal proteins including Tau (76,83,84). BiFC is especially well suited for spatiotemporal analysis of protein–protein interaction as the pre-formed pool of fluorescent protein fragments can be monitored in real time for changes in protein association/dissociation (85). Thus, even sophisticated kinetic studies of protein–protein interactions enter the realm of compound screening feasibility.

Protein–Protein Interaction Biosensors (PPIB)

The PPIB approach currently offered by Cellumen (Pittsburgh, PA) allows one to monitor protein–protein interactions within cells at HTS scale and offers significant advantages over FRET-based and protein complementation–based approaches. At the technical level, the PPIB approach exploits the proven effectiveness of well-characterized fluorescent proteins to act as reporters in whole-cell imaging assays, the availability of routine high-content imaging capabilities to quantify the nuclear/cytoplasmic intensity ratios, and the ability to direct protein expression to specific subcellular compartments. Schematically, the PPIB is comprised of two components—a nuclear anchored component and a nuclear-cytoplasmic shuttling component [Fig. 2(A)]. Each of the components contains three fundamental elements to be expressed as a fusion protein within the cell. First is the protein of interest, which can either encompass the full-length protein or simply the putative binding domain. Second is the reporter, shown here as GFP and RFP, which is intended to monitor the subcellular location of each of the biosensors. Lastly, each of the components is engineered with specific localization sequences to effectively anchor one of the PPIBs in the nucleolus via the use of a nuclear localization sequence (NLS) and to allow the other PPIB to shuttle between the cytoplasm and nucleolus via incorporation of an NLS and a nuclear export sequence (NES) in tandem. PPIB activity is determined by measuring the ratio of fluorescence associated with the shuttling component of the biosensor between the cytoplasm/nucleus. Figure 2(B) demonstrates how the PPIB concept has been applied to monitor the interaction between p53 and HDM2. When both the nuclear anchored p53 component and the HDM2 shuttling component are coexpressed in the untreated state, the two proteins interact and the cytoplasmic/nucleus fluorescence intensity ratio for the shuttling component is $\ll 1$.

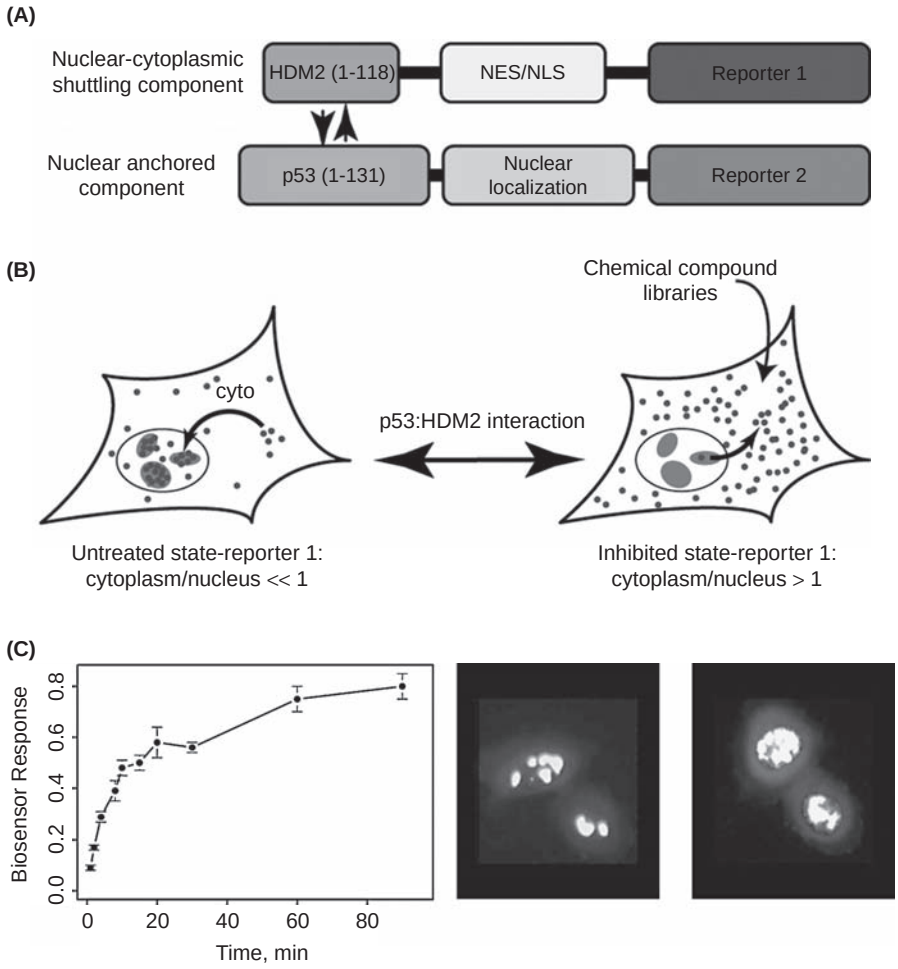

FIGURE 2 Dual color p53:HDM2 protein–protein interaction biosensor. (**A**) Schematic representation of the p53-Hdm2 PPIB 2-construct design. (**B**) PPIB activity is measured by determining the ratio of fluorescence associated with the shuttling component of the biosensor (Hdm2) in the cytoplasm/nucleus. (**C**) Nutlin3 rapidly disrupts the interaction of p53 and Hdm2 observed as an increase in the ratio of cytoplasm/nuclear red fluorescence.

In the presence of an inhibitor such as Nutlin, the components no longer interact and the cytoplasmic/nucleus fluorescence intensity ratio for the shuttling vector is now >1. Representative data from such an experiment are shown in Figure 2(C). In the absence of Nutlin, there is clear colocalization of the two components in the nucleus. Incubation with 25 μM Nutlin results in a rapid and pronounced disruption of binding between p53 and HDM2 as demonstrated by the redistribution of the shuttling component to the cytoplasmic compartment.

The use of PPIBs to monitor protein–protein interactions within cells offers several advantages. The interaction between the two components is reversible, the intensity of the reporters is very bright such that one does not need to express supraphysiologic levels of each of the components in order to observe a signal, the interaction is driven by the binding affinity between the two proteins of interest and not the reporters, and the approach is amenable to HTS. It is also important to note that optimal biosensors would be competent with respect to binding, but otherwise biologically inactive. This allows one to strictly measure protein–protein interaction in the absence of other effects that may themselves confound the interpretation of the data.

ION CHANNELS

Cell-based assays are fundamental for screening ion channel functional activity. Ion channels are heteromultimeric protein complexes within the cell membrane lipid bilayer. They represent a functionally diverse protein class responsible for rapid flux of inorganic ions, such as Na^+, K^+, Ca^{2+}, and Cl^-, through the cellular membrane. These complexes consist of pore forming α-subunits, which contain the selectivity filter and gating apparatus, and auxillary subunits, which modulate these pore-forming proteins to assist trafficking and complex stability. Opening and closing of ion channels regulate multiple physiological cellular phenomena, including membrane potential, secretion and absorption of salt and water, and subsequent cell volume regulation, and many others. Ion channels have been widely explored as attractive targets for drug discovery and numerous modulators are currently on the market to treat different pathologies. However, ion channels have also been implicated in mechanism of action (MOA)-related cardiac toxicity. Several drugs have been withdrawn from the market due to cardiac QT interval prolongation, and in some cases caused life-threatening condition known as *torsade de pointes*, or ventricular arrhythmia (86–89).

Functionally, ion channels can be classified in two groups, ligand-dependent and voltage-gated channels. Screening assays have been developed to monitor both of these functions. Radioligand binding competition assays were extensively utilized in the early 1980s, and subsequently reformatted into scintillation proximity assays (SPA), allowing for a homogenous screening format. Although binding assays provide a direct measurement of drug binding, these assays do not characterize functional activity of these molecules, and thus are unable to distinguish between positive or negative modulators. Most indirect measurement assays monitor changes in the intracellular calcium concentration, which can be detected with Ca^{2+} sensitive dyes. The most commonly used are Fluo-3/4/5, Fura-2, and calcium green dyes in conjunction with a FLIPR detection reader (Molecular Devices, Sunnyvale, CA) (27,87–90). Another method to quantitate ion channel–mediated Ca^{2+} flux is to utilize aequorin as a bioprobe. The binding of calcium ions to aequorin induces a conformational change, resulting in the oxidation of coelenterazine and a fluorescent signal emission (91). Both methodologies require follow-up MOA studies to rule out calcium release from the intracellular stores and/or involvement of calcium transporters.

Voltage-sensing dyes are widely utilized in screening assays for modulators of the membrane potential. The first generation of these assays was based

on changes in fluorescence intensity of negatively charged oxanol when the dye is localized in the inner layer of the membrane (in contrast to the outside aqueous environment) during membrane depolarization. This is a slow responding probe with only limited sensitivity to voltage changes (92). The second-generation voltage-sensitive FRET assay incorporates an additional Coumarin-conjugated phospholipid probe, which acts as a FRET donor for Oxanol. FRET signal can be detected when both probes are colocalized at the outer membrane and are in spatial proximity. Upon membrane depolarization, Oxanol repositions to the inner membrane and the increased physical distance thereby precludes an efficient FRET signal generation (9,89). This method has an advantage of rapid temporal resolution as compared to Ca^{2+}-sensitive dyes, and the ratiometric calculation reduces potential artifacts. The voltage ion probe reader (VIPR), allowing for the kinetic measurement of the FRET signal, was introduced by Aurora Biosciences (presently Vertex, San Diego, CA). Additional modifications utilizing a FRET approach allowed for improvements in signal generation (86), for example pH-insensitive FRET voltage dyes were recently described for the acid-sensing ion channel family (93). Despite recent advancements, these approaches suffer from lack of sensitivity because of the nonlinear nature in the membrane potential change, and can therefore be hard to quantitate.

Patch-clamp real-time measurement is considered the gold standard evaluation of ion channel activity. Traditionally, activity of ion channels is directly evaluated by changes in the membrane potential, which is voltage-clamped through single glass micropipette electrodes. HTS assays have explored automating this time-consuming and tedious methodology. More recently, development of planar-patch multiaperture electrodes with miniaturized recording devices have permitted whole-cell recording. Furthermore, fabrication of the 2D format wells consisting of two chambers that are separated by a substrate, such as glass silicon or plastic polymer, allows separation of cells and formation of high-resistance seals. There are several patch-clamp instruments commercialized by Axon/Molecular Devices (Union City, CA). These include IonWorks Quattro, PatchXpress 7000A, and OpusXpress 6000A. The IonWorks Quattro workstation is suited for cell population patch-clamp technology and is recommended for use with directed compound libraries and secondary screening of hits from HTS assays. The PatchXpress 7000A records from up to 16 cells simultaneously using a giga-Ω seal. The system is supported by advanced analysis software and enables measurements from a wide variety of voltage-gated and ligand-gated ion channels. The OpusXpress 6000A workstation is an automated eight-channel voltage-clamp screening system for oocytes. The design of the OpusXpress 6000A system ensures recordings with high bandwidth from eight oocytes simultaneously. Although oocytes are widely used for electrophysiology, they also present an additional challenge to generate a uniform patch clamp due to their size. Several other patch-clamp automated devices are currently under development and should provide improvements over current technologies (86,88). Recent publications indicate that data generated from the automated systems correlates well with traditional patch-clamp technologies. However, at the current state these technologies still provide medium throughput at best (86) and additional improvements will be required to adapt patch-clamp measurements to HTS.

G-PROTEIN–COUPLED RECEPTORS

GPCRs comprise a large family of cell surface receptors characterized by the presence of seven transmembrane spanning domains. Their ligands include most neurotransmitters and hormones and thereby serve a critical role in normal physiology. As their name implies, these receptors utilize guanine nucleotide-binding proteins or G-proteins to transduce ligand-binding events into intracellular responses. The downstream effectors systems engaged by GPCRs are numerous and broadly include ion channels, enzymes that modulate second messengers (e.g., adenylyl cyclase), kinases, cytoskeletal proteins, and many other molecules involved in normal cellular function (94). Given their critical role in most physiologic systems, it is not surprising that aberrant or dysregulated GPCR function leads to disease.

Early drug discovery screening efforts directed at GPCRs were limited to ex vivo and in vivo responses in a few well-characterized organ systems including smooth muscle contraction/relaxation and ionotropic and chronotropic cardiovascular responses. With the advent of molecular biology, cloning and heterologous expression of specific GPCRs in various cell lines allowed screening to approach the level of molecular and cellular events such as radioligand binding and changes in classical second messengers like cAMP and $Ca^{2+}{}_i/IP_3$. Moreover, a range of modalities could be explored from agonism to antagonism including orthosteric and allosteric mechanisms. Over the last 10 to 15 years, technology gains have driven these types of assays (radioligand binding and second messengers) to the level of commodities for use in industry and academia. When coupled with robust liquid-handling automation for dispensing reagents and compounds and with high-throughput microplate readers, these assays offer ultrahigh-throughput capacity (i.e., >100,000 compounds screened per day). Many excellent reviews have been published on the available screening methodologies to measure GPCR-mediated changes in cAMP, intracellular calcium, and ion conductance (95,96). Names of the current technologies, vendor, and links to the vendor websites are provided in Table 2. The focus of this review is to discuss recent screening technologies that have emerged to complement the toolkit of assayists focused on GPCR drug discovery.

As mentioned above, GPCRs bind to and activate G-proteins by promoting the exchange of guanine nucleotides. In addition to G-proteins, GPCRs recruit another family of proteins called arrestins. They have now been shown to play a critical role in GPCR internalization and trafficking. They have been shown to play a key role in coupling GPCRs to activation of the ERK pathway via a G-protein independent mechanism (97). Recruitment of arrestins to GPCRs is induced by ligand binding much like activation of G-proteins. Thus, the hypothesis was conceived that if one could quantitatively measure arrestin recruitment in microplate formats, then one would have an additional assay platform to measure GPCR function in a cell-based environment. This type of approach would also be amenable to screening orphan GPCRs where the preferred G-protein coupling is unknown.

Today that concept has been reduced to practice. At least two major assay technologies have been exploited to introduce assays of this nature. The first involves the use of fluorescent protein tags in tandem with cellular imaging to quantitatively measure arrestin translocation to the cell surface in response to agonist occupancy of the receptor. The model system first employed by Oakley

TABLE 2 Current Technologies for Cell-Based GPCR Screening Assays

Pathway	Technology	HTS compatible	Vendor	Web link
cAMP	HTRF[a]	Y, 1536	CisBio	www.cisbio.com
	EFC[b]	Y, 3456	DiscoveRx	www.discoverx.com
	AlphaScreen®	Y, 1536	Perkin Elmer	www.perkinelmer.com
	CRE-β-Lactamase	Y, 3456	Invitrogen	www.invitrogen.com
$Ca^{2+}{}_i$	FLIPR[c]	Y, 1536	Molecular Devices	www.moleculardevices.com
	Aequorin	Y, 1536	Perkin Elmer	www.perkinelmer.com
Arrestin	Transfluor	Y, 384	Molecular Probes	www.molecularprobes.com
	EFC	Y, 1536	DiscoveRx	www.discoverx.com
Cell shape	Optical Biosensor	Y, 384	Corning	www.corning.com/epic
	CDS[d], Cell Key	N, 96	MDS Sciex	www.mdssciex.com
ERK	AlphaScreen®	Y, 384	TGR Bioscience	www.tgr-bioscience.com
			Perkin Elmer	www.perkinelmer.com

[a] Homogeneous time-resolved fluorescence.
[b] Enzyme fragment complimentation.
[c] Fluorescent imaging plate reader.
[d] Cellular dielectric spectroscopy.

and colleagues at Norak (now Xsira Pharmaceuticals Inc.) was the Transfluor™ technology, which utilized fluorescently labeled arrestins (98). In one assay prototype, they coexpressed β_2-adrenergic receptors with an arrestin–green fluorescent protein (GFP) fusion protein, and then quantified arrestin translocation in response to challenge with agonists by using the IN Cell Analyzer (GE Healthcare, Piscatway, NJ). In a second version of the assay, they coexpressed vasopressin V2 receptors with GFP-tagged arrestin and demonstrated robust signal to background ratios and $Z' > 0.5$. An additional advantage provided by the confocal imaging capabilities of the IN Cell 3000 Analyzer was the ability to distinguish arrestin distribution patterns and ascribe those patterns to high- and low-affinity binding for arrestin. For example, arrestin–GFP recruitment in response to challenge with a β_2-adrenergic receptors agonist resulted in localization of arrestin into clathrin-coated pits, whereas vasopressin promoted the localization of arrestin to vesicles. The pattern of staining pits versus vesicles is indicative of the affinity of the interaction between the GPCR and arrestin.

As a tool for high-throughput screening, the Transfluor™ assay has been adapted to GPCRs from all three major classes including biogenic amine (Type I), parathyroid hormone (Type II), and metabotropic glutamate receptors (Type III). The assay allows one to identify molecules displaying agonist, antagonist, or potentiator properties and yield similar rank order potencies when compared with other types of functional assays. It is also amenable to screening for ligands of orphan GPCRs (22,99). The assay can be miniaturized to 1536-well format and has been used with other confocal high-content imaging platforms including the Evotec Opera (100).

The second approach that utilizes arrestin recruitment as a means to identify ligands for GPCRs is the PathHunter™ assay platform from DiscoveRx (Fremont, CA). This assay platform exploits enzyme fragment complementation of β-galactosidase as a means to detect arrestin binding to ligand-activated GPCRs. One small fragment termed Prolink is fused to the GPCR of interest. A larger truncated portion of the enzyme is fused to arrestin. As separate fragments there is no enzyme activity; however, upon agonist binding to the GPCR and recruitment of arrestin, the ProLink label associates with the larger fragment of β-galactosidase that is fused to Arrestin and yields a large luminescenct signal. Like Transfluor, the PathHunter™ assay works with GPCRs from each major class. Additionally, the advantages of the PathHunter™ assay are that it is a homogeneous assay, can be run in 384- or 1536-well microplates, and because the read-out is luminescence, it requires only a standard microplate reader that is not as capital intensive an investment as the high-content imaging platforms currently in use. Thus, PathHunter™ serves as an excellent alternative to measure second messengers and is ideal if the G-protein coupling of the receptor is not known. Lastly, it also provides an avenue to identify GPCR ligands that promote activation of downstream pathways in a G-protein independent manner.

The two assay technologies described above require heterologous overexpression of the GPCR of interest in order to obtain a robust functional response that is suitable for HTS. It has long been recognized that receptor signaling properties can be altered with significant receptor overexpression. Therefore, technologies that allow one to measure GPCR function in native cells are desired.

As mentioned above, sometimes the identity of the G-protein that the receptor is coupled to is not known, which then confounds and/or precludes the use of standard assays that measure cAMP, for example, where knowledge of the G-protein coupling is paramount to configuring the assay appropriately. Recently, two label-free technologies, Epic™ from Corning and Cell Key™ from MDS Sciex, have emerged that allow to measure receptor function in native cells with endogenous levels of receptor expression without a precise knowledge of the G-protein subclass to which the receptor is coupled (see also chaps. 4 and 6 in this book). Both systems, while using different underlying detection technologies exploit the dynamic redistribution of cellular components (e.g., changes in cell shape and/or volume) as a means to screen for receptor ligands with the desired pharmacological properties.

The Epic™ system form Corning utilizes optical biosensor technology to report changes in cell-shape induced by receptor activation (101). Optical biosensors have been used in a wide array of applications toward measuring biomolecular interaction, but very recently the technology has been developed for cell-based screening approaches. The underlying principle of the Epic system is the formation of a biological layer of cells on the optical transducer. In contrast to other optical biosensor systems that use surface plasmon resonance, the Epic microplate utilizes a resonant waveguide grating (RWG) optical biosensor. The glass grating diffracts the light impinging on the waveguide film and the wavelength of the reflected light off the film is measured. In the cell-based application, cells adhere to the RWG after a brief period of culturing. The distance between the cell surface and the RWG is sufficiently close such that changes at the cell surface (e.g., receptor endocytosis, plasma membrane ruffling) induced by various stimuli, including GPCR activation, are capable of being detected as changes in the wavelength of the reflected light. Using A431 cells, Fang et al. have demonstrated the ability to detect Bradykinin-induced changes with the Epic system that were comparable in potency to those measured using standard technologies (e.g., FLIPR) (102). The approach has been extended to other receptor types and can detect multiple modalities including agonism, antagonism, and potentiation. The utility of this 384-well technology in screening includes hit identification, lead optimization, and characterizing the type of G-protein coupling utilized by a given receptor.

An alternative to the Epic system is the Cell Key from MDS Sciex. This is also a label-free technology that can distinguish G-protein coupling between G_s, G_i, and G_q-coupled receptors (103). Furthermore, the Cell Key system does offer the opportunity to measure responses in native cell types with endogenous levels of receptor expression under normal or disease contexts. Both adherent and suspension cells can be used with this system. The Cell Key system utilizes cellular dielectric spectroscopy to detect changes in transcellular currents. For example, GPCR ligands that induce cell flattening alter the transcellular current and the changes are recorded as alteration in cellular impedance to electrical currents. As with the Epic system, a unique kinetic signature is obtained depending on the type G-protein the receptor is coupling to mediate the response (104).

Representative data from a Cell Key experiment are shown in Figure 3. HEK cells transiently expressing the GPCR GPR105 with no additional G-protein coexpressed were allowed to adhere by culturing the cells overnight in the wells of the plates. After a challenge with a known agonist, a marked increase in

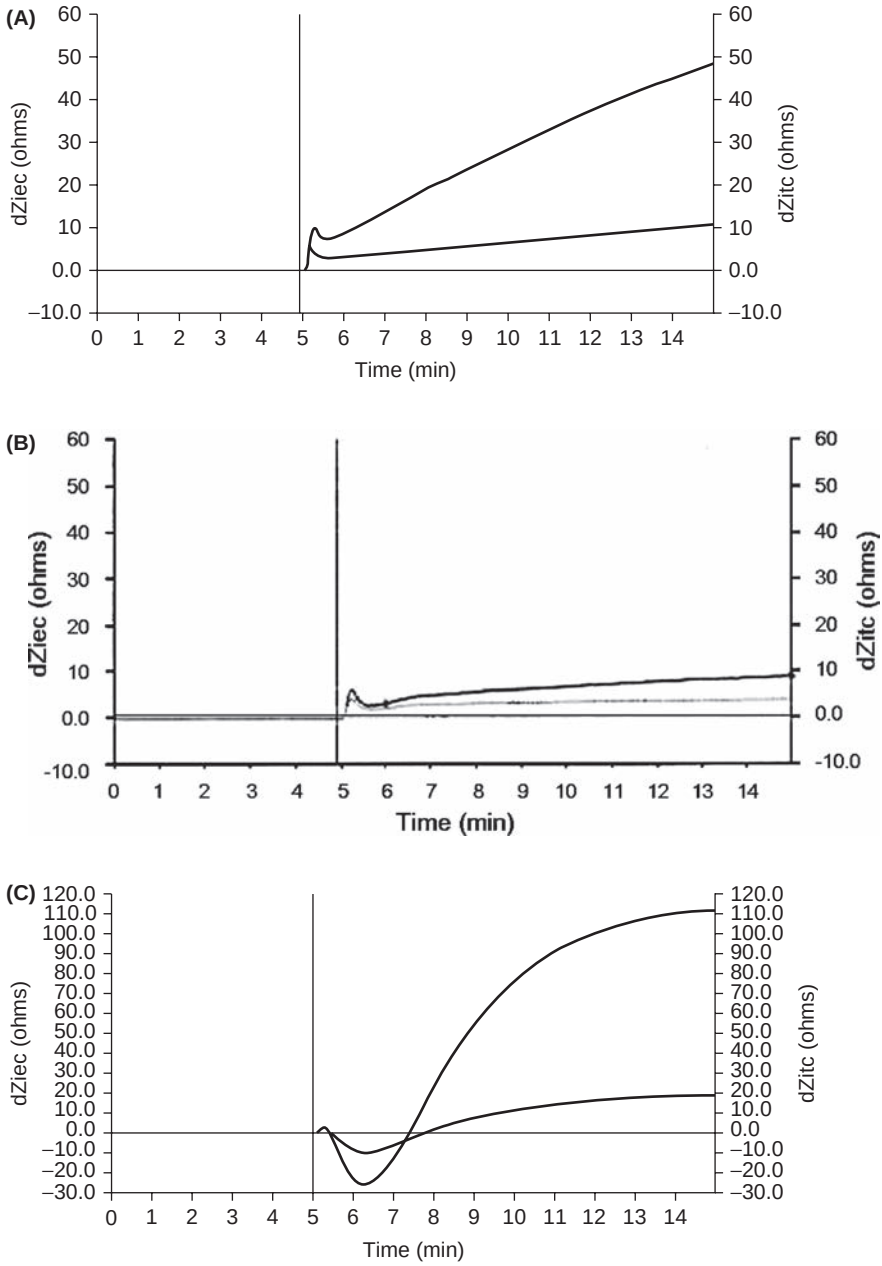

FIGURE 3 GPR105 displays agonist-induced G_i coupling using the Cell Key system. (**A**) HEK cells transiently expressing GPR105 were challenged with agonist (1 μM) and cell response was measured using the Cell Key system from MDS Sciex. The signature obtained is consistent with a G_i-mediated response. (**B**) HEK cells transfected with a control vector lacking GPR105 elicit no response to agonist. **(C)** HEK cells challenged with ADP to activate endogenous G_q-coupled purinergic receptors elicit a Cell Key signature distinct from the GPR105 response.

electrical impedance was observed. Moreover, the signature of the response, an initial sharp spike followed by a steadily increasing impedance was consistent with GPR105 coupling to pertussis toxin-sensitive G-protein from the G_i family. No such response was observed in HEK cells transfected with a control vector lacking the GPR105 cDNA. In addition, the signature elicited by GPR105 was shown to be distinct from that elicited by challenging the HEK cells with ADP, which results in activation of G_q-mediated pathways via purinergic receptors.

HIGH-CONTENT ASSAYS FOR HTS

In the last few years, there has been a dramatic increase in the use of imaging assays for target-based HCS of large numbers of small-molecule compounds or RNA reagents, as well as for toxicity profiling. This is due to the development of several key-enabling technologies. Major advances have occurred on four fronts. First, there has been development of improved labeling reagents for proteins and other cellular components. Second, sophisticated instrumentation for automated collection of multichannel images has been commercialized. Third, increasingly powerful software tools for cellular image analysis and quantification have been developed. Finally, new tools for managing and analyzing complex multivariate and population-based imaging data have become available. New developments in all these areas will be described in this section.

The term HCS is commonly applied to high-throughput and high-resolution imaging of cells growing in microtiter plates either directly on a plastic surface, on coatings such as poly-D lysine and collagen, or within a matrix (see also chaps. 3, 5, 10, and 14 in this book). Recent advances have also begun to allow the analysis of subcellular features within nonadherent cell populations (105). A typical HCS experiment consists of four basic steps: (*i*) Treatment of an appropriate cell line with compounds or RNA molecules; (*ii*) Treatment of the cells with permeabilizers, fixatives, dyes, antibodies, or other reagents required for visualization; (*iii*) Imaging of the cells; and (*iv*) Quantitative analysis. Advances in small molecule and RNA compound management and reagent delivery are outside the scope of this chapter, but recent key technological advances that enable the last three of these basic experimental steps are described below.

HCS Labeling Reagents

HCS assays commonly use multiple fluorescent dyes, which are chosen to allow simultaneous excitation and detection of separate fluorescent wavelengths. In most applications, a DNA-binding dye such a DAPI or Hoechst 33342 is used to stain cell nuclei, thus enabling the identification of individual cells. Cytoplasm and specific subcellular features such as actin filaments, mitochondria, or lysozomes are commonly detected with dye reagents such as rhodamine-phalloidin, MitoTracker, and LysoTracker reagents, respectively (Invitrogen—Molecular Probes, Carlsbad, CA). Specific proteins or phospho-proteins are stained with antibody reagents, either directly fluorescently tagged or employing an additional secondary antibody with a tag. Most common fluorescent tags are conventional organic molecules such at FITC, TRITC, or the Alexa family of dyes (106) (Invitrogen—Molecular Probes). In addition, a new type of biological fluorescent labeling using submicroscopic beads with semiconductor cores, that is "quantum dots" has also become available (107,108). This technology has

the advantage of providing multiple narrow emission spectra with one excitation wavelength, and the beads can be conjugated to streptavidin or antibodies (Invitrogen—Molecular Probes). Fluorescent tagging can also be done using genetically engineered proteins fused with various colored fluorescent protein tags (50), for which many vectors are available (Invitrogen). Indeed, large collections of reagents necessary to run many common HCS assays are now commercially available, either as entire prepackaged kits (Cellomics, Pittsburg PA), or individual validated reagents (BD Biosciences, San Jose CA; Invitrogen—Molecular Probes).

Imaging Hardware

High-quality HCS systems are available from several instrument manufacturers (see also chap. 6). These fluorescent imaging systems fall into three basic types: (*i*) automated conventional wide field microscopes using charge-coupled device (CCD) cameras, (*ii*) automated confocal multichannel fluorescent CCD microscopes, and (*iii*) laser scanning imagers (both confocal and nonconfocal). Standard wide field instruments suitable for HTS are available from several sources and the most widely used are the Array Scan (Cellomics Inc.), ImageXpress Micro (Molecular Devices, Downingtown, PA), IN Cell 1000 (GE Healthcare), and Pathway 435 (BD Biosciences). Wide field microscopes have the advantages of lower cost and resolution sufficient to image well-defined subcellular features, and several models have kinetic reading capabilities. Confocal microscope-based HCS systems include the lamp-based Pathway 855, an instrument with live cell kinetic capability (BD Biosciences) and the laser-based Opera (PerkinElmer, Waltham, MA) and IN Cell 3000 (GE Healthcare). The narrow depth of field achievable with a confocal system allows for the collection of relatively narrow slices through a sample, which can be later compressed into a single image, or reconstructed into a 3D image. Confocal imaging achieves the highest quality images, with lowest background fluorescence, allowing the resolution of very fine subcellular features. However, confocal imaging reduces signal intensities, thereby lengthening the amount of time necessary to collect each image. Use of laser illumination helps to overcome this limitation. Microscope systems, confocal or not, are best suited for HTS experiments with magnifications in the range of 4× to 60×, and as a consequence only sample a portion of the surface area in a microtiter plate.

Laser scanning imagers are now available in both relatively high-magnification confocal instruments, such as the Image Xpress Ultra (Molecular Devices, Downingtown, PA), and in lower magnification nonconfocal systems like the Accumen Explorer (TTP Labtech, Melbourn, U.K.). Low-magnification scanning instruments can image the contents of an entire plate. One recently developed full plate laser scanning instrument is the Isocyte (Blueshift BioTechnologies, Sunnyvale, CA), which, in addition to perform conventional fluorescent imaging, is capable of fluorescence polarization anisotropy measurements. Despite lower magnification, scanning systems such as the Accumen Explorer and Isocyte offer several advantages. Scanning is rapid, and entire 384- or 1536-well plates can be scanned in a few minutes, significantly faster than CCD camera–based image collection. In addition, complete scanning of each well in a microtiter plate is possible, allowing for data to be collected on relatively large populations of cells. Finally, the image depth of field is large, facilitating applications such as the quantification of 3D cultures growing within a matrix (109).

Image analysis on such systems is straightforward; individual cells are identified by nuclear or cytoplasmic staining, and signal intensities are measured in each channel. Subsequent analysis can then focus on calculating the average signal per well, or on threshold-based counting of "positive" cells, including gating based on multiple channels.

In our laboratory, we have used the laser scanning Blueshift Isocyte to develop a robust, rapid multiparametric assay for measuring mitosis, cell number, and apoptosis in high throughput on large numbers of plated cells

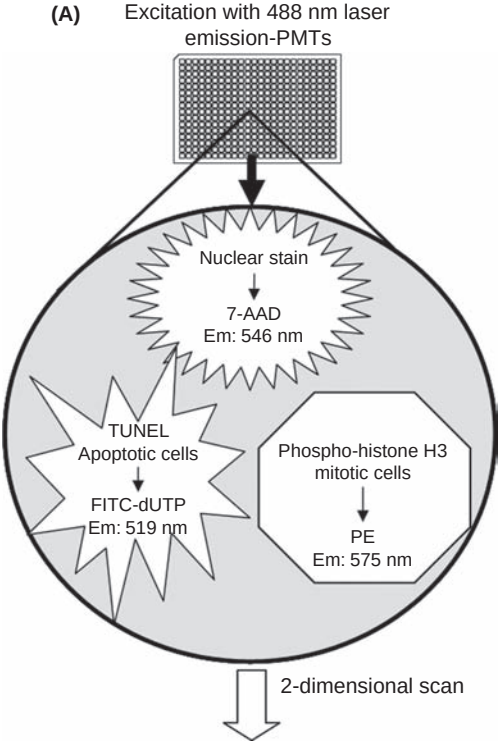

FIGURE 4 Analysis of mitosis and apoptosis by HCS. (**A**) Assay scheme for a three-color assay for mitosis and apoptosis using the Blueshift Isocyte. Cells are plated into a 384-well microtiter plate and allowed to adhere overnight. Compound is added the next day, and the cells are incubated for 24 hours. After compound treatment, the cells are fixed with 1% paraformaldehyde for 30 minutes at 4°C, then washed and permeabilized with 70% ethanol. After treating with TUNEL reagents (including FITC-dUTP) for one hour, the cells are blocked with 5% goat serum for one hour then incubated with a primary anti-phospho-histone H3 antibody for one hour. Following this, the cells are incubated with secondary phycoerythrin (PE)-tagged antibody and 7-aminoactinomycin D (7-AAD) nuclear stain for one hour. The experiment is then read on the Isocyte, using a 488 nm excitation wavelength and detection at 546 nm (7-AAD), 519 nm (FITC-dUTP), and 575 nm (PE). (**B**) Representative images collected on the Isocyte. (*Left column*) Nuclei stained with 7-AAD. (*Middle column*) Apoptosis detected by TUNEL staining. (*Right column*) Mitotic cells detected by phospho-histone H3 staining. Relative to the DMSO control, the mitotic block due to the taxol treatment is readily apparent, as is the simultaneous decrease in cell number and increase in apoptotic cells caused by Staurosporine treatment. (*Continued*)

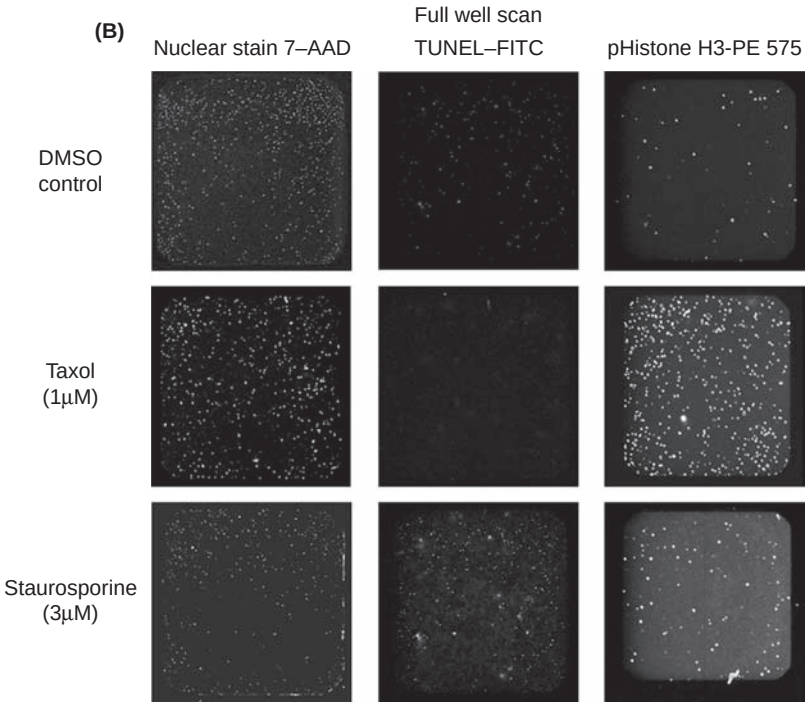

FIGURE 4 (*Continued*)

[Fig 4(A)] (110). As can be seen in Figure 4(B), the mitotic block caused by Taxol is easily observed, as is the apoptotic response stimulated by staurosporine treatment. The drop in cell number due to staurosporine treatment is also easily measured. Typical Z' values for this assay are in the range of 0.6 to 0.7, allowing the accurate measurement of IC_{50} values.

In general, increasing the information density of high-content experiments increases the rate of information output. Another way to accomplish this is to multiplex as many assays as possible. The CellCard system (Vitra Bioscience) is one approach to multiplexing high-content assays. It employs the use of a scanning imager and flat rectangular cell carriers that are "bar coded" with various colors. The system allows scanner-compatible high-content experiments such as TUNEL and proliferation to be run on as many as 10 cell lines simultaneously (111,112).

Image Analysis

Excellent image analysis software packages come bundled with the manufacturer's instruments. These software tools include numerous individual algorithms for analyzing cellular imaging data, many of which have been developed in the last few years (Table 3). The output of these algorithms are typically single numerical values calculated for each cell in a particular channel (wavelength), and then averaged to produce a single value per well, which

TABLE 3 Commercially Available HCS Algorithms

Morphology	Cell viability
Neurite outgrowth	Live/dead
Angiogenesis tube formation	Cell health
Morphology explorer	Micronucleus detection
Receptor internalization	Multiwavelength cell scoring
Transflour	Cell cycle
Granularity	Cell motility
Cell cycle	Multiparameter cytotoxicity
Mitotic index	Mitochondrial localization
Cell cycle	Translocation
Monopole detection	Membrane potential
Fatty acid uptake	Cell health
Cell scoring	Intracellular trafficking
Cell proliferation	Translocation
Count nuclei	Nuclear translocation
Cell proliferation	Compartmental analysis
Cell signaling	Spot detection
Cell health	Protein expression and modification &
Cell cycle	transient transfection
Translocation	Cell scoring
GPCR signaling	Multiwavelength cell scoring

Source: http://www.cellomics.com/content/menu/BioApplications/, http://www.moleculardevices.com/pages/software/metaexpress_modules.html.

can be followed as a function of drug treatment. More sophisticated analysis examines the distribution of intensities or morphological measurements. Some of the commonly available algorithms can be applied to measure nuclear and mitochondrial translocation, GPCR signaling, micronucleus formation, apoptosis, membrane potential, mitosis, DNA content, receptor internalization, kinase activation, fatty acid uptake, cell viability, neurite outgrowth, endothelial tube formation, to name just a few (Table 3). Most of these algorithms rely on some form of intensity thresholding, often used in combination with more sophisticated image analysis routines to help define regions of staining intensity. Many algorithms make use of a nuclear stain to identify individual cells and a cytoplasmic stain to demark cell bodies. As a result, nuclear versus cytoplasmic localization of signals is enabled and hence translocation can be measured. G-protein–coupled receptor signaling can be measured using the Transfluor β-arrestin–GFP translocation assay (98), but it requires the use of an engineered GFP-tagged form of β-arrestin and a cloned GPCR. Interaction of the β-arrestin and activated GPCR initiates the process of receptor internalization, which can be detected by the increase of punctuate GFP staining. A more comprehensive description of these experiments is provided in the GPCR section of this review. Coupled with high-throughput laser confocal high-content screening instrumentation, such assays support a broad platform for GPCR screening (100,113). Another interesting example of a protein redistribution assay is the p53:hdm2 GRIP interaction used to screen for inhibitors of the p53-hdm2 interaction (114). This system is based on the translocation of human cAMP phosphodiesterase PDE4A4 into foci within the cytoplasm. The Hdm2 protein is fused to the PDE4A4B isoform, which acts as an anchor protein. The p53 protein is fused to GFP.

Subsequent treatment with PDE4A4 redistribution agonist RS25344 causes localization PDE4A4 into foci, and recruitment of p53 by the Hdm2 in turn causes GFP labeling of the foci. With well-designed controls, the system could be used to study any two interacting proteins. Another HCS approach to study p53-Hdm2 interactions is illustrated in Figure 2 and described in PPIB section of this chapter.

Morphological measurements of cellular and nuclear shape, size, elongation, and other parameters can also be quantified by most image analysis software. Extracellular features such as neurites (115) and multicellular angiogenic tubules (116) can be measured in the appropriate cell lines. Recently, a novel tracing algorithm for the imaging of neurons that employs methods for segmentation, seed point detection, recursive center-line detection, and 2D curve smoothing has been described (117). Unlike conventional pixel-based methods, the new algorithm is fully automatic and does not require human intervention and is robust enough for poor-quality images. Finally, exciting new methods for analyzing 3D cultures are emerging, and recently a technique for imaging cellular network dynamics in 3D using fast 3D laser scanning has been described (118).

Another recent development in HCS algorithms is the development of object-based hierarchical classification schemes such as the software developed by Definiens, Inc. (119). Such tools have been used to detect complex morphological structures in applications as varied as detecting small intestine crypts in histology samples, measuring phospholipidosis in primary hepatocytes, and monitoring growth cone collapse in sensory neurons.

Imaging Bioinformatics

As image analysis algorithms have matured, a major bottleneck that has emerged is data management and meta-analysis—essentially imaging informatics. In response, several new tools and databases have been developed by high-content screening instrument manufacturers. Two of the more advanced imaging bioinformatics and imaging storage platforms are the Cellomics Store and HCS Explorer (Cellomics), and AcuityExpress/MetaExpress (Molecular Devices, Germantown, PA). Both systems allow archiving and retrieval of annotated imaging, re-analysis of raw image data, and tools for analysis of quantitative results. In an early example of an integrated HCS toolkit, Abraham and coworkers at Cellomics developed a kinetic multiparameter cytotoxicity assay (120).

Analyzing and interpreting large sets of phenotypic data leads to what Giuliano et al. has termed "systems cell biology" (121). Advances in molecular labeling, high-throughput imaging, shape analysis, and machine intelligence are enabling the development of functional tools for understanding cellular biochemistry (122). Multidimensional drug profiling by automated microscopy is useful in many cases; see for example Perlman et al. (123). Mitchison further reviews small-molecule screening and profiling with automated microscopy (124). Tanaka et al., utilizing a Cytometrix automated imaging and analysis system (Cytokinetics, Inc., South San Francisco, CA), conducted an unbiased cell morphology-based screen for small-molecule inhibitors of cellular components not targeted by known protein kinase inhibitors. Screening of several cancer lines resulted in the identification of an inhibitor targeting a previously unknown function for carbonyl reductase 1 (CBR1) (125). In other examples, classification

of compound mechanism has been done using image-based cellular phenotypes (126).

A limitation of vendor-provided HCS informatics systems is the inability to analyze data collected on different hardware platforms. One solution is to create data translators for images collected on other vendor's hardware. Instrument manufacturer Cellomics has implemented gateway software for the GE IN Cell 1000 and the Perkin Elmer Opera that facilitates importation of data into Cellomics storage and analysis software. Another solution is open source software as exemplified by the Open Microscopy Environment data model (127,128), and the open source HCS informatics tool, Cell Profiler (129).

HCS Applications

Applying all these tools together—reagents, hardware, software—is advancing drug discovery by enabling powerful new experiments in high-throughput screening, target identification, compound profiling, and mechanistic studies. Some examples are listed below. Yu et al. have employed protein fragmentation complementation assays to measure drug action in a cellular context (130). Fluorescent imaging of amyloid formation in living cells has been accomplished using functional tetracysteine-tagged α-synuclein (131). In addition, ligand receptor binding can be measured by laser-scanning imaging (132) and HCS for receptor internalization, recycling, and intracellular trafficking is commonly used (133). Oscillations in NFκB signaling controlling dynamics of gene expression have been studied by Nelson et al. (134). An example of HCS with siRNA involving p53 activation in the cellular response to anticancer drugs is described by Giuliano et al. (135) and off target effects and hidden phenotypes have been examined by MacDonald and colleagues (136). Genome-wide screens of gene function as analyzed by HCS are also becoming common (137). Finally, a transgenic mouse has been created with a cell cycle biosensor (138).

AUTOMATED CELL CULTURE

Another key technology that is helping to enable HTS cell-based assays is automated cell culture (ACC) robotic systems. These systems generally include control software, flask and plate incubators, media storage, and flask, plate, and liquid-handling robots all within a HEPA filtered biosafety enclosure. ACC has multiple advantages, including high-throughput cell production, consistent quality, and walk-away 24/7 operation. Several vendors manufacture systems compatible with HTS, including The Automation Partnership (TAP, Royston U.K.), TECAN (Mannedorf, Switzerland), GNF systems (San Diego, CA), and Matrical (Spokane, WA). Of these, TAP has the most extensive product line and has by far the largest number of installed systems. The two units from TAP that are most useful for HTS are the "SelecT" and its smaller version, the "CompacT." Both instruments have the capability to grow multiple cell lines and can create assay ready plates containing cells at a particular density. Each system is anthropomorphic in design, in the sense that the machine is centered around a six axis robotic arm that essentially recapitulates the motions of conventional manual cell culture. One advantage of this is that the instruments use the same flasks, pipettes, and plates as manual cell culture, eliminating the need for purchasing separate supplies of consumables. Other cell culture-related systems available from TAP include the "Cello," a system for automated transfection, expansion,

and harvesting of cells; the "Piccolo," an instrument for parallel purification of recombinant proteins; and the "Cellmate," a platform for bulk cell preparation using roller bottles and T-flasks. These instruments are somewhat less directly applicable to uHTS, but can provide utility for a drug screening laboratory.

In contrast to the SelecT and CompacT robotic arm systems, the TECAN Cellerity automated cell culture system is first and foremost liquid handler, allowing flexible plating of cells and precise handling of small volumes. It includes a TECAN Freedom EVO platform with associated flask and plate manipulators, pipettor heads, and very robust control and scheduling software. The system is designed to use specially designed "roboflasks," which fit the footprint of a microtiter plate. Several Cellerity systems have been installed. Matrical (Spokane, WA) has designed a large capacity automated cell culture instrument, the Matrical Automated Cell Culture System (MACCS). Its design is based on the MatriStore compound storage system, which uses a robotic arm and an innovative tray-based system for sample storage and retrieval. The MACCS is potentially capable of using several different types of cell culture containers, including roboflasks, roller bottles, and conventional T-flasks. A very flexible deck layout and a customizable assortment of pipetting options give the system a lot of capability. Finally as a solution for true uHTS throughput, GNF systems (San Diego, CA) has designed a very robust automated cell culture instrument as part of a larger integrated HTS assay system.

Finally, it should be noted that HTS groups can gain many of the advantages of ACC by outsourcing live cell production to vendors such as Analytical Biological Services (ABS, Wilmington, DE) or GE Cell Factory (GE Healthcare). In addition, the use of cryopreserved batches of division arrested cells for HTS has been validated (139) (see also chap. 13 in this book) and there are several commercial sources for assay ready frozen cells (e.g., PRINCESS cells, CCS Cell Culture Service, Hamburg, Germany).

SUMMARY

Data obtained from cell-based assays not only relates to the target of interest but can potentially predict compound cell permeability, cytotoxicity, targeted pathway specificity, and selectivity. A limitation of cellular assays is that in many cases it is hard to determine the exact mechanism of compound activity without a battery of follow-up assays. The ability to implement multiplexed cell-based assays in high-throughput format creates the additional challenge of developing an appropriate hardware and software infrastructure. Although there have been significant improvements in automated tissue culture equipment, assay robotics, and signal detection hardware, reliable software tools able to process data and to convert cell-assay rich information into scientific knowledge remain in development. Relevant knowledge related to the activity of novel chemical entities against functional disease-relevant genomic targets will increase the chances of success in clinical studies, and accelerate drug discovery of novel medicines.

ACKNOWLEDGMENTS

The authors wish to thank our colleagues at Merck including, Stacia Kargman and Martin Hénault for providing the data from the Cell Key system, Grace Chan and Cem Elbi for the helpful suggestions with imaging assay development, and

Diane Simmons for administrative support. We would also like to thank Lans Taylor and Patricia Johnston from Cellumen for providing their data on Protein–Protein Interaction Biosensors.

REFERENCES

1. Oldenburg KR, Kariv I, Zhang JH, et al. Assay miniaturization: Developing technologies and assay formats. In: Seethala R, Fernandes PB, eds. Handbook of Drug Screening. New York, NY: Marcel Dekker, Inc., 2007:525–562.
2. Hertzberg R, Pope A. High-throughput screening: New technology for the 21st century. Curr Opin Chem Biol 2000; 4(4):445–451.
3. Fox S, Farr-Jones S, Sopchak L, et al. High-throughput screening: Update on practices and success. J Biomol Screen 2006; 11(7):864–869.
4. Balis F. Evolution of anticancer drug discovery and the role of cell-based screening. J Natl Cancer Inst 2002; 94(2):78–79.
5. Ma JN, Schiffer HH, Knapp AE, et al. Identification of the atypical L-type Ca^{2+} channel blocker diltiazem and its metabolites as ghrelin receptor agonists. Mol Pharmacol 2007; 72(2):380–386.
6. Opaluch AM, Aza-Blanc P, Vang T, et al. PTPome-wide functional RNA interference screening methods. Methods 2007; 42(3):306–312.
7. Ovcharenko D, Jarvis R, Hunicke-Smith S, et al. High-throughput RNAi screening in vitro: From cell lines to primary cells. RNA 2005; 11(6):985–993.
8. Borawski J, Lindeman A, Buxton F, et al. Optimization procedure for small interfering RNA transfection in a 384- well format. J Biomol Screen 2007; 12(4):546–549.
9. Gonzalez-Nicolini V, Fussenegger M. In vitro assays for anticancer drug discovery—A novel approach based on engineered mammalian cell lines. Anticancer Drugs 2005; 16(3):223–228.
10. Melnick J, Janes J, Kim S, et al. An efficient rapid system for profiling the cellular activities of molecular libraries. Proc Natl Acad Sci U S A 2006; 103(9):3153–3158.
11. Hug H, Los M, Hirt W, et al. Rhodamine 110-linked amino acids and peptides as substrates to measure caspase activity upon apoptosis induction in intact cells. Biochemistry 1999; 38(42):13906–13911.
12. Buesen R, Visan A, Genschow E, et al. Trends in improving the embryonic stem cell test (EST): An overview. ALTEX 2004; 21(1):15–22.
13. Pouton CW, Haynes JM. Embryonic stem cells as a source of models for drug discovery. Nat Rev Drug Discov 2007; 6(8):605–616.
14. Maffia A III, Kariv I, Oldenburg K. Miniaturization of a mammalian cell-based assay: Luciferase reporter gene readout in a 3 microliter 1536-well plate. J Biomol Screen 1999; 4(3):137–142. doi:10.1177/108705719900400307.
15. Roelan CH, Burns DA, Scheirer W. Accelerating the pace of luciferase reporter gene assays. BioTechniques 1996; 20(5):914–917.
16. Zysk J, Baumbach W. Homogeneous pharmacologic and cell-based screens provide diverse strategies in drug discovery: Somatostatin antagonists as a case study. Comb Chem High Throughput Screen 1998; 1(4):171–183.
17. Giuliano KA, Post PL, Hahn KM, et al. Fluorescent protein biosensors: Measurement of molecular dynamics in living cells. Annu Rev Biophys Biomol Struct 1995; 24:405–434.
18. Giuliano KA, DeBiasio RL, Dunlay RT, et al. High-content screening: A new approach to easing key bottlenecks in the drug discovery process. J Biomol Screen 1997; 2(4):249–259.
19. Rausch O. High content cellular screening. Curr Opin Chem Biol 2006; 10(4):316–320.
20. Lovborg H, Gullbo J, Larsson R. Screening for apoptosis—Classical and emerging techniques. Anticancer Drugs 2005; 16(6):593–599.

21. Krejci P, Pejchalova K, Wilcox WR. Simple, mammalian cell-based assay for identification of inhibitors of the Erk MAP kinase pathway. Invest New Drugs 2007; 25(4):391–395.
22. Crouch S, Slater K. High-throughput cytotoxicity screening: Hit and miss. Drug Discov Today 2001; 6(12 Suppl):S48–S53.
23. Mosmann T. Rapid colorimetric assay for cellular growth and survival: Application to proliferation and cytotoxicity assays. J Immunol Methods 1983; 65(1–2):55–63.
24. Scudiero DA, Shoemaker RH, Paull KD, et al. Evaluation of a soluble tetrazolium/formazan assay for cell growth and drug sensitivity in culture using human and other tumor cell lines. Cancer Res 1988; 48(17):4827–4833.
25. Will Y, Hynes J, Ogurtsov V, et al. Analysis of mitochondrial function using phosphorescent oxygen-sensitive probes. Nat Protoc 2006; 1(6):2563–2572.
26. Riedl SJ, Shi Y. Molecular mechanisms of caspase regulation during apoptosis. Nat Rev Mol Cell Biol 2004; 5(11):897–907.
27. Zhang H, Kasibhatla S, Guastella J, et al. N-Ac-DEVD-N′-(Polyfluorobenzoyl)-R110: Novel cell-permeable fluorogenic caspase substrates for the detection of caspase activity and apoptosis. Bioconjug Chem 2003; 14(2):458–463.
28. Cai SX, Drewe J, Kasibhatla S. A chemical genetics approach for the discovery of apoptosis inducers: From phenotypic cell based HTS assay and structure–activity relationship studies, to identification of potential anticancer agents and molecular targets. Curr Med Chem 2006; 13(22):2627–2644.
29. Yang J, Shamji A, Matchacheep S, et al. Identification of a small-molecule inhibitor of class Ia PI3Ks with cell-based screening. Chem Biol 2007; 14(4):371–377.
30. Ish T, Sootome H, King AJ, et al. A robust, target-driven, cell-based assay for checkpoint kinase 1 inhibitors. J Biomol Screen 2007; 12(6):809–817.
31. Dickey C, Dunmore J, Lu B, et al. HSP induction mediates selective clearance of tau phosphorylated at proline-directed Ser/Thr sites but not KXGS (MARK) sites. FASEB J 2006; 20(6):753–755.
32. Zhang X, Chen H, Warren L, et al. High throughput quantitative measurement of protein phosphorylation in cell based assay for evaluation of small molecule kinase inhibitors. SBS 13th Annual Conference and Exhibition, April 15, 2007, Montreal, Canada. Society of Biomolecular Sciences, 2007.
33. Guenat S, Rouleau N, Bielmann C, et al. Homogeneous and nonradioactive high-throughput screening platform for the characterization of kinase inhibitors in cell lysates. J Biomol Screen 2006; 11(8):1015–1026.
34. Giordano S, Ponzetto C, Di Renzo M, et al. Tyrosine kinase receptor indistinguishable from the c-Met protein. Nature 1989; 339(6220):155–156.
35. Ponzetto C, Giordano S, Peverali F, et al. c-Met is amplified but not mutated in a cell line with an activated met tyrosine kinase. Oncogene 1991; 6(4):553–559.
36. Rege-Cambrin G, Scaravaglio P, Carozzi F, et al. Karyotypic analysis of gastric carcinoma cell lines carrying an amplified c-Met oncogene. Cancer Genet Cytogenet 1992; 64(2):170–173.
37. Yamada T, Tsubouchi H, Daikuhara Y, et al. Immunohistochemistry with antibodies to hepatocyte growth factor and its receptor protein (c-Met) in human brain tissues. Brain Res 1994; 637(1–2):308–312.
38. Zhang JH, Chung TD, Oldenburg KR. A simple statistical parameter for use in evaluation and validation of high throughput screening assays. J Biomol Screen 1999; 4(2):67–73.
39. Alam J, Cook JL. Reporter genes: Application to the study of mammalian gene transcription. Anal Biochem 1990; 188(2):245–254.
40. Bronstein I, Fortin J, Stanley P, et al. Chemiluminescent and bioluminescent reporter gene assays. Anal Biochem 1994; 219(2):169–181.
41. Gailey PC, Miller EJ, Griffin GD. Low-cost system for real-time monitoring of luciferase gene expression. BioTechniques 1997; 22(3):528–534.
42. Tanahashi H, Ito T, Inouye S, et al. Photoprotein aequorin: Use as a reporter enzyme in studying gene expression in mammalian cells. Gene 1990; 96(2):249–255.

43. Berger J, Hauber J, Hauber R, et al. Secreted placental alkaline phosphatase: A powerful new quantitative indicator of gene expression in eukaryotic cells. Gene 1988; 66(1):1–10.
44. Ausseil F, Samson A, Aussagues Y, et al. High-throughput bioluminescence screening of ubiquitin-proteasome pathway inhibitors from chemical and natural sources. J Biomol Screen 2007; 12(1):106–116.
45. Tonary AM, Pezacki JP. Simultaneous quantitative measurement of luciferase reporter activity and cell number in two- and three-dimensional cultures of hepatitis C virus replicons. Anal Biochem 2006; 350(2):239–248.
46. Zlokarnik G, Negulescu P, Knapp T, et al. Quantitation of transcription and clonal selection of single living cells with beta-lactamase as reporter. Science 1998; 279(5347):84–88.
47. Bresnick JN, Skynner HA, Chapman KL, et al. Identification of signal transduction pathways used by orphan G protein-coupled receptors. Assay Drug Dev Technol 2003; 1(2):239–249.
48. Ruocco KM, Goncharova EI, Young MR, et al. A high-throughput cell-based assay to identify specific inhibitors of transcription factor AP-1. J Biomol Screen 2007; 12(1):133–139.
49. Coppola JM, Hamilton CA, Bhojani MS, et al. Identification of inhibitors using a cell-based assay for monitoring Golgi-resident protease activity. Anal Biochem 2007; 364(1):19–29.
50. Chalfie M, Tu Y, Euskirchen G, et al. Green fluorescent protein as a marker for gene expression. Science 1994; 263(5148):802–805.
51. Orengo JP, Bundman D, Cooper TA. A bichromatic fluorescent reporter for cell-based screens of alternative splicing. Nucleic Acids Res 2006; 34(22):e148.
52. Shoemaker BA, Panchenko AR. Deciphering protein–protein interactions. Part I. Experimental techniques and databases. PLoS Comput Biol 2007; 3(3):e43.
53. Ma J, Ptashne M. Deletion analysis of Gal4 defines 2 transcriptional activating segments. Cell 1987; 48(5):847–853.
54. Sadowski I, Ptashne M. A vector for expressing GAL4(1–147) fusions in mammalian cells. Nucleic Acids Res 1989; 17(18):7539.
55. Fields S, Song O. A novel genetic system to detect protein–protein interactions. Nature 1989; 340(6230):245–246.
56. Vidal M, Brachmann RK, Fattaey A, et al. Reverse two-hybrid and one-hybrid systems to detect dissociation of protein–protein and DNA–protein interactions. Proc Natl Acad Sci U S A 1996; 93(19):10315–10320.
57. Bays NW, Margolis J. Yeast as a budding technology in target validation. Drug Discov Today 2004; 1(2):157–162.
58. Eyckerman S, Lemmens I, Catteeuw D, et al. Reverse MAPPIT: Screening for protein–protein interaction modifiers in mammalian cells. Nat Methods 2005; 2(6):427–433.
59. Sapsford KE, Berti L, Medintz IL. Materials for fluorescence resonance energy transfer analysis: Beyond traditional donor–acceptor combinations. Angew Chem Int Ed Engl 2006; 45(28):4562–4589.
60. Tsien RY. The green fluorescent protein. Annu Rev Biochem 1998; 67:509–544.
61. Chan FK, Siegel RM, Zacharias D, et al. Fluorescence resonance energy transfer analysis of cell surface receptor interactions and signaling using spectral variants of the green fluorescent protein. Cytometry 2001; 44(4):361–368.
62. Rizzo MA, Springer G, Segawa K, et al. Optimization of pairings and detection conditions for measurement of FRET between cyan and yellow fluorescent proteins. Microsc Microanal 2006; 12(3):238–254.
63. Ai H, Henderson JN, Remington SJ, et al. Directed evolution of a monomeric, bright and photostable version of Clavularia cyan fluorescent protein: Structural characterization and applications in fluorescence imaging. Biochem J 2006; 400(3):531–540.
64. Karasawa S, Araki T, Nagai T, et al. Cyan-emitting and orange-emitting fluorescent proteins as a donor/acceptor pair for fluorescence resonance energy transfer. Biochem J 2004; 381:307–312.

65. Phizicky E, Bastiaens PI, Zhu H, et al. Protein analysis on a proteomic scale. Nature 2003; 422(6928):208–215.
66. Mena MA, Treynor TP, Mayo SL, et al. Blue fluorescent proteins with enhanced brightness and photostability from a structurally targeted library. Nat Biotechnol 2006; 24(12):1569–1571.
67. Ai HW, Shaner NC, Cheng ZH, et al. Exploration of new chromophore structures leads to the identification of improved blue fluorescent proteins. Biochemistry 2007; 46(20):5904–5910.
68. Ganesan S, Ameer-beg SM, Ng TTC, et al. A dark yellow fluorescent protein (YFP)-based Resonance Energy-Accepting Chromoprotein (REACh) for Forster resonance energy transfer with GFP. Proc Natl Acad Sci U S A 2006; 103(11):4089–4094.
69. Miller LW, Cai YF, Sheetz MP, et al. In vivo protein labeling with trimethoprim conjugates: A flexible chemical tag. Nat Methods 2005; 2(4):255–257.
70. Pfleger KD, Eidne K. Illuminating insights into protein–protein interactions using bioluminescence resonance energy transfer (BRET). Nat Methods 2006; 3(3):165–174.
71. Milligan G. Applications of bioluminescence and fluorescence resonance energy transfer to drug discovery at G protein-coupled receptors. Eur J Pharm Sci 2004; 21(4):397–405.
72. Hamdan FF, Audet M, Garneau P, et al. High-throughput screening of G protein-coupled receptor antagonists using a bioluminescence resonance energy transfer 1-based beta-arrestin2 recruitment assay. J Biomol Screen 2005; 10(5):463–475.
73. Hu K, Clement JF, Abrahamyan L, et al. A human immunodeficiency virus type 1 protease biosensor assay using bioluminescence resonance energy transfer. J Virol Methods 2005; 128(1–2):93–103.
74. Issad T, Blanquart C, Gonzalez-Yanes C. The use of bioluminescence resonance energy transfer for the study of therapeutic targets: Application to tyrosine kinase receptors. Expert Opin Ther Targets 2007; 11(4):541–556.
75. Xu X, Soutto M, Xie Q, et al. Imaging protein interactions with bioluminescence resonance energy transfer (BRET) in plant and mammalian cells and tissues. Proc Natl Acad Sci U S A 2007; 104(24):10264–10269.
76. Morell M, Espargaro A, Aviles FX, et al. Detection of transient protein–protein interactions by bimolecular fluorescence complementation: The Abl-SH3 case. Proteomics 2007; 7(7):1023–1036.
77. Pelletier JN, Campbell-Valois FX, Michnick SW. Oligomerization domain-directed reassembly of active dihydrofolate reductase from rationally designed fragments. Proc Natl Acad Sci U S A 1998; 95(21):12141–12146.
78. Galarneau A, Primeau M, Trudeau LE, et al. Beta-lactamase protein fragment complementation assays as in vivo and in vitro sensors of protein–protein interactions. Nat Biotechnol 2002; 20(6):619–622.
79. Wehrman T, Kleaveland B, Her JH, et al. Protein–protein interactions monitored in mammalian cells via complementation of beta-lactamase enzyme fragments. Proc Natl Acad Sci U S A 2002; 99(6):3469–3474.
80. Paulmurugan R, Gambhir S. Novel fusion protein approach for efficient high-throughput screening of small molecule-mediating protein–protein interactions in cells and living animals. Cancer Res 2005; 65(16):7413–7420.
81. Kerppola TK. Complementary methods for studies of protein interactions in living cells. Nat Methods 2006; 3(12):969–971.
82. Cabantous S, Terwilliger T, Waldo GS. Protein tagging and detection with engineered self-assembling fragments of green fluorescent protein. Nat Biotechnol 2005; 23(1):102–107.
83. Ozawa T, Nishitani K, Sako Y, et al. A high-throughput screening of genes that encode proteins transported into the endoplasmic reticulum in mammalian cells. Nucleic Acids Res 2005; 33(4):e34.
84. Chun W, Waldo GS, Johnson GV. Split GFP complementation assay: A novel approach to quantitatively measure aggregation of tau in situ: Effects of

GSK3beta activation and caspase 3 cleavage. J Neurochem 2007; 103(6):2529–2539.
85. Magliery TJ, Wilson CG, Pan W, et al. Detecting protein–protein interactions with a green fluorescent protein fragment reassembly trap: Scope and mechanism. J Am Chem Soc 2005; 127(1):146–157.
86. Zheng W, Spencer RH, Kiss L. High throughput assay technologies for ion channel drug discovery. Assay Drug Dev Technol 2004; 2(5):543–552.
87. Willumsen NJ, Bech M, Olesen SP, et al. High throughput electrophysiology: New perspectives for ion channel drug discovery. Receptors Channels 2003; 9(1):3–12.
88. Bennett PP, Guthrie HR. Trends in ion channel drug discovery: Advances in screening technologies. Trends Biotechnol 2003; 21(12):563–569.
89. Netzer R, Bischoff U, Ebneth A. HTS techniques to investigate the potential effects of compounds on cardiac ion channels at early-stages of drug discovery. Curr Opin Drug Discov Dev 2003; 6(4):462–469.
90. Galligan JJ. Ligand-gated ion channels in the enteric nervous system. Neurogastroenterol Motil 2002; 14(6):611–623.
91. Dupriez VJ, Maes K, Le Poul E, et al. Aequorin-based functional assays for G-protein-coupled receptors, ion channels, and tyrosine kinase receptors. Receptors Channels 2002; 8(5–6):319–330.
92. Wolff C, Fuks B, Chatelain P. Comparative study of membrane potential-sensitive fluorescent probes and their use in ion channel screening assays. J Biomol Screen 2003; 8(5):533–543.
93. Maher MP, Wu NT, Ao H. pH-Insensitive FRET voltage dyes. J Biomol Screen 2007; 12(5):656–667.
94. Jacoby E, Bouhelal R, Gerspacher M, et al. The 7 TM G-protein-coupled receptor target family. Chem Med Chem 2006; 1(8):761–782.
95. Williams C. cAMP detection methods in HTS: Selecting the best from the rest. Nat Rev Drug Discov 2004; 3(2):125–135.
96. Eglen RM, Bosse R, Reisine T. Emerging concepts of guanine nucleotide-binding protein-coupled receptor (GPCR) function and implications for high throughput screening. Assay Drug Dev Technol 2007; 5(3):425–451.
97. Shenoy SK, Lefkowitz RJ. Seven-transmembrane receptor signaling through beta-arrestin. Sci STKE 2005; 2005(308):cm10.
98. Oakley RH, Hudson CC, Cruickshank RD, et al. The cellular distribution of fluorescently labeled arrestins provides a robust, sensitive, and universal assay for screening G protein-coupled receptors. Assay Drug Dev Technol 2002; 1(1 Pt 1):21–30.
99. Oakley RH, Hudson CC, Sjaastad MD, et al. The ligand-independent translocation assay: An enabling technology for screening orphan G protein-coupled receptors by arrestin recruitment. Methods Enzymol 2006; 414:50–63.
100. Garippa RJ, Hoffman AF, Gradl G, et al. High-throughput confocal microscopy for beta-arrestin-green fluorescent protein translocation G protein-coupled receptor assays using the Evotec Opera. Methods Enzymol 2006; 414:99–120.
101. Fang Y. Label-free cell-based assays with optical biosensors in drug discovery. Assay Drug Dev Technol 2006; 4(5):583–595.
102. Fang Y, Li G, Ferrie A. Non-invasive optical biosensor for assaying endogenous G protein-coupled receptors in adherent cells. J Pharmacol Toxicol Methods 2007; 55(3):314–322.
103. Verdonk E, Johnson K, McGuinness R, et al. Cellular dielectric spectroscopy: A label-free comprehensive platform for functional evaluation of endogenous receptors. Assay Drug Dev Technol 2006; 4(5):609–619.
104. Peters MF, Knappenberger KS, Wilkins D, et al. Evaluation of cellular dielectric spectroscopy, a whole-cell, label-free technology for drug discovery on Gi-coupled GPCRs. J Biomol Screen 2007; 12(3):312–319.
105. George TC, Basiji DA, Hall BE, et al. Distinguishing modes of cell death using the ImageStream multispectral imaging flow cytometer. Cytometry 2004; 59(2):237–245.

106. Panchuk-Voloshina N, Haugland RP, Bishop-Stewart J, et al. Alexa dyes, a series of new fluorescent dyes that yield exceptionally bright, photostable conjugates. J Histochem Cytochem 1999; 47(9):1179–1188.
107. Bruchez M Jr, Moronne M, Gin P, et al. Semiconductor nanocrystals as fluorescent biological labels. Science 1998; 281(5385):2013–2016.
108. Gershon D. Cell signalling: Making connections. Nature 2004; 432(7014):243–249.
109. Miller S, Sarnecki C, Comita PB, et al. High throughput anchorage-independent cell colony growth assay with the IsoCyte™-HTS platform. SBS 13th Annual Conference and Exhibition, April 15, 2007, Montreal, Canada. Society of Biomolecular Sciences, 2007.
110. Smotrov N, Chan GKY, Szewczak AA, et al. Development of a three-color assay for mitosis and apoptosis using the laser-scanning IsoCyte and comparison with the microscope-based INCell Analyzer 1000. SBS 13th Annual Conference and Exhibition, April 15, 2007, Montreal, Canada. Society of Biomolecular Sciences, 2007.
111. Chen T, Hansen G, Beske O, et al. Analysis of cellular events using CellCard cystem in cell-based high-content multiplexed assays. Expert Rev Mol Diagn 2005; 5(5):817–829.
112. Beske OE. Simultaneous screening of multiple cell lines using the cell card system. In: Gad SC, ed. Drug Discovery Handbook. Hoboken, NJ: John Wiley and Sons, Inc., 2005:353–372.
113. Hudson CC, Oakley RH, Sjaastad MD, et al. High-content screening of known G protein-coupled receptors by arrestin translocation. Methods Enzymol 2006; 414:63–78.
114. Heydorn A, Lundholt BK, Praestegaard M, et al. Protein translocation assays: Key tools for accessing new biological information with high-throughput microscopy. Methods Enzymol 2006; 414:513–530.
115. Arden SR, Janardhan P, DiBiasio RB, et al. An automated quantitative high content screening assay for neurite outgrowth. Chem Today 2002; 20:64–66.
116. Kubota Y, Kleinman HK, Martin GR, et al. Role of laminin and basement membrane in the morphological differentiation of human endothelial cells into capillary-like structures. J Cell Biol 1988; 107(4):1589–1598.
117. Zhang Y, Zhou X, Degterev A, et al. A novel tracing algorithm for high throughput imaging screening of neuron-based assays. J Neurosci Methods 2007; 160(1):149–162.
118. Gobel W, Kampa B, Helmchen F. Imaging cellular network dynamics in three dimensions using fast 3D laser scanning. Nat Methods 2007; 4(1):73–79.
119. Baatz M, Arini N, Schape A, et al. Object-oriented image analysis for high content screening: Detailed quantification of cells and sub cellular structures with the Cellenger software. Cytometry 2006; 69(7):652–658.
120. Abraham VC, Taylor DL, Haskins JR. High content screening applied to large-scale cell biology. Trends Biotechnol 2004; 22(1):15–22.
121. Giuliano KA, Cheung WS, Curran DP, et al. Systems cell biology knowledge created from high content screening. Assay Drug Dev Technol 2005; 3(5):501–514.
122. Price JH, Goodacre A, Hahn K, et al. Advances in molecular labeling, high throughput imaging and machine intelligence portend powerful functional cellular biochemistry tools. J Cell Biochem Suppl 2002; 39:194–210.
123. Perlman ZE, Slack MD, Feng Y, et al. Multidimensional drug profiling by automated microscopy. Science 2004; 306(5699):1194–1198.
124. Mitchison TJ. Small-molecule screening and profiling by using automated microscopy. Chembiochem 2005; 6(1):33–39.
125. Tanaka M, Bateman R, Rauh D, et al. An unbiased cell morphology-based screen for new, biologically active small molecules. PLoS Biol 2005; 3(5):e128.
126. Adams CL, Kutsyy V, Coleman DA, et al. Compound classification using image-based cellular phenotypes. Methods Enzymol 2006; 414:440–468.
127. Goldberg IG, Allan C, Burel JM, et al. The Open Microscopy Environment (OME) Data Model and XML file: Open tools for informatics and quantitative analysis in biological imaging. Genome Biol 2005; 6(5):R47.

128. Swedlow JR, Goldberg I, Brauner E, et al. Informatics and quantitative analysis in biological imaging. Science 2003; 300(5616):100–102.
129. Carpenter AE, Jones TR, Lamprecht MR, et al. CellProfiler: Image analysis software for identifying and quantifying cell phenotypes. Genome Biol 2006; 7(10):R100.
130. Yu H, West M, Keon BH, et al. Measuring drug action in the cellular context using protein-fragment complementation assays. Assay Drug Dev Technol 2003; 1(6):811–822.
131. Roberti MJ, Bertoncini CW, Klement R, et al. Fluorescence imaging of amyloid formation in living cells by a functional, tetracysteine-tagged alpha-synuclein. Nat Methods 2007; 4(4):345–351.
132. Zuck P, Lao Z, Skwish S, et al. Ligand-receptor binding measured by laser-scanning imaging. Proc Natl Acad Sci U S A 1999; 96(20):11122–11127.
133. Ghosh RN, Chen YT, DeBiasio R, et al. Cell-based, high-content screen for receptor internalization, recycling and intracellular trafficking. BioTechniques 2000; 29(1):170–175.
134. Nelson D, Ihekwaba AE, Elliott M, et al. Oscillations in NF-kappaB signaling control the dynamics of gene expression. Science 2004; 306(5696):704–708.
135. Giuliano KA, Chen Y, Taylor D. High-content screening with siRNA optimizes a cell biological approach to drug discovery: Defining the role of P53 activation in the cellular response to anticancer drugs. J Biomol Screen 2004; 9(7):557–568.
136. MacDonald ML, Lamerdin J, Owens S, et al. Identifying off-target effects and hidden phenotypes of drugs in human cells. Nat Chem Biol 2006; 2(6):329–337.
137. Carpenter AE, Sabatini DM. Systematic genome-wide screens of gene function. Nat Rev Genet 2004; 5(1):11–22.
138. Burney RO, Lee AI, Leong DE, et al. A transgenic mouse model for high content, cell cycle phenotype screening in live primary cells. Cell Cycle 2007; 6(18):2276–2283.
139. Kunapuli P, Zheng W, Weber M, et al. Application of division arrest technology to cell-based HTS: Comparison with frozen and fresh cells. Assay Drug Dev Technol 2005; 3(1):17–26.
140. Zacharias DA, Violin JD, Newton AC, Tsien RY. Partitioning of lipid-modified monomeric GFPs into membrane microdomains of live cells. Science 2002; 296(5569):913–916.
141. Nagai T, Ibata K, Park ES, Kubota M, Mikoshiba K, Miyawaki A. A variant of yellow fluorescent protein with fast and efficient maturation for cell-biological applications. Nat Biotech 2002; 20(1):87–90.
142. Nguyen AW, Daugherty PS. Evolutionary optimization of fluorescent proteins for intracellular FRET. Nat Biotech 2005; 23(3):355–360.

9 In Vitro Strategies for Ion Channel Screening in Drug Discovery

Ravikumar Peri, Mark Bowlby, and John Dunlop

Neuroscience Discovery Research, Wyeth Research, Princeton, New Jersey, U.S.A.

INTRODUCTION TO ION CHANNEL STRUCTURE AND FUNCTION

Ion channels are defined as proteins forming water-filled pores in cell membranes. Their basic function is to catalyze the movement of ions through the plasma membrane of cells. They are separable from ion transporters by their lack of energy dependence and their high ion conductance rate (often $>10^6$ ions/sec) (1). All ion channels limit the permeation of ions based upon the charge and identity of the permeating ions. Structurally, ion channels at their most fundamental level contain two transmembrane (TM) domains joined by a loop comprising part/all of the selectivity filter of the pore. Most ion channels contain 3, 4, or 5 of these basic units to make up a trimer, tetramer, or pentamer, respectively. Up to five additional transmembrane domains can be attached to the two basic TM domains for each subunit. The macromolecular complex most commonly contains six TM domains in a tetramer format for voltage-gated channels, and three TM domains in a pentamer format for ligand-gated channels (Fig. 1). The voltage sensitivity domain (if present) is carried via a series of charged amino acid residues in a minimum of one TM domain. Ligand sensitivity, in contrast, is via ligand binding to a large extracellular region (usually the N-terminus), similar to what is contained in the 7-TM family of G-protein–coupled receptors. Both voltage and ligand activation methods require coupling of the sensor to a gate region near the inner mouth of the channel, which occurs via other parts of the protein. Opening of the gate allows a flow of charged ions to occur down their electrochemical gradient (passively). Subsequent gating or turning off of ion flow occurs in many ion channels and is termed both inactivation (for voltage-gated) and desensitization (for ligand-gated). For more complete descriptions of the structure of ion channels, the reader is referred to reviews for voltage-gated (2–4), for ligand-gated (5,6), and for mechanosensitive ion channels (7).

ROLE OF ION CHANNELS AS THERAPEUTIC TARGETS AND MODULATION IN DISEASE

Ion channels have been target families of drug receptors for pharmaceutically active agents since the early days of epilepsy research, when phenytoin was discovered as an anticonvulsant agent and later was characterized as a Na^+ channel blocker. Since this time, many other ion channels have been implicated as a causative agent in disease. As in many other genetically linked diseases, however, the majority of mutated ion channels are present only in rare disorders, or are only mutated in a small proportion of more widely distributed diseases. Nevertheless, these mutations can lead to a wider understanding of a disease

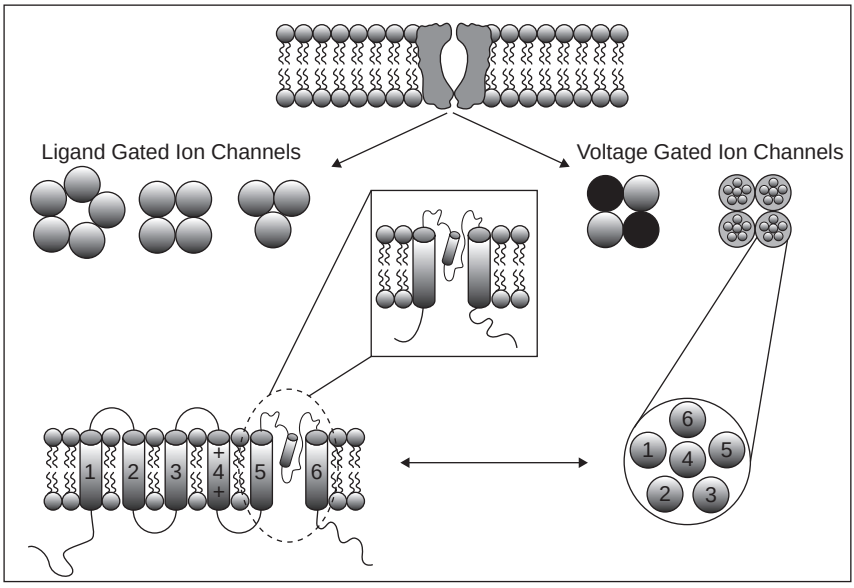

FIGURE 1 Schematic representation of voltage- and ligand-gated ion channels. All ion channels are composed of membrane spanning protein subunits that coassemble into homo- or heteromeric structures. A common feature of all channels is the pore-forming region consisting of two transmembrane domains with a short membrane delimited protein segment in between. Voltage-gated channels such as K^+ channels are commonly tetrameric assemblies of proteins, each of which contains 2 to 6 transmembrane regions. In the case of Na^+ and Ca^{2+} channels, a monomeric assembly is composed of a single protein containing 4 repeats of the standard 6 transmembrane pattern. Ligand-gated channels are more variable in structure, with 3 to 10 transmembrane domains forming one monomer. Fully functioning channels are trimeric, tetrameric, and pentameric assemblies.

phenotype, and thus lead to the discovery of novel drug targets, whether they be the mutated ion channel itself or another protein with a similar (or modulatory) function. A notable exception to this is for the cystic fibrosis transmembrane conductance regulator (CFTR) Cl^- channel, mutation of which results in cystic fibrosis (CF) (8,9). CFTR is the only known cause of CF, with two-thirds of patients containing a ΔF508 truncation mutation, while the rest harbor one of the >1000 other mutations found to disrupt function in CFTR. The mutations all result in a deficit of water movement through epithelial cells, most notably in the lungs. Other disease-causing mutations in Cl^- channels also manifest mainly in nonexcitable cells, notably ClC-5 (endosomal acidification = Dent disease), ClC-7 (bone resorption = osteopetrosis), and ClC-Kb (renal salt loss-–Bartter syndrome type III) (10).

Potassium channels are most commonly associated with disorders present in excitable cells. Loss-of-function mutations generally result in hyperexcitable muscle or nerve tissue, resulting in paralysis, epilepsy, or defective heart rhythms. The most well-known examples occur in cardiac tissue where loss-of-function mutations in KCNQ1, hERG, KCNH2, Kir2.1, KCNE1, or KCNE2 K^+ channels result in long "QT" syndrome and severe cardiac arrhythmia (11–14).

The Kir6.2 and SUR1 channel complex is also critical for pancreatic function, as mutation in either subunit causes insulin hypersecretion and thus hypoglycemia and diabetes (15,16), while the RyR2 mutation causes an unusual exercise-related cardiac tachycardia (17,18).

Hyperexcitability of neurons or muscle (depending on expression pattern of the channel) is often associated with defective Na^+ channel alpha- or beta-subunits. Generalized febrile epilepsies are known to be associated with defective Nav1.1, Nav1.2, and SCN1B, while Nav1.4 defects cause myotonia and periodic paralysis (19,20). An unusual set of mutations in the inactivation gate of the Nav1.5 channel induces a gain of function on a cellular level, but the cardiac expression pattern leads to a long QT syndrome (11). Another set of gain of function mutations has been described for the sensory neuron specific Nav1.7 Na^+ channel, resulting in hypersensitivity to pain in conditions such as primary erythromyalgia (21–23). Lastly, a ClC-1 mutation has also been linked to myotonia (10,24) and KCNQ4 to deafness (25,26), while other more general metabolic disorders have been linked to RyR1 (24,27) mutations.

Reversing a loss-of-function mutation in a protein is not a trivial task, but pharmacological enhancement of function (opening or modulating) can be attempted in some cases. The best-known example for this approach is for the KCNQ2/3 channels that have been linked to benign neonatal familial convulsions (BFNC) in infants (28–30). Soon after the link between this channel and neonatal epilepsy were described, an enhancer of KCNQ channels, retigabine (31–33), was described and characterized as an effective anticonvulsant in animal models and in a clinical trial of partial seizures in adults (34). Thus, the underlying mechanism of KCNQ channel activity was related to multiple types of epilepsy, although in this case the compound retigabine was found serendipitously rather than out of a targeted effort specifically on KCNQ channels.

Most pharmacological agents, however, act on ion channels that are not thought to be mutated in disease, but rather on those channels that affect the function of the biological process altered in the specific disease state. This is most commonly associated with the excitability of nerve and muscle cells, with Na^+ channel blockers being commonly used for epilepsy and pain, and Ca^{2+} channel blockers for cardiac arrhythmias and pain. New targets in this category include K^+ channels such as Kv1.3 and IKCa1 expressed in lymphocytes (for immune suppression and autoimmune diseases) (35), Kv1.3 in pancreas (for type II diabetes) (36,37), and other tissues (obesity) (38,39). There is also significant interest in the "newest" family of ion channels, the transient receptor potential (TRP) family of channels, although most of this work is still in the early stages of drug discovery and target validation. One notable exception is the TrpV1 blocking compounds that have reached early clinical trials for chronic pain conditions (40–43). With respect to ligand-gated ion channels, modulators of nicotinic acetylcholine, γ-aminobutyric acid (GABA), and glutamate (*N*-methyl-D-aspartate subtype) receptors have been successfully developed as therapeutics, and these and other ligand-gated ion channels continue to be important targets for future drug discovery.

ION CHANNEL ASSAY STRATEGIES

Ion channels have been important drug targets for several decades. Several assay strategies have been advocated to assess ion channel activity in drug

discovery. Traditionally, the less-sensitive methods such as radioligand binding and radioactive ion uptake were employed in ion channel screening campaigns. They determined the affinity of ligands for ion channels by using radiolabeled compounds or by competitive displacement of a high-affinity standard radioligand from the channel by the molecules being screened. Functional assessment of ion channel activity was done using medium throughput assays that measured the uptake or release of a radioactive tracer ion. These were followed by low-throughput electrophysiological experiments for detailed biophysical and pharmacological assessment of select few molecules. The lack of good correlation between binding and electrophysiological assays combined with a very low throughput of the latter limited ion channel drug discovery efforts. The development of several functional calcium and membrane potential–based optical ion channel assays and advances in high-throughput optical readers capable of kinetic measurements coupled with automated online robotic pipetting capabilities gave a new dimension to ion channel drug discovery. The development of an ion channel flux technology that works on the principle of atomic absorption spectroscopy gave an alternate, nonradioactive methodology to assess ion channel activity by ion flux via nonradioactive means. Over the past decade, several automated planar electrophysiology platforms have emerged that facilitate medium to moderate increases in screening throughput over the conventional manual patch clamp assays. Each of these approaches has its advantages and shortcomings, and pharmaceutical ion channel drug discovery strategies combine several of these methods in a tiered approach. A schematic of a tiered ion channel screening strategy is illustrated in Figure 2. KCNQ2/3 channel activators have a potential to be used as therapeutic agents for treatment of CNS disorders

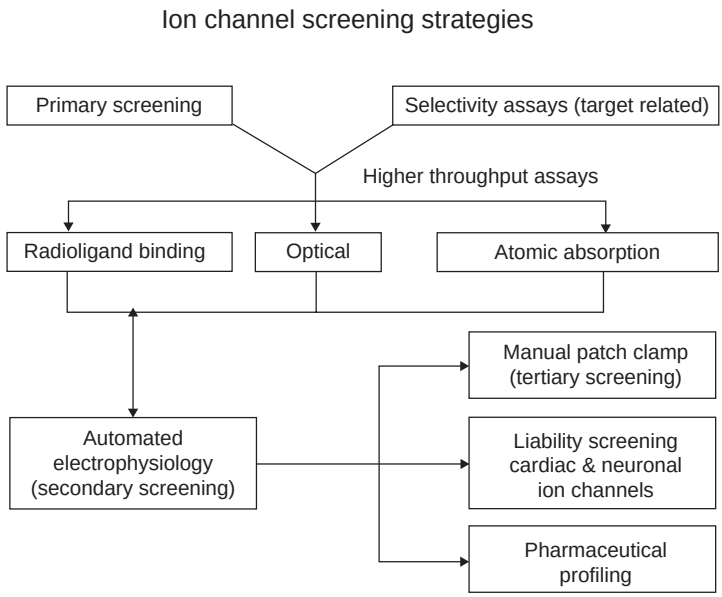

FIGURE 2 Schematic of ion channel screening strategy in pharmaceutical industry.

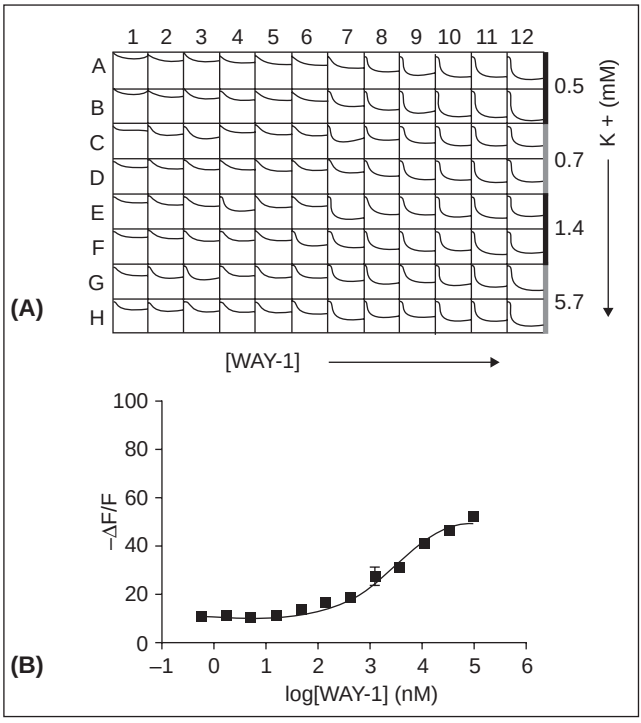

FIGURE 3 Membrane potential dye-based FlexStation (and/or FLIPR) assay can be used as a higher throughput strategy for screening KCNQ2/3 channel activators. Cells stably expressing KCNQ2/3 channels were cultured overnight, loaded with membrane potential dye (Molecular Devices) in a low-potassium buffer, and incubated for 1 to 2 hours. After recording the base line, the cells were stimulated with the compounds and the change in fluorescence was monitored. (**A**) Assay optimization as a function of increasing potassium concentration and increasing concentrations of a test compound WAY-1. (**B**) Concentration–response curve for WAY-1.

such as epilepsy and neuropathic pain. Strategy for identification of KCNQ2/3 activators is illustrated in Figures 3 to 5. Higher throughput optical membrane potential assays in FLEX station and medium throughput rubidium flux assays employing atomic absorption spectroscopy are employed for primary screening. Automated electrophysiology assays in IonWorks HT (or Quattro) constitute secondary assays, and the information rich laborious manual patch-clamp experiments are used for obtaining mechanistic insight of the biophysical modulation of channels. Some of the most commonly used screening methods are discussed later in this chapter.

Test Systems and Reagents

Ion channel assays traditionally relied on native expression systems and employed primary cells such as cardiomyocytes or neurons for cell-based assays and tissue homogenates for radioligand binding assays. Although such systems retain the channel of interest in its native conformation with all the accessory subunits in the correct stoichiometry, they pose a limitation because of

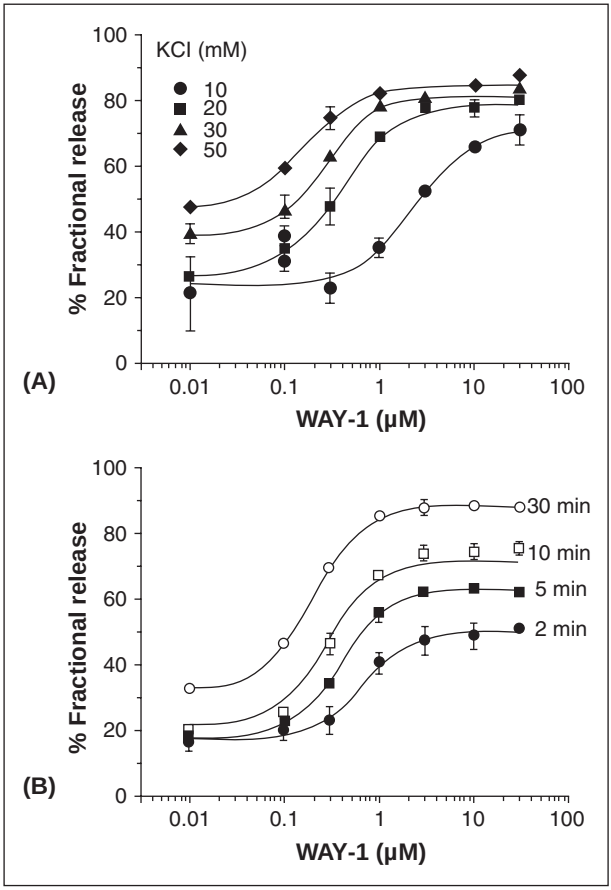

FIGURE 4 Atomic absorption spectroscopy-based rubidium efflux assays can be used with a medium throughput as an alternate screening strategy for KCNQ2/3 channel activators. Cells stably expressing KCNQ2/3 channels were cultured overnight, loaded with Rb^+ loading buffer for three hours. After a wash, the cells were treated with WAY-1 in depolarization buffers containing different K^+. Rubidium efflux into the supernatant was determined by using flame atomic absorption spectroscopy in an ion channel reader ICR 8000. Effect of extracellular K^+ concentration on Rb^+ release in the presence of a KCNQ channel activator WAY-1 in a concentration range of 0.01 to 30 μM are shown. (**A**) EC_{50} values of WAY-1 2.29, 0.37, 0.25, and 0.16 μM were obtained when stimulated with buffer containing 10, 20, 30, and 50 mM KCl, respectively. (**B**) Time course of Rb^+ release following stimulation in 20 mM KCl for different times. EC_{50} values of WAY-1 were 633, 488, 315, and 197 nM corresponding to stimulation times of 2, 5, 10, and 30 minutes, respectively.

interference from coexpression of closely related family members and other ion channels. Recombinant systems are predominantly used for ion channel expression in modern discovery campaigns for both functional assays and binding assays. Because ion channels are heteromeric proteins, a major limitation of the recombinant approach is the challenge to coassemble the functionally and pharmacologically relevant subunits in the correct stoichiometry. Such systems

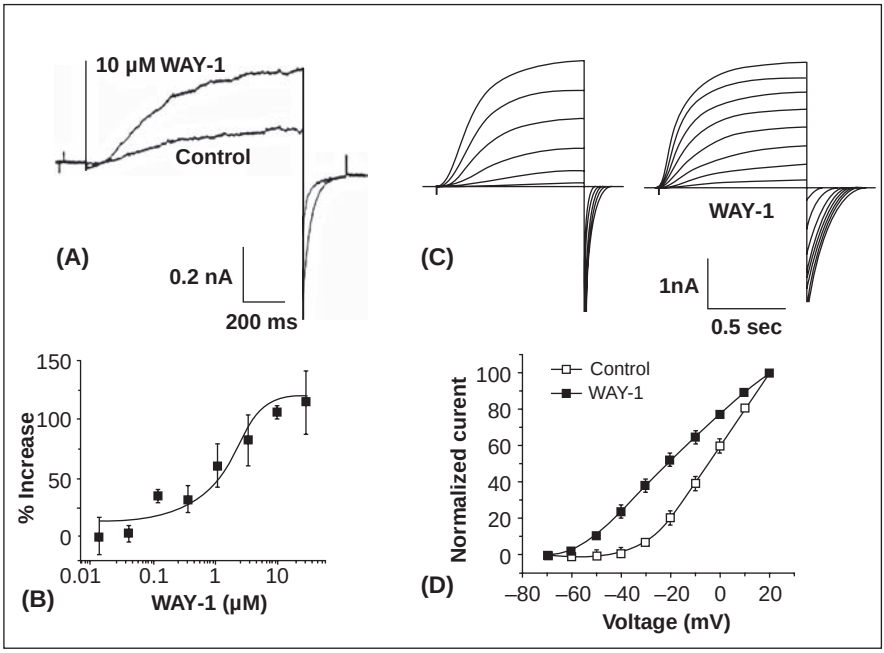

FIGURE 5 Automated electrophysiology assay platforms such as IonWorks provide medium throughput and can be used as secondary screening assays for ion channels. Manual patch-clamp assays, considered a gold standard, have a very low throughput but are extremely information rich and can be used for detailed characterization of compounds, such as on KCNQ2/3 channel currents. (**A**) Raw current traces measured in IonWorks in response to a voltage step to a test potential of −10 mV from a holding potential of −80 mV in the presence and absence of 10 μM WAY-1. (**B**) Concentration–response curve of WAY-1 using the protocol mentioned in (**A**) elicits an EC_{50} of 2.7 ± 0.45 μM. (**C**) Typical KCNQ2/3 current traces elicited from a holding potential of −80 mV by 10 mV voltage steps from −100 to +10 mV, recorded in manual patch-clamp mode in the presence and absence of opener WAY-1 (10 μM). (**D**) Normalized current–voltage relationship in the presence and absence of opener WAY-1 (10 μM). The activation curve is left shifted to hyperpolarizing potentials in the presence of activator.

therefore need functional, biophysical, and pharmacological validations prior to being used in a screening campaign. Recombinant systems include transient expression systems as well as stably transformed cell lines and often have a high level of channel expression compared to native cell systems. Such an overexpression can sometimes alter pharmacological responses and sensitivity of detection. Some channel systems such as the α7 nicotinic acetylcholine receptor require coexpression of chaperone proteins such as RIC-3 for increased cell surface expression in mammalian cells (44). Heterologous mammalian expression systems such as GH_4C_1 and GH_3 cells endogenously express RIC-3 and can be a system of choice for expressing α7 nAChR (45). In addition, adaptability to automated planar electrophysiological systems may require further clonal selections of recombinant cell lines for optimal performance, on the system being used. Achieving successful performance of automated planar electrophysiological platforms requires optimization of intra and extracellular buffers, cell culture,

and dissociation techniques used for dispersing adherent cells. These simple but important considerations are often underappreciated and overlooked prior to implementation.

Optical Methods

Optical fluorescence-based approaches coupled with advances in instrumentation and high-throughput fluidics have revolutionized ion channel drug discovery, enabling the potential to screen libraries of compounds. These techniques have been successfully applied in the pharmaceutical industry to support high-throughput screening (HTS) and lead optimization phases to identify advanced hits. These approaches utilizing fluorescent probes have become an integral part of ion channel drug discovery and have been extensively employed to assess functional activity of ion channels in cell-based assays. These indirect functional ion-channel assays can be broadly categorized into Ca^{2+} dependent or membrane potential dependent assays. Ca^{2+} dependent assays rely on a quantitative flux of Ca^{2+} into cells upon channel activation. Cells are preloaded with Ca^{2+} specific dyes, and an ion–dye interaction produces a fluorescent signal that can be quantitated. Membrane potential assays rely on the principle of a voltage dependent partitioning of a fluorescent dye between the intracellular and extracellular compartments. The dye in the extracellular compartment can complex with a quencher molecule, allowing a specific quantitative assessment of the fraction partitioned into the intracellular compartment, via change in fluorescence intensity, that in turn depends on ion channel activation and a proportional change in membrane potential.

Instrumentation

Improvements in optical instruments, data capture and processing software, integrated multichannel pipetting, and reagents to probe ion channels have enabled the development of new assays that are amenable to high-throughput screening. Several plate readers are available to the users depending on the features desired and assay requirements. The fluorometric imaging plate reader (FLIPR^{TM}) developed by Molecular Devices is one such instrument and allows accurate measurement of fluorescence changes in calcium and voltage-based cellular assays. It utilizes an argon laser for dye excitation, integrated liquid handling in 96- and 384-well formats and CCD detection optics to provide real-time kinetic cellular responses from all the wells simultaneously. The instrument allows multiple solution additions and is coupled with kinetic profiling of target activity. The latest generation FLIPR^{TETRA} employs exchangeable light emitting diode (LED) excitation banks as a source of illumination and exchangeable emission filters coupled with dual camera systems and is capable of being used for both fluorescent and luminescent assays configurable to 96-, 384-, and 1536-well platforms. These innovations provide for significant improvement in throughput.

Microplate readers capable of detecting fluorescence resonance energy transfer (FRET) are available through several manufacturers. Voltage ion probe reader (VIPR) was the earliest among the instruments specifically designed for FRET-based assays. SpectraMax from Molecular Devices, FDSS from Hamamatsu, EuLux^{TM} and EnVision^{TM} from PerkinElmer are a few examples of instruments capable of detecting FRET-based assays in addition to being capable of

performing kinetic fluorescence measurements. These instruments vary in their throughput and kinetic capabilities. They, however, have some limitations that include a limited capability to detect ultrarapid membrane potential changes and applicability to a select group of ion channels.

Fluorescence Assays

Fluorescent dyes are available for qualitative and quantitative assessment of Na^+, Cl^-, and Ca^{2+}. However, the assays for these ions have varying degrees of sensitivity of detection that depends on the specificity of ion–dye interaction and the concentration gradient of the ion in the intra and extracellular compartments or the sensitivity of detection over a dynamic voltage range. Under physiological conditions, cells have a well-regulated ionic homeostasis and maintain a tight transmembrane electrochemical gradient of ions. The gradient is steepest for Ca^{2+} (4 orders of magnitude ~100 nM vs. 2 mM) but is small for K^+, Na^+, and Cl^- (<20 fold) resulting in large transmembrane Ca^{2+} fluxes and significantly smaller changes in the concentration of K^+, Na^+, and Cl^- upon stimulation. Relative differences in the flux of ions and corresponding concentration changes explain to a certain extent the differences in the sensitivity of fluorescence assays employing dyes that complex with K^+, Na^+, and Cl^-, when compared with Ca^{2+}, and the limited implementation of all but the latter.

Ca^{2+} Flux Assays

Calcium mobilization assays are the best characterized fluorescent cell-based assays and measure changes in intracellular Ca^{2+} either by release from intracellular stores upon stimulation of GPCR's or the flux through extracellular compartments upon stimulation of voltage or ligand-gated ion channels. A variety of calcium-sensitive dyes that excite either at single or dual wavelengths are available to monitor Ca^{2+} fluxes. Most commonly used dyes such as Fura, Fluo-3, and Fluo-4 require a wash step after dye loading to eliminate the background fluorescence. Several "No-Wash" Ca^{2+} dyes such as Fluo 4-NW from Invitrogen, FLIPR calcium 3 and calcium 4 from Molecular Devices, and BD™ from Becton-Dickenson, which incorporate a nonpermeant quencher in the extracellular loading buffer and prevent background fluorescence, have become available recently and are routinely incorporated in ion channel screening campaigns. Cells loaded with the dye for a fixed duration either at room temperature or at 37°C are stimulated exogenously to elicit the intracellular Ca^{2+} elevation. The dye-loaded cells are excited at a wavelength of 480 nm and emit a strong signal at 525 nm. The fluorescence intensity is proportional to the concentration of intracellular free Ca^{2+} available to complex with the dye. The extensive use of Ca^{2+} flux assays to study ligand- and voltage-gated channels is documented by their use in the characterization of a wide range of ion channels including nicotinic acetylcholine (46), glycine, glutamate-activated channels, transient receptor potential channels including TRPV1 (47), TRPM2 (48), TRPM7, TRPM8 (49,50) and TRPC6, and voltage-gated calcium channels (51–53). Despite the widespread use of fluorescent assays, there are certain limitations that need to be considered during assay development. These include a lack of control over membrane potential that can cause an altered potency of compounds that exhibit state and/or voltage-dependent inhibition when compared in conventional electrophysiological assays. Interference in the assay due to the intrinsic fluorescence

of compounds being evaluated is yet another shortcoming that can produce artifacts with certain compounds.

Membrane Potential Assays

Optical membrane potential assays utilize fluorescent membrane potential sensitive dyes and rely on the principle that small ionic conductance can generate relatively large changes in membrane potential that can translate to optically quantifiable fluorescence output. The choice of indicators, their sensitivity of detection, and the precision of measurement over a dynamic assay range are critical for the success of these assays. Membrane potential dyes can be broadly binned into two distinct categories, the fast response dyes and the slow response dyes. Fast response membrane potential dyes such as Di-4-ANEPPS and its derivatives and several styryl dyes are available for imaging rapid (millisecond) membrane potential changes in excitable cells such as cardio-myocytes and neurons. They undergo a membrane potential–dependent change in their electronic structure, and consequently in their fluorescence properties. However, the magnitude of fluorescence change over a dynamic membrane potential change is very small, typically in the range of 2% to 10% fluorescence change per 100 mV and hence is of limited use in ion channel screening campaigns despite being great mechanistic tools for investigating rapid membrane potential changes. Traditional membrane potential–based ion channel assay campaigns employ slow response bis-oxanol–based voltage-sensing dyes such as bis-(1,3-dibutylbarbituric acid) trimethine oxonol, or DiBAC4(3) that produce fluorescence changes by partitioning into the cell in a voltage-dependent manner. Membrane depolarization leads to dye internalization, binding to hydrophobic sites, and enhanced fluorescence. Hyperpolarization on the contrary leads to dye extrusion and decrease in fluorescence intensity. Despite an accurate voltage-dependent transmembrane distribution, kinetics of fluorescence changes with DiBAC4(3) are slow and fluctuate with changes in temperature and dilution of the dye, and hence are not suitable for measurement of rapid membrane potential changes. Despite this shortcoming, DiBAC4(3) has been successfully utilized in several potassium channel assay campaigns (54). FLIPR Membrane Potential dye (FMP) from Molecular Devices overcomes some of these shortcomings and enables somewhat faster measurement of membrane potential changes [compared to DiBAC4(3)] with greater accuracy and precision and is routinely used in a number of voltage-dependent ion channel assays (55,56). FMPs are 15 times faster than DiBAC4(3) and utilize a voltage-sensing dye mixed with proprietary fluorescent quenchers in the assay buffer to suppress extracellular dye fluorescence. This eliminates the need for cell wash steps and facilitates assay optimization with enhanced throughput. FMP has been successfully used for measurement of membrane potential changes in several voltage-gated potassium (54) and sodium channel assay (57) campaigns as well as ligand-gated GABA ion channel assay campaigns (58), despite the extremely fast activation and inactivation/desensitization of these channels. To overcome the limitations posed by rapid channel kinetics, sodium channel assays employ reagents such as veratridine and type II pyrethroids deltamethrin and fenvalerate that can lock the channel in an open confirmation (59,60). FMP has also been utilized in excitatory amino acid transporter assays (61) as well as inhibitory amino acid transporter assays (62). In a manner analogous to Ca^{2+}-dependent dyes, voltage sensitive dyes are also prone to

chemical interference when testing fluorescent compounds that may adversely affect assay performance. Hence, the FMPs from Molecular Devices are available as two different dye formulations, namely, the blue FMP and red FMP kits that can individually be optimized for use in an assay. Other membrane potential kits (BD ACT One^{TM}) based on the modification of DISBAC family of membrane potential dyes also allow for measurement of cell membrane potential in homogeneous, single-addition assays with a high degree of sensitivity, precision, and accuracy. Utilizing these reagents, a relatively high-throughput 384-well format assay with relatively low reagent cost can be achieved, facilitating a screening campaign of libraries containing 500,000 to 750,000 compounds in three to four weeks.

Fluorescence Resonance Energy Transfer (FRET) Membrane Potential Assays

FRET-based voltage-sensing dyes incorporate the use of dye-pairs to monitor changes in membrane potential. They use ratiometric measurements and exhibit increased voltage sensitivity over traditional bis-oxanols. FRET-dye pairs comprise a sensitive coumarin-linked phospholipid donor that binds to the outer leaflet of the plasma membrane and a negatively charged oxonol acceptor that partitions across the plasma membrane in a voltage-dependent manner (63). The coumarin–oxanol dye pairs are chosen such that the emission spectrum of the coumarin donor overlaps with the excitation spectra of the oxonol acceptor. The proximity of the two dyes allows excitation of the acceptor dye by the donor dye. At the resting membrane potential, excitation of coumarin produces FRET and excites the oxonol localized in the outer cell membrane thus resulting in increased emission at a wavelength of 580 nm. Depolarization leads to the flux of the oxonol derivative into the inner layer of the cell membrane, increasing the physical distance between dye pairs (>100 nm) and disrupts FRET, resulting in the emission from coumarin at 460 nm. Oxanols such as DiSBAC$_4$(3) with higher hydrophobicity produce fast responses with time constants in the proximity of 10 ms and can accurately measure action potentials. The ratio of fluorescence intensities of the donor and acceptor at the two wavelengths gives a measure of the membrane potential. Ratiometric measurement of changes in membrane potential also helps to reduce assay artifacts. However, the use of two cell wash steps in the assay place some constraints on the throughput and amenability to HTS. FRET assays have been successfully employed in several screening campaigns that include voltage-gated sodium channels that have extremely fast gating and inactivation kinetics (64,65).

Electrophysiological Methods

The use of cell-based microplate formats with fluorescent indicator dyes has emerged as a key technology for ion channel screening, in particular where throughput is a major consideration. That being said, the gold standard assay for measuring ion channel activity, patch-clamp electrophysiology in mammalian cells, is still ultimately necessary, being exceptionally information rich, providing detailed mechanistic insight, and the definitive evaluation of a compound's activity on its cognate ion channel target. Conventional patch-clamp electrophysiology is however fundamentally limited in its broad utility due to the extremely low-throughput nature. Even in the hands of the best trained operator one can achieve only the detailed characterization of one or two compounds in a

working day. Consequently, the continued desire to support compound screening in electrophysiological formats in a higher throughput manner has driven the evolution and implementation of a number of new technology platforms in the last 5 to 7 years.

Two complementary screening approaches have gained prominence in practical use both relying on the use of planar-array or plate/chip-based electrophysiology. The first to gain widespread use was the IonWorksHT platform (66,67), relying on the perforated patch-clamp mode (typically ~100 MΩ seal resistances), utilizing a 384-well PatchPlate design, where each well of the plate is configured with a single 1 to 2 μm hole in the bottom. This design theoretically allows for a single cell from a dispensed cell suspension to be positioned over each hole, achieved via a modest vacuum pressure, followed by the introduction of a pore-forming antibiotic such as amphoterocin C to form a pore in the membrane and thereby gaining electrical access to the cell in the perforated patch clamp mode. Although this may appear to offer a 384-fold increase in screening capacity compared to manual patch clamp, the blinded nature of gaining access to a single cell/well typically leads to a relatively high level of failures, and the use of perforated patch clamp with low seal resistances contributes to high well-to-well variability, requiring multiple wells per condition (e.g., for each compound concentration tested) to be routinely used. Despite these limitations, the IonWorksHT technology has been successfully validated for a number of applications (51,68–70) and has been a major innovation in the electrical screening of ion channels. As an illustrative example, we have experienced throughput on the IonWorksHT of up to 8 PatchPlates per day for screening potential hERG channel blockers corresponding to 25 to 50 compound IC_{50}s per day using a 7-point concentration response and running a positive control on each plate for data validation. Clearly, this is a major advance in capacity over conventional electrophysiology.

A more recent significant advance with the IonWorks technology is the introduction of the Quattro, using a PatchPlate design with 64 holes/well, termed the population patch clamp (PPC) mode (65,71,72). The PPC mode overcomes one of the aforementioned limitations of the IonWorksHT providing a population average recording per well and not relying on the successful recording from only a single cell per well. As a result the Quattro typically allows for a two to fourfold increase in screening capacity when compared with the IonWorksHT. This single advance has for the first time offered the real possibility of screening small compound libraries for ion channel targeted drugs using an electrical read-out and this has been validated in practical use in the search for new Ca^{2+}-activated K^+ channel modulators (73). This same study also demonstrated the benefit of the PPC mode in overcoming the often significant well-to-well variability observed in the single hole format.

Although the IonWorks platforms have unquestionably revolutionized ion channel screening using an electrical read-out, their use of the perforated patch clamp mode has not faithfully reproduced the highest quality gigaohm seal recordings afforded by manual patch clamp electrophysiology. In addition, the instrument design does not allow for simultaneous add and record capability achieved by manual recordings, limiting the use to voltage-gated and slowly inactivating ligand-gated channels. The second screening approach taken in the development of plate/chip-based electrophysiology has endeavored to

recapitulate the same high-quality seal and continuous recording characteristics of manual patch-clamp leading to the introduction of three validated platforms, the PatchXpress, QPatch, and Patchliner, with many others still in the development stage. Each of these takes its own proprietary approach to the challenge, for example, the PatchXpress uses a 16-channel SealChip substrate with electrodes separated from the chip, while the QPatch uses a 16- or 48-channel QPlate with embedded recording and ground contacts. Despite this, all these platforms share in common the ability to perform true gigaohm seal quality patch-clamp recordings in a parallel manner, best exemplified by the 16-channel SealChip or QPlate formats where the validation is strongest. A number of studies have now described the use of these platforms in support of ion channel screening (46,74–78). In practical use, the blind nature of patching cells in the chip/plate formats employed leads to some failures as discussed above; however, it would not be impossible to routinely achieve in the region of 12 successful recordings from each 16 channel chip, again representing a very significant enhancement compared to manual patch clamp. In this regard, the most recent innovation toward even higher throughput is the introduction of the 48-channel QPlate for the QPatch platform, although at the time of writing there is little published validation data on its practical implementation.

The availability of these higher throughput electrical platforms for ion channel screening does not come without some important limitations. Each requires significant capital investment for initial set-up and plate consumables are expensive when compared to the per well cost achieved with nonelectrophysiological approaches. Another "cost" is typically in the form of resources dedicated to transitioning assays from manual to automated format, and this can be significant. Despite these considerations, automated electrophysiology has now been firmly established as a complementary strategy for ion channel screening and can be very effectively integrated with the various other approaches discussed in this chapter.

Other Methods

Despite the fact that modern ion channel drug discovery strategies rely predominantly on a combination of high-throughput fluorescence methods and follow on automated electrophysiological assays, there are several other approaches of interrogating ion channel activity. Historically, radioligand binding assays and radioactive tracer ion uptake assays were the only in vitro tools available for ion channel drug discovery but they enabled the discovery of several important drugs for the treatment of disorders of the cardiovascular and central nervous system. These assays traditionally relied on membranes derived from native tissues and more recently exploit channels expressed in recombinant systems as a source of protein. Although radioactive tracer ion uptake assays have given way to nonradioactive methods, radioligand binding assays still have an important role in drug discovery to determine the affinity of ligand for receptor or channel and in vivo to study receptor occupancy. They work on the principle of mass action and rely on a high-affinity interaction of radioligand in a saturable and reversible manner with the channel of interest. Filtration binding assays traditionally used in the past have given way to nonseparation-based homogenous scintillation proximity assays (SPA). SPA's can be configured to 96- and 384-well platforms and

offer moderate throughput. However, a fundamental limitation of radioligand binding assays is the presumption that ligands/compounds being investigated interact with the specific binding site of the radioligand either directly or allosterically.

The invention of the ion channel readers that use the flame atomic absorption spectrophotometry has renewed interest in nonfluorescent approaches to functional assessment of ion channel activity (79). Ion flux assays are medium to high throughput cell-based functional end point assays and quantify tracer ions either in cellular extracts or supernatants using ion-specific detectors but lack the ability to provide kinetic information, unlike optical or electrophysiological assays. Atomic absorption based Rb^+ efflux assays have been used successfully to assess the activity of a variety of potassium channels such as hERG (80), Kv1.1, 1.3 (81), 1.4, 1.5, and KCNQ (82,83) and also for ligand-gated ion channels such as KATP. Data obtained by this method correlates reasonably well with the data obtained using traditional electrophysiology methods, though often with right-shifted EC_{50}/IC_{50} values observed with the flux assays. Ion flux assays to investigate other channels such as Na^+ and Cl^- have been developed but lack extensive validation. Li^+ flux can be used for the analysis of sodium channel activity. Cl^- channel and transporter activity can indirectly be measured postefflux by precipitating the Cl^- by treatment with an excess of $AgNO_3$ and determining the concentration of the free residual Ag^+ ions using atomic absorption spectrophotometry.

APPLICATION OF IN VITRO ION CHANNEL ASSAYS IN SAFETY PHARMACOLOGY

Ion channels play a critical role in mediating cardiac excitability. The QT interval of electrocardiogram (ECG) is a measure of the duration of ventricular depolarization and repolarization. It is determined by the duration of cardiac action potential and results from the concerted activity of ion channels and transporters. Action potential prolongation due to increased depolarizing Na^+ or Ca^{2+} currents (either by decreased inactivation or increased activation) or decreased repolarizing delayed rectifier K^+ currents (IKr, IKs) can lead to prolongation of QT interval. Drug-induced inhibition of hERG potassium channel (IKr) by compounds of diverse chemical structure, the subsequent prolongation of QT interval accompanied with fatal polymorphic ventricular arrhythmia, "Torsades-de-pointes" (TDP) has led to withdrawal from market of several non-antiarrhythmic drugs (NARDS) such as astemizole, sertindole, cisapride, terfenadine, and grepafloxacin in the past 10 years (84). Regulatory agencies from US (FDA), Europe (EMEA), and Japan have issued guidance (ICH S7B) on preclinical integrated risk assessment strategies for testing the pro-arrhythmic potential of human pharmaceuticals (85). These primarily include in vitro IKr assays and in vivo QT assessment. Preclinical in vitro screening for effects of new pharmaceuticals on heterologoulsy expressed hERG channels constitutes an important part of pharmaceutical screening tree and has gained prominence in early drug discovery. A demand for higher throughput in early discovery employs indirect hERG channel assays that include radioligand binding assays (86), optical assays employing membrane potential dyes (55), and ion-flux assays employing atomic absorption spectroscopy (69,70). Lower throughput high fidelity patch-clamp assays are traditionally incorporated later in the

screening tree, as the compounds progress towards development. The advent of planar patch-clamp technologies has led to increased utilization of platforms that include IonWorksTM HT, IonWorks Quattro, Patchxpress, Qpatch, and Patchliner in safety pharmacology studies (69,70,77,78,87,88). These automated electrophysiology platforms allow direct assessment of potency of compounds on cardiac ion channels and give reliable information to medicinal chemists to enable structure–activity optimization. Potency shifts can be expected in these automated platforms with hydrophobic compounds and are caused by lack of extracellular perfusion, excess of cells per well and high surface to volume ratios.

Although IKr inhibition and QT prolongation are the characteristics of most Torsadogenic drugs, hERG channel block does not always cause QT prolongation nor induce TDP (89). This may be attributable to inhibitory effects of drug on channels such as Cav1.2 counterbalancing the effects of pure IKr inhibition. Thus, hERG inhibition is not always a perfect predictor for proarrhythmic risk in vivo. Specific inhibition or activation of other cardiac ion channels such as Nav1.5, Cav1.2, and HCN4 in the absence of hERG activity can also contribute to proarrhythmic risk. When discrepancies exist between in vitro and in vivo data, ICH S7B recommends additional follow-up studies to understand the mechanistic basis for QT prolongation and proarrhythmic risk. These can include testing the effects of the drug on other ion cardiac channels such as Nav1.5, Cav1.2, and HCN4 in a frequency and state-dependent manner. Ex vivo repolarization assays employing tissues such as cardiac Purkinje fibers (rabbit/dog) (90), ventricular wedge preparations (91), and Langendorff perfused isolated heart (92) are also used as follow-up mechanistic assays to understand proarrhythmic potential of drugs. Ex vivo assays allow assessment of liability in the native environment of the cell where multiple ion channels and transport proteins are expressed with all the accessory subunits in the right stoichiometry. In ex vivo studies, careful consideration should be given to study design with intent to maximize the information obtained from such studies. For example, while Purkinje fiber studies can assess the effects of drugs on multiple action potential parameters (action potential durations for 50% and 90% repolarizations APD_{50} and APD_{90}, the maximum upstroke velocity V_{max}, etc.), adding frequency of stimulation as a variable allows the investigator to assess compound effects on use- and state-dependent inhibition of multiple ion channels that may contribute to proarrhythmia. Analysis of triads, a set of three features of cardiac action potential (namely, the effects on triangulation of action potential, reverse use dependence, and instability) are thought to give a very good assessment of proarrhythmic risk leading to TDP (93,94). Species and gender specific differences that exist in ion channels governing cardiac excitability, repolarization and action potential duration can have a profound impact on the outcome of ex vivo studies and should be carefully considered while selecting test systems. Rabbits have a higher distribution of IKr relative to IKs and may be the species of choice for measuring IKr-mediated proarrhythmic risks. Rodents on the contrary do not express IKr. In a similar manner, Guinea pig is the species of choice to measure IKs-mediated effects. Gender also plays a critical role in proarrhythmic risk and females have longer QT intervals and have a greater propensity for TDP then males (95).

Data from in vitro ion channel assays, in vivo QT studies, and any follow-up mechanistic studies forms an important component of the safety pharmacology data package for regulatory submission. A comprehensive analysis of this

data along with the pharmacokinetic profile of the drug and its physicochemical properties allows integrated risk assessment and ensures safety of drugs in clinics and in human patients.

CONCLUSION

In modern drug discovery, multiple screening approaches are available for both voltage- and ligand-gated ion channels. In practice, these are employed in an integrated manner using the highest throughput assays, representing the least direct index of ion channel function (binding, optical, ion flux), first to support hit identification and initial lead optimization. This results in follow-up evaluation on a smaller subset of compounds using more information-rich electrophysiological techniques, both automated and manual, to gain a high degree of understanding of compound potency and mechanism of action. In this way, the best candidates can be selected for further evaluation.

REFERENCES

1. Hille B. Ion Channels of Excitable Membranes, 3rd ed. Sunderland, MA: Sinauer Associates, Inc., 2001.
2. Tombola F, Pathak MM, Isacoff EY. How does voltage open an ion channel? Annu Rev Cell Dev Biol 2006; 22:23–52.
3. Miller C. ClC chloride channels viewed through a transporter lens. Nature 2006; 440(7083):484–489.
4. Ramsey IS, Delling M, Clapham DE. An introduction to TRP channels. Annu Rev Physiol 2006; 68:619–647.
5. Mayer ML. Glutamate receptors at atomic resolution. Nature 2006; 440(7083):456–462.
6. Sine SM, Engel AG. Recent advances in Cys-loop receptor structure and function. Nature 2006; 440(7083):448–455.
7. Kung C. A possible unifying principle for mechanosensation. Nature 2005; 436(7051):647–654.
8. Riordan JR, Rommens JM, Kerem B, et al. Identification of the cystic fibrosis gene, cloning and characterization of complementary DNA. Science 1989; 245(4922):1066–1073. [Erratum appears in Science 1989; 245(4925):1437].
9. Gadsby DC, Vergani P, Csanady L. The ABC protein turned chloride channel whose failure causes cystic fibrosis. Nature 2006; 440(7083):477–483.
10. Jentsch TJ, Maritzen T, Zdebik AA. Chloride channel diseases resulting from impaired transepithelial transport or vesicular function. J Clin Invest 2005; 115(8):2039–2046.
11. Moss AJ, Kass RS. Long QT syndrome, from channels to cardiac arrhythmias. J Clin Invest 2005; 115(8):2018–2024.
12. Moss AJ, Zareba W, Kaufman ES, et al. Increased risk of arrhythmic events in long-QT syndrome with mutations in the pore region of the human ether-a-go-go-related gene potassium channel. Circulation 2002; 105(7):794–799.
13. January CT, Gong Q, Zhou Z. Long QT syndrome, cellular basis and arrhythmia mechanism in LQT2. J Cardiovasc Electrophysiol 2000; 11(12):1413–1418.
14. Furutani M, Trudeau MC, Hagiwara N, et al. Novel mechanism associated with an inherited cardiac arrhythmia, defective protein trafficking by the mutant HERG (G601S) potassium channel. Circulation 1999; 99(17):2290–2294.
15. Flechtner I, de Lonlay P, Polak M. Diabetes and hypoglycaemia in young children and mutations in the Kir6.2 subunit of the potassium channel, therapeutic consequences. Diabetes Metab 2006; 32(6):569–580.
16. Gloyn AL, Siddiqui J, Ellard S. Mutations in the genes encoding the pancreatic beta-cell KATP channel subunits Kir6.2 (KCNJ11) and SUR1 (ABCC8) in diabetes mellitus and hyperinsulinism. Hum Mutat 2006; 27(3):220–231.

17. George CH, Jundi H, Thomas NL, et al. Ryanodine receptors and ventricular arrhythmias, emerging trends in mutations, mechanisms and therapies. J Mol Cell Cardiol 2007; 42(1):34–50.
18. Scheinman MM, Lam J. Exercise-induced ventricular arrhythmias in patients with no structural cardiac disease. Annu Rev Med 2006; 57:473–484.
19. Meisler MH, Kearney JA. Sodium channel mutations in epilepsy and other neurological disorders. J Clin Invest 2005; 115(8):2010–2017.
20. George AL Jr. Inherited disorders of voltage-gated sodium channels. J Clin Invest 2005; 115(8):1990–1999.
21. Cheng X, Dib-Hajj SD, Tyrrell L, et al. Mutation I136V alters electrophysiological properties of the Na(v)1.7 channel in a family with onset of erythromelalgia in the second decade. Mol Pain 2008; 4:1.
22. Waxman SG. Nav1.7, its mutations, and the syndromes that they cause. Neurology 2007; 69(6):505–507.
23. Sheets PL, Jackson JO II, Waxman SG, et al. A Nav1.7 channel mutation associated with hereditary erythromelalgia contributes to neuronal hyperexcitability and displays reduced lidocaine sensitivity. J Physiol 2007; 581(Pt 3):1019–1031.
24. Jurkat-Rott K, Lehmann-Horn F. Muscle channelopathies and critical points in functional and genetic studies. J Clin Invest 2005; 115(8):2000–2009.
25. Kharkovets T, Hardelin JP, Safieddine S, et al. KCNQ4, a K^+ channel mutated in a form of dominant deafness, is expressed in the inner ear and the central auditory pathway. [See comment]. Proc Natll Acad Sci U S A 2000; 97(8):4333–4338.
26. Van Hauwe P, Coucke PJ, Ensink RJ, et al. Mutations in the KCNQ4 K^+ channel gene, responsible for autosomal dominant hearing loss, cluster in the channel pore region. Am J Med Genet 2000; 93(3):184–187.
27. Priori SG, Napolitano C. Cardiac and skeletal muscle disorders caused by mutations in the intracellular Ca^{2+} release channels. J Clin Invest 2005; 115(8):2033–2038.
28. Hirose S, Zenri F, Akiyoshi H, et al. A novel mutation of KCNQ3 (c.925T → C) in a Japanese family with benign familial neonatal convulsions. Ann Neurol 2000; 47(6):822–826.
29. Yang WP, Levesque PC, Little WA, et al. Functional expression of two KvLQT1-related potassium channels responsible for an inherited idiopathic epilepsy. J Biol Chem 1998; 273(31):19419–19423.
30. Zhu G, Okada M, Murakami T, et al. Dysfunction of M-channel enhances propagation of neuronal excitability in rat hippocampus monitored by multielectrode dish and microdialysis systems. Neurosci Lett 2000; 294(1):53–57.
31. Main MJ, Cryan JE, Dupere JR, et al. Modulation of KCNQ2/3 potassium channels by the novel anticonvulsant retigabine. Mol Pharmacol 2000; 58(2):253–262.
32. Rundfeldt C, Netzer R. The novel anticonvulsant retigabine activates M-currents in Chinese hamster ovary-cells tranfected with human KCNQ2/3 subunits. Neurosci Lett 2000; 282(1–2):73–76.
33. Wickenden AD, Yu W, Zou A, et al. Retigabine, a novel anti-convulsant, enhances activation of KCNQ2/Q3 potassium channels. Mol Pharmacol 2000; 58(3):591–600.
34. Porter RJ, Partiot A, Sachdeo R, et al. Randomized, multicenter, dose-ranging trial of retigabine for partial-onset seizures. Neurology 2007; 68(15):1197–1204.
35. Beeton C, Wulff H, Standifer NE, et al. Kv1.3 channels are a therapeutic target for T cell-mediated autoimmune diseases. Proc Natl Acad Sci U S A 2006; 103(46):17414–17419.
36. Xu J, Wang P, Li Y, et al. The voltage-gated potassium channel Kv1.3 regulates peripheral insulin sensitivity. Proc Natl Acad Sci U S A 2004; 101(9):3112–3117.
37. Tschritter O, Machicao F, Stefan N, et al. A new variant in the human Kv1.3 gene is associated with low insulin sensitivity and impaired glucose tolerance. J Clin Endocrinol Metab 2006; 91(2):654–658.
38. Xu J, Koni PA, Wang P, et al. The voltage-gated potassium channel Kv1.3 regulates energy homeostasis and body weight. Hum Mol Genet 2003; 12(5):551–559.

39. Michelakis E. Anorectic drugs and vascular disease, the role of voltage-gated K+ channels. Vasc Pharmacol 2002; 38(1):51–59.
40. Chizh BA, O'Donnell MB, Napolitano A, et al. The effects of the TRPV1 antagonist SB-705498 on TRPV1 receptor-mediated activity and inflammatory hyperalgesia in humans. Pain 2007; 132(1–2):132–141.
41. Levine JD, Alessandri-Haber N. TRP channels, targets for the relief of pain. Biochim Biophys Acta 2007; 1772(8):989–1003.
42. Facer P, Casula MA, Smith GD, et al. Differential expression of the capsaicin receptor TRPV1 and related novel receptors TRPV3, TRPV4 and TRPM8 in normal human tissues and changes in traumatic and diabetic neuropathy. BMC Neurol 2007; 7:11.
43. Szallasi A, Cortright DN, Blum CA, et al. The vanilloid receptor TRPV1, 10 years from channel cloning to antagonist proof-of-concept. Nat Rev Drug Discov 2007; 6(5):357–372. [Erratum appears in Nat Rev Drug Discov 2007; 6(6):442].
44. Castillo M, Mulet J, Gutierrez LM, et al. Role of the RIC-3 protein in trafficking of serotonin and nicotinic acetylcholine receptors. J Mol Neurosci 2006; 30(1–2):153–156.
45. Williams ME, Burton B, Urrutia A, et al. Ric-3 promotes functional expression of the nicotinic acetylcholine receptor alpha7 subunit in mammalian cells. J Biol Chem 2005; 280(2):1257–1263.
46. Dunlop J, Roncarati R, Jow B, et al. In vitro screening strategies for nicotinic receptor ligands. Biochem Pharmacol 2007; 74(8):1172–1181.
47. Gunthorpe MJ, Rami HK, Jerman JC, et al. Identification and characterisation of SB-366791, a potent and selective vanilloid receptor (VR1/TRPV1) antagonist. Neuropharmacology 2004; 46(1):133–149.
48. Song Y, Buelow B, Perraud AL, et al. Development and validation of a cell-based high-throughput screening assay for TRPM2 channel modulators. J Biomol Screen 2008; 13(1):54–61.
49. Behrendt HJ, Germann T, Gillen C, et al. Characterization of the mouse cold-menthol receptor TRPM8 and vanilloid receptor type-1 VR1 using a fluorometric imaging plate reader (FLIPR) assay. Br J Pharmacol 2004; 141(4):737–745.
50. Liu Y, Lubin ML, Reitz TL, et al. Molecular identification and functional characterization of a temperature-sensitive transient receptor potential channel (TRPM8) from canine. Eur J Pharmacol 2006; 530(1–2):23–32.
51. Xie X, Van Deusen AL, Vitko I, et al. Validation of high throughput screening assays against three subtypes of Ca(v)3 T-type channels using molecular and pharmacologic approaches. Assay Drug Dev Technol 2007; 5(2):191–203.
52. Benjamin ER, Pruthi F, Olanrewaju S, et al. Pharmacological characterization of recombinant N-type calcium channel (Cav2.2) mediated calcium mobilization using FLIPR. Biochem Pharmacol 2006; 72(6):770–782.
53. Rogers KL, Fong WF, Redburn J, et al. Fluorescence detection of plant extracts that affect neuronal voltage-gated Ca^{2+} channels. Eur J Pharm Sci 2002; 15(4):321–330.
54. Whiteaker KL, Gopalakrishnan SM, Groebe D, et al. Validation of FLIPR membrane potential dye for high throughput screening of potassium channel modulators. J Biomol Screen 2001; 6(5):305–312.
55. Baxter DF, Kirk M, Garcia AF, et al. A novel membrane potential-sensitive fluorescent dye improves cell-based assays for ion channels. J Biomol Screen 2002; 7(1):79–85.
56. Wolff C, Fuks B, Chatelain P. Comparative study of membrane potential-sensitive fluorescent probes and their use in ion channel screening assays. J Biomol Screen 2003; 8(5):533–543.
57. Smith JA, Amagasu SM, Hembrador J, et al. Evidence for a multivalent interaction of symmetrical, N-linked, lidocaine dimers with voltage-gated Na^{+} channels. Mol Pharmacol 2006; 69(3):921–931.
58. Joesch C, Guevarra E, Parel SP, et al. Use of FLIPR membrane potential dyes for validation of high-throughput screening with the FLIPR and {micro}ARCS technologies, identification of ion channel modulators acting on the GABAA receptor. J Biomol Screen 2008; 13(3):218–228.

59. Benjamin ER, Pruthi F, Olanrewaju S, et al. State-dependent compound inhibition of Nav1.2 sodium channels using the FLIPR Vm dye, on-target and off-target effects of diverse pharmacological agents. J Biomol Screen 2006; 11(1):29–39.
60. Vickery RG, Amagasu SM, Chang R, et al. Comparison of the pharmacological properties of rat Na(V)1.8 with rat Na(V)1.2a and human Na(V)1.5 voltage-gated sodium channel subtypes using a membrane potential sensitive dye and FLIPR. Receptors Channels 2004; 10(1):11–23.
61. Alaux S, Kusk M, Sagot E, et al. Chemoenzymatic synthesis of a series of 4-substituted glutamate analogues and pharmacological characterization at human glutamate transporters subtypes 1–3. J Med Chem 2005; 48(25):7980–7992.
62. Benjamin ER, Skelton J, Hanway D, et al. Validation of a fluorescent imaging plate reader membrane potential assay for high-throughput screening of glycine transporter modulators. J Biomol Screen 2005; 10(4):365–373.
63. Gonzalez JE, Oades K, Leychkis Y, et al. Cell-based assays and instrumentation for screening ion-channel targets. Drug Discov Today 1999; 4(9):431–439.
64. Liu CJ, Priest BT, Bugianesi RM, et al. A high-capacity membrane potential FRET-based assay for NaV1.8 channels. Assay Drug Dev Technol 2006; 4(1):37–48.
65. Trivedi S, Dekermendjian K, Julien R, et al. Cellular HTS assays for pharmacological characterization of Na(V)1.7 modulators. Assay Drug Dev Technol 2008; 6(2):167–179.
66. Schroeder K, Neagle B, Trezise DJ, et al. Ionworks HT, a new high-throughput electrophysiology measurement platform. J Biomol Screen 2003; 8(1):50–64.
67. Dunlop J, Bowlby M, Peri R, et al. High-throughput electrophysiology, an emerging paradigm for ion-channel screening and physiology. Nat Rev Drug Discov 2008; 7(4):358–368.
68. Jow F, Shen R, Chanda P, et al. Validation of a medium-throughput electrophysiological assay for KCNQ2/3 channel enhancers using IonWorks HT. J Biomol Screen 2007; 12(8):1059–1067.
69. Bridgland-Taylor MH, Hargreaves AC, Easter A, et al. Optimisation and validation of a medium-throughput electrophysiology-based hERG assay using IonWorks HT. J Pharmacol Toxicol Methods 2006; 54(2):189–199.
70. Sorota S, Zhang XS, Margulis M, et al. Characterization of a hERG screen using the IonWorks HT, comparison to a hERG rubidium efflux screen. Assay Drug Dev Technol 2005; 3(1):47–57.
71. Finkel A, Wittel A, Yang N, et al. Population patch clamp improves data consistency and success rates in the measurement of ionic currents. J Biomol Screen 2006; 11(5):488–496.
72. Harmer AR, Abi-Gerges N, Easter A, et al. Optimisation and validation of a medium-throughput electrophysiology-based hNav1.5 assay using IonWorkstrade mark. J Pharmacol Toxicol Methods 2008; 57(1):30–41.
73. John VH, Dale TJ, Hollands EC, et al. Novel 384-well population patch clamp electrophysiology assays for Ca^{2+}-activated K^{+} channels. J Biomol Screen 2007; 12(1):50–60.
74. Kutchinsky J, Friis S, Asmild M, et al. Characterization of potassium channel modulators with QPatch automated patch-clamp technology, system characteristics and performance. Assay Drug Dev Technol 2003; 1(5):685–693.
75. Asmild M, Oswald N, Krzywkowski KM, et al. Upscaling and automation of electrophysiology, toward high throughput screening in ion channel drug discovery. Receptors Channels 2003; 9(1):49–58.
76. Trepakova ES, Malik MG, Imredy JP, et al. Application of PatchXpress planar patch clamp technology to the screening of new drug candidates for cardiac KCNQ1/KCNE1 (I Ks) activity. Assay Drug Dev Technol 2007; 5(5):617–627.
77. Guo L, Guthrie H. Automated electrophysiology in the preclinical evaluation of drugs for potential QT prolongation. J Pharmacol Toxicol Methods 2005; 52(1):123–135.
78. Dubin AE, Nasser N, Rohrbacher J, et al. Identifying modulators of hERG channel activity using the PatchXpress planar patch clamp. J Biomol Screen 2005; 10(2):168–181.

79. Terstappen GC. Functional analysis of native and recombinant ion channels using a high-capacity nonradioactive rubidium efflux assay. Anal Biochem 1999; 272(2):149–155.
80. Rezazadeh S, Hesketh JC, Fedida D. Rb^+ flux through hERG channels affects the potency of channel blocking drugs, correlation with data obtained using a high-throughput Rb^+ efflux assay. J Biomol Screen 2004; 9(7):588–597.
81. Gill S, Gill R, Wicks D, et al. A cell-based Rb(+)-flux assay of the Kv1.3 potassium channel. Assay Drug Dev Technol 2007; 5(3):373–380.
82. Jow F, Tseng E, Maddox T, et al. Rb^+ efflux through functional activation of cardiac KCNQ1/minK channels by the benzodiazepine R-L3 (L-364,373). Assay Drug Dev Technol 2006; 4(4):443–450.
83. Scott CW, Wilkins DE, Trivedi S, et al. A medium-throughput functional assay of KCNQ2 potassium channels using rubidium efflux and atomic absorption spectrometry. Anal Biochem 2003; 319(2):251–257.
84. Preziosi P. Science, pharmacoeconomics and ethics in drug R&D, a sustainable future scenario? Nat Rev Drug Discov 2004; 3(6):521–526.
85. Guidance for industry S7B Nonclinical evaluation of the potential for delayed Ventricular Repolarization (QT interval prolongation) by human pharmaceuticals.
86. Finlayson K, Turnbull L, January CT, et al. [^{3}H]Dofetilide binding to HERG transfected membranes, a potential high throughput preclinical screen. Eur J Pharmacol 2001; 430(1):147–148.
87. Guthrie H, Livingston FS, Gubler U, et al. A place for high-throughput electrophysiology in cardiac safety, screening hERG cell lines and novel compounds with the ion works HTTM system. J Biomol Screen 2005; 10(8):832–840.
88. Ly JQ, Shyy G, Misner DL. Assessing hERG channel inhibition using PatchXpress. Clin Lab Med 2007; 27(1):201–208.
89. Sanguinetti MC, Tristani-Firouzi M. hERG potassium channels and cardiac arrhythmia. Nature 2006; 440(7083):463–469.
90. Gintant GA, Limberis JT, McDermott JS, et al. The canine Purkinje fiber, an in vitro model system for acquired long QT syndrome and drug-induced arrhythmogenesis. J Cardiovasc Pharmacol 2001; 37(5):607–618.
91. Liu T, Brown BS, Wu Y, et al. Validation of the isolated arterially perfused rabbit ventricular wedge in preclinical assessment of drug-induced proarrhythmias. Heart Rhythm 2006; 3(8):948–956.
92. Lawrence CL, Bridgland-Taylor MH, Pollard CE, et al. A rabbit Langendorff heart proarrhythmia model, predictive value for clinical identification of Torsades dePointes. Br J Pharmacol 2006; 149(7):845–860.
93. Hondeghem LM. Relative contributions of TRIaD and QT to proarrhythmia. J Cardiovasc Electrophysiol 2007; 18(6):655–657.
94. Hondeghem LM. Use and abuse of QT and TRIaD in cardiac safety research: Importance of study design and conduct. Eur J Pharmacol 2008; 584(1):1–9.
95. Lu HR, Marien R, Saels A, et al. Are there sex-specific differences in ventricular repolarization or in drug-induced early after depolarizations in isolated rabbit purkinje fibers? J Cardiovasc Pharmacol 2000; 36(1):132–139.

10 Wheat from Chaff: General and Mechanistic Triage of Screening Hits for Enzyme Targets

Mark R. Harpel

Heart Failure Biochemistry and Cell Biology, Metabolic Pathways Center of Excellence in Drug Discovery, GlaxoSmithKline, King of Prussia, Pennsylvania, U.S.A.

INTRODUCTION

Since the 1990s, high-throughput screening (HTS) has been, and will likely continue to be, a key engine to discover novel chemical starting points for optimization into enzyme-targeted, small-molecule therapeutics. But even from the introduction of HTS into the pharmaceutical industry, there has been ongoing debate surrounding the effectiveness of this approach, its total impact on drug discovery, and its benefits versus cost to the bottom line of building strong drug pipelines and delivering new drugs to patients (for example, see Ref. 1). Pursuing false leads from a screening campaign is therefore unacceptable, given the associated cost, loss of time, and loss of opportunity to deliver much-needed new drug product.

As screening technologies mature, there will continue to be a need to efficiently triage the results in order to uncover valid inhibitors from the potential quagmire of false positive hits, and delineate those compounds with the best chance of success for conversion into bona fide leads and (eventually) drugs. Indeed, it is generally agreed that selection of a lead inhibitor class and dedication of chemistry resources to its optimization are usually the most important and expensive decisions made in the early drug discovery process (2).

Reviews, chapters, and entire texts (including the previous edition of this series) have been devoted to the design and analysis of enzyme-based screens (for examples, see Refs. 3–5), and the reader is referred to these for general discussions and specific details. This chapter is not intended to supersede these sources, and in fact I draw upon them throughout, as I have in laboratory practice. The chapter deals little with such issues as chemical tractability, detailed selectivity screening, and pharmacokinetics and toxicity screening, but instead focuses on postscreening activities designed to validate screening hits as true inhibitors of the target enzyme and to prioritize them according to desirable and progressible mechanisms of action. Although newer affinity-based technologies are becoming more prevalent as screening tools (2,6–8), activity-based biochemical screening continues to be a mainstay of the pharmaceutical industry and so will be the major emphasis; validation of screening hits as target-based inhibitors and selection of best hits for progression as leads are common postscreening goals, regardless of discovery engine employed.

This chapter considers two general aspects of postscreening analysis: "general triage" and "mechanistic triage". Presented under the topic of general

triage are those activities that immediately follow a screening campaign and are designed to confirm the inhibitory activity of the original screening hit, eliminate obvious artifacts due to assay interference, filter any reactive compounds or hits deemed undesirable from a physicochemical standpoint, and provide an initial analysis of structure–activity relationships (SAR) and clustering of hits. The mechanistic triage provides a further confirmation of inhibitory activities and allows for binning of hits for further prioritization according to mechanism of action. These studies provide the program team with a quantitative understanding of true inhibitor potencies and other information required to select which class(es) of inhibitor(s) should receive further chemistry funding, as well as more advanced biological and biochemical support.

THE SCREEN

Screening strategies and basic enzymology considerations involved in screening assay design will not be discussed to great extent in this chapter. However, it is important to briefly discuss screening goals and options in order to understand requirements for postscreen follow-up activities. In broad terms, the goal of a screen is to discover small-molecule starting points for chemical elaboration and optimization into a candidate drug molecule. In many companies, this phase is called "Lead Identification"; for the purposes of this chapter, the screen is used to find "hits" from which "leads" (or lead series, also referred to as chemotypes) are selected for optimization.

How a screen is carried out often reflects the level of understanding of the enzyme's in vitro chemical and kinetic mechanisms, as well as in vivo function and physiological environment. This knowledge provides the researcher with the luxury of designing whether the screen should be poised to find the widest range of inhibitor types (a "balanced" screen) or directed towards one given mechanism (5). For example, the discovery of allosteric inhibitors for kinases has raised much interest in searching for similar inhibitors that might drive kinase-inhibitor selectivity (9), whereas a search for inhibitors of a less-characterized enzyme might cast a wide net with a balanced screen. An ideal screen would target a certain mechanism of inhibition (corresponding to a rate-limiting kinetic step or susceptible conformation of the enzyme), utilize full-length protein and native substrate (in complex with associated cofactors and accessory proteins) and employ substrate concentrations as found in vivo or with the best chance of selecting a physiologically active inhibitor (5). However, the reality (and pace) of industrial biochemical screening is often such that, for example, the full kinetic mechanism for the enzyme may not yet be fully understood, the physiological substrate may not yet be known, only recombinant enzyme may be available for screening, or the only screening assay that is available with sufficient signal-to-noise entails a technology prone to interference. These are the types of restrictions that dictate the level of care that must be taken after the screen to sort through hits for false positives and may dictate the course for follow-up evaluation as potential leads. For example, if the catalytic domain of an enzyme is used for HTS, then it is incumbent on the research team to evaluate the effects of inhibitors using full-length enzyme, and preferably in a physiologically representative context, during postscreen follow-up. At a more basic level are questions of hit validation and determination of initial inhibition mechanisms. Studies to answer these questions will be guided by the criteria for hit progression.

CRITERIA FOR A PROGRESSIBLE HIT

Recognizing the importance of selecting the best hits for promotion to lead status, there has been much discussion within the industry of what characteristics of a hit will produce a good lead. Accordingly, there is now a realization that potency alone is not sufficient [a "false predictor" (10)] for success, and that an ideal lead molecule must exhibit a balance of potency, selectivity, and favorable physicochemical properties. An in-depth discussion of this topic is out of the scope of this chapter. However, retrospective surveys (see Refs. 1,10–12 and references therein) have led to new concepts of druggability and lead-likeness, from the now-famous "rule-of-five" of Lipinski and coworkers (12) to the concept of ligand efficiency as a "per-atom" normalized measure of binding energy (10), which are now evaluated during hit analyses for early enrichment of desirable physicochemical properties. Aided through computational analyses (13–15), screening libraries are increasingly being evaluated with these concepts in mind (1). As an example of the difficulty in achieving the best balance of properties, one recent analysis of drugs in the clinic and trends in patent literature showed that lipophilicity is a primary determinant of the clinical success of a drug. However, lipophilicity is also predictive of later stage attrition due to lack of selectivity (11). An earlier emphasis on other causes of late-stage attrition, such as ADME-Tox (absorption, distribution, metabolism, excretion, and toxicity) liabilities, has also been advocated to increase the chances of success from hit through preclinical development (10).

At the top of all of these considerations, and for even the best designed inhibitor screen, is the need to sort through the (potentially) thousands of HTS hits with the most basic question in mind: Is the positive signal from the screen a true representation of enzyme inhibition or an assay artifact? Thus, criteria have been established for a valid hit from a screening campaign. As reviewed by Wunberg et al. (10) such a compound should be inherently stable and nonreactive, exhibit a defined structure and purity (hopefully those expected from the library annotation), show reasonable and confirmable potency (usually defined by the target, the assay, and needs of the team), and be free from known nuisance mechanisms of inhibition. These will be the starting points for discussion in the next few sections. For progression to lead status, it is desirable for the selected series to exhibit some degree of selectivity for the target enzyme and an emerging SAR among compounds of similar structure from the screening library. As addressed in the rest of the chapter, a confirmed (and preferred) mechanism of action is ultimately what should trigger the commitment to lead progression for a given hit class, followed by advancement into further studies that probe the ability of the compound to inhibit the enzyme under conditions approaching its physiological and pathological state.

GENERAL TRIAGE TO VERIFY HITS

Upon completion of the primary screen, the immediate tasks for the discovery team are to reconfirm the inhibitory activity of screening hits, carry out sufficient counterscreens to identify any assay artifacts and eliminate false hits, and provide an initial quantification of potency to determine SAR trends (Fig. 1). Further selection of compounds usually involves the combined expert judgment of medicinal chemists, with informatics input for nearest-neighbor clustering analysis of hits and evaluation for general properties of "lead-likeness" (15). These

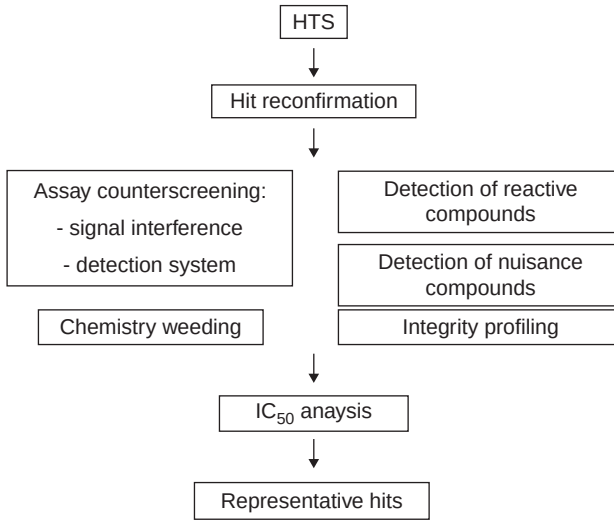

FIGURE 1 Example work flow for general triage of screening hits.

efforts identify the true enzyme inhibitors and provide the basis for selecting compounds for further study.

Depending on the nature of the primary enzyme target and the screening assay format, both false negatives and false positives can occur. False negatives are generally more tolerated for several reasons: Most libraries are perceived to contain sufficient diversity that significant information will not be lost with the elimination of a few hits due to false negatives, and it is thought that "lost" compounds will frequently be found during postscreen hit clustering and testing of analogs. On the other hand, the presence of false positives may confound overall hit analysis and mislead follow-up efforts. Therefore, these are the major focus for the sections to follow.

False positive screening hits may arise for a number of reasons (2–4). In broad terms, these can be classified into off-target interactions between assay components and screening compounds, direct interference of the screening compound with assay signal, interfering physicochemical properties of the screening hit, and/or unsatisfactory sample purity. These topics are described in more detail in the following sections.

Spectral Interference

Almost all assay platforms suffer from the potential for direct interference of assay readouts by screening compounds, the most straightforward interference resulting from spectral overlap between screening compounds and reporter groups in optical and fluorescence assay formats (16). Fluorescence assays dominate HTS platforms because of their high sensitivity, flexibility across multiple homogeneous formats, ease of miniaturization, and applicability across a wide range of targets. However, fluorescent readouts are also highly sensitive to spectral artifacts. For instance, false negatives occur due to light scattering, colored, or fluorescent compounds that contribute to the net fluorescence signal. In

contrast, spectral overlap between the reporter fluorophore and a strongly absorbing compound will quench the reporter signal and produce a false positive reduction in signal. These effects may in part be ameliorated if rates are measured as slopes from multi-timepoint kinetic-read assays, but are particularly troublesome for extrapolated rates measured by endpoint assays.

Available fluorescent platforms are generally classified into several categories: simple fluorescence intensity measurements as described above, fluorescence polarization (FP), radiation-independent energy transfer (FRET), and time-resolved measurements (HTRF, TR-FRET). The practical and theoretical bases of these formats are reviewed elsewhere (4,16–18). Each of these approaches exhibits a varying degree of sensitivity to spectral interference. However, the newer technologies have been designed, in part, to minimize some of the interference inherent in standard fluorescence intensity measurements. For example, in TR-FRET measurements, resonance energy transfer is detected between a lanthanide chelate donor and fluorescent acceptor molecule. Many variants of this format exist, including capture of donor (or acceptor)-labeled product of the enzymatic reaction by a product-specific antibody, or displacement by unlabeled enzyme product of a preformed FRET pair between donor (or acceptor)-labeled product and an acceptor (or donor)-labeled antibody. Lanthanide-chelate donors are characterized by long fluorescence lifetimes. By introducing a delay between excitation and emission detection, TR-FRET is theoretically able to discriminate between a real signal and the short-lived fluorescence of interfering assay components, including screening compounds. In addition, the measurement incorporates the ratio of emission from donor and acceptor, and thus normalizes for direct compound interference given the close proximity of emission wavelengths between donor/acceptor pair. However, even in this instance, screening compounds may preferentially enhance or quench one or the other of the emission wavelengths, and with sufficiently long lifetime, to affect the TR-FRET signal.

Frequently, false hits due to fluorescence interference fall out of consideration in the reconfirmation stage or during IC_{50} analysis, based on anomalous concentration response characteristics (discussed further below) or inconsistent (or absent) SAR among related compounds. Careful inspection of primary data may also detect symptomatic abnormalities, for example high initial reads. In those cases of an obviously high hit rate or a particularly sensitive assay format, fluorescence interferences due to absorption or fluorescence of screening compounds can be determined by direct reads of compounds in the presence of the fluorescent detection signal.

Signal quenching by colored and fluorescent compounds is also a common issue for scintillation proximity assays (SPA) used to detect radioactive reaction products. As above, these can be detected by direct titration of compound into preformed SPA complexes. The impact of colored compounds on the SPA signal can also be lessened by the use of a color quenching correction (19).

Inhibition of Detection System

Another source of false inhibition is interference of secondary reagents required for signal generation. For example, any format that requires antibody-based capture of product to form reaction signal (e.g., ELISA, antibody-capture SPA, TR-FRET, etc.) may exhibit apparent inhibition of the target enzyme if a screening

compound is able to disrupt the product/antibody complex. Although usually not an issue for optimized product and antibody pairs, such false positives may be detected by directly assaying for the ability of compounds to disrupt complex formation between reaction product and antibody.

Screens that employ enzyme-coupling systems are another example of a complex system that may suffer from detection interference. Many enzymes form reaction products that are not amenable to direct detection. To obtain a convenient spectral readout, the primary enzyme's reaction may be monitored by coupling its product to the reaction of an additional enzyme (or enzyme cascade). The coupling reaction in turn produces a colorimetric (e.g., lactate dehydrogenase-coupled NADPH oxidation to detect pyruvate formation) or fluorescent (e.g., horseradish peroxidase-coupled fluorescent dye oxidation to detect H_2O_2 formation) signal. As first shown by Easterby (20) and Cleland (21), formation of a reporter signal by a coupled reaction is limited by the coupling enzyme's ability to keep up with formation of product by the primary enzyme, as dictated by the concentration and efficiency of the coupling enzyme(s). Thus, the steady-state concentration of the target enzyme's reaction product (P) is a function of the target enzyme's reaction velocity (v) and a lag factor (τ), dependent on the properties of the coupling enzyme(s):

$$[P]_{ss} = v\tau, \tag{1}$$

$$\text{where } \tau = \sum \frac{K_{m,n}}{V_{\max,n}} \tag{2}$$

$$\text{and } V_{\max,n} = k_{\text{cat},n}[E]_{\text{coupling},n} \tag{3}$$

K_m, $V_{\max}$, k_{cat}, and $[E]_{\text{coupling}}$ all correspond to properties of the coupling enzyme. The coupling system may require a multienzyme cascade (22) and "n" in the above equations refers to the number of coupling enzymes in the system. The overall signal produced by this cascade is then described by the equation:

$$[\text{signal}] = v(t + \tau\, e^{-t/\tau} - \tau). \tag{4}$$

The net result of this theory is that a certain kinetic lag, τ, precedes the steady-state production of signal in all coupled assays. But given enough time, such reactions reach a rate of signal formation that equates to the rate of formation of primary reaction product, P. The extent of this lag is modulated by the kinetic parameters of the coupling enzyme and how much of it (and its associated secondary reaction substrates and cofactors) can be tolerated in the reaction, as shown in Figure 2(A) (traces a and b). However, there is a balance between coupling efficiency, cost of assay, and availability of reagents in the design of a coupled assay (21), which may limit the coupling efficiency. Substantial inhibition of the coupling enzyme can be tolerated in a highly optimized coupling assay, but would nonetheless result in a diagnostic extension of the lag phase [Fig. 2(A), traces c and d]. If only the coupling enzyme(s) is inhibited, the kinetic traces should eventually exhibit the same steady-state rate as control. However, this may not be readily apparent, especially in screens that rely on an endpoint read. Endpoints by definition extrapolate back to a zero time point to estimate slopes, which leads to an artifactual reduction of rate in the presence of an undetected lag phase (Fig. 2B).

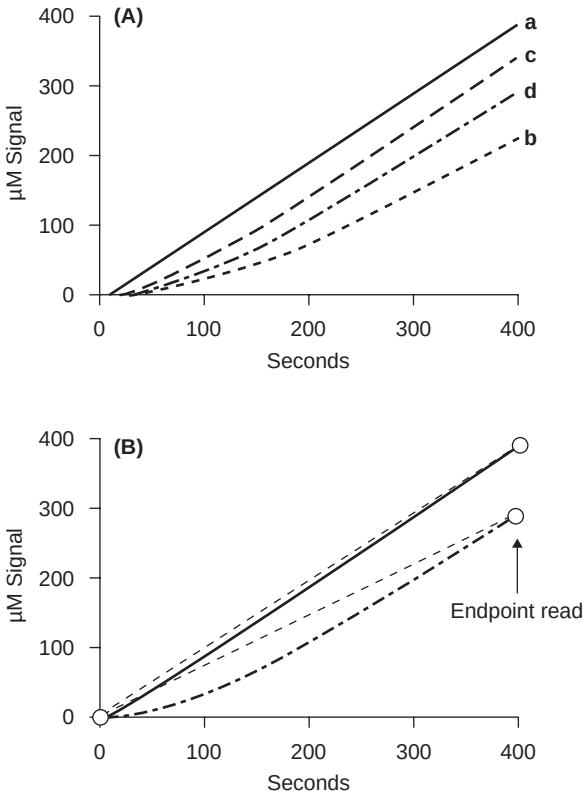

FIGURE 2 Simulated time courses for an enzyme-coupled assay system. The theoretical treatment is as described in the text. In all cases, the turnover rate of the primary enzyme ("v") is assumed to be 1 μM/s, and the inherent kinetic constants for the coupling enzyme ("E") are $K_m = 250$ μM (using product of the primary reaction as substrate) and $k_{cat} = 25\ s^{-1}$. (**A**) Conditions: (a) optimized coupling reaction ($[E] = 1$ μM; $\tau = 10$ sec); (b) system limited by level of coupling enzyme ($[E] = 0.05$ μM; $\tau = 200$ sec); (c,d) system limited by inhibition of coupling enzyme (conditions as in a but with $[I]/K_i = 5$, which increases τ to 60 sec, and $[I]/K_i = 10$, which increases τ to 110 sec). (**B**) Time courses for conditions (a) and (d) in black, with grey dashed lines representing the extrapolated slopes that would be derived from a single-read analysis at $t = 400$ sec.

Several strategies may be taken to weed out compounds that interfere with the coupling enzyme's turnover of primary reaction product in a coupled assay system. Direct assays can be carried out for inhibition of the coupling enzyme. Inhibitors of the coupling system may also be eliminated by counterscreening hits using the same coupling system, but with a different primary enzyme that produces the same reaction product as the screening target enzyme. If the related enzyme is judiciously chosen to also address selectivity considerations, any compound that is positive in this counterscreen may then be eliminated from consideration regardless of whether it inhibits the coupling enzyme(s) or the undesired counterscreening enzyme.

Reconfirmation: Utility of an Orthogonal Assay

Reconfirmation of screening hits is routinely carried out as one of the first steps of a general screening triage and therefore usually utilizes the same assay format as the original screen. The discussion thus far has focused on potential causes for false screening positives that may be related to either general interference with the screening assay technology components or by direct, but undesired, interference with the target enzyme; these false positives would likely be retained during reconfirmation at a single inhibitor concentration using the original screening assay format. One logical test to discriminate assay-specific versus target-specific inhibition would therefore be to test for enzyme inhibition under similar reaction conditions but using an alternative assay format that employs a direct detection method independent of the original screening technology (referred to as an "orthogonal" assay). This step may require a low-throughput assay more suitable for the work described under the mechanistic triage section of this chapter (e.g., HPLC or filter-capture of radiolabeled product). However, it is also worth considering whether an orthogonal format could be incorporated into a general screening scheme, if not during initial reconfirmation then when determining initial IC_{50} values for the hits.

Reactive Compounds

Chemical reactivity of a screening hit must be detected early in the discovery process to avoid distracting the program from productive hit optimization or derailing it in later stages of development (23–26). The ability of a compound to chemically modify components of the screening assay may lead to false positive screening hits (e.g., modification of substrate or components of the detection system) or select for undesirable inhibition mechanisms (e.g., covalent inactivation of target enzyme). Further along the pathway, the potential for in vivo modification of proteins by reactive compounds may elicit direct toxic effects (24,26) or lead to idiosyncratic drug reactions due to covalent drug–protein adducts (26,27). The latter effects may in many cases result from downstream in vivo metabolites of the compounds, which will not be discussed here but are reviewed elsewhere (27). Frequently, these compounds also suffer from low inherent stability, which confounds SAR and presents a pharmacokinetic liability for advancement into plasma-based, cellular, and in vivo evaluations.

The presence of electrophilic substituents in library compounds is a primary cause of false screening hits, because of their ability to alkylate (or acylate) and consequently inactivate, the screening enzyme and/or other assay components (23,28). This reactivity may either reflect a general reactivity towards nucleophilic assay components or a specific inhibition of the target enzyme's catalytic mechanism. For example, enzymes that employ nucleophilic catalysis, such as serine hydrolases, are particularly sensitive to active-site modification and inactivation by reactive electrophiles that access the catalytic serine residue. Such reactive compounds may be detected during general screening approaches (discussed in this section) or in target-specific follow-up assays (discussed further below in the section on reversibility).

Visual inspection and computational analysis of screening hits for potentially reactive structural features (29,30) are often sufficient to remove a reactive compound from postscreen consideration. However, these are often subjective analyses and are limited by the experiences or databases upon which they

are built. Hence, reactive hits often remain undetected and must be identified through other means. Additionally, the actual chemical entity responsible for the observed inhibition may not reside in the parent compound, but in an undetected (and perhaps minor) impurity such as a synthetic intermediate or a decomposition product that arose during compound storage (25).

Experimentally, several approaches have been described to identify and evaluate inherent reactivity of compounds according to their propensity to form adducts with reactive nucleophiles, usually thiols. Historically, the most widely applied approach was that of Epps and Taylor (31), which monitors the reactivity of reduced glutathione with test compounds according to their ability to interfere with the fluorimetric reaction between glutathione and fluorescein-5-maleimide (or some other colorimetric or fluorimetric thiol–reactive probe). This method is readily carried out with high throughput and does not require specialized equipment. However, there are limitations to the method, in particular interferences and reliance on a small molecule surrogate to mimic the reactivity of cysteines in a native protein environment (25).

To address some of these concerns, Huth et al. developed a new assay, termed ALARM-NMR (a La assay to detect reactive molecules by nuclear magnetic resonance) (25). This assay uses NMR to monitor the environments of two cysteines in a 224–amino acid portion of the human La antigen protein. One of these cysteines is particularly reactive and seems not to reside in a well-defined binding pocket on the protein. Because small molecules can thus freely access the cysteine, modification of the cysteine primarily reflects the inherent reactivity of the electrophile instead of binding phenomena. Furthermore, ALARM-NMR can also sense oxidation of the primary cysteine. Although the approach requires more sophisticated equipment and methodologies, it provides greater flexibility (e.g., it can be run in the presence of dithiothreitol), is more sensitive to reactive compounds, is less prone to interference, and provides a more protein-centric analysis of compound reactivity than the fluorescent glutathione method.

Redox-active compounds are another source of false positives. As with electrophilic compounds, the sensitivity of an assay towards a redox-active screening compound will reflect the properties of the primary screening target and/or assay detection technology employed. Thus, enzymes containing redox-active cofactors or readily oxidized catalytic residues (if inactivating), and assays utilizing redox-based substrates, will be most impacted (32). Redox reactive compounds may also confound further downstream analyses and present a general liability (e.g., if associated with mitochondrial toxicity).

Redox-active compounds were traditionally detected by assessing the damage that they did to target proteins, or by inference from a related event such as oxidative toxicity. However, Lor and colleagues recently described an elegant and robust assay for the detection and characterization of oxidizing compounds (32). Following up on the results of a screen for activators of glucokinase, they observed that a large number of primary hits (discovered with an assay that coupled gluose-6-phosphate formation to diaphorase-catalyzed reduction of resazurin via NADH formed by glucose-6-phosphate dehydrogenase) failed to confirm in an orthogonal absorbance assay. Rather, these false positives directly catalyzed the reduction of resazurin in the presence of dithiothreitol contained in the reaction buffer. Application of resazurin and dithiothreitol to hits from a number of screens with target enzymes that contain a readily oxidizable active

site (e.g., mononuclear nonheme iron enzymes, cysteine proteases, etc.) showed its general utility for detecting oxidizing compounds and its superior sensitivity over an approach of simply monitoring disulfide formation (oxidation) of dithiothreitol. This enhancement was attributed to a catalytic amplification of resazurin reduction by the interfering compounds. This reaction also demonstrates the potential for direct interference by oxidizing compounds in screening assays; for example, oxidation of resorufin to resazurin (the reverse direction as above) is a common read-out for systems that can be coupled to horseradish peroxidase, and so will be susceptible to interference from redox-active compounds.

Regardless of the assay utilized to detect inherent chemical reactivity of screening hits, further experiments must be carried out if the goal is to determine how these compounds inhibit the screening assay. If the observed inhibition stems from interference with the assay detection system or by substrate modification, there would be no further interest in the compound. These possibilities can be tested by direct analysis for adduct formation or modification of the impacted reaction components via, for example, mass spectrometric analysis. Use of an orthogonal assay may also discriminate between assay-technology/component-specific and target enzyme-specific effects. Additional biochemical analyses, such as evaluation of reversibility of inhibition by the compound, would provide confirmation of an on-target inactivation mechanism (see section below on reversibility).

Although there is valid concern over progressing an inhibitor that acts via covalent modification of the target enzyme, there may be interest in pursuing such a compound as a mechanistic tool. Furthermore, there has been a recent re-evaluation of whether inhibitors that exhibit a long residency time on the target enzyme, including inhibitors that act according to a covalent mechanism, may elicit the greatest efficacy in vivo (33,34). Should their inherent reactivity be mechanism (or active-site)-specific and not a liability for general toxicity or pharmacokinetics, such reactive compounds may provide valid starting points for lead optimization. But pursuit of such a lead requires dedication from the program team to progress them with downsides of a covalent mechanism in mind (23).

Structural Integrity of Hits

False positives, or at least confounding SAR, can arise when the structure of a screening hit cannot be verified. Initial operator errors (e.g., sample misidentification or sample impurity upon library deposition) or routine sample mishandling of library compounds have now been largely resolved, as most companies have optimized their infrastructure for compound management and submission criteria (35). But sample integrity may still be an issue, especially with acquired compounds. More frequently, compound integrity issues arise from compound degradation during storage. Solution stores in dimethyl sulfoxide (DMSO) are known to react with oxygen and water with age and during freeze/thaw cycles, which may lead to degradation and/or insolubility (25). Even compounds stored as solids may react with water, oxygen, and counterions. In addition, there is always the potential, even with well-characterized compounds, for carryover of reactive synthetic reagents that are not readily detected during standard post-synthesis compound characterization or those that are at sufficiently low

levels to fail detection yet affect a screen. These may not interfere with all classes of enzymes, and so may not be detected as general interfering compounds; for example, serine hydrolases are generally more reactive towards common electrophilic synthetic reagents than other types of enzymes, and so may be more sensitive to low-level reactive contaminants.

Understanding the potential loss of productivity that results from such issues, several initiatives have been launched within the industry to address library integrity through robust compound profiling. These efforts represent a balance between management of risk with the resources required for profiling and the cost of consuming precious compound stocks. In one such report, researchers at Wyeth prioritized the depth of analysis required to address compound identity and purity according to stage of the discovery process (35). Thus, higher resolution profiling approaches are appropriate later in discovery or with a few select compounds, whereas lower resolution methods may suffice to build confidence in overall screen performance and SAR for earlier or more general analyses. Similar approaches have also been a large component of library enhancement efforts taken by other companies in the industry (1).

Even with a well-characterized library, there is still benefit in considering the purity of hits prior to commitment of chemistry resourcing for SAR. In the best of worlds, screening hits would be quickly resynthesized and reconfirmed as inhibitors of the target enzyme. But resynthesis requires time and resourcing that may slow down other aspects of the program. Therefore, it is usually reserved for compounds that are selected for further evaluation, such as the mechanistic triaging described below. In our experience, in the absence of resynthesis, advanced studies are best carried out using solid, resupplied material that has undergone rigorous quality control. For further study of compounds that have questionable integrity, repurification from liquid stocks may suffice until resynthesis of the original hit and analogs is accomplished.

Pertinent to this discussion is what one does with a compound that does not confirm upon integrity profiling. This may not always eliminate a hit from further consideration. But it does bring with it considerable risk, a requirement to define the structure of the actual inhibitory species, elimination of concerns about untoward reactivity by contaminating species, and an organizational commitment to resource such a venture. Pursuit of an unknown species is usually based on consideration of potency alone, and so does not consider properties that may be more optimal in other screening hits. Obviously, such a decision depends upon the prioritization of this type of hit relative to others, and is usually undertaken only in the absence of better options.

Concentration–Response Curves

Following reconfirmation, couterscreening for assay artifacts and elimination of obviously reactive compounds, the screening group usually provides the program team with a concentration–response analysis of hits for enzyme inhibition. Beyond providing a more quantitative definition of inhibitor potencies for early rank ordering of hits and initial SAR, the characteristics of inhibitor concentration–response curves may provide indications of nonideal behavior and propensity for nonspecific inhibition of the target enzyme. Thus, concentration–response curves should receive careful analysis beyond delivery of a potency index.

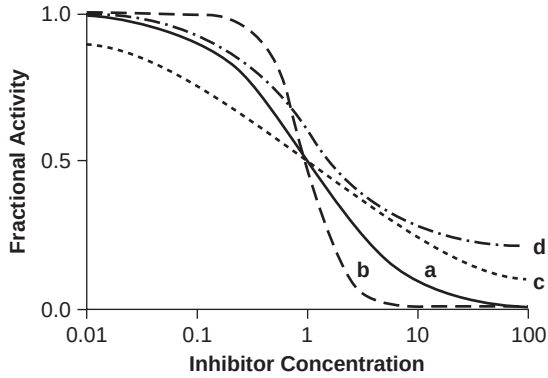

FIGURE 3 Example IC_{50} curves: (a) ideal response (full inhibition, Hill slope = 1), (b) steep dose response (Hill slope = 2.5), (c) shallow dose response (Hill slope = 0.5), and (d) partial inhibition with normal Hill slope (80% inhibition; Hill slope = 1).

Concentration–Response Curves: Data Fitting and the Ideal Response

Most enzyme–inhibitor titration response curves can be fitted by the four-parameter equation:

$$y = \frac{y_{\max} - y_{\min}}{1 + ([I]/\mathrm{IC}_{50})^h} + y_{\min}, \tag{5}$$

where y = fractional activity = $v_{\text{inhibited}}/v_{\text{control}}$, $y_{\max}$ and $y_{\min}$ describe the respective maximal and minimal responses, and h is the Hill coefficient describing the steepness of the dose response. This formulation is usually viewed as a semilogarithmic plot, as shown in Figure 3. IC_{50} relates the half-saturation point for inhibitor action under these conditions and is a well-acknowledged parameter of potency for initial rank ordering of screening hits within and between chemical series. Unfortunately, issues may arise if data are fitted to this full form of the equation and only the value for IC_{50} is reported for hit evaluation. Namely, an ideal enzyme inhibitor, analyzed with a properly designed assay, is expected to follow a defined set of behaviors: $y_{\max}$ should equal unity (full activity of control), $y_{\min}$ should achieve a value equal to zero (i.e., complete inhibition), and the Hill coefficient should also equal unity (as expected for a 1:1 binding stoichiometry between enzyme and inhibitor), according to the simpler equation:

$$\frac{v_i}{v_0} = \frac{1}{1 + ([I]/\mathrm{IC}_{50})} \tag{6}$$

Departure from this ideal behavior, without mechanistic justification or commitment to follow-up by further detailed analysis, may provide sufficient reason for prompt discontinuation of a particular compound or series. This information is lost if all values are not reported (or departures noted) for data fitted to equation (5). Thus, aside from visual inspection of data, many screening groups now have within their analysis routine triggers to warn of nonideal behavior in dose–response curves.

Another word of caution relates to the quantitative interpretation of IC_{50} values to assess the relative potency of screening hits. At this early stage of

analysis, IC_{50} is usually the most quantitative measure of enzyme–inhibitor affinity. But this value is determined under only one defined set of conditions and is therefore an *apparent* measure of inhibitor potency that reveals nothing about the mechanism or kinetics of inhibitor binding. As discussed below (see section on substrate competition analysis), an apparent IC_{50} may shift leftward (more potent) or rightward (less potent) from the true inhibition constant (K_i), depending on the inhibitor's mechanism of action and the substrate concentration used in the assay (36). Care should therefore be taken when comparing IC_{50} values between compounds until more detailed work is carried out on chemotype exemplars to define mechanism. Similarly, the impact of assay conditions on IC_{50} should be taken into account when values obtained with different enzymes (potentially using different assay formats) are used to determine inhibitor selectivity for the primary target.

Departures from Ideal Behavior

Departures from an idealized concentration–response relationship may make one consider a hit class more skeptically. However, there may be valid reasons for the departure, such as may result from the enzyme's and/or inhibitor's kinetic mechanisms. Both cases can manifest in the steepness of the dose response (Hill slope) or in the extent of inhibition observed (3,37). Both low and high Hill slopes are common in dose–response curves of screening hits. Thus, positive allosteric inhibitor binding by an oligomeric enzyme can increase the apparent Hill slope (Fig. 3, trace b), whereas multisite binding to the same enzyme molecule or negative allosteric binding to an oligomeric enzyme can produce a shallow Hill slope (depending on the separation of affinities in the latter case, which may or may not reflect nonspecific binding of inhibitor) (Fig. 3, trace c). A high Hill slope might also indicate inhibition under conditions in which the enzyme concentration is high relative to inhibitor K_i. This situation arises when assay conditions require a relatively high concentration of enzyme for robust signal generation and defines the lower level for apparent IC_{50} quantification according to the relationship (3):

$$IC_{50,\mathrm{app}} = K_i^{\mathrm{app}} + \frac{[E]}{2} \tag{7}$$

At lower inhibitor concentrations, a substantially greater proportion of free inhibitor is depleted by binding to enzyme (E), which give rise to a steep dose–response curve as the system deviates from pseudo–first-order inhibition kinetics. Such curves are more properly analyzed by a more detailed equation that introduces a quadratic term to quantify the level of inhibitory species ($[EI]$) relative to total enzyme ($[E]_T$) and total inhibitor ($[I]_T$) throughout the titration range, although care must be taken to properly define conditions and interpret the results of these analysis (38,39):

$$\frac{v_i}{v_0} = 1 - \frac{([E]_T + [I]_T + K_i^{\mathrm{app}}) - \sqrt{([E]_T + [I]_T + K_i^{\mathrm{app}})^2 - 4[E]_T[I]_T}}{2[E]_T} \tag{8}$$

Nuisance inhibitor mechanisms can also produce nonideal concentration–response curves. For example, inhibitors that act through nonspecific, aggregating mechanisms elicit steep dose responses, as will be discussed in the following section. Assuming that the target enzyme is sufficiently purified so that it is the

only activity being measured, a shallow Hill slope may indicate insolubility at higher inhibitor concentrations. At the extreme, insolubility might manifest as partial inhibition (Fig. 3, trace d) in which, past a certain threshold of inhibitor added, only a maximum (but less than fully inhibitory) amount of inhibitor is able to partition into solution and inhibit the enzyme.

Beyond insolubility and other nuisance mechanisms, partial inhibition might also have mechanistic origins directly related to inhibitor binding, such as observed for binding of peptidic inhibitors to an exosite on coagulation factor VIIa. Reflective of incomplete allosteric communication between sites, inhibitor binding to the exosite cannot fully inhibit enzyme activity, leading to a circumstance of true partial inhibition (40). Only after further elaboration to extend beyond that site do these inhibitors sufficiently influence the enzyme's active site to cause full inhibition (41,42). Partial inhibition is also observed with processive enzymes (43). Occurrence of partial inhibition might therefore provide an important mechanistic context to an enzyme–inhibitor interaction, but must be approached with some caution and verified by further experimentation.

Nonspecific Enzyme Inhibitors

Other major causes of false positive inhibition are nuisance mechanisms linked to the physicochemical properties of screening compounds. The existence of nonspecific inhibitors in screening libraries has long been known, but poorly understood, in the pharmaceutical industry. Only within the last approximately five years has there been a general understanding of the properties of perhaps the most prevalent group of these, initially referred to as "promiscuous" inhibitors. Due in large part to the work of Schoichet and coworkers (44,45), in addition to early contributions by workers at GlaxoSmithKline (46), it is now proposed that this class of inhibitor acts by sequestering enzyme molecules into colloidal aggregates of inhibitor molecules that associate even at submicromolar concentrations of inhibitor. As determined by transmission electron microscopy and dynamic light scattering experiments, these aggregates produce particles of up to 1 μm in diameter. Biophysical analyses demonstrated that enzymes associate with these particles, likely residing on the surface but without denaturation, thereby making them inaccessible to substrate and inactive (47). The general signature of these aggregating inhibitors includes (45) a steep concentration–response relationship; time-dependent, noncompetitive, reversible inhibition; tendency to inhibit multiple unrelated enzymes; and attenuation of inhibition by detergents at levels below their critical micellar concentrations (e.g., as low as 0.01% Triton X-100), high levels of introduced protein, small (subdenaturing) levels of urea or guanidine-HCl, or increased amounts of enzyme.

In practice, not all of these signature characteristics may be readily apparent for every enzyme, aggregating inhibitor, or varied assay condition, and so should be viewed in composite. Nonetheless, individual observations merit further study. For example, a high Hill slope observed during general triage of screening hits may be the first indication of a potential aggregating inhibitor, and should trigger experiments directed at determining whether the inhibitor fits the rest of the profile. Some of these experiments may be carried out within the context of the general triage, for example, determining whether including a small amount of detergent or increasing enzyme concentration relieves inhibition, as predicted for aggregating inhibitors but not standard inhibitors. The

effect of detergent reflects disruption of the aggregate, whereas adding more enzyme overcomes sequestration by oversaturating enzyme-binding sites on the aggregate particle. Other experiments are part of the further mechanistic triaging of hits (i.e., time-dependency, reversibility, and substrate competition). However, the most convincing test of this mechanism is whether the inhibitor binds with a 1:1 stoichiometry of enzyme:inhibitor or a much higher ratio. These studies may entail more detailed biophysical binding studies and are thus restricted to advanced studies with a small number of compounds.

It is difficult to predict from structure alone whether any given compound will form inhibitory aggregates, although efforts to develop predictive algorithms that may assist early identification of this class of nuisance hits are in progress (48,49). In fact, there are several reports of compounds selected by virtual screening to be active-site ligands for enzymes, which indeed inhibit the target enzymes but by nonspecific means (50,51). Higher-throughput schemes for experimentally detecting compounds that form inhibitory aggregates are being developed and may aid this process (13,49,52). In part to bypass the general phenomenon, many screening groups routinely include a small level of detergent in HTS assays.

Ultimately, two concerns arise concerning this sort of inhibitor: "Is it a progressible mechanism?" and "could it be an effective therapeutic?". Given current knowledge, the answer to the first question is "no." There is generally no path for SAR advancement and their lack of selectivity for the target enzyme introduces a built-in liability. Beyond these critical concerns, the utility of this class of inhibitor as therapeutics may (at best) depend upon the clinical indication. Consistent with the sequestration model, Schoichet and coworkers have shown that previously reported inhibitors of protein aggregation actually work by sequestering protein monomers into inhibitor aggregates and therefore keeping them from self-associating to form the undesired protein aggregates (53). Although the biological effect of these aggregating inhibitors is generally unclear, these authors point out that several amyloid-directed compounds actively inhibit protein polymerization in cell culture, thereby showing the potential of these inhibitors to act in a more biological setting. In other cases, proteins and other components of plasma and cellular environments may disrupt the aggregates. Thus, one survey of marketed drugs found some able to inhibit off-target enzymes, but at levels higher than required to inhibit the drugs' targets and in most cases higher than targeted therapeutic concentration (48). Thus, aggregating screening hits should be viewed with caution. They should be identified and, given other options, prioritized low on the list of hits for further progression.

MECHANISTIC TRIAGE

Once confirmed as valid hits through a general triage, selected screening hits are next evaluated with respect to mechanistic criteria: demonstration of reversibility, preliminary binding kinetics, determination of inherent potency, and initial determination of binding mechanism. These analyses further confirm the nature of the hits as true inhibitors of the target enzyme and begin to address more advanced questions surrounding hit prioritization: Does the hit fit a desirable mechanistic profile? Is there any basis for differentiated hit prioritization and preferential initiation of chemistry on any one series?

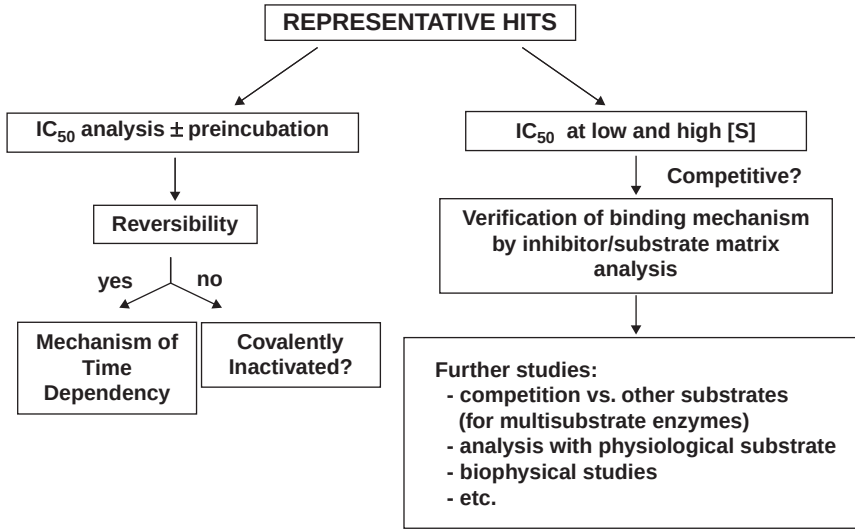

FIGURE 4 Representative mechanistic triage of hits for advancement of compounds selected from the general triage.

A typical triage scheme for mechanistic evaluation of screening hits is shown in Figure 4. Similar schemes have been presented elsewhere (2–5) and we have used variants of this basic decision tree to routinely triage hits in daily operations, with modifications according to enzyme being studied, assay(s) used for screening and follow-up, and types of inhibitors being looked for in the screen. Although mechanistic triage of hits may be carried out on larger scale within screening groups, they are frequently the responsibility of more specialized compound profiling or enzymology departments. Correspondingly, the number of compounds analyzed may also vary, from comprehensive screening of large hit lists to analysis of chemotype exemplars, depending upon the detail of analysis required and the capacity of the group carrying out the analysis.

Concentration Response Reconfirmation

The assays used for mechanistic work may be the same as the primary screening assay or may be substantially different to better fit the requirements of mechanistic evaluations. Regardless, when the mechanistic triage is to be carried out by a group other than the primary screening team, an IC_{50} analysis should be re-run with the attention to detail noted in the section above and ideally with an independent supply of compound. Not only does this provide independent confirmation of potency between research teams, but it allows the researchers tasked with understanding more detailed aspects of the enzyme–inhibitor interaction to establish conditions for the next steps of the mechanistic triage. An orthogonal assay format also provides additional confidence in the enzyme-specific nature of the observed inhibition.

Time-Dependent Inhibition

The discussion to this point has assumed that enzyme and inhibitor reach complete binding equilibrium rapidly and within the time frame of the kinetic assay; this is not always the case. The rate (and extent) at which the enzyme–inhibitor binding equilibrium is attained is a function of the overall association and dissociation rates of the enzyme–inhibitor complex and will vary depending on the character of this interaction. These rates can be complex functions encompassing multiple internal equilibria, with the result that rate-limiting microscopic kinetic constants may in fact produce a nonequilibrium system that results in a slow onset of true equilibrium inhibition (3–4,54–55).

There are several reasons for evaluating time-dependent inhibition. Most important is the desire to determine the true potency of an inhibitor: if enzyme and inhibitor have not had sufficient time to equilibrate fully during standard potency assays, then the inhibitor's potency will be underestimated and the program team will be left chasing a misleading SAR. Second, observation of time-dependent inhibition may highlight further issues within a given screening hit series. For example, although slow onset of inhibition need not be associated with irreversible inhibition, a compound that covalently inactivates an enzyme often shows slow onset of inhibition. Third, time-dependent analysis establishes conditions and types of experiments required for further studies. As examples, analysis of the reversibility of inhibitor binding requires that the researcher establish sufficient conditions for enzyme and inhibitor to attain a fully inhibited state. Identification of time dependence will also dictate how competition between substrate and inhibitor binding is properly evaluated.

The most straightforward way to detect time-dependent inhibition is to compare inhibition in the presence and absence of a preincubation period between enzyme and inhibitor. IC_{50} is determined for one set of inhibitor concentrations with minimal preincubation between enzyme and inhibitor. Another set (inclusive of controls lacking inhibitor) is first allowed to incubate with enzyme for a period of time allowable by the enzyme stability, then reactions are initiated by addition of substrate and monitored as normal. A shift of IC_{50} towards greater potency for the preincubated set indicates the presence of a time-dependent inhibitor. Varying the preincubation time allows one to estimate time to equilibrium. Notably, high-throughput screens are often run with inclusion of an enzyme–inhibitor preincubation step, with the express purpose of capturing time-dependent inhibitors. But even in these cases, confirmation of time dependency is warranted during postscreen follow-up; this can readily be carried out by the mechanistic team during the process of re-evaluating inhibitor potency by IC_{50} analysis.

Time-dependent onset of inhibition may also be observed in primary data as nonlinearity of reaction progress curves for inhibitor-containing reactions initiated with enzyme, as shown in Figure 5. Such curves can be fit to an equation that describes a first-order process for conversion between an initial velocity (equivalent to an uninhibited control reaction or an initial weak binding complex between enzyme and inhibitor) and a final rate corresponding to the final equilibrium binding state between enzyme and inhibitor (54,55):

$$[P] = v_s t + \frac{v_i - v_s}{k_{obs}}(1 - e^{-k_{obs}t}), \tag{9}$$

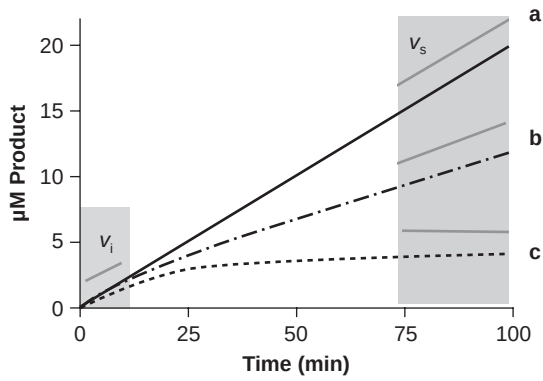

FIGURE 5 Progress curves for time-dependent inhibition. (a) Uninhibited reaction corresponding to $v_i = 0.2$ μM/min and $v_s = 0.2$ μM/min. (b) Slow-onset inhibitor exhibiting 50% inhibited reaction at steady state: $v_i = 0.2$ μM/min, $v_s = 0.1$ μM/min, and $k_{obs} = 0.05$ min^{-1}. (c) Irreversible, slow-onset inhibitor with otherwise comparable kinetic parameters: $v_i = 0.2$ μM/min, $v_s = 0$ μM/min, and $k_{obs} = 0.05$ min^{-1}.

where [P] is the product concentration at time "t," v_i is the initial reaction velocity, v_s is the reaction velocity in steady state, and k_{obs} is the first-order rate constant for progression from v_i to v_s. In theory, the final equilibrium rate (v_s) should be equivalent to that obtained when enzyme and inhibitor are allowed to fully preequilibrate prior to initiation of reaction.

Detection of time dependency is relatively straightforward for a stable, single-substrate enzyme. However, the experimenter must always keep in mind other nuances of the enzyme and its reaction. For example, a built-in assumption with preincubation analyses is that enzyme stability does not differ significantly in the absence or presence of inhibitor. On the contrary, one could imagine instances in which the inhibitor may actually protect an unstable enzyme from thermal denaturation, resulting in ambiguous interpretation of "inhibited" activity relative to "uninhibited" control. In addition, the kinetic mechanism of an enzyme may preclude detection of time dependence by simple preincubation. Hence, in the case of a two-substrate enzyme that preferentially binds substrate "A" before it binds substrate "B" (i.e., an obligate ordered binding mechanism), a "B"-competitive inhibitor may not bind (or would bind poorly) to the enzyme unless "A" is present; preincubation between inhibitor and enzyme would not reveal any time-dependent onset of inhibition related to ordered substrate binding.

Beyond the recognition of time-dependent onset of inhibition, it is important to understand how one obtains meaningful data to support SAR for time-dependent inhibitors, given that they may present out of equilibrium under standard assay conditions. As mentioned above, introduction of a standard preincubation period into IC_{50} measurements will suffice for a simple enzyme–inhibitor series, provided sufficient time is given the enzyme and inhibitor to reach binding equilibrium prior to analysis. If monitoring progress curves, one may also rely on the rate of the second phase of reaction, v_s in Figure 5, to obtain inhibition rates. However, these treatments are not appropriate for inhibitors that exhibit irreversible (or slowly reversed) mechanisms (discussed in the next

section), and simple equilibrium measurements (i.e., IC_{50} or K_i) may not appropriately describe time-dependent inhibitors.

Using Eq. [9], quantitative analysis of progress curves at varied concentrations of inhibitor and substrate can be used to obtain kinetic details concerning inhibitor binding mechanism and rate constants for the inhibitor association/dissociation rates (3,54,55). Briefly, such studies allow determination of a second-order rate constant that incorporates terms for initial binding and onset of final equilibrium states, which provide a measure of relative potency comparisons: $k_{obs,max}/K_i$ using the formalism of Eq. [9], or $k_{inact,max}/K_i$ for true covalent enzyme inactivators (4,56). An example of the use of these constants to drive SAR is found in reference (57).

Reversibility

A tight-binding complex between enzyme and inhibitor may arise from covalent inactivation of the enzyme, such as by electrophilic compounds as discussed above. But it may also indicate a stable, yet slowly reversible, complex between enzyme and inhibitor. As already discussed, the former mechanism brings with it certain risks for progression as a potential lead candidate, whereas the latter may in fact represent an inhibitor class that could confer an advantage for certain disease indications by enhancing therapeutic efficacy due to its increased on-target residency time (33,34). The ease of inhibitor reversibility will also dictate the approach taken to define binding mechanism relative to substrate. A qualitative evaluation of inhibitor reversibility is therefore important for detecting undesirable hits that may have escaped detection during general hit triage and for guiding further experiments. More quantitative analysis is important to better understand the basis of compound potency and perhaps predict the potential for in vivo efficacy.

Inhibitor reversibility may be assessed through several means. Observation of "flat" rates in the equilibrium phases of enzyme-initiated reaction time courses is a first indication of irreversible inhibition (see trace c in Fig. 5). For analysis of a few suspect compounds, qualitative demonstration of reversibility may also be obtained by using any method that physically separates free from bound inhibitor and enzyme. Dialysis against a large volume of buffer may be used to remove excess inhibitor as well as any that dissociates from pre-equilibrated enzyme–inhibitor complex during the time of dialysis. Dissociation is gauged by the activity level of enzyme after dialysis, in comparison to a separately dialyzed control sample (never exposed to inhibitor). This approach may be limited by the slow diffusion of even small molecules out of the dialysis chamber, and thus is not appropriate for defining kinetics of inhibitor dissociation within a less than multi-hour time frame. Compound retention within the dialysis chamber, by adsorption to the membrane or formation of aggregates larger than the membrane pore size, may also lead to a false assignment of irreversible binding. Similar analysis can be performed using gel-permeation chromatography. Likewise, if radiolabeled compound is available (not likely for screening hits), reversibility may be analyzed by competitive displacement of label from the enzyme–inhibitor complex by unlabeled material.

A more versatile and higher throughput method for determining inhibitor reversibility involves directly monitoring recovery of enzyme activity as inhibitor dissociates and substrate binds in an activity-based preincubation/

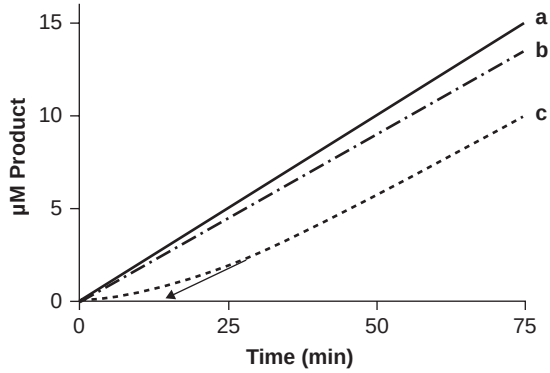

FIGURE 6 Simulated reversibility evaluation by dilution analysis. (a) Uninhibited reaction (0.2 μM/min). (b) Control reaction containing the carryover level of inhibitor (not preincubated). (c) Progress curve for dilution of preincubated enzyme–inhibitor complex into an otherwise complete reaction. Dissociation is gauged by the extent of lag time prior to restoration of normal activity. As extrapolated from the steady-state rate according to the grey arrow or from fitting to Eq. [9], the $t_{1/2}$ for dissociation in this example is 14 minutes. In this simulation, the preincubation is carried out by incubating enzyme (100x final) at an inhibitor concentration equivalent to 10x IC_{50}, then diluted 100-fold into a reaction mixture to give a carryover level of inhibitor equal to 0.1x IC_{50}. Missing from the figure is an additional control reaction usually run in the presence of the preincubation concentration of inhibitor, which demonstrates complete inhibition of enzyme at the preincubation concentration.

dilution experiment (3,55). Thus, enzyme (at high concentration) is allowed to fully equilibrate with a sufficiently high concentration of inhibitor to effect full inhibition, then diluted into an otherwise complete assay mixture to an extent sufficient to reduce inhibitor concentration well below the condition-specific IC_{50}. The substrate level in this assay is usually maintained at a saturating level in order to reduce inhibitor rebinding by competitive inhibitors. As shown in Figure 6, reversibility is qualitatively determined as the restoration of activity rate to the level exhibited by a "carryover" control that contains the same small amount of residual inhibitor as that brought along with enzyme into the enzyme–inhibitor dilution reaction. Ideally, the reaction can be run long enough to demonstrate full restoration of activity within a time frame that still maintains a linear response in the control reaction. Quantitatively, the length of the lag period reflects the half-life for inhibitor dissociation (shown by the arrow in Fig. 6). This can be more precisely determined by fitting the progress curve to Eq. [9] to derive the rate constant for this process (k_{obs}), which converts to half-life as:

$$t_{1/2} = \frac{0.693}{k_{obs}}. \tag{10}$$

In all of these experiments, it is important to demonstrate that the enzyme and inhibitor have fully equilibrated prior to analysis for reversibility. Thus, appropriate preincubation time and concentration of inhibitor must be employed, as guided by the experiments discussed above (see section on time-dependent inhibition). For the dilution experiment, it is even advisable to demonstrate by direct experimentation that the high concentrations of enzyme

used for preincubation are inhibited by the chosen level of inhibitor. As discussed above, inclusion of other components for multisubstrate system should also be evaluated as requirements for binding.

Whether inhibition is reversible for a time-dependent inhibitor will determine the next step for analysis. Rapidly reversible, fast-associating inhibitors are amenable to steady-state competition analysis, as discussed in the next section. Reversible, yet time-dependent inhibitors should be further analyzed to obtain inhibitor mechanism and rigorously confirm potency determinations, as discussed above. A slowly reversing inhibitor requires a rigorous evaluation of whether the compound forms a covalent adduct with the enzyme or arises from noncovalent interaction of inhibitor with enzyme. As mentioned above, an inhibitor that forms a covalent adduct will usually be of lower interest to the program team than a noncovalent inhibitor.

Several approaches have been described to assess covalent binding and characterize the (putative) enzyme–inhibitor adduct. Traditionally, this may involve demonstration that compound is retained with the protein after denaturation of the enzyme–inhibitor complex, followed by physical demonstration of an adduct. In the past, this entailed Edman degradation of isolated, trypsin-digested peptide fragments of the inhibited enzyme in order to demonstrate a modified amino acid. This was assisted by any knowledge of suspect target groups in the protein, for example, an active-site serine for inactivators of serine hydrolases. These experiments were also facilitated by the availability of radiolabeled compound, which will not be the case with initial screening hits. Modern approaches of high-resolution mass spectrometry have greatly facilitated the identification and chemical-structure determination of enzyme–inhibitor adducts and are now methods of choice. Ultimately, correlation between extent of adduct formation and rate (and level) of inhibition and inactivation is required to make a decision regarding the impact of the covalent modification on whether to progress a compound towards lead status, especially if adduct formation is not associated with a known catalytic residue in the enzyme. As discussed above (see section on reactive compounds), correlation of inhibition with a covalent mechanism may still provide a route forward towards a lead series, but requires full commitment and understanding within the program team of the issues associated with progressing such a series.

Substrate Competition Analysis

One of the clearest roles of the enzymologist in drug discovery is to help medicinal chemists understand how inhibitors bind to the enzyme in relation to substrate(s) and other inhibitors, in the hopes of defining inhibitor binding sites, understanding SAR, and differentiating between inhibitor classes. Mechanistic evaluations also provide new or confirmatory validation of screening hits as target-based inhibitors of the enzyme reaction and would identify hits that follow a preferred inhibitor binding mechanism. Thus, there is benefit in gathering this information early in the discovery process, even if only for initial binning of chemotypes, to prioritize compounds for further detailed investigation.

The general framework for binding of a simple, reversible inhibitor to an enzyme is well known and discussed in many texts and reviews (3,4,58). On the basis of enzyme forms to which it can bind, an inhibitor may be broadly categorized as competitive, noncompetitive, or uncompetitive (Fig. 7).

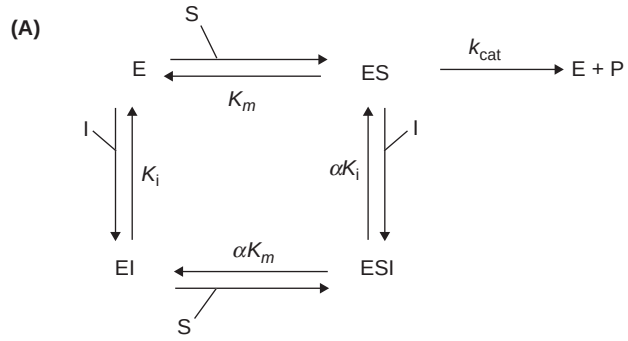

(B)

Competitive ($\alpha \rightarrow \infty$)	Noncompetitive ($0 < \alpha < \infty$)	Uncompetitive ($\alpha << 1$)
$v = \dfrac{V_{max}[S]}{[S]+K_m\left(1+\dfrac{[I]}{K_i}\right)}$	$v = \dfrac{V_{max}[S]}{[S]\left(1+\dfrac{[I]}{\alpha K_i}\right)+K_m\left(1+\dfrac{[I]}{K_i}\right)}$	$v = \dfrac{V_{max}[S]}{[S]\left(1+\dfrac{[I]}{\alpha K_i}\right)+K_m}$

FIGURE 7 Simple substrate and inhibitor binding equilibria (**A**) with corresponding inhibition equations (**B**). A competitive inhibitor will bind only to the free state of the enzyme ("E") in the equilibrium shown on the left-hand side of the thermodynamic box. A noncompetitive inhibitor may bind to either free enzyme or enzyme bound by substrate (or any form of enzyme that proceeds from substrate binding). Therefore, noncompetitive inhibitor binding is described by two apparent inhibition constants, K_i and αK_i, where α describes the preference for one side of the cycle over the other; for a pure noncompetitive inhibitor with no preference, $\alpha = 1$. An uncompetitive inhibitor is described only by αK_i. In this treatment, substrate binding is assumed to be equivalent to K_m, which need not always be the case.

Competitive inhibitors bind exclusively to the unliganded form of the enzyme (E) in competition with substrate. Thus, competitive inhibitors increase the apparent K_m for substrate (in the simplest case, by decreasing the apparent affinity for substrate by directly competing for the same binding site on the enzyme) without effect on apparent V_{max}; if introduced at high enough levels, substrate will always out-compete binding of a competitive inhibitor and saturate the ES complex to promote maximal reaction velocity. At the other extreme are uncompetitive inhibitors, which bind to the enzyme only after substrate binding (ES). As shown in Figure 7(A), an uncompetitive inhibitor may bind to enzyme at the same time as substrate (ESI), although an inhibitor that binds to any form of the enzyme *after* substrate binding (e.g., an enzyme–product complex) will appear uncompetitive. Thus, uncompetitive inhibitors decrease the apparent K_m for substrate (enhances formation of enzyme–substrate complex by pulling the binding equilibrium to the right) and also decrease the apparent V_{max} (forms a dead-end inhibited complex that is not overcome, but rather enriched with increasing levels of substrate). Noncompetitive inhibitors are able to bind to both states of the enzyme. In the case of a pure noncompetitive inhibitor [$\alpha = 1$ in the formalism shown in Fig. 7(A)], the apparent K_i values for binding to the E and

ES forms of the enzyme are equivalent, so there is no effect on apparent K_{m} for substrate. However, $V_{\max}$ is reduced due to formation of nonproductive complexes. Noncompetitive inhibitors with $\alpha \neq 1$ arise from nonuniform synergy in binding to the two forms of the enzyme, and therefore elicit changes in both the apparent K_m and $V_{\max}$ values. Beyond active-site binding, all three modes of inhibition can result from binding of inhibitor to allosteric sites elsewhere on the enzyme, reflective of the inherent conformational flexibility of many enzyme molecules (59).

From this simplistic framework, the key point of an early binding mode analysis is twofold: to verify that the hit fits a possible binding mechanism, and to select those hits that demonstrate a preferred modality (if there is one). For a simple reversible inhibitor, the modality of inhibitor binding can be kinetically determined in the classic manner of measuring initial-velocity enzyme activities over a matrix of substrate and inhibitor concentrations, then analyzing for best global fit to the standard (or otherwise reasonable) models of inhibition by using one of many pieces of commercial fitting software (4,58). If limited to a smaller number of exemplars for each chemotype of interest, these experiments are readily carried out by the bench scientist without requirement for automation. Wang et al. (60) have also detailed the use of an automated system to obtain steady-state inhibition mechanism data, in which the use of liquid handling provides very reproducible data and allows analysis of larger number of compounds with throughput compatible with analysis of screening hits. However, the user of these large-scale analyses is still bound by the need for careful attention to data processing and analysis in order to notice irregularities and signatures of mechanistic flaws that could be readily missed in the wholesale processing of these large data sets.

Another option for analysis of a large set of screening hits is to mechanistically bin compounds according to predicted effect of substrate concentration on observed IC_{50}. Such an approach is readily carried out within a screening group, as recently described by Wei et al. (61). As first noted by Cheng and Prusoff (36), the observed IC_{50} for an inhibitor shifts from the inherent (and therefore mechanism-independent) K_{i} value as a function of substrate concentration according to the following relationships:

$$\mathrm{IC}_{50} = K_{\mathrm{i}}\left(1 + \frac{[S]}{K_m}\right) \quad \text{Competitive} \tag{11}$$

$$\mathrm{IC}_{50} = \alpha K_i\left(1 + \frac{K_m}{[S]}\right) \quad \text{Uncompetitive} \tag{12}$$

$$\mathrm{IC}_{50} = \frac{[S] + K_m}{(K_m/K_i) + ([S]/\alpha K_i)}, \quad \mathrm{IC}_{50} = K_i \text{ when } \alpha = 1 \quad \text{Noncompetitive} \tag{13}$$

The impact of substrate concentration on apparent IC_{50} values for various inhibitors is shown in Table 1. A pure noncompetitive inhibitor ($\alpha = 1$) shows no shift in IC_{50}, whereas other values of α produce intermediate shifts. Note that adequate discrimination for competitive inhibition occurs between $[S] = K_{\mathrm{m}}$ and $[S] > 5\mathrm{x} - 10\mathrm{x}\ K_{\mathrm{m}}$, whereas that for an uncompetitive inhibitor requires lower

TABLE 1 Example Substrate- and Mechanism-Dependent Shifts in IC_{50}

			IC_{50} (nM)[a]		
Inhibition mechanism	K_i (nM)	αK_i (nM)	$[S] = 0.1x\ K_m$	$1x\ K_m$	$10x\ K_m$
Competitive	1	–	1.1	2.0	11.0
Uncompetitive	–	1	11.0	2.0	1.1
Noncompetitive	1	1	1.0	1.0	1.0
Noncompetitive	1	5	1.1	1.7	3.7

[a]Calculated according to the Cheng–Prusoff relationships given in Eqs. [11–13] in the text.

concentrations of substrate. Although this approach is an expedient way to bin inhibitors into different modalities, there are limitations. For example, the experiment is usually carried out by measuring IC_{50} values at two concentrations of substrate; as shown in Table 1, these concentrations might best be $[S] = 0.1 \times K_m$ and $[S] = 10 \times K_m$ in order to accommodate all modes of inhibition. But depending on assay constraints and flexibility in varying the substrate concentration (on either the low or the high end), the method may not have suitable dynamic range for full differentiation. Thus, inability to derive adequate signal for IC_{50} analysis at a lower substrate concentration may mean that inhibitors can only be binned as "competitive" and "other." Yet even this exercise might provide sufficient information for hit prioritization.

Several comments are warranted concerning the use and interpretation of information obtained from these initial determinations of inhibitor binding modality. These experiments are at best thorough analyses using purity-confirmed (potentially resynthesized) inhibitor, and at worst binning analyses using screening hits obtained directly from DMSO library stocks. In all cases, results must be considered in the context of the enzyme's overall kinetic mechanism, and the investigator needs to be aware of reasons for artifacts in the inhibition patterns observed. For example, the preferred substrate binding order, the assay conditions used in the study, and even the choice of substrate itself may dictate the interpretation and choices for inhibitor mechanism (4,58,59). Multisubstrate enzymes raise possibilities of random versus obligate ordered substrate binding, with attending conformational adjustments that could yield multiple (yet predictable) possible interactions between substrate(s) and inhibitors (59). One specific example is the observation of NADPH-uncompetitive inhibition of 5 alpha-reductase, as eventually explained by the formation of a ternary complex between enzyme, inhibitor, and $NADP^+$ product (62). Only after further experimentation is such a mechanism clearly understood, but can confound initial inhibitor analyses. Ideally, the kinetic mechanism with respect to substrate binding and product dissociation will already be defined for the target enzyme, and conditions for the initial mechanistic triage described here can be optimized to provide required categorization of "hits."

A second consideration is the interpretation of noncompetitive inhibition patterns, or patterns that otherwise deviate from expectation. Noncompetitive inhibitors may result for a number of bona fide reasons related to an enzyme's kinetic mechanism. However, apparent noncompetitive inhibition may also occur by suspect means. As mentioned above, noncompetitive

inhibition is one of the hallmarks of nonspecific, aggregating inhibitors. Taken alone, the observation of noncompetitive inhibition does not demonstrate a colloidal inhibitor. But along with other information obtained in the mechanistic triage, it directs the researcher to consider the possibility of nonspecific inhibition. Unrecognized inhibitor time dependency, especially if resulting from irreversible binding of inhibitor to the enzyme, may also lead to improper assessment of reaction rates and improper assignment of kinetic mechanism.

Although of clear value in the context of sorting hits in a mechanistic triage, initial assignments of inhibitor modality must therefore be followed up with further detailed kinetic and biophysical studies. In the case of multisubstrate enzymes this means, but is certainly not limited to, immediate follow-up for inhibition mechanism with respect to other required substrate(s). As already mentioned, time-dependent inhibitors are most appropriately analyzed for substrate competition according to specialized methodologies (for examples, see references 63–65; reviewed in 3,54,55). In practice, we have also found that early analysis of multiple members of a chemotype is very useful for confirming mechanisms. This is especially true in cases of ambiguous results or where departures from expected modalities may provide an additional flag of potential nuisance mechanisms with either a single exemplar or an entire chemotype.

ADVANCED MECHANISTIC LEAD OPTIMIZATION

The mechanistic triage separates true inhibitors from false positives and provides initial insight into mechanism of action for lead prioritization. But, as introduced in the prior section, further analyses are in most cases required to verify these results and better understand the kinetic and thermodynamic details of enzyme/inhibitor interactions. The needs of the particular target–inhibitor pair will determine the sort of experiments that are necessary. Examples include detailed steady-state and time-dependent kinetic experiments, presteady state kinetic and equilibrium binding measurements, and biophysical approaches such as isothermal calorimetry and surface plasmon resonance measurements. These determinations will confirm the initial assignment of inhibition mechanism for a given inhibitor, confirm whether it fits a desired mechanism of action for the target and indication, and provide more detailed information (e.g., association and dissociation rates) that might explain small differences between compounds and chemotypes. This information will also help place emerging SAR into an enzyme-functional context, and more precisely define the binding site of the inhibitor to help medicinal chemists and structural biologists understand and optimize enzyme–inhibitor interactions; often this information may be delivered prior to the attainment of an x-ray crystal structure of the enzyme in complex with appropriate compounds. Evaluation of inhibition with physiological substrates and analysis of the temperature dependency of inhibition (especially at 37°C, because most initial analyses during the screening phase are carried out at room temperature) would provide higher confidence in the targeted inhibitor modality and expected potency in cells or in vivo. Along with information derived by biologists and pharmacologists, this information allows the program team to better place emerging in vitro knowledge into a physiological context for eventual extension to inhibition in the in vivo pathological setting.

CONCLUSION

The choice of a lead series from an assortment of screening hits is a critical decision point for a drug discovery effort. In doing so, a program team sets its immediate and short-term strategies and convinces the organization to commit medicinal chemistry resources to these efforts. A poor decision at this juncture not only results in wasted resources and decreased institutional productivity, but also costs precious time and may delay (or even block) delivery of a new therapeutic to the patient population. In reality, it is rare to progress only one chemical series. But even one false series may be a critical distraction for the team.

This chapter defined some of the major causes and symptoms of screening artifacts, set out criteria for validating hits as true enzyme inhibitors, and laid out workflows and experimental approaches for identifying the best hits for progression into lead optimization. Although the emphasis was on characterizing screening hits from biochemical activity-based screens for enzyme inhibitors, some of the basic questions remain the same and the described approaches apply to other enzyme-based screens, in particular those seeking enzyme activators (66) and using cell-based assessment of enzyme targets. Space limitations precluded a more detailed treatment of every aspect of this process. However, the reader is hopefully left with a comprehensive overview, key references, and practical insights sufficient to understand the critical concepts and to pursue appropriate paths for processing screening hits from initial discovery through a well-informed lead declaration.

ACKNOWLEDGMENTS

I wish to acknowledge past and present colleagues, in particular Dr. Robert Copeland, for their influence on my approach to many of the strategic concepts captured in this chapter. I also thank Robert Copeland, Jay Edelberg, Greg Gatto, Dennis Murphy, Mark Pullen, and Min Wei for critically reading this manuscript.

REFERENCES

1. Gribbon P, Sewing A. High-throughput drug discovery: What can we expect from HTS? Drug Discov Today 2005; 10:17–22.
2. Keserü GM, Makara GM. Hit discovery and hit-to-lead approaches. Drug Discov Today 2006; 11:741–748.
3. Copeland RA. Evaluation of Enzyme Inhibitors in Drug Discovery. Hoboken, NJ: Wiley-Interscience, 2005.
4. Copeland RA. Enzymes: A Practical Introduction to Structure, Mechanism and Data Analysis, 2nd ed. Hoboken, NJ: Wiley-Interscience, 2000.
5. Copeland RA. Mechanistic considerations in high-throughput screening. Anal Biochem 2003; 320:1–12.
6. Hadjuk PJ, Greer J. A decade of fragment-based drug design: Strategic advances and lessons learned. Nat Rev Drug Discov 2007; 6:211–219.
7. Scheuermann J, Dumelin CE, Melkko S, et al. DNA-encoded chemical libraries. J Biotechnol 2006; 126:568–581.
8. Karaman MW, Herrgard S, Treiber DK, et al. A quantitative analysis of kinase inhibitor selectivity. Nat Biotechnol 2008; 26:127–132.
9. Bogoyevitch MA, Fairlie DP. A new paradigm for protein kinase inhibition: Blocking phosphorylation without directly targeting ATP binding. Drug Discov Today 2007; 12:622–633.

10. Wunberg T, Hendrix M, Hillisch A, et al. Improving the hit-to-lead process: Data-driven assessment of drug-like and lead-like screening hits. Drug Discov Today 2006; 11:175–180.
11. Leeson PD, Springthorpe B. The influence of drug-like concepts on decision-making in medicinal chemistry. Nat Rev Drug Discov 2007; 6:881–890.
12. Lipinski CA, Lombardo F, Dominy BW, et al. Experimental and computational approaches to estimate solubility and permeability in drug discovery and development settings. Adv Drug Deliv Res 2001; 46:3–25.
13. Feng BY, Simeonov A, Jadhav A, et al. A high-throughput screen for aggregation-based inhibition in a large compound library. J Med Chem 2007; 50:2385–2390.
14. Walters WP, Namchuk M. Designing screens: How to make your hits a hit. Nat Rev Drug Discov 2003; 2:259–266.
15. Harper G, Pickett SD. Methods for mining HTS data. Drug Discov Today 2006; 11:694–699.
16. Gribbon P, Sewing A. Fluorescence readout in HTS: No gain without pain? Drug Discov Today 2003; 8:1035–1043.
17. Seethala R. Homogeneous assays for high-throughput and ultrahigh-throughput screening. In: Seethala, R, Fernandes, PB, eds. Handbook of Drug Screening. New York: Marcel Dekker, 1999:69–124.
18. Bronson D, Hentz N, Janzen WP, et al. Basic considerations in designing high-throughput screening assays. In: Seethala, R, Fernandes, PB, eds. Handbook of Drug Screening. New York: Marcel Dekker, 1999:5–30.
19. Neumann K, Kolb A, Englert D, et al. Scintillation proximity assay on the TopCount microplate scintillation counter. TopCount Topics, 1994; 19 (http://las.perkinelmer.com/content/ApplicationNotes/APP_TopCountScintProxAssays.pdf. 2001).
20. Easterby JS. Coupled enzyme assays: A general expression for the transient. Biochim Biophys Acta 1973; 293:552–558.
21. Cleland WW. Optimizing coupled enzyme assays. Anal Biochem 1979; 99:142–145.
22. McElroy KE, Bouchard PJ, Harpel MR, et al. Implementation of a continuous, enzyme-coupled fluorescence assay for high-throughput analysis of glutamate-producing enzymes. Anal Biochem 2000; 284:382–387.
23. Rishton GM. Reactive compounds and in vitro false positives in HTS. Drug Discov Today 1997; 2:382–384.
24. Evans DC, Watt AP, Nicoll-Griffith DA, et al. Drug–protein adducts: An industry perspective on minimizing the potential for drug bioactivation in drug discovery and development. Chem Res Toxicol 2004; 17:3–16.
25. Huth JR, Mendoza R, Olejniczak ET, et al. ALARM NMR: A rapid and robust experimental method to detect reactive false positives in biochemical screens. J Am Chem Soc 2005; 127:217–224.
26. Zhou S, Chan E, Duan W, et al. Drug bioactivation, covalent binding to target proteins and toxicity relevance. Drug Metab Rev 2005; 1:41–213.
27. Uetrecht J. Screening for the potential of a drug candidate to cause idiosyncratic drug reactions. Drug Discov Today 2003; 18:832–837.
28. Rishton GM. Nonleadlikeness and leadlikeness in biochemical screening. Drug Discov Today 2003; 8:86–96.
29. Metz JT, Huth JR, Hajduk PJ. Enhancement of chemical rules for predicting compound reactivity towards protein thiol groups. J Comput Aided Mol Des 2007; 21: 139–144.
30. Roche O, Schneider P, Zuegge J, et al. Development of a virtual screening method for identification of "frequent hitters" in compound libraries. J Med Chem 2002; 45:137–142.
31. Epps DE, Taylor BM. A competitive fluorescence assay to measure the reactivity of compounds. Anal Biochem 2001; 295:101–106.
32. Lor LA, Schneck J, McNulty DE, et al. A simple assay for detection of small-molecule redox activity. J Biomol Screen 2007; 12:881–890.

33. Swinney DC. Biochemical mechanism of drug action: What does it take for success? Nat Rev Drug Discov 2004; 3:801–808.
34. Copeland RA, Pompliano DL, Meek TD. Drug-target residency time and its implications for lead optimization. Nat Rev Drug Discov 2006; 5:730–739.
35. Kerns EH, Di L, Bourassa J, et al. Integrity profiling of high throughput screening hits using LC-MS and related techniques. Comb Chem High Throughput Screen 2005; 8:459–466.
36. Cheng Y, Prusoff WH. Relationship between the inhibition constant (K1) and the concentration of inhibitor which causes 50 percent inhibition (I50) of an enzymatic reaction. Biochem Pharmacol 1973; 22:3099–3108.
37. Schoichet BK. Interpreting steep dose–response curves in early inhibitor discovery. J Med Chem 2006; 49:7274–7277.
38. Morrison JF. Kinetics of the reversible inhibition of enzyme-catalyzed reactions by tight-binding inhibitors. Biochim Biophys Acta 1969; 185:269–286.
39. Murphy DJ. Determination of accurate K_I values for tight-binding enzyme inhibitors: An in silico study of experimental error and assay design. Anal Biochem 2004; 327:61–67.
40. Lazarus RA, Olivero AG, Eigenbrot C, et al. Inhibitors of tissue factor/factor VIIa for anticoagulant therapy. Curr Med Chem 2004; 11:2275–2290.
41. Roberge M, Peek M, Kirchofer D, et al. Fusion of two distinct peptide exosite inhibitors of factor VIIa. Biochem J 2002; 363:387–393.
42. Maun HR, Eigenbrot C, Lazarus RA. Engineering exosite peptides for complete inhibition of factor VIIa using a protease switch with substrate phage. J Biol Chem 2003; 278:21823–21830.
43. Spence RA, Kati WM, Anderson KS, et al. Mechanism of inhibition of HIV-1 reverse transcriptase by nonnucleoside inhibitors. Science 1995; 267:988–993.
44. McGovern SL, Caselli E, Grigorieff N, et al. A common mechanism underlying promiscuous inhibitors from virtual and high-throughput screening. J Med Chem 2002; 45:1712–1722.
45. Schoichet BK. Screening in a spirit haunted world. Drug Discov Today 2006; 11:607–615.
46. Ryan AJ, Gray NM, Lowe PN, et al. Effect of detergent on "promiscuous" inhibitors. J Med Chem 2003; 46:3448–3451.
47. McGovern SL, Helfand BT, Feng B, et al. A specific mechanism of nonspecific inhibition. J Med Chem 2003; 46:4265–4272.
48. Seidler J, McGovern SL, Doman TN, et al. Identification and prediction of promiscuous aggregating inhibitors among known drugs. J Med Chem 2003; 46:4477–4486.
49. Feng BY, Shelat A, Doman TN, et al. High-throughput assays for promiscuous inhibitors. Nat Chem Biol 2005; 1:146–148.
50. Liu H-Y, Wang Z, Regni C, et al. Detailed kinetic studies of an aggregating inhibitor; inhibition of phosphomannomutase/phosphoglucomutase by Disperse Blue 56. Biochemistry 2004; 43:8662–8669.
51. Malvezzi A, de Rezende L, Izidoro MA, et al. Uncovering false positives on a virtual screening search for cruzain inhibitors. Bioorg Med Chem Lett 2008; 18:350–354.
52. Feng BY, Schoichet BK. A detergent-based assay for the detection of promiscuous inhibitors. Nat Protoc 2006; 1:550–553.
53. Feng BY, Toyama BH, Wille H, et al. Small-molecule aggregates inhibit amyloid polymerization. Nat Chem Biol 2008; 4:197–199.
54. Williams JW, Morrison JF. The kinetics of reversible tight-binding inhibition. Methods Enzymol 1979; 63:437–467.
55. Morrison JF. The slow-binding and slow, tight-binding inhibition of enzyme-catalysed reactions. Trends Biochem Sci 1982; 7:102–105.
56. Silverman RB. Mechanism-based inactivators. Methods Enzymol 1995; 249:240–283.
57. Kuang R, Epp JB, Ruan S, et al. Utilization of the 1,2,5-thiazolidine-3-one 1,1 dioxide scaffold in the design of potent inhibitors of serine proteases: SAR studies using carboxylates. Bioorg Med Chem 2000; 8:1005–1016.

58. Segel IH. Enzyme Kinetics: Behavior and Analysis of Rapid Equilibrium and Steady-State Enzyme Systems. New York, NY: John Wiley & Sons, 1975.
59. Copeland RA, Harpel MR, Tummino PJ. Targeting enzyme inhibitors in drug discovery. Expert Opin Ther Targets 2007; 11:967–978.
60. Wang A, Huang Y, Taunk P, et al. Application of robotics to steady state enzyme kinetics: Analysis of tight-binding inhibitors of dipeptidyl peptidase IV. Anal Biochem 2003; 321:157–166.
61. Wei M, Wynn R, Hollis G, et al. High-throughput determination of mode of inhibition in lead identification and optimization. J Biomol Screen 2007; 12:220–228.
62. Levy MA, Brandt M, Heys JR, et al. Inhibition of rat liver steroid 5 alpha-reductase by 3-androsterone-3-carboxylic acids: Mechanism of enzyme–inhibitor interaction. Biochemistry 1990; 29:2815–2824.
63. Williams JW, Morrison JF, Duggleby RG. Methotrexate, a high-affinity pseudosubstrate of dihydrofolate reductase. Biochemistry 1979; 18:2567–2573.
64. Betz A, Wong PW, Sinha U. Inhibition of factor Xa by a peptidyl-α-ketothiazole involves two steps. Evidence for a stabilizing conformational change. Biochemistry 1999; 38:14582–14591.
65. Harpel MR, Horiuchi KY, Luo Y, et al. Mutagenesis and mechanism-based inhibition of *Streptococcus pyogenes* Glu-tRNA^{Gln} amidotransferase implicate a serine-based glutaminase site. Biochemistry 2002; 41:6398–6407.
66. Groebe DR. Screening of positive allosteric modulators of biological targets. Drug Discov Today 2006; 11:632–639.

11 Protein Kinases and Phosphatases

Pirthipal Singh
Singh Consultancy, Shire Home, Wilmslow, Cheshire, U.K.

INTRODUCTION

Many key processes of cellular activity are regulated by the opposing action of protein kinases and phosphatases, which phosphorylate and dephosphorylate proteins, respectively. The human genome encodes 518 different kinases (1,2) and 142 different protein phosphatases (3). The human "kinome" has been subdivided into seven groups (4) comprising (*i*) TK (tyrosine kinases, including receptor kinases), (*ii*) TKL (tyrosine kinase–like kinases), (*iii*) STE (homologues of yeast sterile 7, 11, and 20 kinases), (*iv*) CK1 (casein kinase 1), (*v*) AGC (containing the cyclic nucleotide–dependent protein kinase A & G families and the lipid-dependent protein kinase C family), (*vi*) CaMK (calcium/calmodulin-dependent protein kinase), and (*vii*) CMGC [containing the CDK (cyclin-dependent kinase), MAPK (mitogen-activated protein kinase), GSK3 (glycogen synthase kinase), and CLK (Cdc-2-like kinase) families]. Phosphatases have been similarly grouped by substrate specificity into ser/thr, tyr, and dual-specificity classes. Furthermore, the "conventional" Tyr phosphatases have been classified as those specific for phosphorylated Tyr residues (PTPs), whereas dual-specificity phosphatases (DSPs) act at phosphorylated Tyr and Ser/Thr residues (5). Similarly, the 107 PTPs have been divided into four families based on the amino acid sequences of their catalytic domains (6), each having a range of substrate specificities. Most of the PTPs are posttranslationally modified but glycosylation is apparently restricted to the transmembrane PTPs. Like kinases, the most common form of modification of PTPs is ser, thr, or tyr phosphorylation and this has been shown to regulate their catalytic activity. This key role played by PTPs in maintaining the level of tyr phosphorylation of various proteins in cells may be an important contributing factor in the physiological regulation of cellular activity.

Protein kinases catalyze the transfer of γ-phosphate of ATP to tyr, ser, or thr residues on protein substrates and play key roles in signaling pathways that regulate cellular processes such as differentiation, proliferation, cell cycle, and apoptosis. Protein-tyrosine kinases (90, in the human genome) can be either present as soluble cytoplasmic proteins (32 soluble kinases) or integral membrane proteins (58 membrane kinases) containing an extracellular ligand binding domain. In the cell, there are many signaling pathways that operate sequentially (Fig. 1), each consisting of a series of distinct proteins. Each kinase phosphorylates and alters the conformation of the protein substrate, resulting in the modulation of that protein—exemplified by the MAP kinases. Many of the protein substrates are themselves enzymes that gain activity on

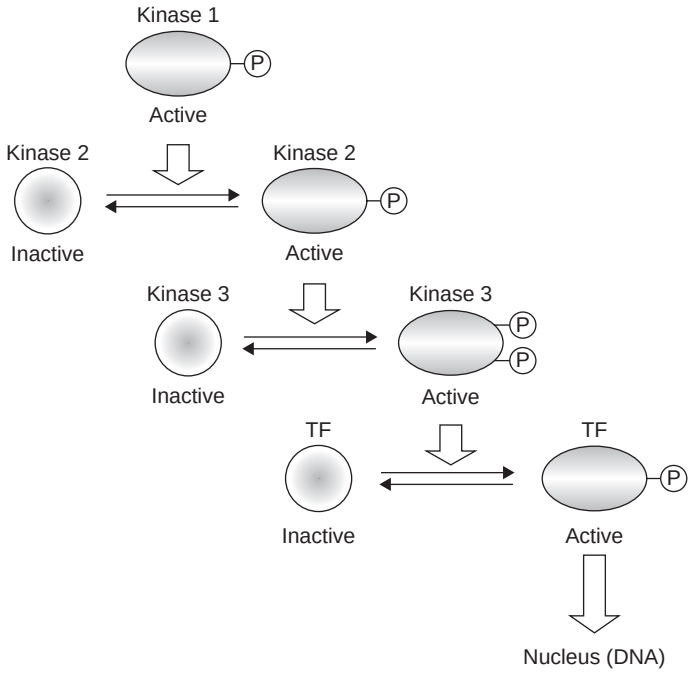

FIGURE 1 Signal transduction pathway comprising several kinases that catalytically change the conformation and activity of downstream proteins [kinases and trascription factor (TF)], as a result of phosphorylation. Each phosphorylation step can potentially be reversed by the action of a phosphatase.

phosphorylation (Fig. 1); other substrates include transcription factors, ion channels, and regulatory proteins. The phosphorylation status of most proteins is temporally and spatially modulated by the complementary process, dephosphorylation, which is regulated by protein phosphatases (7). This balance has been well demonstrated by Akt/PKB in the PI3 pathway. As a result of PI3 kinase activation, PIP3 is generated, which is believed to facilitate the recruitment of Akt to the plasma membrane via interaction with its PH (Pleckstrin Homology) domain and promotes binding to PDK1. While PDK1 phosphorylates Akt on Thr 308 in the activation loop, the level of phosphorylated Akt is regulated by the phosphatase PP2A. However, for full activation, Akt complexes with mTOR (TORC2 complex) and is also phopsphorylated on Ser 473. Once again, this site is regulated by phosphatase PHLPP. Akt, itself a kinase, has been shown to phosphorylate over 40 substrates including kinases and transcription factors.

Kinase-dependent phosphorylation, therefore, may be reversed by protein phosphatases such that the phosphorylation state regulates the activity of many different proteins. Different proteins are phosphorylated by specific kinases, thus mediating selective regulation of the kinases and offering therapeutic potential. Abnormalities in kinase activity are linked with various forms of cancer,

diabetes, and inflammatory diseases such as rheumatoid arthritis. Many tyrosine kinases are implicated in cancers, either through gene amplification (e.g. HER2, or erbB2), overexpression (e.g. Src), gain-of-function mutations (e.g. c-Kit, BRAF, JAK), or chromosomal translocation (e.g. Bcr-Abl). Kinases, therefore, have become an important focus for drug discovery programs in the pharmaceutical industry. To date, there are several hundred kinase inhibitors at various stages of development, ranging from early preclinical discovery to marketed drugs. The potential of kinase inhibitors has been exemplified by the success of Gleevec (imatinib mesylate), a small molecule inhibitor of Abl, PDGFR, and c-Kit, which generated sales of more than $2.5 billion in 2006 (8) and the emergence of several drugs targeting tyrosine kinases, including VEGFR (e.g., Sutent, Nexavar) and EGFR (e.g., Iressa, Tarceva). However, the chemical properties of prototype phosphatase inhibitors have hampered the development of suitable pharmaceuticals against this target class.

ASSAY APPROACHES

The activity of kinases and phosphatases can be measured in various cell-based assays or in biochemical assays using the isolated enzyme and a variety of substrates ranging from simple model substrates to physiological proteins. Such diverse approaches offer a variety of assay formats and assay signal read-outs; some are based on the use of radiolabeled ATP, while others require specific detection reagents including phospho-site specific antibodies.

Cell-Based Assays

The key strength of a cell-based assay is the near-physiological relevance that it offers in understanding the status of the individual target, under the influence of a variety of regulatory factors. Such assays can be used in a variety of different ways. One method is to stimulate the cells, in the absence and presence of inhibitor and prepare a cell lysate. On the other hand, cells can be fixed following stimulation and the phosphorylation status of individual targets monitored by using an appropriate antibody-based detection system. Fixed cell assays can also be conducted in 96-well and 384-well microplates. The plates are scanned and images analyzed using specific software algorithms.

Alternatively, the target protein can be enriched by immunoprecipitation (IP) from the cell lysate and the extent of phosphorylation quantified in an immunoassay or enzyme activity measured in a biochemical assay method. Another approach is to utilize recombinant cells engineered to express the target protein, as a GFP-fusion protein and monitor its translocation (cytoplasm to nucleus) to assess the activity of the target in the pathway. In other cases, the reporter activity of an enzyme protein (e.g. β-galalctosidase or luciferase) is measured from cell lysates to identify inhibitors in a cellular assay. Often, several factors can influence the outcome of the end result and this can require careful data interpretation. It should also be noted that while cell-based assays are commonly considered to be "more physiological," they generally demand a higher level of resource. Furthermore, reagent concentrations (within the cell) cannot be easily modulated and the assay data is likely to have a higher level of variation, reflecting biological variability amongst the cells in different preparations. In addition, early chemical leads may have poor cell-penetration properties, although they could represent useful starting points for the development of effective drugs.

Isolated Protein Assays

Large batch preparation of purified reagents can often result in the development of a robust and reproducible assay, ideally suited for the identification of inhibitors of the target protein. A variety of methods ranging from those employing separation and wash steps to the simple "mix-and-measure" (homogeneous) formats, are now available to monitor kinase (Fig. 2) and phosphatase (Fig. 3) activity. Some methods require specific antibodies or other detection reagents, while others are more versatile, based on the use of generic reagents. The key advantage of this format is that the assay can be conducted with known reagent concentrations and protocols can be "tailored" to potentially address the customized needs of each target. Buffer compositions and assay components can be adjusted as required for each assay. However, certain additional cofactors (e.g., divalent ions, reducing agents, detergents) can significantly influence enzymatic activity. This assay format allows the key parameters (K_m and V_{max}) to be easily measured (Fig. 4). Assays can be developed in kinetic mode to ensure that the rate of reaction is constant over the incubation time. It should also be noted that the value of parameters such as K_m and V_{max} are assay dependent and can be affected by changes in buffer composition and reaction conditions. Thus, the buffer composition can dramatically change the enzymatic activity and this must be kept in mind when a compromised buffer is used to run a panel of assays for generating compound selectivity data.

Heterogeneous Assay Formats

Historically, separation assays such as ELISA (enzyme-linked immunosorbant assay) and FCA (filter capture assay) are well established and understood methods used in screening format to remove any interference from assay reagents, including test compounds. The FCA method has typically been used with radioactive [^{32}P]ATP and more recently, [^{33}P]-ATP in measuring kinase activity by using either peptide-based or full-length protein substrates. The ELISA method (9) on the other hand, is reliant on the availability of suitable antibodies, requiring multiple wash steps to remove excess reagents and can be extremely resource intensive. However, sensitivity can be optimized by amplification of signal from the enzymatic step—the final reagent being an enzyme-conjugated (HRP, horseradish peroxidase or AP, alkaline phosphatase) antibody. The key benefit is the lack of interference from compounds or assay reagents, and although the throughput can be limiting, such assays can be run continuously on robotic platforms. Both assay formats can be used for measuring kinase and phosphatase activities, as signal increase and decrease assays, respectively. Introduction of time-resolved fluorescence (TRF) to the ELISA format resulted in the availability of DELFIA® (dissociation-enhanced lanthanide fluorescent immunoassay). TRF makes use of the long-lived fluorescence lifetime of lanthanides (such as europium) and the large Stoke shift, permitting differentiation of the short-lived background fluorescence from various biological components of assay reagents. DELFIA requires the addition of an enhancement solution that dissociates the lanthanide from the original chelate to form a highly fluorescent chelate.

Homogeneous Assay Formats

There are numerous assay methods that are claimed as homogeneous formats, although some require the use of beads (e.g., SPA, scintillation proximity

assay; ALPHAscreen, amplified luminescent proximity homogeneous assay; IMAP, immobilized metal assay for phosphochemicals). The limited throughput offered by the heterogeneous methods led to the development of these "mix-and-measure" approaches, particularly to address high-throughput screening (HTS) needs. Many assay technology principles (e.g., FRET, fluorescence resonance energy transfer; TR-FRET, time-resolved fluorescence resonance energy transfer; FP, fluorescence polarization) are sufficiently versatile that they can be used to develop assays for many target classes, including kinases and phosphatases. An important benefit offered by this format is the ability to run extremely large-size batches, often as a simple two-step assay method. The first step is the enzymatic reaction (± test compound) and the second step is the addition of detection reagents, frequently incorporating a stop reagent, to quench the enzyme activity. Frequently, the assay signals (following equilibration) are very stable, providing flexibility in reading times. Many HTS assays are currently developed and routinely run in standard or low volume 384-well microplates. Selective assay types such as FP (10) and ALPHAscreen (11) have been successfully miniaturized further and can be run in 1536-well microplates. However, it should be noted that although homogeneous assays are highly desirable and favored by HTS groups, there is an increased potential for compound interference. Often this can lead to high hit-rates, some of which may be "false positives," and additional assays (counter-screens) are implemented to identify "true" hits.

SIGNAL DETECTION

Most assay endpoints rely on the measurement of light, be it optical absorbance, fluorescence, or luminescence. Quantification of the light signal may involve simple photodetectors or for more sophisticated applications, photomultiplier tubes (PMTs) or charge-coupled device (CCD)–based cameras may be used. In most imaging devices, the CCD camera is cooled to low temperatures to improve the sensitivity, especially for measuring low light intensity signals from very small assay volumes in high density (e.g., 1536-well) microplates. In general, using an imaging instrument compared to single well detection can dramatically reduce plate-reading times, particularly for the higher density microplates. For measuring fluorescence signal, the samples can be excited with light from a high-intensity lamp (mercury or xenon) source and the excitation wavelength selected using an appropriate filter, or a laser light (or LED, light emitting device) is used at a single wavelength. Fluorescence assays, for example, can be considered to be advantageous in that an increased level of excitation often results in higher emission signals, compared to radiochemical assays, where the signal is based on natural decay of the isotope used. However, all methods have associated advantages and disadvantages, regarding flexibility and sensitivity.

Radiochemical Assays

Historically, kinase assays were based on the incorporation of radiolabeled phosphate onto the tyr, ser, or thr residue, from using [^{32}P]- or [^{33}P]-ATP. The product can be quantified by autoradiography following electrophoresis to separate product from unchanged substrate. FCA format uses glass-fiber filter to remove unused radiolabeled ATP and the product is measured by scintillation counting. FCA format can also be used with phosphocellulose filter plate to capture the radiolabeled product and measured by scintillation counting. Many scientists in

the field of kinase reasearch are still using the FCA format for compound screening and it is often considered as the "gold-standard" assay, especially when comparing newer (mostly nonradiochemical) assay formats.

Technology developments have led to the availability of "mix-and-measure" assays, avoiding the separation step. One of these formats is based on the use of beads (available with a variety of surface coatings, including streptavidin, protein A, and various secondary antibodies) where the scintillant is incorporated within the bead, and close proximity of the captured radiolabeled product results in the production of a signal in the assay. This method is referred to as the SPA and has been not only widely used with peptide and protein substrates to monitor kinase activity, but can also be adapted to monitor phosphatase activity as a signal decrease assay. Several methodological modifications have been introduced over the years to decrease the nonspecific signal in the SPA format—centrifugation of the microplate or addition of ceasium chloride (in the final step) to increase the density of the stopped kinase reaction mix to float the polyvinyl toluene (PVT) beads, commonly preferred for HTS assays, due to their physical properties. An example of an SPA-based method for measuring MAPKAP-K2 (kinase) activity, using a biotinylated peptide substrate, [^{33}P]-ATP, and streptavidin-coated SPA beads, was recently reported (12).

Further developments of this approach led to the "second-generation" of SPA beads (LEADseeker^{TM}) with signal emission at higher wavelengths (610–620 nm), compared to the emission from classical SPA beads (400–500 nm) to overcome signal quenching when testing colored (mainly yellow and orange) compounds. This notwithstanding, quenching in standard SPA can be corrected by incorporating a quench correction standard curve, using a yellow dye such as tartrazine, although this is only applicable in a satisfactory manner over a limited range of the quenched signal.

Absorbance Assays

Absorbance signal detection is commonly used with chromogenic substrates in ELISA-based methods and phosphatase assays, where a visible color change occurs following enzyme activity. The sample is measured at a single wavelength and the absorbance is proportionally related to the extinction coefficient, concentration of the reagent, and the path length described by the Beer–Lambert law. It should be noted that the absorbance signal deviates from linearity at very high concentrations, although modern plate readers claim to measure absorbance in excess of a value of 3, which is equivalent to more than 99.9% light absorbed.

An example of a microplate method, based on absorbance signal readout, for measuring phospho-Hsp-27 from HeLa cell lysate using a capture (monoclonal anti-Hsp-27) and a detection (polyclonal antiphospho-Hsp-27) antibody for Ser-82 was recently described (12). The hydrolysis of TMB substrate by HRP on the goat anti-rabbit IgG antibody was stopped by the addition of sulfuric acid and the absorbance signal measured at 450 nm. An analogous ELISA-based assay format was reported for measuring phospho-CREB/ATF1, from HeLa cell lysate.

Fluorescence Assays

Fluorescence is the result of a process that occurs in certain molecules (generally aromatic or heterocyclic) called fluorophores and can be divided into three parts.

In the first part, a photon of energy $h\nu_{EX}$ is supplied by an external source (lamp or a laser) and absorbed by the fluorophore, creating an excited electronic singlet state (S_1'). During the second part, the energy of S_1' is partially dissipated, yielding a relaxed singlet excited state (S_1) from which fluorescence emission originates. Finally, in the third part of the process, a photon of energy $h\nu_{EM}$ is emitted, returning the fluorophore to its ground state S_0. The Jablonski diagram, named after the Polish physicist Aleksander Jablonski, is commonly used to illustrate this process. Emission of light always occurs at a longer wavelength, compared to excitation, as some energy is lost as molecular vibrational energy and heat. The quantum yield provides an indication of the efficiency of the fluorescence process, and the fluorescence lifetime indicates the average time the molecule is in the excited state, before returning to the ground state.

In terms of fluorescence application, biological molecules can be tagged with a fluorescent molecule such as fluorescein by chemical modification, and the fluorescence of the tag enables sensitive and quantitative detection of the parent molecule. Fluorescein isothiocyanate (FITC) is a common reagent used to link fluorescein onto primary amine groups. Other frequently used fluorophores are derivatives of rhodamine, coumarin, BODIPY®, and cyanine. Newer generation of fluorophores, such as Alexa® fluor (Invitrogen), DyLight™ (Thermo Fisher Scientific) and Hilyte Fluor™ dyes (AnaSpec) are generally brighter, more photostable and less pH sensitive than older comparable fluorescent dyes. Yet another interesting area of fluorescence is represented by quantum dot (Q-dot) nanocrystals, which are nanometer-scale clusters, containing from a few hundred to a few thousand atoms of a semiconductor material (cadmium mixed with selenium or tellurium) and coated with an additional semiconductor shell (zinc sulfide) to improve the optical properties. The wavelength of fluorescence emission has a predictable relationship with the physical size of the quantum dot and therefore this can be "tuned," and Q-dots have been widely exploited in multicolor (multiplex) assays. Q-dot nanocrystals are also extremely efficient in generating fluorescence, compared with conventional fluorophores. Their emission spectra are narrow and symmetric, with minimal overlap with other colors, allowing their use in multiplex assays. In this respect, there are many examples of Q-dot applications in multicolor immuno-fluorescence imaging with Q-dot–labeled secondary antibody conjugates and in vivo imaging

Fluorescence Intensity

Although fluorescence can be used in many ways, fluorescence intensity (highly dependent of the lifetime of the fluorophore) provides a measure of the concentration of the fluorescent molecules. It is one of the commonly used fluorescence modes, available on all multimode microplate readers.

In terms of application examples in drug discovery, fluorescence intensity signal output is used in the ADP Quest™ HS assay, (DiscoverX), IQ™-based signal quench assay (Pierce) and Omnia™ Kinase Assay (Invitrogen) for measuring kinase activity.

ADP Quest™ HS assay is based on ADP detection for profiling kinase enzyme activity. This is a generic, nonantibody-based, homogeneous method capable of being used with ATP (up to 200 μM) and can be used in both kinetic

and endpoint modes. It is a useful format that provides flexibility regarding the nature of the substrate used and permits kinase assays to be run with high substrate concentrations to investigate the nature of inhibition.

Both IQ-based and Omnia™ kinase assays use a fluorescently labeled peptide substrate to monitor kinase activity in a noncompetitive, homogeneous, format and also do not require any antibodies. In the IQ assay, following phosphorylation of the peptide, a proprietary iron-containing reagent binds to the phosphorylated residue and quenches the fluorescent signal resulting in a decrease in signal intensity. The signal quench is directly proportional to the extent of phosphorylation, and a calibration curve can be used to ascertain the level of substrate conversion. It is commonly used in an endpoint mode and can also be used to monitor phosphatase activity, by employing a phosphorylated peptide substrate. Both assays have been shown to be compatible with physiological (mM) concentrations of ATP. In the Omnia™ kinase assay, signal increases with increasing phosphorylation and it can also be run in kinetic mode. It is claimed to efficiently correct for false positives (compound auto fluorescence) and false negatives (quenching) to overcome compound interference.

Proximity (Energy-Transfer; FRET)

Fluorescence resonance energy transfer (FRET), developed by Theodor Förster, is widely used in drug discovery. It relies on transfer of energy between a donor molecule that is frequently a fluorophore and an acceptor molecule, which may be a fluorophore or a quencher. This is a distance-dependent interaction between the electronic excited states of two fluorescent dye molecules in which energy from the excited donor molecule is transferred to an acceptor molecule, in close proximity (typically <10 nm), without emission of a photon. The efficiency of FRET is proportional to the inverse sixth power of the intermolecular separation (13), making it useful over distances comparable with the dimensions of biological macromolecules. In addition, the spectral overlap of the donor emission and acceptor absorption spectra contributes to the efficiency of FRET, as well as the relative orientation of the donor and acceptor emission dipole moments.

An example of FRET application in a biochemical assay is the Z′-LYTE™ from Invitrogen for monitoring kinase activity. The homogeneous assay format is based on a FRET peptide substrate and does not require any antibodies. It is highly compatible with automation, making it an attractive method for HTS. The subtlety of the method lies in the differential sensitivity of phosphorylated and nonphosphorylated peptides to the protease-based development reagent. Following cleavage of the nonphosphorylated peptide, FRET no longer occurs between the donor (coumarin) and the acceptor (fluorescein) molecule. Kinase activity is therefore monitored as a decrease in the emission ratio, from the emission signals of the donor and acceptor. In principle, although not yet published, it could also be used in "reverse," with FRET-peptide containing the phosphorylated residue to monitor phosphatase activity. A significant benefit of the ratiometric approach helps to minimize well-to-well variations in FRET-peptide concentration and signal intensities. Consequently, high Z′-factor values (>0.7) can be obtained with relatively low levels of phosphorylation.

Time-Resolved Fluorescence (TRF)

TRF-based assays take advantage of the long lifetime of fluorescence emission from the lanthanide (rare earth) ions, including europium, samarium, terbium, and dysprosium. The emission of the TRF reagents is measured over hundreds of microseconds, compared to nanoseconds for conventional fluorescent dyes. In addition, compared to traditional fluorophores, the lanthanides exhibit a large Stoke shift. For example, a commonly used lanthanide (europium) has an emission signal at 620 nm when excited at 340 nm. TRF-based reagents have been used in a number of different formats, taking advantage of the long-lived fluorescence to reduce undesirable background fluorescence while increasing assay sensitivity.

TR-Intensity

A common application of TRF in intensity mode has been in the heterogeneous assay format referred to as DELFIA® based on the ELISA format. The assay is gradually built (sometimes referred to as sandwich assays) by the sequential addition of reagents with wash-steps in between to remove unused reagent. DELFIA-based kinase assays (14) use a lanthanide-labeled antibody and the final reagent added is a detergent-based enhancement solution, which dissociates the lanthanide from the original chelate forming highly fluorescent micelles. The background fluorescence signal can be gated out by using a time-delayed reading, which results in increased assay sensitivity.

TR-FRET

This has been applied in various homogeneous assay formats, including HTRF® (Cisbio), LANCE™ and LANCE *Ultra*™ (PerkinElmer), and Lanthascreen™ (Invitrogen), all of which use the FRET principle with a lanthanide as the donor and a suitable acceptor. The long-lived emission from the acceptor, as a result of FRET, is used as an indication of the proximity between the donor and the acceptor. Moreover, the use of lanthanide donor (TRF-based reagent) takes advantage of the long-lived fluorescence to reduce background fluorescence signal and helps significantly increase assay sensitivity. Traditional TR-FRET assays have used europium as the donor label and the fluorescent protein allophycocyanin (APC or XL-665) as the acceptor species. However, LANCE *Ultra*™ uses a small-molecular-weight red-shifted emission acceptor dye (U*Light*), which is ideally suited for most biochemical enzyme assays using peptide substrates. LanthaScreen™ TR-FRET platform represents another alternative format by using terbium in place of europium as the long-lifetime donor species and fluorescein as the acceptor species.

Distance over which energy transfer can efficiently take place in TR-FRET assays is much smaller (~7 nm), compared to ALPHAscreen® (~200 nm) and they are often perceived to be limited in their use for peptide-based assays. However, assays employing antibody-based detection reagents with XL665 (cross-linked APC protein; molecular weight around 104 kD) linked to streptavidin have been shown to be successful in detecting kinase activity with co-polymer (poly-Glu-Ala-Tyr) and other immunoassays. Signal from TR-FRET assays can be read on many PMT-based microplate readers and CCD-based imagers.

An assay to measure the mitogen- and stress-activated protein kinase-1 (MSK1) activity by using a biotinylated peptide substrate has been reported (12). The method uses a europium-labeled phosphospecific antibody and streptavidin-allophycocyanin (APC) conjugate to bind the phosphoserine and biotin, respectively. Homogeneous time-resolved fluorescence quenching assay (TruPoint^{TM}) has also been applied to nucleic acid detection (15) and measuring protease activity.

Fluorescence Polarization (FP)

FP measures the polarization of light emitted from a fluorescent probe, following excitation with a plane-polarized light (14,16,17). Most microplate readers used in FP mode provide polarization data as milli-Polarization (mP), where $P = 1000$ mP. Theoretical maximum value for polarization is 500 mP. The polarization value is calculated by using the emission intensity (I) signals measured in two planes (parallel and perpendicular, relative to the excitation plane) from the fluorescent sample, as shown in the equation below:

$$P = \frac{\left(I_{\text{parallel}} - G.I_{\text{perpendicular}}\right)}{\left(I_{\text{parallel}} + G.I_{\text{perpendicular}}\right)}$$

The G-factor can be used to "calibrate" different instruments with a standard (e.g. fluorescein solution with a known theoretical mP value), if absolute milli-Polarization values are required. Polarization (P) and anisotropy (r) are comparable techniques (18) and are closely related, as shown below:

$$P = \frac{3r}{2} + r$$

Anisotropy (r) can be defined as

$$r = \frac{\left(I_{\text{parallel}} - I_{\text{perpendicular}}\right)}{\left(I_{\text{parallel}} + 2I_{\text{perpendicular}}\right)}$$

An approximation of the total intensity can be made using the following equation:

$$I_{\text{total}} = I_{\text{parallel}} + 2I_{\text{perpendicular}}$$

The extent of polarization is dependent on several factors one of which is the rotation rate of the probe, which in turn is dependent on its molecular size. Thus, when polarized light is applied to a fluorescent solution, molecules that are aligned with the plane of excited light are preferentially excited. If they remain close to stationary, the emitted signal will also remain mainly polarized. However, as the free probe molecules are spinning randomly, the emitted signal is polarized to a lower extent and this results in a low milli-Polarization value. Conversely, when the probe is bound to a large protein molecule, the slower rotational movement of the complex (protein-probe) causes the emitted signal to remain polarized, resulting in a higher milli-Polarization value. Most FP assays are based on the change in milli-Polarization (ΔmP), as a result of binding or displacement of the probe in a competition assay. Furthermore, the milli-Polarization value is independent of the probe concentration and this assay format does not require the separation of the bound and free probe molecules in

order to study the association or dissociation interaction between the probe and a larger molecule. A common misconception regarding the avoidance of using tight binding fluorescent probes in FP competition assays in screening has been addressed (19). Use of simulated plots, clearly illustrates that the higher affinity of the probe can allow a wider range of inhibitor potencies to be resolved. Moreover, compounds that enhance, or quench, the fluorescence signal can be easily identified (20).

Fluorescence Correlation Spectroscopy (FCS)

FCS is a specialized technique in the area of fluorescence, which examines the diffusion of fluorescent molecules in an extremely small volume ($\sim 10^{-15}$ L) as fluctuations in the fluorescence signal. The fluorescence fluctuation data is computed and an autocorrelation plot generated, from which diffusion times are obtained. The increase in the diffusion time, as the probe binds a large molecule can be used as a measure of biomolecular interactions at the level of a single molecule. Evotec has successfully applied this approach commercially for many target classes, based on their proprietary FCS$^+$ *plus* platform. Most assays are based on confocal fluorescence signals including intensity, polarization, lifetime combined with single-molecule resolution, in specially designed high-density 1536-well and 2080-well microplates, using Insight^{TM} FCS$^+$ *plus* readers. Moreover, availability of suitable fluorescent reagents has led to FCS being applied in cell-based assays.

A detailed guide to the application of FCS to cellular systems was recently provided (21), highlighting the importance of fluorophore selection, labeling method, and the position of labeling on the success of this application. Furthermore, the application of dual color fluorescence cross-correlation spectroscopy (FCCS), which is an extension of FCS, provides an ability to study the interaction of differently labeled molecules with greater precision than the single-color FCS.

Fluorescence Lifetime (FLT)

A key advantage in using FLT-based approach, compared to intensity-based assays, is that the lifetime of a fluorophore is independent of the intensity signals. However, it can be influenced by changes in the surrounding microenvironment. Thus, the lifetime of a fluorophore can change upon binding to a biological molecule, particularly if it is bound in a deep binding pocket and this change can be used to quantify the level of binding in a homogeneous format. Two methods of measuring FLT are time-domain and frequency-domain (22). The latter method is also referred to as phase modulation (121).

Although intensity changes reflect a global result following binding of the fluorescent probe, FLT data can provide a greater level of detail with two lifetimes (for free and bound forms) and their relative contribution to the overall intensity signal. Thus, from the actual free and bound fractions, the extent of binding can be calculated.

Application of FLT in a binding assay to characterize kinase inhibitors has been recently reported (22). FLT also provides a particular advantage in microscope-based immunohistological studies where the relatively low amounts of fluorescently labeled reagent (e.g. antibody) can undergo photobleaching to a significant extent, causing a reduction in signal intensity with negligible effect on

the lifetime of the fluorophore. This application is referred to as FLIM (fluorescence lifetime imaging microscopy).

Luminescence

Luminescent reagents generate a light signal that is emitted either as an extremely bright flash with a very short half-life, or a lower energy glow that has a much longer half-life. On-board injectors are necessary for flash-based assays readers, and since these assays need to be conducted on a single well at a time basis, HTS groups have not favored this format. In contrast, there is an emerging increase in the use of glow-based chemiluminescent substrates for various enzymes as direct assay, for both biochemical assays and cell-based reporter assays.

For example, substitution of a chromogenic substrate with a chemiluminescent substrate (CSPD; Tropix), for measuring alkaline phosphatase (conjugated onto the detection antibody) in an ELISA method can significantly increase assay sensitivity. This has been exemplified (23), for measuring kinase activity using a biotinylated peptide substrate captured in strepavidin-coated wells of a microplate.

Other additional applications are illustrated by electrochemiluminescence (ECL)-based assays (14) including IGEN (based on ORIGEN® technology; 24) and MSD (MesoScale Discovery, based on MULTI-ARRAY® technology; 25). The light signal is generated by the application of a low voltage to an electrode initiating a cyclic oxidation–reduction reaction of the ruthenium ion, frequently conjugated onto the detection antibody. In the IGEN method, paramagnetic beads are used to capture molecules of interest on their surface and the detection antibody is labeled with ruthenium, bound in a *tris*-bipyridine chelate. The redox reaction, which takes place in the presence of an excess reducing agent (tripropylamine), results in a 620 nm emission signal.

Application of chemiluminescence, using donor and acceptor beads, has also been exemplified in the ALPHAscreen method (26). ALPHAscreen is based on a pair of 250 nm beads (27), with various surface coatings to allow the capture of biomolecules for proximity-based signal detection. Upon excitation with a laser at 680 nm, the photosensitizer in the donor bead converts ambient oxygen into an excited singlet state, which has a half-life of $\sim$4 μsec. Each donor bead can generate up to 60,000 singlet oxygen molecules per second, upon excitation. Diffusion of the singlet oxygen reacts with the thioxene derivative in the acceptor bead (that is in close proximity; up to 200 nm) activating the fluorophores contained with the acceptor bead, resulting in light (520–620 nm) emitted. The relatively large diffusion distance is an advantage in detecting large macromolecular interactions and represents a clear advantage over conventional FRET and TR-FRET assays. However, there is a drawback in that the AlphaScreen beads undergo a "photo-bleaching" effect upon first read. Thus, repeat readings cannot be made from the same well, to obtain kinetic data and separate incubation wells are needed for time-course studies.

Label-Free Technologies

Optical biosensors have traditionally been used to study molecular interactions, for their ability to provide detailed kinetic information and to allow the determination of rate constants (k_{on} and k_{off}) from association and dissociation

reactions, respectively. In addition to surface plasmon resonance (SPR), biosensors have been developed using resonant waveguide grating (RWG) and resonant mirrors. Examples of instruments, using SPR include BIACORE (Biacore), Plasmon Imager (Graffinity), IBIS I and II (IBIS Technologies), and SensiQ® (ICx Nomadics Bioinstrumentation Group). In addition, Epic® (Corning) and BIND® (SRU Biosystems) are based on RWG, IAsys (Thermo) uses resonant mirror and Octet™ System (FortéBio) is based on Biolayer Interferometry (BLI). Both SPR and RWG use evanescent waves to study molecular interactions at, or near, the sensor surface. The principles of these methods have been reviewed (28), with application examples in both biochemical and cell-based assays. Furthermore, extensive ranges of optical and nonoptical biosensors currently available on the market have been reviewed (29,30).

An example of SPR application in studying two small-molecule kinase inhibitors (SB-203580 and SKF-86002) binding to immobilized unphosphorylated p38α the biosensor surface, with the Biacore 3000 instrument has been described (31). It highlights the important issue of retaining a high level of biological activity, following the immobilization step, using the amine coupling method. Apparently, if the coupling to the biosensor surface was conducted in the presence of an excess concentration of SB-203580, it stabilized the protein, resulting in more than 90% active protein on the biosensor surface, compared with the conventional (<20%) immobilization procedure.

Application of surface plasmon resonance (SPR) to measure PKA activity and a universal approach to quantify the extent of phosphorylation in a covalently immobilized peptide substrate (Kemptide) array has been reported (32). This includes the application of a biotinylated zinc(II) complex (Zn_2L^{3+}) where the chelate compound is based on two zinc(II) ions that bridge a phosphate group regardless of the nature of the phosphorylated amino acid. Streptavidin is used to enhance the SPR signal. This method was also used to study the kinetics of on-chip phosphorylation, and the versatile nature of the detection method is advantageous in exploring peptide library arrays for the identification of suitable substrates for new kinase targets. Additional methods reported used phospho-site specific antibodies, followed by SPR measurement and autoradiography with radiolabeled ATP.

The diverse nature of the SPR instruments permits assays of varying throughputs as reagents flow over the thin gold layer surface in the biosensor chip (Biacore) or in 384-well microplates (Epic) with optical sensors. The Octet system uses disposable tips that can be dipped into microplates with minimal reagent consumption and all platforms offer a variety of surfaces, for either direct capture of biomolecules (via tags) or conducting chemical coupling reactions for immobilization.

ASSAY FORMATS

Assays formats can range from the multistep reagent additions (ELISA-like) with multiwash steps, to remove unwanted materials that are particularly demanding in time and resource, to the simple two-step methods. Examples include TR-FRET (Cisbio), ALPHAscreen (PE Biosciences), antibody-based FP (DiscoveRx) comprising (*i*) enzyme reaction and (*ii*) detection step. They are "mix-and-measure" methods, frequently referred to as homogeneous assays, although some require the use of beads. Over the years, the desire to reduce radioactive

reagents in relation to safety issues and environmental concerns has led to the development of numerous nonradioactive assays, most of which exploit fluorescence and luminescence. Most assays methods are used in endpoint mode with a fixed incubation period. However, Omnia™ from Invitrogen and luciferase-based ATP detection methods such as PKLight® (33), Kinase-Glo™ (34), and Biothema kinase reaction rate assay (35), which measure ATP depletion, can be used in kinetic mode. Thus, repeat readings from a single well can be used to generate time-course data, with significant savings in assay reagents. Endpoint-based assays frequently incorporate a stop solution, used to terminate enzyme activity, enabling the assays to be run in a batch-mode. A commonly used stop solution for kinase assays is EDTA to chelate Mg^{2+}, which is normally essential for enzyme activity. Use of robotics can enable the synchronized addition of reagents, to start and stop enzyme reactions. Once the detection step (often a binding reaction) has reached equilibrium, there can be considerable flexibility in the reading of plates providing the assay signal is stable over time.

While several examples of ELISA format have been commonly used for measuring tyrosine kinase activity, an ELISA-based assay has been reported to measure serine phosphorylation, by protein kinase D (PKD) 1. PKD1 is also referred to as protein kinase C (PKC) μ, which belongs to a novel protein kinase family and is activated by a wide range of growth factors. The assay is based on the use of full-length myelin basic protein (MBP) to follow the phosphorylation of Ser-160 residue, on MBP (9). It also illustrates an important point in that the early attempts to set up the ELISA using biotinylated PKD substrate peptides onto streptavidin-coated plates were unsuccessful, due to inefficient phosphorylation. The assay has been shown to be useful to identify PKD inhibitors and measuring cellular PKD activity.

Microplates

A variety of microplates, which satisfy the SBS standards agreed in 1999 (36), are available from 96-wells to 3456-wells, although 384-well microplates are in common use for biochemical assays. A low-volume version of the 384-well plate adequately serves to run miniaturized assays, which can also be run in 1536-well plates. While high-density plates can deliver economies in terms of reagent use and overall costs, there is an increased requirement on the precision of dispensing reagents into microplate wells and the readers to ensure that signal measurements are not compromised from errors arising from small repetitive movements. The large numbers of miniaturized incubations in small wells also raise an important issue regarding incubation temperature and evaporation of the reaction mixture. This can lead to potential "edge effects," where the outer part of the plate can become warmer much more quickly than the inner section, when plates are transferred into incubators with higher than ambient temperature.

There are many vendors including Corning® Costar (37), Greiner bio-one (38), and Nunc™ (39), who provide microplates in a variety of well shapes and various materials including polypropylene and polystyrene in natural and assorted colors. In addition, there are many well surface coatings that are specially designed to facilitate the capture of biomolecules or minimizing background signal from passive adsorption of assay reagents. Some surfaces are designed to permit chemical reactions for performing covalent coupling of molecules.

In general, clear plates are used in reactions with an absorbance signal output while solid black or white plates are used for fluorescence and luminescence assays, respectively. Moreover, clear glass bottom plates are also available (MatriCal™; 40) with flatness better than 2 μm over a 0.75 mm^2 and <150 μm over the entire plate. This is particularly important when using confocal imaging platforms to ensure that the laser remains in focus across the entire area being imaged. Most plates designed for cell-based assays are available with a variety of surface coating to enable cells to adhere to the well surface. Further developments have led to the availability of sensor plates used for label-free technologies on instruments like Epic® (Corning) and BIND® (SRU Biosystems). Similarly, plates with integrated electrodes have led to the emergence of MULTI-SPOT® technology by Mesoscale Discovery (MSD).

Additional uses of microplates include the filter-based plates, used in radioactive filter-capture assays, and deep well microplates used for sample storage and dilution.

Microchips

In addition to highly miniaturized incubations that can take place in extremely small volumes, the use of microchips offer a closed system that eliminates the issue of evaporation. Moreover, the microchannels provide a means of highly accurate internal dispensing and this has been utilized as an effective dilution process with minimal reagent consumption, in the microfluidic gCard™ (SpinX; 41). In terms of separation assays (Caliper; 42 and Nanostream; 43), the microchips offer a miniaturized process for conducting chromatographic-based separation with the ability to measure both substrate and product.

So far, microchips have predominantly been used in detection mode, although "on-chip" assays are also a possibility. A comparison of on-chip and off-chip assay formats for kinases has been reported (44). While it concluded a good correlation between the two formats with significant savings in enzyme and substrate, it also highlighted an important issue regarding compound aggregation with the on-chip assay format. Currently, the off-chip format can be considered as a highly desirable approach. Compound interference can be virtually eliminated and the use of ratiometric data analysis can result in highly reproducible assays with negligible effects arising from reagent dispensing errors.

It should also be noted that the binding properties of both assay reagents and surface characteristics of the channels can be critically important, since the surface area-to-volume ratio significantly increases. Therefore, a simple transfer of protocols for assays developed in a microplate may not always be possible.

The importance of substrate specificity is particularly important during assay development. In a study reported recently (45), two kinase peptide substrates were investigated using the microparallel liquid chromatography (μPLC). The μPLC approach, based on nanostream technology, can analyze 24 samples in parallel by aspirating reaction samples from a 384-well microplate. This study was based on measuring protein kinase A (PKA) activity using two N-terminal fluorescently labeled peptide substrates (Kemptide and CREBtide), with ATP. Both substrate and product were quantified to provide kinetic data with both substrates. Interestingly, although Kemptide had higher V_{max} and k_{cat} values, compared to CREBtide, both substrates had a similar k_{cat}/K_m value suggesting both substrates having similar specificity for PKA. However, when the

PKA/substrate complexes were studied with respect to ATP, there was a five-fold difference for the two substrates. Thus, although the sequence differences between the two substrates did not affect their interaction with PKA, there was an apparent secondary effect on the interaction of the complex with ATP. This could have a profound effect on the selection of appropriate substrate during assay development. While traditional methods employing radioactive labeling and high-performance liquid chromatography (HPLC) are time-consuming and lead to higher variability, the ratiometric measurement of substrate and product (in μPLC) was considered to enhance the reproducibility and robustness of the assay.

Microarrays

This assay format represents a combination of multiplexing capability, where more than one assay can be conducted in a single well of a microplate, or a free-format with proteins spotted on a glass slide or similar support, removing the need for discrete wells. These approaches are exemplified by various technology platforms, like PamChip® (46), SearchLight® (47), and MULTI-SPOT® (25) in microplate formats. In all cases, a microarray of several spots is created within the single well of a microplate.

Examples of slide-based (free-format) microarrays include Protoassay® (48) and Kinome 2.0^{plus} protein function arrays (49), which can be used for the identification of protein substrates for the kinase target. Alternatively, competitive binding assays can be run with a probe to identify additional inhibitors or profile a known inhibitor against a large kinase panel. Such formats have led to the development of Panorama® antibody micoarray (50), spotted onto a nitrocellulose-coated glass slide, providing profiling with over 220 antibodies.

A versatile and generic application has been reported, which uses γ-biotin-ATP with gold nanoparticles modified with avidin, to detect the phosphorylation of a kinase peptide substrate (kemptide) by PKA (51) in a microarray format assay. This assay is also applicable to assess enzymatic phosphatase activity using a phosphorylated peptide substrate. The signal is measured by resonance light scattering (RLS) and the binding of nanoparticles can be enhanced by silver deposition. Potentially, this can be used to detect a single biomolecular-binding event. This microarray method has been claimed to be potentially applicable in HTS, with a significantly reduced demand for assay reagents.

Similarly, a peptide array developed for measuring protein kinase activity, based on fluorescence imaging, has been reported (52). The report uses the nonreceptor tyrosine kinase c-Src as a model to evaluate the peptide array, using positive and negative peptides for quantification of phosphorylation ratio. The method was shown to be successful in measuring c-Src kinase activity, from both purified sample and cell lysate, where Cy^5-labeled antiphosphotyrosine antibody was used to monitor the level of phosphorylation. Surprisingly, the extent of phosphorylation of c-Src substrate was higher, when compared to that in solution—perhaps this was due to apparently high concentrations of both substrate and enzyme in the spotted area. The c-Src inhibitor (SU6656) was able to inhibit the purified enzyme and MCF-7 cell lysate–based reaction on the peptide array. This approach is claimed to be sufficiently sensitive and specific with potential for HTS application in drug discovery.

Peptides are generally considered to be more reliable than the comparable proteins because they are likely to be more resistant to denaturation and have been used for measuring tyrosine kinase activity in cell lysates (53). A method has also been reported (54) to assess the heterogeneity of immobilization.

Multiplexing

With increasing availability of high-affinity antibodies and microarrays (described previously), it is now possible to conduct several assays in the same well of a microplate by using a spotting technique to immobilize several capture antibodies. A number of antigens can be captured from a complex sample, followed by quantification using appropriate detection antibodies.

Examples of this application are commercially available, such as SearchLight® (47), using DyLight™-labeled secondary reagents or using chemiluminescence signal output and Mesoscale discovery (25), using MULTI-SPOT® technology with MULTI-ARRAY® footprints, in specially designed microplates with integrated electrodes. Assays with chemiluminescence signals are measured on CCD imaging systems while signal from the DyLight 800 fluor can be measured with the Odyssey® or Aerius® infrared imaging systems (55). An elegant combined use of microarrays in a microplate well with a porous base is referred to as the 3-D flow through microarray technology (46). Amongst its many diverse applications is kinase activity profiling with a range of immobilized peptide substrates. These plates can be used for substrate identification for new kinase targets or testing clinical samples to monitor fluctuations in kinase pathway activity for kinase profiling, following patient treatment. The arrays are available for measuring activity of tyrosine and ser/thr kinases, using fluorescently labeled antibodies, generating a "fingerprint" based profile. Furthermore, peptide substrates can be immobilized at a single fixed or varying concentrations to assess substrate dependency on the potency of inhibition.

Beads have been used as an alternative to the microplate well surfaces for the immobilization of capture antibodies and thereby enabling multiplex assays. Examples include the well-established Luminex color-coded microsphere-based (xMAP) technology (56), which provides 100 unique bead identity signatures. They can be used to identify each bead in order to interrogate the identity of the biomolecular complex captured on the bead. Essentially, this approach permits the development of multiplex assays where several immunoassays can be conducted in a single incubation, with a single sample. A common application has been in the quantification of multiple cytokines (57) from cell lysates, primarily due to the availability of antibody pairs, originally developed for ELISA-based assays. Nowadays, many vendors supply similar reagents, including Bioplex (58) and LINCOplex (59). A limited multiplexing capability based on different fluorophores and bead sizes is also available with FMAT™ technology, which has a 633-nm helium neon red laser as the excitation source and two PMTs. In this respect, FMAT 8100 HTS system has been used for measuring Src tyrosine kinase activity (60) with a biotinylated substrate tethered onto streptavidin-coated beads and Cy^5-conjugated secondary antibody.

MODES OF INHIBITION

Although a compound can bind to an enzyme and reduce its catalytic activity, the mechanism can be highly specific because it will depend on the site of binding

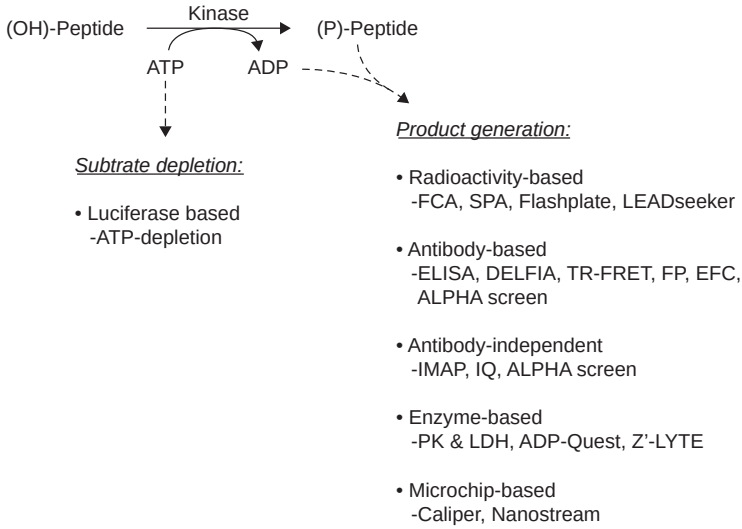

FIGURE 2 Various assay technologies for measuring kinase activity, using a peptide substrate, based on measuring product generation and substrate depletion.

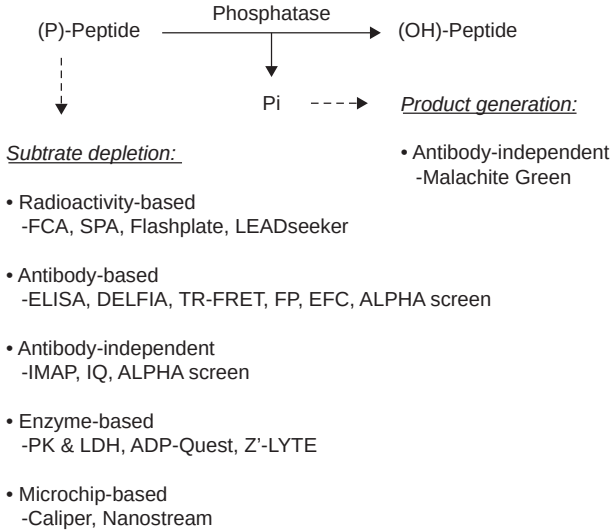

FIGURE 3 Assay technology options for measuring phosphatase activity, with a phosphorylated-peptide substrate, based on measuring product generation and substrate depletion.

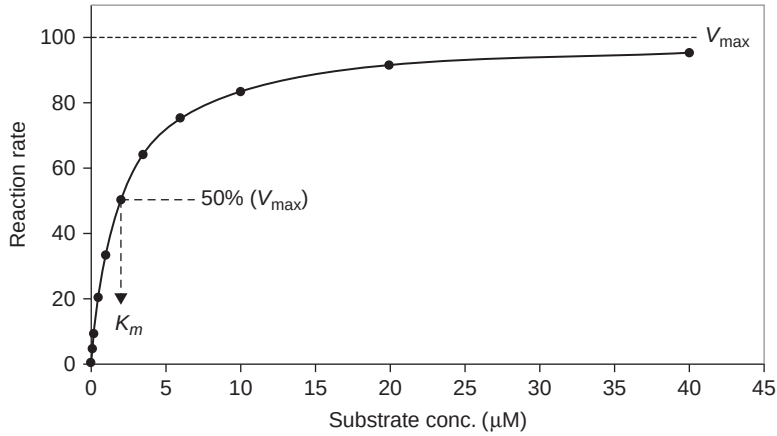

FIGURE 4 Saturation plot showing dependency of reaction rate with respect to substrate concentration and the key parameters (K_m) and (V_{max}), at a fixed enzyme concentration, for a given set of assay conditions including buffer composition, assuming $K_m = 2$ μM and $V_{max} = 100$, for simplicity.

and the enzyme form. The route, by which the compound binds, has traditionally been classified into several types—referred to as the "mode of inhibition." Two common examples are briefly discussed below to illustrate the different ways a compound may inhibit an enzyme. While most inhibitors are assumed to bind in a reversible manner, a diagnostic method for the analysis of inhibitor reversibility has been reported (61).

Competitive Vs Noncompetitive

Competitive inhibition is probably the most common mode of inhibition. Such inhibitors are frequently designed to be substrate analogues and are likely to compete with the substrate for the binding site. An example in the kinase area is staurosporine, which is an ATP-competitive inhibitor. Compared to the control enzyme reaction, the competitive inhibitor increases the apparent K_m value of the substrate, while the parameter V_{max} remains unaffected. Here, the inhibitor can only bind to the free enzyme prior to substrate. During compound screening, apparent potency (IC_{50}) is highly influenced by the substrate concentration when used at higher than its K_m value (Fig. 5). Thus, substrates are often used at a concentration that is equal to (or lower than) their K_m value so that the observed potency (IC_{50}) is not more than twofold different to the inhibition constant (K_i), for a pure competitive inhibitor.

In contrast, pure noncompetitive inhibitors can bind both free enzyme and enzyme–substrate complex, before and after substrate binding. Here, the result is that both apparent K_m is increased and V_{max} is decreased. During inhibition studies, the observed IC_{50} is unaffected by the substrate concentration used and reflects the inhibition constant (K_i) for an inhibitor acting in a pure noncompetitive manner.

When biochemical assays are used for screening inhibitors, the concentration of substrate used, with respect to its K_m value is a key determinant in the

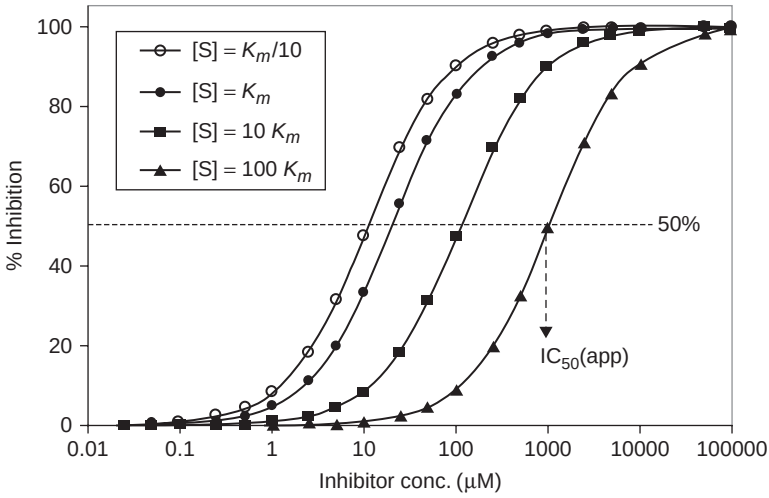

FIGURE 5 Inhibition plot with theoretical dose–response curves for a competitive inhibitor (K_i = 10 μM), at various substrate concentrations, illustrating a rightward shift in the apparent inhibitor potency, IC_{50} (app), when substrate is used at higher concentrations than the K_m value. At substrate concentration equal to K_m, IC_{50} (app) = 20 μM (= $2K_i$). A secondary plot of IC_{50} (app) versus substrate concentration can be used to estimate the inhibitor constant (K_i).

ability of the assay to identify competitive inhibitors. Since apparent potency (IC_{50}) for a competitive inhibitor is affected by substrate concentration, when used at higher than K_m value, it is important that IC_{50} values are transformed into K_i values using the appropriate Cheng–Prusoff equations (62) reflecting their respective inhibition modes.

Inhibition of Catalysis (IOC)

Most kinase activity assays use the activated (phosphorylated, in most cases) form of the target enzyme with a physiological or a model substrate to identify inhibitors of the target enzyme. This format is considered as "Inhibition of Catalysis" (IoC) of the target enzyme (Fig. 6). Historically, nearly all biochemical assays for enzyme targets have been based on this concept.

Prevention of Activation (PoA)

This is a relatively recent application in the kinase area, which considers the use of target kinase (inactive; nonphosphorylated form, in most cases) as the substrate and uses the upstream kinase (active; in most cases, phosphorylated at one or more sites) as the enzyme. This type of assay can enable the identification of inhibitors that may bind to the inactive form of the target kinase and prevent its phosphorylation, in addition to identifying inhibitors (IoC) of the upstream kinase (Fig. 6). Hence, the format is referred to as "Prevention of Activation" (PoA) type assay. It is considered to be particularly advantageous for identifying inhibitors of adjacent kinases in a signal transduction pathway (63).

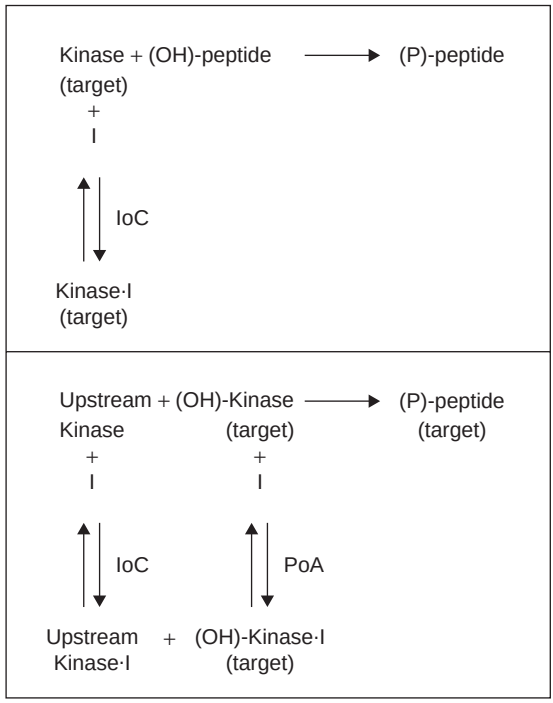

FIGURE 6 Identification of a competitive inhibitor of the kinase target, via IoC (*top panel*), which primarily inhibits the active form of the target kinase, and an alternative assay design (*bottom panel*) can enable the identification of inhibitors of the target kinase (PoA) and upstream kinase (IoC), in the same assay.

Identification of Inhibitors in Binding Assays

In addition to enzyme activity assays, binding assays can be used to identify inhibitors of the target protein (Fig. 7), using active or inactive forms of the enzyme. Moreover, binding assays do not require substrate, ATP, or any additional detection reagents such as phospho-site specific antibodies. Furthermore, binding assays can be conducted with different forms (e.g., phosphorylation status, full length or kinase domain, and mutants) of the enzyme. However, an additional step is essential to confirm that binding leads to inhibition.

A homogeneous assay based on the concept of enzyme fragment complementation (EFC) has been developed into commercial reagents (DiscoveRx; 64) with *E. coli* β-galactosidase to provide a versatile assay platform (65). The proprietary technology is based on the complementation of a small α fragment peptide (~4 kDa; ProLabel or Enzyme Donor) with a ω deletion mutant of the enzyme (Enzyme Acceptor), which occurs with high affinity (K_d ~1 nM), and the enzyme (β-gal) activity can be measured with fluorescent or chemiluminescent substrates. This approach has been reported to confirm the slow association of BIRB 796, with p38α, although BIRB 796 and SB 203580 did not show any selective preference for the active or inactive form of p38α (66). SPR confirmed

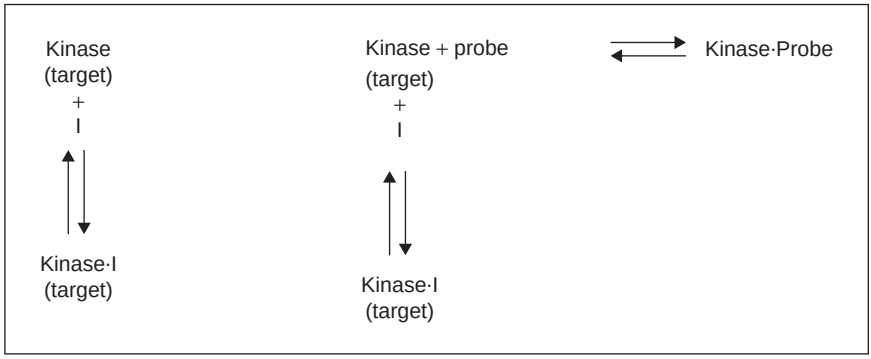

FIGURE 7 Binding assay formats with a direct binding assay approach (*left*) and a competition assay (*right*), using a known inhibitor of the target kinase. This can permit the use of various forms of the kinase target, such as nonactivated, activated, full length, catalytic domain, and mutant forms for compound profiling.

the slow binding kinetics with good agreement between enzyme and cellular activity data.

KINOME*scan*™ (67) is an innovative high-throughput method for screening small-molecule compounds against large numbers of human kinases. The method is a competition-binding assay in which human kinases of interest are fused to a proprietary tag. The amount of kinase bound to an immobilized active site directed ligand is measured in the presence and absence of the test compound.

A recently published comprehensive study of this technology has provided kinase inhibitor selectivity data (68) for 38 kinase inhibitors tested against a panel of 317 kinases. Binding data was summarized on the kinase dendrogram as interaction maps illustrating binding affinity (K_d) values between 1 nM and 10 μM. Apparently, Ambit has recently expanded its commercial KINOMEscan profiling panel to greater than 400 kinases, including therapeutically relevant lipid, mutant, and atypical kinases providing a large coverage of the kinome.

Another binding assay approach has been illustrated by the use of *Kinobeads*™ (69) to measure the potency of compounds, for around 300 different kinases. The beads bind not only a large number of proteins, primarily kinases, but also other enzymes that can bind ATP. In total, more than 1000 different proteins can be bound and their identity monitored by mass spectrometry. The technology permits the compounds to be uniquely "finger-printed" for their kinase interactions. The resulting information is claimed to be sufficiently informative to demonstrate mode of action and to point out potential side effects, thus providing a complementary approach to current methods for screening and selectivity profiling of kinase inhibitors.

In addition, methods such as competitive fluorescence (FP)–based homogeneous polarization ligand binding assays, using a fluorescently labeled kinase inhibitor, can also be run in HTS mode. Also, label-free methods such as SPR-based and isothermal titration calorimetry (ITC) can also be used at lower throughputs, although a large amount of protein or specialized instrumentation is required.

ASSAYS FOR COMPOUND SCREENING

Wide selections of assay types are available for monitoring kinase activity (Fig. 2), most of which measure product generated. They are predominantly nonradioactive and can be chosen on the basis of substrate preference and antibody availability. In addition to the FP assay for ADP quantification (70), a TR-FRET version has recently become available (Adapta™; 48), which uses an Alexa Fluor® 647 labeled ADP analog (tracer) and a europium-labeled anti-ADP antibody. It is also claimed to require much less enzyme, compared to the Kinase-Glo® plus (34) luminescent kinase assay, thereby making it possible to resolve tight-binding inhibitors. Although the use of phospho-site directed antibodies can help increase the assay specificity, it can add a significant cost to the assay. On the other hand, substrate (ATP) depletion can also be used to monitor phosphorylation, as well as ATPase activity displayed by some kinases. Furthermore, the ATP depletion and the ADP quantification assays represent universal kinase approaches, enabling assaying difficult kinase targets, including lipid kinases. While many assay methods have been described in other sections, it is noteworthy that most methods are used in endpoint mode. The type of inhibitors identified can be influenced by the assay format used, in terms of an activity (Fig. 6), or a binding (Fig. 7) assay. Similarly, the apparent potency of a pure competitive inhibitor is highly dependent on the substrate concentration (Fig. 5).

Amongst the examples of various biochemical assays reported is the use of IMAP TR-FRET assay for Polo-like kinase (Plk) (71) which is a ser/thr protein kinase, expressed predominantly during the late G_2 and early M phase of the cell cycle. Following assay validation, by duplicate screening of the LOPAC library, it was used to screen a compound library of more than 97,000 compounds. The assay was run at 25 μM ATP ($\sim 3K_{m,ATP}$) to bias the types of inhibitors detected. Compound interference was also tested in the same assay format, and actives were tested for selectivity against protein kinase D (PKD) by using the IMAP-based FP assay.

Although a large number of assay methods used for kinases can be used "in-reverse" for measuring phosphatase activity (Fig. 3), a homogeneous microplate assay for measuring phosphatase enzyme activity for a ser/thr protein phosphatase type 5 (PP5) has been described (72). This method used 4-methylumbelliferyl phosphate (MUP) and 6,8-difluoro-methylumbelliferyl phosphate (DiFUMP) with fluorescence intensity signal readout; potentially suitable for screening inhibitors from chemical libraries and natural extracts. Progress curves were obtained using fluorescent substrates and both assays were claimed to be suitable for HTS, with Z′-values of greater than 0.8. The report also described the use of an endpoint assay based on the use of *p*-nitrophenyl phosphate (pNPP) as a chromogenic substrate, for monitoring the expression and purification of PP5c, (catalytic subunit). In addition, a radiolabeled assay based on ^{32}P liberated from phosphohistone (prepared by incubating bovine brain histone (type-2AS), with [γ-^{32}P]-ATP and PKA, from rabbit muscle) was used to validate the assay. Although the inhibition profiles from [^{32}P]-phosphohistone was similar to that obtained with DiFMUP, it should be noted that the radiolabeled proteins probably closely mimic physiological substrates. In addition, enzyme activity of alkaline phosphatase (AP) is frequently based on the hydrolysis of MUP to the fluorescent product 4-methylumbelliferone (4-MU).

Although pNPP has been a commonly used substrate, a doubt has been raised on its reliability with newly identified phosphatases (73). An mRNA transcription/processing factor (Ssu72) was reported to hydrolyze pNPP, but not dephosphorylate, a phosphopeptide substrate. A fluorescence intensity–based assay using phospho-peptide substrates (rhodamine 110, *bis*-phosphopeptide amide) has been reported (74) with a very low fluorescence signal and is resistant to aminopeptidase. Upon dephosphorylation, the peptides are hydrolyzed by the protease activity liberating the free form of rhodamine 110, which is highly fluorescent. In order to identify compounds, which do not inhibit phosphatase but inhibit aminopeptidase, an additional peptide AAF-AMC was used concurrently.

Use of an alternative substrate (3-*O*-methyl fluorescein phosphate; OMFP) in a homogeneous 384-well fluorescence intensity assay, for measuring mitogen-activated protein kinase (MAPK) phosphatase-1 (MKP-1) dual-specificity phosphatase activity, was described (75). MKP family members dephosphorylate MAPKs on thr and tyr residues and are encoded by 11 human genes (6). As MKP-1 is highly expressed in various cancers (76–78), it is an attractive therapeutic target. This assay was previously reported as a 96-well format (79) and the current format has been used in the endpoint format, where the phosphatase reaction is terminated by the addition of NaOH and fluorescence intensity is measured to monitor enzyme activity. The assay was used to screen over 65,000 compounds at 10 μM, from an NIH diversity library, to identify MKP-1 inhibitors with 100 compounds resulting in 50% or higher inhibition, representing a hit rate of approximately 0.15%. Subsequently, follow-up studies revealed four potent compounds, with IC_{50} values below 1 μM.

Assay Throughput

This can vary extensively depending on the target class, nature of the assay type, assay robustness, complexity of assay protocol, and size of the compound library. For targets run in HTS mode where the throughputs can be very high, assay designs are typically based on simple "mix-and-measure" protocols. Numerous examples have been provided in this chapter, in various sections.

Reagents and Readers

Assay reproducibility and robustness, especially in homogeneous assays, are highly dependent on the quality of reagents used. Background signal in non-separation assays is usually higher due to the presence of unused reagents, especially in radioactive assays. Assays using crude preparations of target kinase may contain protease or ATPase activity, resulting in peptide and ATP degradation, respectively. Peptide substrates are also more prone to such contaminants over the long contact periods, especially in homogeneous assay formats when screening in large batch sizes. Progressive unwanted "side-reactions" can result in significant drifts in assay signal and this may need to be taken into account during data analysis. Good reagent stability can also contribute favorably to the success of automating a screening protocol. Thus, reagent purity, activity (in the case of enzymes), and stability are all important factors in influencing the outcome of an assay. Appropriate use of tags, used during protein expression and purification, can provide flexibility in selecting appropriate assay technology format. Although normal expression systems only permit the introduction of peptide-like tags like 6-His, c-myc, and FLAG, fusion proteins with SNAP-tag™ (80)

offer the selective introduction of tags via N- or C-terminal, including fluorescent dyes, to generate custom proteins. When using bead-based reagents, continuous agitation is required to ensure that they remain as a consistent suspension throughout the duration of reagent addition. Cost-effective exploitation of various fluorescent-based methods is facilitated by the availability of multimode readers; assays can be designed such that compound interference is minimized during primary screening of large compound libraries.

Recent developments in multimode microplate readers have given rise to instruments such as the Synergy™ 4 multimode detection reader (81) incorporating Hybrid Technology™, providing both filter-based and quadruple monochromator-based fluorescence detection. Additional modes include fluorescence polarization, time-resolved fluorescence, luminescence, and UV-visible absorbance, with fast wavelength switching enabling fast reading for HTS. The combination of filters and monochromator options provides greater flexibility and opportunities to explore new assay designs. Similarly, FLUOstar Omega (82) is a multimode microplate reader offering high-speed read ability and full spectrum (220–850 nm) absorbance, with 1 nm resolution, including reagent injectors for kinetic assays.

Evaporation from microplates, particularly where low incubation volumes are used in high-density plates, can often lead to variation in the signal. This is typically seen as "edge effects" where signals in the outermost wells of the plates are different to those observed elsewhere in the plate. The MicroClime™ environmental lid (83) is a recently developed microplate lid incorporating a fluid-absorbing matrix. The fluid creates a vapor barrier to protect the sample from the exterior environment, especially near the edges of the microplate. The lid is compatible with both manual and robotic systems. It is claimed to prevent DMSO hydration, during compound storage and stop evaporation of ultralow-volume samples during assay incubation.

Assay Development

Good assay design is a crucial step in producing robust and reproducible protocols that will deliver good performance at high throughputs. Assay type (activity vs binding), throughput, and the level of automation implemented can influence the selection of appropriate assay technology and format used. Additional factors, such as radiochemical storage, license limits and safety issues can also influence the extent of radioactive reagents used.

Interestingly, some kinases also display intrinsic ATPase activity (84,85), which can result in the hydrolysis of ATP, in addition to ATP utilization in the phosphorylation reaction, as shown below:

$$\begin{aligned} \text{Kinase activity (phosphorylation):} \quad & \text{(OH)-substrate} + \text{ATP} \\ & \rightarrow \text{(P)-substrate} + \text{ADP} \\ \text{ATPase activity (intrinsic):} \quad & \text{H}_2\text{O} + \text{ATP} \rightarrow \text{ADP} + \text{P}_\text{i} \end{aligned}$$

Luciferase-based ATP depletion assay (86) is a conveniently suitable homogeneous assay format, which can be used to study these reactions, without the need for any tagged substrate or phospho-site antibody.

In terms of defining the assay protocol, although it is important to select the optimal composition of assay buffer, the same importance needs to be placed

on the detection buffer to ensure that assay sensitivity is not compromised. Similarly, concentrations of assay reagents like peptide, ATP, and kinase during the phosphorylation reaction need to be selected such that the rate of reaction is near constant during the incubation period. It has been highlighted previously that the substrate is often used at a concentration equal to, or lower than, the K_m value. Likewise, enzyme is selected such that the reaction rate is proportional to the enzyme concentration. Several interactions from buffer components and assay reagents can be measured in parallel and are more easily revealed using statistical methods than the one-factor-at-a-time (OFAT) approach. These include design of experiment (DOE; 87) and SAGIAN™ (88) automated assay optimization (AAO) from Beckman Coulter. AAO can be run on Biomek® 2000 Laboratory Automation Workstation (88), where several experimental conditions may be tested (Fig. 8) in a single run, avoiding the tedious task of manual pipetting. Moreover, assay optimization process can be enhanced by the use of statistically designed experiments (89). During data analysis, it is strongly recommended that nonlinear curve fitting be used to determine parameters like K_m and $V_{\max}$ (Fig. 4). It is also important to consider the impact on assay signal from using higher concentrations of assay reagent, during the kinase reaction, with respect to detection reagents. For example, an excess of biotinylated peptide can result in a progressive decrease in the assay signal (called the "hook" effect) for a "mix-and measure" assays format like ALPHAscreen (90), where a limited concentration of the detection reagent (streptavidin-linked bead) can bind to both the substrate and product. During experimental planning stages, it is also important to consider the type of plot that will be used for data analysis (linear or logarithmic scale) and select the concentrations of reagents accordingly, to ensure that the data points are relatively equally spaced. This can lead to better estimates of parameters during data analysis. For enzyme-activity assays, it is also important to confirm the linearity of reaction by monitoring the product generated (or substrate depleted) over time in kinetic mode. Again, assay technologies that permit repeat reading of the same well can enable a significant reduction in the consumption of reagents.

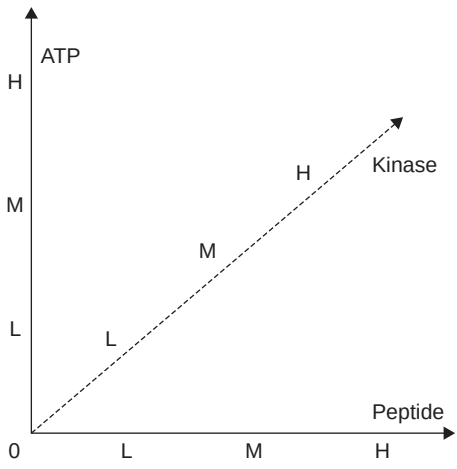

FIGURE 8 Key assay reagents can be simultaneously tested in a single experiment at several concentrations (low, medium, and high; L, M, and H, respectively), as well as zero controls to identify their contribution to the assay signal. For a full DOE or AAO study, this will require 64 individual incubations to measure all interactions.

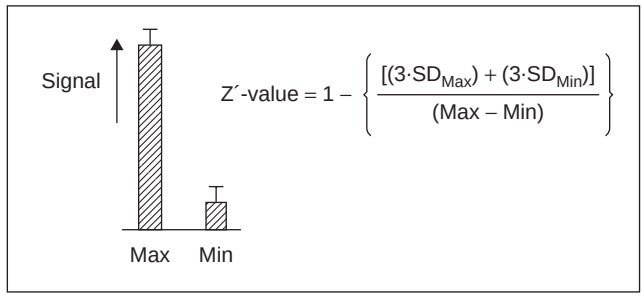

FIGURE 9 Calculation of the Z′-value, for a given set of assay control incubations (noninhibited, Max signal and fully inhibited, Min signal), takes into account the variation (SD) for the control signals, as well as specific (Max − Min) signal.

An extremely useful parameter (Z′-value) can be used (91) to assess the ability of an assay and an indication of the confidence with which inhibitors can be identified, particularly for HTS applications. The calculation is generic and simply takes into account the specific signal and the variability in the maximum and minimum signal values (Fig. 9). Although, it is highly desirable to have assays with a large signal-to-background ratio, satisfactory Z′-values can still be obtained for assays with a high background signal (as much as 50%), provided the variability in maximum and minimum signals is less than 4% (Table 1). In most homogeneous assays, this is achievable because the errors are mainly from pipetting assay reagents. For assays with a high signal-to-background ratio and a large specific signal, there is more tolerance for signal variability.

Assay Validation

Once an assay has been developed, it requires validation. This procedure can cover several aspects relating to both the validity of the assay and the processes being used. With respect to an enzyme-activity assay, reproducibility of the signal for a given incubation (with or without inhibitor), sensitivity to commonly used organic solvent for dissolving test compounds (dimethyl sulfoxide; DMSO), and confirmation of known active inhibitors are integral parts of assay validation. Similarly, automated processes, from dilution and transfer of test samples

TABLE 1 Inverse Dependency of Signal Variability (%cv) on Z′ value for an Assay with a Relatively High (50%) Background (Min) Signal

Max signal	SD	%cv	Min signal	SD	%cv	Z′ value
100	10	10.0	50	5	10.0	0.10
100	8	8.0	50	4	8.0	0.28
100	6	6.0	50	3	6.0	0.46
100	4	4.0	50	2	4.0	0.64
100	2	2.0	50	1	2.0	0.82

If the variability can be reduced to 4%cv, or less, satisfactory Z′ values (>0.6) can be achieved. Note: SD = standard deviation and %cv is calculated as: 100 × SD/signal value.

to assay assembly, require validation to ensure that the cycle time for each step is commensurate for the size of the batch to be processed.

In addition to single concentration (primary) screening, active hits are tested over a concentration range to estimate their respective potency. Although serial dilutions can be performed by robotics, in different ways, an evaluation of interplate and intraplate layout formats has recently been reported (92), using an SPA and a β-lactamase reporter gene assay to highlight the issues associated with both formats, from a practical perspective in compound screening. As expected, the potency data from both formats is in good agreement but the time taken to prepare plates in the intraplate format increases proportionally with increasing compound numbers, while it is practically independent for the interplate format and the number of concentration points used.

Assay Automation

For assays requiring multiple repetitive processes, use of automation can remove the tedious aspects as well as improve the assay reproducibility. The extent to which automation should be considered will depend on factors such as screening capacity required, assay component stability, assay signal stability, plate reading capability, and the automation friendliness of the assay method. Automation can help improve the reproducibility of the assay by enabling the synchronized addition of assay reagents, both to start and stop the reactions, at the appropriate time. In this way, automation can help standardize reaction conditions in each well of the microplates. Ideally, assays should be developed in an appropriate manner, depending on the throughput required and whether or not automation is planned. Simply applying automation to a manually developed assay to achieve high throughput will often fail if the basic assay design is faulty.

CELL-BASED METHODS

Cell-based assays can often be carried out in 384-well microplates, and a common assay format to measure the level of phosphorylation uses fixed cells. Following stimulation of cells incubated with or without test compound, the distribution of phosphorylated protein may be located with fluorescently labeled primary or secondary antibodies. For example, phosphohistone H3 staining in normal human dermal fibroblast (NHDF) cultures, using Cy-labeled antibody and imaged with the ArrayScan™ HCS reader, has been reported (93).

Similarly, NIH 3T3 and HeLa cell-based assays have been reported (94) for the identification of inhibitors of dual specificity phosphatases (DUSPs), which catalyze the removal of phosphate groups from thr and tyr residues on the same substrate. DUSPs appear to play a key role in the regulation of many signaling pathways including mitogen-activated protein kinase (MAPK) and cyclin-dependent kinase (Cdk) activation.

Cell-Lines

Cell-based assays are often based on the use of recombinant cells that have been "designed" to maximize assay signal to improve robustness and reliability. Although it is desirable to use stable, transfected cell lines for reproducible results, transiently transfected cells have also been used. Many cell lines, which either prefer to grow in suspension or adhere onto surfaces, have been used in drug discovery. Examples of cells used in the area of measuring protein

phosphorylation include human chondrosarcoma cell line (SW1353), Baby Hamster Kidney (BHK), THP-1, Chinese Hamster Ovary (CHO), Human Bone Osteosarcoma (U2OS; 95), A431 (28), NIH 3T3, and HeLa cells (94), normal human dermal fibroblast (NHDF) cultures (93).

Reagents and Assays

Cellular translocation of kinases, following their activation, can be studied using suitable antibodies after fixation of the cells. Such assays can provide a highly relevant functional endpoint to study the action of inhibitors. This approach can be used as an alternative to measure enzymatic activity from a cell lysate or the phosphorylation status of the kinase in an immunoassay. Naturally fluorescent proteins [e.g. green fluorescent protein (GFP) and its variants] represent a class of very useful reagent for cell-based assays due to their intrinsic fluorescence that can be measured by a variety of fluorescence imagers and plate readers. An elegant example of this type of assay development was reported (96), where PKCζ–GFP fusion protein was expressed in the human breast cancer cell line (MDA-MB-231) and inhibitors of chemotaxis were used to validate the assay. EGF-induced PKCζ phosphorylation resulted in its translocation from the cytosol to plasma membrane. Although it was initially developed as a microscope-based assay, it may be converted into a 96-well format to study cancer cell migration and metastasis. It could also be used for screening pharmacological agents that either stimulate or inhibit PKCζ translocation.

Similarly, a cell-based assay, using the fluorescent imaging plate reader (FLIPR®), can be used to develop an assay that measures calcium mobilization, regulated by kinase activation. An assay of this type was reported (97) to identify inhibitors of Bruton's tyrosine kinase (Btk) and interleukin-2-inducible T cell kinase (Itk)—members of the TEC family of nonreceptor tyrosine kinases. Such compounds could prove to be useful in treating inflammatory and autoimmune conditions.

A high-content screening assay for the dual specificity mitogen-activated protein kinase phosphatase-1 (MKP-1) has been described (79). Following treatment (± test samples, from a natural product library), HeLa cells grown in collagen-treated 384-well microplates were fixed and immunostained with a variety of primary and secondary antibodies that were labeled with Alexa fluors. The microplates were analyzed by three-channel multiparametric analysis on the ArrayScan II (Cellomics) reader. A plant alkaloid with known antitumor activity, but no known primary cellular target, was identified as a potent inhibitor of MKP-1, with selectivity for MKP-1 over MKP-3. Moreover, it was 5 to 10-fold selective for MKPs over $Cdc25B_2$ and protein-tyrosine phosphatase 1B (PTP1B).

Application of DELFIA to monitor the degree of phosphorylation as an indicator of receptor activation has also been reported (98) using cell lysate. The assay was modified from the trkA assay and satisfactorily validated (with Z′ values >0.5) on the Zymark Allegro™ uHTS robotic platform (99). This method represented a significant and beneficial advance over previously used Western blot assays.

Imagers for High-Content Screening (HCS)

A variety of cell imaging instruments are available that permit high-content screeing (HCS) including ArrayScan® (Cellomics), Acumen Explorer® (TTP

LabTech), IN Cell Analyzer (GE Healthcare), BD Pathway™ (BD Biosciences), and Opera™ (PerkinElmer). A number of these platforms have been reviewed (100) to illustrate how multiplexed HCS assays can be used to increase systems cell biology knowledge for drug discovery. HCS assays have been conducted in HTS mode, with an IN Cell Analyzer 3000 (101).

Many of these platforms provide information-rich fluorescence-based cellular images that can enable a broad range of applications, such as neurite outgrowth, angiogenesis, protein translocation, colocalization, for simultaneously monitoring an extensive number of parameters. Assays based on using GFP-fusion proteins can provide temporal and spatial data, in real-time, to study compound-related changes in live cells. Furthermore, they can enable the use of cell-based assays to study cell signaling, gene expression, membrane receptor binding and internalization, cellular morphology, and immunochemical detection to investigate the expression of proteins and their phosphorylation status. Data files can be extremely large and if storage of all image files is required following an HTS campaign, this can challenge data storage and management infrastructures.

ADDITIONAL TECHNOLOGIES

A new approach Duolink™ (102), based on the proximity ligation assay (PLA) technology, is claimed to be a highly sensitive method for detecting protein interaction (e.g., dimerization) and modification (e.g., phosphorylation). This has been adapted from the method previously described in the literature (103) and is claimed to be highly sensitive, compared to other fluorescence approaches such as fluorescence resonance energy transfer (FRET; 104), bioluminescence resonance energy transfer (BRET; 105,106), and bimolecular fluorescence complementation (BiFC; 107). PLA technology can be apparently applied to study signaling pathways in native cells and tissues. Proteins can be studied at their endogenous level, replacing the need to tag and overexpress proteins.

Given that data from radioactive assays is frequently recognized as the "Gold Standard," Reaction Biology Corporation (RBC) offers a screening service using a nanoliter low-volume method, referred to as Kinase HotSpot℠ (108). This service is offered with 200 kinases and there are several key benefits including reduced false positives from compound interference, and the cost is claimed to be as low as fluorescent screens. However, it should be noted that the highest concentration of ATP that can be used in this method is approximately 10 μM.

Regarding multiplex assays, WideScreen™ assays are available from Novagen (109) based on the Luminex® xMAP® technology platform. Essentially, WideScreen EpiTag™ assays are the next generation of bead-based assays for the quantification of phosphoproteins. Similarly, WideScreen RTK assays can be used to simultaneously monitor several receptor tyrosine kinases (RTKs) for their respective tyrosine phosphorylation status and enable the examination of changes in cellular signaling, caused by disease states or drug treatment.

An elegant semi-synthetic reaction scheme making use of an ATP analogue (ATPγS), followed by alkylation of the thiophosphorylated amino acid, resulting in a semi-synthetic epitope (for thiophosphate ester–specific antibody) of kinase substrates has been reported (110). Several kinases have been reported to use ATPγS as a phosphodonor, although the catalytic rate (k_{cat}) is often reduced

(111). Given that nearly 87% of the kinases tested were successful in using the ATP analogue, and the polyclonal antibodies recognized each thiophosphorylated and alkylated (with *p*-nitrobenzylmesylate; PNBM) substrate, irrespective of the modified residue (serine, threonine, or tyrosine) and the amino acids surrounding the phosphorylation site, this approach potentially offers a wide area of application.

CONCLUSIONS

As a result of reagent developments over the past few decades, in vitro biochemical HTS assays have predominantly used the homogeneous format, due to their mix and measure approach and easy adaptation onto automation platforms to screen compound libraries. Many microplate-based assays utilizing various assay technologies, including SPA (112) and FP (16), several versions of TR-FRET (71) have been used in drug discovery. Emerging methods including the gold nanoparticle-based calorimetric method (113), deep quench (114), and an ATP assay using molecular beacon (115) may provide alternative approaches. Thus, there are many assay technology options available for measuring kinase and phosphatase enzymatic activity, using a variety of substrates. However, it is only by careful consideration of their strengths and weaknesses, specific reagent requirements (e.g., antibody or chemical modification), that the appropriate assay technology can be selected, due to the lack of a single "one-size-fits-all" method.

Generic assay platforms based on ATP depletion (86) or ADP generation (70) can enable rapid and economical assay development of homogeneous microplate-based biochemical assays, suitable for primary screening in HTS mode. Although these approaches provide total flexibility in the nature of substrate and do not require phospho-site antibodies, they are also applicable for developing assays for nonprotein kinases.

Regarding the mechanistic nature of the inhibitor, assays using the active form of the enzyme with model substrates will primarily identify IoC inhibitors. However, the same technology platforms such as TR-FRET and ALPHAscreen can be applied to develop alternative assays that can potentially identify PoA inhibitors (116). Similarly, a fluorescently labeled peptide may serve to be an adequate substrate in many assay technology platforms (TR-FRET, ALPHA, IMAP, IQ, FP-IA, Caliper, etc.). Such IoC assays can also serve as secondary tests to classify the primary hits from a PoA assay into target kinase and upstream kinase inhibitors.

In addition to the use of enzyme-activity assays, binding assays can be used to assess compound affinity to the target protein. These assays can be based either on surface immobilization of the target protein or on homogeneous competition-based assay formats. Furthermore, facilitating screening for new targets with unsuitable substrates, or with very low catalytic activity, they can also aid compound profiling with different forms of the target kinase (nonphosphorylated/phosphorylated/mutant/full length/catalytic domain) that may be prevalent in certain diseases, or subpopulations of the world.

Use of cellular assay methods can provide physiologically relevant phosphorylation status of the kinases in response to stimuli and their dependency in cell transduction pathway. Because of the intricacy with which the kinases and phosphatases interact in the cell, a combination of microarray and multiplex

assay platforms permit clinical samples to be tested more efficiently. These formats also offer a way forward to compound profiling by assessing the phosphostatus of a relatively large number of kinases (within the cellular environment), using biochemical detection methods.

Although several groups have conducted assay technology comparison studies (14,112,117,118), the overall conclusion has been that many assay technologies produce similar relative potencies but some methods can be more susceptible to interference than others. Consequently, the choice of method used will frequently depend on many factors such as ease of use, reproducibility, robustness, assay throughput, sensitivity, cost, and compound interference. Interestingly, a combination of activity (luciferase and luciferin-based, ATP depletion) and binding (competition FP-based) assay methods were recently reported (119) as part of the strategy to facilitate screening across the human kinome. The FP probes were based on known kinase inhibitors, including indolinones and 2, 4, 5-substituted pyrimidine scaffolds. These two assay formats were used to screen over 100 unique human protein kinases to provide selective coverage across the kinome. Furthermore, several kinases were screened more than once to answer the question of differential sensitivity between nonactivated and catalytically active forms of the kinase.

Appropriate selective inhibition of kinases associated within a pathways and a specific disease, with minimal side effects, remains an important goal in the design of future kinase inhibitors (120). Perhaps the next generation of kinase inhibitors (e.g., allosteric, ATP-noncompetitive), acting via new mechanisms of action (115), will help to introduce the desired level of selectivity in kinase inhibition, providing exciting therapeutic opportunities. The rate of progress is likely to be accelerated by the emergence of new technologies and their selective use in drug discovery programs. These will be used to elucidate the complexity of signal transduction pathways and promote the identification of novel therapeutic agents for the treatment of many human diseases.

ACKNOWLEDGMENTS

I would like to express my sincere thanks to John Major for his help from inception to culmination, with supportive comments and invaluable discussions. I would also like to thank my colleagues at AstraZeneca (Alderley Park, UK), Dave Tonge, Geoff Holdgate, Dermott O'Callaghan, Walter Ward, Pete Broad, and Andy Thomas, for their helpful suggestions and critical reading of various sections of the manuscript, and Kevin Hudson, for useful comments.

REFERENCES

1. Manning G, Whyte DB, Martinez R, et al. The protein kinase complement of the human genome. Science 2002; 298:1912–1934.
2. Park J, Hu Y, Murthy TVS, et al. Building human kinase gene repository: Bioinformatics, molecular cloning, and functional validation. Proc Natl Acad Sci U S A 2005; 102(23):8411–8419.
3. Bhaduri A, Sowdhamini R. Domain architectural census of eukaryotic gene products containing O-protein phosphatases. Gene 2006; 366(2):246–255.
4. http://www.cellsignal.com.
5. Jeffrey KL, Camps M, Rommel C, et al. Targeting dual-specificity phosphatases: Manipulating MAP kinase signalling and immune responses. Nat Rev Drug Discov 2007; 6:391–403.

6. Alonso A, Sasin J, Bottini N, et al. Protein tyrosine phosphatases in the human genome. Cell 2004; 117:699–711.
7. Karp G. Cell and Molecular Biology (Concepts and Experiments), 5th ed. New York: John Wiley & Sons, Inc., 2007.
8. Norman D. Kinase Therapeutic Pipelines: An Assessment of Targets and Agents in Development. Needham, MA: Insight Pharma Reports, 2007.
9. Rykx A, Vancauwenergh S, Kimpe Lde, et al. An enzyme-linked immunosorbent assay for protein kinase D activity using phosphorylation ste-specific antibodies. Assay Drug Dev Technol 2007; 5(5):637–643.
10. Gaudet EA, Huang K-S, Zhang Y, et al. A homogeneous fluorescence polarization assay adaptable for a range of protein serine/threonine and tyrosine kinases. J Biomol Screen 2003; 8(2):164–175.
11. Leoprechting AV, Kumpf R, Menzel S, et al. Miniaturization and validation of a high-throughput serine kinase assay using the AlphaScreen platform. J Biomol Screen 2004; 9(8):719–725.
12. Ishii T, Sootom H, Toyoda H, et al. Dual enzyme-linked immunosorbent assay system for detection of endogenous kinase activities of mitogen- and stress-activated protein kinase-1/2. Assay Drug Dev Technol 2007; 5(4):523–533.
13. Stryer L, Haugland RP. Energy transfer: A spectroscopic ruler. Proc Natl Acad Sci U S A 1967; 58(20):719–726.
14. Kadkhodayan S, Elliott LO, Mausisa G, et al. Evaluation of assay technologies for the identification of protein–peptide interaction antagonists. Assay Drug Dev Technol 2007; 5(4):501–513.
15. Ylikoski A, Elomaa A, Ollikka P, et al. Homogeneous time-resolved fluorescence quenching assay (TruPoint) for nucleic acid detection. Clin Chem 2004; 50:1943–1947.
16. Seethala R. Fluorescence polarization competition immunoassay for tyrosine kinases. Methods 2000; 22(1):61–71.
17. Sportsman JR, Gaudet EA, Boge A. Immobilized metal ion affinity-based fluorescence polarization (IMAP): Advances in kinase screening. Assay Drug Dev Technol 2004; 2(2):205–214.
18. Owicki JC. Fluorescence polarization and anisotropy in high throughput screening: Perspectives and primer. J Biomol Screen 2000; 5(5):297–306.
19. Huang X. Fluorescence polarization competition assay: The range of resolvable inhibitor potency is limited by the affinity of the fluorescent ligand. J Biomol Screen 2003; 8(1):34–38.
20. Singh P, Lilleywhite B, Bannaghan C, et al. Using IMAP Technology to identify kinase inhibitors: Comparison with a substrate depletion approach and analysis of the nature of false positives. Comb Chem High Throughput Screen 2005; 8:319–325.
21. Kim S, Heinze KG, Schwille P. Fluorescence correlation spectroscopy in living cells. Nat Methods 2007; 4(11):963–973.
22. Lebakken CS, Kang HC, Vogel KW. A fluorescence lifetime based binding assay to characterize kinase inhibitors. J Biomol Screen 2007; 12:828–841.
23. Lehal C, Daniel-Issakani S, Brasseur M, et al. A chemiluminescent microtitre plate assay for sensitive detection of protein kinase activity. Anal Biochem 1997; 244:340–346.
24. Kibbey MC, MacAllan D, Karaszkiewicz JW. Novel electrochemiluminescent assays for drug discovery. J Assoc Lab Autom 2000; 5(1):45–58.
25. http://www.mesoscale.com.
26. Ullman EF, Kirakossian H, Singh S, et al. Luminescent oxygen channelling immunoassay: Measurement of particle binding kinetics by chemiluminescence. Proc Natl Acad Sci U S A 1994; 91:5426–5430.
27. http://www.perkinelmer.com.
28. Fang Y. Label-free cell-based assays with optical biosensors in drug discovery. Assay Drug Dev Technol 2006; 4(5):583–595.
29. Cooper MA. Optical biosensors: Where next and how soon? Drug Discov Today 2006; 11(23/24):1061–1067.

30. Cooper MA. Non-optical screening platforms: The next wave in label-free screening? Drug Discov Today 2006; 11(23/24):1068–1074.
31. Casper D, Bukhtiyarova M, Springman EB. A Biacore biosensor method for detailed kinetic binding analysis of small molecule inhibitors of p38α mitogen-activated protein kinase. Anal Biochem 2004; 325:126–136.
32. Inamori K, Kyo Y, Nishiya Y, et al. Detection and quantification of on-chip phosphorylated peptides by surface plasmon resonance imaging techniques using a phosphate capture molecule. Anal Chem 2005; 77:3979–3985.
33. http://www.lonzabioscience.com.
34. http://www.promega.com.
35. http://www.biothema.com.
36. http://www.sbsonline.org/msdc/pdf/text1999–04.pdf.
37. http://www.corning.com.
38. http://www.greinerbioone.com.
39. http://www.nuncbrand.com.
40. http://www.matrical.com.
41. http://www.spinx-technologies.com.
42. http://www.caliperls.com.
43. http://www.nanostream.com.
44. Dunne J, Reardon H, Li VTE, et al. Comparison of on-chip and off-chip microfluidic kinase assay formats. Assay Drug Dev Technol 2004; 2(2):121–129.
45. Wu J, Vajjhala S, O'Connor S. A MicroPLC-based approach for determining kinase-substrate specificity. Assay Drug Dev Technol 2007; 5(4):559–566.
46. http://www.pamgene.com.
47. http://www.piercenet.com.
48. http://www.invitrogen.com.
49. http://www.procognia.com.
50. http://www.sigmaaldrich.com.
51. Sun L, Liu D, Wang Z. Microarray-based kinase inhibition assay by gold nanoparticle probes. Anal Chem 2007; 79(2):773–777.
52. Han X, Shigaki S, Yamaji T, et al. A quantitative peptide array for evaluation of protein kinase activity. Anal Biochem 2008; 372:106–115.
53. Brueggemeier SB, Wu D, Kron SJ, et al. Protein-acrylamide copolymer hydrogels for array-based detection of tyrosine kinase activity from cell lysates. Biomacromolecules 2005; 6:1765–1775.
54. Vijayendran RA, Leckband DE. A quantitative assessment of heterogeneity for surface-immobilized proteins. Anal Chem 2001; 73:471–480.
55. http://www.licor.com.
56. http://www.luminexcorp.com.
57. Shi Y, White D, He L, et al. Toll-like receptor-7 tolerizes malignant B cells and enhances killing by cytotoxic agents. Cancer Res 2007; 67(4):1823–1831.
58. http://www.bio-rad.com.
59. http://www.millipore.com.
60. Lee JY, Miraglia S, Yan X, et al. Oncology drug discovery applications using the FMAT™ 8100 HTS system. J Biomol Screen 2003; 8(1):81–88.
61. Lai C-J, Wu JC. A simple kinetic method for rapid mechanistic analysis of reversible enzyme inhibitors. Assay Drug Dev Technol 2003; 1(4):527–535.
62. Cheng Y, Prusoff WH. Relationship between the inhibition constant (K_i) and the concentration of inhibitor which causes 50 percent inhibition (I_{50}) of an enzymatic reaction. Biochem Pharmacol 1973; 22(23):3099–3108.
63. Lu Z, Yin Z, James, L, et al. Development of a fluorescent polarization bead-based coupled assay to target different activity/conformation states of a protein kinase. J Biomol Screen 2004; 9(4):309–321.
64. http://www.discoverx.com.
65. Eglen R. Enzyme fragment complementation: A flexible high throughput screening assay technology. Assay Drug Dev Technol 2002; 1(1):97–104.

66. Zaman GJR, van der Lee MMC, Kok JJ, et al. Enzyme fragment complementation binding assay for p38α mitogen-activated protein kinase to study the binding kinetics of enzyme inhibitors. Assay Drug Dev Technol 2006; 4(4):411–420.
67. http://www.ambitbio.com.
68. Karaman MW, Herrgard S, Treiber DK, et al. A quantitative analysis of kinase inhibitor selectivity. Nat Biotechnol 2008; 26(1):127–132.
69. http://www.cellzome.com.
70. Lowery RG, Kleman-Leyer K. Transcreener™: Screening enzymes involved in covalent regulation. Expert Opin Ther Targets 2006; 10:179–190.
71. Sharlow ER, Leimgruber S, Shun TY, et al. Development and implementation of a miniaturized high-throughput time-resolved fluorescence energy transfer assay to identify small molecule inhibitors of polo-like kinase 1. Assay Drug Dev Technol 2007; 5(6):723–735.
72. Ni L, Swingle MS, Bourgeois AC, et al. High yield expression of serine/threonine protein phosphatase type 5, and a fluorescent assay suitable for use in the detection of catalytic inhibitors. Assay Drug Dev Technol 2007; 5(5):645–653.
73. Meinhart A, Silberzahn T, Cramer P. The mRNA transcription/processing factor Ssu72 is a potential tyrosine phosphatase. J Biol Chem 2003; 278:15917–15921.
74. Kupcho K, Hsiao K, Bulleit B, et al. A Homogeneous, nonradoioactive high-throughput fluorogenic protein phosphatase assay. J Biomol Screen 2004; 9(3):223–231.
75. Johnston PA, Foster CA, Shun TY, et al. Development and implementation of a 384-well homogeneous fluorescence intensity high-throughput screening assay to identify mitogen-activated protein kinase phosphatase-1 dual-specificity protein phosphatase inhibitors. Assay Drug Dev Technol 2007; 5(3):319–332.
76. Magi-Galluzzi C, Mishra R, Fiorentino M, et al. Mitogen-activated protein kinase phosphatase-1 is overexpressed in prostate cancers and is inversely related to apoptosis. Lab Invest 1997; 76:37–51.
77. Denkert C, Schmitt WD, Berger S, et al. Expression of mitogen-activated protein kinase phosphatase-1 (MKP-1) in primary human ovarian carcinoma. Int J Cancer 2002; 102:507–513.
78. Wang HY, Cheng Z, Malbon CC. Overexpression of mitogen-activated protein kinase phosphatases MKP1, MKP2 in breast cancer. Cancer Lett 2003; 191:229–237.
79. Vogt A, Tamewitz A, Skoko J, et al. The benzo[*c*]phenanthridine alkaloid, sanguinarine, is a selective, cell-active inhibitor of mitogen-activated protein kinase phosphatase-1. J Biol Chem 2005; 280(19):19078–19086.
80. http://www.covalys.com.
81. http://www.biotek.com.
82. http://www.bmglabtech.com.
83. http://www.labcyte.com.
84. Paudel HK, Carlson GM. The ATPase activity of phosphorylase kinase is regulated in parallel with its protein kinase activity. J Biol Chem 1991; 266:16524–16529.
85. Kashem MA, Nelson RM, Yingling JD, et al. Three mechanistically distinct kinase assays compared: Measurement of intrinsic ATPase activity identified the most comprehensive set of ITK inhibitors. J Biomol Screen 2007; 12(4):70–83.
86. Singh P, Harden BJ, Lillywhite BJ, et al. Identification of kinase inhibitors by an ATP depletion method. Assay Drug Dev Technol 2004; 2(2):161–169.
87. http://www.isixsigma.com.
88. http://www.beckmancoulter.com.
89. Altekar M, Homon CA, Kashem MA, et al. Assay optimization: A statistical design of experiments approach. J Assoc Lab Autom 2006; 11(1):33–41.
90. DeForge LE, Cochran AG, Yeh SH, et al. Substrate capacity considerations in developing kinase assays. Assay Drug Dev Technol 2007; 5(4):501–513.
91. Zhang JH, Chung TD, Oldenburg KR. A simple statistical parameter for use in evaluating and validation of high-throughput screening assays. J Biomol Screen 1999; 4:67–73.

92. Rodrigues DJ, Lyons R, Laflin P, et al. A three-stage experimental strategy to evaluate and validate an interplate IC_{50} format. Assay Drug Dev Technol 2007; 5(6): 805–813.
93. Gasparri F, Mariani M, Sola F, et al. Quantification of the proliferation index of human dermal fibroblast cultures with the ArrayScan™ high-content screening reader. J Biomol Screen 2004; 9(3):232–243.
94. Vogt A, Cooley KA, Brisson M, et al. Cell-active dual specificity phosphatase inhibitors identified by high-content screening. Chem Biol 2003; 10:733–742.
95. Almholt DLC, Loechel F, Nielsen SJ, et al. Nuclear export inhibitors and kinase inhibitors identified using a MAPK-activated protein kinase 2 redistribution® screen. Assay Drug Dev Technol 2004; 2(1):7–12.
96. Zhao C, Mi C, Zhang Y, et al. Development of a microscopy-based assay for protein kinase Cζ activation in breast cancer cells. Anal Biochem 2007; 362:8–15.
97. Douhan J III, Miyashiro JS, Zhou X, et al. A FLIPR-based assay to assess potency and selectivity of inhibitors of the TEC family kinases Btk and Itk. Assay Drug Dev Technol 2007; 5(6):751–758.
98. Minor LK, Westover L, Kong Y, et al. Validation of a cell-based screen for insulin receptor modulators by quantification of insulin receptor phosphorylation. J Biomol Screen 2003; 8(4):439–446.
99. Armstrong JW. A review of linear robotic systems for high throughput screening—New developments result in more flexibility and lower cost. J Assoc Lab Autom 1999; 4(4):28–29.
100. Taylor DL, Giuliano KA. Multiplexed high content screening assays create a systems cell biology approach to drug discovery. Drug Discov Technol 2005; 2(2): 149–154.
101. Ross S, Chen T, Yu V, et al. High-content screening analysis of the p38 pathway: Profiling of structurally related p38α kinase inhibitors using cell-based assays. Assay Drug Dev Technol 2006; 4(4):397–409.
102. http://www.olink.com.
103. Söderberg O, Gullberg M, Jarvius M, et al. Direct observation of individual endogenous protein complexes *in situ* by proximity ligation. Nat Methods 2006; 3(12):995–1000.
104. Sohn HW, Tolar P, Jin T, et al. Fluorescence resonance energy transfer in living cells reveals dynamic membrane changes in the initiation of B cell signalling. Proc Natl Acad Sci U S A 2006; 103(21):8143–8148.
105. De A, Loening AM, Gambhir SS. An improved bioluminescence resonance energy transfer strategy for imaging intracellular events in single cells and living subjects. Cancer Res 2007; 67(15):7175–7183.
106. Blanquart C, Gonzalez-Yanes C, Issad T. Monitoring the activation state of insulin/insulin-like growth factor-1 hybrid receptors using bioluminescence resonance energy transfer. Mol Pharmacol 2006; 70(5):1802–1811.
107. Hu CD, Chinenov Y, Kerppola TK. Visualization of interactions among bZIP and Rel family proteins in living cells using bimolecular fluorescence complementation. Mol Cell 2002; 9(4):789–798.
108. http://www.reactionbiology.com.
109. http://www.novagen.com.
110. Allen JJ, Li M, Brinkworth CS, et al. A semisynthetic epitope for kinase substrates. Nat Methods 2007; 4(6):511–516.
111. Sondhi D, Xu W, Songyang Z, et al. Peptide and protein phosphorylation by protein tyrosine kinase Csk: Insights into specificity and mechanism. Biochemistry 1998; 37(1):165–172.
112. Park YW, Cummings RT, Wu L, et al. Homogeneous proximity tyrosine kinase assays: Scintillation proximity assays versus homogeneous time-resolved fluorescence. Anal Biochem 1999; 269(1):94–104.
113. Oishi J, Asami Y, Mori T, et al. Measurement of homogeneous kinase activity for cell lysates on the aggregation of gold particles. ChemBioChem 2007; 8(8):875–879.

114. Sharma V, Agnes RS, Lawrence DS. Deep quench: An expanded dynamic range for protein kinase sensors. J Am Chem Soc 2007; 129:2742–2743.
115. Ma C, Yang X, Wang K, et al. A novel kinase-based ATP assay using molecular beacon. Anal Biochem 2008; 372:131–133.
116. Singh P, Ward WHJ. Alternative assay formats to identify diverse inhibitors of protein kinases. Expert Opin Drug Discov 2008; 3(7):819–831.
117. Sills MA, Weiss D, Pham Q, et al. Comparison of assay technologies for a tyrosine kinase assay generates different results in high throughput screening. J Biomol Screen 2002; 7:191–214.
118. Hubert CL, Sherling SE, Johnston PA, et al. Data concordance from a comparison between filter binding and fluorescence polarization assay formats for identification of ROCK-II inhibitors. J Biomol Screen 2003; 8(4):399–409.
119. Kashem MA, Nelson RM, Jakes S. Design of an assay strategy to facilitate screening the human kinome. Am Drug Discov 2008; 3(1):8–14.
120. Bogoyevitch MA, Fairlie DP. A new paradigm for protein kinase inhibition: Blocking phosphorylation without directly targeting ATP binding. Drug Discov Today 2007; 12(15/16):622–633.
121. Lakowicz JR. Principles of Fluorescence Spectroscopy, 2nd ed. New York: Plenum Publishing, 1999.

12 MicroRNA Strategies in Drug Discovery

Wishva B. Herath, Dwi S. Karolina, Arunmozhiarasi Armugam, and Kandiah Jeyaseelan

Department of Biochemistry, Yong Loo Lin School of Medicine, National University of Singapore, Singapore

INTRODUCTION

Discovery of MicroRNAs

Wightman et al. (1) and Lee et al. (2) found that two genes, lin-4 and lin-14, are important in the regulation of the larval development of a nematode, *Caenorhabditis elegans*, and noted that lin-4 gene product represses the lin-14 gene (1). Subsequently, in 1993, it was also discovered that lin-4 does not code for a protein but codes for two short RNA transcripts, which are 22 and 61 nt (nucleotide) long (2) and that it had complementary repeated sequences to the 3′ UTR of the lin-14 mRNA (2,3). These observations led to the understanding that the transcriptional product of lin-4 targeted the lin-14 mRNA leading to translational repression (2,3). Later it became clear that this class of small (∼22 nt long) noncoding RNAs termed microRNAs (miRNA) could regulate animal and plant gene expression either by cleaving or by inhibiting the messenger RNA (mRNA) from taking part in translation.

Progress and Impact

The discovery of such miRNAs and their targets soon resulted in the emergence of a new area of research known as RNA interference (RNAi) that resulted in an extensive utilization of exogenous synthetic small RNAs called siRNAs (small interfering RNAs) for RNAi.

To date, PubMed citations for the MeSH term "miRNA" has 3756 entries and 70% of them have been found to be recent articles from the past two years (4).

Furthermore, currently there are 706 miRNAs that have been identified in humans (5). Of these, 690 have been experimentally confirmed in human (5).

Current Status

From its humble beginnings as a mere scientific curiosity, miRNAs have developed into an extensively studied class of molecules that show great promise as a therapeutic agent. Currently investigations on various areas of miRNA biology are being pursued with vigor all around the world. Studies on miRNAs are not only restricted to academia, but have engaged many private ventures, including big pharma as well as start-up companies. Even though currently miRNA-based therapies are still in their infancy, the performance of oligo-based therapeutics as viable treatment option has been considered very promising. Vitravene® from ISIS Pharmaceuticals Inc., USA, is an FDA approved antisense drug

for Cytomegalovirus retinitis in HIV patients (6). Macugen® co-developed by Eyetech Pharmaceuticals, Inc., and Pfizer Inc., is another oligonucleotide-based drug that is also FDA approved and effective against age-related macular degeneration (7). There are also quite a few other RNA-based drugs that are undergoing phase 2 and 3 clinical trials. For example, Genasense® from Genta Inc., which is a Bcl-2 inhibiting anticancer agent, is in the phase 3 of clinical trials (8). Some of the oligonucleotide-based therapeutic agents that are currently undergoing final clinical trials and have been approved by FDA are listed in Table 1. The progress of these oligonucleotide-based drugs shows that miRNA-based drugs, once optimized, could also have a good potential as therapeutic agents and targets.

BIOGENESIS AND FUNCTION OF miRNAs

Biogenesis

The genes that code for miRNAs are found in intragenic or intergenic regions (9) as well as in the untranslated regions of genes (10, 11). The miRNAs could exist singularly or in clusters (12, 13). Their biogenesis is a multistep process (Fig. 1), which involves several posttranscriptional modification steps. Biogenesis of miRNA is initiated in the nucleus and ends in the cytoplasm. MicroRNA genes are usually transcribed by RNA polymerase II (14, 15) giving rise to a single stranded RNA known as primary miRNA (pri-miRNA). The pri-miRNA contains a 7-methylguanosine cap and a poly A tail (14–16), and it can form a stem-loop structure. The pri-miRNA in mammals is then processed by microprocessor complex that contains the RNAse III enzyme, Drosha (17), cofactor DGCR8/Pasha, and a dsRNA binding domain (18, 19). The microprocessor complex cleaves the pri-miRNA liberating the ~70-nt stem-loop structure, which is termed the precursor miRNA (pre-miRNA). The pre-miRNA stem-loop contains a 5′-phosphate and a 3′-hydroxyl end and is usually flanked by 2 to 3 nt overhangs (20). The pre-miRNA is then exported out of the nucleus into the cytoplasm via a nuclear membrane protein, Exportin5 (21, 22). In the cytoplasm, the pre-miRNA is cleaved by an enzyme complex, which consists of a RNAse III enzyme known as Dicer and a dsRNA binding domain transactivator RNA binding protein (TRBP) or PACT in humans (23, 24), giving rise to a ~22-nt RNA duplex. This RNA duplex forms a precomplex with a multiprotein complex, the RNA-induced silencing complex (RISC). The RISC comprises of the endonuclease Dicer, human immunodeficiency virus (HIV-1), transactivating response (TAR), RNA-binding protein (TRBP) (25), and a human argonaute protein (hAgo2) (26). The miRNA strand of the duplex having the lower internal stability at the 5′ end is retained within the RISC, while the other strand is degraded. This activated miRNA-RISC complex (miRISC) is the main functional unit of the miRNA (27)

Mechanism of Action

The miRISC binds to the target mRNA based on its sequence complementarity. Generally, the miRISC cleaves the mRNA if the complementarity between the miRNA and the target mRNA is complete. Partial complementarity between the miRNA and mRNA will inactivate the target mRNA generally by translational repression and in some cases by miRNA-directed cleavage of mRNA (28). The binding between miRNA and the target mRNA with partial complementarity

TABLE 1 Oligonucleotide-Based (Antisense) Therapeutic Agents that Have Been Approved by the FDA or Currently Undergoing Clinical Trials

Drug	Developed and marketed	Function/mechanism of action	Mode of administration	Trial/approval stage
Vitravene®	Isis Pharmaceuticals, Inc.	Antisense inhibitor of CMV replication, the virus that causes retinitis. CMV retinitis is a degenerative opportunistic infection that affects people with AIDS and results in blindness.	Intravitreal injection	FDA approved
Macugen®	Eyetech Pharmaceuticals, Inc. and Pfizer Inc.	Pegylated anti-VEGF aptamer (pegaptanip sodium injection), which binds to and inhibits the activity of vascular endothelial growth factor (VEGF) in vision loss associated with neovascular AMD (age-related macular degeneration).	Intravitreous injection	FDA approved
Genasense®	Genta Inc. and Aventis	Antisense molecule that targets and inhibits production of Bcl-2 that is believed to block chemotherapy-induced apoptosis. Genasense (in combination with chemotherapy) may enhance the effectiveness of current anticancer treatment.	Continuous intravenous injection	Phase 3
Mipomersen (ISIS 301012)	ISIS Pharmaceuticals	Reduces the production of apolipoprotein B-100, preventing it from carrying certain forms of cholesterol and triglyceride particles in blood in familial hypercholesterolemia.	Subcutaneous injection	Completed Phase 3
Alicaforsen (ISIS 2302)	ISIS Pharmaceuticals and Atlantic Healthcare	Phosphorothioate-modified antisense oligodeoxynucleotide inhibitor of intercellular adhesion molecule 1 (ICAM-1), inhibits protein expression/activity in subjects with ulcerative colitis and pouchitis (and inhibitor for several inflammatory disorders).	Enema	Completed Phase 3
SPC2996	Santaris Pharma	Antisense molecule that targets and inhibits production of Bcl-2 that blocks chemotherapy-induced apoptosis. Enhance the effects of chemotherapy in chronic lymphocytic leukemia (CLL).	Intravenous injection	Phase 2

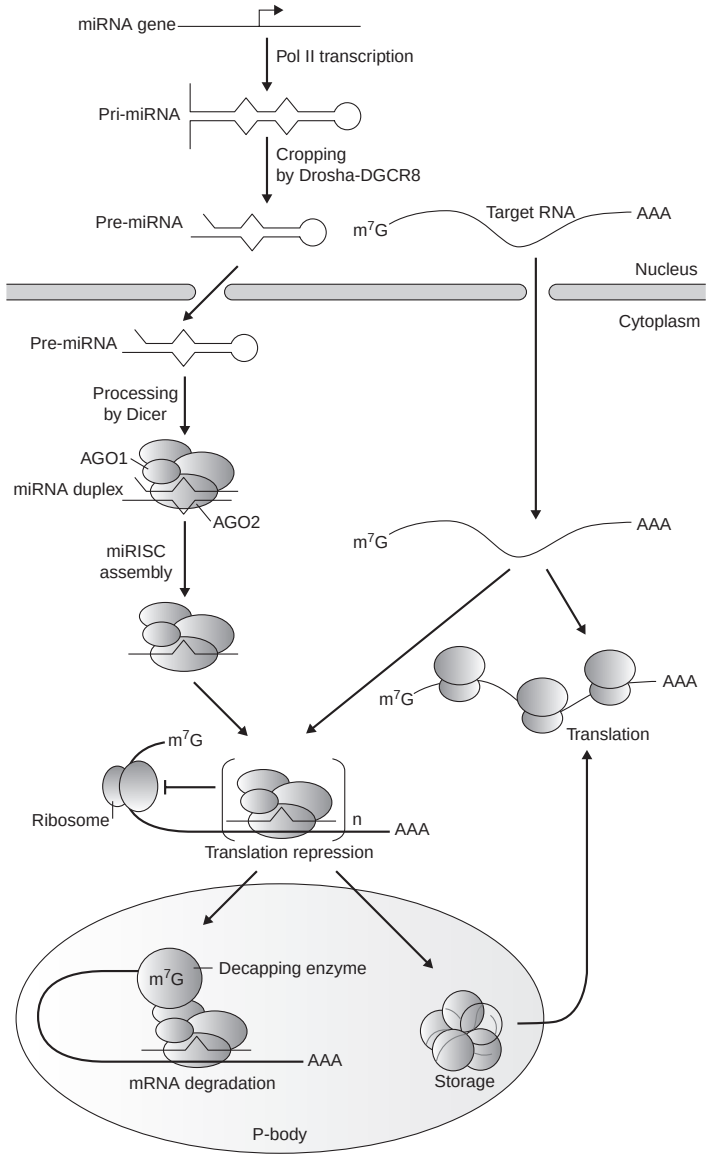

FIGURE 1 Biogenesis of miRNA. *MiRNA* genes are transcribed by RNA polymerase II (pol II) in the nucleus to generate the primary transcripts (pri-miRNAs). Pri-miRNAs are then processed by Drosha, a nucleus RNase III enzyme, and cofactor DGCR8 complex (microprocessor complex) to form the ~70-nucleotide (nt) stem-loop pre-miRNA containing an ~2-nt 3′ overhang. The nuclear export factor exportin-5 exports the pre-miRNA out to the cytoplasm. Subsequently, the cytoplasmic RNase III, Dicer, process the pre-miRNA into small (~22nt) miRNA duplexes. This mature miRNA will then be incorporated with RISC components to form the miRISC complex, the RNAi execution unit. The miRSC binds to target mRNA in the cytoplasm and subsequently arrest the translation process. The fate of the mRNA (recycled or degraded) that is stored in the P-bodies depends on the requirements and conditions of the cell. *Source*: From Ref. 94.

TABLE 2 Comparison of miRNA and siRNA

	miRNA (miRNA)	Small interfering RNA (siRNA)
Presence	Endogenous only (genetically inherited-in built in genome)	Exogenous (introduced by viral or induced by transposon activation) Endogenous (tasiRNA, rasiRNA, scnRNA, and piRNA)
Origin/precursor	Single-stranded (ss)RNA	Coding double-stranded (ds)RNA
Biogenesis processor	Drosha (nucleus) and Dicer (cytoplasmic)	Dicer (cytoplasmic)
Length	19–25 nt	21–22 nt
Complementarity to target (mRNA)	Partial	Complete
Targets (mRNA)	Multiple	Single
Mode of action	Translational repression	Translational inhibition (cleavage of target)
Regulation	Gene specific regulators—regulators of gene expression in genome (*trans* regulators)	Gene specific inhibitors—guardian of genome (*cis* regulators)
Mode of action	Repression of protein translation; acceleration of mRNA degradation; sequestration of mRNA to storage (P-bodies)	mRNA cleaved and degraded by cellular exonucleases
Fate of target	miRNA repressed mRNA can be recycled	Depletion of gene pool

Sources: From Refs. 30, 31, 94, and 95.

enables the miRNA to regulate multiple targets, and it has been estimated that a single miRNA is capable of targeting ~200 different transcripts (29).

miRNA and siRNA

Both miRNA and siRNA are small RNA molecules that regulate the mRNA expression in the cell. However, there are several distinct differences between them (Table 2). miRNAs originate from single stranded RNAs that are coded by the genome of the organisms in which they are found and sequentially processed from the encoding gene to form 20- to 22-nt RNA end product. The siRNAs are processed from long double stranded RNA to form ~19- to 22-nt RNA end product. The siRNAs are normally introduced exogenously in mammals but have been found within the cells in plants and lower animal kingdom. In the cell, miRNAs have multiple targets, thus controlling the regulation of multiple genes, while siRNAs usually target a specific gene. Nevertheless, both of these molecules utilize the same RNAi machinery for their activity with siRNA, entering the pathway at the cleavage by Dicer prior to formation of RISC complex (30).

Both miRNA and siRNA have been reported to have distinct function in the biology of the cell. miRNAs are acquired genetically and are programmed

to regulate expression of genes and are crucial in development and growth of an organism. On the other hand, siRNAs play crucial roles in antiviral defense, silencing/cleaving of the overexpressed or translationally abandoned mRNA, and protecting the genome from interference by transposons (31). Both siRNA and miRNA processing show a symbiotic relationship, one benefiting from the other. Hence, the tools or methods developed for utilization and delivery of siRNA can be used for miRNA with little or no modification. As for therapeutic strategies, siRNA could be used to subdue/inhibit a specific gene (32), while the miRNA could be utilized to suppress a pool of genes (33)

miRNA IN DRUG DISCOVERY

Advantages and Benefits

MicroRNA is a unique molecule that has the capacity to specifically regulate multiple gene targets at the translational level. In conventional therapies, mainly proteins are targeted at specific domains using a single agent. For example, statins, a group of drugs that is widely being used against hypercholesterolemia, targets the HMGCoA reductase, the rate-limiting enzyme of the cholesterol biosynthesis pathway. In contrast, miRNA-based methods give the ability to regulate multiple gene targets with a single miRNA.

It has been shown that several disease states including cancer have a strong relationship with the aberrant expression of miRNAs or have defects in the miRNA biogenesis machinery. The most effective way in treating this type of diseases would be by restoring the normal miRNA profile. Thus, by using miRNA therapy we would be directly treating the cause of the disease instead of the symptoms. Apart from treatment, miRNAs can also be used as biomarkers for early detection and progression/regression of diseases.

Challenges

The major challenges in developing miRNA-based therapy will involve delivery of the therapeutic agent, making it the target agent specific for a particular organ or gene (prevention of off target effects) and possibly the requirement of a larger dose of therapeutic agents.

SCOPE FOR miRNA AS DRUG

MicroRNAs have a tight and wide ranging control over the translation of proteins in the cell. In a disease state, the phenotype may be seen when a defect occurs in either the miRNAs or the targets or the RNAi machinery. Thus, an interference with the RNAi machinery or the restoration of normal miRNA level is needed to revert into normal state.

A mutation in the miRNA transcript can also cause the miRNA to lose or reduce the efficiency of its binding ability with its target mRNAs or allow a broad spectrum nonspecific target binding ability. Either of these scenarios is hazardous as they change the regulation framework of the given cell. As miRNAs have multiple targets, this characteristic can result in widespread changes in the biology of the cell. Similarly, a mutation in a gene encoding protein can also lead to a disease state. This can occur if the mutation affects the miRNA binding site, and therefore, either makes a specific miRNA unable to bind to its target mRNA or allow unrelated miRNA to bind to the (mutated) mRNA. Defects in the RNAi

machinery could also cause a disease state. Here, defects can be widespread and can affect the miRNA profile of the cell.

In some cases, a totally unrelated phenomenon can also cause alterations in the miRNA profile of a cell and subsequently altering the biology of the cell. In cases like these, restoring the normal miRNA profile will not be able to treat/restore but would help in reducing the symptoms.

MicroRNA-related technology could also be used in cases where the cell biology needs to be fine-tuned in a specific manner. For example, if a disease state is caused by an overexpression of a group of related proteins, a specific miRNA targeting the mRNAs of those proteins can be utilized to bring down the levels of the proteins.

If we are to see miRNAs as effective and practical tools for disease therapy, strategies should be developed to control the disease states as in scenarios mentioned above. This mainly involves methods to alter the levels of miRNA in vivo. When the cellular miRNA level needs to be increased, synthetic miRNA (pre-miRNA) can be introduced into the cell by using an effective delivery method. On the other hand, to reduce the expression level of a miRNA molecule, anti-miRNA oligonucleotides (AMOs), 2′-*O*-methyl-antimiRNA oligonucleotides (2′-*O*-Me), 2′-O-methoxyethyl AMOs (MOE), or antagomirs can be delivered into the cells.

CURRENT METHODS AND TOOLS IN miRNA RESEARCH

An investigator working on miRNA has the option of using a wide array of experimental tools and methods. These tools enable them to study all facets of miRNA biology. The methodologies/tools available can be divided into two broad categories: (a) molecular biology methodologies and (b) computational tools. It should be noted that the following compilation of the methods is by no means comprehensive. The highlighted methods are intended to give the reader an understanding on the type of tools available and the ways in which they are used.

Molecular Biology Methodologies

Within the last few years, many molecular biology methods have evolved to facilitate the study of miRNAs. Based on the currently available and effective miRNA target prediction tools, thousands of datasets have become available for miRNA studies. Because there is a considerable amount of false positives in the predicted dataset (bioinformatics based), weeding out the false targets is a daunting task. In cases like these, the most common tool that is used to experimentally verify the targets of a specific miRNA is the luciferase reporter assay (LRA). In this procedure, the 3′ UTR region is cloned into a luciferase reporter plasmid and its expression is measured in the presence and absence of the miRNA under investigation. Northern blotting, RNAse protection assays, quantitative PCR methods can also be used to assess the miRNA-mediated mRNA stability. Another popular method is miRNA profiling. miRNA profiles give the investigator a "snapshot" of the miRNA expression levels at selected time point in the cell. They can be used to study the changes that occur in the known miRNA component of the cell and thus give a broader picture of the effects of a particular condition or a treatment.

MicroRNA microarrays follow the same principle as the "traditional" mRNA microarray but the chip, consumables, and the protocol have been optimized to be sensitive to miRNAs that are much smaller than mRNAs. It contains antisense oligonucleotide probes that hybridize with their specific miRNAs. The acquisition and analysis of data follows the same steps as a normal microarray and finally the results show the expression pattern (upregulation or downregulation) of a specific miRNA in relation to the control with a statistical score, which shows the reliability of the results. Recently, Illumina sequencing technology (Solexa sequencing) has enabled sequencing of small RNAs (<30nt). This high throughput sequencing technology produces highly accurate, reproducible, and quantitative readouts of small RNAs, including those expressed at low levels (Illumina Inc., CA, USA).

When the number of miRNAs that is to be studied is in a more manageable range, several PCR techniques can be used. Real-time stem-loop PCR can be used to quantitate the expression levels of miRNAs. Stem-loop PCR involves using a stem-loop primer to reverse transcribe the miRNA followed by quantitative real-time PCR. The stem-loop primers enable the amplification of the very small miRNA. Alternatively, a low-density array (LDA) could be utilized in order to quantitate the miRNA in the expression profile. The LDA functions as the same chemistry as stem-loop PCR, but could be used to quantitate and detect hundreds of miRNA simultaneously. This technique just like the microarray also gives a quantitative value for the expression level of the specific miRNA. Bead-based flow cytometric methods have also been used in the profiling of miRNAs (34) and if the number of miRNAs is very small then even cloning methods can also be utilized (35).

Bioinformatic Tools

The rapid adaption of computers for the storage of the huge amount of miRNA-related data and the development of bioinformatic tools for the computational study of miRNA are some factors that contributed to the explosive growth of the field of miRNA biology. In most cases, these bioinformatic tools and databases are available online and are freely accessible.

There are several databases that contain information relating to miRNA (Table 3). These databases fall into two broad categories. The first is the databases that contain data on published miRNA and the other contains data on miRNA that have been computationally predicted. miRBase (36–38) is one of the most comprehensive online databases on miRNA (miRBase) in the web. It contains three main tools: (*i*) The first tool miRBase:Sequences is a database that contains details of all published miRNA (39). The latest version is release 13.0 that contains 9539 entries (39). Using this tool one can obtain information such as the sequence details, genomic location, annotation, and references for a particular miRNA. (*ii*) The second tool miRBase targets contains predicted targets of the miRNA in the miRBase::Sequences database (40). It uses the popular miRanda algorithm for the identification of potential target sites in the genome for specific miRNAs (41). (*iii*) The third tool offered by miRBase is miRBase registry, which assigns nomenclature for newly discovered miRNAs prior to its publication (42).

ARGONAUTE 2 is an online database that contains information on mammalian miRNAs and their known or predicted targets (43,44). The site also contains a miRNA motif finder tool that predicts miRNA motifs, which bind to a given sequence (45).

TABLE 3 Public Databases for miRNA Compilation and Target Prediction

Database	Features/functions	URL
miRBase	Published miRNA and their predicted targets	http://miRNA.sanger.ac.uk/
ARGONAUTE 2	Mammalian miRNAs and their predicted targets	http://www.ma.uni-heidelberg.de/
TarBase	Experimentally validated targets of miRNA	http://www.diana.cslab.ece.ntua.gr/tarbase/
miRNAMAP	Published and predicted miRNA and their targets	http://mirnamap.mbc.nctu.edu.tw/
PicTar	Predicted targets by the PicTar algorithm	http://pictar.mdc-berlin.de/
TargetScan	Predicted targets by the TargetScan algorithm.	http://www.targetscan.org/
miRDB	Software for target prediction and functional annotation of animal miRNAs.	http://mirdb.org/miRDB/
ViTa	A database on viral miRNA and their predicted host miRNA targets.	http://vita.mbc.nctu.edu.tw/intr.php
miRNA—target gene prediction at EMBL	Predicted targets for *Drosophila* miRNA.	http://www.russell.embl-heidelberg.de/miRNAs/

The miRNA database TarBases (46,47) contains information on experimentally supported targets of miRNA. Currently, the TarBase5.0 database contains data on 1333 experimentally supported miRNA targets (46) miRNAdb (48) is a database that contains information on reported miRNA genes and their validated targets. The database miRNAMap (49,50) contains information on published as well as predicted miRNA and their targets. Target prediction algorithms have the capacity of going through a particular genome and based on a set of rules, to find potential binding sites for a given miRNA. Because of the high processing power of modern computers such a search takes only a limited amount of time.

miRanda (51,52) is the most widely used algorithm for the identification of miRNA targets. It takes the nucleotide sequence of the miRNA and a genomic sequence as an input and the prediction is done in a two-step process (51). First a local alignment search is performed between the given RNA sequence and the genomic sequence. A score is given to each match based on the sequence complementarity. The matches above a certain threshold score is taken into the next step where their thermodynamic stability is analyzed using the RNAlib (53) library from the ViennaRNA package, and a statistical (Z) score is given to each final predicted target site. The TargetScanS algorithm (54–57) predicts the miRNA targets by looking for the conserved 8mer and 7mer sites that match the seed region

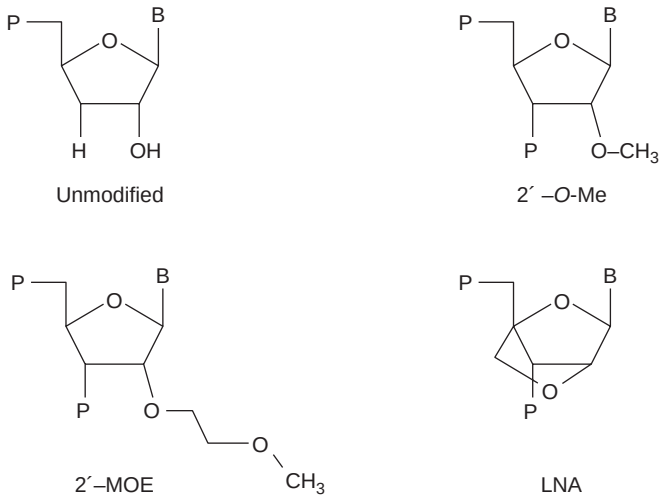

FIGURE 2 Chemically modified anti-miRNA oligonucleotides. *Abbreviations*: P, phosphate bridge; B, base.

of the specific miRNA and it contains separate search tools for mammal, worm, and fly miRNA. There are also other algorithms for miRNA target prediction such as PicTar (58), DIANA (59), RNAhybrid (60), etc. It should be kept in mind that integrative approaches that combine more than one of these algorithms provide a more accurate picture on miRNA targets.

MODULATION OF miRNA LEVELS IN THE CELL

Various tools and protocols have been developed to specifically increase and decrease the miRNA level of the cell with varying degrees of efficiency. These tools and methods would lay the foundation for the treatment strategies of miRNA-based therapy.

Potential Therapeutic Agents

There are several molecules that can be used to inhibit specific miRNAs in a cell. Generally, they have a sequence complementarity with the specific miRNA and in most cases chemically modified (Fig. 2) to increase their inhibiting ability. The following molecules are commonly used as miRNA inhibitors.

Anti-miRNA Oligonucleotides (AMOs)

AMOs are short DNA molecules that has the ability to bind with their target miRNAs and inactivate them. Ideally, they are of the same length as the target miRNA and have full sequence complementarity, so as to increase the binding affinity and the stability of the resulting DNA/miRNA hybrid. Nevertheless, microinjection of 11 AMOs for 11 miRNA targets in *Drosophila* has led to interference to normal development only in four of the cases (61). The poor stability of unmodified DNA in vivo has been attributed with the low efficiency of inhibition.

2′-O-Methyl-Anti-miRNA Oligonucleotides (2′-O-Me)

2′-*O*-Me molecule is an AMO with a methyl substitution at 2′ carbon of the sugar ring. The methyl group improves the efficiency by improving the binding affinity to miRNA and also conferring a limited amount of nuclease resistance (62). 2′-*O*-Me miRNA has been effectively used to inhibit the miRNA let-7 in *C. elegans* (63).

2′-O-Methoxyethyl AMOs (MOE)

As compared to 2′-*O*-Me, MOE has a higher affinity and specificity to its target miRNA (64). MOE has been used to identify and inhibit miR-143 in regulation of adipocyte differentiation (64)

Locked Nucleic Acid AMOs (LNA)

LNAs contain one or more LNA nucleotide monomers with a bicyclic furanose unit, which is locked in an RNA mimicking sugar conformation (65). They have a very high affinity towards their targets (65). LNA-based conjugation of miR-122 showed more effective inhibition than the 2′-*O*-Me modified oligonucleotides (66).

Cholesterol Conjugated miRNA-Antagomirs

Antagomirs (67) are single stranded RNA molecules of 21 to 23 nt in length, complementary to the target miRNA sequence. Antagomirs are cholesterol conjugated miRNA with modified (2′-*O*-Me) ribose sugars (68). They have been effectively used to identify the effects of miR-122 in cholesterol biosynthesis (67).

The molecules described above reduce the amount of miRNA in the cell. Interestingly, there are several studies that hint at the potential of using synthetic molecules to increase the amount of specific miRNAs in the cell. In one study it has been shown that dsRNAs targeting the promoter regions of E-cadherin, P21, and VEGF brings about a long-lasting induction of the target genes (69). In another study, dsRNAs complementary to the promoter of the progesterone receptor have been shown to increase the expression of the progesterone receptor protein (70). If we are able to design dsRNAs that target a promoter region that affects a miRNA gene then we may be able to cause the upregulation of that gene, thus increasing the amount of that specific miRNA.

Delivery Methods

MicroRNA delivery methods should be able to efficiently introduce miRNAs to the cell and also be able to target the molecule to a particular site. The delivery method greatly depends on the modulating molecule/agent that is being administered. Simple transfection and electroporation methods have been utilized to deliver the dsRNA molecules into cells in vitro. However, the expression vector based delivery to express the dsRNA within the cells is proposed to be most effective in expressing or introducing the gene regulator. The polycistronic RNA polymerase II expression vector known as SIBR vectors is regarded as one of the most effective vector for dsRNA deliveries (71). SIBR vector uses a modified miR-155 precursor stem-loop and flanking BIC sequences, BIC being the gene that codes for the precursor of miR-155 (71).

It is now known that conjugation of the mediator molecule to bile acids, long fatty acids, or cholesterol controls the siRNA uptake into the cells and

that the uptake process depends on the interactions with lipoprotein particles, lipoprotein receptors, and transmembrane proteins (72). The study also states that the siRNA could be used to target an organ or a tissue based on the conjugated molecule. For example, antagomirs, which are anti-miRNAs conjugated with cholesterol, could be directly injected to the animal model. Intraperitoneal injection has been proved to be effective in obese mice model (67). The low-density lipoprotein (LDL) conjugation is reported to deliver siRNA primarily to the liver (72). It has also been shown that siRNA incorporated neutral liposome 11,2-dioleoyl-sn-glycero-3 phosphatidylcholine (DOPC) can be used for siRNA delivery (73). There is a potential for this method to be used in miRNA delivery.

SEARCH FOR NEW MICRORNAs AND THEIR FUNCTIONS

The typical identification workflow of new miRNA includes isolation of total RNA, cloning of small RNA, sequencing, and database search to identify telltale sequence patterns of miRNA (74). To date, all the miRNAs have been identified by molecular cloning (74) followed by sequencing, and in one isolated case, the oligonucleotides was identified as polyribosomes bound molecules (75). However, it is believed that the majority of miRNAs have not been discovered. It is suspected that the "junk" sequences in our genome may largely code for miRNAs. Thus, an effort such as the human genome project will be very useful in revealing the miRNA profile in any organisms. Characterization of the newly identified miRNA, however, needs an integrated approach using bioinformatic and molecular biology strategies. Gene databases can be used to predict for potential targets. Nevertheless, molecular biology and protein biochemistry intervention must be utilized to validate or prove the molecular target and functionality of the new miRNAs.

POTENTIAL THERAPEUTIC APPLICATIONS OF miRNAs

Cancer

The link between cancer and miRNA is supported by the extensive amount of scientific evidence that the subject has generated in recent years. It has been shown that a considerable number of miRNA are coded by regions in the genome, which are known to be associated with initiation and progression of tumor, and that the normal expression of miRNA is deregulated in various types of cancer. Currently, the entire mechanism in which miRNA contributes to cancer is not fully elucidated.

The mir-15 and mir-16 that are located in chromosome 13 have been shown to be either deleted or downregulated in most of the B-cell chronic lymphocytic leukemias (76). Similarly, it has also been shown that miR-143 and miR-145 are downregulated in the adenomatous and cancer stages of colorectal neoplasia (77). In fact, the general observation has been that downregulation of miRNAs occurs in tumors as compared with normal tissues (34). However, it should be noted that the above observation does not hold true for all miRNAs. miR-21, miR-141, and miR-200b have been observed to be highly expressed in malignant cholangiocytes (78). The miR-21 is also known to be highly expressed in breast tumors (79). Thus, it is quite complex to provide a general hypothesis for the role played by miRNAs in cancer, as different miRNAs have different

effects on cancer. In some cases, cancer is attributed to a cluster of miRNAs. miRNA cluster miR-17–92 have been found to highly expressed in B-cell lymphoma patients (80).

Although there is a tight relationship between cancer and miRNAs, the relationship differs greatly with types of cancer. Thus, it is safe to assume that the miRNA-based therapies for cancer would be aimed mainly at correcting the abnormal expression of miRNA in the disease state and that the treatment strategy would very much depend on the type of cancer that is being treated.

Metabolic Disease

Diabetes

The overexpression of the pancreatic islet specific miRNA miR-375 has been shown to suppress glucose-induced insulin secretion (81). It is proposed that miR-375 acts via the inhibition of mRNA that encodes the protein Myotrophin (81). It is known that the insulin secretory pathway in tightly controlled at multiple levels from its biosynthesis to exocytosis (82), hence, miR-375 is believed to be one of the modulating agents to the insulin regulatory network. Myotropin inhibits F-actin assembly via CapZ (83). Even though several hypotheses exist, which link the myotrophin inhibition by miR-375 (82) with the suppression of insulin secretion, to date, none has been conclusively proven. In another study, it has been reported that miR-9 diminishes the expression of the transcription factor Onecut-2, which leads to a series of events, eventually exerting a negative control on insulin release (84). Further studies on miR-375, miR-9, and related miRNA regulation of insulin secretion can be used in a clinical condition to modulate the insulin levels in blood.

Hypercholesterolemia

Inhibiting miR-122, an abundant liver specific miRNA, leads to the reduction in levels of plasma cholesterol (67). It has also been shown that inhibition of miR-122 results in improvement in liver steatosis and reductions in several lipogenic genes in an obesity mouse model (85). Thus, the current evidence supports that inhibition of miR-122 could prove to be beneficial in the treatment of hypercholesterolemia.

Neurological Disorders

Apart from the changes in miRNA levels, deregulation of miRNA biogenesis or its component could also contribute to a disease state. In neurological/developmental disorders (not neurodegenerative), defects in the miRNA biogenesis/processing stage largely contribute to the disease conditions.

Fragile X Syndrome

The fragile X syndrome is caused by a mutation in the fmr1 gene, which silences the FMRP (Fragile X mental retardation protein). Studies have shown that the dFMR1P, the *Drosophila* ortholog of the human FMR1P gene, is associated with the RISC complex (86). It has also been shown that human FMRP can act as a miRNA acceptor protein for Dicer and that it facilitates the assembly of miRNAs on its target RNA sequence (87). Thus, these observations suggest that the root cause of the symptoms shown by the patients of the fragile X syndrome is due to the alterations in the RNAi machinery as a result of the mutation of the gene

encoding FMRP. This is a special case because the disease is caused by a protein that is vital for the miRNA processing machinery. Because of this reason, the therapeutic strategies involving modulating the miRNA levels cannot be used directly in this instance.

DiGeorge Syndrome

Most patients suffering from DiGeorge syndrome have a deletion in a region of the 22nd chromosome known as the DiGeorge syndrome chromosomal region (DGCR) (88). The gene DGCR8 is located in the DGCR (79). It has been reported that the enzyme Drosha, which participates in the RNAi machinery, interacts with DGCR8 (19). Thus, the disease phenotype in DiGeoroge syndrome may be due to the irregularities of the RNAi mechanism.

Viral Infections

Simian Virus 40 (SV40)

It has been observed that miRNA from Simian Virus 40 accumulates at the late phase of infection in an infected cell. The miRNAs are reported to have a full complementarity to early viral mRNAs, leading to its translational inhibition (89). The SVmiRNA suppresses the expression of the T-antigen from the infected cell, making it more resistant to lysis by cytotoxic T-cells, thus, giving the viral particles a higher rate of survival (89). Cases like these can be exploited in a clinical setting whereby knocking out the SVmiRNAs would make the infected cells more susceptible to the T-cells, thus help in controlling the spread of viral particles.

Human Immuno-Deficiency Virus (HIV)

miR-N367 that is coded by the *nef* gene in HIV-1 virus is reported to suppress HIV virulence in human T-cells by reducing the HIV-1 LTR promoter activity (90). Mechanisms such as these can be therapeutically enhanced to limit the HIV infection.

Apart from regulating its own mechanisms using viral miRNAs, HIV also changes the miRNA levels of the infected host cells. During an HIV infection, the cellular miRNAs: miR-122, miR-370, miR-373, and miR-297 are upregulated and the miR-17/92 cluster is downregulated (91). The viral replication was inhibited by Dicer and Drosha (91) in peripheral blood mononuclear cells from HIV-1 infected donors and in latent infected cells. The details of these mechanisms would shed more light on the regulation of HIV life cycle by the virus itself and the infected cell, making pharmaceutical intervention feasible.

Other Viral Diseases

When the level of miR-122, a miRNA that is abundantly found in the human liver, was reduced, it led to the reduction of autonomously replicating hepatitis C viral RNAs (92). miR-122 is thought to bind to the 5′ noncoding region of the viral genomic RNA and because manipulation of miR-122 levels did not affect the translation or stability of the viral mRNA, it is believed that miR-122 affects the replication of the hepatitis C virus (92).

Cellular miRNA, miR-32, has been shown to restrict the accumulation of the primate foamy virus type-1 in human cells. Furthermore, the virus itself produces a protein, Tas, which suppresses miRNA directed functions (93). This

is an example on how viruses and hosts have co-evolved machineries for infection/evasion. Knowledge on mechanisms such as these would enable the scientists to manipulate in such a way that the balance is tipped in the favor of protecting the host cells from infection.

FUTURE OF MICRORNA THERAPEUTICS

miRNA is a fascinating molecule. It sheds light on the efficient "hierarchy" of regulatory agents, which exist in the cell so that the complex mechanisms and processes inside the cell can be controlled with much accuracy. Given the ability to modulate specific miRNA levels in the cells, scientists now have the power to control the cell at the systems level. This as opposed to controlling a specific protein in the conventional methods, is more effective in a clinical setting as the cell's own natural regulatory pathways would be exploited in the treatment of diseases. The exploitation of the RNAi pathway via siRNA in developing therapeutics is a positive sign that shows that miRNAs could also be used in similar applications. The exponential growth of research and the initiation of pharmaceutical ventures to develop therapies based on miRNAs show that the emergence of miRNA as therapeutics is not far fetched.

However, there are several issues that need to be resolved to secure the growth of the field of miRNA. We believe that these would be resolved in time and would not pose a major threat for miRNA-based therapeutics. The knowledge on the various regulatory mechanisms of the miRNA-mediated processes is vital to the understanding of miRNA biology. In light of the fact that the expression of hundreds of genes is controlled by a single type of miRNA, the question what triggers/regulates the expression of miRNA is an interesting one.

Based on the human genome sequence informations, the majority of miRNAs in the cell have not been discovered yet, and a large number of targets for the known miRNAs are also unknown. Comprehensive understanding of various miRNAs and their targets are vital to develop an effective therapeutic strategy. However, because of the vast number of miRNAs that are thought to exist in the cell and the considerable number of targets that a single miRNA has, the process of classifying the entire miRNA component in a cell has become a colossal one. Thus, there is a pressing need for a large-scale collaborative project, designed on the same lines as the human genome project, to be completed experimentally to identify and verify the targets of the currently unknown miRNAs. The knowledge resulting from such a project would greatly accelerate the development of miRNA-based therapeutics.

REFERENCES

1. Wightman B, Burglin TR, Gatto J, et al. Negative regulatory sequences in the lin-14 3′-untranslated region are necessary to generate a temporal switch during *Caenorhabditis elegans* development. Genes Dev 1991; 5:1813–1824.
2. Lee RC, Feinbaum RL, Ambros V. The C. *elegans* heterochronic gene lin-4 encodes small RNAs with antisense complementarity to lin-14. Cell 1993; 75:843–854.
3. Wightman B, Ha I, Ruvkun G. Posttranscriptional regulation of the heterochronic gene lin-14 by lin-4 mediates temporal pattern formation in *C. elegans*. Cell 1993; 75:855–862.
4. http://www.ncbi.nlm.nih.gov. "MiRNAs"[Mesh]—PubMed Results (accessed December 2007).

5. http://miRNA.sanger.ac.uk/sequences/browse-Homo sapiens (accessed April 2009).
6. http://www.isispharm.com. Isis Pharmaceuticals + Vitravene® (accessed April 2009).
7. http://www.macugen.com. Macugen, An Exciting Treatment for AMD (accessed April 2009).
8. http://www.genta.com. Genasense® (oblimersen sodium) Injection—GENTA (accessed April 2009).
9. Rodriguez A, Griffiths-Jones S, Ashurst JL, et al. Identification of mammalian miRNA host genes and transcription units. Genome Res 2004; 14:1902–1910.
10. Smalheiser NR. EST analyses predict the existence of a population of chimeric miRNA precursor-mRNA transcripts expressed in normal human and mouse tissues. Genome Biol 2003; 4:403.
11. Cullen BR. Transcription and processing of human miRNA precursors. Mol Cell 2004; 16:861–865.
12. Kim VN, Nam JW. Genomics of miRNA. Trends Genet 2006; 22:165–173.
13. Wu W, Sun M, Zou GM, et al. MiRNA and cancer: Current status and prospective. Int J Cancer 2007; 120:953–960.
14. Lee Y, Kim M, Han J, et al. MiRNA genes are transcribed by RNA polymerase II. EMBO J 2004; 23:4051–4060.
15. Cai X, Hagedorn CH, Cullen BR. Human miRNAs are processed from capped, polyadenylated transcripts that can also function as mRNAs. RNA 2004; 10:1957–1966.
16. Kim VN. MiRNA biogenesis: Coordinated cropping and dicing. Nat Rev Mol Cell Biol 2005; 6:376–385.
17. Lee Y, Ahn C, Han J, et al. The nuclear RNase III Drosha initiates miRNA processing. Nature 2003; 425:415–459.
18. Gregory RI, Yan KP, Amuthan G, et al. The microprocessor complex mediates the genesis of miRNAs. Nature 2004; 432:235–240.
19. Han J, Lee Y, Yeom K-H, et al. The Drosha-DGCR8 complex in primary miRNA processing. Genes Dev 2004; 18:3016–3027.
20. Du T, Zamore PD. microPrimer: The biogenesis and function of miRNA. Development 2005; 132:4645–4652.
21. Bohnsack MT, Czaplinski K, Gorlich D. Exportin 5 is a RanGTP-dependent dsRNA-binding protein that mediates nuclear export of pre-miRNAs. RNA 2004; 10:185–191.
22. Lund E, Guttinger S, Calado A, et al. Nuclear export of miRNA precursors. Science 2004; 303:95–98.
23. Grishok A, Pasquinelli AE, Conte D, et al. Genes and mechanisms related to RNA interference regulate expression of the small temporal RNAs that control *C. elegans* developmental timing. Cell 2001; 106:23–34.
24. Lee Y, Hur I, Park SY, et al. The role of PACT in the RNA silencing pathway. EMBO J 2006; 25:522–532.
25. Haase AD, Jaskiewicz L, Zhang H, et al. TRBP, a regulator of cellular PKR and HIV-1 virus expression, interacts with Dicer and functions in RNA silencing. EMBO Rep 2005; 6:961–967.
26. Hammond SM, Boettcher S, Caudy AA, et al. Argonaute2, a link between genetic and biochemical analyses of RNAi. Science 2001; 293:1146–1150.
27. Bennasser Y, Yeung ML, Jeang K-T. HIV-1 TAR RNA subverts RNA interference in transfected cells through sequestration of TAR RNA-binding Protein, TRBP. J Biol Chem 2006; 281:27674–27678.
28. Yekta S, Shih I-h, Bartel DP. MiRNA-directed cleavage of HOXB8 mRNA. Science 2004; 304:594–596.
29. Krek A, Grun D, Poy MN, et al. Combinatorial miRNA target predictions. Nat Genet 2005; 37:495–500.
30. Tang G. siRNA and miRNA: An insight into RISCs. Trends in Biochem Sci 2005; 30:106–114.

31. Vaucheret H. MiRNA-dependent trans-acting siRNA production. Sci STKE 2005; 2005:pe43.
32. Fire A, Xu S, Montgomery MK, et al. Potent and specific genetic interference by double-stranded RNA in *Caenorhabditis elegans*. Nature 1998; 391:806–811.
33. Olsen PH, Ambros V. The lin-4 regulatory RNA controls developmental timing in *Caenorhabditis elegans* by blocking LIN-14 protein synthesis after the initiation of translation. Dev Biol 1999; 216:671–680.
34. Lu J, Getz G, Miska EA, et al. MiRNA expression profiles classify human cancers. Nature 2005; 435:834–838.
35. Chen PY, Manninga H, Slanchev K, et al. The developmental miRNA profiles of zebrafish as determined by small RNA cloning. Genes Dev 2005; 19:1288–1293.
36. Griffiths-Jones S, Grocock RJ, van Dongen S, et al. miRBase: miRNA sequences, targets and gene nomenclature. Nucleic Acids Res 2006; 34:D140–D144.
37. Griffiths-Jones S. The miRNA registry. Nucleic Acids Res 2004; 32:D109–D111.
38. http://miRNA.sanger.ac.uk (accessed April 2009).
39. http://miRNA.sanger.ac.uk/sequences/.miRBase::Sequences (accessed April 2009).
40. http://miRNA.sanger.ac.uk/targets/v5/ (accessed April 2009).
41. http://miRNA.sanger.ac.uk/targets/v5/info.html (accessed April 2009).
42. http://miRNA.sanger.ac.uk/registry/ (accessed April 2009).
43. Shahi P, Loukianiouk S, Bohne-Lang A, et al. Argonaute—A database for gene regulation by mammalian miRNAs. Nucleic Acids Res 2006; 34:D115–D118.
44. http://www.ma.uni-heidelberg.de. ARGONAUTE (accessed April 2009).
45. http://www.ma.uni-heidelberg.de/apps/zmf/argonaute/motif.php (accessed April 2009).
46. http://diana.cslab.ece.ntua.gr/tarbase Diana TarBase: Experimentally supported miRNA targets (accessed April 2009).
47. Sethupathy P, Corda B, Hatzigeorgiou AG. TarBase: A comprehensive database of experimentally supported animal miRNA targets. RNA 2006; 12:192–197.
48. http://bioinfo.au.tsinghua.edu.cn/micrornadb/MiRNAdb-a comprehensive database for miRNAs (accessed April 2009).
49. Hsu PW, Huang HD, Hsu SD, et al. miRNAMap: Genomic maps of miRNA genes and their target genes in mammalian genomes. Nucleic Acids Res 2006; 34:D135–D139.
50. http://mirnamap.mbc.nctu.edu.tw. miRNAMap—Genomic maps of studying genes regulation by metazoan miRNAs (accessed April 2009).
51. http://www.miRNA.org (accessed April 2009).
52. Enright AJ, John B, Gaul U, et al. MiRNA targets in *Drosophila*. Genome Biol 2003; 5:R1.
53. Hofacker IL, Fontana W, Stadler PF, et al. Fast folding and comparison of RNA secondary structures. Monatshefte für Chemie/Chemical Monthly 1994; 125:167–188.
54. http://www.targetscan.org/ TargetScan 5.1 (accessed April 2009).
55. Lewis BP, Shih IH, Jones-Rhoades MW, et al. Prediction of mammalian miRNA targets. Cell 2003; 115:787–798.
56. Lewis BP, Burge CB, Bartel DP. Conserved seed pairing, often flanked by adenosines, indicates that thousands of human genes are miRNA targets. Cell 2005; 120:15–20.
57. Grimson A, Farh KK, Johnston WK, et al. MiRNA targeting specificity in mammals: Determinants beyond seed pairing. Mol Cell 2007; 27:91–105.
58. http://pictar.mdc-berlin.de/ (accessed April 2009).
59. http://diana.cslab.ece.ntua.gr/ (accessed April 2009).
60. http://bibiserv.techfak.uni-bielefeld.de. (accessed April 2009).
61. Boutla A, Delidakis C, Tabler M. Developmental defects by antisense-mediated inactivation of micro-RNAs 2 and 13 in Drosophila and the identification of putative target genes. Nucleic Acids Res 2003; 31:4973–4980.
62. Weiler J, Hunziker J, Hall J. Anti-miRNA oligonucleotides (AMOs): Ammunition to target miRNAs implicated in human disease? Gene Ther 2005; 13:496–502.

63. Hutvágner G, Simard MJ, Mello CC, et al. Sequence-specific inhibition of small RNA function. PLoS Biol 2004; 2(4):E98.
64. Esau C, Kang X, Peralta E, et al. MiRNA-143 regulates adipocyte differentiation. J Biol Chem 2004; 279:52361–52365.
65. Vester B, Wengel J. LNA (locked nucleic acid): High-affinity targeting of complementary RNA and DNA. Biochemistry 2004; 43:13233–13241.
66. Fabani MM, Gait MJ. miR-122 targeting with LNA/2′-*O*-methyl oligonucleotide mixmers, peptide nucleic acids (PNA), and PNA peptide conjugates. RNA 2008 14(2):336–346.
67. Krutzfeldt J, Rajewsky N, Braich R, et al. Silencing of miRNAs in vivo with 'antagomirs'. Nature 2005; 438:685–689.
68. Mattes J, Yang M, Foster PS. Regulation of miRNA by antagomirs: A new class of pharmacological antagonists for the specific regulation of gene function? Am J Respir Cell Mol Biol 2007; 36:8–12.
69. Li L-C, Okino ST, Zhao H, et al. Small dsRNAs induce transcriptional activation in human cells. Proc Natl Acad Sci U S A. 2006; 103:17337–17342.
70. Janowski BA, Younger ST, Hardy DB, et al. Activating gene expression in mammalian cells with promoter-targeted duplex RNAs. Nat Chem Biol 2007; 3:166–173.
71. Chung K-H, Hart CC, Al-Bassam S, et al. Polycistronic RNA polymerase II expression vectors for RNA interference based on BIC/miR-155. Nucleic Acids Res 2006; 34:e53.
72. Wolfrum C, Shi S, Jayaprakash KN, et al. Mechanisms and optimization of in vivo delivery of lipophilic siRNAs. Nat Biotechnol 2007; 25:1149–1157.
73. Landen CN Jr, Chavez-Reyes A, Bucana C, et al. Therapeutic EphA2 gene targeting in vivo using neutral liposomal small interfering RNA delivery. Cancer Res 2005; 65:6910–6918.
74. Lagos-Quintana M, Rauhut R, Yalcin A, et al. Identification of tissue-specific MiRNAs from mouse. Curr Biol 2002; 12:735–739.
75. Kim J, Krichevsky A, Grad Y, et al. Identification of many miRNAs that copurify with polyribosomes in mammalian neurons. Proc Natl Acad Sci U S A 2004; 101:360–365.
76. Calin GA, Dumitru CD, Shimizu M, et al. Frequent deletions and down-regulation of micro- RNA genes miR15 and miR16 at 13q14 in chronic lymphocytic leukemia. Proc Natl Acad Sci U S A 2002; 99:15524–15529.
77. Michael MZ, O'Connor SM, van Holst Pellekaan NG, et al. Reduced accumulation of specific miRNAs in colorectal neoplasia. Mol Cancer Res 2003; 1:882–891.
78. Meng F, Henson R, Lang M, et al. Involvement of human micro-RNA in growth and response to chemotherapy in human cholangiocarcinoma cell lines. Gastroenterology 2006; 130:2113–2129.
79. Si ML, Zhu S, Wu H, et al. miR-21-mediated tumor growth. Oncogene 2007; 26:2799–2803.
80. He L, Thomson JM, Hemann MT, et al. A miRNA polycistron as a potential human oncogene. Nature 2005; 435:828–833.
81. Poy MN, Eliasson L, Krutzfeldt J, et al. A pancreatic islet-specific miRNA regulates insulin secretion. Nature 2004; 432:226–230.
82. Gauthier BR, Wollheim CB. MiRNAs: 'Ribo-regulators' of glucose homeostasis. Nat Med 2006; 12:36–38.
83. Taoka M, Ichimura T, Wakamiya-Tsuruta A, et al. V-1, a protein expressed transiently during murine cerebellar development, regulates actin polymerization via interaction with capping protein. J Biol Chem 2003; 278:5864–5870.
84. Plaisance V, Abderrahmani A, Perret-Menoud V, et al. MiRNA-9 controls the expression of granuphilin/Slp4 and the secretory response of insulin-producing cells. J Biol Chem 2006; 281:26932–26942.
85. Esau C, Davis S, Murray SF, et al. miR-122 regulation of lipid metabolism revealed by in vivo antisense targeting. Cell Metab 2006; 3:87–98.

86. Caudy AA, Myers M, Hannon GJ, et al. Fragile X-related protein and VIG associate with the RNA interference machinery. Genes Dev 2002; 16:2491–2496.
87. Plante I, Davidovic L, Ouellet DL, et al. Dicer-derived MiRNAs are utilized by the fragile X mental retardation protein for assembly on target RNAs. J Biomed Biotechnol 2006; 2006:64347.
88. Shiohama A, Sasaki T, Noda S, et al. Molecular cloning and expression analysis of a novel gene DGCR8 located in the DiGeorge syndrome chromosomal region. Biochem Biophys Res Commun 2003; 304:184–190.
89. Sullivan CS, Grundhoff AT, Tevethia S, et al. SV40-encoded miRNAs regulate viral gene expression and reduce susceptibility to cytotoxic T cells. Nature 2005; 435:682–686.
90. Omoto S, Fujii YR. Regulation of human immunodeficiency virus 1 transcription by nef miRNA. J Gen Virol 2005; 86:751–755.
91. Triboulet R, Mari B, Lin Y-L, et al. Suppression of MiRNA-silencing pathway by HIV-1 during virus replication. Science 2007; 315:1579–1582.
92. Jopling CL, Yi M, Lancaster AM, et al. Modulation of hepatitis C virus RNA abundance by a liver-specific MiRNA. Science 2005; 309:1577–1581.
93. Lecellier C-H, Dunoyer P, Arar K, et al. A cellular MiRNA mediates antiviral defense in human cells. Science 2005; 308:557–560.
94. Rana TM. Illuminating the silence: Understanding the structure and function of small RNAs. Nat Rev Mol Cell Biol 2007; 8(1):23–36.
95. Chu CY, Rana TM. Small RNAs: Regulators and guardians of the genome. J Cell Physiol 2007; 213(2):412–419.

13 Strategies for Screening of Biologic Therapeutics

Ian Foltz

Department of Protein Sciences, Amgen Inc., Burnaby, British Columbia, Canada

Francesca Civoli

Department of Clinical Immunology, Amgen Inc., Thousand Oaks, California, U.S.A.

INTRODUCTION

The development of biologic therapies has been a major biomedical advancement in recent times. With the development of recombinant DNA technology, the large-scale production of human homologues such as the interferons (IFNs), growth factors (e.g., Epogen), and hormones (e.g., insulin) became feasible. More recently, other types of biologic therapeutics, such as monoclonal antibodies and engineered fusion proteins, have been developed and used in the clinic. The United States sales of biologic therapeutics amounted to $40.3 billion in 2006, with several biologics reaching the status of "blockbuster" with more than $1 billion in sales (1). There are more than 160 biologic therapeutics available today (2), and more than 370 new biologics are currently in various stages of clinical testing. Biologic therapeutics are being used in the clinic for a wide range of disorders, including cancer and rheumatoid arthritis, psoriasis, anemia, hepatitis C, muscular dystrophy, and diabetes.

In general, a biologic therapeutic has higher success rate from discovery to market. One of the reasons is that the toxicity of a biologic is usually low, with few off-target effects that may compromise the drug development program (3). However, not all molecular targets are amenable; although antibodies able to penetrate the plasma membrane (intrabodies) are being pursued, at the moment only extracellular targets are amenable to protein therapeutics. Also, protein therapeutics are more difficult to manufacture and require a stricter quality control program. Even apparently small changes in the manufacturing process, equipment, or facilities could result in changes in the biological product, which are difficult to detect by using bioanalytical methods and may require additional clinical studies to demonstrate the product's safety, identity, and potency. In addition, because biologic therapeutics are generally large proteins, they can generate an unwanted immune response in the patients. Depending on the patient's condition and the type of biologic therapeutic, this immune response can have an impact from minimal to severe, and can affect the safety of the therapeutic. Therefore, immunogenicity of a large protein therapeutic needs to be assessed during drug development and in some cases it may prevent further development or approval.

TABLE 1 Examples of Antibody-Based Therapeutics Currently on the Market

Drug	Molecule type	Company	Therapeutic area	Target
Infliximab (Remicade™)	Chimeric Mab	Centocor/J&J	Inflammation	TNF
Adalimumab (Humira™)	Fully human Mab	Abbott	Inflammation	TNF
Rituximab (Rituxan™)	Chimeric Mab	Genentech	Hematology/ oncology	CD-20
Panitumumab (Vectibix™)	Fully human Mab	Amgen	Oncology	EGFR
Cetuximab (Erbitux™)	Humanized Mab	ImClone/BMS	Oncology	EGFR
Bevacizumab (Avastin™)	Humanized Mab	Genentech	Oncology	VEGF
Trastuzumab (Herceptin™)	Humanized Mab	Genentech	Oncology	HER 2
Alemtuzumab (Campath™)	Humanized Mab	Genzyme/ Bayer	Hematology/ oncology	CD52

Monoclonal antibodies represent the most rapidly expanding class of biologic therapeutics; examples of some of the most successful therapeutic monoclonal antibodies on the market are presented in Table 1. The selection of lead candidates for the discovery of therapeutic monoclonal antibodies requires the application of screening technologies and tools to select a candidate for development, in a similar fashion to small molecule or natural product therapeutics. In this chapter, we will focus on the discovery process of monoclonal antibody therapeutics (mAbs) from the generation of antibody libraries to the identification of lead molecules.

DISCOVERY OF ANTIBODY THERAPEUTICS

The development of the hybridoma technology in 1975 to generate specific monoclonal antibodies in mice lead to the approval of the first murine monoclonal antibody by the FDA, OKT3, in 1986. However, early studies determined that rodent mAbs had properties that could limit their utility, including the induction of an immune response against the protein (15). In an effort to reduce these unwanted effects, chimeric mAbs, consisting of rodent variable regions fused to human constant domains, have been developed and approved for human use. Other methods to further reduce the potential immunogenicity of mAbs have led to "humanized mAbs." There are many ways to humanize a mAb, but in its simple terms humanization consists of replacement of the CDR (complementary-determining regions) from the parental murine antibody to a human acceptor antibody (CDR grafting). Most recently, the development of transgenic mice with the human IgG germlines instead of the normal murine germline has allowed the generation of fully human mAbs, like Panitumumab (Vectibix) (4). In addition to the hybridoma technology, phage display techniques can be used to design and generate antibody libraries with specific characteristic. In this chapter, we will describe a strategy to select lead mAb candidates from hybridoma libraries, including primary screening, purification, secondary screening, and characterization.

Generation of Monoclonal Antibodies

The process of monoclonal antibody generation has seen many improvements over recent years, but the basic processes of hybridoma technology has remained unchanged since its advent by Kohler and Milstein in 1975 (5). The technology

still relies on the successful administration of an immunogen to a naïve animal, typically a wild-type mouse or a genetically modified animal expressing fully human antibodies (6,7), in an attempt to generate a specific humoral immune response. Generally, after several boosts with the antigen, the animals are bled and the immune serum from each animal is analyzed for the presence of antibodies against the target antigen. Once a successful antigen-specific antibody response has been detected, B cells from the spleen or lymph nodes of hyperimmune animals are isolated and fused with a myeloma fusion partner (SP2/0 or P3 cells generally) by using either polyethylene glycol or more recently electrofusion technology (8). The resulting cells known as hybridomas are cultured under selection media to kill unfused B-cells, unfused myeloma cells, and unstable hybrid cells. After a couple weeks in culture, the successfully generated hybridomas will produce an antibody with the same specificity as the original B cell and will be able to grow indefinitely as the myeloma cells. During the process, the hybridomas are normally plated in 96-well microtiter plates as an oligoclonal mixture containing many antibody specificities in each well. These plates are often split into at least two 96-well daughter plates during the culture process: one plate frozen for archiving the hybridomas at -80°C for future use during the subcloning process and the other for the generation of exhaust supernatant for the screening process. The process of exhaust supernatant generation maximizes antibody production by allowing the hybridomas to grow and produce antibody until they have exhausted the nutrients in the media and perish. At this point, the supernatants containing the antibodies can be removed from the hybridomas and used for screening purposes.

Antibody Design Goals

Before starting the hybridoma process, it is important to take some time to determine the design goals of the monoclonal antibody against the antigen. These antibody design goals are important, because the efforts required to generate an antibody that simply binds to its antigen is significantly less than the effort required to generate a high-affinity, functionally active antibody against a target that is highly conserved with the mouse ortholog. Thus, the scale of the hybridoma process should reflect the perceived difficulty of the goal. There are many different criteria that should be considered for antibody design goals that can be grouped into several broad categories—specificity, affinity, in vitro, and in vivo functional activity (Table 2).

Specificity is simply the ability to bind to its cognate antigen and not to other proteins. However, the required affinity of this binding interaction should

TABLE 2 Considerations for Antibody Design Goals

Specificity	Binding to target antigen or epitope of interest
Isotype	Required antibody effector function
Affinity	Requirement for in vivo efficacy based on target-specific knowledge
Cross-reactivity to orthologs	Cross-reactivity required to support in vivo models
Cross-reactivity to homologs	Binding to related proteins—may be desirable or undesirable
In vitro functional assays	Target specific or nonspecific assays to characterize antibody function
In vivo functional assays	Required in vivo activity, pharmacodynamic and pharmacokinetic profile

be defined based on the expression and bioavailability of the target. If one is targeting highly potent molecules that are expressed at low levels or in areas of low antibody biodistribution, one might require a high-affinity antibody. In contrast, a lower affinity antibody might be sufficient for a therapeutic target that it expressed at higher levels primarily in regions with good bioavailability such as blood. The specificity requirement of the antibody also needs to consider binding to related human proteins (homologs) and the same protein from other species (orthologs). For homologs, antibodies can sometimes cross-react to highly related proteins, so it is important to consider if this binding is advantageous, unimportant, or a toxicology risk for the antibody product. For example, one might need an antibody that binds to all related proteins to truly inhibit a signaling pathway or, if this information is unclear, one may need to characterize the lead antibodies for this specificity so that the theory can be tested during the clinical path. The concept of cross-reactivity against orthologs is also extremely important for the clinical path of a therapeutic antibody. For oncology targets, one can often identify human cell lines that will grow as xenografts in immunocompromised mice, making cross-reactivity to the murine ortholog less important. However, for many targets where the grafting of human cells or tissues are not an option, the ability to bind to the murine ortholog is extremely helpful to effectively advance the lead antibodies. Of greater importance is the ability of the lead antibodies to bind to and functionally inhibit the target antigen of a nonhuman primate for toxicology and possibly preclinical efficacy studies. Based on the needs of the downstream screening pathways, one should put in place assays to confirm binding to the antigen of any preclinical species required by the design goals. The other specificity consideration worth mentioning is the binding of the antibody to the endogenous antigen. As stably or transiently transfected proteins are not always going to be expressed with the appropriate co-receptors or with relevant posttranslational modifications, it is always important to have binding to the native protein for a soluble antigen or a primary cell line or primary tumor tissue for a cell-based antigen in the design goals.

Functional activity is often the most significant characteristic of an antibody. Antibodies have been selected for a variety of functional activities including ability to deliver a toxin, antagonist activity, partial or full agonist activity, to name a few. The in vitro assays that can be used for screening antibody supernatants or purified antibodies will encompass most of the discussion for the remainder of this chapter. The assays outlined in the in vitro design goals should be specific and reflective of the desired in vitro activity required to select the lead antibodies from the larger antibody panel prior to in vivo experiments. It is important to highlight at this time that an antibody has two identical antigen-binding sites and an Fc domain that may provide additional functional activity to the final antibody product. This is an important aspect of the antibody therapeutic that differentiates it from most other therapeutic modalities. The two antigen-binding sites may allow an antibody to cross-link its target antigen, and therefore antibodies may function as agonists by delivering a biological signal or antagonists by stimulating the internalization of a target and effectively neutralizing it. An agonist antibody may also deliver different bioactivity depending on its saturation of its target antigen. For example, at low concentrations the antibody would cross-link the antigen effectively, whereas at high concentrations the antibody would predominantly be bound with a single binding domain and may not cross-link the target effectively. The Fc domain is involved in maintaining

antibody half-life in vivo, altering antigen clearance, directly mediating effector function through complement fixation (CDC) and indirectly mediating effector function through antibody-dependent cellular cytotoxicity (ADCC). The functional differences are all defined by the use of different antibody isotypes including IgG1, IgG2, IgG3, or IgG4. For therapeutic antibodies, only IgG1, IgG2, and IgG4 are generally considered due to their long serum half-life and manufacturability advantages. Therefore, it is important to consider in vitro functional activity delivered by the antigen binding domain and the Fc domain of an antibody when determining the antibody design goals. The in vivo preclinical functional activities will not be the focus of this overview, but it is important to consider this during the design phase of any antibody program to ensure that assays and reagents can be generated to allow programs to advance efficiently. In addition to the ortholog cross-reactivity assays described above, one might need to develop assays to demonstrate functional inhibition of the orthologous protein. For oncology targets, ortholog cross-reactivity is not generally an issue, but one should identify or generate a cell line that expresses the target of interest and validate that the target is involved in the growth or survival of the tumor xenografts as early as possible. For inflammatory targets, angiogenesis targets, and oncology targets, where both the host and the tumor cell provide the target protein, one might consider creating a humanized mouse strain with the mouse ortholog of the target protein replaced by the human ortholog (9). This approach should be validated to show that the knocked-in gene recreates a functional system, but when successful, the path is greatly simplified to the clinic because one no longer needs surrogate antibodies or having to go directly to nonhuman primates for preclinical studies, significantly reducing cost and risk. The generation of the humanized mice on the appropriate background strain or the identification of appropriate tumor xenografts for in vivo studies can take a significant effort and time, so it is essential that this is factored into the program during the antibody design goal stage so that the program has the best chance of success.

Screening Assays

The process of screening hybridomas supernatants for the presence of antigen-specific antibodies is a fairly straightforward process. However, there are several factors that one needs to be aware of prior to screening. One factor is that the supernatants may be polyclonal for antigen-specific antibodies at the primary screening stage, which can complicate the downstream screening assays. This can generally be predicted from the percentage of supernatants containing antigen-specific antibodies in the early binding screens. If the percentage of positive wells is below 20%, then the majority of the supernatants are most likely monoclonal for antigen binding, although a few could contain multiple antigen-specific antibodies. If the percentage of positive wells is well above 20%, then care should be taken in interpreting any screening data prior to subcloning, as many of the wells will contain multiple antigen-specific antibodies. Another factor worth considering during screening assay development is that each supernatant will contain a variable concentration of antigen-specific antibody. This will vary depending on the number of competing hybridomas in each well, the time of culture, and culture conditions. The amount of antigen-specific antibody in each well could vary by more than 10-fold, so it is important to understand relatively how much antibody is produced in the system prior to screening to ensure that

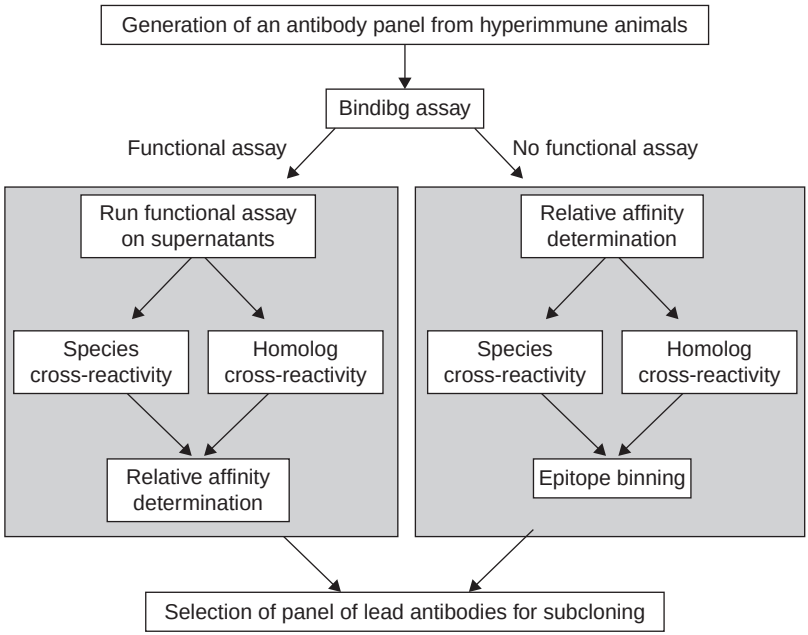

FIGURE 1 Schematic of primary screening strategy for hybridoma supernatants.

the assays are developed appropriately. A third factor that can affect screening assays, particularly bioassays, is the growth factors and other proteins present in supernatant. As such, the assay window and read-out should be tested with a control that includes exhaust supernatant from irrelevant hybridomas during screening assay development.

There are several different techniques for identifying antigen-specific antibodies from hybridomas supernatants. As outlined in Figure 1, the primary binding assay is almost always the first step of the hybridomas process and it should be run as soon as possible to allow a consolidation of positive wells onto a small number of plates for use in all downstream screening from the dozens or potentially hundreds of culture plates initially used to generate the hybridomas. This assay needs to be sufficiently robust to identify the antigen-specific antibodies in the concentration range of the antibodies in the supernatants. The nature of the screening assay will largely depend on the target antigen and should closely reflect the native form of the protein to ensure that the screen is relevant. This overview will focus its discussion on the techniques that are commonly used to identify antigen-specific antibodies against soluble antigens and cell-associated antigens in many hybridoma laboratories: the enzyme-linked immunosorbent assay (ELISA) and on-cell binding assays such as FMAT, respectively.

ELISA Assays

One of the most commonly used platforms to identify antigen–antibody complexes is the ELISA. As this basic assay can be applied for many different purposes, the generic protocol is described in some detail below.

Coating the Microtiter Plate

The plates used for running an ELISA should be flat-bottomed and made of a material such as polystyrene that allows for high protein binding. The format of the plate (96 well or 384 well) will depend on the liquid handling available for screening and the number of plates to be run. The antigen-coating step can be critical for the success of the screening cascade. Direct coating of an antigen can be successfully applied to many antigens, and most proteins can be coated at concentrations between 1 and 10 μg/mL. However, some antibody-binding epitopes can be lost if one face of the antigen preferentially coats the plate or if the coating causes an allosteric change in the conformation of the antigen. This can lead to binding screens that weakly detect or fail to detect antibodies of interest. Therefore, it is important to test your antigen coating with a positive control antibody against a neutralizing epitope or epitope with the same functionality as the antibody from the design goals if possible. Alternatively, if the antigen is a receptor–ligand pair, it is important to show that this binding interaction is still functional on the coated material. To minimize these coating issues, one can coat a biotinylated form of the antigen onto streptavidin- or neutravidin-coated plates. Protein antigens can be easily biotinylated on different residues using several different chemistries [for example, primary amine residues with Sulfo-NHS-LB-biotin (Pierce)] and peptide antigens can be synthesized with C-terminal or biotinylated lysine residues. The advantages of this technique include that it exposes different epitopes for antibody binding and it takes significantly less protein to coat a plate. The disadvantage of this approach is that the labeling process can also destroy epitopes if the protein is overbiotinylated. For example, Sulfo-NHS-LB-biotin reacts with any primary amines in the antigen such as the epsilon amino group of any exposed lysine. The incorporation of a single biotin residue should be sufficient to coat the antigen to the plate, but if the reaction is left to go to completion the protein could literally be coated with biotin residues. To minimize any issues with this approach, one can shorten the reaction time or run the reaction at a more neutral pH, as this reaction proceeds most effectively at basic pH (~8.5). Prior to use, the biotinylated protein should be tested activity to show little or no change has occurred. When optimizing the protein coating it is important to use a positive control antibody or other binding reagent to ensure that the coating is high enough to detect antibody binding at concentrations found in diluted supernatants. Appropriate control antibodies include monoclonal or polyclonal antibodies against the antigen or against protein tags that may have been engineered into the protein during production. To determine the optimal coating, it is a good practice to run a checkerboard screen during assay development with a titration of both the positive control antibody and the coating to select a condition with a robust signal to background window and at least 1 OD difference at the expected antibody concentration.

Blocking the Microtiter Plate

As irrelevant antibodies in hybridomas supernatant will nonspecifically bind to ELISA plates, it is important to ensure that the ELISA plates are well blocked after washing away the unbound antigen. This is an important step that will keep the background low and help to maintain a good signal-to-noise ratio in the assay. Blocking the plate is generally performed with a short incubation of the ELISA plate with a high concentration of a protein such as bovine serum albumin

or nonfat skim milk powder. The blocking protein can usually be dissolved in phosphate-buffered saline. There are other blocking proteins and buffers to use, and the final decision on what to use should be determined empirically in one's own system.

Primary Antibody Binding
After washing away the blocking solution, a volume of hybridomas supernatant (generally 10–15 μL) for a 96-well microtiter plate diluted in blocking buffer to 100 μL is incubated in the antigen-bound microtiter plate. The antibody is generally left to bind for an hour and then the plate is washed several times to remove any unbound antibody.

Secondary Antibody Binding
The antibody–antigen complexes bound to the microtiter plate can be detected with a secondary antibody that recognizes the constant region of the primary antibody. The secondary antibody can either be directly labeled with an enzyme [typically horse radish peroxidase (HRP)] or a tag such as biotin, which further amplifies the signal and can be detected with an enzyme conjugated to streptavidin. The latter option cannot be used with biotinylated antigen-coated plates, as the detection reagent will bind directly to the antigen on the plate. The secondary antibody is normally a goat or rabbit polyclonal antimouse IgG antibody, but it can also be an antihuman IgG antibody if antibodies are being generated from transgenic animals, such as the XenoMouse® animals. The secondary antibody is also left to bind for an hour and then the plate is washed several times to remove any unbound antibody.

Detection of Antibody–Antigen Complexes
The final step of the process involves the addition of substrate for the enzyme conjugated to the secondary antibody. The most common detection enzymes are HRP and alkaline phosphatase, because they are robust, inexpensive, and maintain their activity after conjugation. There are many different substrates for both enzymes that can be classified as colorimetric (such as TMB), chemiluminescent (such as SuperSignal ELISA Pico), or chemifluorescent substrates (such as QuantaBlu). The different substrates have different sensitivities, linear ranges, costs, and may require different ELISA plate readers. The substrate should be allowed to incubate with the enzyme for a consistent time within the linear range of the enzyme that significantly separates positive from negative control wells. The development of the substrate should be stopped by the addition of acid prior to reading. In the case of TMB, the stopped reaction can be read at 450 nM. It is also important to ensure that sodium azide is not included in any of the steps of the ELISA protocol after the primary binding step, as it will inhibit the enzyme activity of the HRP.

On-Cell Binding Assays
Although the ELISA technique is more commonly used, the on-cell or native binding screen is the most important screen for cell-associated targets. Many antibody generation programs will take advantage of the relative ease of generating antibodies against the extracellular domain of a transmembrane protein. However, it is critical to take the binding screen for these antibodies back to native

antigen to ensure that the antibodies recognize a native conformation of the antigen. Also, for multiple transmembrane receptors for which purified material can be difficult to generate, a native binding screen is the most appropriate choice. There are many different platform technologies available to identify antibodies, which bind to cell-expressed antigens such as the Arrayscan (Cellomics) and the fluorometric microvolume assay (FMAT) instrument (PE Biosystems). The FMAT has been our instrument of choice at this stage of the screening cascade primarily as it allows high-throughput "mix and read" screening on live cells without having to wash the plates. The reader requires the secondary antibodies to be labeled with a fluorescent dyes (Cy5, Cy5.5, or FMAT Blue), and primarily functions as a single channel instrument, although it can simultaneously detect two dyes for well-optimized assays. The amount of secondary antibody required for screening needs to be very well optimized for this assay format. If the concentration of secondary antibody is too low, the concentration of antibody in the supernatants could sequester the fluorescent signal from the cells, resulting in no detectable binding signal. If the concentration of secondary is too high, the background will be higher and could obscure the identification of positive wells. The other important considerations for screening with the FMAT system are the antigen expression and quality of the cells. To determine the antigen expression, cells should be screened by fluorescence-activated cell sorting (FACS) by using a positive control antibody. Generally, the expression of an antigen is sufficient for screening if the cells express about a 2 log shift as detected by FACS. If the antigen expression is lower than this, one can sometimes still detect binding by incorporating a wash step into the assay, which reduces the background and improves the assay sensitivity. The other approach that works well with FMAT screening is the use of transiently transfected cells. These cells generally express very high levels of the antigen that can be easily detected by FMAT and if mixed with untransfected parental cells can allow for the multiplexing of positive and negative cell screening in the same well. As the reader only reads a small portion of the entire well, it is important to have the cells well distributed on the plate to ensure there are many events in the field of view. Depending on the size of the cells, there should be 2000 to 25,000 cells per well. It may also be advantageous to have the cells seeded onto the FMAT plates overnight prior to screening, allowing the cells to adhere to the plate, as positive binding on adherent cells is easier to visually confirm than similar binding on nonadherent cells. In general, the analysis for FMAT data can be done with cut-offs defined by positive and negative controls using the variables of size, number of counts, or total fluorescence of the well.

Functional Assays

Once hybridomas producing antigen-specific antibodies of interest have been identified, a robust and biologically relevant functional assay is generally the next critical step for the identification of therapeutic monoclonal antibodies (Fig. 1). The goal of these initial assays is not to identify antibodies meeting design goals, but rather to cull the antibody panel down to a subset of antibodies with the best chance of meeting the antibody design goals. During assay development for a soluble antigen, the goal should be to reduce the concentration of antigen in the assay as much as possible, without compromising the assay window. As antibody concentrations in hybridoma supernatants are variable, this

will allow for low-concentration, high-affinity antibodies to completely saturate the antigen and be identified as positive in the assay. This should also allow for the differentiation of higher affinity antibodies, because when the antigen concentration is pushed to low levels the assay becomes more and more affinity driven rather than antibody concentration driven. This is also true for a cell surface antigen, but the potency of the assay is driven by two factors, the number of receptors on the cells and the total cell number in the well. For most functional cell-based assays, antigen levels will be low and thus the assay results will be driven by the affinity of the antibodies as well as by their functional properties. The exception to this might be stably transfected cell lines, so it is important to isolate high- and low-expressing cell lines for binding assays and functional assays, respectively. For both soluble and cell-based antigens, reducing the concentration of antigen in the bioassay will focus the panel toward the highest affinity and potency antibodies in the panel. Detailed below is an incomplete list of functional assays that can be applied to antibody-based screening of hybridoma supernatants or the purified antibodies. The purpose of this discussion is to provide an overview of the different kind of screens that can be applied, some of the pitfalls to be avoided and some of the differences between small molecule and antibody-based screening. However, before discussing these assays, it is important to discuss how the hybridoma supernatant impacts these assays. Functional assays can be easily broken down into two groups, assays that generally work in hybridoma media and assays that generally do not work in hybridoma media. The hybridoma media often contains 10% fetal calf serum and is essentially conditioned media from the exhausted hybridomas. This rich and complex media greatly affects many different functional assays. Although it is possible to purify the antibody from the hybridoma supernatants by using protein A or protein G chromatography, this will normally require thawing the hybridomas and producing 5 to 10 mL exhaust supernatant from the polyclonal well. As protein A or G beads have relatively low affinity for IgG, this is generally not practical on the small volumes of supernatant generated hundreds or thousands of antigen-specific hybridomas. The supernatant effects can sometimes be mitigated through dilution; however, this lowers the concentration of antibody in the assay and often affects the quality of the screen.

Survival, Apoptosis, and Proliferation Assays

These three assay formats are being considered together as they are related assays and they are generally unsuitable for screening hybridoma supernatants due to supernatant effects. The read-outs for these assays can include metabolic read-outs (MTT, Alamar Blue, CellTiterGlo), DNA content (CyQuant), and DNA synthesis (BrDU incorporation). In addition, there are many cellular processes specific for apoptosis that provide unique assay read-outs such as caspase activation (PARP cleavage, fluorescent caspase substrates), DNA fragmentation (TUNEL), and cellular permeability (propidium iodide). These are all robust read-outs for these assays and several different read-outs should be attempted during assay development to ensure that the optimal assay is developed.

For survival or apoptosis assays, the cells are generally cultured under serum-starved conditions at a high cell density such that the cells are forced to use the pathway of interest to survive. The assay is generally run over several days and the window increases as the cells die off. As antibodies are noncell

permeable and nontoxic molecules, it is not necessary to differentiate necrotic and apoptotic death in the screening assays because any cell death observed during the assay will be a result of apoptosis. For proliferation assays, the cells are generally cultured in the presence of a specific growth factor at a relatively low cell density with a low concentration or without serum. This assay window can generally be seen after a couple days based on a rapid increase in cell numbers. Assays involving factor independent cell lines, which use growth factors found in serum, are generally both unsuitable for screening as both the FCS in the hybridoma media and growth factors produced by the hybridomas can reduce the assay window. However, assays involving factor-dependent cell lines can often be run successfully by using hybridomas supernatants. One can utilize factor-dependent cell lines to develop proliferation assays by introducing signaling pathways through transfection, such as the introduction of the EGFR family into the murine IL-3 dependent pro-B cell line Ba/F3 cells, and forcing the cells to grow in response to a different growth factor to survive (10).

Phosphorylation Assays

Signal transduction pathways are good assay read-out option when assays that directly interrogate the desired biological function, such as proliferation, cannot be used as an upfront screening assay. These pathways are more specific to the target antigen and are thus less likely to be activated by hybridoma supernatant. Phosphorylation is one of the easier signal transduction pathways to interrogate, as there are a lot of commercially available antibodies against phosphoproteins or phosphorylated tyrosine residues. These assays can be used for screening hybridoma supernatants when the pathway being targeted is membrane proximal such as the phosphorylation of a tyrosine kinase receptor or the phosphorylation of a protein fairly unique to the signaling axis such as STAT6 by the IL4 pathway. However, focal points of many signaling axes such as MAPK or AKT phosphorylation should be avoided because they are activated by hybridoma media and generally cannot be used as the assay readout.

Cytokine Release Assays

The downstream consequence of many signaling pathways is the production of cytokines or other secreted proteins. As the read-out for these assays would be an ELISA specific for the secreted cytokine or protein, there is an additional amplification step in the readout that makes these assays very robust and sensitive. These advantages allow one to aggressively reduce the concentration of the soluble antigen or cell number and focus the screen to identify high affinity and potency antibodies. The difficult and time-consuming aspect of cytokine-release assays is the identification of two antibodies that can bind to the cytokine simultaneously for quantitation, also known as a sandwich ELISA. Fortunately, sandwich ELISA antibody pairs have been identified and are commercially available for many cytokines, simplifying this aspect of assay development. In general, this is a very robust screening approach for hybridoma supernatants as the culture supernatant does not normally induce or interfere with cytokine release assays.

Co-stimulation Assays

Generally, co-stimulation assays are required to screen for antibodies that can modulate immune cell activation. Multiple cell types may be required for these

assays including T cells, B cells, dendritic cells, and macrophages. These assays are difficult to develop as they often require the use of primary cells, which have a lot of day-to-day variability compared with cultured cell lines. These assays also require a precise stimulation of these primary cells to ensure that co-stimulation occurs and effects of the antigen-specific antibody can be assessed. For example, murine T-cell stimulation assays will often signal through CD3 using plate-bound 2C11, a mouse monoclonal antibody against CD3. If the coating concentration of 2C11 is too high, a maximal signal will be delivered by anti-CD3, preventing the detection of any co-stimulatory signal. In contrast, if the anti-CD3 coating concentration is too low then the signal may be insufficient for co-stimulation to occur. Although the assay development for these assays can be difficult, these assays are not generally affected by components of hybridoma media and thus can perform very well for supernatant screening.

Receptor–Ligand Competition Assays
Although this assay is not technically a functional assay, it is a very robust screening assay that is likely to predict whether an antibody is neutralizing if the antigen has a known ligand or receptor. This assay can be run using soluble antigen in an ELISA format by coating a plate, for example, the receptor onto the microtiter plate, and detecting the receptor–ligand complex with an HRP-conjugated polyclonal antibody against the ligand or by using a biotinylated ligand and SA-HRP detection. Generally, the assay is best performed when the antigen is kept in solution, as the concentration of antigen required to detect the complex will often be lower than if the antigen was coated onto the plate. The assay can also be run with the receptor expressed on cells. In this instance, the ligand can be detected as above, but may also include fluorescent detection and quantitation by FACS or FMAT.

Adhesion Assays
This assay is essentially a cell-based format for a receptor–ligand competition assay. The assay involves coating a plate with a ligand for a receptor such as an integrin, allowing cells to adhere to the ligand, an aggressive washing step to remove any unbound cells and then a total cell readout such as CyQuant to quantitate the relative amount of plate-bound cells. If you are targeting an antigen on the cell, this assay can be extremely good at identifying high affinity and potency neutralizing antibodies and is not normally affected by components of hybridoma media. However, if ligand is targeted, this assay is not going to effectively screen antibody supernatants, as the concentration of ligand required to get strong binding is high enough to prevent discrimination between high- and low-affinity neutralizing antibodies.

Chemotaxis Assays
Signaling through chemokine receptors induces the movement of cells toward a chemokine gradient, which can be detected using chemotaxis assays. These assays require 96-well transwell plates with a top chamber for the cells and antibody, a filter with 3 to 8 μm pores and a lower chamber for the chemotactic agent. The chemotactic gradient will induce the cells to move from the top chamber to the bottom chamber where the cells can be quantitated by using CyQuant. In general, this assay is unaffected by components of hybridoma media.

Antibody Effector Function Assays

In addition to assessing the bioactivity of the antigen-binding domain of the antibody, there are several assays to evaluate the effector function of the constant region of the antibody. For these assays one must consider the isotype of the constant domain of the antibody. Antibodies of the murine IgG2a or the human IgG1 isotype are capable of both complement-dependent cytotoxicity (CDC) and antibody-dependent cellular cytotoxicity (ADCC). If the antibody is of another isotype class, the antibody variable domains will need to be cloned and grafted onto the appropriate constant domain and re-expressed prior to assaying. ADCC and CDC activities are epitope dependent, and antibodies will have different activity despite having the correct isotype. For both these assays, the read-out can be increased cell permeability by FACS or release of intracellular fluorescent signal from preloaded target cells. These assays can be run at the hybridoma supernatant level on antibodies of these isotypes, but it is more realistic to perform these assays on purified antibodies.

Affinity Determination

It is important to attempt to understand the affinity of the antibodies with the desired activity at this stage of the screening cascade. Otherwise, the program may advance through the process of hybridoma subcloning, antibody production, and antibody purification before there is an understanding if the antibody panel is likely to have met affinity design goals. The importance of this assay is minimized if one has a robust, affinity driven functional assay; however, it is still worthwhile running this assay to identify the highest affinity antibodies within the pool of functional antibodies to help focus the subcloning efforts.

ELISA-Based Affinity Techniques

The ELISA protocol can be easily modified to address affinity for soluble antigens by altering the incubation time and the antigen coating. The incubation time for most binding ELISA assays is around an hour, however, this isn't sufficient time to truly interrogate an antibody affinity. The easiest protocol change is to extend the incubation time to at least an overnight incubation to allow the antibody binding to approach equilibrium. The antigen coating concentration is also an easy variable to change to make the assay more affinity focused than simply binding. If one coats an ELISA plate with a low concentration of antigen, the assay becomes more affinity based. It may be necessary to run the binding assay with a titration of antigen to empirically find a concentration where the assay can effectively discriminate the antibodies based on affinity. In contrast, if one coats an ELISA plate with a very high concentration of antigen, the assay can be used to relatively quantitate the amount of antigen-specific antibody rather than affinity. This will likely require an extensive titration of antibody supernatant on a high antigen coating to ensure that the ELISA signal is in a linear range.

FACS-Based Binding Assays

FACS is a very powerful technique that should be an important aspect of any screening cascade. Although primary binding assays need to be run on the FMAT platform as it has sufficient throughput to handle hundreds of plates, the FACS should be considered as the platform of choice for all other binding assays on smaller panels of antigen-specific antibodies. These assays include binding to primary cells, tumor cells, other human homologous proteins and mouse or

monkey orthologous proteins. As the FACS is quantitative over a large dynamic range and most proteins are expressed on cells under affinity controlled conditions, the FACS can serve as a relative affinity screen for antibodies at the screening stage. The lower the expression of the target antigen on cell lines, the more the antibody binding is affinity related and the amount of antibody in the supernatants becomes less relevant. For transiently transfected or other highly expressed proteins, the amount of cell surface antigen may not effectively differentiate the affinity of antibodies as the antigen expression can be high enough that the binding is no longer related to the antibody affinity or avidity.

Epitope Binning

This assay can be effectively applied to an antibody screening cascade, but it should really only be considered if functional assays are not available (Fig. 1). Epitope binning is a process of determining how different antibodies bind to the same antigen at the same time and is different from epitope mapping, which determines the actual amino acids contacts of an antibody on its antigen. The easiest form of epitope binning involves the use of a monoclonal antibody of a known activity that you want to screen against other antibodies in a competition format to identify antibodies that bind to the same epitope. This assay works best if the antibody is a different species or isotype than the antibodies that are being screened so these antibodies can be detected without interference from the blocking antibody. An ELISA plate coated with the soluble antigen or an FMAT plate containing antigen-expressing cells needs to first be saturated for binding with the known monoclonal antibody. Then the antibody supernatants can be added to the plate and detected with an appropriately labeled secondary detection antibody. A lack of signal will usually indicate the identification of an antibody binding the same epitope bin as the known antibody. This can be confirmed by detecting the binding of the antibody supernatant in a separate well in the absence of blocking antibody. The epitope binning assay is more difficult to perform in the reverse orientation, as the antibody supernatants contain variable antibody concentrations and it is impossible to know if all wells contain sufficient antibody to block all of the antigen binding sites in the ELISA or FMAT plate. In this format, the binding observed from the known antibody could be due to either a non-competing epitope or insufficient antigen-specific antibody in the supernatants. As an alternative approach, multiplexed competitive antibody binding can also be used for epitope mapping panels of antigen-specific antibodies using Luminex technology (11).

Subcloning, Purification, and Characterization

The data collected so far should have characterized the binding specificity, the relative affinity, and either the functional activity or the epitope binning of the antibody panel. Collectively, these data can be used to select lead antibodies from the original panel of hybridomas for subcloning. The process of subcloning involves thawing the frozen plates from the initial hybridoma plating and then replating the hybridomas from the selected wells at a clonal density. After a couple weeks in culture, the cultures should be rescreened for binding specificity to identify at least one hybridoma secreting the antigen-specific antibody of interest from each well. The hybridoma should be sequenced at this point to learn

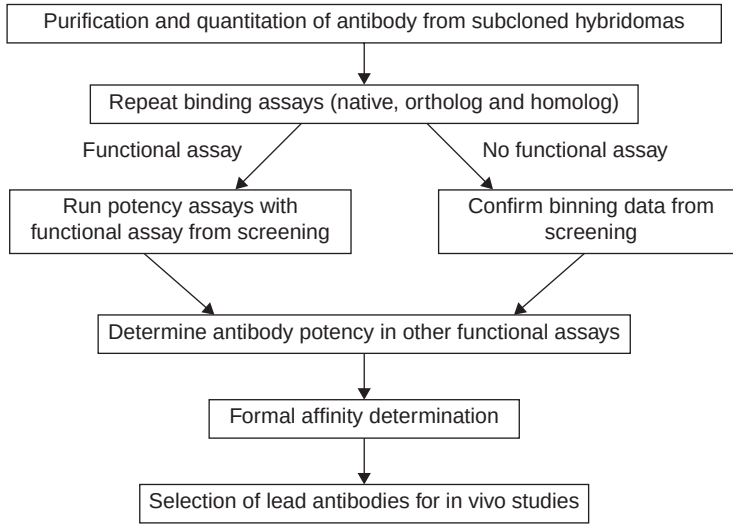

FIGURE 2 Schematic of secondary screening strategy for purified antibodies.

the primary nucleotide sequence for the variable heavy chain and the variable light chain genes. In parallel, the hybridoma should be scaled up and allowed to produce sufficient antibody to use for all subsequent screening assays. After scale up, the antibodies should be purified from the supernatant with protein A or protein G chromatography and eluted at an acidic pH. The eluate containing the antibody should be neutralized and then buffer-exchanged or dialyzed into a physiological buffer such as phosphate buffered saline. The concentration of the purified antibody should be quantitated by spectrophotometry and purity should be confirmed by visual inspection using SDS-PAGE. These purified and quantitated antibodies are now ready for further characterization.

Screening Purified Antibodies

The goal of the screening assays used for screening hybridoma supernatants was to identify antibodies that were likely to have the characteristics to meet the antibody design goals. In contrast, the goal of the assays run on purified antibodies is to characterize the antibodies against the design goals. As outlined in Figure 2, the screening process should start with a repeat of the assays used to identify these antibodies for subcloning. These assays should now be set up with full dose–response curves with multiple replicates at each point to determine and compare antibody potencies. As the complications involved with screening hybridoma supernatants have been removed at this stage of the process, other functional assays such as proliferation assays can also be used to characterize the lead antibody panel.

Formal Affinity Determination

At this time in the screening process, the antibody panel has been characterized for its binding profile and potency, and the lead antibodies should satisfy most of the in vitro antibody design goals. The last antibody characteristic to be

determined is the formal affinity of the antibody for the antigen. Depending on the binding profile, it may also be important to determine the affinity of the antibodies for the cynomolgus monkey ortholog of the antigen and the mouse ortholog of the antigen to support in vivo studies. If the antibody is against a soluble protein, there are several different technologies available to determine the antibodies affinity including the Biacore instrument (GE Healthcare) and the Kinetic Exclusion Assay or KinExA instrument (Sapidyne). It is more difficult to determine the affinity of endogenously expressed cell-based antigens. The traditional method for determining the affinity in these situations is a Scatchard assay, but recent efforts have successfully applied the KinExA to determine on cell affinity (12).

Selection of Lead Antibodies

The selection of the lead antibodies is the fruition of the significant effort from the characterization of a panel of hybridoma supernatants to the careful evaluation of a small panel of interesting antibodies against the predetermined antibody design goals. While this has been an extensive process, the real cost and effort of drug development are just beginning. It is for this reason that it is important that the lead antibodies have met the specificity, affinity, and potency goals that were deemed necessary for advancement to animal and possibly clinical trials.

CONCLUSIONS

Over the past two decades monoclonal antibodies and biologic therapeutics in general have become a major part of the therapeutic repertoire available to physicians to treat diseases. Industrial R&D is investing more in biologics, with more than 200 companies now working on antibody therapeutics (13). Recombinant protein products are the largest class of biologic therapeutic on the market. However, most of the future growth of biologic therapeutics is anticipated to be due to the development of therapeutic monoclonal antibodies, particularly fully human or humanized antibodies and conjugated antibodies (14). Undoubtedly, new advances will be made in the next few years in the field of antibody generation, selection, and development.

REFERENCES

1. IMS Health. IMS Reports U.S. Prescription Sales Jump 8.3 Percent in 2006, to $274.9 billion. March 8, 2007 at http://www.imshealth.com/ims/portal/front/articleC/0,27776599_3665_80415465,00.html. Accessed September 2007.
2. Walsh G. Biopharmaceuticals: Recent approvals and likely directions. Trends Biotechnol 2005; 23(11):553–558.
3. Projan SJ, Gill D, Lu Z, et al. Small molecules for small minds? The case for biologic pharmaceuticals. Expert Opin Biol Ther 2004; 4:1345–1350.
4. Jakobovits A, Amado RG, Yang X, et al. From XenoMouse technology to panitumumab, the first fully human antibody product from transgenic mice. Nat Biotechnol 2007; 25(10):1134–1143.
5. Kohler G, Milstein C. Continuous cultures of fused cells secreting antibody of predefined specificity. Nature 1975; 256:495–497.
6. Lonberg N, Taylor LD, Harding FA, et al. Antigen-specific human antibodies from mice comprising four distinct genetic modifications. Nature 1994; 368:856–859.

7. Mendez MJ, Green LL, Corvalan JR, et al. Functional transplant of megabase human immunoglobulin loci recapitulates human antibody response in mice. Nat Genet 1997; 15:146–156.
8. Vienken J, Zimmermann U. An improved electrofusion technique for production of mouse hybridoma cells. FEBS Lett 1985; 182:278–280.
9. Bolon B. Genetically engineered animals in drug discovery and development: A maturing resource for toxicologic research. Basic Clin Pharmacol Toxicol 2004; 95(4):154–161.
10. Riese DJ, Kim ED, Elenius K, et al. The epidermal growth factor receptor couples transforming growth factor-alpha, heparin-binding epidermal growth factor-like factor, and amphiregulin to Neu, ErbB-3, and ErbB-4. J Biol Chem 1996; 271:20047–20052.
11. Jia XC, Raya R, Zhang L, et al. A novel method of multiplexed competitive antibody binning for the characterization of monoclonal antibodies. J Immunol Methods 2004; 288:91–98.
12. Rathanaswami P, Babcook J, Gallo M. Anal Biochem 2008; 373(1):52–60.
13. Maggon K. Monoclonal antibody "gold rush". Curr Med Chem 2007; 14(18):1978–1987.
14. Pavlou AK, Belsey MJ. The therapeutic antibodies market to 2008. Eur J Pharm Biopharm 2005; 59(3):389–396.
15. Kuus-Reichel K, Grauer LS, Karavodin LM, et al. Will immunogenicity limit the use, efficacy, and future development of therapeutic monoclonal antibodies? Clinical and Diagnostic Laboratory Immunology 1994; 1(4):365–372.

14 Cryopreserved Cells in Functional Cell–Based HTS Assays

Geetha Shankar

Clinical Development, Exelixis Inc., South San Francisco, California, U.S.A.

Kirk McMillan

New Lead Discovery and Pharmacology, Exelixis Inc., South San Francisco, California, U.S.A

INTRODUCTION

High-throughput screening (HTS) is a key process in modern drug discovery, as it serves to reveal novel chemical leads from large compound libraries. Efficient and rapid translation of HTS efforts in to lead optimization, and subsequently, clinical candidates, requires that HTS campaigns yield near drug-like hits with substantial structure–activity relationship (SAR) information upfront to get a head start. A recent analysis of HTS practices in the industry revealed that on an average about 50% of the targets screened in HTS resulted in leads (1). Of the leads, 104 drug candidates made it into human testing and clinical trials. This number is trending upwards, due in part to the increasing number of laboratories that undertake HTS campaigns, which further underscores the importance of HTS in drug discovery. Thus, HTS necessitates the screening of increasingly large compound libraries in a highly industrialized and automated setting. Although the chemical composition of the library is unarguably a critical component of this process, the other equally important step is the design of sensitive and reliable assays that will serve as markers of compound activity. This chapter focuses on the use of cell-based assays as primary high-throughput screens, and more specifically, the recent advances in availability of cells for large-scale screens that are resulting in noteworthy trends in HTS practices.

HIGH-THROUGHPUT SCREENING

The term HTS typically refers to the testing of 10,000 to 100,000 compounds per day. Prior to formal screening practices, the pharmaceutical industry relied on discovering biological activity in naturally occurring substances. It was not until the 1990s that laboratory automation allowed researchers to break through significant barriers in the scale and speed of drug discovery from a growing collection of chemical probes (2). Current expectations dictate that leads from primary screens lend themselves to rapid structural optimization to potential drugs. In order to accomplish these goals, a key criterion is a highly diverse chemical library with high-quality compounds. At the same time, it is important to have sufficient breadth within a chemical scaffold to yield early structure activity information. It follows that selection of appropriate assay methodologies and

technology platforms to test compound libraries in a high-throughput manner is equally important.

Advances in assay detection technologies, increased use of combinatorial chemical synthetic methods, and laboratory automation have allowed for HTS campaigns to be embarked on a scale that had previously not been possible. HTS assays are increasingly done on fully automated and integrated screening platforms. As the scale and speed of these assays are significantly higher than routine bench top formats, the assay development parameters are carefully planned. Key criteria include homogenous assay formats that are amenable to miniaturization. Miniaturization allows the use of microtiter plates (MTP) ranging from 384-wells to 3456-well plates to maximize throughput and minimize reagent costs. Typically, the quality and source of reagent supplies are carefully monitored in order to minimize assay variability. Ideally, reagents for an HTS campaign are confined to one single batch, and all steps in the assay are highly standardized; thus, the only variable from day to day or well to well is the test compound itself, with all other parameters operating within a strict window of acceptability. The preferred assay duration is minutes to hours. Similarly, assay formats that utilize stable endpoints are far more reliable than those with kinetic endpoints. This is primarily because of the logistics and lack of flexibility of timing on plate readers and the increased variability that results when the kinetics of a signal has a rapid downward trend. Thus, in the aggregate, it is imperative that in order to be a reliable HTS assay, the performance is consistent and robust and the variability is minimal.

Given the stringent requirements for a successful HTS campaign, early HTS efforts focused on biochemical and cell-free systems: these include enzyme-based assays and receptor ligand binding assays. However, rapid progress in genomics and proteomics has greatly expanded the repertoire of "druggable" targets and necessitated the use of more complex assay formats. Thus, an unexpected finding from the 2004 study on HTS practices was an increased use of cell-based assays in HTS (1).

CELL-BASED ASSAYS IN HTS

Modes of Screening

Cell-based assays were reserved as secondary or tertiary line of screening where the throughput was significantly lower and the assays were significantly more complex. However, it was soon recognized that this approach has some serious limitations. The high rate of compound attrition observed was partly due to lack of cell-based activity and inability of compounds to permeate natural membrane barriers. Furthermore, with increased understanding of the biology of targets and the expanding repertoire of therapeutically attractive targets, it became clear that certain targets are not amenable to biochemical-based approaches. Examples of the latter include targets that require agonists or allosteric modulators; targets that dimerize upon activation and display altered pharmacology in a natural membrane setting; and, cell surface targets or intracellular targets such as G-protein–coupled receptors (GPCRs), ion channels, nuclear hormone receptors, and transporters that are better studied in a functioning milieu. Thus, the use of cell-based assays as a primary screening tool has become more routine, and less restricted to secondary or tertiary assays for hits and leads.

Cell-based assays in HTS offer many advantages including the fact that (a) intact, live cells are more representative of a functioning milieu than an isolated protein or a membrane preparation; (b) functional cell–based assays offer insight into the mode of action of a compound, and, unlike binding assays, can be exploited to identify agonists, antagonists, and related pharmacological modulators; (c) the assays yield higher content, specifically with regards to membrane permeability and availability within cells; (d) undesirable effects such as cytotoxicity can be identified from the outset and suboptimal compounds weeded out of the lead identification process; (e) cell-based assays offer an avenue to screen targets that are refractory to biochemical methods, such as GPCRs and ion channels.

Limitations and Pitfalls

The risks and disadvantages of cell-based assays are obvious: (a) the consistent use of large scale, live cells in various assays is highly labor intensive; (b) cell-based assays are necessarily fraught with variability, as cells are repeatedly harvested over the duration of assay development; (c) cell-based assays are significantly more expensive due to the resource-intense nature of the assays; (d) cell-based assays require special equipment required to maintain cell lines in a contamination free environment, as well as specialized plates and plate readers in some instances; and, (e) cell-based assays can potentially have less impact on driving SAR, particularly in cases where off-target effects of compounds are difficult to tease out with appropriate counter screens.

With cell-based assays averaging >50% of all HTS assays (1), it is clear that the benefits offered by cell-based HTS campaigns far outweigh the risks. Although primary cells of human origin are the most physiologically relevant, they are difficult to come by in quantities required for an HTS campaign. Although the advantages of using primary human cells are compelling, their short supply has made them lower-throughput secondary assays at best. Recent advances that allow using low cell numbers in assays without compromising assay quality and function, may favorably impact the more widespread use of primary cells—these include the use of labchips, microcarriers, and microfluidics to significantly lower cell and reagent use (3). However, the need for specialized cell carriers and chips still hampers industry-wide acceptance of this approach for cell-based HTS practices and may well be a number of years away from being common practice.

A majority of HTS formats utilize immortalized cell lines of human origin, or rodent cell lines that are transfected to express the human target of interest. In order to support HTS campaigns that span weeks or even months, cell culture activities needs to be scaled up to support the availability of hundreds of microtiter plates (MTPs) everyday. This can be partially offset by the use of a miniaturized assay format that can be performed in 1536-well or 3456-well MTPs. Not only does this approach significantly increase the daily throughput of an assay, but it also significantly reduces the duration of the HTS campaign. Like all assay reagent supplies, cell culture reagents have to be carefully monitored for quality and lot-to-lot variability. However, unlike other assay reagents, cell culture supplies have to be even more tightly regulated, as they are susceptible to contamination over prolonged use and lack of stringent aspectic practices. As with all assay reagents, single lots should be utilized for the duration of the screen. Adequate liquid handling instrumentation should be employed for

accurate delivery of small volumes of cells into microtiter plates. Assay parameters such as cell density should also be tightly controlled as this can affect the overall assay performance.

CRYOPRESERVATION OF CELLS

It has long been assumed that for cells to function "normally," it is required that cells are thawed, placed in cell culture flasks, allowed to acclimatize, and finally propagated and scaled up. For most cell-based HTS campaigns, this meant having to scale up cells to support daily testing of 50 to 100 MTPs for an extended period of time. The cell culture demands were intense and prone to variability depending on cell passage number, occasional contamination, and changes in growth during the course of the HTS campaign. One solution to controlling this variability is to screen cells within a narrow window of harvesting cycles. This necessitated that after a fixed number of passages, fresh cells had to be thawed, scaled up, and the cycle of thawing-scaling up-screening continued until the HTS campaign was done.

As the practice of cell-based HTS campaigns becomes common place in drug discovery settings, it is inevitable that discoveries are made that significantly impact the ease of the use of live cells in HTS laboratories. One such discovery is the observation that, for some assays, cells may be used directly from frozen vials into assay plates, thus skipping the cumbersome, labor-intensive cell culture phase in between.

All immortalized cells in culture are derived from cryopreserved cells. The concept of using cryopreserved cells in cell-based assays, is therefore, not necessarily revolutionary. However, the concept of using cells *directly* from a frozen vial into an assay plate is starting to revolutionize the practice of cell-based HTS assays in the pharmaceutical industry. Thus, one of the more innovative ideas to come along in the 21st century has been to uncouple the process of cell culture and HTS: in this setting, the highly labor-intensive and variable component of the assay, the living cells, is transformed into a reagent.

Benefits of Cryopreserving Cells

The idea that all cells may not require to be thawed and cultured several days or weeks before they are applied to an HTS campaign was received with skepticism by most scientists. However, data from several HTS laboratories shows that, for a majority of cell lines and assay formats, cells can indeed be thawed from a vial directly into an MTP, and treated much like any other reagent in a biochemical assay format. The advantages of this approach cannot be overemphasized. The first and perhaps the most important consequence of using cryopreserved cells is that it offers tremendous flexibility from an operational perspective. For cells that had to be plated and cultured overnight, it offered the ability to be able to screen every day of the week, significantly reducing the overall duration of the screen. Since cells can be scaled up and cryopreserved independent of HTS activities, the overall planning of the HTS campaign is significantly simpler and easier. Prior to the use of cryopreserved cells, it was not uncommon to have to repeat many days worth of screening simply because of underperforming cells. In some instances, cells were contaminated in the midst of an HTS campaign, causing long disruptions and significant loss in reagents, time, and money.

Use of Cryopreserved Cells in HTS

One of the earliest documentations on the use of cryopreserved cells in a homogeneous cell-based assay was in 2001 by Weetall et al. (4). The assay described a novel method to study binding of very late antigen-4 (VLA-4) to the adhesion molecule VCAM-1. The authors were able to successfully demonstrate that they could use cryopreserved, fluorescently labeled, divalent cation–activated cells for 50 experiments at a time and utilize these cells as reagents for all subsequent assays. This approach was significant in that it increased both the throughput and the reproducibility of the assay dramatically, as cells could be rapidly prepared on the day of the screen. Most importantly, this approach also preserved the biological integrity of the function and behavior of the cells. Following this initial demonstration, several laboratories have demonstrated similarly successful outcomes over a wide range of cells and assay methodologies. Some of these studies are briefly described below.

A large proportion of early lead compounds have poor pharmacokinetic properties that prevent evaluation in their in vivo efficacy. Numerous approaches have been taken to develop a reliable, predictive in vitro assay so that unsuitable compounds can be identified earlier. One of the cells routinely used in determining hepatic clearance are hepatocytes from various animal species as well as human sources. Studies demonstrated that cryopreserved hepatocytes have significant predictive potential and have the added advantage of flexibility in use because they can be preserved in liquid N_2 for up to a year with minimal loss of enzyme activity (5,6).

Another cell-based assay format that lends itself well to cryopreservation and HTS methods is the reporter gene assay. Commonly used reporters include luciferase, β-galactosidase, and β-lactamase. The β-lactamase format was used recently to discover inhibitors to hepatitis C virus (HCV) replication (7). Special HCV replicon-permissive cells were transfected with β-lactamase and cryopreserved. For the latter step, transfected cells were prepared in two large batches (>1.4 billion cells per batch) in order to minimize lot-to-lot variability. The cells were frozen at 1×10^7 cells per vial, and found to have >90% viability with no loss of β-lactamase activity after thawing. The primary HTS campaign included 270,000 compounds, and the assay was conducted in 384-well MTPs. After confirmatory assays, 563 compounds were identified as leads, and the assay was also successfully miniaturized into a 3456-well MTP format with no loss of signal and a projected decrease in HTS duration to two days (vs six weeks for 384-well plates).

More recently, the use of cryopreserved cells in cell-based assays has been augmented by the introduction of yet another technology called division-arrested cells. This discovery stemmed from the observation that for rapidly growing cells, some of the assay-to-assay variability may be controlled by ensuring that the cells are blocked in cell cycle, thus making them more homogeneous. To achieve this, cells are treated with low doses of the natural antibiotic and antitumor agent Mitomycin C. Thus, cells can be grown in large batches, growth-arrested, and frozen in assay-ready formats. Cells were found to be functional following this procedure with no apparent toxicity observed. The dose of Mitomycin C varies from cell line to cell line. This method was successfully applied for various assay methods including reporter-based assays (8), Ca^{2+}-mobilization (FLIPR) assays (8,9), receptor tyrosine kinase ELISA assay (10),

cAMP assay, and ion channel assay using a membrane potential sensitive dye (9). In all cases, the division-arrested cells performed as well as frozen cells, and in many cases better than fresh cells. For example, in the reporter assay using division-arrested HEK293-NF-κB cells, the coefficient of variation (CV) was 7.5% (compared to 20% for unarrested cells) and Z′ was 0.79 (compared to 0.35 for unarrested cells). Similarly, in a GPCR Ca^{2+}-mobilization assay, the average Z′ ranged from 0.58 to 0.78 at 24 and 48 hours, respectively (as compared to 0.61–0.43 at the same time points) (8).

The use of cryopreserved cells can also be demonstrated in hERG (human ether-a-go-go) ion channel assay using Rb^+ efflux as the readout (11). The data showed that cryopreserved cells perform as effectively as fresh hERG expressing cells in this assay format. The method has been especially well suited for yet another channel, the transient receptor potential A1 (TRPA1) channel, which is difficult to express in cells due to toxicity and loss of function over time (12). The authors successfully utilized transient transfection of TRPA1 followed by cryopreservation. Thus, the cells were made in large batches and were shown to have strong expression for as long as 35 weeks after transfection with storage at −80°C. The cells were also functional in Ca^{2+}-influx assays and secondary electrophysiological assays. Approximately 10 billion cells were transfected and frozen: >700,000 compounds were screened and statistical analysis of the overall HTS campaign demonstrated that the assay performance was excellent (Z′ of 0.75, S/B of 13.2, and CV of 5.9%).

Cryopreservation has been applied to yet another important assay in the drug discovery assay suite—the pregnane X receptor assay (PXR) (13). PXR is a nuclear hormone receptor that upon activation can induce transcription of cytochrome P450 (CYP) 3A4. Thus, this assay can be used in various drug discovery programs to eliminate PXR activating compounds with potentially liable CYP induction profiles. Transiently transfected HepG2 cells were cryopreserved and tested in the PXR assay with no significant differences in pharmacology compared to freshly transfected cells.

Finally cryopreserved cells have most recently been applied for compound profiling in measuring intracellular calcium using FLIPR in about 10 different GPCR antagonist and agonist assays (14). There was good correlation between pEC50 values from cryopreserved cells and continuously cultured cells with correlation coefficients of 0.90 to 1.00.

Methods of Cryopreservation

Freezing and thawing procedures have to be optimized for each cell line. The standard method for cryopreservation of cells consists of 10% dimethylsulfoxide/10% serum (15) and has been shown to work well for the majority of standard cell lines used in HTS laboratories. DMSO has been shown to be a cryoprotectant with good aqueous solubility and low toxicity (13). Recrystallization during thawing can be avoided by thawing rapidly in a 37°C water bath with agitation.

CASE STUDIES: USE OF CRYOPRESERVED CELLS IN VARIOUS ASSAY FORMATS

This section focuses on cell-based HTS campaigns that have utilized cryopreserved cells in-house. In order to screen the in-house compound library of

>4.5 million compounds, the HTS criteria applied are fairly stringent. For most cell-based assays, S/B is expected to be ≥3, and Z′ ≥ 0.5. During the assay development phase, emphasis is placed on miniaturization and scalability with the preferred format being 1536-well MTPs. Compounds are screened in orthogonal pools (10 compounds per well) and hit identification is enabled by deconvolution of the sum total of hits in the assay. Cell-based assays are required to be stable, reproducible, and robust over the duration of the screen, which is typically four to six weeks. For all cell-based assays, appropriate counter screens are run at the compound confirmation stage to eliminate nonspecific hits.

G_S-Coupled GPCR Agonist Assay

One of the major advantages of using a functional cell–based assay is the ability to screen for agonist effects of compounds. In a recently conducted HTS campaign, we utilized a cell line overexpressing G_s-coupled GPCR together with a CRE-Luc reporter gene. Luciferase activity was used to determine compounds that activated the receptor of interest (Fig. 1). The assay was performed in 1536-well MTPs using 5000 cells per well. In order to conduct the HTS campaign using cryopreserved cells, two large batches of cells were cultured and frozen down to yield approximately 15 billion cells. Briefly, cells were thawed and plated into 1536-well plates and incubated overnight. Following compounds addition, cells were further incubated for six hours, at which time plates were read on a standard luminescence plate reader (EnVision, Perkin Elmer).

The primary HTS campaign identified 2942 compounds that were tested in a 10-point dose response format. The overall S/B was 5.1, and mean Z′ was 0.5. The results were as follows: a total of 450 compounds were identified as hits with EC_{50} of <1 μM; of these, 82 compounds had EC_{50} < 100 nM, including 5 compounds with EC_{50} < 10 nM. Over 90% of the compounds showed no activity in cells overexpressing CRE-Luc in the absence of the receptor of interest. EC_{50}s of the top compounds are shown in Table 1. A subset of these compounds

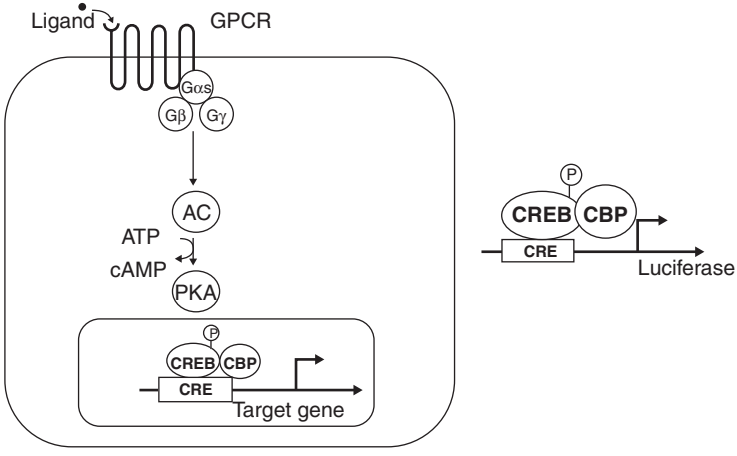

FIGURE 1 Schematic of a Gs-coupled GPCR reporter assay. In this particular example, responses induced by agonists of the Gs-GPCR pf interest are measured by quantification of cyclic AMP-dependent expression of firefly luciferase protein.

TABLE 1 GPCR Agonists Using Reporter Assay Format: Summary of Top 10 Compounds (Primary Hits)

Compound #	Batch	GPCR_HEK 293_CRE_LUC G_S agonist (EC_{50}, nM)	GPCR_HEK 293_CRE_LUC G_S agonist associated results
1	1	2.8	Efficacy: 89.7 rEC_{50}: 3.4 Mean activation: 97.4
2	1	3.1	Efficacy: 78.2 rEC_{50}: 3.2 Mean activation: 88.3
3	1	4.6	Efficacy: 55.9 rEC_{50}: 98.8 Mean activation: 72.3
4	1	4.8	Efficacy: S3.9 rEC_{50}: 10.2 Mean activation: 86.5
5	1	6.6	Efficacy: 34.2 rEC_{50}: 9.5 Mean activation: 97.1
6	2	10.2	Efficacy: 81.2 rEC_{50}: 14.0 Mean activation: 88.1
7	1	10.6	Efficacy: 86.3 rEC_{50}: 17.3 Mean activation: 91.7
8	2	11.2	Efficacy: 82.7 rEC_{50}: 16.5 Mean activation: 94.8
9	1	11.9	Efficacy: 86.8 rEC_{50}: 30.2 Mean activation: 87.5

was further tested after resynthesis of the compounds and structure confirmation (Table 2). These compounds were found to be comparable in activity to the HTS hits, and the assay was found to be extremely valuable as it yielded potent hits with significant SAR information directly from the HTS campaign. This was largely enabled by the fact that this assay was not prone to as much variability as a typical cell-based assay and we attribute this to the use of cryopreserved cells in this campaign.

TABLE 2 GPCR Agonist Reporter Assay: Summary of Hit Confirmation

Compound #	GPCR_HEK293_CRE_Luc G_S agonist HTS (HTS EC_{50}, nM)	GPCR_HEK293_CRE_Luc G_S agonist resynthesized compounds (EC_{50}, nM)
2	3.1	13.3
3	4.6	2.9
4	4.8	5.1
8	11.2	1
10	18.2	3

β-Arrestin Recruitment Assays

β-Arrestin recruitment is widely used as an indication of receptor activation because it has many advantages. Important among them is the fact that β-arrestin recruitment is an almost universal downstream effect of GPCR activation and unlike other readouts, such as Ca^{2+} and cAMP, is not dependent on the specific G-protein interaction with the GPCR. β-Arrestins play a crucial role in the termination of GPCR signals following receptor activation. The process is initiated by phosphorylation of GPCRs by GRKs (members of the G-protein–coupled receptor kinase family), which in turn causes binding of arrestins to the phosphorylated receptor and inhibits further activation by G-proteins. The bound receptor–arrestin complexes are ultimately sequestered in clathrin-coated pits and targeted for recycling to the cell surface or degradation. There are a few technologies that exploit β-arrestin recruitment and apply it towards a screening format. One such technology that has been tested and applied in HTS is based on cell lines where the GPCR of interest is engineered such that it has a specific protease cleavage site in the C-terminal region of the receptor. Additionally, the C-terminal tail is fused to a transcriptional factor. Finally, the β-arrestin protein is also fused to a protease, such that, upon receptor activation, β-arrestin recruitment results in the cleavage of the transcription factor, which triggers downstream gene reporter cascade that can be tailored to various readouts (Invitrogen, WI). This technology was also utilized to screen for an agonist of a G_i-coupled receptor. Approximately 26 billion cells were cultured in an automated cell culture unit (SelecT, TAP systems) and frozen (20 million cells per vial). Cells were thawed and tested periodically for activity and showed no loss of signal at least for nine months postfreezing.

Biosenor-Based cAMP Assays

Although many downstream effectors of GPCRs have served as suitable endpoints for assay design of HTS campaigns, cost-effective cAMP assays have been relatively late to join the category. Until recently, screening of G_s- and G_i-coupled receptors has been limited to using chimeric G-proteins such as G_{qi} or G_{qs}. These G-proteins have the advantage of binding to the GPCRs of interest as normal, but are altered in their signaling and instead of cAMP are now involved in stimulating mobilization of intracellular calcium, which is adaptable in a format that is HTS friendly.

Most of the cAMP assays to date have been based on the use of a labeled cAMP–cAMP antibody complex that is competed off upon formation of cAMP in live cells. These formats have ranged from radioactive labels to fluorescent labels amenable to a homogeneous time-resolved fluorescence (HTRF) method. Recently, the use of a biosensor such as the cyclic nucleotide gated (CNG) channel to monitor changes in cAMP has come to the forefront. In this assay format, cells overexpress the G_s- or G_i-coupled GPCR of interest in addition to a modified CNG channel that is sensitive to changes in cAMP (BD Biosciences, CA). This technology offers several advantages: (a) changes in cAMP cause the CNG channel to open, which in turn allows an influx of Ca and Na ions ensuing in a change in membrane potential; (b) the use of cell-permeable membrane potential sensitive fluorescent dyes adds ease and homogeneity to the assay; (c) CNG channel activation is fairly stable, thus allowing for an endpoint assay, which in turn also allows for tremendous flexibility in the HTS scheme; (d) the assay

format is well suited for agonist, antagonists, inverse agonists, and allosteric modulators of GPCRs; (e) for the G_i-antagonist format, the cells are treated with an agonist of an endogenous receptor such as Isoprotenerol (β-adrenergic receptor agonist) or NECA (adenosine receptor agonist) in order to stimulate cAMP, which is subsequently inhibited in the presence of a Gi agonist. Potential G_i-GPCR antagonists thus inhibit the ligand-induced suppression of cAMP and cause a net increase in cAMP and a net increase in fluorescence. This format is especially attractive as it will not pick up fluorescence inhibitors, which can typically manifest as false positives. This technology has been successfully applied to the identification of G_i-GPCR agonists and antagonists, and G_s-GPCR antagonists.

In summary, the use of cryopreserved cells in HTS assays has transformed cell-based assays. Cells have transitioned from being real-time laboratory processes to "on demand" reagents. This has in turn had tremendous impact on the cost, quality, and robustness of cell-based HTS assays. The increase in use of cell-based assays as primary screening tools will also reduce attrition of compounds that fail due to lack of permeability across living membranes or lack of stability in a more physiological milieu.

ACKNOWLEDGMENTS

The authors would like to thank Jason Munderloh (New Lead Discovery), and Levina Goon, Neema Parikh, and the Drug Discovery Cell Facility at Exelixis for their support in preparation of cryopreserved cells for HTS activities.

REFERENCES

1. Fox S, Farr-Jones S, Sopchak L, et al. High-throughput screening: Update on practices and success. J Biomol Screen 2006; 11:864–869.
2. Macarron R. Critical review of the role of HTS in drug discovery. Drug Discov Today 2006; 11:277–279.
3. Zaman GJR. Cell-based screening. Drug Discov Today 2004; 9:828–830.
4. Weetall M, Hugo R, Friedman C, et al. A homogeneous fluorometric assay for measuring cell adhesion to immobilized ligand using V-well microtiter plates. Anal Biochem 2001; 293:277–287.
5. McGinnity DF, Soars MG, Urbanowicz RA, et al. Evaluation of fresh and cryopreserved hepatocytes as in vitro drug metabolism tools for the prediction of metabolic clearance. Drug Metab Dispos 2004; 32:1247–1253.
6. Lau YY, Sapidou E, Cui X, et al. Development of a novel in vitro model to predict hepatic clearance using fresh, cryopreserved, and sandwich-cultured hepatocytes. Drug Metab Dispos 2002; 30:1446–1454.
7. Zuck P, Murray EM, Stec E, et al. A cell-based β-lactamase reporter gene assay for the identification of inhibitors of hepatitis C virus replication. Anal Biochem 2004; 334:344–355.
8. Fursov N, Cong M, Federici M, et al. Improving consistency of cell-based assays by using division-arrested cells. Assay Drug Dev Technol 2005; 3:7–15.
9. Kunapuli P, Zheng W, Weber M, et al. Application of division arrest technology to cell-based HTS: Comparison with frozen and fresh cells. Assay Drug Dev Technol 2005; 3:17–26.
10. Digan ME, Pou C, Niu H, et al. Evaluation of division-arrested cells for cell-based high-throughput screening and profiling. J Biomol Screen 2005; 10:615–623.
11. Ding M, Stjernborg L, Albertson N. Application of cryopreserved cells to hERG screening using a non-radioactive Rb^+ efflux assay. Assay Drug Dev Technol 2006; 4:83–88.

12. Chen J, Lake MR, Sabet RS, et al. Utility of large-scale transiently transfected cells for cell-based high-throughput screens to identify transient receptor potential channel A1 (TRPA1) antagonists. J Biomol Screen 2007; 12:61–69.
13. Zhu Z, Puglisi J, Connors D, et al. Use of cryopreserved transiently transfected cells in high-throughput pregnane X receptor transactivation assay. J Biomol Screen 2007; 12:248–254.
14. Wigglesworth MJ, Lawless KJ, Standing DJ, et al. Use of cryopreserved cells for enabling greater flexibility in compound profiling. J Biomol Screen 2008; 13:354–362.
15. Zaman GJR, de Roos JADM, Blomenrohr M, et al. Cryopreserved cells facilitate cell-based drug discovery. Drug Discov Today 2007; 12:521–526.

15 High-Content Screening with a Special Emphasis on Cytotoxicity and Cell Health Measurements

Ralph J. Garippa and Ann F. Hoffman
Roche Discovery Technologies, Roche, Inc., Nutley, New Jersey, U.S.A.

INTRODUCTION

High-content screening (HCS) has evolved over the past 10 years to transform processes and techniques for fluorescence microscopy from the single representative sample on a glass slide to the fully automated high-throughput screening (HTS) process (1). This process has been embraced by microscopists and cellular biologists alike to query multiple therapeutic areas of study in order to better characterize disease processes, "on and off target" perturbances of potential target molecules as well as monitoring the impact on cellular homeostasis of silencing RNA treatments (2). Cellular biologists have integrated these autonomous platforms that can serve to industrialize the experimental process: acquiring images, performing image analysis to quantify detectable fluorescent changes of probes and biosensors, and finally, analyzing the numerical data with visualization tools to present the information in an interpretable fashion (3). HCS is often used in the drug discovery process to provide information on mechanism of action when deciphering disease states or alterations due to compound treatment and has brought many successes and enlightenments of cellular processes and pathways (4). These platforms inherently have enabled both a high-resolution, detailed view of biological processes as well as have the ability to exponentially examine tens of thousands of samples per day (5). Therefore, profiling applications where evaluations of scores of compounds or of many distinct cell types for a particular function or event have become commonplace. A significant area of study has been cellular profiling for early safety evaluations where the goal is to quantify multiple cell health parameters and cytotoxicity assessments to detect early compound liabilities (6). Analogously, profiling studies utilizing cytotoxicity read-outs for compounds with similar functions, such as kinase inhibition, have been done to characterize the kinase targets and the nonspecificity of kinase action (7). High-content imaging instrumentation and techniques are expanding to encompass the latest advancements in physics and biology to achieve submicron resolution imaging and multimodal optical properties. At present, studies such as those described here are significantly impacting the drug discovery process and its strategic approach in developing new molecules.

ASSAY DEVELOPMENT CHOICES

One of the attractive features of HCS is the myriad of cellular functions which can be queried by this technique. Early in the assay development stage, a choice

must be made as to what approach will be taken to create access to the protein of interest with a fluorescent marker. This aspect takes advantage of the wide variety of fluorescent probes available such as primary or secondary antibodies (8), stably expressed fluorescent proteins such as GFP, dyes such as Cy3 from GE, tags (such as SnapTag from Covalys or HaloTag from Promega), or selenium-based particles [e.g., Quantum Dots (9,10) from Invitrogen]. Basically, if a marked protein translocates from one intracellular compartment or organelle to another, activates [as in the case of cellular biosensors (11)], rearranges itself into multimers or combines with another protein, moves into or out of an intracellular area, which has been masked in an algorithm, is imported into the cell or exported from the cell, then one has a chance to devise a high-content screen to quantify the intracellular dynamics (12). Limitations will be put on the system by accounting for such variables as the photobleaching of the fluorophore, spatial constraints of the cell area being addressed, and the overall cell health and background in which the measurement is made. For example, a useful tool for adding an element of quality control to HCS assays is the use of a cellular viability measurement immediately prior to the experiment (13). A small benchtop microcapillary flow system such as the Guava EzCyte can be employed to gauge the degree of protein expression (which gives an indication of the patency of the endoplasmic reticulum and Golgi apparatus), precise cell counting, and an assessment of cell viability.

At present many types of cellular drug discovery assays rely on the overexpression of the protein of interest in order to query activation states of the protein, interactions with ligands or other binding partners, leading to cascading signal transduction events. High-content assays are able to make use of both endogenous cellular systems and those modified to overexpress or silence (as discussed thereafter) given genes. In such cases, the overexpression of a given protein may be tunable with vector systems such as the Tet-on tet-off promoters, or the BacMam expression systems, which are regulated by the multiplicity of infection (MOI) of the virally transduced protein and the time point of expression (14). Aside from the level of the expression of the protein of interest, the effects of the experimentally introduced fluorescent probes may themselves also alter the natural cellular processes and pathways. Failure to monitor the effects of these manipulations is a justifiable criticism of experimental design and may later enter into the question of data interpretation. General methods can be commonly used to ultimately query the properties of the protein (fluorescently tagged or not) to ascertain the mechanism of action, regulation of, for example, changes of intracellular calcium concentrations, or activation of transcription. Cell health assays have been used to quantify the impact of newly synthesized small molecules on theses processes. We have utilized various HCS measurements to monitor adverse effects. These include quantifying nuclear morphology and effects on mitochondrial activity and lysosomal activity (15). Additionally, when specific high-affinity antibodies to the protein of interest are available, localization studies may significantly support interpretations from a wide source of cellular assay formats.

SECONDARY ASSAYS

The use of HCS for secondary assays was the first point of establishment in bringing forward known fluorescent microscopy techniques onto automated

platforms. The list of secondary assays and applications that can be performed in HCS has been constantly expanding, and the more common, long-established applications such as neurite outgrowth, cytonuclear translocation, apoptosis, nuclear morphology, and tube formation have been evolved over the years into more sophisticated packages (16). Two popularly deployed assays, micronucleus detection, and the measurement of cells arrested in a particular mitotic phase (re: mitotic index) are not well adapted to any other experimental format (17). Simply put, HCS enables the objective quantification of experimental parameters that are not easily obtained using alternative experimental methods. Within drug discovery, secondary assays continue to have a firmly established place among the vital metrics needed to bring potential candidate molecules forward.

HCS assays may be parsed and deployed based upon general cell signaling pathways, therapeutic areas, proliferation, activation, or induction of a cellular function or a specific protein (18). With development of additional sophistication in image analysis, probe development and the need to obtain the maximum amount of information from each experiment, there is a trend to integrate and multiplex more cytotoxicity parameters (19). Analysis of multiplexed data, in turn, serves to "qualify" and cluster the mechanistic results as to function, of for example, how a compound affects a receptor activation event, and the acute effects of that compound on viability (20). HCS platforms easily allow multiple feature measurements on each and every cell within the image field. Automated data analysis has now progressed such that software options offer the ability to classify and perform principal component analysis (PCA) on the multiple feature measurements whether as few as 5 or as many as 50 are collected (21). Additionally, a number of software packages are able to identify and itemize the few key features, constituting the majority of the measured response of a cell to a compound (22). Presently, HCS use is split between mechanism of action studies and cell health/cytotoxicity assays. A reason for this is the need to identify the most promising functional compounds lacking potential liabilities as quickly as possible in the development of a new drug.

USE OF RNAi

The use of RNAi for the determination of the role of a target protein via loss-of-function studies is one of the mainstays of modern drug development and was the second point of establishment of HCS (23). In a sense, RNAi and HCS were two technologies that could never have reached their full potential without the ability to exploit the power of each other's platform. Early proponents of RNAi sought a visual experimental endpoint, which could characterize a wide diversity of cellular phenotypes (24). Such a platform needed to be flexible in terms of which cellular compartments would be queried, and algorithms to address these images had to be modifiable to the extent of picking-up both expected and unexpected phenotypes. These unforeseen morphological presentations either portended off-target effects of the siRNA or they intimated at profound on-target alterations in normal cellular physiology. It is this aspect of discovering the therapeutic potential of interventions in and around these novel protein targets, along with the recent deciphering of the human genome and the genomes of other species (25), which ensures the long-term utility of combining siRNA and HCS techniques. Time and time again, HCS results have shown the progression of cellular data toward tissue relevance and ultimately being representative of whole

animal studies in the laboratory. It is expected that these correlations will eventually follow through in human validation studies.

In combining efforts to evaluate new drug targets and monitor the effects of an automated large-scale siRNA transfection scheme, we chose to implement both a secondary HCS assay and a profiling HCS cytotoxicity assay in parallel. In obtaining these dual results simultaneously, not only was there a clear time savings but the interpretation of results was also greatly facilitated. We encountered examples where multiple siRNAs for a single gene gave >90% knockdown in the branched DNA assay used to measure of gene expression. In a subset of these, we also noted that the number of cells in the HCS assay was diminished due to cellular death (fragmented nuclei and changes in cellular morphology), which implied that the actual gene that was knocked down may not be the preferred "new drug target" candidate. In the course of further studies on a gene-by-gene basis, we were able to clearly sort out the adverse "off target" toxicities with regard to cell health using multiple probe sets. Because candidate gene targets were analyzed for the common off-target cytokine expression markers, as evidenced from either up- or downregulated gene expression, the data revealed further supportive evidence for utilizing the HCS CT assays. As an exponential rise in the use of siRNA silencing tools for target validation grew, there was also an increased use of nonimaging cellular assays (glucose uptake, triglycerides, proliferation assays such as MTT), which also was shown to further support the data generated from a dual HCS cytotoxicity/cell health assay.

CYTOTOXICITY AND CELL HEALTH

An exciting new deployment of HCS strategies and the third point of establishment of HCS assays in drug discovery is the realm of early safety profiling in the preclinical setting (26). Although non-HCS assays such as MTT and Alamar blue exclusion assays remain as effective straightforward methodologies to assess cell viability, HCS offers a much more sophisticated means to determine a cell's reaction to noxious substances. HCS assays can be set-up in live cell or fixed cell mode, although it is appropriate to remind the reader that the purpose of a fixed cell HCS assay is to stabilize by fixation (typically by soaking the cells in formalin or ethanol) an event that was recorded in a live cell. In cytotoxicity or cell health assays, the ability of HCS to pinpoint the area of integrity breach becomes obvious. Parameters in the plasma membrane, nucleus, lysosomes, endosomal compartments, mitochondria, Golgi, ER, or adherence properties can be measured in parallel. Key selections that must be made in the experimental design include the choice of cell (which can be relevant to target organ toxicity or perhaps a more generalized, sensitive cell to act as a cytotoxicity sentinel), the preference of the concentration of toxicant exposure (multiple doses are preferred, spanning the micromolar to the high nanomolar range), and the time of exposure (typically, 24, 48, or 72 hours) (27). As might be expected, it is not unusual to find a much greater toxicant effect at the later timepoints. For discrete kinetic analysis of evolving toxic events, one may utilize live-cell environmentally controlled HCS instruments (Cellomics Vti) and gather a detailed timecourse of the cell's reaction to an onslaught of cellular disrupting agents (28). Therefore, early safety profiling efforts in the preclinical setting have taken on multiple meanings (29)—for example, HCS that revolves around specific cell types (cardiomyocytes, hepatocytes), HCS assessments revolving around general cellular functions, HCS

profiling designed to differentiate compounds based upon similar MOA (protein kinase example), and HCS profiling to potentially reduce or replace animal testing for specific known safety liabilities (in vitro micronucleus assay) (30,31). A natural extension of HCS cellular imaging is in the area of imaging small animals such as zebrafish; however, full automation of all of the steps in hatching, embryo sorting, and visualization techniques of single macroscopic living organisms, to date, lags far behind the area of HCS applications for adherent and nonadherent cell types (32). Further confirmation of HCS cytotoxicity results may be accomplished by applying toxicogenomic techniques (33,34).

As shown in Figure 1, a workflow for conducting a profiling high-content cell-based assay for cytotoxicity profiling entails two parts. In part I, the cells are plated, incubated with test compounds, labeled, fixed, read, and analyzed. In part II, the analysis may go beyond the straightforward observation of results and attempt to forecast and categorize future results with other compounds based upon the measurements and their correlations to specific cellular outcomes. Using linear regression and Baysean statistical models, support vector machines and neural networks are beginning to appear in publications (35,36). By taking an iterative approach, additional compounds may be screened and compared to the predictive models created in the initial exercise. Numerous iterative cycles serve to refine the model. There can be great flexibility in the HCS assay choices, depending on the selection of fluorophores and their inherent excitation and emission spectra (Table 1). Although a nuclear stain is a nearly nonnegotiable measurement, which ensures accurate cell counting while gaining a nuclear metric, the fluorophores in channels two and three can be substituted

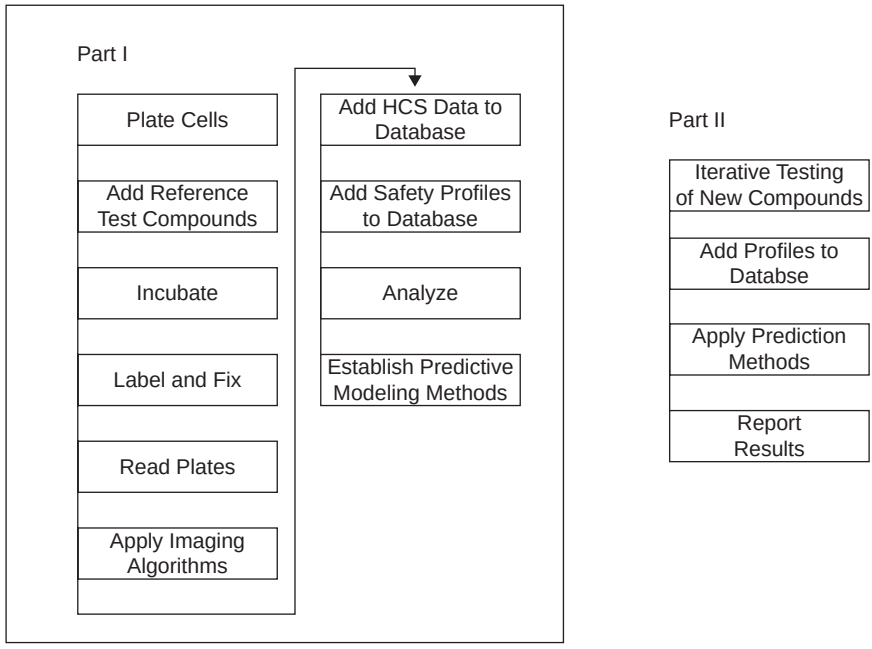

FIGURE 1 Typical workflow diagram for cytotoxicity and cell health high-content assays.

TABLE 1 Example of Seven Different Assay Development Choices for Setting-Up a High-Content Multiplex Experiment for Cytotoxicity and Cell Health

	Channel 1	Channel 2	Channel 3
Module 1	Nuclear morphology	Cell Permeability	Lysosomal mass/pH
Module 2	Nuclear morphology	Cell Permeability	Mitochondrial potential
Module 3	Nuclear morphology	Membrane potential dye	Cytochrome C
Module 4	Nuclear morphology	Oxidative stress	Reactive oxygen species
Module 5	Nuclear morphology	Phospho-histoneH3	–
Module 6	Nuclear morphology	Phospho-gH2AX	–
Module 7	Nuclear morphology	Mitochondrial mass/potential	Cytoskeletal changes

for other markers. In Figure 2, the dose response characteristic of the cytotoxicity index is seen with a candidate compound. Within this HCS bioapplication, parameters are measured in multiplex fashion, taking advantage of the differences in emission spectra of the fluorescent emitters: nuclear morphology, cell number, cell permeability, and changes in lysosomal mass and lysosomal pH. At 10 and 30 μM concentrations of the test compound, the cytotoxicity index was raised ~60%. At the 100 μM concentration of the test compound, there was a complete loss of cells from the plate surface, which is reflected as a paradoxical drop in the cytotoxicity index. The numerical data that accompanies Figure 2 is seen in Table 2. A new cytotoxicity assay with potentially greater sensitivity for detecting noxious agents is shown in Figure 3. The phosphorylation of the histone variant H2AX at double-stranded breaks in DNA is thought to be crucial for the recognition and repair of DNA damage. Phosphorylation of the C-terminal Ser139 only occurs at sites surrounding double-stranded breaks. The phosphor-Ser139 H2AX colocalizes with known repair enzymes at the site of DNA breaks. It presents an opportunity to measure both direct and indirect cell killing, as well

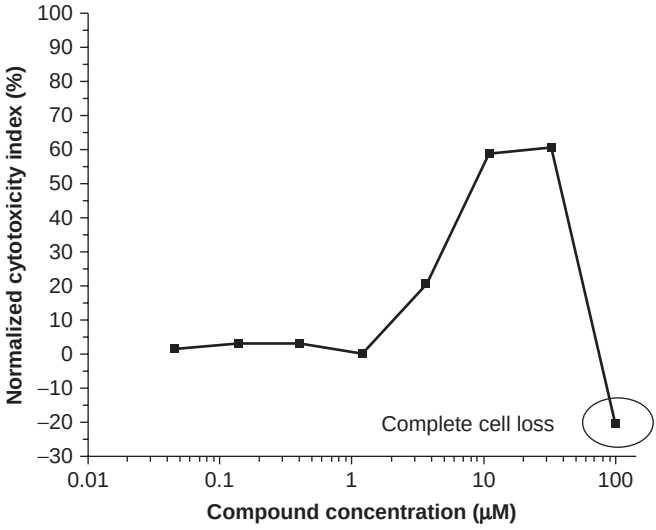

FIGURE 2 The dose response characteristics of the of the cytotoxicity index are shown in the context of a candidate compound.

TABLE 2 Dose Response Characteristics of the Cytotoxicity Index as Shown with a Candidate Drug

Concentration (μM)	Average norm cytotox index	Average norm mean cell perm	Average norm meanLyso mass	Average norm mean-NucFragCon-den	% Cell count	Comment
100	−20.55	−10.74	−159.28	−19.51	0.00	Low cell count
33.3333	60.60	49.07	682.68	3.61	35.79	Low cell count
11.1111	58.76	50.84	479.12	4.76	25.43	Low cell count
3.7037	20.47	29.74	320.56	1.76	95.57	
1.2346	0.46	1.98	24.26	−0.19	97.02	
0.4115	3.25	2.30	22.58	0.14	104.13	
0.1372	3.05	3.03	13.27	−0.12	102.92	
0.0457	1.68	3.48	5.35	0.60	98.10	

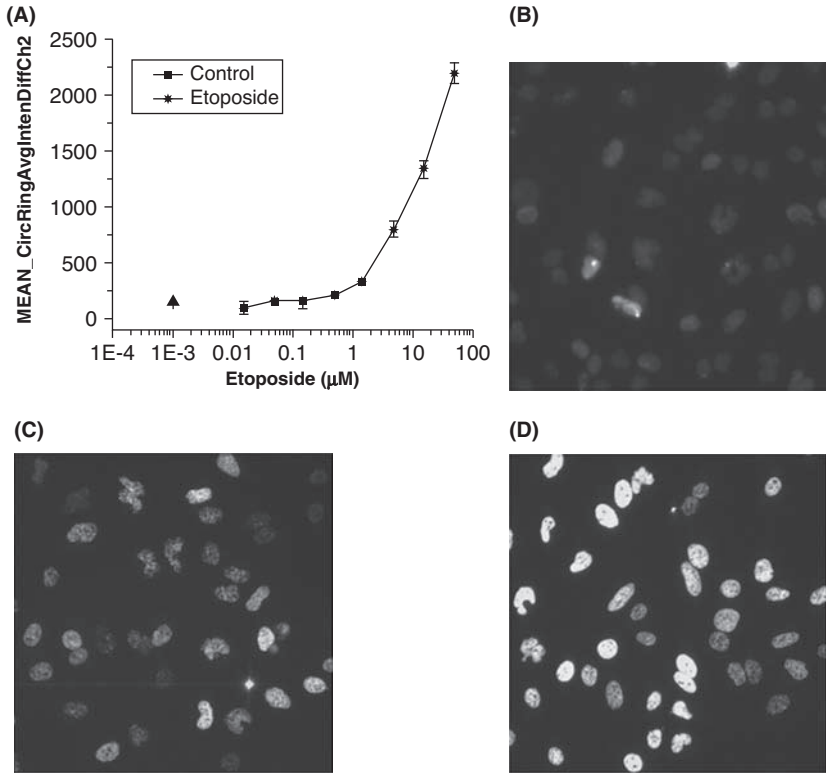

FIGURE 3 A new cytotoxicity assay with potentially greater sensitivity for detecting noxious agents. (**A**) Exposure to etoposide at concentrations above 1 μM resulted in consecutive increases in the amount of serine 139 phosphorylated gH2AX. The control untreated cellular phenotype is shown in panel (**B**) as a comparison to the 5-μM etoposide-treated cells shown in panel (**C**) and the 50-μM treatment of etoposide exposure in panel (**D**).

TABLE 3 Signal-to-Noise Ratios for 10 Cytotoxicity Assays as Shown with Their Respective Positive Control Reference Compound

Biological function (stain or antibody)	Reference compound	HeLa S/N	HepG2 S/N
Cell loss (nuclear stain)	Valinomycin	8	~5
Nuclear size (nuclear stain)	Valinomycin	1.2	~1.2
Mitotic arrest (histone H2AX)	Nocodazole	~7	~7
ROS & oxidative stress (DHE)	Rotenone/CCCP		~30
Oxidative stress (histone H2AX)	Etoposide	~12	~12
Plasma membrane integrity (permeability dye)	Valinomycin	~10	~10
Mitochondrial function (mito dye MTO)	Valinomycin	~2–3	~2–3
Lysosomal function (lyso dye)	Valinomycin	~4	~4
Cytoskeletal integrity (tubulin)	Paclitaxel	1 : 5	
CellTiter-Glo luminescent cell viability	Valinomycin	~30	~30

as the underlying DNA lesion, which produces the chromosomal damage. As shown in Figure 3, panel (A), exposure to etoposide at concentrations above 1 μM resulted in consecutive increases in the amount of Ser139 phosphorylated gH2AX detected in the masked area. The change from the control untreated cellular phenotype shown in the photomicrograph in panel (B) is highly evident when compared to the 5 μM concentration shown in panel (C) and the 50 μM concentration of etoposide exposure in panel (D).

Although not renown for having high signal-to-noise (S/N) ratios, high-content assays can be developed, which display more than adequate S/N values. In Table 3, the S/N ratios for 10 cytotoxicity assays are shown along with their respective positive control reference compound. Across two different cell lines, HeLa and HepG2, the S/N values range from 1.2 to 30 (37). This is compared to standard non-HCS plate-based assays where S/N values are typically in the range of 4 to >30. Further utility of HCS assays in drug development is prominent in Figure 4. A comparison of noninhibitors to known inhibitors of protein kinases, as measured by their activity in several high-throughput screens each for a different kinase, is shown. A multiplexed cytotoxicity HCS was performed after a 48-hour compound exposure measuring nuclear parameters, membrane permeability, and lysosomal mass and pH. Clearly, the mean cytotoxicity index was significantly higher ($P = 0.008$) when comparing the specific inhibitors with the noninhibitory compounds. The same significant difference held true when comparing compounds with moderate promiscuity with the specific inhibitors ($P = 0.0001$). However, the mean toxicity index for highly promiscuous inhibitors was not significantly different from mildly promiscuous inhibitors. One interpretation of this result is that active kinase-inhibitory small molecules have a significantly greater chance of exhibiting a toxic response than inactive, kinase non-inhibitory molecules, and that mildly to highly promiscuous compounds hold a much higher risk potential for exhibiting cytotoxic effects than do specific mono on-target compounds.

Shown in Figure 5 is a Spotfire representation of the distribution of baseline controls from vehicle-treated wells in a 384-well plate where high-content cytotoxicity is being measured. On each plate of this compound library screen, 16 wells were dedicated to basal controls. The average data for the test compounds was normalized to the average results for the basal wells for all measured HCS

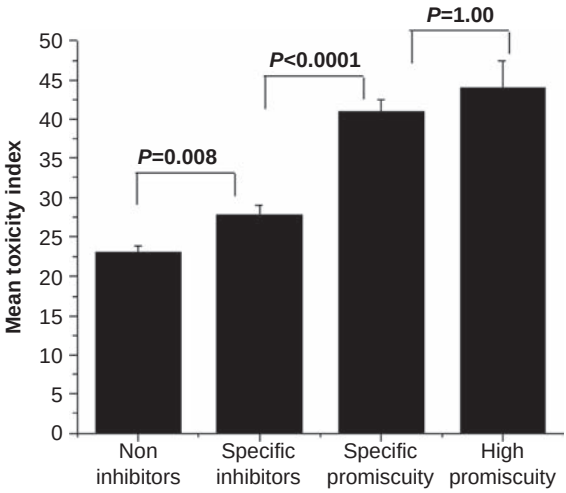

FIGURE 4 A comparison of noninhibitors, selective inhibitors, and promiscuous kinase inhibitors. The mean cytotoxicity index is significantly higher ($P = 0.008$) when comparing the specific inhibitors with the noninhibitory compounds. The same significant difference holds true when comparing compounds with moderate promiscuity with the specific inhibitors ($P > 0.0001$). However, the mean toxicity index for highly promiscuous inhibitors was not significantly different from mildly promiscuous inhibitors ($P = 1.00$).

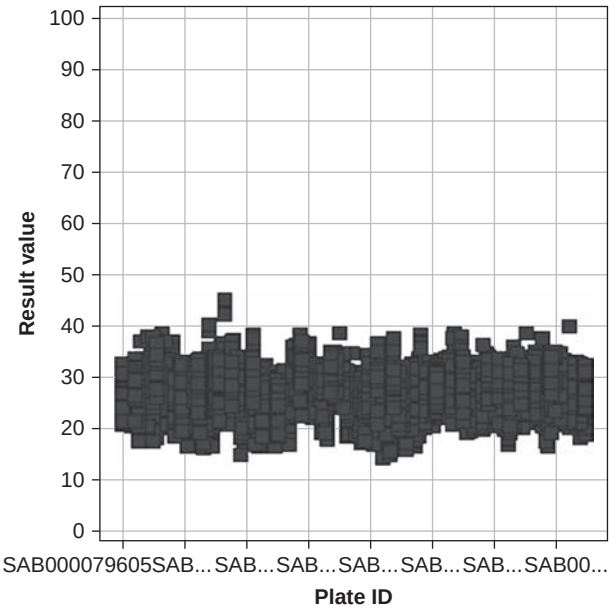

FIGURE 5 Spotfire representation of baseline control compounds. The result value of cytotoxicity index is measured on 16 untreated wells from each microtiter plate. The average cytotoxicity index as measured in the basal wells was ~25%.

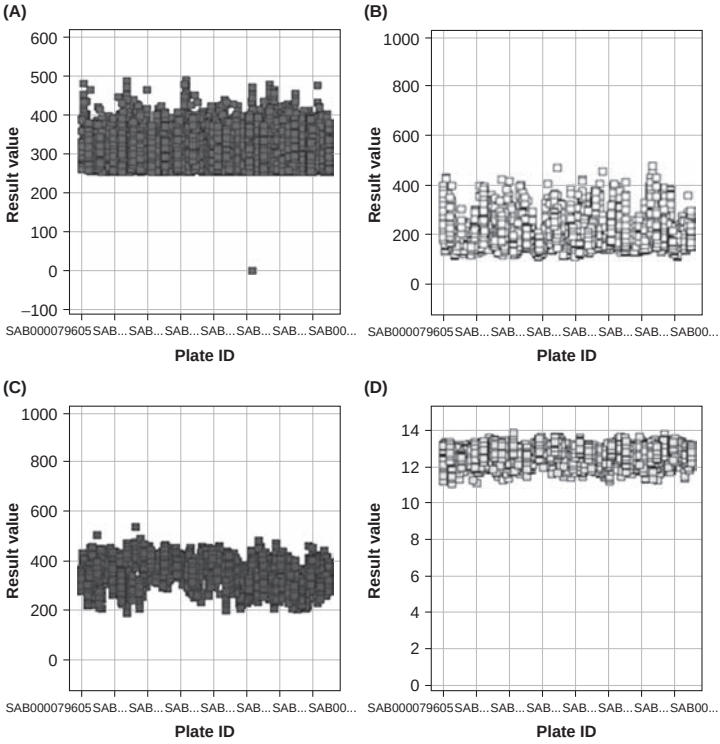

FIGURE 6 Spotfire representation of baseline values for four CT features. The four cytotoxicity features are cell count in panel (**A**), the cell permeability in panel (**B**), the lysosomal mass and pH determination in panel (**C**), and the degree of nuclear condensation and fragmentation in panel (**D**). A highly consistent baseline is evident on each plate over day-to-day experimentation.

parameters. The average cytotoxicity index as measured in the basal wells was ~25%. The baseline values can be further broken down into the four individual features in Figure 6. For the cell count in panel (A), the cell permeability in panel (B), the lysosomal mass and pH determination in panel (C), and the degree of nuclear condensation and fragmentation in panel (D), one sees a highly consistent baseline, from plate to plate and from day to day. It is not unusual that a significant amount of time upfront is needed in the assay development stage of HCS in order to develop standard operating procedures (SOPs), which greatly facilitate the generation of consistent baseline values. The breakdown and interpretation of four HCS parameters following exposure to a toxic test compound are shown in Figure 7. In panel (A), the average normalized cell permeability is markedly increased from the range of 3 to 30 μM but seems to paradoxically recover at 100 μM concentration of the compound. However, as is seen in panel (D), the amount of cells remaining attached and therefore assayable on the plate is extremely low, thereby contributing to the high experimental error at the highest doses. In panel (B), the average lysosomal mass and pH measurement drastically increases at 1 and 3 μM concentrations of the compound but exhibits

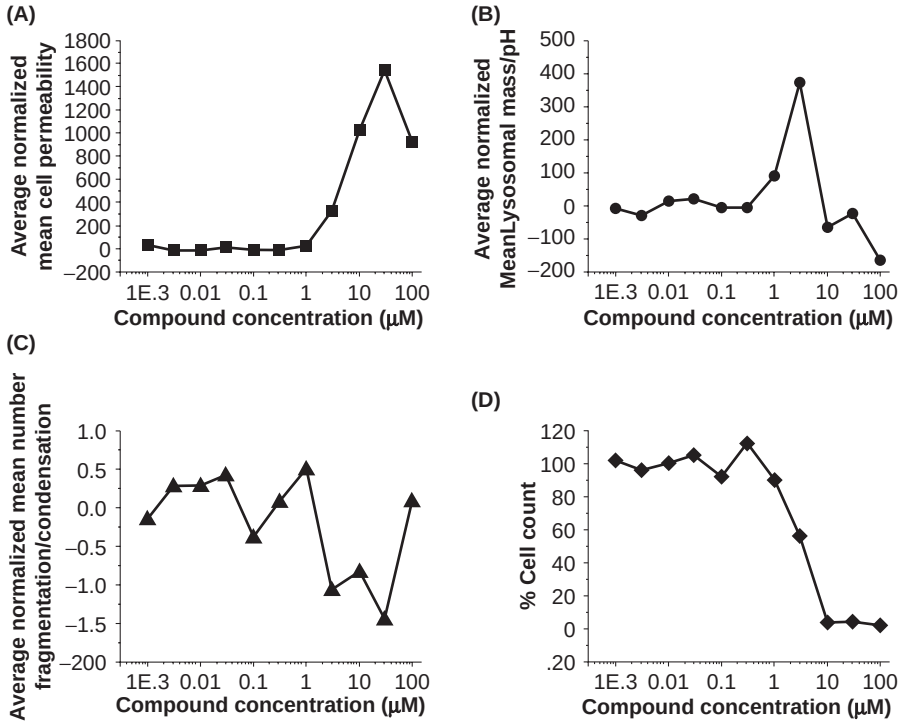

FIGURE 7 Breakdown and interpretation of four HCS parameters following exposure to a toxic test compound. Panel (**A**) describes the average normalized cell permeability, panel (**B**) the average lysosomal mass and pH measurement, panel (**C**) the nuclear condensation and fragmentation measurement, and panel (**D**) the percent of cells remaining after compound treatment and processing. These measurements, taken together, allow the investigator a higher level of rational interpretation of the progression of cytotoxicity.

a sharp decrease below baseline at 10, 30, and 100 μM concentrations. For this parameter, either a significant increase or decrease from baseline would be indicative of a cytotoxic event. In panel (D), the cell count drops approximately 50% at the 3 μM concentration of the compound, whereas above 10 μM the adherent cell count approaches zero. These concentration-related phenomena, taken together, allow the investigator a higher level of rational interpretation of the concentration-dependent progression of cytotoxicity.

The cytotoxicity index distribution of 25 lead candidate compounds from an anticancer drug program are shown in Figure 8. Eleven of these compounds were without any cytotoxicity flags. Three compounds were flagged for low cell number and high degree of cell permeability. Another compound was fluorescent and produced a low cell number. Two more compounds were flagged for a low cell number with concurrent high cell permeability and nuclear condensation and fragmentation. One compound demonstrated a significant change in lysosomal pH and another in nuclear condensation and fragmentation. These results demonstrate that multiplex HCS can be enabled, so as to present a gauntlet of experimental tests to identify potentially noxious compounds, those

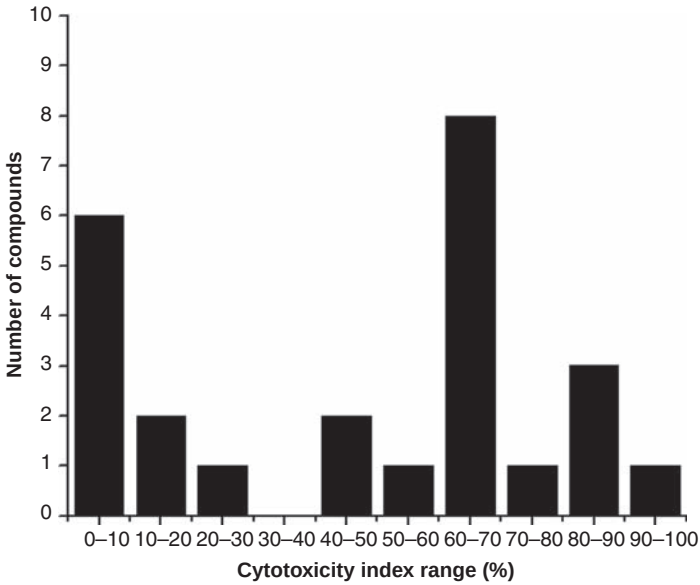

FIGURE 8 Cytotoxicity index distribution of 25 lead candidate compounds from an anti-cancer drug program. Approximately half of the compounds were without any cytotoxicity flags, while the remaining displayed multiple combinations of flags for the four parameters.

producing unwanted on- or off-target effects, at an early stage in preclinical drug development. By comparison, the cytotoxicity distribution for 12 lead candidate compounds from an antiobesity drug program are shown in Figure 9. Only one of these compounds was without any toxicity flags. The remaining 11 compounds were either flagged for indices of high cell permeability, changes in lysosomal mass and pH, nuclear condensation and fragmentation, a decrease in cell number, or some combination of the above parameters. As these two examples demonstrate, as applied in two distinct disease biology areas, HCS assays can provide an effective way to rank order or cull compounds within the lead advancement stage of drug development programs.

HTS SIMILARITIES AND OVERLAPS

Similarities and overlaps between HTS and HCS abound. Although the field of HTS came to the forefront of drug discovery approximately one decade ahead of HCS, the field of HCS itself has a long and storied history (38). In actuality, it was the early successes of HTS that drove the business case for developing automated cell-based assays, which could provide further detailed functional information regarding the early hits identified in either biochemical (absorbance, luminescence, radiometric binding, or fluorescence intensity) read-outs or cell-based (typically reporter gene assays, calcium flux, or cAMP determination) read-outs. This kind of information was and is still used to guide structure–activity relationships (SAR) and to advance drug candidates from the post-HTS to lead optimization phases right through clinical candidate selection for a particular project. One must be able to make the distinction between when it is appropriate

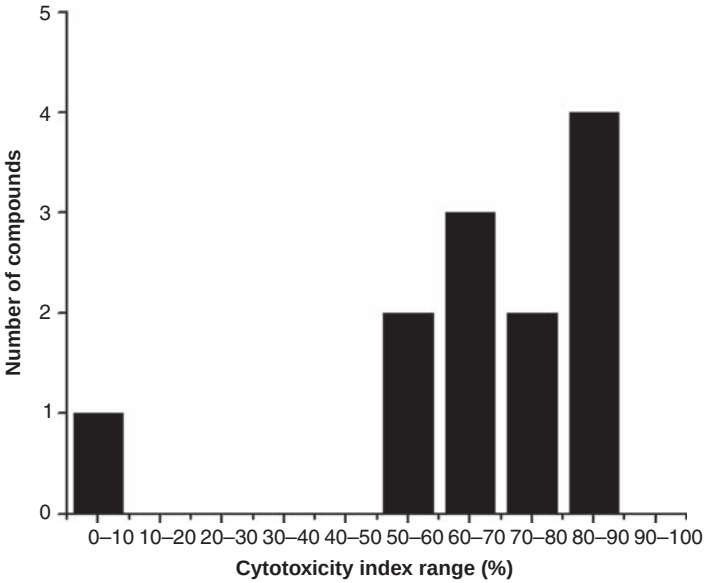

FIGURE 9 Cytotoxicity index distribution of 12 lead candidate compounds from an antiobesity drug program. Only one of these compounds was without any toxicity flags. The remaining compounds were flagged for indices of high cell permeability, changes in lysosomal mass and pH, nuclear condensation and fragmentation, a decrease in cell number, or some combination of the above parameters.

to separate HTS and HCS, and when it is beneficial to merge the two (39). In certain cases of the former, the HTS is better served by employing a noncell-based format because of reasons of higher throughput at a lower cost using smaller volumes of expensive reagents (40). In certain cases of the latter, it is generally agreed that the advantages of using the HCS as the basis of the HTS outweigh the potential drawbacks. These advantages include but are not exclusive to the ability to query the target protein in a relevant cellular context, obtain a metric, which is associated with the protein's known physiological role, and gather more than one measurable feature (the act of multiplexing) on a cell-by-cell basis.

VENDOR LANDSCAPE AND INSTRUMENTATION

Through mergers and acquisitions, the vendor landscape has drastically changed for the field of HCS. One of the earliest pioneer companies, Cellomics, is now owned by ThermoFisher. A trailblazer in the area of confocal HCS was Praelux, a Princeton (New Jersey)-based company, which was subsequently purchased by Amersham and then by General Electric Life Sciences. Another early player in the field was Universal Imaging that went through successive rounds of acquisition, first by Molecular Devices Corporation (MDC, Sunnyvale, CA), which had also acquired Axon Instruments and then by MDX Sciex. The Evotec Opera confocal imager is now the property of Perkin Elmer (Waltham, MA). Atto Bioscience is now owned by Becton-Dickinson. An important take-home message from all of the above business activity is that HCS remains a high viable scientific and

business entity. The research and drug discovery markets are constantly looking for new and better ways to render fluorescent-based cellular imaging experiments into databased information, which can drive project decisions. The base of HCS users seems to have an almost insatiable appetite for improved algorithms and choices in instrument capabilities and cost point. One would anticipate that the opportunity to bring forward new HCS imaging formats such as FLIM, FRET, FISH, brightfield, darkfield, and multispectral analysis would enhance the prospects of extending HCS endeavors into broader scientific disciplines.

ROLLOUT AND RETURN ON INVESTMENT

A number of questions beg to be addressed. Has HCS served to advance drug pipelines or is it too early to tell? Has there been a good return on investment (ROI)? A way of answering the first question is to look at the almost universal penetration of HCS in all of the major Pharma company's drug development strategies. Furthermore, one needs only to glance at the adoption of HCS techniques in academic screening labs to realize that most researchers recognize HCS as a means to a defined experimental end, namely, a powerful cellomic tool to generate chemogenomic information (41). The answer to the second question posed above, concerning ROI, in our experience, is a resounding "yes." The reason for this is the basic need for project teams to gather trustworthy information that will experimentally differentiate early drug candidates. Like any other new technology destined for Pharma rollout, once the initial barriers of instrument purchase costs, training of personnel, mainframe, and database considerations were addressed, HCS became a facile resource available to a wide variety of project teams and therapeutic areas. In the early days of HCS, proponents wrestled with the choice of which instrument (singular) to purchase. In recent years, the effort has been more focused on the integrated management of a diverse panel of HCS instrumentation, one with the flexibility to handle a full range of higher throughput lower resolution assays, all the way to lower throughput higher resolution assays.

CHALLENGES STILL TO BE OVERCOME

What challenges still need to be overcome? This question can be answered on an experimental level as well as on a data management level. First, on an experimental basis, one must consider the almost certain influx of stem cells (42) and primary-derived cells into HCS paradigms (43–45). These will present certain problems in terms of differentiation, handling, and passage that are not evident when carrying clonal cell populations. Although steps have been underway to bridge these gaps, they are not, for example, universally agreed upon methods for handling nonadherent suspension cells for HCS.

Experimental

Advances by Molecular Cytomics has been to develop single-cell honeycombed wells in a microtiter plate geometry for the staining of cells using both dyes and antibodies which includes washing steps to support image acquisition. Additional advances include BioStatus Limited's (U.K.) products, CyGel™, and CyGel Sustain™, which when mixed with suspension cells locks the cells in a matrix for visualization and study in three and four dimensions. One product

is a thermoreversible gel that can be used to immobilize nonadherent cells by simple warming, and conversely allowing recovery by simple cooling, while the second is used for extended imaging of live cells over several hours. A common technique in the in vivo laboratory is to utilize a cytospin centrifuge to obtain a concentrated representative sampling of blood, bronchoalveolar lavage, or other fluid containing a limited cellular population on standard glass slides. The development of multichambered "slide holders" for the HCS platforms assists in acquiring both fluorescent and brightfield images for further automated image analysis. Challenges arise in the field of pathology and immunohistochemistry regarding tissue samples, both an increase in the numbers of samples prepared for analysis as well as an increase in the need to automate image analysis of tissue sections and tissue microarrays (TMA). TMAs are commonly used to determine the correlation of a candidate drug targets expression or localization within specific tumor types, cell types, or disease states. Currently, the newer slide-based automated platforms vie for speed and sensitivity and market share; however, adaptation to similar if not the same image analysis and data/image management solutions may be a consideration. Furthermore, there is a need for more fluorescent biosensors, compartment-selective dyes, and protein-specific antibodies to better query targets of interest.

Data Management

On the data management level, many of the initial barriers in the field such as encoded headers in the file format (which would severely restrict the automated analysis and file sharing) are succumbing to user requests for more open file formats. The easy import and export of image files into image databases has vastly improved; however, it remains the end user's choice to determine which image features and files will remain in long-term storage and which ones will be jettisoned in favor of terabyte management costs. Encouragingly, HCS imaging management systems such as the Cellomics Store and the PE Evotec Columbus System suggest that future HCS laboratories will be able to enjoy the defined standardized types of file-sharing capability that are present in the field of flow cytometry and the open microscopy environment. This, in turn, will facilitate the development of faster algorithm construction for more rare, first-time visual biologies by widely enabling image access. Additional challenges beyond the image access include how the art of visualization and restoration will permit the science of three- and four-dimensional quantification of HCS parameters. As new findings in HCS assays for cytotoxicity and cell health determinations pinpoint key attributes, future specialization with respect to cell types, environmental conditions, and time-lapse video microscopy remain on the horizon.

What will be the future drivers for the continued use of HCS in Pharma? Pharma has supported HCA or HCI and HCS as HTS over the past five years, as it has become a mainstay in the industry. Most characteristically, fluorescence microscopy is imbedded as a core competency of the cellular biologist. However, that too is evolving as automation and computerization know-how is adopted and more scientists from various disciplines make use of these techniques and platforms. Presently, pharma laboratories may be specialized with an automated microscopy platform in an HTS setting with robotic automation and liquid handling support equipment, or the HCS platforms may be in a core laboratory also housing flow cytometry, multiphoton or super-resolution microscopes,

confocal intravital microscopes or such specialized custom-built instruments for total internal reflection fluorescence microscopy (TIRF). Pharma has found that high-content techniques are amenable to unlocking queries ranging from target identification to data for clinical study and clinical outcome. This track record is also supported by the world-wide HCS facilities of many Pharmas (institutes, biotechs, and academia) over multiple sites. The future drivers for the continued use of HCS will likely be the new biosensors and new probes that allow detection of the key sentinels of signal transduction pathways in disease processes, which upon transduction/transfection cause minimal perturbations in cellular homeostasis. Additionally, a likely rise in the preclinical use of HCS will also revolve around key predictivity findings supporting the use of HCS, as correlations between in vitro cytotoxicity and in vivo toxicity results become stronger. The higher the correlations, the more rapid the "best targeted compounds" will move forward in the discovery process and tested in vivo, advanced for further testing, and achieve a lead status for entry into human studies. HCS will likely play a key role in the clinic as we currently acknowledge flow cytometry does today.

REFERENCES

1. Harrison C. High-content screening–Integrating information. Nat Rev Drug Discov 2008; 7(2):121.
2. Evans DM, Azorsa DO, Mousses S. Genome scale cytometry: High content analysis for high throughtput RNAi phenotype profiling. Drug Discov Today: Technol 2005; 2(2):141–147.
3. Pipalia N, Huang A, Ralph H, et al. Automated microscopy screening for compounds that partially revert cholesterol accumulation in Niemann-Pick C cells. J Lipid Res 2006; 47:284–301.
4. Hoffman AF, Garippa RJ. A pharmaceutical company user's perspective on the potential of high content screening in drug discovery. In: Taylor DL, Haskins JR, Giuliano K, eds. Methods in Molecular Biology, Vol 356. Totowa, NJ: Humana Press Inc., 2007:19–31.
5. Garippa RJ, Hoffman AF, Gradl G, et al. High-throughput confocal microscopy for B-arrestin-green fluorescent protein translocation G protein-coupled receptor assays using the Evotec Opera. In: Inglese J, ed. Meth Enzymol 2006; 414:99–120.
6. Abraham VC, Towne DL, Waring JF, et al. Application of high-content multiparameter cytotoxicity assay to prioritize compounds based on toxicity potentials in humans. J Biomol Screen 2008; 13(6):527–537.
7. Pelkmans L, Fava E, Grabner H, et al. Genome-wide analysis of human kinases in clathrin- and caveolae/raft-mediated endocytosis. Nature 2005; 436:1–9.
8. Szent-Gyorgyi C, Schmidt BF, Creeger Y, et al. Fluorogen-activating single-chain antibodies for imaging cell surface proteins. Nat Biotech 2008; 26(2):235–240.
9. Michalet X, Pinaud FF, Bentolila LA, et al. Quantum dots for live cells, in vivo imaging, and diagnostics. Science 2005; 307:538–544.
10. Wylie PG. Multiple cell lines using quantum dots. Methods Mol Biol 2007; 374:113–123.
11. Fan F, Binkowski BF, Butler BL, et al. Novel genetically encoded biosensors using firefly luciferase. ACS Chem Biol 2008; 3(6):346–351.
12. Carpenter AE. Image-based chemical screening. Nat Chem Biol 2007; 3(8):461–465.
13. Miret S, De Groene EM, Klaffke W. Comparison of in vitro assays of cellular toxicity in the human hepatic cell line HepG2. J Biomol Screen 2006; 11(2):184–193.
14. Kost TA, Condreay JP, Ames RS, et al. Implementation of BacMam virus gene delivery technology in a drug discovery setting. Drug Discov Today 2007; 12(9/10):396–403.

15. Vogt A, Kalb EN, Lazo JS. A scalable high-content cytotoxicity assay insensitive to changes in mitochondrial metabolic activity. Oncol Res 2004; 14:305–314.
16. Radio NM, Breier JM, Shafer TJ, et al. Assessment of chemical effects on neurite outgrowth in PC12 cells using high content screening. Toxicol Sci 2008; 105(1):106–118.
17. Bowen WP, Wylie PG. Application of laser-scanning fluorescence microplate cytometry in high content screening. Assay Drug Dev Technol 2006; 4(2):209–221.
18. Ross DA, Lee S, Reiser V, et al. Multiplexed assays by high-content imaging for assessment of GPCR activity. J Biomol Screen 2008; 13(6):449–455.
19. Lynch C. How do your data grow? Nature 2008; 455(4):28–29.
20. Li F, Zhou X, Zhu J, et al. High content image analysis for human H4 neuroglioma cells exposed to CuO nanoparticles. Biotechnology 2007; 7:66–70.
21. Durr O, Duval F, Nichols A, et al. Robust hit identification by quality assurance and multivariate data analysis of a high-content, cell-bases assay. J Biomol Screen 2007; 12(8):1042–1049.
22. Shamir L, Orlov N, Eckley D, et al. Wndchrm—An open source utility for biological image analysis. Source Code Biol Med 2008; 3:13.
23. Martin M, Reidhaar-Olson JF, Rondinone CM. Genetic association meets RNA interference: Large-scale genomic screens for causation and mechanism of complex diseases. Pharmacogenetics 2007; 455–464.
24. Wang J, Zhou X, Bradley PL, et al. Cellular phenotype recognition for high-content RNA interference genome-wide screening. J Biomol Screen 2008; 13(1):29–39.
25. Moffat J, Grueneberg DA, Yang X, et al. A lentiviral RNAi library for human and mouse genes applied to an arrayed viral high-content screen. Cell 2006; 1238–1298.
26. Houck KA, Kavlock RJ. Understanding mechanisms of toxicity: Insights from drug discovery research. Toxicol Appl Pharmacol 2008; 227(2):163–178.
27. Guillouzo A, Guguen-Guillouzo C. Evolving concepts in liver tissue modeling and implications for in vitro toxicology. Expert Opin Drug Metab Toxicol 2008; 4(10):1279–1294.
28. Xia M, Huang R, Witt KL, et al. Compound cytotoxicity profiling using quantitative high-throughput screening. Environ Health Perspect 2008; 116(3):284–291.
29. Peters TS. Do preclinical testing strategies help predict human hepatotoxic potentials? Toxicol Pathol 2005; 33:146–154.
30. Walum E, Hedander J, Garberg P. Research perspectives for pre-screening alternatives to animal experimentation: On the relevance of cytotoxicity measurements, barrier passage determinations and high throughput screening in vitro to select potentially hazardous compounds in large sets of chemicals. Toxicol Appl Pharmacol 2005; 207(2) Suppl 1:393–397.
31. Collins FS, Gray GM, Bucher JR. Transforming environmental health protection. Science 2008; 319:906–907.
32. Milan DJ, Peterson TA, Ruskin JN, et al. Drugs that induce repolarization abnormalities cause Bradycardia in zebrafish. Circulation 2003; 107:1355–1358.
33. Boess F, Kamber M, Romer S, et al. Gene expression in two hepatic cell lines, cultured primary hepatocytes, and liver slices compared to the in vivo liver gene expression in rats: Possible implications of toxicogenomics use of in vitro systems. Toxicol Sci 2003; 73:386–402.
34. Koppal T. Toxicogenomics warns of drug danger. Drug Discov Dev 2004; 7(7):30–34.
35. Tao CY, Hoyt J, Feng Y. A support vector machine classifier for recognizing mitotic subphases using high-content screening data. J Biomol Screen 2007; 12(4):490–496.
36. Loo L-H, Wu LF, Altschuler SJ. Image-based multivariate profiling of drug responses from single cells. Nat Methods 2007; 4:445–453.
37. Flynn TJ, Ferguson MS. Multi-endpoint mechanistic profiling of hepatotoxicants in HepG2/C3A human hepatoma cells and novel statistical approaches for development of a prediction model for acute hepatotoxicity. Toxicol In Vitro 2008; 22:1618–1631.
38. Pereira DA, Williams JA. Origin and evolution of high throughput screening. Br J Pharmacol 2007; 152(1):53–61.

39. Hoffman AF, Garippa RJ. HCS for HTS. In: Haney S, ed. High Content Screening. Hoboken, NJ: John Wiley & Sons, Inc., 2008:227–247.
40. Blow N. New ways to see a smaller world. Nature 2008; 456:825–828.
41. Lazo JS, Brady LS, Dingledine R. Building a pharmacological lexicon: Small molecule discovery in academia. Mol Pharmacol 2007; 72(1):1–7.
42. Ivanova N, Dobrin R, Lu R, et al. Dissecting self-renewal in stem cells with RNA interference. Nature 2006; 442:533–538.
43. Xu JJ, Henstock PV, Dunn MC, et al. Cellular imaging predictions of clinical drug-induced liver injury. Toxicol Sci 2008; 105(1):97–105.
44. O'Brien PJ, Irwin W, Diaz D, et al. High concordance of drug-induced human hepatotoxicity with in vitro cytotoxicity measured in a novel cell-based model using high content screening. Arch Toxicol 2006; 80(9):580–604.
45. Chan K, Jensen NS, Silber PM, et al. Structure–activity relationships for halobenzene induced cytotoxicity in rat and human hepatoctyes. Chem Biol Interact 2007; 165:165–174.

16 Effective Application of Drug Metabolism and Pharmacokinetics in Drug Discovery

Sharon Diamond and Swamy Yeleswaram

Incyte Corporation, Experimental Station, Wilmington, Delaware, U.S.A.

INTRODUCTION

Twenty years back, Prentis et al. (1) upon reviewing pharmaceutical innovation and the factors that limited productivity concluded that approximately 40% of failures in early clinical development are due to inappropriate pharmacokinetics in man. This survey served as a wake-up call to the pharmaceutical industry, and the ensuing 20 years have brought a sea of changes in the attitude, strategy, investment, and practice of drug discovery in the pharmaceutical and biotechnology industry. More recent reviews peg the attrition rate due to pharmacokinetic issues at less than 10% (2), although some of the attrition attributed to "lack of efficacy" can still be due to the drug metabolism and pharmacokinetic (DMPK) profile, for example, less than optimal distribution into the relevant biospace, especially in the case of CNS and oncology targets. This impressive turnaround was made possible by easy availability of appropriate tools, for example, Caco-2 cells, recombinant cytochrome P450 (CYP) isozymes, pooled human liver microsomes, and importantly the integration of DMPK into drug discovery at an early stage such that DMPK properties can be optimized in parallel with potency and selectivity. While a lot has been accomplished to screen for and build-in critical pharmacokinetic properties like oral absorption, microsomal stability, lack of CYP inhibition, etc., several DMPK issues and challenges remain. This chapter will focus on some best practices for tackling the well-known DMPK issues and trends in dealing with the emerging ones.

UNDERSTANDING THE NEEDS FOR DMPK ASSAYS AT VARIOUS STAGES OF THE FUNNEL

Advances in automation technology and commercial availability of human tissues, cell lines, and recombinant enzymes have created both opportunities and challenges for the drug discovery process with respect to optimization of DMPK properties. In a general sense, more data is better than less and to be sure most medicinal chemists believe that any additional data could be incrementally beneficial in understanding the structure–activity relationship and in driving lead optimization. However, attempting to gather a data point for every compound against every assay may not be the smartest investment of resources. This dilemma led to the concept of "staging" assays at various stages of the discovery project. How this is executed in a particular company is often as much influenced by management philosophy at that company as the unique needs of the project. Some of the factors to consider in staging the assays are discussed below.

High-Throughput Screening Hits

Depending upon the size of the compound library, threshold for potency, and the nature of the target, the number of screening hits could be from less than 100 to a few thousands. One technique often employed by computational chemists is "scaffold binning," which bins the hits to a handful of scaffolds or structural backbones. This enables a few representative molecules from each scaffold bin to be profiled across a number of DMPK assays (see section "DMPK Assays in Current Drug Discovery" below). If the hits are in the thousands and not readily amenable to scaffold binning, in silico evaluation is worth considering. The options range from simple rules like "Lipinski's Rule of 5," polar surface area, and hetero-atom count to proprietary software packages.

Lead Optimization

Typically, lead optimization process starts with a "lead" identified either through in-house screening efforts or from the public domain. Since lead optimization is a resource intensive process involving several medicinal chemists and biologists and often represents significant opportunity cost within drug discovery organizations, it is important to make sure that the liabilities of the starting point for chemistry optimization are well understood. This not only ensures optimal staging of DMPK, pharmacology, and toxicology assays but can also avoid a nasty surprise down the road during candidate profiling or still worse, early clinical development. The profiling of the lead should be centered on three main questions: Does the molecule have acceptable PK profile that is consistent with the desired dose target, for example, <100 mg once daily, is there potential for drug–drug interactions, and is there potential for safety concerns due to chemical reactivity? The first question can be addressed with routine PK studies in a rodent and nonrodent using intravenous and oral dosing. From these studies, an estimate of systemic clearance, absolute oral bioavailability, percentage dose absorbed following oral administration, and half-life in animals can be obtained. The second question on drug interaction potential can be addressed with a panel of in vitro assays to assess the inhibition of the seven major CYPs, induction of CYP3A4 and P-gp, and inhibition of P-gp. The third question on reactivity should be addressed with an assay for glutathione adduct formation. These assays are explained in detail in section "DMPK Assays in Current Drug Discovery" below. Depending upon the results from these assays, follow-up experiments may be required; for example, if percentage dose absorbed is <50%, experiments to determine solubility, intrinsic permeability, acid lability, etc. will be helpful in understanding the reason for limited oral absorption. Results from profiling of the lead, as detailed above, should also form the basis for the screening strategy to drive lead optimization, for example, a lack of interaction of the starting chemical lead with CYPs and hERG could justify dropping these assays from the critical path for lead optimization and could be substituted with periodic spot checks of the submissions to ensure that the initial profile is maintained. Besides the aforementioned assays, an effort to characterize PK/PD in animal models is highly desirable. For further discussion on PK/PD, please see section "DMPK Assays in Current Drug Discovery" below.

Development Candidate Evaluation

The goal of the discovery effort is to identify compounds that are worthy of preclinical and clinical development. Current estimates on average cost incurred during early development is $3 to $5 MM, which includes scale-up of compound, toxicology evaluation to enable clinical trials, and first-in-man clinical study. These are just the direct costs. Therefore, a thorough evaluation of DMPK properties is justified before declaring a development candidate. It is recommended that multiple assays be used to address the three questions around PK, drug interaction potential, and reactivity. It is critical to understand the clearance pathways and the primacy of each pathway in the case of multiple pathways. For compounds that are cleared by metabolism, the major metabolites should be identified and their contribution to pharmacology and toxicology delineated. In addition, a good handle on preclinical pharmacokinetic (PK)/phramacodynamics (PD) based on data from multiple experiments involving different treatment regimen, for example, oral dosing and intravenous infusion is essential to guide early clinical development. Estimation of human dose for efficacy should be attempted based on PK/PD and projected human pharmacokinetics.

DMPK Evaluation During Development

The following studies are conducted typically during early clinical development and the timing of these studies is limited by the availability of radiolabeled material: mass balance studies in a rodent and nonrodent species, tissue distribution studies in pigmented rodents, for example, Long Evans rats and quantitative assessment of metabolites in the two species used for safety assessment studies, and in humans. Conducting some of these studies earlier should be considered under certain circumstances, for example, to address any concerns around distribution to specific tissues or metabolic profile.

DMPK ASSAYS IN CURRENT DRUG DISCOVERY

Assays for Absorption

The physiological barrier that a drug will invariably encounter is the lipid bilayer in the form of epithelium or endothelium; thus, drug permeability is evaluated early in the drug discovery process. Since most marketed drugs are administered orally, the most frequently used assays focus on the permeability across the intestinal mucosa (epithelial cells). While intestinal permeability is dependent on the physiochemical properties of a compound (lipophilicity, partitioning coefficient, hydrogen bonding, molecular size, etc.), making predictions based on these properties alone are complex and limited in scope. Instead, at the discovery stage, permeability is most often predicted using in vitro cell culture systems. In vivo, a soluble drug moves from the apical side (lumen) of the intestinal epithelial cell (enterocyte) to the basolateral side (blood) by passive diffusion (trancellular or paracellular transport), or by a carrier-mediated process (Fig. 1). Alternately, a drug may not reach the blood because of degradation by drug metabolizing enzymes in the intestine (e.g., cytochrome P450s, UDP glucuronosyltransferases, glutathione S-tranferase, sulfotransferase) or efflux by transporters (e.g., P-gp, MRP, BCRP) expressed in the intestinal epithelial cells. While there are several in vitro cell culture lines available (Caco-2, MDCK, LLC-PK1, HT29, and TC7), the human colon adenocarcinoma cell line (Caco-2 cells) is the most widely used

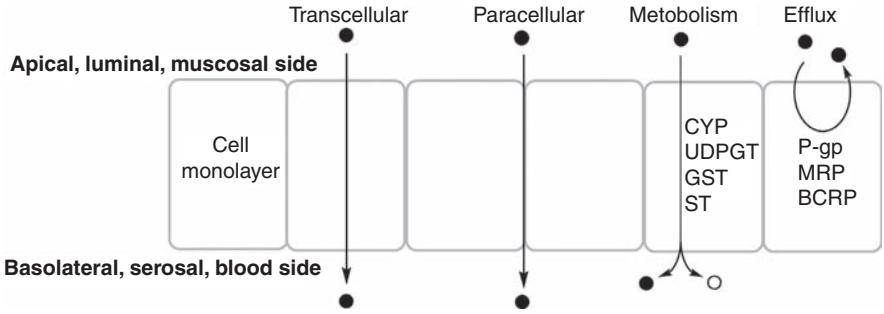

FIGURE 1 Possible pathways for the intestinal absorption of a drug (•) across the intestinal epithelium by transcellular or paracellular transport. Also, drugs may be excluded by efflux or converted to a metabolite (○).

because it mimics the function of the in vivo intestinal epithelium. These characteristics include tight intercellular junctions, microvilli, and the expression of intestinal enzymes and transporters, notably, P-glycoprotein (P-gp).

The Caco-2 assay requires both tissue culture facilities and analytical (LC/MS) resources. Briefly, Caco-2 cells are grown at 37°C in an atmosphere of 5% CO_2 in supplemented growth medium. Confluent cell monolayers are subcultured every seven days by treatment with trypsin and are seeded on porous filters usually supported using welled plates. Culture conditions and the number of passages can influence confluence and the expression of active transport systems (3). Cells typically are fully differentiated at approximately three weeks. The cell membrane confluence is confirmed by measuring transepithelial electrical resistance for each well to ensure tight intercellular junctions, and only Caco-2 cell monolayers with an acceptable value (typically $\geq$300 $\Omega \cdot cm^2$) are used. For absorption studies, compound (typically 10–25 μM) is added to the top chamber (apical, A) of the well, and sampled at the receiver chamber (basolateral, B) after a two-hour incubation. The donor and receiver chambers are filled with Hank's balanced buffer solution adjusted to pH 7.4, although it is possible to keep the donor chamber solution pH adjusted to 5.0 to better mimic the intestinal pH. It is important to make sure that the compound is soluble enough under the conditions used, and some laboratories routinely filter the donor chamber solution and analyze the concentration so that the permeability is more accurately calculated. This additional step is only necessary if a large number of poorly soluble compounds are under investigation. While solubilization of compound in the apical side is important to determine the intrinsic permeability, the solubility in the receiver chamber is critical to maintain the sink condition so that the Fick's law is valid and the permeability can be reliably calculated as shown below. More and more laboratories are using 4% bovine serum albumin (BSA) in the receiver chamber to improve the solubilization of lipophilic compounds. The presence of 4% BSA on the basolateral side is also physiological. At the end of incubation, the supernatants are collected following centrifugation for LC/MS analysis, and the permeability coefficient (P_{eff}) calculated from the following equation:

$$\text{Papp(cm/sec)} = \frac{(F \times V_D)}{(SA \times M_D)}$$

Where the flux rate (F, mass/time) is calculated from the slope of the cumulative amount of compound on the receiver side, SA is the surface area of the filter, V_D is the donor volume, and M_D is the initial amount using mass, of the solution in the donor chamber.

Since interexperimental and interlaboratory variability is somewhat expected for Caco-2 cells, especially for the active transport systems, appropriate controls must be included for each experiment. These controls could either be literature reference compounds (e.g., atenolol and metoprolol for low- and high-transcellular permeability) or in-house compounds to bracket the permeability range of interest.

Importantly, Caco-2 cells are also used to characterize the efflux or bidirectional transport of a compound (B to A/A to B). For these studies, compound is added in the absorptive direction (A to B) as described above, and in a separate, well studied in the secretory direction (B to A). To minimize any bias in the directional transport, 4% BSA is not included in the basolateral side in these experiments. A net flux ratio greater than 2 is considered positive, that is, indicative of transporter involvement. To further characterize the transporter responsible for efflux, experiments are conducted with and without known inhibitors of P-gp, for example, quinidine and verapamil. If the known P-gp inhibitor reduces the flux ratio by half, the compound is considered a P-gp substrate. If a significant amount of flux is not inhibited by a known P-gp inhibitor, then involvement of other transporters are implied, but are difficult to elucidate since specific trasporter inhibitors are not available (4). In addition to determining the potential for a compound to act as a P-gp substrate, a compound should be evaluated for its potential to inhibit P-gp. One drawback of the Caco-2 assay is that it can be labor intensive, so to increase high throughput many pharmaceutical companies have turned to automation. This platform has been quite successful and a fully automated system using a 96-well format can process approximately 800 compounds a week (5).

Two alternate in vitro cell systems to access permeability that are used include the Madin-Darby Canine Kidney (MDCK) and the Lewis Lung Carcinoma-Porcine Kidney (LLC-PK1) cell lines. The advantage of these cell lines is that they grow to confluency in a short period of time. MDCK and LLC-PK1 cell lines are derived from dog and pig, respectively, and do not always express enzymes and transporters reflective of humans (6). However, these cell lines can be transfected, to express transporters, notably P-gp. The MDCK cell line transfected to express P-gp (MDR-MDCK) has been widely used to screen permeability at the intestine, as well as the blood–brain barrier (7).

Assays to Identify Metabolic Liabilities

Intrinsic Clearance

There are several aspects of metabolism that are important to characterize very early in the discovery process. Perhaps the most central of these assays is the determination of the in vitro metabolic stability (intrinsic clearance, Cl_{int}) of a test compound. Hepatic Cl_{int} is defined as the rate of metabolism by liver enzymes in the absence of blood flow or tissue binding. Rapid metabolism (clearance) is a liability that limits systemic exposure and results in poor oral bioavailability. At the discovery stage, the Cl_{int} assay effectively eliminates high-clearance compounds from consideration and focuses valuable resources on viable drug leads. While

viable compounds move forward, the metabolic "soft" spots can be determined for high-clearance compounds giving medicinal chemistry a path forward to an improved ADME profile.

The in vitro Cl_{int} assay assumes that the liver is the major site of metabolism, and that the in vitro rate of metabolism is reflective of the in vivo. Since liver microsomes contain most of the major metabolizing enzymes, particularly CYP, it is the most popular in vitro system used. For most compounds, this is a reasonable approach unless non-CYP oxidations/reductions or direct conjugation (phase II reactions) pathways are suspected to contribute significantly to the rate of metabolism. It is prudent to determine the metabolic pathway responsible for metabolism using an in vitro panel as described in the Pharmaceutical Research and Manufacturers of America position paper (8), to choose the in vitro system that includes all possible metabolic pathways for a representative compound (hepatocytes, cytosol, S9). Table 1 shows the major pathways for drug metabolism, the enzymes responsible, and the in vitro system containing those enzymes. There is evidence that hepatocytes provide an accurate estimation of clearance (9), but hepatocytes are generally considered cost prohibitive for large screening efforts.

In most discovery laboratories, the Cl_{int} assay is conducted using a high-throughput platform. Generally, compounds at a final concentration of 1 μM are incubated at 37°C with potassium phosphate buffer (100 mM, pH 7.4), pooled human liver microsomal protein (1 mg/mL), and NADPH (1 mM), a cofactor necessary for CYP metabolism. In parallel, compounds are incubated under identical conditions without NADPH, to ensure that the compounds are stable under these incubation conditions. Also, a high-clearance compound should be included as a positive control to ensure that protein and cofactors are functioning properly. The incubation is typically initiated with NADPH and terminated with acetonitrile or methanol at 5 or 10 minute increments from 0 to 40 minutes. After centrifugation, the resulting supernatants are analyzed by LC/MS. The peak area of the test compound for the time zero sample is used as 100%, and the percentage remaining is calculated for the rest of the time course. An internal standard for the LC/MS analysis is typically not required for this experiment. There are

TABLE 1 General Biotransformation Pathways, the Enzymes Responsible, and the Corresponding In Vitro System That Should Be Used

Reaction		Enzymes	In Vitro System
Phase I	Hydrolysis	Esterase	S9, microsomes, hepatocytes
		Epoxide hydrolase	S9, microsomes, hepatocytes
	Reduction	Quinone reduction	S9, microsomes, hepatocytes
		Sulfoxide reduction	S9, hepatocytes
		Nitro reduction	S9, hepatocytes
	Oxidation	Cytochrome P450	S9, microsomes, hepatocytes
		Alcohol dehydrogenase	S9, hepatocytes
		Aldehyde oxidase	S9, hepatocytes
		Xanthine oxidase	S9, hepatocytes
		Monoamine oxidase	S9, hepatocytes
		Flavin-monooxygenase	S9, microsomes, hepatocytes
Phase II	Conjugation	Glucuronidation	S9, microsomes, hepatocytes
		Sulfation	S9, hepatocytes

three major models described to calculate in vivo clearance from in vitro clearance (10,11), but the "well-stirred model" is most frequently used. Accordingly, the percentage remaining data is transformed to its natural logarithm and plotted versus time, and the slope determined to calculate the in vitro half-life. The in vivo Cl_{int} (L/h/kg) is then calculated from the in vitro half-life value and conventional biological scaling factors specific to a species (11,12). To strengthen the human clearance value estimated in vitro, an in vitro–in vivo correlation should be established for a representative molecule in at least two preclinical species.

Potential for Reactivity

Compounds may undergo bioactivation to a reactive electrophilic metabolite(s) that covalently binds to nucleophilic tissue proteins possibly resulting in toxicity. A comprehensive catalog and discussion of possible reactive functional groups has been summarized by Kalgutkar et al. (13). The question that challenges ADME scientists is what level of reactivity should be considered the threshold for deselection. Not only organ toxicities are a concern but drug-protein adducts formed may act as a hapten resulting in immune-mediated toxicities in humans. While safety assessment studies can identify organ toxicities in preclinical species, it is generally accepted that there is no preclinical model to predict immune-mediated toxicities in humans. Obviously, reactivity should be minimized, and there are both in vitro and in vivo approaches to access the reactivity of a test compound, or its metabolite(s). In both approaches, ADME scientists search for evidence of a glutathione adduct, since metabolite-protein adducts are not easily detected by conventional analytical methods. Glutathione is a tripeptide of glutamic acid, glycine, and cysteine, with the cysteine residue providing the nucleophilic sulfhydryl group that traps the electrophilic compound. This reaction can occur chemically or enzymatically via glutathione S-tranferase(s) present at high levels in the liver along with the obligatory cofactor glutathione (10 mM).

At the discovery stage, often the first assay conducted is the in vitro "trapping" assay, using glutathione (or possibly cyanide) as an agent to trap the electrophilic moiety. Generally, compounds at a final concentration of 5 μM are incubated at 37°C with potassium phosphate buffer (100 mM, pH 7.4), pooled human liver microsomal protein (1 mg/mL), NADPH (1 mM), and reduced glutathione (5 mM). Glutathione ethyl ester may also be used to increase mass spectral sensitivity (14). Parallel incubations are conducted without NADPH and glutathione, to serve as negative controls for metabolism-mediated adduct formation. A positive control such as diclofenac may be used to demonstrate reactivity under the conditions used in the experiment (15). The incubation is terminated with organic solvent and supernatants are analyzed by LC/MS/MS for the neutral loss of 129 mass units, which denotes a characteristic loss of glutamic acid from the glutathione adduct. A frank positive result will dismiss a compound from the lead track. However, if a minor glutathione adduct is detected qualitatively, it is a challenge to put this data into perspective without quantitative data. Usually, such observations are flagged and if the compound moves forward, in vivo studies should be conducted to address the relevance of in vitro finding, for example, presence of adducts in rat urine or bile as discussed below.

The superior in vitro technique to access reactivity is the covalent-binding assay using radiolabeled material. While this technique is preferred because it

provides quantitative data, it is unusual to have radiolabeled material available during the discovery process. The radiolabeled compound is incubated in vitro with human microsomes and the appropriate buffers and cofactors as described above. The reaction is terminated with an organic solvent, or 10% trichloroacetic acid. The pellet is harvested via centrifugation or filtration, and washed with the appropriate organic solvent optimized to extract all noncovalently bound material. After several exhaustive washes to remove all noncovalently bound material, the radioactivity covalently bound to the protein is determined and expressed as picomole drug-related material per milligram of microsomal protein. Scientists at Merck have proposed a decision tree to access covalent-binding values, and suggest that a target threshold for advancement is 50 pmol/mg of protein (16).

In addition to in vitro techniques described, evidence of glutathione adducts can be detected from in vivo samples. Understanding the catabolism pathway of the glutathione adduct is useful in selecting the appropriate matrix for metabolite identification. In preclinical samples, the intact glutathione adduct can be detected in the bile, while the catabolism products (cysteine-glycine conjugates to the mercapturate metabolites) are normally detected in the urine. This is because enzymes responsible for the catabolism of the glutathione conjugate are predominantly located in the kidney (17).

Assays to Predict Drug–Drug Interactions

It is very likely that a marketed drug will be coadministered with others drugs, raising the possibility of drug–drug interactions (DDI). A drug–drug interaction results when the administration of one drug alters the properties of a coadministered drug, potentially affecting clinical efficacy or toxicity. Several drugs (Seldane®, Posicor®, Duract®, Lotronex®) have been withdrawn from the market because of DDIs (18). Therefore, it is crucial to understand the metabolism and excretion mechanisms of a compound to predict DDI before reaching the clinic. In vitro methods are widely used in discovery to access the risk of DDIs related to the inhibition and induction of drug metabolizing enzymes, and the possibility of metabolism by a polymorphic enzyme. Most assays focus on CYP as three quarters of the marketed drugs cleared by metabolism are metabolized by CYPs (18). Given the importance of these assays to clinical efficacy and safety, pharmaceutical industry leaders defined the best practices to conduct these DDI studies (8), which are referenced in the FDA draft guidance (19).

CYP Inhibition

The most common type of DDI is caused by a compound inhibiting the metabolism of a coadministered drug, increasing the exposure and possibly the toxicity of the coadministered medication. Inhibition can occur via both reversible and irreversible mechanisms. The major human CYPs that are studied include CYP1A2, CYP2B6, CYP2C8, CYP2C9, CYP2C19, CYP2D6, and CYP3A4. Each CYP isozyme can be assessed separately by using a probe substrate selective for that isozyme. The rationale is that the probe substrate is metabolized selectively by a CYP isozyme to a metabolite that is monitored. If the CYP isozyme is inhibited, the formation of the metabolite will be diminished. A list of preferred and acceptable probe substrates for these in vitro experiments can be found at the FDA Web site http://www.fda.gov/cder/drug/druginteractions/default.htm (19).

For reversible inhibition studies in discovery, fluorescent probe substrates are most often used with individually expressed human recombinant CYPs using a high-throughput platform. While this is a useful robust assay, the inhibition of fluorescent probe substrates does not always correlate with that of conventional drug-like substrates, which are considered the gold standard (20). Confirmatory experiments using drug-like probe substrates that require LC/MS analysis are recommended for compounds being considered for development. In both cases, the probe substrate is incubated at a sub-K_m concentration so that the IC_{50} of the test compound is similar to the K_i. Generally, the probe substrate is incubated along with compound at multiple concentrations (so that an IC_{50} can be determined), potassium phosphate buffer (50–100 mM, pH 7.4), NADPH (1 mM), and the individual CYP or human liver microsomes at 37°C. For in vitro incubations, methanol and acetonitrile are the preferred solvents to solubilize substrates/compounds, and the final volume must be less than 1.0% as solvents can inhibit CYPs (21). Appropriate controls should be included to demonstrate inhibition for each CYP studied. To access the likelihood of inhibition in vivo, the calculated in vitro IC_{50} (K_i) can be compared to the expected maximum steady state clinical plasma concentration for total drug [I] and the threshold K_i for deselection could be 10% of highest anticipated exposure in clinical studies.

Irreversible inhibition occurs when a compound binds to an active site and is transformed to a metabolite that irreversibly binds to the enzyme, rendering the enzyme inactive. This process called time-dependent or metabolism-dependent inhibition should be evaluated for lead discovery compounds, especially for known structural alerts (22). Essentially, this assay involves two incubations. First, the compound (at therapeutically relevant concentrations) is preincubated without and with NADPH (1 mM), potassium phosphate buffer (100 mM, pH 7.4), and human liver microsomes (10 × more than required for linear range of CYP isozyme assay). Aliquots are removed over time and used to start a second assay to measure functional activity of a specific CYP isozyme. To minimize any effects of reversible inhibition, the dilution of the aliquot into the second incubation should be 10-fold. The CYP assay conditions are generally similar to those used for reversible inhibition, except the CYP substrate concentration used should exceed V_{max} concentration to minimize any CYP inactivation after the initial preincubation. For each compound concentration, the log of the percentage of CYP activity remaining in the presence of NADPH is plotted against preincubation time to determine K_I and K_{inact} (23). Often, this assay is conducted using a high-throughput platform, typically focused on CYP3A4, the most clinically relevant CYP.

CYP Induction

Enzyme induction is a process involving transcriptional activation of a gene or stabilization of mRNA/protein that increases the drug metabolizing enzyme(s). While many drug metabolizing enzyme(s) can be induced, discovery screening strategies often focus on CYP induction since these are the enzymes responsible for the bulk of metabolism. CYP induction by a compound can alter the metabolism of the compound itself, termed "auto-induction," or a coadministered drug. Not only clinical efficacy will potentially be affected but the safety profile may also worsen if the formation of a toxic metabolite(s) is enhanced. Before a compound reaches the clinic, the potential to induce human CYP(s)

can be assessed using two types of in vitro techniques, cell-based receptor gene assays and cultured human hepatocytes.

Drugs alter gene expression by activation of ligand-activated transcription factors such as the aryl hydrocarbon (Ah) receptor for CYP1A, the constitutive androstane receptor (CAR) for the CYP2B6 and CYP2C9, and the pregnane X receptor (PXR) for the CYP3A family. Given the clinical importance of CYP3A4, at the discovery stage, activation of PXR is often monitored with cell-based receptor assays using high-throughput platforms. PXR activation is used as a surrogate for CYP3A4 induction. Briefly, mammalian cells (HepG2 cells) are transfected with a reporter gene (*Firefly* luciferase) under the control of the human CYP3A4 promoter, which includes the PXR–responsive element (PXRE). In addition, a construct for the expression of human PXR is included in the transfection, while a third plasmid, expressing the *Renilla* luciferase reporter gene, is added as a transfection control (24,25). Transfected cells are cultured in 96-well plates and exposed to either DMSO vehicle (0.6%), test compound (3, 10, and 30 μM), or rifampicin (3, 10, and 30 μM) as a positive control. The ability of the compounds to activate the PXR-mediated pathway of gene induction is measured using the luminometric luciferase assay. The hPXR data for a compound is expressed as a percentage of vehicle control or the positive control run at the same concentrations. The threshold for positive readout is usually threefold over vehicle control or 20% of that observed with rifampicin at 10 μM.

The cultured hepatocyte assay for induction using either cryopreserved of freshly isolated cells is considered the gold standard assay for CYP induction because multiple CYP isozymes can be evaluated at once, and functional enzyme activity is measured (not just gene activation). However, this assay is not a high-throughput assay and is practically applied at the lead selection stage. Briefly, freshly isolated or cryopreserved hepatocytes are cultured for two to three days to return CYPs to basal levels. Cells are then incubated with compound (at least three concentrations spanning the therapeutic range), as well as the appropriate positive and negative controls for approximately three days. Microsomes are prepared from the hepatocytes, and microsomal protein, mRNA, CYP enzyme activity or immunoreactive protein, and cell toxicity are measured. A compound is considered an inducer if the increase in activity is equal to or greater than 40% of the positive control. There are disadvantages to cultured human hepatocytes, mainly the availability of tissue and significant variability among liver samples.

CYP Isozyme Mapping

CYP isozyme mapping or "phenotyping" refers to in vitro experiments conducted to identify the CYP isozymes responsible for the metabolism of a compound. This information is important not only to foresee potential DDIs and plan clinical drug interaction studies but also to predict the variability for drug exposure in clinical studies. While several isozymes exhibit polymorphism, most of the pharmacogenomic attention has focused on CYP2C9, CYP2C19, and CYP2D6, since the genetic variability of these genes has significantly influenced therapeutic outcome for 20% to 25% of drug treatments (26).

The major human P450 isozymes are available commercially as recombinant cytochrome P450s, and often, the first CYP mapping study is conducted with a panel of microsomes prepared from individual CYPs. Compound (at a therapeutically relevant concentration) is incubated at 37°C with the appropriate

buffer that may be isozyme specific (pH 7.4), each individual recombinant CYP (1 pmol/mL), and NADPH (1 mM). The incubation is terminated with organic solvent usually at 20-minute increments from 0 to 60 minutes. After centrifugation, the resulting supernatants are analyzed by LC/MS and the percentage compound remaining determined over time. While disappearance of compound indicates the CYP isozyme(s) involved in metabolism, this approach does not determine the relative contribution of the each individual CYP(s) to metabolism. This is because these experiments are conducted with a single isozyme and lack competing enzymatic pathways. Moreover, the activity of enzyme per unit of recombinant microsomal protein is not the same as in human liver microsomes or reflective of the in vivo CYP levels. As reported by Shimada et al. (27), the concentration of CYP1A2, CYP2B6, CYP2C, CYP2D6, CYP2E1, and CYP3A represents 13, 4, 18, 2, 7 and 29%, respectively, of total P450 in microsomes prepared from human livers.

To assign the relative contributions of individual CYPs to the metabolic clearance of a compound, additional studies are required. CYP mapping experiments are conducted with human liver microsomes using chemical inhibitors or inhibitory antibodies to selectively inhibit a particular CYP isozyme. Incubations are carried out as described above except (*i*) pooled human liver microsomes (0.5 mg/mL) and (*ii*) a panel of chemical inhibitors or inhibitory antibodies known to selectively inhibit individual CYP isozymes is used. A list of isozyme-selective chemical inhibitors can be found at the FDA Web site (19). For these experiments, the fraction of compound metabolized in the presence of an inhibitor is compared to the fraction of compound metabolized in the absence of an inhibitor. Alternatively, the relative activity factor method can be used and combines CYP and human microsomal data to determine the ratio of clearance for individual isozymes (28). If the contribution of a CYP to the clearance of a compound is substantial (>25%), clinical drug-interaction studies should be considered. An alternate approach is to determine the turnover rate of compound in individual (as opposed to the pooled) liver microsomes and conduct a correlation analysis against activity of each of the major CYPs. This requires the availability of liver microsomes from at least a few dozen individual subjects and that the preparations are fully characterized for catalytic activity using marker substrates.

Assays for Distribution

After a compound is absorbed and reaches the systemic circulation, it distributes into tissues based on its affinity for plasma proteins versus tissue proteins, thus drug-protein binding plays a role in the distribution of a compound. Most compounds bind to plasma proteins to some extent, and the drug then exists in plasma in equilibrium as unbound (or free) drug and bound drug. It is generally accepted that it is the unbound compound that is free to interact with receptors and elicit a pharmacological response. Experiments to determine the unbound fraction of drug are necessary to develop an understanding of pharmacokinetic–pharamcodynamic relationships, understand the distribution of a drug, and may be used to calculate safety margins among species.

Protein-binding experiments involve separating, and then measuring the unbound compound from compound that is bound to plasma proteins. In vitro protein-binding samples are typically prepared by spiking pooled blank human plasma (10 donors) with compound at a therapeutically relevant concentration.

Solvents used to dissolve the compound in plasma should be minimized to less than 1% of total volume. Additionally, the ex vivo unbound fraction can be determined when plasma from toxicokinetic studies becomes available to calculate safety margins. Since compounds can affect plasma pH, which may in turn affect plasma protein binding, the plasma pH should be adjusted to physiological pH before the experiment is started (29). The most commonly used methods of separation include ultrafiltration and equilibrium dialysis techniques. Ultrafiltration devices are commercially available and consist of two reservoirs separated by a filter with a molecular weight cut-off of typically between 8000 and 10,000 Da. The compound-containing plasma is added to the top reservoir, and centrifuged for typically 20 minutes until the plasma water and low-molecular-weight compounds are forced through the filter. The resulting ultrafiltrate is then analyzed for compound along with the initial compound-containing plasma. The fraction unbound is determined by dividing the compound concentration in the buffer by the concentration in the plasma. The limitation of this assay, particularly for hydrophobic compounds, is that a portion of the unbound compound may adsorb to the filter, affecting the unbound concentration. Buffer spiked controls (at a concentration similar to the expected fraction unbound) should be included to evaluate adsorption, and if there is measurable adsorption, this technique may not provide reliable results.

There is no standard assay for protein binding, but many consider equilibrium dialysis the preferred method. The main reason is that the equilibrium of protein binding is not affected by this technique during the experiment. Basically, a Teflon® dialysis cell is divided into two reservoirs separated by a dialysis membrane. Compound-containing plasma is added to one reservoir, and physiological potassium phosphate buffer (0.133 M, pH 7.4) is added to the second reservoir. The cell is sealed and incubated at 37°C until equilibrium is reached. Although time to equilibrium is compound dependent, the design of the device can greatly accelerate this such that most compounds reach equilibrium within a few hours. The time to reach equilibrium depends on the size of the cell and system used and should be established using reference compounds with low-, medium-, and high-protein binding. After reaching equilibrium, buffer and serum samples are removed and analyzed for compound typically by LC/MS. The fraction unbound is determined by dividing the compound concentration in the buffer by the concentration in the plasma. Equilibrium dialysis can be time-consuming depending on the system used; however, rapid and high-throughput dialysis methods have gained acceptance in discovery laboratories and are widely used (30).

In Vivo PK Studies

One of the central criteria for lead selection/optimization is demonstrating that a compound has an acceptable pharmacokinetic profile consistent with the desired PD profile and dosing regimen. PK is the time course study of a compound within a body and incorporates the processes of absorption, distribution, metabolism, and excretion (ADME). A compound is dosed via intravenous and oral routes, and the plasma concentration of compound determined by LC/MS analysis. The resulting plasma drug concentration-time data is analyzed using noncompartmental modeling by commercially available software. The most important PK parameters governing drug disposition are clearance

(the efficiency of the body to remove compound), apparent volume of distribution (a parameter that relates the administered dose to the observed concentration), elimination half-life (the rate of which the body removes the drug), and oral bioavailability (the fraction of drug absorbed into the systemic circulation). A thorough discussion of pharmacokinetic modeling and parameters is beyond the scope of this chapter, but many excellent resources are available (31–33).

There is a limited amount of compound available at the discovery stage, so PK profiling usually starts with a rodent PK study. With approximately 10 mg of compound, two groups of rats ($N = 3$ per group) can be given a single IV and oral 5 mg/kg dose of a compound. It is unlikely that formulation has been optimized at the discovery stage, so most laboratories use a generic IV formulation such as 5% dimethylacetamide (DMAC), 10% propylene glycol in saline. For oral dosing, a compound is typically formulated in 0.5% methylcellulose and sometimes includes a solubilizing agent. The oral exposure values obtained with dosing solution that contained a solubilizing agent should be interpreted with caution as such solubilizing agents are typically not used in first-in-man studies and the extrapolation of fractional dose absorbed may not be valid. The conventional in vivo PK paradigm calls for a compound to be dosed discretely, that is, one compound examined within one group of animals. During the 1990s, scientists developed the N-in-1 (or cassette) dosing approach to increase throughput, and to use less animals and analytical resources (34).

For cassette dosing, a mixture of several compounds (including one benchmark compound) is formulated together and given to a group of animals. Analytical considerations include avoiding a compound that could potentially be a metabolite of another coadministered compound in the cassette. The pharmaceutical industry is divided regarding the utility of cassette dosing and about half of those surveyed employ the technique (35). The drawback of this approach is that the PK obtained using cassette dosing may not be reflective of discrete dosing, due to drug–drug interactions, as the clearance of a compound may be inhibited by a coadministered compound in the cassette. While this concern cannot be dismissed, drug–drug interactions can be minimized by eliminating compounds that score positive in CYP inhibition screen, and by using low doses in cassettes (typically $\leq$1 mg/kg per compound). In fact, a useful correlation between PK parameters obtained from cassette and discrete dosing has been established in some laboratories (36). A discrete PK study should always be conducted as a follow-up to confirm any strong PK leads that emerge from cassette dosing. If a compound exhibits a favorable PK profile in rodents (low clearance, high oral bioavailability), it often proceeds to nonrodent species (dog or monkey), using either a discrete or cassette approach.

Pharmacokinetic/Pharmacodynamic Evaluations

It is important to understand the relationship between pharmacology and exposure for three reasons, (*i*) to project human dose: human PK is predicted as outlined in section "Prediction of Human Pharmacokinetics for Lead Compounds" and if the target exposure for optimal pharmacology is known, it is then possible to come up with projected human dose. This in turn allows the estimation of pill burden, cost of goods, etc. at a very early stage in the drug discovery process, (*ii*) to confirm that the pharmacology is on target: although biomarkers often serve to track the mechanism of action, a pharmacokinetic–pharmacodynamic (PK–PD)

relationship can extend that result. The desired pharmacology, that is, efficacy in animal model, should be associated with exposure that is equivalent to the potency of the molecule in vitro, after taking into account necessary corrections. If much higher exposures are required to achieve efficacy than is expected based on in vitro data, off-target effects should be investigated (*iii*). If efficacy measures are observed at a fraction of the target exposure, generation of active metabolite(s) should be investigated. It is possible that one of the metabolites is a better candidate overall than the parent molecule.

The first step in establishing a PK–PD relationship is the selection of the in vitro assay for potency readout. Functional assays are better than binding displacement assays and cell-based assays and whole-blood assays are better suited for this exercise than cell-free assays. If multiple options are available, the one that comes close to the in vivo readout should be preferred, for example, cytotoxicity assay for tumor growth inhibition. The second step is to determine the extent of activity required for efficacy, that is, 50% inhibition versus 90% inhibition of activity for an antagonist, etc. In many instances, this information is not available and 50% inhibition can be the default. If PD readout (as opposed to efficacy readout) from animal study is available, the exposure–PD relationship can be established ahead of exposure–efficacy relationship, and this may also provide some granularity on the extent of inhibition that is minimally required. The third step is to figure out the correction factors for bridging the in vitro potency to in vivo efficacy. The most important correction factor is serum protein binding in the animal model. Other correction factors like ligand concentration can also be considered on a case-by-case basis. The final step is to understand the most sensitive PK parameter for efficacy, for example, maximum (C_{max}), trough (C_{min}), or average (C_{ave}) plasma concentration. This is often discerned by conducting pharmacology studies using different dosing schedules, for example, oral dosing and infusion to steady state. Using these information and dose–response data for efficacy, an in vivo EC_{50} as well as target clinical exposure (C_{max} or C_{min} or C_{ave}) can be determined. The serum protein binding adjusted (and any other appropriate correction factor applied) in vitro IC_{50} should be close to the in vivo EC_{50} (within two- to threefold of each other) to gain confidence around on-target pharmacology.

DECISION MAKING BASED ON DMPK ASSAY RESULTS

As discussed above, the DMPK assays at various stages of development are put in place to predict disposition in humans and thereby insure selection of compounds with a high probability of success in clinical development. While there is general agreement across the industry in terms of list of assays used in a given stage of a discovery project, the respective protocols, and data analysis, there is a lack of consensus when it comes to making decisions based on DMPK data. In this context, decision making refers mostly to "deselection" of compounds. It is often straightforward to deal with results that are close to the extreme ends of the range of possible values, for example, aqueous solubility >1 mg/mL, IC_{50} for inhibition of CYP isozymes <1 μM. For results that fall in the gray zone, the key factors that drive deselection are discussed below.

"Soft" determinants: For the vast majority of compounds for which the data does not readily translate into a clear "yes" or "no" readout, decision making is influenced by (*i*) the diversity of compounds available: If the compound

collection is diverse and the deselection impacts only a fraction of these compounds, it is reasonable to not expend additional resource to further investigate the data but rather focus on the winners. In actual practice, this is easier said than done as the readout from various assays does not become available at the same time and therefore the relative attractiveness of compounds change over time. To deal with this, compounds are "quarantined" rather than "deselected." (*ii*) Relative tractability of the target: Setting up threshold value for assays and deselection have to consider the tractability of the target. For example, it has been generally challenging to come up with inhibitors of phosphotases with good transcellular permeability. In such cases, it is good to lower the threshold and move compounds into rodent PK studies even if the odds of positive outcome in those resource-intensive investigations are low. (*iii*) Novelty of chemical structure: One of the overarching goals of drug discovery is to identify proprietary chemical structures, that is, compounds with a high probability of securing a patent. This is increasingly becoming a challenge, especially in heavily mined areas like "receptor tyrosine kinase inhibitors." Therefore, the rules for deselection for innovative scaffolds are kept more lenient than usual. (*iv*) Overall organizational philosophy: The mindset of leadership in the organization, the prevailing culture, and earlier experience of team leaders tend to shape the deselection strategy. While this is unavoidable, it is important to stay as objective as feasible and constantly reevaluate the strategy to insure timely identification of high-quality leads.

Pharmacodynamics

The term, pharmacodynamics, refers to the temporal pharmacology and, in combination with pharmacokinetics, is critical to the understanding of the dose–concentration–effect relationship. Simplistically, the potency, bioavailability, and half-life determine the daily dose and the average daily exposure, which in turn provide the frames of reference for assessing the therapeutic index as well as the potential for interaction with other drugs. The target daily dose range (e.g., $\leq$100 mg) helps to determine the threshold values for various assays, for example, solubility, permeability, clearance, volume of distribution, protein binding, CYP and P-gp interactions, for a given potency range. The threshold values should be periodically revisited as more molecules are profiled and pharmacology is better defined. Follow-up animal studies may be warranted on a case-by-case basis depending upon the confidence in establishing the threshold and structural novelty of compound being deselected by the assay result etc. The projected human pharmacokinetics (see section "Prediction of Human Pharmacokinetics for Lead Compounds" below) and the anticipated exposure at therapeutically relevant doses help to understand the potential for drug interactions. The potential for drug interactions increase when the ratio of $[I]/K_i$, where $[I]$ refers to the concentration of the molecule of interest and K_i refers to its inhibitory potency, exceeds 0.1 and the FDA guidance recommends conducting clinical studies to explore the interaction in such situations (19). It is important to consider what $[I]$ refers to in the above ratio. In most cases, $[I]$ refers to maximum plasma concentration or total C_{max} but in some situation it could be concentration at a different site, for example, first-pass hepatic concentration for CYP interaction or intestinal concentration for interaction with transporters involved in intestinal uptake or efflux.

Potential for Aberrant Readouts

The potential for false-positive as well as false-negative readouts in some of the DMPK assays should be kept in mind just like one would do with any screening. Aberrant readouts are possible due to incomplete solubilization of compound in the assay system, use of inappropriate assay system, chemical instability under the conditions used, etc.

PREDICTION OF HUMAN PHARMACOKINETICS FOR LEAD COMPOUNDS

Human pharmacokinetics must be predicted from preclinical data to demonstrate that a compound has the desired PK profile to justify development, and to select first-in-man doses that will be safe and efficacious. While progress has been made, this process remains a challenge for ADME scientists. It is important to rigorously examine and understand the disposition of a compound before the most appropriate method for PK prediction is considered. Allometric scaling is a widely used tool, and uses animal data to predict human pharmacokinetics. The most uncomplicated of the allometric approaches is called simple allometry, and this method assumes that species variation in pharmacokinetics stems from differences in organ sizes and blood flow and that these differences are captured by the average body weight of those species. The main limitation of this approach is that it assumes that the absorption and metabolism, factors that greatly influence pharmacokinetics, are invariant among species. Thus, this simple approach is most successfully used if a compound is completely absorbed, primarily cleared by renal elimination, and protein binding is similar among species. Several additional approaches to allometric scaling use correction factors to improve accuracy. Mahmood and Balian (37) used allometric scaling with the "rule of exponents," which uses brain weight and life span as corrections, to successfully predict human clearance. Other researchers have integrated the fraction unbound among species as a correction factor (38) to improve accuracy, and in fact, this has reported to be the most accurate approach (39). Besides allometric scaling, human clearance can also be estimated from in vitro experiments as described in section "DMPK Assays in Current Drug Discovery". Once a reasonable estimate of human CL has been obtained from an in vitro study, the clearance value along with model-dependent parameters is entered into the pharmacokinetic compartmental model to generate time-plasma drug concentration data. To select the model-dependent parameters used for human predictions, it is useful to fit animal PK data to understand the disposition of the compound (one or two compartmental fit, rate of absorption, etc.).

The chimpanzee (*pans troglodytes*), with 98.8% genetic similarity to humans, is also a reasonable pharmacokinetic model to estimate human pharmacokinetics. Wong et al. have reported that the chimpanzee most successfully rank ordered the oral clearance for compounds in humans compared to the rat, dog, and monkey (40). Before the chimpanzee is considered, it is important to complete CYP isozyme mapping experiments, as the hepatic catalytic activities of CYP1A and CYP2D isozymes in the chimpanzee are 10-fold greater than in humans, while CYP2C and CYP3A isozymes appear similar among the species. While this species appears to be a reasonable surrogate for humans if compounds are metabolized via CYP2C9 and CYP3A isozymes, other important enzyme/transporter systems are not yet fully characterized.

EMERGING ISSUES AND TECHNOLOGIES IN DMPK

Over the last couple of decades, the focus of DMPK assays has been on drug metabolizing enzymes and in particular, the P450 family of enzymes. Tremendous progress has been made in understanding the expression level, catalytic activity, substrate selectivity, and polymorphism of these enzymes and this has provided robust assays to screen and characterize compounds for P450 metabolism. More recently, the focus has shifted to enzymes and proteins that are not involved in biotransformation but nonetheless have a significant impact on the disposition of small molecules. Some of the emerging knowledge base around nonmetabolizing proteins and technological developments are highlighted below. Since the emphasis of this chapter is on DMPK assays in drug discovery, we have limited discussion to issues that directly impact the screening and profiling practice today.

Transporters

Much of the focus in the post-P450 era has been on transporters that limit the uptake, distribution, and elimination of drug-like molecules. There are two major classes of transporters that are known to be involved in drug disposition—the ATP-binding cassette proteins (ABC) and the solute-linked carrier proteins (SLC). The former is ATP dependent while the later function in an ATP-independent manner.

P-glycoprotein

The most widely studied transporter protein involved in drug disposition is P-glycoprotein or P-gp, which is expressed, among other tissues, in the small intestinal epithelium and the blood–brain barrier and functions in an energy-dependent manner to efflux xenobiotics. P-gp is also the most well-characterized member of the ABC family. Drug efflux at the level of the intestine could limit absorption as well as lead to drug–drug interactions depending upon the K_m for efflux and the dose. Generally, for compounds with a dose >10 mg, the impact on oral absorption is minimal since the intestinal concentration often exceeds the K_m, thereby saturating the transporter. However, the impact on tissue distribution, in particular to the central nervous system, is significant since blood concentrations are usually well below the K_m for P-gp. While this is desirable for drugs designed to interact with peripheral targets, this poses a significant challenge for neuropharmacology. Therefore, it is critical to understand the interaction of compounds with P-gp regardless of the target or site of action as this interaction impacts both efficacy and safety. Compounds could either be substrates or inhibitors of P-gp and hence the need to evaluate both these potential interactions. Our understanding of the function of P-gp was greatly enhanced by the availability of mdr1a and mdr1b (mouse orthologs of human MDR1, the gene that encodes P-gp) knockout mice. The differences in tissue distribution between wild-type mice and mdr1 knockout mice could be close to 100-fold for compounds with high affinity for P-gp (41). Such compounds could also exhibit higher clearance due to significant intestinal secretion in wild-type animals. The commercial availability of these knockout animals has enabled the conduct of confirmatory as well as mechanistic studies to follow up on in vitro evaluations. In vitro assays to screen for substrates and inhibitors of P-gp are discussed in section "DMPK Assays in Current Drug Discovery".

Other Transporters

A comprehensive review of transporters with potential role in drug disposition is beyond the scope of this book and readers are referred to excellent reviews on transporters that have been published (42,43). Besides P-gp, four other transporters are worthy of mention here. (1) MRP1-–this ABC protein is expressed ubiquitously and could play a role in brain uptake and biliary excretion. Cell lines stably transfected with MRP1 are available for in vitro assays, (2) MRP2-–this is another ABC protein that is expressed predominantly in the liver, intestine, and kidney. Typical substrates of MRP2 are glutathione and glucuronide conjugates. The active metabolite of irinotecan, SN-38, and its glucuronide conjugate are known substrates of MRP1 (44). The organic anion transporters are primarily expressed in the renal epithelial cells and are capable of transporting both endogenous (e.g., para-amino-hippurate, riboflavin) substrates and wide variety of weakly acidic drugs. The recently approved DPP4 inhibitor, sitagliptin (Januvia®), is predominantly cleared by renal excretion by a member of the OATP group, hOAT-3 (45). The organic cation transporters are primarily expressed on the basolateral membrane of epithelial cells in the renal proximal tubule and are capable of transporting heterocyclic weak bases, including both endogenous compounds (e.g., dopamine, epinephrine and choline) as well as a variety of drugs like procainamide and cimetidine that undergo substantial net tubular secretion (46).

In Vivo Models for Drug Interaction

Currently, extrapolation of in vitro metabolism-based interaction data to clinical setting is empirical at best. Drug interaction studies in animals are hampered by differences in substrate selectivity as well as kinetic parameters for a given substrate between human enzyme and their respective orthologs in animals. To overcome this limitation, attempts have been made to generate transgenic mice that express human enzyme. Humanized transgenic mice expressing CYP3A4 and PXR have been generated as well as transgenic mice expressing each of the other major human P450 enzymes (47,48). The commercial availability of these models is limited at present, but this could change in the coming years if further studies show a clear advantage in using these animals to model drug interactions. In terms of studying interaction with transporters, both transgenic and chemical knockout models have been described for routine use in drug discovery (49).

REFERENCES

1. Prentis RA, Lis Y, Walker SR. Pharmaceutical innovation by the seven UK-owned pharmaceutical companies (1964–1985). Br J Clin Pharmacol 1988; 25(3):387–396.
2. Kola I, Landis J. Can the pharmaceutical industry reduce attrition rates? Nat Rev Drug Discov 2004; 3(8):711–715.
3. Sambuy Y, De Angelis I, Ranaldi G, et al. The Caco-2 cell line as a model of the intestinal barrier: Influence of cell and culture related factors on Caco-2 cell functional characteristics. Cell Biol Toxicol 2005; 21(1):1–26.
4. Wang Q, Strab R, Kardos P, et al. Application and limitation of inhibitors in drug-transporter interactions studies. Int J Pharm 2008; 356(1–2):12–18.
5. Marino AM, Yarde M, Patel H, et al. Validation of the 96-well Caco-2 culture model for high throughput permeability assessment of discovery compounds. Int J Pharm 2005; 297(1–2):235–241.
6. Balimane PV, Chong S. Cell culture-based models for intestinal permeability: A critique. Drug Discov Today 2005; 10(5):335–343.

7. Wang Q, Rager JD, Weinstein K, et al. Evaluation of the MDR-MDCK cell line as a permeability screen for the blood brain barrier. Int J Pharm 2005; 288(2):349–359.
8. Bjornnson TD, Callaghan JT, Einolf HJ. The conduct of *in vitro* and *in vivo* drug-drug interaction studies: A pharmaceutical research and manufacturers of America (PhRMA) Perspective. Drug Metab Dispos 2003; 31(7):815–832.
9. Brown HS, Griffin M, Houston JB. Evaluation of cryopreserved human hepatocytes as an alterantive *in vitro* system for the prediction of metabolic clearance. Drug Metab Dispos 2007; 35(2):293–301.
10. Houston JB. Utility of *in vitro* drug metabolism data in predicting metabolic clearance. Biochem Pharamcol 1994; 47(9):1469–1479.
11. Obach RS, Baxter JG, Liston TE, et al. The prediction of human pharmacokinetic parameters from preclinical and *in vitro* metabolism data. J Pharmacol Exp Ther 1997; 2839(1):46–58.
12. Davies B, Morris T. Physiological parameters in laboratory animals and humans. Pharm Res 1993; 10(7):1093–1095.
13. Kalgutkar AS, Gardner I, Obach RS, et al. A comprehensive listing of bioactivation pathways of organic functional groups. Curr Drug Metab 2005; 6(3):161–225.
14. Soglia JR, Harriman SP, Zhao S, et al. The development of a higher throughput reactive intermediate screening assay incorporating micro-bore liquid chromatography-micro-electrospray ionization-tandem mass spectrometry and glutathione ethyl ester as an *in vitro* conjugating agent. J Pharm Biomed Anal 2004; 36(1):105–116.
15. Yu LJ, Chen Y, Deninno MP, et al. Identification of a novel glutathione adduct of diclofenac, 4′-hydroxy-2′-glutathion-deschloro-diclofenac, upon incubation with human liver micorosmes. Drug Metab Dispos 2005; 33(4):484–488.
16. Evans DC, Watt AP, Nicoll-Griffith DA, et al. Drug-protein adducts: An industry perspective on minimizing the potential for drug bioactivation in drug discovery and development. Chem Res Toxicol 2004; 17(1):3–16.
17. Commandeur JN, Stijntjes GJ, Vermeulen PE. Enzymes and transport of systems involved in the formation and disposition of gluathione S-conjugates. Pharmacol Rev 1995; 47(2):271–330.
18. Wienkers LC, Heath TG. Predicting *in vitro* drug interactions from *in vitro* drug discovery data. Nat Rev Drug Discov 2005; 4(10):825–833.
19. http://www.fda.gov/cder/drug/druginteractions/default.htm
20. Cohen LH, Remley MJ, Raunig D, et al. *In vitro* drug interactions of cytochrome P450: An evaluation of fluorogenic to conventional substrates. Drug Metab Dispos 2003; 31(8):1005–1015.
21. Chauret N, Gauthier A, Nicoll-Griffith DA. Effect of common organic solvents on *in vitro* cytochrome P450-mediated metabolic activities in human liver microsomes. Drug Metab Dispos 1998; 26(1):1–4.
22. Kalgutkar AS, Obach RS, Maurer TS. Mechanism based inactivation of cytochrome P450 enzymes: Chemical mechanisms, structure-activity relationships and relationship to clinical drug-drug interactions and idiosyncratic drug reactions. Curr Drug Metab 2007; 8(5):407–447.
23. Silverman RB. Mecahnism based enzyme inactivators. In: Purich DL, ed. Contemporary Enzyme Kinetics and Mechanism, 2nd ed. San Diego: Academic Press, Inc., 1996:291–334.
24. Grover GS, Brayman TG, Voorman RL, et al. Development of *in vitro* methods to predict induction of CYP1A2 and CYP3A4 in humans. Assay Drug Dev Technol 2007; 5(6):793–804.
25. Moore JT, Kliewer SA. Use of nuclear receptors PXR to predict drug interactions. Toxicology 2000; 153:1–10.
26. Ingelman-Sudberg M, Sim SC, Gomez A, et al. Influence of cytochrome P450 polymorphisms on drug therapies: Pharmacogenetic, pharmacoepigenetic and clinical aspects. Pharmacol Ther 2007; 116(3):496–526.
27. Shimada T, Yamazaki H, Mimura M, et al. Interindividual variations in human liver cytochrome P450 enzymes involved in the oxidations of drugs, carcinogens, and toxic

chemicals: Studies with liver microsomes of 30 Japanese and 30 Caucasians. J Pharmacol Exp Ther 1994; 270(1):414–423.
28. Venkatakrishnan K, von Moltke LL, Greenblatt DJ. Application of the relative activity factor approach in scaling from heterologously expressed cytochromes P450 to human liver microsomes: Studies on amitriptyline as a model substrate. J Pharmacol Exp Ther 2001; 297(1):326–337.
29. Kochansky CJ, McMasters DR, Lu P, et al. Impact of pH on plasma protein binding in equilibrium dialysis. Mol Pharm 2008; 5(3):438—448.
30. Water NJ, Jones R, Williams G, et al. Validation of a rapid equilibrium dialysis approach for the measurement of plasma protein binding. J Pharm Sci 2008; 97(10):4586–4595.
31. Rowland M, Tozer TN. Clinical Pharmacokinetics Concepts and Applications, 3rd ed. Philadelphia, PA: Lea & Febiger, 1995.
32. Gibaldi M. Biopharmaceutics and Clinical Pharmacokinetics, 4th ed. Philadelphia, PA: Lea & Febiger, 1991.
33. Ritschel WA, Kearns GL. Handbook of Basic Pharmacokinetics Including Clinical Applications, 6th ed. Washington, DC: American Pharmacists Association, 2004.
34. Berman J, Halm K, Adkison K, et al. Simultaneous pharmacokinetics screening of a mixture of compounds in the dog using API LC/MS/MS analysis for increased throughput. J Med Chem 1997; 40(6):827–839.
35. Manitpisitkul P, White RE. Whatever happened to cassette dosing pharmacokinetics. Drug Discov Today 2004; 9(15):652–658.
36. He K, Qian M, Wong H, et al. N-in-1 dosing pharmacokinetics in drug discovery: Experience, theoretical and practical considerations. J Pharm Sci 2008; 97(7):2568–2580.
37. Mahmood I, Balian JD. Interspecies scaling: Predicting clearance of drugs in humans. Three different approaches. Xenobiotica 1996; 26(9):887–895.
38. Feng MR, Lou X, Brown RR, et al. Allometric pharmacokinetics scaling: Towards the prediction of human oral pharmacokinetics. Pharm Res 2000; 17(4):410–418.
39. Sinha VK, De Buck SS, Fenu LA, et al. Predicting oral clearance in humans, how close can we get with Allometry? Clin Pharmacokinet 2008; 47(1):35–45.
40. Wong H, Grossman SJ, Bai S, et al. The chimpanzee (pan troglodytes) as a pharmacokinetic model for selection of drug candidates: Model characterization and application. Drug Metab Dispos 2004; 32(12):1359–1369.
41. Schinkel AH, Smitt JJ, van Telligan O, et al. Disruption of the mouse mdr1 a P-glycoprotein gene leads to a deficiency in the blood brain barrier and to increased sensivity to drugs. Cell 1994; 77(4):491–502.
42. Girardin F. The role of transporters in drug interactions. Eur J Pharm Sci 2006; 27(5):501–517.
43. Girardin F. Membrane transporter proteins: A challenge for CNS drug development. Dialogues Clin Neurosci 2006; 8(3):311–321.
44. Horikawa M, Kato Y, Tyson CA, et al. The potential for an interaction between MRP2 (ABCC2) and various therapeutic agents: Probenecid as a candidate inhibitor of the biliary excretion of irinotecan metabolites. Drug Metab Pharmacokinet 2002; 17(1):23–33.
45. http://www.merck.com/product/usa/pi_circulars/j/januvia/januvia_pi.pdf
46. Somogyi A, McLean A, Heinzow B. Cimetidine-procainamide pharmacokinetic interaction in man: Evidence of competition for tubular secretion of basic drugs. Eur J ClinPharmacol 1983; 25(3):339–345.
47. Gonzalez FJ. CYP3A4 and pregnane X receptor humanized mice. J Biochem Mol Toxicol 2007; 21(4):158–162.
48. van Herwaarden AE, Wagenaar E, van der Kruijssen CM, et al. Knockout of cytochrome P450 3A yields new mouse models for understanding xenobiotic metabolism. J Clin Invest 2007; 117(11):3583–3592.
49. Xia CQ, Milton MN, Gan LS. Evaluation of drug-transporter interactions using *in vitro* and *in vivo* models. Curr Drug Metab 2007; 8(4):341–363.

17 Compound Management for Drug Discovery: An Overview

Moneesh Chatterjee and Martyn N. Banks

Lead Discovery, Profiling and Compound Management, Applied Biotechnology, Bristol-Myers Squibb, Wallingford, Connecticut, U.S.A.

CREATING A COMPOUND INVENTORY

Compound management is a critical hub in all drug discovery programs providing one of the essential ingredients in hit identification and lead optimization (Fig. 1). Most compound inventories have been constructed with small molecules from a range of sources. Historical medicinal chemistry programs have provided the backbone of the inventory, and in the last 20 years, these have been complemented by combinatorial libraries using in-house resources or through acquisition from alliance partnerships, academics, and commercial vendors. Another viable source of compounds is for two companies to exchange or trade compounds within their individual collections. The main objective of supplementing internal medicinal chemistry compounds is to diversify the internal compound collection. However, the selection of compounds needs to be carefully considered because these need to be relevant to the biological targets that are to be screened. Additionally, the compounds need to contain chemical and physical characteristics that will yield a high probability of enabling future medicinal chemistry programs.

To ensure biological relevance, a variety of computational tools and databases is used to assess available compounds, or to design specific libraries to be synthesized. For example, special sets of compounds could be assembled that contain functional groups known to interact with a particular biological target class. Most drug discovery companies have these focused sets for the common druggable targets, for example, kinases, G-protein-coupled receptors, ion channels, proteases. These are usually subdivided to cover a particular type of receptor or enzyme within a target class. To aid in the procurement of compounds, there are a range of commercially available knowledge bases that contain all the published information including patents around a biological target class that can be used to select compounds of interest. Although beyond the scope of this chapter there are also a range of computational modeling techniques to facilitate this type of compound selection (1,2), certain targets do not conveniently lend themselves to a particular target class and a diverse set of compounds will also need to be available for drug discovery programs.

If compound structures are available from a vendor or partner, the compounds can be selected based on calculated physical or topological properties. One method is to use the "Rule of Five" as an estimate as to whether compounds may have pharmacokinetic problems further down the drug discovery process (3). Lipinski's Rule of Five, formulated in 1997, is a rule of thumb to determine if

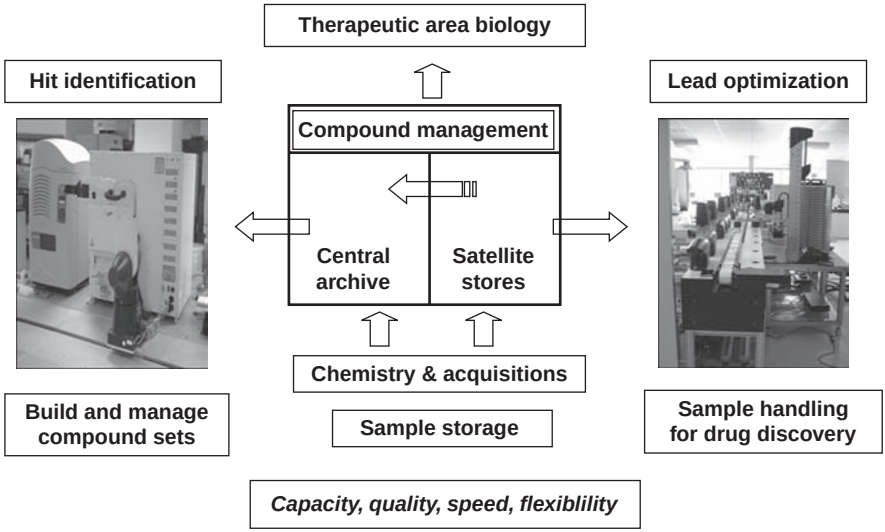

FIGURE 1 Compound management's role in drug discovery.

a chemical compound has properties that would make it a likely orally active drug in humans (4). The rule was based on the observation that most drugs are relatively small lipophilic molecules. The rule describes molecular properties important for a drug's pharmacokinetics in the human body, including their absorption, distribution, metabolism, and excretion (ADME). While the rule does not predict if a compound is pharmacologically active, it is an important tool for drug development where a pharmacologically active lead structure is optimized stepwise for increased activity and selectivity, as well as for drug-like properties. Others have elaborated and refined the rule to evaluate "druglikeness" (5). The term "Lead Like" has also been introduced in the literature for compounds identified from HTS campaigns. In these cases, compounds may be suitable for optimization but may not have properties that fully reflect the Lipinski values (6–8).

An alternative approach, "fragment-based" discovery (9–12), is used for the construction of fragment libraries for lead generation. In this instance, the hits identified generally obey a "Rule of Three." Using this approach, small molecular-weight fragment libraries are screened using high-throughput X-ray crystallography or nuclear magnetic resonance. Binding interactions that may be weak, but important interactions with the protein are identified using this method. As X-ray crystallography is very effective at identifying weak interactions (μM–mM), fragment hits can be identified that have no measurable activity in a biological assay. This information is then used to augment current structure–activity analysis or provide the basis for further chemical elaboration.

In all instances, it is essential to identify and eliminate compounds that have unwanted functionality. The compounds should be soluble, physically stable, and not chemically modify the protein. Certain compounds are promiscuous and appear positive in a range of unrelated assays, for example, compound aggregates can appear as false positives in a range of biochemical assays (13)

and overtly toxic compounds confound cellular assays. The aforementioned as well as other considerations (14) contribute the concept of "Lead Like" being the basis for compound acquisition as these compounds are better candidates for hit identification and progression into medicinal chemistry (15).

Having assembled the necessary databases, used the chemoinformatic tools to select compounds of interest, the next significant challenge is to purchase the compounds, ensure that the compounds are in the correct container types, and most importantly ensure that the purity and absolute identity of the compounds is known.

CONSIDERATIONS FOR THE STORAGE OF COMPOUNDS

Appropriate storage conditions for compounds are a key to the success for the drug discovery process. A number of factors have been taken into account in terms of compound storage, both for short-term and for archival purposes. Temperature, inert atmosphere, container types, and humidity are prime factors for consideration for storage of solids. Additionally, concentration, freeze-thaw cycles, and water content become increasingly important for liquid stocks in dimethyl sulfoxide (DMSO) (16–19). Appropriate storage conditions for samples are dependent on the company and there is no industrywide standard, probably because of process variations in each company. Typical temperatures used in the archive range from -20°C to 4°C to room temperature; although recently, storage at -80°C has emerged for biological samples (20). The majority of pharmaceutical companies store samples at -20°C for long-term storage. This is driven primarily by degradation and decomposition issues that arise at higher temperatures. Room temperature storage is most common when samples are being stored for short periods (weeks to months), especially because repeated freezing and thawing of samples is avoided. Use of argon, nitrogen, or dry air in the sample containers is also common practice. Coupled with lower temperatures, inert atmosphere is used to prevent degradation of samples. Other methods to reduce degradation and aid solubility of dried compounds include the possible use of cyclodextrins (21), although no commercial use has been reported. DMSO is used almost exclusively as the solvent of choice for dissolving compounds for delivery into in vitro biological assays. This is due to the ability of DMSO to dissolve a variety of chemical entities and its compatibility with aqueous biological buffers. There is literature precedence that freeze/thaw of samples in hydrated DMSO results in samples being driven to their crystalline form and limits solubility (11). However, if dry DMSO is used, this is not an issue. In certain instances, the compound collections are stored in a mix of DMSO/water (90/10) or DMSO/ethanol (90/10). The hydrated DMSO stocks are then replenished at regular intervals. In order to determine the effects of degradation in DMSO under a variety of storage conditions, a consortium of pharmaceutical companies (AstraZeneca, Bristol-Myers Squibb, Eli Lilly, Hoffmann-La Roche, GlaxoSmithKline, Merck, and UCB-Pharma) has embarked on a long-term study to evaluate appropriate storage conditions. The COMDECOM project involves a stability study, monitoring the stability in DMSO solution of a diverse selection of 15,000 compounds from the Specs' stock (22). From the generated dataset, a predictive model will be developed, to flag potentially "unstable" compounds in the library, and indicate preferred storage conditions.

THE COMPOUND DISPENSARY

With the accelerated growth of compound collections and screening formats in the last few years, increasing demands are being placed on organizations that oversee research sample inventories—to supply samples more quickly, in greater numbers, and in multiple formats. These escalating requirements are being met with more efficient storage systems that track compounds accurately. In the mid-1990s, the science underlying drug discovery had outpaced engineering. With the advent of HTS and combinatorial chemistry, it was possible to grow the compound collection and screen faster than it was possible for CM (Compound Management) organizations to provide sufficient numbers of compounds for screening. This required a fundamental transition from the manual compound store to the automated store. Thus, compound management has grown from dispensaries that manually handled and delivered a few hundred compounds to automated systems that manipulate millions of compounds per year. In the early 1990s, manual stores were typically shelved in cabinets, with limited tracking of sample containers. By the late 1990s, the prototype-automated stores were the norm, with storage possible in a variety of formats and inventory systems that provided the basis for foolproof tracking of compounds and efficient screening (Table 1).

With the proliferation of the automated stores, industrialization of CM process flows has occurred. A number of options have emerged for storage and distribution of samples across multiple sites. Typically, in a single-site model, the central archive serves the purpose for long-term storage as well as for quick distribution of samples for biological assays (Fig. 2). In the case of multisite operations, a hub and spoke model is more prevalent (Fig. 3). Large deck sets for lead discovery tend to be the purview of the central archive, whereas local stores tend to pick up the workflows for lead optimization studies.

The flow of compounds from receipt into the archive to the assay platforms for testing usually consists of a dry dispensation from/to vials. Sample solutions can then be prepared by dissolving in DMSO and easily dispensed into assay ready formats for high-throughput testing and analysis. One of the challenges posed by the growth of the compound collection is the manual weigh process for compound distribution. This is a time-consuming task that is not easily scalable. Automation to perform this process has seen limited use due to the

TABLE 1 Examples of Automated Storage Options

Company	Format	Temperature	Software	Tubes	Vials	Plates
TAP	High Density Double Aisle	−80°C to RT	Concerto/ OSCAR	X	X	X
REMP	Modular or High Density Double Aisle	−80°C to RT	Sample Administrative System	X	X	X
TTP	Modular	−20°C to RT	ComPound	X	X	X
RTS	High density	−80°C to RT	d-Sprint/SIS	X	X	n/a
Tekcel-Hamilton	Low Density	−20°C to RT	ASM	X	n/a	X
Matrical	High Density	−20°C to RT	n/a	X	X	X
Nexus	High Density/ Modular	−20°C to RT	Yes	X	X	X

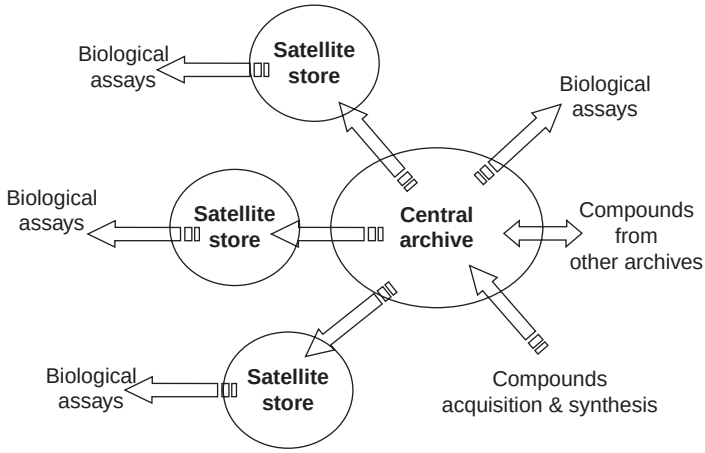

FIGURE 2 Distributive model in compound management.

varied nature of the compounds. Free-flowing powders can be dispensed using automated methods but the problem with gums and oils persists. Solid dispensing has been automated using the Archimedes screw (Mettler-Toledo), vibratory shakers (CyBio), and by the use of charged rods (Zinsser). Biodot DisPo 1500 performs volumetric delivery of dry powders and solids using an adjustable plunger. Fill height and diameter of the probe determine the sampling volume of powder. Each of these methods has its problems and works on approximately 50% to 75% of the sample population. Other options, especially for gums and oils, include using a volatile solvent transfer, followed by lyophilization of samples to

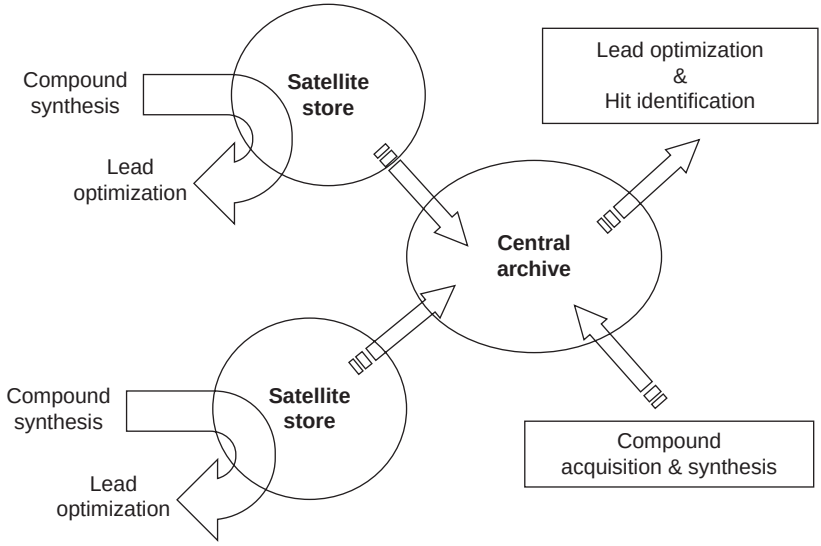

FIGURE 3 Hub and spoke model in compound management.

change the physical characteristics of the compound. When volatile solvents are used, the sample is dissolved in an appropriate solvent to a known concentration, the required volume transferred and then dried down. This method is capable of handling the variation in physical characteristics of the compounds and is amenable to greater throughputs by using automated liquid handlers. However, this process can change the amorphous to crystalline ratio of the compound, which in turn can change the solubility of the compound in biological media.

For the creation of samples as DMSO solutions, a variety of liquid-handling systems are used. Typically, solid samples are accurately weighed in vials or solubilization tubes; DMSO is added to it using a variable volume liquid dispenser (Tecan Genesis/Evo®, Hamilton Star®, Biomek® FX, Perkin Elmer Janus®, etc.) and then sonicated to ensure dissolution to a fixed concentration. DMSO stock solutions are usually maintained in the archives at a 1- to 10-mM range. Once solubilized, the samples are easily transferred using liquid handlers to a variety of formats for storage in the archive.

A number of vendors have "stand-alone" archive systems for ease of storage and retrieval. In some instances, these systems may also be capable of integrating additional automation for delivery of samples in a variety of formats. The large, automated stores are capable of storing millions of vials or tubes and can be maintained at temperatures ranging from -80°C to room temperature in dry conditions (relative humidity control). The systems consist of integrated robotics and software that allow for the completely automated handling of archived samples. Users can place orders for samples in a variety of formats through a web-based ordering systems that show inventory in real time (Table 1). There is no human intervention in the processes of storage, manipulation, or dilution. This approach ensures that (1) precious samples are handled to best minimize hydrolysis and oxidation, (2) minimal quantities of samples are dispensed for each assay, and (3) virtual loss of compound is avoided by unambiguously tracking compounds and containers to a relational database.

The storage units consist of large cold rooms with redundant cooling systems that are filled by the storage racks and robotics. The walls of the cold room are lined from floor to ceiling with high-density trays that hold racks into which either vials or microtubes can be loaded. Samples are usually stored randomly within the system. When a vessel is placed in the store, the software picks the most efficient location without regard to the content in the vessel. This process is repeated every time the vessel is picked from, or placed into, the store. Over time, the individual vessels move through the store with the software tracking each movement by means of a barcode for vials or a microtube rack barcode for the tubes. Each store is capable of retrieving approximately 5000 to 20,000 samples stored in tubes in a 20-hour workday. The retrieval capacity is somewhat slower for samples stored in vials (1000–6000).

The second component of the system is the associated location database and the scheduling software. In such complex systems, the greatest challenge is not physical storage, but data handling. One of the paramount concerns is knowledge of the location of an individual sample. The software needs to track the position of all compounds concomitantly without error. To mitigate this issue, data backup is done in real time. Efficient sorting algorithms are in place to optimize picking and placing of samples. This is achieved by registering each sample container with a vessel identifier and tracking this identifier electronically

through each operation. Sophisticated scheduling is part of the software to ensure that multiple operations of picking and placing of vessels proceed efficiently. Audit trails are available to track samples routinely and ensure accuracy.

Overall, all these elements work together to ensure that sample integrity is preserved, the archive is managed to maximize the utility of each sample, and that samples required for downstream processes are in the required format and composition. The use of industrial scale robotics for these activities provides low error rates and errors that are traceable. They also remove the need for a large number of staff for mundane and tedious tasks that are error prone.

PROCESS DEMANDS ON COMPOUND MANAGEMENT

Process and data demands on CM vary greatly depending on which of the drug discovery processes is being supported. For hit identification, strategies include providing large diverse compound sets (millions), at starting points for screening a variety of targets (Fig. 4). These predetermined sets are then further augmented by the use of smaller subsets (tens of thousands) of compounds for specific target classes. In each of these instances, the creation and storage of multiple copies of compound "master plates" for ease of replication and distribution is the norm. Formats include either 96-, 384-, or 1536-well microtiter plates, with the majority of users employing 384-well technology. However, the trend is shifting to the higher density 1536-well plate in recent years. Typically, multiple copies of master plates are made at a time to be able to replicate the entire deck set (millions of samples) in a matter of days. Additional needs of the hit identification include sequential screening, whereby smaller subsets of compounds are created and screened in an iterative fashion to enrich the hits at each stage of screening. This approach needs the efficient creation of relatively large (10,000–30,000) subsets through "cherry picking" of sample from the archive. In this case, the ability to turn around the subsets in a timely manner is imperative (1–2 days) and the hardware in the archive needs to be able to support the throughput. This approach

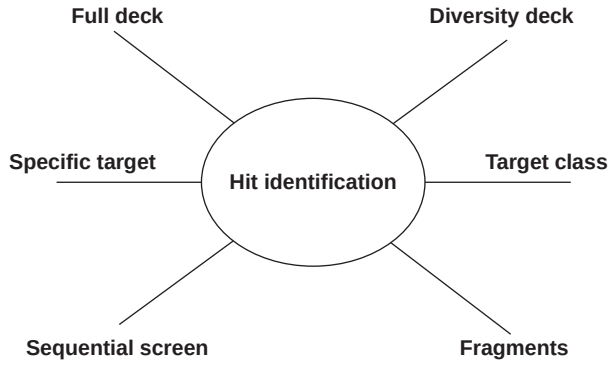

- Capture and integrate all historical and new compounds
- Synthesis and external acquisition of novel chemotypes
- Rapid turnaround for storage and supply of customized compoud sets

FIGURE 4 Hit identification strategy.

also holds good for focused screening, which relies on constructing and delivering a custom set of compounds based on knowledge of the target. In all these cases, rapid retrieval and reformatting of samples in appropriate screening formats for retests and concentration–response curve determination are needed to complete hit identification. In most cases, the samples are retrieved from the central archive, especially if high-speed-picking hardware is already in place. However, in some instances, closed-loop screening of samples is enabled whereby the sample is dispersed from the original screening plate on the screening system.

While the initial foray into automation in CM was based on the advances in HTS capabilities, the advent of lead optimization has become the priority in recent years (Fig. 5). This has made necessary the integration of CM into the discovery process, with close working relationships with biology and chemistry. Although dealing with smaller numbers of samples, process flows for lead optimization are more complex and the data dossier for decision making much more intricate. Thus, compound management needs to support structure–activity relationship studies, in vivo efficacy, and ADME and Toxicology studies. The complexities in process for supporting a variety of assays have proved to be a challenge for most organizations. Processes and automation for weighing, solubilization, and just-in-time plate preparation in assay ready formats are needed with the emphasis on low-volume dispensing (Fig. 6). Typically, a fully integrated software system comes into play as soon as the sample is synthesized by the chemist and registered to be run in panels of assays. Compounds are dissolved in DMSO and plated on the day that the assay is run; thus, data transfer and cycle times are critical. This effective and seamless integration of samples and the associated biological data drives improved productivity for the lead optimization process.

QUALITY CONTROL

The quality of data-driving decisions in hit identification and lead optimization depends a great deal on the sample inputs and the quality of the CM processes. To achieve inputs with high physicochemical character, samples are monitored for purity, solubility (in DMSO and assay buffer), concentration, and water content of the DMSO stock solutions. Process quality is also monitored by ensuring balances for weighing and liquid handler dispensing is accurate and precise. Integration of inert environment into the processes to prevent water uptake in the

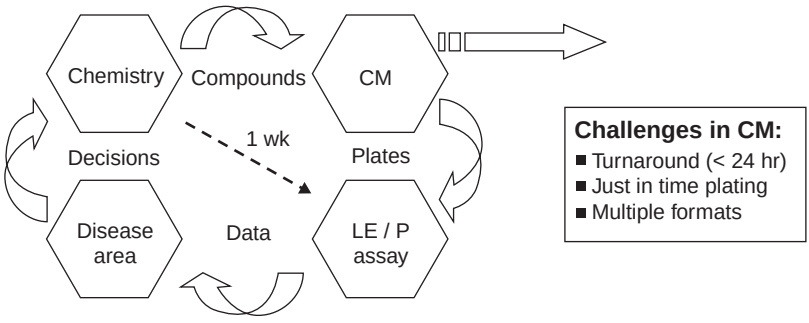

FIGURE 5 Lead optimization compound life cycle.

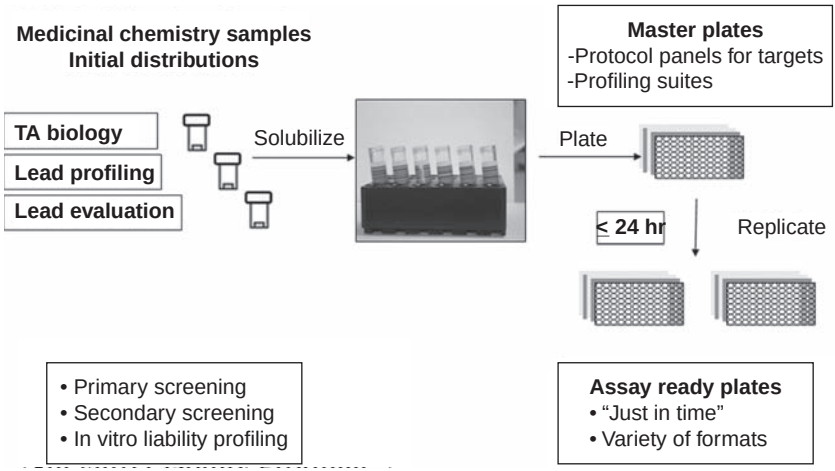

FIGURE 6 Lead optimization sample processing.

samples is also important. For large sample collections, monitoring purity of each individual compound over time is an onerous task, in terms of both data interpretation and cost. High-throughput analytical techniques have not kept pace with the HTS paradigm, making purity checks of large libraries difficult. While the purity of the compound is well known at the time of incorporation into the sample collection, over time the purity can change, and purity checks must be done periodically to evaluate each sample. High-throughput methods in mass spectroscopy and nuclear magnetic resonance spectroscopy have recently been employed to look at purity of samples on a rotating basis, so that the entire collection can be checked over a period of years. Quality control of liquid handlers is routinely practiced by the industry (Fig. 7). Volumes dispensed can vary from the low nanoliter range (10–100 nL) using Labcyte's acoustic technology. For larger volumes (100–100 μl), systems like the Velocity11 BioCel® are used. Accuracy and precision are tested routinely and typically are less than 10% of dispensed volume.

SUPPORTING AUTOMATION AND IT

IT and automation are intertwined to provide synergy in moving samples and data through the path of a sample's life cycle through compound management. A number of applications need to be integrated with the compound archive and dispensary. Sample registration is initiated upon receipt of compound into the archive and then tracked through each process. Compound characteristics, including weight, physical characteristics, structure, etc., are incorporated in the database. Once samples are picked from the archive, processing could take place using automation and informatic applications either directly integrated with the archive or off-line. Each pathway has its advantages. In the case of completely integrated systems (Table 1), samples can be thawed, decapped, transferred, recapped, and returned to the archive with minimal manual intervention. This is clearly an efficient process with efficient FTE (Full Time Equivalent) utilization, and works well for well-defined, simple processes that do not change often. Data

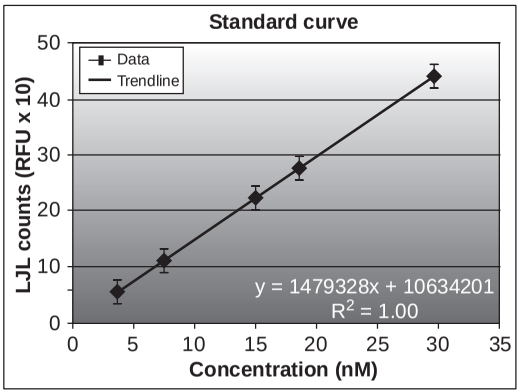

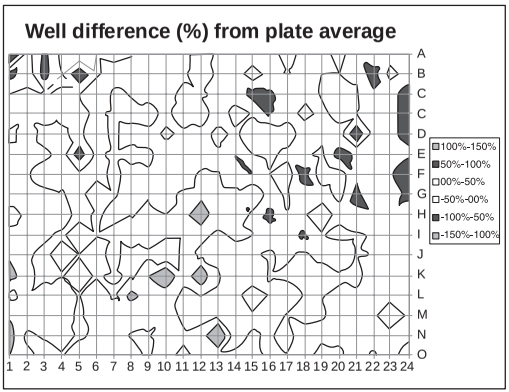

Well accuracy:
100 nL ± 10 nL
1 µ L ± 0.1 µL

Plate Precision:
100 nL CV range:
4.5–9.7%
1µL CV range:
2.8–5%

Carryover:
< part in a 10,000,000

FIGURE 7 Quality control: Dispensing.

is resident with one vendor and minimizes issues in case of problems. On the other hand, decoupled systems have the advantage of flexibility. New automation and applications can be incorporated and upgraded as they become available as long as open architecture is available in the archive for data uploads. As changes to technology take place or as processes evolve, they can be quickly added to the repertoire of compound management. However, in these instances, data transfer between the archive and sample processing automation can be a challenge.

FUTURE DIRECTIONS

Compound Management will continue to remain a central core service to drug discovery. In the past, CM focused primarily on services for hit identification through HTS. More recently, CM has had to expand its services into the lead optimization arena as well. Expansion of the infrastructure to include biologics (cells, RNA, DNA, proteins, peptides, serum, etc.) is a logical extension of CM's capabilities since the hardware is now available to handle low temperatures. A number of "Bio-Banks" have already been instituted. Integration of analytical QC for determining purity, solubility, and concentration of samples is also within reach from a scientific perspective. The change in focus from processing large numbers of samples to one of providing a dossier of quality with the samples is imminent.

REFERENCES

1. Chan JA, Hueso-Rodriguez, JA. Compound library management. Methods Mol Biol 2002; 190:117–127.
2. Yao N, Nilar S, Stoisavljevic V, et al. Managing the collection of HTS compounds through suppliers. Abstracts of Papers, 223rd ACS National Meeting, Orlando, FL, United States, April 7–11, 2002.
3. Lipinski CA. Drug-like properties and the causes of poor solubility and poor permeability. J Pharmacol Toxicol Methods 2000; 44(1):235–249.
4. Lipinski CA, Lombardo F, Dominy BW, et al. Experimental and computational approaches to estimate solubility and permeability in drug discovery and development settings. Adv Drug Deliv Rev 2001; 46:3–26.
5. Ghose AK, Viswanadhan VN, Wendoloski JJ. A knowledge-based approach in designing combinatorial or medicinal chemistry libraries for drug discovery. J Comb Chem 1999; 1:55–68.
6. Oprea TI. Is there a difference between leads and drugs? A historical perspective. J Chem Inf Comput Sci 2001; 41:1308–1315.
7. Teague S, Davis AM, Leeson PD, et al. The design of leadlike combinatorial libraries. Angew Chem Int Ed Engl 1999; 38:3743–3748.
8. Carr R, Jhoti H. Structure-based screening of low-affinity compounds. Drug Discov Today 2002; 7:522–527.
9. Congreve M, Carr R, Murray Coti H. A "Rule of Three" for fragment-based lead discovery. Drug Discov Today 2003; 8(19):876–877.
10. Erlanson DA, Braisted CA, et al. Site-directed ligand discovery. Proc Natl Acad Sci U S A. 2000; 97:9367–9372.
11. Vetter D. Chemical microarrays, fragment diversity, label-free imaging by plasmon resonance—a chemical genomics approach. J Cell Biochem 2002; 39:79–84.
12. Lipinski, CA, Lombardo F, Dominy BW, et al. Experimental and computational approaches to estimate solubility and permeability in drug discovery and development settings. Adv Drug Deliv Rev 2001; 46(1–3):3–26.
13. McGovern SL, Caselli E, Grigorieff N, et al. A common mechanism underlying promiscuous inhibitors from virtual and high-throughput screening. J Med Chem 2002; 45:1712–1722.

14. Rishton GM. Nonleadlikeness and leadlikeness in biochemical screening. Drug Discov Today 2003; 8:86–96.
15. Irwin JJ. How good is your screening library?. Curr Opin Chem Biol 2006; 10:352–356.
16. Ilouga PE, Winkler D, Kirchhoff C, et al. Investigation of 3 industry-wide applied storage conditions for compound libraries. J Biomol Screen 2007; 12(1):21–32.
17. Schopfer U, Engeloch C, Stanek J, et al. The Novartis Compound Archive—from concept to reality. Comb Chem High Throughput Screen 2005; 8(6):513–519.
18. Kozikowski BA, Burt TM, Tirey DA, et al. The effect of room-temperature storage on the stability of compounds in DMSO. J Biomol Screen 2003; 8(2):205–209.
19. Cheng X, Hochlowski J, Tang H, et al. Studies on the repository compound stability in DMSO under various conditions. J Biomol Screen 2003; 8(3):292–304.
20. Owens J. Successful Automation of Specimen Storage at −80°C. Biorepositories Conference, Philadelphia, PA, September 8–10, 2008.
21. Arvidsson P, Divers M, Petersen-Mahrt S. Use of cyclodextrin for protective storage of chemical compound libraries. Astrazeneca, AB: European Patent EP 1212270, 2004.
22. www.specs.net.

18 Practical Approach to Quantitative High Throughput Screening

Wei Zheng, Ke Liu, and James Inglese
NIH Chemical Genomics Center, NHGRI, NIH, Bethesda, Maryland, U.S.A.

INTRODUCTION

High throughput screening (HTS) has progressively evolved since the late 1980s as an important approach for new lead discovery and a chemistry starting point (1). The size of compound collections used in HTS campaigns has also increased significantly from under 100,000 to a few million in major pharmaceutical companies. In the 1990s, pooling approaches, in which 10 to 20 compounds were contained in one well, were widely used for compound screening due to the limited screening throughput (2). Frequent interference from compounds in pooled samples and time-consuming hit deconvolution from the primary screen impaired the ability of lead identification using early pooling strategies. In the late 1990s and early 2000s, single-compound screening became the main platform with the advances in HTS technology and increases in screening throughput. However, primary screening of compound collections is routinely performed at a single concentration, typically as a single replicate, due to the high cost and time requirement for screening such large compound collections (usually in millions of compounds). Screening at a single concentration provides only a limited window of opportunity to identify the useful lead compounds.

Several weaknesses persistently exist in HTS in the single-compound concentration screen despite the advances in robotic instrument, assay technologies, and miniaturization. The false positive rate varies, depending on the assay type and assay format. Because of the high false positive rate in HTS, the primary screening results are usually less decisive and hits must be retested to confirm their activity. This is equal to a 10,000-compound retest for a 1% hit rate against a 1 million member library. Furthermore, the confirmed hits must then be subjected to concentration-response testing since the potencies of active compounds are not available. Significant time is lost due to these confirmation and potency tests as well as the consumption of precious compound stocks. Importantly, false negatives (unidentified active compounds) are a common concern in HTS conducted at a single concentration.

Recently, the NIH Chemical Genomics Center has developed a new screening paradigm—quantitative high-throughput screening (qHTS), in which all compounds are screened in a seven-concentration titration (3). qHTS has greatly improved the data quality in the primary compound screen and the resulting information-rich data have transformed the process for selection and prioritizing of active compounds. Taken together, (*i*) robotic assay optimization is simplified in qHTS. In HTS with single-compound concentration screening, pilot screening trails with different compound concentrations must be performed to assess the

optimal concentration that yields an acceptable hit rate (usually 0.1–1%). This step is not required in qHTS paradigm. (*ii*) The rate for failed plates in qHTS is much smaller, usually under 5%, because of the use of compound titration. The occasional one "bad" plate of a set of seven titration plates can often be ignored without detriment to data analysis and interpretation. (*iii*) Prioritization of active compounds becomes much easier in qHTS because the potency and efficacy of active compounds are immediately revealed after primary screen, avoiding time-consuming process of hit cherry-picking/confirmation and determination for compound potency. Selection of active compounds based on potency and efficacy is more pharmacologically relevant than typical "hit" selection based on the data from a single concentration. (*iv*) Information on structure–activity relationships (SAR) can be obtained directly from the qHTS results, which greatly facilitates the process of hit-to-lead data refinement. It also accelerates lead optimization, since additional analogs of lead structures from the SAR information can be purchased together with the lead compounds from the commercial sources. Thus, SAR of lead compounds can be expanded quickly. (*v*) Certain false positives may be avoided in qHTS because of the selection of active compounds based on the concentration–response curve. The random interferences from instrument glitches, compound carryover, and interference from dust/lint fluorescent "sparks" can be easily eliminated during data analysis (Fig. 1). (*vi*) Certain false negatives can also be avoided in qHTS, including those compounds with biphasic responses ("bell" type of concentration response), commonly because of nonspecific cytotoxicity at high compound concentrations and compounds showing low efficacy that would fall below a standard-percent activity cutoff threshold.

Over 100 projects in our laboratory have been screened in qHTS format in last three years and data have been published in PubChem as open access. To help readers set up a qHTS facility, we include here the detailed descriptions of instrument selection, compound dilution plate preparation, and two examples of assay implementation for qHTS.

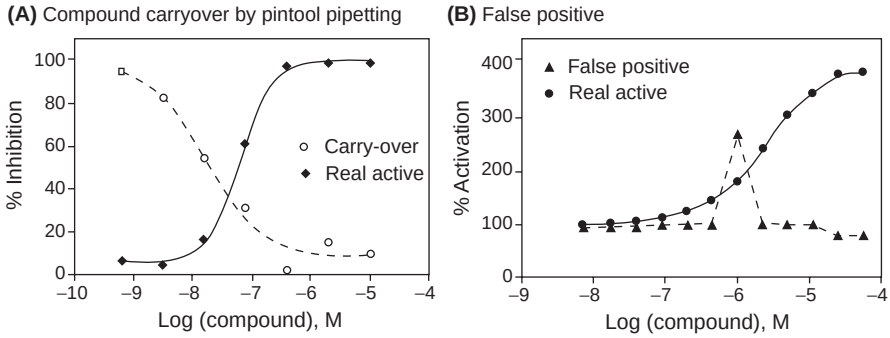

FIGURE 1 Certain false positives can be avoided in qHTS. (**A**) Compound carryover due to a "sticker" compound that stuck on the pipetting pins and tips firmly and washed off slowly. It can be easily distinguished by the shape of curve since the compound concentration is usually placed from low to high in qHTS. (**B**) Lint, dust, or instrument glitch can result in the false positives in the single-concentration screen. It is easily eliminated due to no concentration–response curve for this type of problems.

Since multiple compound concentrations are used in qHTS, the well numbers for each compound increase compared to one well per compound in traditional HTS relying on a single-compound concentration. The assay miniaturization in 1536-well plates is beneficial for qHTS to reduce the cost and increase screening efficiency. Thus, qHTS in 1536-well plate format is described here. If the 384-well plate format is considered for qHTS, formatting 384-well compound plates to 1536-plates and 1536-well dispensing described in following sections can be omitted.

LIQUID HANDLING FOR qHTS IN 1536-WELL PLATE FORMAT

Multidrop dispenser (Thermo-Fisher Scientific, Waltham, Massachusetts, U.S.A) is used for dispensing DMSO to 384-well plates for compound dilution. An automated pipetting station equipped with a 384-tip head and changeable tips can be used for the interplate compound dilution in 384-well plates. For example, Cybiwell (Cybio, Jena, Germany) and Evolution P3 dispenser (PerkinElmer, Waltham, Massachusetts, U.S.A), both equipped with two pairs of plate stackers, can be used for a semiautomated preparation of these plates. The 1536-well compound plates are generated by the indexing pipetting using the same 384-well pipetting head from the diluted 384-well compound plates. Compounds in DMSO solution are transferred at 20 nL/well to assay plates using a Pintool station (Kalypsys, San Diego, California, U.S.A) with three tip washers containing DMSO, ethanol, and methanol, respectively. Different sizes of transferring pins (e.g., 10, 15, 20, 30, 40, or 50 nL) for compound transfer can be selected dependent on the applications (V&P Scientific, San Diego, California, U.S.A). Reagents dispensing for assays in 1536-well plates is carried out at 0.5 to 5 μL/well with a BioRAPTR FRD™ Workstation (Beckman Coulter, Fullerton, California, U.S.A.).

PLATE READERS FOR 1536-WELL ASSAYS

CCD-imaging-based multifunctional plate readers such as the ViewLux™ (PerkinElmer) as well as PMT-based plate readers including the EnVision™ (PerkinElmer) and Safire™ (Tecan, Männedorf, Switzerland) are recommended for detection of 1536-well assay plates.

COMPOUND PREPARATION FOR qHTS

As described recently (4), 10 mM compounds in DMSO solution are dispensed at 50 μL/well to 384-well polypropylene U-bottom plates that are used as the compound source plates. The wells in columns 1 and 2 are empty and will be used for controls in qHTS. An interplate dilution at 1:5 ratio is used for serial titration of all compounds in library collections. A set of seven 1536-well compound plates is prepared from four sets of 384-well compound dilution plates and contains 1408 compounds as a seven-concentration titration (wells in column 1–4 are empty). As briefly described in Figure 2, 40 μL/well of DMSO is dispensed to 24 polypropylene U-bottom 384-well plates except wells in columns 1 and 2. Four compound 384-well source plates containing 50 μL/well of 10 mM compound solution are needed to produce one set of 1536-well plates. Thus, each of 384-well compound source plate is paired with six plates containing 40 μL/well DMSO for a dilution series; 10 μL/well of 10-mM compound solution is transferred with a 384-well pipetting head to a 384-well plate containing 40 μL/well DMSO and mixed; subsequent serial dilutions are made for all remaining five

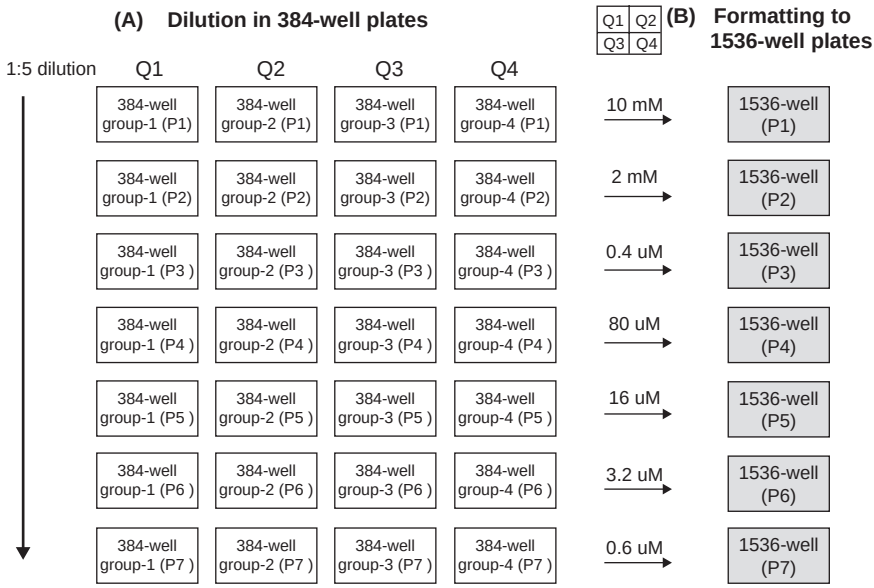

FIGURE 2 Schematic illustration of the process of 1:5 dilution in 384-well plates that are reformatted into 1536-well plates. (**A**) P1 contains 50 μL/well of 10 mM compounds from which 10 μL/well is added to 40 μL DMSO in P2 and mixed. Same dilutions subsequently made from P2 to P7 to complete the dilution for each set (Q1, Q2, Q3, and Q4). (**B**) 7 μL/well of compounds from four 384-well plates with the same compound concentration (Q1, Q2, Q3, and Q4) is added to one 1536-well plate to form one set of 1536-well plate. A total of four sets of 1536-well compound plates can be made in this method.

plates with the same 10 μL liquid transfer. Four sets of seven 384-well compound plates with 1:5 serial dilutions are produced with the same method. Then, each of four 384-well compound plates with the same concentration is transferred with a 384-well pipetting head at 7 μL/well to a specified quadrant of a 1536-well plate. One set of seven 1536-well compound plates is thus produced by repeating the above quadrant transfer step. A total of four sets of 1536-well plates can be made at once in approximately 2.5 hours. The resulting compound plates are heat sealed (PlateLoc® , Velocity 11, Menlo Park, California, U.S.A.) for long-term storage. A set of compounds is kept at room temperature for qHTS and will be discarded after six months. The other three sets of 1536-well dilution plates are stored at −80°C. The concentrations in 1536-well compound plates range from 0.64 μM to 10 μM (0.64 μM, 3.2 μM, 16 μM, 80 μM, 0.4 mM, 2 mM, and 10 mM). In addition, a 1:2.236 ($\sqrt{5}$) dilution can be made to add one concentration point between two concentrations in above dilution series to form a 15-concentration titration ranged from 0.13 μM to 10 mM.

qHTS DATA ANALYSIS

Primary screen data with titrations for all compounds are loaded into a internally developed database. Concentration responses are fit with a four-parameter Hill equation using a customized program that minimizes the residual error between

the modeled and observed responses. Since the primary screening data contain the concentration responses for all compounds, the potency and efficacy of each compound are available after the data analysis. Active compounds ("Hits") can be selected by information-rich criteria such as IC_{50} values < 10 μM and curve classes of 1.1, 1.2, 2.1, and 2.2 (reflecting efficacy, details described in next chapter). This curve-fitting software for qHTS data is now available for open access (www.ncgc.nih.gov). To prioritize the qHTS hits, clustering analysis of active compounds from the primary screening is then performed with Leadscope® Hosted Client (Leadscope Inc., Columbus, Ohio, U.S.A.). The active compounds are then grouped in clusters based on their similarity in structure that are used for cherry-picking of compounds for confirmation and follow-up studies. The EC_{50} values of compounds in the confirmation and follow-up experiments are calculated by nonlinear regression analysis using a Prism computer program (GraphPad Software, San Diego, California, U.S.A.). The more detailed description of data analysis for qHTS results is included in the next chapter "Enabling the Large Scale Analysis of Quantitative High-Throughput Screening Data." The Z' factor, an index for screening assay quality control (5), was determined by the equation of $Z' = 1-(3 \times SD_{high} + 3 \times SD_{low})/(Mean_{high} - Mean_{low})$.

GLUCOCEREBROSIDASE ASSAY: ENZYME SCREENING IN qHTS FORMAT

Glucocerebrosidase (GC) is a lysosomal enzyme that catalyzes the hydrolysis of β-glucocerebroside to glucose and ceramide. Mutations in this enzyme cause degradation, misfolding, and mistrafficking of the protein, leading to the Gaucher disease. Chemical chaperone therapy using small-molecule GC activators or inhibitors represents a new potential therapeutic approach to treat Gaucher disease (6–8). The mutant protein misfolding/mistrafficking can be corrected by small-molecule chaperones partially restoring enzyme function in the lysosome. A fluorogenic enzyme assay (Fig. 3) has been optimized in 1536-well plate format for HTS to identify activators and inhibitors that may serve as a starting point for chemistry development of lead compounds for chaperone therapy (9,10). The activity of GC can be measured using a profluorescent substrate, 4-methylumbelliferyl β-D-glucopyranoside (4 MU-β-Glc, Sigma-Aldrich, St. Louis, MO). Purified GC was obtained from the residual solution after clinical infusions of imiglucerase (Cerezyme®, Genzyme Co., Cambridge, Massachusetts, U.S.A., Mr = 60,430), which showed a specific activity of 42.2 units/mg and 14 units/mL. The enzyme stock was prepared in 30% glycerol

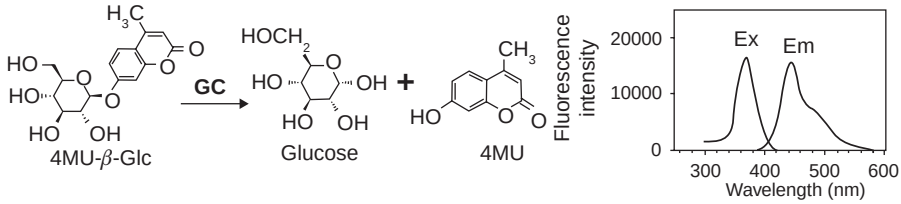

FIGURE 3 Schematic illustration of the GC enzyme assay. Hydrolysis of substrate 4MU-β-Glc yields resorufin that emits at red end of spectrum. To obtain the maximal signal-backgroud ratio, an excitation of 370 (±20 nm) and emission of 440 (±10 nm) are used for detection in this assay.

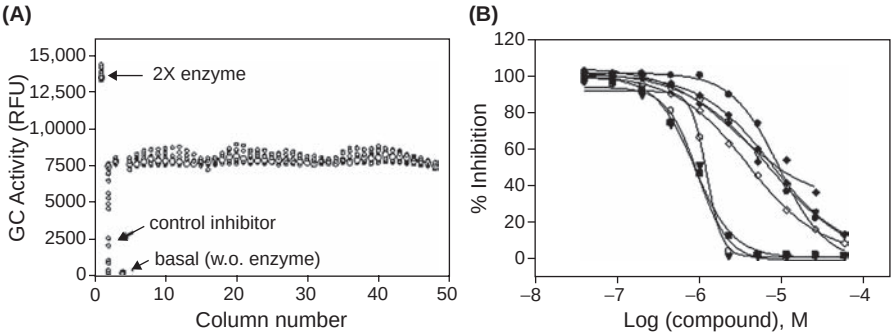

FIGURE 4 Results of a GC screen with the LOPAC library screen. (**A**) Scatter plot of the results from a DMSO plate. The signal-to-basal ratio was 32.8-fold with a CV of 3.7% and Z′ factor of 0.91. Wells in column 1 with 2X enzyme were used as a positive control for activator discovery (**B**) Concentration–response curves of hits with an IC50 $\leq$10 mM identified from the LOPAC library screen. Thirteen active compounds were identified with a hit rate of approximately 1.0%. The potency and efficacy of active compounds were revealed in the primary screen data.

at 3.82 μM, aliquoted and stored at −80°C. Before the assay, the enzyme and substrate were diluted in the assay buffer composed of 50 mM citric acid, 176 mM K_2HPO_4, pH 5.9, 0.01% Tween-20, and 10-mM sodium taurocholate. The GC assay started with the incubation of 2 μL/well of enzyme solution with 20 nL library compound in 1536-well black plates for five minutes at room temperature (Table 1). The negative controls received 2 μL/well of assay buffer without enzyme. The enzyme reaction was initiated by addition of 1 μL of substrate solution, followed by 20 min incubation at room temperature and stopped by an addition of 3 μL stop solution containing 1 M sodium hydroxide and 1 M glycine at pH 10. The substrate consumption in this enzyme assay was under 5%. The final concentrations of enzyme and substrate (4MU-β-Glc) were 1.9 nM and 30 μM, respectively. Fluorescence was read at an excitation of 370 (±20) nm and an emission of 440 (±20) nm, which yielded the optimal signal-to-basal ratio.

A compound library containing 1280 pharmacologically active compounds (LOPAC collection) was selected for screening assay validation (11,12). This GC enzyme assay was screened in qHTS format. The average signal-to-basal ratio from the DMSO plate was 32.8-fold, and the CV and Z′ factor were 3.7% and 0.91, respectively [Fig. 4(A)]. With a cutoff at IC_{50} <10 μM and efficacy > 50% inhibition, eight compounds were actives that inhibited GC activity with a hit rate of 0.25% [Fig. 4(B)]. Their activities were all confirmed in the subsequent experiments (9).

IP-ONE ASSAY: CELL-BASED SCREENING IN qHTS FORMAT

G-protein coupled receptors (GPCRs) are a family of cell surface receptors important for drug development. After binding to their ligands, GPCRs transfer extracellular stimuli to intracellular signals by activation of subtypes of heterotrimeric G-proteins including Gs, Gi, and Gq. The Gs subtype activates adenylyl cyclase (AC), and thus increases the concentration of intracellular adenosine 3′,5′-cyclic monophosphate (cAMP), a secondary messenger that signals through the activation of protein kinase A (PKA). The Gi subtype inhibits AC and suppresses

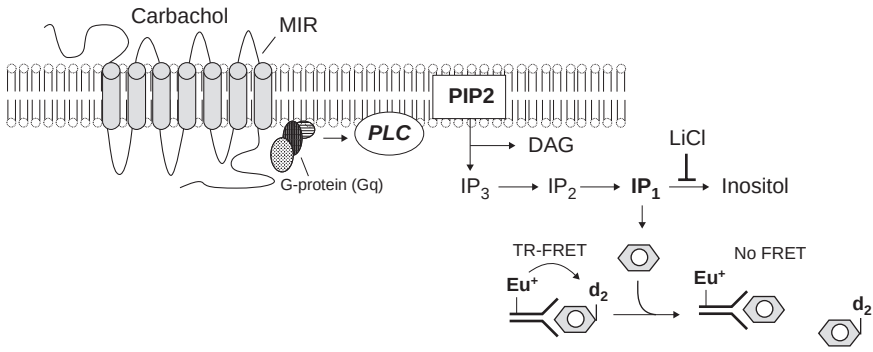

FIGURE 5 Schematic representation of the assay design for the IP-One assay in a HTRF format. The detection reagents including d_2-conjugated IP_1 and Eu+ cryptate-conjugated anti-IP_1 antibody in a cell lysis buffer enables a homogenous measurement of IP_1 production in the M1R-CHO cells stimulated by Carbachol.

signaling in the cAMP/PKA pathway. The Gq subtype activates phospholipase C (PLC), which increases the second messengers inositol 1,4,5-trisphosphate (IP_3) and diacyl glycerol (DAG), resulting in an increase of intracellular free Ca^{2+} and activation of protein kinase C. Recently, antibody-based assays in a TR-FRET (Time Resolved–Fluorescence Resonance Energy Transfer) detection mode have been developed for measurements of cAMP and IP_1 in compound library screening (13,14). The IP-One assay measures the accumulation of intracellular inositol-1-phosphate (IP_1) that correlates with the level of IP_3 (Fig. 5). Here, we describe a compound library screen using this IP-One assay to search for antagonists of the M1 muscarinic acetylcholine receptor (M1R) expressed in Chinese hamster ovary (CHO) cells.

A CHO cell line stably expressing the rat MIR was purchased from American Type Culture Collection (#CRL-1984, Manassas, Virginia, U.S.A.). Cells were cultured in F-12 Kaighn's medium supplemented with 0.05 mg/mL G418, 100 units/mL penicillin, 100 μg/mL streptomycin, and 10% fetal bovine serum at 37°C, 5% CO_2. To store the cells, cells harvested at approximately 95% confluence were resuspended in a cell freezing medium (#12,648–010, Invitrogen, Carlsbad, California, U.S.A.) and aliquoted to 1 mL per vial at 40 to 50 million cells per milliliter. Vials of cells were placed in a Cryo 1°C freezing container (Nalgene Nunc, Rochster, New York, U.S.A.) and slowly frozen overnight in a −80°C freezer at approximately 1°C/min. The frozen cells were then transferred to liquid nitrogen for storage for up to two years.

Before the assay, frozen cells were thawed, resuspended in fresh culture medium, and plated into tissue culture-treated, white 1536-well plates at 4 μL/well containing 2000 cells/well (Table 2). Assay plates with cells were incubated at 37°C, 5% CO_2 for overnight. The library compounds in serial dilutions were added at 20 nL/well to assay plates, followed by a 10-min incubation. Carbachol, an agonist of M1R, was prepared in the stimulation buffer (10 mM Hepes, 1 mM $CaCl_2$, 0.5 mM $MgCl_2$, 4.2 mM KCl, 146 mM NaCl, 5.5 mM glucose, and 250 mM LiCl, pH 7.4) and added to the assay plate at 1 μL/well. After incubation with Carbachol at 37°C, 5% CO_2 for 30 min, 1 μL/well of d_2-conjugated IP_1

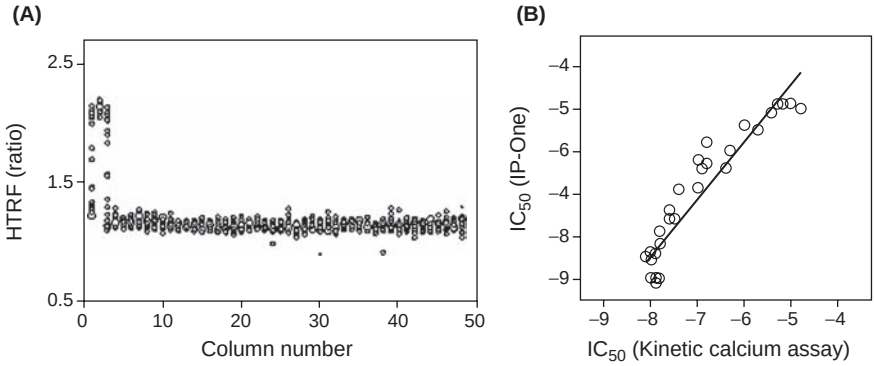

FIGURE 6 (**A**) Scatter plot of the results from IP-One assay. Plate map—the whole plate was stimulated with 12-μM Carbachol (EC_{80}) with serial titrations of atropine and pirenzepine in column 1 and 2 respectively, and column 4 of 50-μM atropine (IC100). (**B**) Correlation of known cholinergic antagonist activities between the IP-One and intracellular calcium assays. The LOPAC collection was screened in the qHTS format with both the IP-One assay and the calcium assay. The IC_{50} values of 30 know cholinergic antagonists determined from both screens were correlated well.

(d_2-IP_1), and 1 μL/well of Eu^{+3} cryptate-conjugated anti-IP_1 antibody (Eu^{+3}-Ab) were dispensed. Both reagents were from the HTRF® IP-One kit (Cisbio, Bedford, Massachusetts, U.S.A.) and prepared in the cell lysis buffer supplied in the kit. After 10 min incubation at room temperature, the assay plates were measured in the TR-FRET detection mode with a ViewLux plate reader (Ex = 320 nm, Em = 590 and 665 nm). The results were calculated as the ratio of acceptor fluorescence intensity (665 nm)/donor fluorescence intensity (590 nm). The cells without agonist stimulation (added with 1 μL/well of buffer) were used as a control.

A DMSO plate test in this IP-One assay revealed robust statistical results [Fig. 6(A)]. The LOPAC compound library (σ) was screened with this IP-One assay using the M1R-CHO cell line in qHTS format that yielded a hit rate of 2.2% with a cutoff of IC_{50} value <1 μM and curve class 1.1, 1.2, 2.1, and 2.2. The hits rate was relatively high because many of the compounds in the LOPAC collection are known for their pharmacological function as receptor antagonists for M1R or other GPCRs. We have compared the activities of 30 known antagonists

TABLE 1 A Protocol for the Glucocerebrosidase Assay in 1536-Well Plate Format

Step	Parameter	Value	Description
1	Reagent—1	2 μL	1.5 × enzyme solution
2	Compound or control	23 nL	Control plate and compound library plate
3	Incubation	5 min	Room temperature
4	Reagent—2	1 μL	3 × substrate
5	Incubation	20 min	Room temperature
6	Stop solution	3 μL	1 × stop solution
7	Time for incubation	1 min	Room temperature
8	Detection	Ex = 365, Em = 440 nm	ViewLux (1 sec)

TABLE 2 A Protocol for the IP-One HTRF Assay in 1536-Well Plate Format

Step	Parameter	Value	Description
1	Cells	4 μL	2000 cells/well
2	Incubation	20–30 hrs	37°C, 5% CO_2
3	Compound	23 nL	0.128 μM to 10 mM in DMSO dilution
4	Reagent	1 μL	Carbachol at a concentration of EC_{80}
5	Incubation	30 min	37°C, 5% CO_2
6	Reagent	1 μL	IP_1-d_2 in cell lysis buffer
7	Reagent	1 μL	Eu-anti-IP_1-Ab in cell lysis buffer
8	Incubation	30 min	Room temperature
9	Detection	HTRF mode	ViewLux plate reader

determined from this assay in an intracellular calcium assay using a fluorescence kinetic plate reader, the FDSS-7000 (Hamamatsu, Japan). A good correlation of IC_{50} values of these 30 known antagonists was found between two assay methods [Fig. 6(B)].

SUMMARY

Primary compound screening in qHTS format has greatly improved the data quality and facilitated the selection and prioritization of active compounds for follow-up screens and lead optimization. Application of qHTS in primary screening can increase the prospect for discovering high-quality leads, reducing costly follow-up of false positives and lowering the probability of false negatives. One issue with qHTS is a significant increase in plate numbers as well as cost compared with the HTS with a single compound concentration. This apparent limitation of qHTS can be partly overcome by application of new assay technologies, assay miniaturization, increased diversity/quality in compound collections (to reduce the size), and careful selection of the number of titration concentrations for each screening (e.g., three or four concentrations vs. seven concentrations), but in reality is more than compensated by the effort and resources eliminated in the protracted follow-up of false positives common in traditional HTS.

REFERENCES

1. Pereira DA, Williams JA. Origin and evolution of high throughput screening. Br J Pharmacol 2007; 152(1):53–61.
2. Devlin JJ, Liang A, Trinh L, et al. High capacity screening of pooled compounds: Identification of the active compound without re-assay of pool members. Drug Dev Res 1996; 37:80–85.
3. Inglese J, Auld DS, Jadhav A, et al. Quantitative high-throughput screening: A titration-based approach that efficiently identifies biological activities in large chemical libraries. Proc Natl Acad Sci U S A 2006; 103(31):11473–11478.
4. Yasgar A, Shinn P, Jadhav A, et al. Compound management for quantitative high-throughput screening. JALA Charlottesv Va 2008; 13:79–89.
5. Zhang JH, Chung TD, Oldenburg KR. A simple statistical parameter for use in evaluation and validation of high throughput screening assays. J Biomol Screen 1999; 4(2):67–73.
6. Chang HH, Asano N, Ishii S, et al. Hydrophilic iminosugar active-site-specific chaperones increase residual glucocerebrosidase activity in fibroblasts from Gaucher patients. FEBS J 2006; 273(17):4082–4092.

7. Lieberman RL. Wustman BA, Huertas P, et al. Structure of acid beta-glucosidase with pharmacological chaperone provides insight into Gaucher disease. Nat Chem Biol 2007; 3(2):101–107.
8. Sawkar AR, Adamski-Werner SL, Cheng WC, et al. Gaucher disease-associated glucocerebrosidases show mutation-dependent chemical chaperoning profiles. Chem Biol 2005; 12(11):1235–1244.
9. Urban DJ, Zheng W, Goker-Alpan O, et al. Optimization and validation of two miniaturized glucocerebrosidase enzyme assays for high throughput screening. Comb Chem High Throughput Screen 2008; 11(10):817–824.
10. Zheng W, Padia J, Urban DJ, et al. Three classes of glucocerebrosidase inhibitors identified by quantitative high-throughput screening are chaperone leads for Gaucher disease. Proc Natl Acad Sci U S A 2007; 104(32):13192–13197.
11. Benjamin ER, Pruthi F, Olanrewaju S, et al. State-dependent compound inhibition of Nav1.2 sodium channels using the FLIPR Vm dye: On-target and off-target effects of diverse pharmacological agents. J Biomol Screen 2006; 11(1):29–39.
12. Rickardson L, Wickström M, Larsson R, et al. Image-based screening for the identification of novel proteasome inhibitors. J Biomol Screen 2007; 12(2):203–210.
13. Liu K, Titus S, Southall N, et al. Comparison on functional assays for Gq-coupled GPCRs by measuring inositol monophospate and intracellular calcium in 1536-well plate format. Curr Chem Genomics 2008; 1:70–78.
14. Titus S, Neumann S, Zheng W, et al. Quantitative high-throughput screening using a live-cell cAMP assay identifies small-molecule agonists of the TSH receptor. J Biomol Screen 2008; 13(2):120–127.

19 Enabling the Large-Scale Analysis of Quantitative High-Throughput Screening Data

Noel T. Southall, Ajit Jadhav, Ruili Huang, Trung Nguyen, and Yuhong Wang

NIH Center for Chemical Genomics, NHGRI, NIH, Rockville, Maryland, U.S.A.

INTRODUCTION

High-throughput screening (HTS) is a scalable methodology for identifying modulators of biological activity from vast libraries of potential modulators through automation and miniaturization. It employs a specialized, highly sensitive biological test system (assay, e.g., a reconstituted protein activity or a cellular system) to measure the specific activity of a biological process in response to perturbations by a library of samples, either chemical compounds or natural product extracts (a compound library), or even libraries of siRNAs. HTS opened a new, broad avenue for pharmacological research (1,2) alongside rational drug design approaches (3–8), and recently, it has been used to search the vast area of chemical, genomic, and biological space for bioactive samples of potential in probing complex biological systems and pathways (9).

The NIH Chemical Genomics Center (NCGC) has recently proposed a quantitative high-throughput screening (qHTS) approach that determines the concentration-response profile of a sample during primary screening (10). The development of qHTS was aimed at leveraging high-capacity HTS technologies to improve the quality of HTS data while maintaining sufficient throughput and flexibility. In qHTS, a concentration–response curve is generated for every compound by integrating together the data from sequential single-concentration assay plates. Generating concentration–response curves (CRCs) for each compound transforms the analysis of the screening data from a statistical evaluation to a pharmacological one. The cost of increasing the scope of the primary screen is offset by improving the efficiency of the follow-up process coupled with recent advances in miniaturization. A seven-point concentration screen using 1536-well plates consumes less sample, uses the same amount of enzyme or cells and other reagents, and requires only twice the number of plates as a traditional single-point concentration screen (10). The additional plate handling is offset by streamlining the cherry-picking and confirmation process, conserving time and valuable samples. This novel approach to screening has been widely recognized as an important advance in HTS (11).

The benefits of qHTS include reducing false positives (FP) and capturing false negatives (FN), allowing the data to be mined to determine a compound's pharmacological profile, to identify and filter assay-related artifacts, and to construct structure–activity relationships (SAR) from the primary screening

data to drive probe optimization immediately after completion of the screen. Overall, a better estimate of compound significance is provided. Novel algorithms have been developed at our center to leverage this information and improve the screening process. For example, we have used compound activity profiling at the NCGC to explore the nature of biological activity in complex cell-based assays (12). As an example of eliminating assay artifacts, a biochemical screen for a dehydrogenase target reported approximately 10-K actives with more than 500 clusters of related compounds (31). Much of the SAR was due to fluorescent artifacts and we used background fluorescence data and our spectral profiling data (13) to deprioritize these SAR series. In addition to these direct advantages, concentration-response profiles enable new types of HTS experimental design and the exploration of a richer activity space, as in the case of toxicological screening (14,15). This allows follow-ups to be performed in a more selective way on fewer samples (saving time) and allows direct purchase of the most promising chemotypes (which saves money). On average, NCGC has required far fewer "cherry picks" from its screening collection to initiate optimization and, furthermore, can initiate series optimization immediately following screening rather than waiting the three to six months typically required for reconfirmation, IC_{50} determination, and initial SAR using traditional approaches.

While the qHTS approach provides richer data, it also poses a daunting informatics challenge: how to process and store the massive amount of concentration-response data that is generated and how to enable rapid SAR analysis using large-scale pharmacology data. The biggest limitation of existing software is that it requires close supervision during the data analysis process, often requiring manual curation of individual data in order to ensure quality control. The challenge for the current system is to be able to scale the quality control components of data analysis to the throughput of modern robotic systems. Storing and retrieving large amounts of data can be efficiently handled by modern relational databases.[1] Likewise, computing hardware and algorithmic improvements continue to expand overall computational capacity. However, there remains a significant number of manual tasks in the curation of HTS data, especially in the expert evaluation of data quality. This includes identifying screening artifacts due to dispensing, detector, and execution errors, and applying cleanup to automated analyses, especially the fitting of CRC. The solution to this problem is to develop quality metrics that can be used to drive automated decisions and then either proceed or flag for expert intervention. In particular, we focus on automated solutions to the problem of curve fitting to improve the scaling of the data analysis pipeline to qHTS needs.

In order to address the challenges posed by the qHTS paradigm and at the same time to provide those wishing to implement qHTS with an alternative, free, scalable, and robust solution, we have developed the current approach and software. This software has enabled the annotation of over 7 million CRCs by NCGC in just the last three years and has facilitated the development of numerous small-molecule modulators of diverse biological systems. It provides automated

[1] Current off-the-shelf solutions for HTS data management are not tailored to the task of storing large numbers of concentration–response curves; some performance gains can be achieved simply by improving existing data schemas.

processing of qHTS data with robust algorithms for data masking and curve fitting, identifies cases when manual curation is required, and provides facile access to qHTS tools and data. Robustness of data analysis is the paramount concern. As few assumptions as possible are made during data analysis, and as few restrictions put upon the experimental design, allowing the full depth of the data to be realized. NCGC-developed software and source code implementing this approach are freely available from the authors at www.ncgc.nih.gov.

For the purposes of illustrating the finer points of each of step of the analysis, examples are provided from the analysis of qHTS assays. The first is the in vitro biochemical assay of a dehydrogenase target (31). The second is a cell-based, multiplexed assay of IκBα protein stability (12,16). This assay is concerned with discovering compounds that stabilize the IκBα protein without adversely affecting the cells themselves. This is measured by simultaneously capturing data about the relative expression of two proteins and provides an example of how multiplexed data is treated and ultimately interpreted.

qHTS DATA ANALYSIS OVERVIEW

qHTS generates a concentration-response profile for every compound during the primary run of the assay. Assays are optimized for robotic screening using 1536-well plates (between 3 and 10 μL assay volume). Details of compound preparation, storage, registration, and tracking of the vertically developed plate dilution series (i.e., interplate titrations) are described elsewhere (17). The compound collection is stored in DMSO and plated into the rightmost 1408 wells of 1536-well plates; the remaining wells are reserved for control samples that are run in each plate. The first four columns of 1536-well plates are reserved for the inclusion of appropriate controls onto each assay plate, to monitor assay performance and for the normalization of data. These controls comprise some or all of: (*i*) blank controls—wells without reagent, to monitor background signal; (*ii*) neutral controls—wells treated with DMSO vehicle, to monitor signal and noise in the baseline assay; (*iii*) maximum effect controls—reference agonist or antagonist of the reporter at saturating concentrations, to monitor the dynamic range of the signal; and (*iv*) control titrations, to track the reproducibility of the response dynamic and AC_{50} determinations. Compound titration series are plated in dilution across several plates, with each sample recurring at the same location on a plate. This allows flexibility in screening the collection; individual titration points can be omitted for assays with limited reagents. Compound collections with known bioactivity are typically plated in 15-point titration, starting at 10-mM compound concentration using a square root of fivefold dilution factor. Other screening compounds are typically plated in seven-point titration using fivefold dilution, starting at 10-mM compound concentration. Compound titration series are run in order of increasing concentration, which limits sample carryover between plates in the experiment (the tendency of certain samples to contaminate dispensing equipment and downstream assay wells). Typical assay protocols consist of (*i*) an initial uniform dispense of reagents into assay plates, (*ii*) a pinning (1536 aliquots are transferred in parallel using pins; the volume of transfer is not adjustable, approximately 20 nL) of 128 control samples from a control plate (a 1536-well plate with only the leftmost four columns occupied with samples), (*iii*) a pinning of 1408 compound samples from a compound plate, (*iv*) incubation of the assay mixture, and (*v*) measurement of activity. Measurements

of activity from each plate are parsed and then loaded into the database for analysis along with secondary information about the design of the experiment, including information on the type of plate used, the time the data was recorded, the location and concentration of tested samples, and the location and concentration of control samples.

INITIAL ASSESSMENT OF ASSAY PERFORMANCE

Gross assay performance is assessed using quality metrics from each plate and also visually. For each plate, CV (coefficient of variation), S/B (signal to background ratio), and RZ′ (robust Z-prime) are calculated (18). Trends in these metrics can indicate problems during the execution of the primary screen and corrective action can sometimes be taken, for example, by more frequent changes of reagents. "Failed plates" identified by abnormally poor values are inspected visually and, if necessary, excluded from further analysis. All plates are briefly inspected visually to identify other subtle abnormalities such as tip effects or blotting from cell dispenses. Unfortunately, there are no hard and fast rules for the use of these metrics in excluding plates and data. However, the number of plates from an experiment is usually limited to 1000 or 2000, so brief visual inspection is at least tenable. It is interesting to note that data from plates with very poor metrics can still be robust, depending on the type of failure observed. We have successfully identified active series from plates with RZ′s of zero (this problem reflected variability in the control compound used, not the ability of the assay to detect signal) and S/B ratios of one (control compound was accidentally omitted). Because assays are first validated on the production system with a modest screen before the production run, we already have a sense for the expected performance and robustness of an assay and can usually recover useful data when minor problems are encountered during the production run.

INTRAPLATE NORMALIZATION OF DATA

To control for minor deviations in experimental protocols like exposure time, incubation times, and other plate-handling artifacts, the raw data for each plate is normalized to the median responses of the positive- and neutral-control wells on that plate (19). The neutral-control response, measured using DMSO (which is the vehicle used to transfer samples), is normalized to 0% activity and the positive control is normalized to either 100% or −100% activity, depending on the type of assay. Typically, negative values are used to describe decreases in activity and positive values are used to describe increases in activity, although this is arbitrary. Ideally, assays are designed to monitor both increase and decrease in signal to capture of activation and inhibition activity within one execution of an assay protocol.

INTERPLATE CORRECTION OF DATA

While data normalization controls for some aspects of experimental variability between plates, it does not control for response variability within plates and for changes in that intraplate variability over time. For example, the detector itself may distort the measured data, and how a reagent is dispensed may affect total signal produced at the top of the plate relative to the bottom (time of dispense differences) or may manifest as striping across the plate (tip effects), or if there is a temperature gradient in an incubator, there may be a variation in background

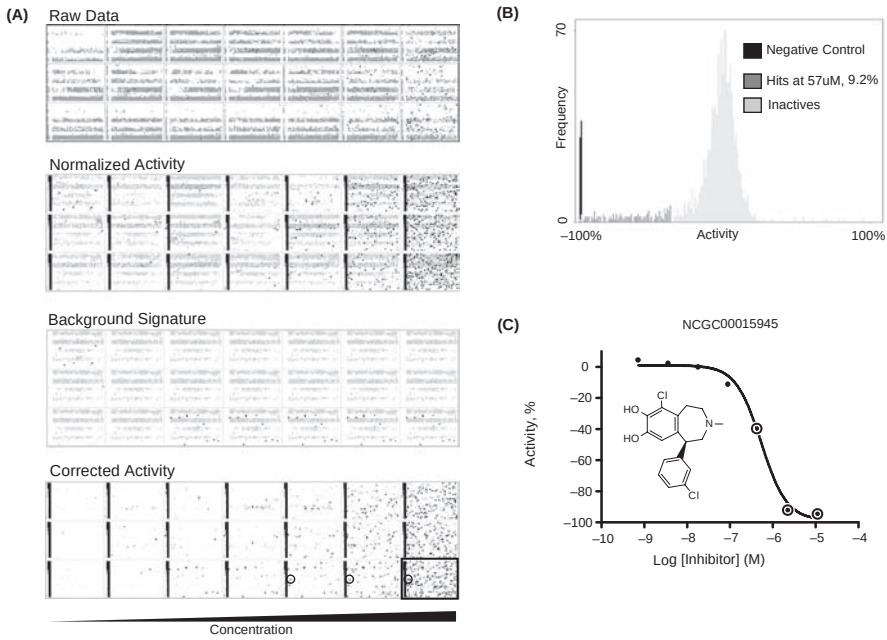

FIGURE 1 Data Normalization and Correction of Systematic Errors in qHTS: (**A**) An example set of three separate 1536-well plate series is shown on each row of plate heatmaps. Raw data represents the background fluorescent read (Read 1) of a 2-min time course. Normalized data revealed a background pattern that was detected and corrected for in final activity calculations. (**B**) Activity distribution of top concentration of one of the plate series is shown. Such normal distributions are used in traditional single-point screening and hits are typically determined using 3-σ or 6-σ thresholds. (**C**) qHTS leads directly to CRCs from the primary screen. Such CRCs are captured for all channels and time course reads available in assay systems.

from left to right across the plate. Most patterns in background response are not linear and change over the course of the experiment, reflecting some combination of multiple effects. These background perturbations are measured explicitly by using vehicle-only (DMSO) plates inserted at points during the course of the experiment, and the contribution to any particular assay plate well is modeled by interpolating between the nearest vehicle-only plates. This effect is then subtracted from the normalized data to produce "corrected" data [Fig. 1(A)].

The correction algorithm interpolates time and well location effects by identifying time-dependent, linear patterns. In other words, if the correlation between signal and time on the DMSO plates is statistically significant, we perform least-square linear fitting of the signal and calculate the correction factors for assay plates based upon their measurement time. If no significant correlation is observed (linear regression $p > 0.05$), the function resolves to a simple median correction algorithm (median per well across all DMSO plates in a run-set). Also, single-well outliers (wells greater than three standard deviations from the median value) are substituted with the median value. Other software (19,36) correct data using two basic algorithms: median and pattern based. In the median

correction algorithm, the median signal from control plates is simply subtracted. For pattern based correction, algorithmic details have not been published, although the results are superficially similar to the algorithm described above (20).

Data normalization and correction procedures attempt to control for normal experimental variability, while making as few assumptions as possible. Other analysis methods that depend on the distribution of activity across plates (19) often break down in the most interesting cases, because they tend to assume (*i*) a low hit rate and (*ii*) uniform distribution of those hits. They can be used to rescue individual plates, but the results can also be of dubious quality. For instance, sometimes an active library of related congeners appears on a single-assay plate, not distributed throughout the screening plates. There are some assays, for example, cytochrome P450s, where over half the molecules tested are reproducibly active. On the other hand, there are some cases where assumptions must be made to analyze the data, such as when an appropriate control cannot be found. Another challenging case is when significant edge effects are observed in the control-well region of the plate. Edge effects occur when the signal from wells at the edge of a plate is distorted with respect to the rest of the plate (21). Because the control wells are located on the far left of the plate, significant edge effects can render the control data useless—the variability in edge effects being on order the same as the difference between the neutral and positive controls. In these less than ideal cases, additional assumptions are introduced, and higher false-positive and false-negative rates are to be expected. We have treated data from such plates using several correction methods including median, tip, and discrete cosine transform (DCT) (22) approaches. The key idea for the empirical tip correction algorithm is that experimental noises tend to have patterns that reflect what instrument was used to perform assay, such as an eight-tip parallel dispenser. The DCT algorithm is designed to remove background noise, and it is based upon the fact that background noise tends to be signals of low frequency. In this algorithm, two-dimensional plate data is treated as an image, and the data are transformed by DCT into image space. In the image space, data of low-frequency spectra are removed, and then the image data is transformed back to real space using inverse DCT.

In addition to censoring bad plates during analysis, individual wells, rows, and columns on plates are also sometimes masked. This is done during the visual inspection of the corrected dataset, and also during the analysis of unusual CRCs (which tends to identify plates with strong artifacts more often than random compounds with bizarre concentration-responses). Common row artifacts include transient-tip problems from the multi-tip dispensers (e.g., clogged tips). Column artifacts are more often associated with edge effects, perhaps because of evaporation during long incubation times or unexpected temperature gradients across the plate (and condensation onto plate lids). Individual wells are less often masked, as these are usually appropriately flagged as outlier data during the curve-fitting process. But individual wells that are outliers over the entire course of the screen (e.g., a bad pin in the pin tool) are also sometimes masked.

LARGE-SCALE CONCENTRATION-RESPONSE DATA ANALYSIS

At this point, data analysis proceeds by formatting the data into arrays of concentration-response titrations as opposed to working with the data in

plate-associated matrices. It is assumed that the majority of plate-related artifacts have been identified, normalized, corrected, and, if necessary, censored, and that the remaining data can be interpreted in the concentration-response framework. Sample titration points are typically found at the same plate location across several plates and are tested in order of increasing concentration to help control for carryover effects (confirmation plates and some small libraries are fitted onto single plates). Sample titrations are first curve fitted to model the sample's concentration response and then these curves are classified to assess the significance of the observed concentration response.

Concentration responses are fitted using the Hill equation, although qHTS curve-fitting process is not necessarily limited to use of Hill model. Most software packages use one of several nonlinear optimization routines to efficiently fit this four-parameter model (23). However, most packages for fitting the Hill equation simply are not robust enough to fit the large numbers of CRCs from qHTS ($\gg$100,000 curves) without a great deal of visual inspection and manual curation. The biggest obstacle to the automation of curve fitting is the robust identification and masking of spurious outlier data points. Other packages which fit CRCs one-at-a-time do themselves a great disservice by assuming that each sample has a different variance, instead of using the observed variance across the entire screen to handicap outlier data points.

Outlier detection is inseparable from the task of CRC fitting. The present algorithm is designed to do both simultaneously, with the goal of minimizing human intervention. In common statistical practice, outlier points are detected by their deviation from the statistical mean. For example, if a data point is more than three standard deviations away from the expected mean, it may be considered an outlier. However, it is difficult to do this with dose–response data as we are assessing if a given data point is unusually larger than the mean at the same time that we are assessing what the mean (as a function of concentration) might be. Instead, we rely upon data trends to help detect data outliers and couple to curve fitting in three steps. The first calculates the deviation of a data point from an interpolated one on the line connecting the previous two data points or the previous and next data points. The second calculates the deviation of a data point from the expected value; for example, the data point at the lowest concentration is expected to be close to zero. The third is iteration; iterative curve fitting is performed, and if excluding a data point yields a much better fitting, the data point will be masked. The result is a fit of the four Hill parameters and a vector describing which points are masked.

Occasionally, a sample will exhibit a complicated concentration response involving both an initial increase in signal followed by a decrease in signal at higher concentrations, or vice versa. In most cases, this reflects a sample's multiple mechanisms of action, one at low concentrations and the other at higher concentrations, such as activating a signaling pathway at low concentrations while being cytotoxic at higher concentrations. In these cases, the most potent concentration response is fitted and the remaining higher concentration points are masked. Other more complicated responses are also possible. Now, these are only considered in follow-up, after the primary screen, where experiments can be designed to inspect and replicate the activity in detail. In the case of simple enzymatic assays, when bell-shaped curves are not anticipated, this masking

strategy is not used (though even with enzymatic assays, nonspecific activating compounds can sometimes inhibit at higher concentrations) (24).

$$y = S_0 + \frac{S_{\text{inf}} - S_0}{1 + (10^{\text{Log}\,AC50 - x})^n}$$

The Hill equation (25) taken as the basic concentration-response model and is fitted in log concentration space (23). The Hill equation has four parameters: S_0—activity level at zero concentration, S_{inf}—activity level at infinite concentration, AC_{50}—concentration at which activity reaches 50% of maximum level, and Hill coefficient (n)—measure of slope at AC_{50} (26). The goal in curve fitting is to determine the optimal values of the four parameters that best fit the experimental data. One commonly used quantitative measure for fitness of a model and the one we use here is R^2, which is defined as:

$$R^2 = 1.0 - \frac{\text{SS(Hill fit)}}{\text{SS(constant fit)}}$$

SS is the sum-of-square of the vertical distances of the points from the curve (Hill fit) or the line (constant fit). Typical nonlinear optimization algorithms (Levenberg-Marquardt, Simplex) start from randomly initialized values of the parameters, and iterate by evaluating partial derivatives of Hill equation with respect to each variable and then adjusting these parameters to optimize a target function like R^2. These algorithms are usually efficient and fast in optimization, but occasionally, algorithmic issues crop up (e.g., when derivatives are close to zero). These local optimization algorithms are also susceptible to being trapped in local minima. The present approach exhaustively samples a discretized parameter space during fitting. All possible values of the four parameters are enumerated to find the combination having the best R^2. Hill slope is bounded by the values 0.3 and 5.0 (values greater than 5.0 have little effect on the data fit given the sampling of titration points). AC_{50} values are bounded by the tested concentrations plus a set value. Parameters are optimized in two rounds. In the first round, it enumerates all possible values at relative large intervals (AC_{50}: 0.5, S_0 and S_{inf}: max[2.0 or range of $S/20$], slope: 0.2). In the second round, only the configuration space near the solution from the first round is sampled, and smaller intervals are used (AC_{50}: 0.05 or smaller, S_0 and S_{inf}: max[0.5 or range of $S/200$], slope: 0.1).

Ninety-five percent confidence intervals (95% CI) are generated for the Hill equation parameters to aid in the assessment of activity. Ninety-five percent CI is defined to be the interval that has a 95% chance of containing the true value of the parameter. Generally, there are three different algorithms for generating these intervals (23): (*i*) estimating the intervals based on measured response error and error propagation, (*ii*) simulating replicate experiments using the observed distribution of data, and (*iii*) using statistical significance to map possible parameter intervals. The third algorithm starts from a p-value, for example, 0.05 for a confidence of 95%, and estimates the F ratio based upon the given p-value and number of degrees of freedom. Parameter space is then sampled to find the intervals of these parameters in which the corresponding mean sum-of-squares are less than the F ratio times the sum-of-squares of the best-fit model. We adopt the third approach for several reasons. Simulating data via Monte Carlo is too slow for qHTS data processing, and it tends to produce optimistic confidence

intervals. Moreover, the curve-fitting algorithm already sweeps parameter space during parameter optimization, and so the computational cost in adopting this approach is small.

STATISTICAL ASSESSMENT OF CURVE SIGNIFICANCE

Having fitted a sample's concentration response to the Hill equation, we can then ask the questions, with what confidence can one reject the null hypothesis that a given sample has no concentration response and how significant is this concentration response relative to other sample responses in the assay? Note that these two questions are not addressed by the same test—the first assesses whether a compound may be considered an "active" and gives some idea whether one can expect to reproduce the result upon retesting. The second relates more specifically to what activity profile is of interest for a probe, whether it is potency or efficacy, or a particular mechanism of action, etc. We discuss statistical approaches to addressing the first question here and will discuss the second question in the next section.

Two common statistical tests for rejecting the null hypothesis (that no concentration response exists) are the F-test, where data are assumed to meet the normality assumption of analysis of variance, and the nonparametric Kruskal–Wallis test, for which there are no normality assumptions. The F-test is preferred, as it is a much better powered test with small sample sizes. It provides a p-value from the difference in residuals of the two models, accounting for differences in degrees of freedom and sample size. However, it is often the case that the F-test underestimates the true frequency with which single-point outliers do occur in HTS. Instead of assuming any particular data distribution, the Kruskal–Wallis test assesses whether the mean ranks of sampled points are the same. Deciding which test should be used is really a question of whether the assay data is normally distributed.

In general, for the several assay platforms that have been used at NCGC, we find that the data near the mean is very close to being normally distributed [Fig. 2(A)], but that there are very long tails on the distributions—in other words, dramatic outliers do occur with some regular frequency [Fig. 2(B)]. This probability distribution is characteristic of systems with two different scales of physics involved (such as in cavity formation in liquids) (27). One is the kind of run-of-the-mill noise that we encounter every day: random, normally distributed. The other, although very rare, is propagated with surprising strength. Example probability distributions from a few assays along with models of normally distributed data are plotted below and we can see that normality assumptions may be problematic. Some example concentration responses and their significance as estimated by the F-test and the Kruskal–Wallis test are shown in Figure 3. Neither is universally useful; the F-test seems to overestimate the significance of a curve with a single point of activity as compared to the complete curve with several points of significant activity, while the Kruskal–Wallis test is liable to overestimate the significance of inactive compounds that exhibit any regular trend (which are likely uncorrected background effects as opposed to a true compound response). The Kruskal–Wallis test is also underpowered for the typical CRC that qHTS generates (seven-point titrations).

The F-test compares a flat line fit model with the Hill equation fit model. In this test, the F ratio of the average sum-of-square of differences (SS) between the

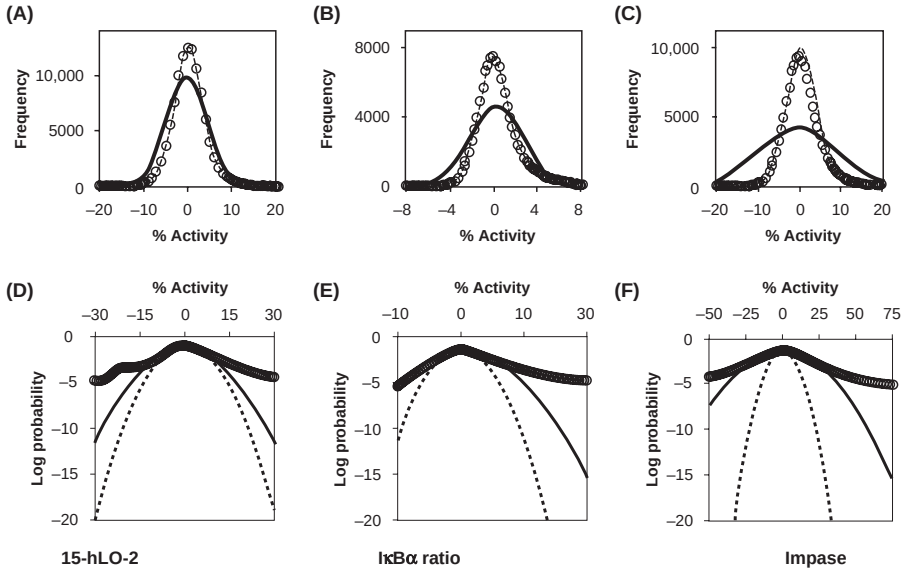

FIGURE 2 Error in activity measurements is normally distributed near the mean, but that distribution has very long tails, so that normality assumptions underestimate the true occurrence of large, random deviations in signal. Results from three very different types of assays are shown here and each gives similar results, including (*left*) a fluorescence-based enzymatic assay for dehydrogenase activity (31), (*center*) a cell-based luciferase reporter assay of IκBα stabilization (16), and (*right*) a cell-based fluorescence-polarization assay of impase inhibition. Activity at the lowest concentration tested was taken as a surrogate for untreated. Signal error (*circles*) is closely approximated by a normal distribution near the mean (*dotted line*), but not by one using the standard deviation over the entire dataset (*solid line*). Far from the mean (>3 SD), error is not well approximated by a normal distribution. Instead large error values are much more likely than predicted by normality assumptions. The probability of very large deviations in signal may be underestimated by normality assumptions by as much as 10^{15}.

flat and Hill models is calculated, and the corresponding significance or p-value is obtained from the F distribution. There are several modifications one could make to the F-test to improve the test: pooled variance (each compound does not possess its own unique variance; rather, the expected variance is a property of the assay technology/signal detector), concentration-dependent variance (the expected variance is larger near the AC_{50} of a compound owing to uncertainty in compound concentration in addition to typical signal noise), and bounds on residuals to balance overestimates of the significance of single-activity points. But none of these attempts have satisfactorily resolved the issue at present.

CURVE CLASSIFICATION IS A HEURISTIC ASSESSMENT OF CONCENTRATION-RESPONSE SIGNIFICANCE

As an alternative to the calculation of a p-value, NCGC characterizes concentration responses by placing them into curve classes (Fig. 4). A major advantage of this approach is that it is simple to understand and use because it segments along simple, useful characteristics like efficacy and the shape of the observed curve. A

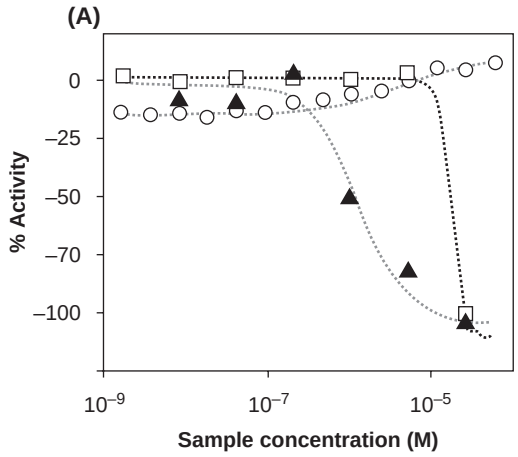

(B)

Sample	Curve Class	F Test p-value	Kruskal-Walls p-value
○	4	1×10^{-7}	3×10^{-4}
□	3	5×10^{-6}	0.65
▲	1.1	0.03	0.06

FIGURE 3 The F-Test and Kruskal–Wallis test do not appropriately rank significant sample responses. Shown are three concentration responses obtain from screening. The most potent concentration response has the least significant *p*-value using an F-Test.

major limitation, as with all classification approaches, is that very similar curves can have very different curve classes near the descriptor boundaries. Nevertheless, it is an efficient way to summarize the diversity of curve types found in a screen and prioritize compounds for analysis and confirmation. Curves are first sorted by the number of "significant" points in the curve. "Significant" here means a point greater than three standard deviations from zero. Standard deviation is measured from a fit of data at the lowest concentration tested to a normal distribution. Inactive curves, class 4, have no significant data points. Partial curves, class 2, have at least one significant point and one supporting point (an adjacent point with activity greater than one standard deviation), as opposed to class 3 curves with only a single point of activity at their highest (unmasked) concentration. Complete curves, class 1, have more than one point within 80% of the maximum efficacy. Classes 1 and 2 are then subdivided by efficacy (>80% of control) and by R^2 of fit (>0.9).

Curve class	Asymptotes	r^2	Efficacy	Description
1	Higher and lower	≥ 0.9	> 80%	1.1: Complete curve; high efficacy
			Min - 80%	1.2: Complete curve; partial efficacy
		< 0.9	> 80%	1.3: Complete curve; high efficacy; poor fit
			Min - 80%	1.4: Complete curve; partial efficacy; poor fit
2	Lower only	≥ 0.9	> 80%	2.1: partial curve; high efficacy
			Min - 80%	2.2: partial curve; partial efficacy
		< 0.9	> 80%	2.3; partial curve; high efficacy; poor fit
			Min - 80%	2.4; partial curve; partial efficacy; poor fit
3	Lower only		≥ Min	3: Single point of activity
4			< Min	4: Inactive
5			≥ Min	5: Inconclusive

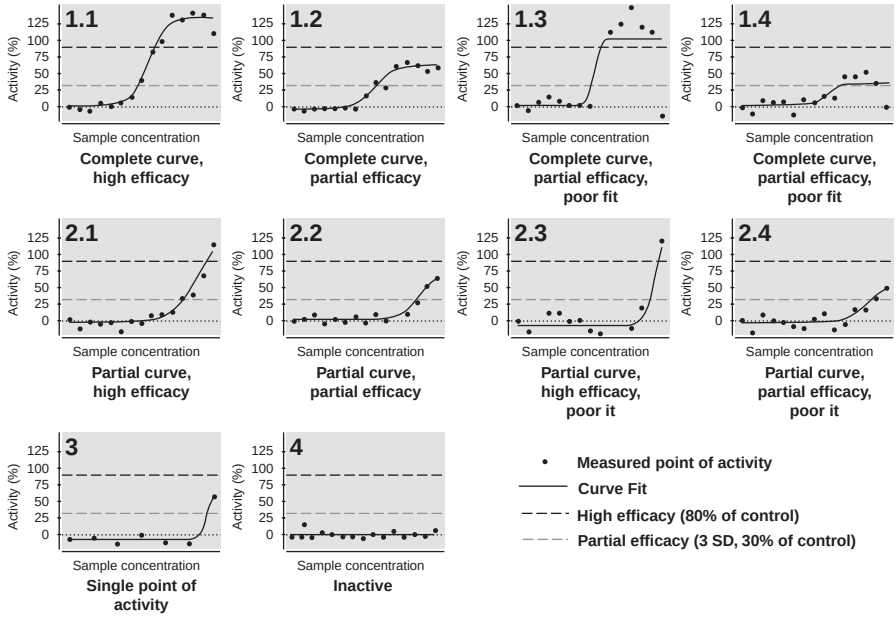

FIGURE 4 Curve classification as a heuristic assessment of significance. Shown are the criteria used to classify concentration responses, and example concentration responses for each class, taken from actual screening data.

Samples with the highest confidence are those in curve class 1.1. For most projects, active compounds are those in curve classes 1.1, 1.2, 2.1, and possibly 2.2. Occasionally, one can afford to be stringent enough and only consider those samples with responses greater than six standard deviations as opposed to three. Class 4 compounds, typically the vast majority of assayed samples, are considered inactive, with sample AC_{50}s estimated to be at least greater than twice the highest concentration tested, if not higher. The remaining classes are considered less confident or inconclusive.

Curve class is not static once it has been assigned after curve fitting, instead curve classes are used to drive decisions about which curve fits require manual curation. Manually curating which data points are masked can sometimes improve an R^2 and can cause a curve class to change, and those in curve class 5 always require manual curation. The most problematic concentration responses are automatically assigned curve class 5 based on considerations like the direction of activity (observing alternately both increases and decreases in signal over a short concentration range) and unusually large signal at low sample concentrations (zero compound effect is estimated to be >30% of control). Typically, there are only a handful to perhaps a few score of such curves from any qHTS screen. Assays with large numbers of class 5 curves generally have doubtful utility. After class 5, curve class 1.3 and 2.3 deserve the most attention. Curve class 1.4 activity more often reflects problems correcting baseline artifacts rather than true compound activity. These curve classes speed the analysis process by directing curation efforts to the CRCs most in need of curation. In general, we do not observe many inconclusive CRCs with qHTS, which reflects the robustness of the cumulative assay, curve fitting, and classification process.

Curve classification is a useful measure of significance, as measured by the confirmation rate of samples from the different curve classes. While curve classification does not generate a calibrated estimate of significance, a *p*-value, this heuristic measure can indicate which samples are most likely to reproduce upon confirmation. Table 1 shows the confirmation rate of screening hits as a function of curve class. Confirmation here means that the sample either showed activity in both the original and confirmation experiments or that it was inactive (curve class 4) in both—subtle changes in curve class upon confirmation are still counted as having confirmed. As expected, the high-efficacy curve classes have better confirmation rates. Class 4 samples' confirmation rate (86%) is probably an underestimate of the true reproducibility of this class; this set was highly enriched for samples expected to be FN in the original screen based on observed

TABLE 1 Example Confirmation Rates as a Function of Curve Class for Four Selected Projects

	Project (confirmed/ tested)				Summary (all projects)	
Curve class	CRE	PK	TSHR	15-hLO-2	Confirmed/ tested	Confirm rate (%)
1.1	44/44	7/9	12/14	2/2	65/69	94
1.2	11/12	1/9	3/9	11/17	26/47	55
1.4	2/2	1/4	1/2	0/1	4/9	44
2.1	21/21	9/11	46/69	4/5	80/106	75
2.2	3/3	1/4	-	6/19	10/26	38
2.4	-	-	0/1	-	0/1	0
3	1/1	0/1	3/3	1/3	5/8	63
4	16/21	36/47	81/88	58/66	191/222	86

Two of the curve class 1.1 samples that did not reproduce were extensively characterized by analytical chemistry, but no significant differences in sample composition were found between the original and confirmation samples. The original perceived activity is likely because of experimental noise. Confirmation rates here underestimate the true accuracy of qHTS. Suspected false-positive and false-negative samples were often prioritized for confirmation based on SAR considerations; the samples reported here are accordingly biased. Screens are described in PubChem (31,33–35).

structure–activity relationships and similarity to other active compounds. The most important factor affecting the overall confirmation rate of qHTS is the number of hits found in a screen; with more hits, the confirmation rate improves. When there are very few hits in a screen, there is a higher probability of noise and other assay artifacts conspiring to produce concentration responses that look real.

It is interesting to compare these observed confirmation rates with the *p*-value estimates from the F-test exercise above. The F-test was designed to estimate how often by chance a sample would appear to have the observed concentration response while in reality the sample actually had no concentration response. This is very similar to the confirmation rates being measured here, although the selection of tested samples in this case was biased by structure–activity relationship considerations; the best series were tested in confirmation, which may bolster hit rates. Nevertheless, curve class 1.1 curves confirm only 94% of the time across these four projects, even though all these sample curves had *p*-values less than 0.001 in the original assay. In fact, the correlation between confirmation rates and *p*-value is modest in comparison to curve class. Using a threshold α of 0.00001 (the *p*-value below which results are considered significant) only increases the confirmation rate to 88% versus the confirmation rate for all samples, which was 78%.

ACTIVITY IN MULTICHANNEL ASSAYS IS CHARACTERIZED USING PHENOTYPE

Following primary data analysis, each compound is sorted by phenotype, which is compiled from the responses of the individual data layers to provide one unified assessment of a sample's activity. For example, if the assay is an in vitro fluorescence-based enzymatic assay, and there is only one layer of data obtained, then the phenotype simply reflects whether the signal increased, decreased, or was unaffected by the compound—activator, inhibitor, or inactive. For more complicated assays that combine a primary readout like protein expression with a secondary readout like viability, the phenotype reflects combined readouts from both data layers—inhibitor if expression decreases but viability is unaffected, or cytotoxic if both decrease. A more complicated example is shown for a β-lactamase reporter assay (28) in Table 2. For each phenotype, one representative data layer is chosen for use in reporting a sample's AC_{50} etc. That data layer can differ depending on the type of activity observed, for instance inhibitors in a β-lactamase reporter assay use the ratio channel (which is more robust than the 460-nm channel), while the 530-nm channel activity is reported for cytotoxic compounds.

While assessing sample phenotypes, a distinction is made between secondary assays and secondary data channels. Secondary data channels are tightly controlled for performance with the primary data channel by virtue of the fact that the same assay mixture is being interrogated twice. Secondary assays, on the other hand, having been run on different days, on different sets of library plates, with different reagents, introduce new sources of experimental variability into the analysis process. Sample phenotypes are generally used to integrate secondary data where experimental variability has been as tightly controlled as possible (although this is a gray area). Counterscreens using different buffer

TABLE 2 β-Lactamase Reporter Assay Phenotypes

Phenotype	Ratio (530/460)	530 Channel (green)	460 Channel (blue)
Inhibitor	Inhibition	Inactive	Inhibition
Activator	Activation	Inactive	Activation
Fluorescent[a]	Inactive	Activation	Activation
Cytotoxic[a]	Inactive	Inhibition	Inhibition
Inactive	Inactive	Inactive	Inactive
Possible inhibitor	Inhibition	Activity(460) > activity(530)	Inhibition
Possible activator	Activation	Activity(460) > activity(530)	Activation
Possible fluorescent[a]	N/A	Activation	Activation/inactive
Possible cytotoxic[a]	N/A	Inhibition	Inhibition/inactive
Possible inactive	Inactive	N/A	N/A
Inconclusive	N/A	N/A	N/A

GeneBLAzer® (28) assays measure fluorescence activity at 530 nm and 460 nm, which reflects the distribution of a cell-permeable dye into a cell, and the presence of the β-lactamase reporter.
[a]These phenotypes are consistent with fluorescence and cytotoxicity artifacts, but are not conclusive for them.

conditions, different cell lines, etc. are employed at the structure–activity relationship (SAR) stage of analysis rather than at the sample level, to add an extra level of robustness into the analysis (29).

qHTS FACILITATES HIT TO LEAD PROGRESSION

Decisions on which activity to follow-up are ultimately made for compound series (if SAR exists), or on potent singletons (if no SAR exists) and known bioactives, not sample phenotypes. Establishing SAR strengthens the results of data analysis by selecting for a kind of self-consistency. To generate SAR, we developed a workflow that is systematic and exhaustive. First, we define rules of determining an active set of compounds for the assay. These include decisions on inhibitors and activator phenotypes, target selectivity and counterscreen information, curve class, cytotoxicity filters, etc. This process eliminates many false-positive series that appear to have SAR and show reasonable CRCs, and has been validated by our follow-up experiments. To cluster compounds, hierarchical agglomerative clustering with a 0.7-Tanimoto cutoff is performed using Leadscope fingerprints (30). For each cluster, maximal common substructures (MCS) are extracted and each MCS is trimmed manually to create a list of scaffolds. Each scaffold is then precisely defined to indicate the number of attachments, ring size variability, etc. Negative assay data is also included in the series analysis. Singletons are reported separately with their individual profiles. SAR series are ranked by their activity profile and other set criteria. When analysis of primary screen is complete, the assay description and data are deposited into PubChem. Two detailed examples of the analysis process are provided in subsequent sections.

In addition to the analysis of the screening collection for SAR, active samples with previously reported activity are analyzed in depth. The NCGC library has been enriched with such samples both to help validate the assay biology and to provide useful starting points for new projects. Samples with known bioactivity help to validate assays by confirming expected sources of activity modulation (known targets) and by identifying novel ones (e.g., histone deacetylase inhibitors that can modulate a cellular response to G-protein coupled receptor activation) that challenge the conventional interpretation of an assay's results. These results help generate new questions and experiments that can help us

understand the utility of an assay in modeling a biological process, as well as gaining a deeper understanding of the biological process itself.

CASE STUDY: DEHYDROGENASE DATA ANALYSIS

HADH2, 17β-hydroxysteroid dehydrogenase type 10, was screened by using β-hydroxybutyryl coenzyme A as an electron donor and nicotinamide adenine dinucleotide (NAD^+) as an electron acceptor/cofactor to identify novel small-molecule inhibitors of the enzyme (31). An increase in the fluorescence intensity due to conversion of NAD^+ to NADH was used to measure the enzyme activity. HADH2 catalyzes the NAD^+-dependent oxidation of a variety of substrates including acyl-CoAs, androgens, and neurosteroids as well as bile acids (31,32). The role in neurodegeneration by binding to amyloid-peptide led to its identification, and mutations in its gene appear to be causative for 2-methyl-3-hydroxybutyryl-CoA dehydrogenase deficiency. The enzyme was produced by *Escherichia coli* fermentation as His-tagged recombinant for the purpose of X-ray structure determination, and had been mass spectrometry characterized.

A 1536-well miniaturized qHTS protocol was developed for HADH2 (31). The substrate and cofactor solution consisted of 1-mM NAD^+ and 90-μM β-hydroxybutyryl coenzyme A, 100 mM, and Tris-HCl pH 9.0 with 0.01% Tween-20 was used as the buffer, and 20 nM of the enzyme was used in the protocol. A qHTS of 527 1532-well plates consisting of 73,177 diverse small molecules was run against HADH2. Final sample concentrations in the assay ranged from 2.9 nM to 57 μM. Plates were read on a ViewLux™ CCD imager (Perkin-Elmer, Waltham, Massachusetts, U.S.A.) using 360-nm excitation and 450-nm emission fluorescence protocol. Time course data were collected for each assay plate and kinetic data were processed using in-house developed software. For each sample at each concentration, five time points were collected over the course of two minutes. Data were processed using ordinary least-square regression to determine slope and intercept of linear fit. A calculated layer of activity was generated using the difference of last and first time points, and data were normalized to neutral (uninhibited) and no enzyme controls. Tip dispense problems were observed during the qHTS [Fig. 1(A)]. DMSO control plates inserted uniformly throughout the validation were used to capture trends in the underlying dispense pattern and were applied on a per-plate, per-well basis on the normalized data. The resulting corrected activity improved the RZ′ of the screen from 0.72 to 0.84, but more importantly, it eliminated a significant source of potential FP in the screen. Such pattern corrections applied in single-point screening can lead to questionable under- or over correction of activity data leading to increased FP or FN. The redundancy of qHTS plate-based titrations of the same set of samples across 7 to 15 plate series gives more confidence in the application of such correction algorithms.

Typically, activity from a screening campaign is assumed to be normally distributed. Figure 1(B) shows such a distribution for one of the plates in the HADH2 screen. One common approach for hit identification is to determine 3-σ and 6-σ thresholds for the screen and categorize compounds as inactive (<3 σ), moderate actives (between 3 and 6 σ), and actives (>6 σ). In qHTS, activity is defined in terms of concentration-dependent pharmacological profiles [Fig. 1(C)]. Additionally, CR profiles are captured across multiple channels of data and across time courses in the case of kinetic-based reads. While traditional

single-point distributions give a slice of apparent activity, qHTS provides additional valuable information on concentration-dependent artifacts such as autofluorescence of compounds.

An apparent active in qHTS is a sample that shows a significant concentration-dependent response. To identify actives in the HADH2 screen, all curves were first fit through an automated data analysis process. Curves were classified into full-titration inhibitors and activators, partial modulators, partial curves with weak potencies, and single-point actives and inactives based on the curve classification scheme. Figure 5(A) shows an activity plot of all samples screened against all of their respective concentrations. Samples that were classified as class 4s were considered inactive. Samples showing signal increase were likely suspect fluorescent artifacts or were potential activators of HADH2. Likewise, ones that gave a decrease in signal were fluorescent artifacts and real actives. Because of the blue-shifted fluorescence readout of this assay, we anticipated a high level of fluorescence interference when assessing the activity outcomes of the screen (13). Of the 73,177 compounds tested against HADH2, 15% gave concentration-dependent response. To eliminate compounds that gave false inhibition solely because of fluorescence, the concentration-response profile of the background fluorescence read was analyzed (the CR from the first read of the time course of each sample). Figure 6(A) shows the distribution of the raw background reads for all compounds at their highest concentration tested. A threshold for read 1 cutoff was determined using the distribution of read 1 of the neutral control wells in the screen. All compounds greater than this threshold (1.6 in log RFU for this screen) were flagged as potentially autofluorescent for the spectral region for this assay. The slopes of the kinetic plots were used to retrieve potential real actives from the flagged compounds. Using this triaging, >12% of the compounds screened were flagged as fluorescent artifacts.

Once filters based on auxiliary information such as background fluorescence are applied in the qHTS data analysis process, a starting point for SAR analysis is established [Fig. 5(B)]. In the HADH2 screen, 2088 filtered actives were used for compound clustering using Leadscope fingerprints. Hierarchical agglomerative clustering with a 0.7-Tanimoto cutoff was used to generate 140 clusters and 113 singletons. By contrast, clustering on the full 15% apparent actives leads to 529 clusters and 334 singletons. The chemical series extracted from clusters leads to numerous potential starting points for chemistry optimization. Thus the filtering of qHTS data provides a significant advantage in the prioritization of chemotypes. To validate informatics prediction of separating autofluorescent series from real actives, two HADH2 series were selected for follow-up [Fig. 6(B) and 6(C)]. A triazolo thiadiazole series showed high background fluorescence and steady slopes in the time course data whereas the benzo[d]azepines were shown to be likely real actives. Subsequent follow-up confirmed both findings. Thus large-scale filtering of qHTS data based on proper assay design leads to information that can be used to allow proper prioritization of chemical series, thus saving valuable chemistry resources and time.

Case Study: IκBα Data Analysis

A cell-sensor assay for stabilization of IκBα was developed in the activated B cell-like diffuse large B-cell lymphoma cell line OCI-Ly3 (12). This cell line expresses known nuclear factor κB (NFκB) target genes due to high constitutive activity of

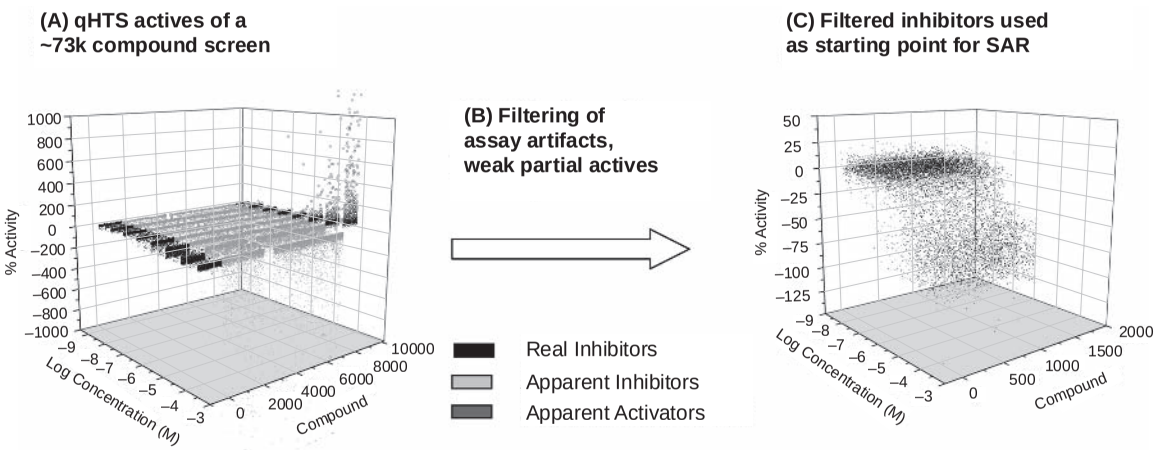

FIGURE 5 Filtering of qHTS data for analysis activity: (**A**) 73,177 compounds were screened against an oxidoreductase, HADH2; 15% of compounds demonstrated activity response in the assay those responses are shown; (**B**) Data analysis filters maximized use of qHTS design to eliminate fluorescent compounds and compounds showing weak partial response; (**C**) 2088 filtered inhibitors (20% of all actives) were used as a starting point for compound clustering and SAR.

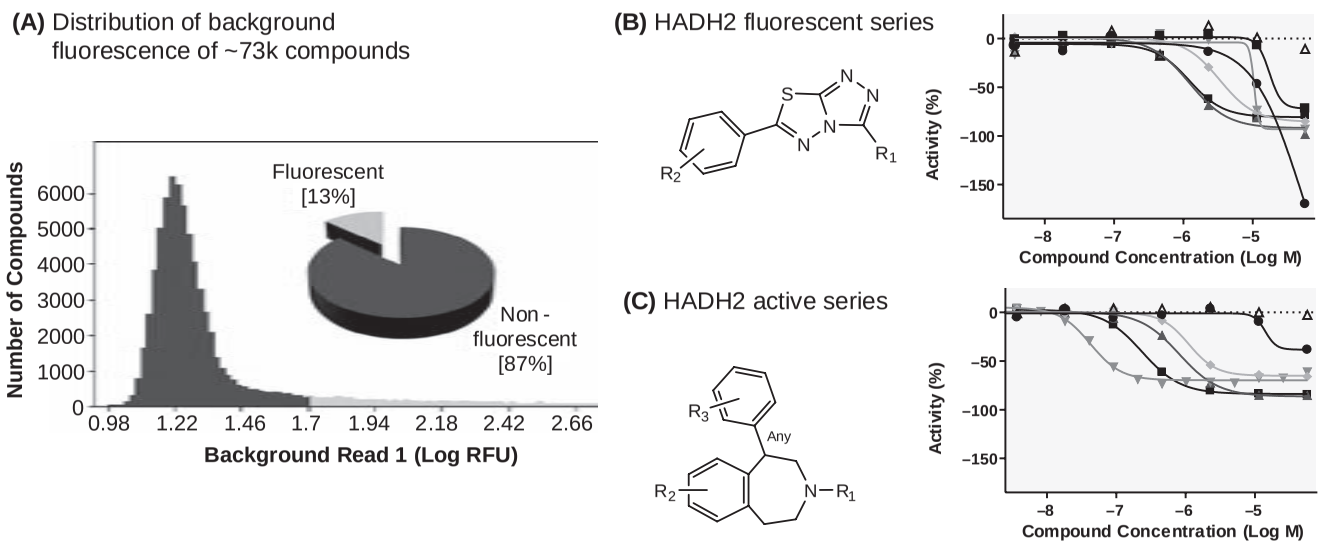

FIGURE 6 Elimination of fluorescent SAR series: (**A**) Distribution of the raw background fluorescence read captured for all compounds screened against HADH2; compounds in red designate highly fluorescent ones. (**B**) An example fluorescent series, triazolo thiadiazoles, whose SAR is due to intrinsic fluorescence and not activity. (**C**) An active series, benzo[d]azepines, whose response in the assay was due to HADH2 activity and not fluorescence.

IκB kinase (IKK), which phosphorylates the protein IκBα leading to proteasomal degradation of IκBα and activation of NFκB. The cell-sensor assay uses green- and red-light-emitting beetle luciferases, with the green luciferase fused to IκBα (IκBα-CBG68) and the click beetle red luciferase (CBR) present in its native state. The IκBα-CBG68 reporter functions as a sensor of IKK and proteasome activity, while CBR serves to normalize for cell number and nonspecific effects. Both reporter constructs were stably integrated and placed under the control of an inducible promoter system, which increased fold responsiveness to inhibitors when assay incubations were performed simultaneously to reporter induction by doxycycline. The assay was miniaturized to a 1536-well plate format and showed a Z' of 0.6. The CRCs for the IκBα-CBG68 and CBR signals were then used to identify specific stabilizers of IκBα, such as IKK inhibitors or proteasome inhibitors, which increased the doxycycline-induced rise in IκBα-CBG68 without affecting the rise in CBR. Known and unexpected inhibitors of NFκB signaling were identified. The development and merits of this assay are discussed in detail in Davis et al. (12).

Concentration-response titrations were first fitted to the Hill equation and then classified. For the two-color dual luciferase assay, these curve classes were assigned for all three data layers (green and red luminescence and the green/red ratio). The curve classification used was a modification from that used in Inglese et al. (10). The earlier curve classification scheme was devised for use with an enzymatic screen. In the present assay, we observed that the noise in this cell-based dataset was generally larger than what is typically found for such enzymatic screens. We therefore modified the curve classification in three significant ways. (*i*) The efficacy cutoff that was considered statistically significant was set to six standard deviations above the mean. The mean and standard deviations were calculated by fitting the distribution of percentage activity at the lowest concentration tested to a normal distribution. (*ii*) The r^2 requirements for curve fits were relaxed from 0.9 to 0.8. This was not necessary with the enzyme screen, as none of the curve fits had an $r^2 < 0.9$. (*iii*) We tailored the fitting of titration data to the Hill equation to allow for "bell-shaped" curves. This was because we observed reproducible activities for several compounds where the observed activity first increases, then decreases, with increasing concentration, potentially indicating that the compound has two mechanisms of action—one at lower concentrations, the other at high concentrations of compound. Sets of points at higher concentrations were iteratively masked to maximize r^2 of these bell-shaped type curves. After assignment, curve classes of all three datasets were used to sort the compounds into phenotypic categories. This was achieved by a script that uses the CRC classes of the ratio and the green and red readouts as inputs. All three datasets are necessary to characterize the full range of responses. The script was constructed by iteratively applying heuristic criteria to compounds and examining the classification of the compounds by hand. The first decision point examined the performance in the green layer, and so forth, until a phenotypic class number was assigned to each compound.

Use of the algorithm to sort the concentration–response curve classes into categories resulted in partitioning compounds into four phenotypic categories: IκBα stabilizers, signal activators, signal inhibitors, and inactive. IκBα stabilizers were consistent with compounds that were selective for stabilization of the IκBα-CBG68 fusion. Signal activators (Fig. 7) exhibited both the green and

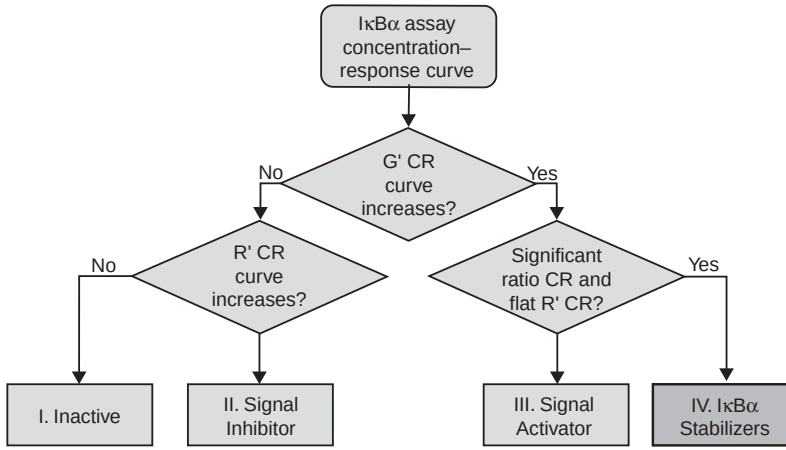

FIGURE 7 IκBα phenotype classification. Flow chart for triaging concentration–response (CR) curves into phenotypic categories for the IκBα assay. Compounds are triaged using the concentration–response curve classes of the G′/R′ ratio and G′ (IκBα-CBG68) and R′ (CBR) readouts. The first decision point considers whether a significant increase in G′ readout has been observed. If it has not, and the R′ readout has also been flat, the compound is considered Inactive. If the G′ readout did not increase, but a decrease in the R′ readout was observed, the compound was categorized as a Signal Inhibitor. If an increase in G′ readout was observed, then depending on whether that increase was selectively observed in the G′ readout and not also the R′ readout, the compound was categorized as a Signal Activator (not selective) or an IB Stabilizer (selective). Compounds that increased the red luminescence without increasing the green luminescence showed curve fits of low confidence and were placed in the Inactive category. Specific criteria for differentiating IB Stabilizers from Signal Activators included either of the following statements being true: (*i*) no significant change in R′ was observed, or (*ii*) if R′ increased, the ratio was also increasing, and if so, the increase in R′ was 50% of G′.

red luminescent responses, with 89% of these compounds showing an inactive concentration–response relationship in the ratio layer. For this category, we also observed inactive fits in the red luminescent data. This is because the red luminescent data was nosier than the other datasets; therefore, marginal increases in the red luminescent were often fit to an inactive curve class. The ratio layer also showed these compounds to be inactive. Overall, this category is consistent with compounds that showed nearly equal activation of the green and red luminescent signals. Signal Inhibitors showed inhibitory CRCs in the red and green luminescent dataset, with 45% of these compounds showing an inactive concentration–response relationship in the ratio layer. As mentioned above, the green luminescence showed less sensitivity to inhibitors than the red luminescence, and we observed 68 compounds showing an inactive concentration–response relationship within the green luminescence. An artificial rise in the ratio results when this is associated with an inhibitory curve within the red luminescent dataset. Inhibition curves within the ratio dataset were also found within this category, suggesting the presence of compounds that decreased the stability of the IκBα-CBG68 reporter, although, as mentioned above, these curves were of low quality. Finally, the Inactive category was categorized by compounds that did not show any concentration-effect dependence in any of three datasets.

REFERENCES

1. Cox B, Denyer JC, Binnie A, et al. Application of high-throughput screening techniques to drug discovery. Prog Med Chem 2000; 37:83–133.
2. Spencer RW. High-throughput screening of historic collections: Observations on file size, biological targets, and file diversity. Biotechnol Bioeng 1998; 61(1):61–67.
3. Schneider G, Clement-Chomienne O, Hilfiger L, et al. Virtual screening for bioactive molecules by evolutionary De Novo design. Angew Chem Int Ed Engl 2000; 39(22):4130–4133.
4. Marriott DP, Dougall IG, Meghani P, et al. Lead generation using pharmacophore mapping and three-dimensional database searching: Application to muscarinic M(3) receptor antagonists. J Med Chem 1999; 42(17):3210–3216.
5. Milne GW, Nicklaus MC, Wang S. Pharmacophores in drug design and discovery. SAR QSAR Environ Res 1998; 9(1–2):23–38.
6. Gane PJ, Dean PM. Recent advances in structure-based rational drug design. Curr Opin Struct Biol 2000; 10(4):401–404.
7. Huang N, Jacobson MP. Physics-based methods for studying protein-ligand interactions. Curr Opin Drug Discov Dev 2007; 10(3):325–331.
8. Coupez B, Lewis, RA. Docking and scoring—theoretically easy, practically impossible? Curr Med Chem 2006; 13(25):2995–3003.
9. Hillenmeyer ME, Fung E, Wildenhain J, et al. The chemical genomic portrait of yeast: Uncovering a phenotype for all genes. Science 2008; 320(5874):362–365.
10. Inglese J, Auld DS, Jadhav A, et al. Quantitative high-throughput screening: A titration-based approach that efficiently identifies biological activities in large chemical libraries. Proc Natl Acad Sci U S A 2006; 103(31):11473–11478.
11. Kozarich JW. New LSD therapies unfolding. Chem Biol 2007; 14(9):976–977.
12. Davis RE, Zhang Y-Q, Southall N, et al. A cellular assay for IκBα stabilization using a two-color dual luciferase-based sensor. Assay Drug Dev Technol 2007; 5:85–103.
13. Simeonov A, Jadhav A, Thomas CJ, et al. Fluorescence spectroscopic profiling of compound libraries. J Med Chem 2008; 51(8):2363–2371.
14. Xia M, Huang R, Witt KL, et al. Compound cytotoxicity profiling using quantitative high-throughput screening. Environ Health Perspect 2008, 116(3): 284–291.
15. Huang R, Southall N, Cho MH, et al. Characterization of diversity in toxicity mechanism using in vitro cytotoxicity assays in quantitative high throughput screening. Chem Res Toxicol 2008; 21(3):659–667.
16. PubChem, IkB Signaling qHTS Assay. http://pubchem.ncbi.nlm.nih.gov/assay/assay.cgi?aid=445.
17. Yasgar A, Shinn P, Jadhav A, et al. Compound management for quantitative high-throughput screening. JALA 2008; 13(2):79–89.
18. NCGC, Eli Lilly and Company. Assay Guidance Manual. http://www.ncgc.nih.gov/guidance/index.html.
19. Malo N, Hanley JA, Cerquozzi S, et al. Statistical practice in high-throughput screening data analysis. Nat Biotechnol 2006; 24(2):167–175.
20. Heyse S, Brodte A, Bruttger O, et al. Quantifying bioactivity on a large scale: quality assurance and analysis of multiparametric ultra-HTS data. JALA 2005; 10(4):207–212.
21. Lundholt BK, Scudder KM, Pagliaro L. A simple technique for reducing edge effect in cell-based assays. J Biomol Screen 2003; 8(5):566–570.
22. Britanak V, Yip P, Rao KR. Discrete Cosine and Sine Transforms. Academic Press, 2006.
23. Motulsky H, Christopoulos A. Fitting models to biological data using linear and nonlinear regression: A practical guide to curve fitting. New York: Oxford University Press, 2004.
24. Goode DR, Totten RK, Heeres, JT, et al. Identification of promiscuous small molecule activators in high-throughput enzyme activation screens. J Med Chem 2008; 51(8):2346–2349.
25. Hill AV. The possible effects of the aggregation of the molecules of haemoglobin on its dissociation curves. J Physiol 1910; 40(Suppl):iv–vii.

26. Weiss JN. The Hill equation revisited: uses and misuses. FASEB J 1997; 11(11):835–841.
27. Huang DM, Chandler D. Cavity formation and the drying transition in the lennard-jones fluid. Phys Rev E Stat Phys Plasmas Fluids Relat Interdiscip Topics 2000; 61(2):1501–1506.
28. Invitrogen, GeneBLAzer® Technology Overview. http://www.invitrogen.com/site/us/en/home/Products-and-Services/Applications/Drug-Discovery/Target-and-Lead-Identification-and-Validation/g-protein_coupled_html/GPCR-Cell-Based-Assays/GeneBLAzer-Theory.html.
29. Yan SF, Asatryan H, Li J, et al. Novel statistical approach for primary high-throughput screening hit selection. J Chem Inf Model 2005; 45(6):1784–1790.
30. Leadscope Leadscope, Columbus, OH: Leadscope.
31. PubChem, qHTS Assay for Inhibitors of HADH2. http://pubchem.ncbi.nlm.nih.gov/assay/assay.cgi?aid=886.
32. Shafqat N, Marschall HU, Filling C, et al. Expanded substrate screenings of human and Drosophila type 10 17beta-hydroxysteroid dehydrogenases (HSDs) reveal multiple specificities in bile acid and steroid hormone metabolism: Characterization of multifunctional 3alpha/7alpha/7beta/17beta/20beta/21-HSD. Biochem J 2003; 376(Pt 1):49–60.
33. PubChem, Cell signaling CRE-BLA (Fsk stim). http://pubchem.ncbi.nlm.nih.gov/assay/assay.cgi?aid=662.
34. PubChem, Pyruvate Kinase. http://pubchem.ncbi.nlm.nih.gov/assay/assay.cgi?
35. PubChem, qHTS Assay for Agonists of the Thyroid Stimulating Hormone Receptor. http://pubchem.ncbi.nlm.nih.gov/assay/assay.cgi?aid=926.
36. GeneData GeneData Screener, GeneData AG, Basel, Switzerland.

20 Application of Nanobiotechnologies for Drug Discovery

K. K. Jain

Jain PharmaBiotech, Blaesiring, Basel, Switzerland

INTRODUCTION

Nanotechnology is the creation and utilization of materials, devices, and systems through the control of matter on the nanoscale, that is, at the level of atoms, molecules, and supramolecular structures. Given the inherent nanoscale functional components of living cells, it was inevitable that nanotechnology will be applied in biotechnology giving rise to the term nanobiotechnology, which will be used in this chapter. An up-to-date description of nanobiotechnologies and their applications in healthcare is given in a special report on this topic (1). This chapter will discuss the use of nanotechnologies—nanoparticles and various nanodevices such as nanobiosensors and nanobiochips—to improve drug discovery. Microfluidics has already proven useful for drug discovery. Through further miniaturization, nanotechnology will improve the ability to fabricate massive arrays in small spaces using nanofluidics and the time efficiency. This would enable direct reading of the signals from nanofluidic circuits in a manner similar to a microelectronics circuit where one does not require massive instrumentation. This would increase the ability to do high-throughput drug screening. Application of nanobiotechnologies to various stages of drug discovery is shown schematically in Figure 1. A classification of various nanobiotechnologies used for drug discovery is presented in Table 1.

APPLICATION OF NANOPARTICLES FOR DRUG DISCOVERY

Nanoparticles—gold nanoparticles, quantum dots, micelles, dendrimers, and carbon nanotubes—have received a considerable attention recently with their unique properties for potential use in drug discovery. Role of some of these will be described briefly.

Gold Nanoparticles

It is important to track drug molecules in cells. Gold nanoparticles can be observed by multiphoton absorption-induced luminescence (MAIL), in which specific tissues or cells are fluorescently labeled using special stain. However, gold nanoparticles can emit light so strongly that it is readily possible to observe a single nanoparticle at laser intensities lower than those commonly used for MAIL—sub-100-fs pulses of 790-nm light (2). Moreover, gold nanoparticles do not blink or burn out, even after hours of observation. These findings suggest that metal nanoparticles are a viable alternative to fluorophores or semiconductor nanoparticles for biological labeling and imaging. Other advantages of the technique are that the gold nanoparticles can be prepared easily, have very low

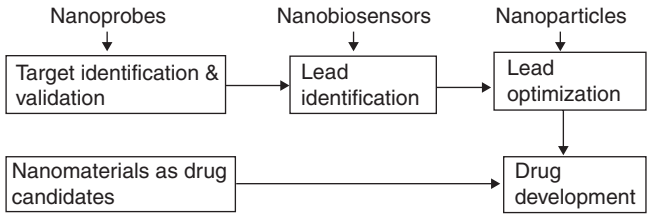

FIGURE 1 Application of nanobiotechnology at various stages of drug discovery.

TABLE 1 Basic Nanobiotechnologies Relevant to Drug Discovery

Nanoparticles
Gold nanoparticles
Lipoparticles
Magnetic nanoparticles
Micelles
Polymer nanoparticles
Quantum dots
Nanofibers
Nanowires
Carbon nanofibers
Nanoconduits
Nanotubes
Nanopipettes
Nanoneedles
Nanochannels
Nanopores
Nanofluidics
Nanobiotechnology applications in proteomics relevant to drug discovery
Nanoflow liquid chromatography
High-field asymmetric waveform ion mobility mass spectrometry
Use of nanotube electronic biosensor in proteomics
Fluorescence planar wave guide technology
Miscellaneous nanobiotechnologies
Visualization and manipulation at biological structures at nanoscale
Surface plasmon resonance
Drug discovery through study of endocytosis on nanoscale
Nanomaterials as drug candidates
Dendrimers
Fullerenes
Nanobodies
Use of nanodevices for drug discovery
Atomic force microscopy
Cantilevers
Nanoarrays and nanobiochips
Nanobiosensors
Nanowire devices

toxicity, and can readily be attached to molecules of biological interest. In addition, the laser light used to visualize the particles is a wavelength that causes only minimal damage to most biological tissues. This technology could enable tracking of a single molecule of a drug in a cell or other biological samples.

Surface plasmon resonance (SPR) has also been successfully applied with colloidal gold particles in buffered solution (3). This application offers many advantages over conventional SPR. The support is cheap, easily synthesized, and can be coated with various proteins or protein-ligand complexes by charge adsorption. With colloidal gold, the SPR phenomenon can be monitored in any UV-vis spectrophotometer. For high-throughput applications, the technology has been adapted in an automated clinical chemistry analyzer. Among the label-free systems currently available, the use of metal nanocolloids offers enhanced throughput and flexibility for real-time biomolecular recognition monitoring at a reasonable cost (4).

Quantum Dots

The use of quantum dots (QDs) for drug discovery has been explored extensively. Both advantages and drawbacks have been investigated (5).

Advantages of the use of QDs for drug discovery are as follows:

1. Enhanced optical properties as compared with organic dyes. QDs offer great imaging results that could not be achieved by organic dyes. They have narrow band emission together with large UV absorption spectra, which enables multiplexed imaging under a single light source.
2. Multiple leads can be tested on cell culture simultaneously. Similarly, the absorption of several drug molecules can be studied simultaneously for a longer period of time.
3. Using the surface functionalization properties of QDs, targeting capabilities can be added as well.
4. Because of the inorganic nature of QDs, their interaction with their immediate environment at in vivo states can be minimal compared with their organic counterparts.

QDs have not been totally perfected and some of the drawbacks of their use for drug discovery are as follows:

1. Size variation during the synthesis of single-color dots is 2% to 4% as reported by Evident Technologies and Invitrogen for Qdot. For applications such as capillary electrophoresis or gel electrophoresis, it could create false results. Therefore, QD synthesis techniques need to have improved quality control with respect to size distribution before they can be seriously used in drug discovery research.
2. For absorption, distribution, metabolism, and excretion (ADME) purposes, blue QDs (diameter of 3.7 nm) are the smallest class of the QD family, but they are considerably larger than organic dyes. Hence, the use of QDs for this purpose might not be desirable in special cases.
3. Similarly, the number of functional groups attached to an organic dye is usually one, or it can be controlled very precisely. However, in the case of QDs, the functional groups usually decorate the entire surface and thus cause multiple attachments of target molecules.

4. The transport of a large volume (because of multiple attachments of drug molecules to a single QD) across the membrane will be more difficult than a single molecule itself.
5. To satisfy all the available surface groups, larger numbers of target molecules are needed; this could affect the cost of the experiment. Although several methods have been reported to reduce the number of surface groups around a single dot, each of these methods adds to the final size of the QDs, which might not be desired in many cases, especially in studies related to kinetics and transport of drug molecules.
6. The "blinking" characteristics of QDs when they are excited with high-intensity light could be a limiting factor for fast scan systems such as flow cytometry.
7. Under combined aqueous-UV excitation conditions, QDs demonstrate oxidation and release of Cd ions into the environment. This is a definite concern for in vivo applications. As an alternative, capping the surface of a core dot with a large band-gap-semiconductor or proteins can eliminate or reduce the toxicity. But each additional step on the QDs will add to their final size and could even affect their final size distribution during these additional process steps.

ROLE OF NANOPROTEOMICS IN DRUG DISCOVERY

Nanoproteomics—application of nanobiotechnology to proteomics—improves on most current protocols including protein purification/display and automated identification schemes that yield unacceptably low recoveries with reduced sensitivity and speed while requiring more starting material. Low abundant proteins and proteins that can only be isolated from limited source material (e.g., biopsies) can be subjected to nanoscale protein analysis by nanocapture of specific proteins and complexes and optimization of all subsequent sample-handling steps leading to mass analysis of peptide fragments. This is a focused approach, also termed targeted proteomics and involves examination of subsets of the proteome, for example, those proteins that are either specifically modified, or bind to a particular DNA sequence, or exist as members of higher order complexes, or any combination thereof.

Development of miniaturized devices that enable rapid and direct analysis of the specific binding of small molecules to proteins could be of substantial importance to the discovery of and screening for new drug molecules. Highly sensitive and label-free direct electrical detection of small-molecule inhibitors of ATP binding to Abl has been reported by using silicon nanowire field-effect transistor devices (6). Abl, which is a protein tyrosine kinase, whose constitutive activity is responsible for chronic myelogenous leukemia, was covalently linked to the surfaces of silicon nanowires within microfluidic channels to create active electrical devices. Concentration-dependent binding of ATP and concentration-dependent inhibition of ATP binding by the competitive small-molecule antagonist imatinib were assessed by monitoring the nanowire conductance. In addition, concentration-dependent inhibition of ATP binding was examined for four additional small molecules, including reported and previously unreported inhibitors. These studies demonstrate that the silicon nanowire devices can readily and rapidly distinguish the affinities of distinct small-molecule inhibitors and thus could serve as a technology platform for drug discovery.

The use of liquid chromatography (LC) in analytical chemistry is well established but relatively low sensitivity associated with conventional LC makes it unsuitable for the analysis of certain biological samples. Furthermore, the flow rates at which it is operated are not compatible with the use of specific detectors, such as electrospray ionization mass spectrometers. Therefore, because of the analytical demands of biological samples, miniaturized LC techniques were developed to allow for the analysis of samples with greater sensitivity than that afforded by conventional LC. In nanoflow LC (nanoLC), chromatographic separations are performed using flow rates in the range of low nanoliter per minute, which result in high analytical sensitivity due to the large concentration efficiency afforded by this type of chromatography. NanoLC, in combination to tandem mass spectrometry, was first used to analyze peptides and as an alternative to other mass spectrometric methods to identify gel-separated proteins. Gel-free analytical approaches based on LC and nanoLC separations have been developed, which are allowing proteomics to be performed in faster and more comprehensive manner than by using strategies based on the classical 2-D gel electrophoresis approaches (7).

Protein identification using nanoflow liquid chromatography-mass spectrometry (MS-) MS (LC-MS-MS) provides reliable sequencing information for low femtomole level of protein digests. However, this task is more challenging for subfemtomole peptide levels.

APPLICATION OF VARIOUS NANODEVICES FOR DRUG DISCOVERY

Several nanodevices are commonly used in nanobiotechnology research in life sciences. Some of these are useful in drug discovery, for example, atomic force microscopy, and will be described here.

Atomic Force Microscopy

In its most basic form, atomic force microscopy (AFM) images topography by precisely scanning a probe across the sample to "feel" the contours of the surface. In contrast to light microscopy and scanning electron microscopy, AFM provides the most optimal means to investigate the surface structures in three dimensions, with resolutions as high as 0.1 to 0.2 nm. An approach called TREC (topography and recognition imaging) uses any of a number of different ligands such as antibodies, small organic molecules, and nucleotides bound to a carefully designed AFM tip-sensor, which can, in a series of unbinding experiments, estimate affinity and structural data (8). If a ligand is attached to the end of an AFM probe, one can simulate various physiological conditions and look at the strength of the interaction between the ligand and receptor under a wide range of circumstances. By functionalizing the tip, one can use it to probe biological systems and identify particular chemical entities on the surface of a biological sample. This opens the door to more effective use of AFM in drug discovery.

AFM has been used to study the molecular-scale processes underlying the formation of the insoluble plaques associated with Alzheimer's disease (AD). As one of a class of neurological diseases, caused by changes in a protein's physical state, called "conformational" diseases, it is particularly well suited for study with AFM. Extensive data suggest that the conversion of the Aβ peptide from soluble to insoluble forms is a key factor in the pathogenesis of AD. In recent years, AFM has provided useful insights into the physicochemical processes

involving Aβ morphology. AFM was the key in identifying the nanostructures that are now recognized as different stages of Aβ aggregation in AD and has revealed other forms of aggregation, which are observable at earlier stages and evolve to associate into mature fibrils. AFM can now be used to explore factors that either inhibit or promote fibrillogenesis. Use of AFM enabled the comparison of two monoclonal antibodies being studied as potential treatments for AD to select the one that did a better job of inhibiting the formation of these protofibrils. M266.2, which binds to the central portion of the Aβ, completely inhibited the formation of protofibrils, while the other antibody, m3D6, slowed but did not totally stop their growth (9). These results indicate that AFM can not only be reliably used to study the effect of different molecules on Aβ aggregation, but that it can also provide additional information such as the role of epitope specificity of antibodies as potential inhibitors of fibril formation.

Nanolasers

Nanolasers could be helpful in discovering drugs for neurodegenerative diseases such as Parkinson's and Alzheimer's as well as illnesses caused by radiation and chemical nerve agents. Mitochondria are involved in these diseases. Because mitochondria are so small, current techniques to find protective compounds are arduous and slow. By flowing mitochondria through a solid-state microscopic laser-making cavity that is powered up to just below the threshold of emitting laser light, the nanoscale mitochondria will do the "lasing" themselves. The laser light frequency given off by the mitochondria reveals their state of health. Healthy mitochondria "lase" light at one frequency, while disordered mitochondria lase at another. Using the nonlaser technique, laboratory researchers should be able to give large numbers of healthy mitochondria the "die" signal that they get from neurodegenerative diseases and then test to see if there are any compounds that block the "die" signal and can save the mitochondria. The nanolaser technique would enable screening of thousands of compounds.

Among the more promising drugs already known to protect mitochondria is cyclosporine, but its drawback is that it also weakens patients' immune systems. However, there are many variants of the compound that the nanolaser technique could quickly screen to see if they might be effective as well. One of those variations might have few or no side effects.

Biosensors for Drug Discovery

A biosensor is defined as an analytical device consisting of a biological component enzyme (antibody, entire cell, and DNA) and a physical transducer such as an optical device. Optical biosensors are gaining widespread uses in drug discovery because of recent advances in instrumentation and experimental design that enable label-free cell-based assays (10). Several biosensors use nanotechnology and can be termed nanobiosensors. Biosensors are currently being used in target identification, validation, assay development, lead optimization, and ADMET (absorption, distribution, metabolism, elimination, and toxicity) studies, but are best suited for soluble molecules. A primary application of current biosensor technologies is the optimization of limited-scope drug libraries against specific targets.

One example of application is drug discovery for HIV-1 as the virus entry into cells is a multifaceted process involving target cell CD4 and the chemokine

receptors, CXCR4, or CCR5. HIV-1 envelope (Env) protein mediates entry into cells by binding CD4 and an appropriate coreceptor, which triggers structural changes in Env that lead to fusion between the viral and cellular membranes. Virus–receptor interactions are among the therapeutic targets. A biosensor assay was developed for studying ligand–membrane receptor interactions: binding of antibodies and HIV-1 Env to chemokine receptors (11).

Paired with lipoparticle technology being developed by Integral Molecular Inc., biosensors can be used to address some of the most complex biological problems facing the drug discovery industry, including cell–cell recognition; cell–adhesion, cell–signaling, cell–lipid interactions; and protein–protein interactions. Potential applications in drug discovery are as follows:

- Where high-throughput screening of random libraries does not work.
- Only weak ligands are known and ultrasensitivity is required.
- When high-content information is needed (affinity, kinetics).
- For structure-based rational drug design.
- ADMET studies: drug binding to cytochromes, serum proteins, and lipid solubility.
- For peptide-based ligand design where no ligand is available.

Role of Nanofluidics, Nanoarrays, and Nanobiochips

Microfluidics, microarrays, and biochips have established their usefulness in drug discovery. The next level of miniaturization is on nanoscale and would further extend and refine applications in this area. An assay has been described for a kinase screen based on the electrophoretic separation of fluorescent product and substrate using a Caliper nanofluidics platform in on-chip incubation mode (12). The screen in on-chip mode was characterized by high precision as well as good sensitivity and led to the identification of four novel chemical series of inhibitors.

A biochip measuring 1 cm^2 has been devised that holds thousands of tiny cylindrical vessels, which are open at the top and sealed at the bottom with alumina containing numerous pores measured in nanometers (13). This "nanoporous" material makes it possible to carry out reactions inside the vessels. The goal is to produce "laboratories-on-a-chip" less than a half-inch square that might contain up to a million test chambers, or "reactors," each capable of screening an individual drug.

NANOBIOTECHNOLOGY FOR TARGET VALIDATION

Multivalent attachment of small molecules to nanoparticles can increase specific binding affinity and reveal new biological properties of such nanomaterial. Multivalent drug design has yielded antiviral and antiinflammatory agents several orders of magnitude more potent than monovalent agents. Parallel synthesis of a library has been described, which is comprised of nanoparticles decorated with different synthetic small molecules (14). Screening of this library against different cell lines led to discovery of a series of nanoparticles with high specificity for endothelial cells, activated human macrophages, or pancreatic cancer cells. This multivalent approach could facilitate development of functional nanomaterials for applications such as differentiating cell lines, detecting distinct cellular states, and targeting specific cell types. It has potential applications in high-throughput drug discovery, target validation, diagnostics, and human therapeutics (15).

NANOTECHNOLOGY-BASED DRUG DESIGN AT CELL LEVEL

To create drugs capable of targeting some of the most devastating human diseases, scientists must first decode exactly how a cell or a group of cells communicates with other cells and reacts to a broad spectrum of complex biomolecules surrounding it. But even the most sophisticated tools currently used for studying cell communications suffer from significant deficiencies and typically can detect only a narrowly selected group of small molecules, or for a more sophisticated analysis, the cells must be destroyed for sample preparation. A nanoscale probe, the scanning mass spectrometry (SMS) probe, can capture both the biochemical makeup and the topography of complex biological objects. The SMS probe can help map all those complex and intricate cellular communication pathways by probing cell activities in the natural cellular environment, which might lead to better disease diagnosis and drug design on the cellular level.

NANOMATERIALS AS DRUG CANDIDATES

In addition to the use of nanobiotechnology for drug discovery, some drugs are being developed from nanomaterials. Well-known examples of these are dendrimers, fullerenes, and nanobodies.

Dendrimers as Drug Candidates

Dendrimers are a novel class of 3-D nanoscale, core-shell structures that can be precisely synthesized for a wide range of applications. Specialized chemistry techniques enable precise control over the physical and chemical properties of the dendrimers. They are most useful in drug delivery but can also be used for the development of new pharmaceuticals with novel activities. Polyvalent dendrimers interact simultaneously with multiple drug targets. They can be developed into novel-targeted cancer therapeutics. Polymer–protein and polymer–drug conjugates can be developed as anticancer drugs. These have the following advantages:

- Tailor-made surface chemistry
- Nonimmunogenic
- Inherent body distribution enabling appropriate tissue targeting
- Possibly biodegradable

Dendrimer conjugation with low-molecular-weight drugs has been of increasing interest recently for improving pharmacokinetics, targeting drugs to specific sites, and facilitating cellular uptake. Opportunities for increasing the performance of relatively large therapeutic proteins such as streptokinase (SK) using dendrimers have been explored in one study (16). Using the active ester method, a series of streptokinase-poly (amido amine) (PAMAM) G3.5 conjugates was synthesized with varying amounts of dendrimer-to-protein molar ratios. All of the SK conjugates displayed significantly improved stability in phosphate buffer solution, compared to free SK. The high-coupling reaction efficiencies and the resulting high enzymatic activity retention achieved in this study could enable a desirable way for modifying many bioactive macromolecules with dendrimers.

Fullerenes as Drug Candidates

A key attribute of the fullerene molecules is their numerous points of attachment, allowing for precise grafting of active chemical groups in 3-D orientations. This attribute, the hallmark of rational drug design, allows for positional control in matching fullerene compounds to biological targets. In concert with other attributes, namely, the size of the fullerene molecules, their redox potential, and its relative inertness in biological systems, it is possible to tailor requisite pharmacokinetic characteristics to fullerene-based compounds and optimize their therapeutic effect.

Fullerene antioxidants bind and inactivate multiple circulating intracellular free radicals, giving them unusual power to stop free radical injury and to halt the progression of diseases caused by excess free radical production. Fullerenes provide effective defense against all of the principal damaging forms of reactive oxygen species. C60 fullerene has 30 conjugated carbon–carbon double bonds, all of which can react with a radical species. In addition, the capture of radicals by fullerenes is too fast to measure and is referred to as "diffusion controlled," meaning the fullerene forms a bond with a radical every time it encounters one. Numerous studies demonstrate that fullerene antioxidants work significantly better as therapeutic antioxidants than other natural and synthetic antioxidants, at least for CNS degenerative diseases. In oxidative injury or disease, fullerene antioxidants can enter cells and modulate free radical levels, thereby substantially reducing or preventing permanent cell injury and cell death. Fullerenes have potential applications in the treatment of diseases where oxidative stress plays a role in the pathogenesis. Mechanisms of action of fullerene are as follows:

- Fullerenes can capture multiple electrons derived from oxygen free radicals in unoccupied orbitals.
- When an attacking radical forms a bond with fullerene creating a stable and relatively nonreactive fullerene radical.
- A tris-malonic acid derivative of the fullerene C60 molecule (C_3) is capable of removing the biologically important superoxide radical.
- C_3 localizes to mitochondria, suggest that C_3 functionally replaces manganese superoxide dismutase (SOD), acting as a biologically effective SOD mimetic (17).

The first-generation antioxidant fullerenes are based on the C_3 compound, produced by the precise grafting of three malonic acid groups to the C60 fullerene surface. C_3 has shown significant activity against a spectrum of neurodegenerative disorders in animal models. These animal models replicate many of the features of important human neurodegenerative diseases, including amyotrophic lateral sclerosis and Parkinson's disease.

The second-generation antioxidant fullerenes are based on DF-1, the dendrofullerene, produced by attaching a highly water-soluble conjugate to the C60 fullerene core. In preclinical testing, C60 has shown DF-1 to be highly soluble, nontoxic, and able to retain a high level of antioxidant activity in both cultured cells and animals.

A number of water-soluble C60 derivatives have been suggested for various medical applications. These applications include neuroprotective agents, HIV-1 protease inhibitors, bone-disorder drugs, transfection vectors, X-ray

contrast agents, photodynamic therapy agents, and a C60–paclitaxel chemotherapeutic.

Another possible application of fullerenes is to be found in nuclear medicine, in which they could be used as an alternative to chelating compounds that prevent the direct binding of toxic metal ions to serum components. This could increase the therapeutic potency of radiation treatments and decrease their adverse effect profile, because fullerenes are resistant to biochemical degradation within the body.

Nanobodies

Nanobodies, derived from naturally occurring single-chain antibodies, are the smallest fragments of naturally occurring heavy-chain antibodies that have evolved to be fully functional in the absence of a light chain. The Nanobody technology (Ablynx, Ghent, Belgium) was originally developed following the discovery that camelidae (camels and llamas) possess a unique repertoire of fully functional antibodies that lack light chains (18). Like conventional antibodies, nanobodies show high target specificity and low inherent toxicity; however, like small-molecule drugs they can inhibit enzymes and can access receptor clefts. Their unique structure consists of a single variable domain (VHH), a hinge region, and two constant domains (CH_2 and CH_3). The cloned and isolated VHH domain is a perfectly stable polypeptide harboring the full antigen-binding capacity of the original heavy chain. This newly discovered VHH domain is the basic component of Ablynx's Nanobodies®. Ablynx's Nanobodies are naturally highly homologous to human antibodies. They can also be humanized to within 99% sequence homology of human VH domains. Ablynx's Nanobody platform can quickly deliver therapeutic leads for a wide range of targets. Advantages of Nanobodies are as follows:

- They combine the advantages of conventional antibodies with important features of small-molecule drugs.
- Nanobodies can address therapeutic targets not easily recognized by conventional antibodies such as active sites of enzymes.
- Nanobodies are very stable.
- They can be administered by means other than injection.
- They can be produced cost-effectively on a large scale.
- Nanobodies have an extremely low immunogenic potential. In animal studies, the administration of Nanobodies does not yield any detectable humoral or cellular immune response.

The cloning and selection of antigen-specific nanobodies obviate the need for construction and screening of large libraries and for lengthy and unpredictable in vitro affinity maturation steps. The unique and well-characterized properties enable nanobodies to excel conventional therapeutic antibodies in terms of recognizing uncommon or hidden epitopes, binding into cavities or active sites of protein targets, tailoring of half-life, drug format flexibility, low immunogenic potential, and ease of manufacture. Moreover, the favorable biophysical and pharmacological properties of nanobodies, together with the ease of formatting them into multifunctional protein therapeutics, leave them ideally placed as a new generation of antibody-based therapeutics. They have a potential as cancer therapeutic agents (19).

Another example of use of nanobodies as novel drugs is nanobody-conjugated human trypanolytic factor for treatment of human African trypanosomiasis (HAT). Normal human serum (NHS) contains apolipoprotein L-I (apoL-I), which lyses African trypanosomes except resistant forms such as *Trypanosoma brucei rhodesiense*, which expresses the apoL-I–neutralizing serum resistance–associated (SRA) protein, endowing this parasite with the ability to infect humans and cause HAT. A truncated apoL-I (Tr-apoL-I) has been engineered by deleting its SRA-interacting domain, which makes it lytic for *T. b. rhodesiense*. Tr-apoL-I has been conjugated with a nanobody that efficiently targets conserved cryptic epitopes of the variant surface glycoprotein of trypanosomes to generate a new type of immunotoxin with potential for trypanosomiasis therapy (20). Treatment with this engineered conjugate resulted in clear curative and alleviating effects on acute and chronic infections of mice with both NHS-resistant and NHS-sensitive trypanosomes.

DISCOVERING PERSONALIZED MEDICINES

Personalized medicine simply means the prescription of specific treatments and therapeutics best suited for an individual. It is also referred to as individualized or individual-based therapy. Personalized medicine is based on the idea of using a patient's genotype as a factor in deciding on treatment options but other factors are also taken into consideration. Molecular diagnostics is an important component of personalized medicine and nanobiotechnologies are already being used in molecular diagnostics. Although current efforts using pharmacogenomics and pharmacogenetics include matching the existing drugs to the right patients for optimal efficacy and safety, future personalized medicines could be discovered and designed for specific groups of patients using pharmacoproteomics. Nanobiotechnology shows promise of facilitating discovery of personalized medicines apart from facilitating integration of diagnostics and therapeutics (21).

FUTURE OUTLOOK

None of the nanoparticles available are ideal for all requirements of drug discovery. The choice may depend on the needs. QDs can be used for high-throughput cell-based studies with the advantage of multiplexing (i.e., multiple leads can be tested at the same time). However, as discussed earlier there are some limitations yet to be resolved for their use in the drug discovery studies, namely, toxicity, size variation, agglomeration, potential multiple drug attachment to a single QD, and blinking.

An increasing use of nanobiotechnology by the pharmaceutical and biotechnology industries is anticipated. Nanotechnology will be applied at all stages of drug development—from formulations for optimal delivery to diagnostic applications in clinical trials. In the near future, it may be possible to fully model an individual cell's structure and function by computers connected to nanobiotechnology systems. Such a detailed virtual representation of how a cell functions might enable scientists to develop novel drugs with unprecedented speed and precision without any experiments in living animals.

In another promising area of application is the development of non-biodegradable 3-D scaffolds to hold stem cells for pharmaceutical and biological

research. These tissue constructs can be used to test new drugs. Since tissues grow in 3-D and not 2-D, 3-D would be more suitable for early drug screening.

REFERENCES

1. Jain KK. Nanobiotechnology: Applications, Markets and Companies. Basel, Switzerland: Jain PharmaBiotech Publications, 2009:1–724.
2. Farrer RA, Butterfield FL, Chen VW, et al. Highly efficient multiphoton-absorption-induced luminescence from gold nanoparticles. Nano Lett 2005; 5:1139–1142.
3. Englebienne P, Van Hoonacker A, Verhas M. Surface plasmon resonance: Principles, methods and applications in biomedical science. Spectroscopy 2003; 17:255–273.
4. Englebienne P, Van Hoonacker A, Verhas M, et al. Advances in high-throughput screening: Biomolecular interaction monitoring in real-time with colloidal metal nanoparticles. Comb Chem High Throughput Screen 2003; 6:777–787.
5. Ozkan M. Quantum dots and other nanoparticles: What can they offer to drug discovery? Drug Discov Today 2004; 9:1065–1071.
6. Wang WU, Chen C, Lin K, et al. Label-free detection of small-molecule-protein interactions by using nanowire nanosensors. Proc Natl Acad Sci U S A 2005; 102:3208–3212.
7. Cutillas PR. Principles of nanoflow liquid chromatography and applications to proteomics. Curr Nanosci 2005; 1:65–71.
8. Ebner A, Kienberger F, Kada G, et al. Localization of single avidin-biotin interactions using simultaneous topography and molecular recognition imaging. Chemphyschem 2005; 6:897–900.
9. Legleiter J, Czilli DL, Gitter B, et al. Effect of different anti-Abeta antibodies on Abeta fibrillogenesis as assessed by atomic force microscopy. J Mol Biol 2004; 335:997–1006.
10. Fang Y. Label-free cell-based assays with optical biosensors in drug discovery. Assay Drug Dev Technol 2006; 4:583–595.
11. Hoffman TL, Canziani G, Jia L, et al. A biosensor assay for studying ligand-membrane receptor interactions, binding of antibodies and HIV-1 Env to chemokine receptors. Proc Natl Acad Sci U S A 2000; 97:11215–11220.
12. Perrin D, Frémaux C, Scheer A. Assay development and screening of a serine/threonine kinase in an on-chip mode using caliper nanofluidics technology. J Biomol Screen 2006; 11:359–368.
13. Wang Z, Haasch RT, Lee GU. Mesoporous membrane device for asymmetric biosensing. Langmuir 2005; 21:1153–1157.
14. Weissleder R, Kelly K, Sun EY, et al. Cell-specific targeting of nanoparticles by multivalent attachment of small molecules. Nat Biotechnol 2005; 23:1418–1423.
15. Jain KK. Nanoparticles as targeting ligands. Trends Biotechnol 2006; 24:143–145.
16. Wang X, Inapagolla R, Kannan S, et al. Synthesis, characterization, and in vitro activity of dendrimer-streptokinase conjugates. Bioconjug Chem 2007; 18:791–799.
17. Ali SS, Hardt JI, Quick KL, et al. A biologically effective fullerene (C60) derivative with superoxide dismutase mimetic properties. Free Radic Biol Med 2004; 37:1191–1202.
18. Conrath KE, Wernery U, Muyldermans S, et al. Emergence and evolution of functional heavy-chain antibodies in Camelidae. Dev Comp Immunol 2003; 27:87–103.
19. Revets H, De Baetselier P, Muyldermans S. Nanobodies as novel agents for cancer therapy. Expert Opin Biol Ther 2005; 5:111–124.
20. Baral TN, Magez S, Stijlemans B, et al. Experimental therapy of African trypanosomiasis with a nanobody-conjugated human trypanolytic factor. Nat Med 2006; 12:580–584.
21. Jain KK. A Textbook of Personalized Medicine. Springer Science, New York, 2009.

Index